GEOTHERMAL ENERGY:

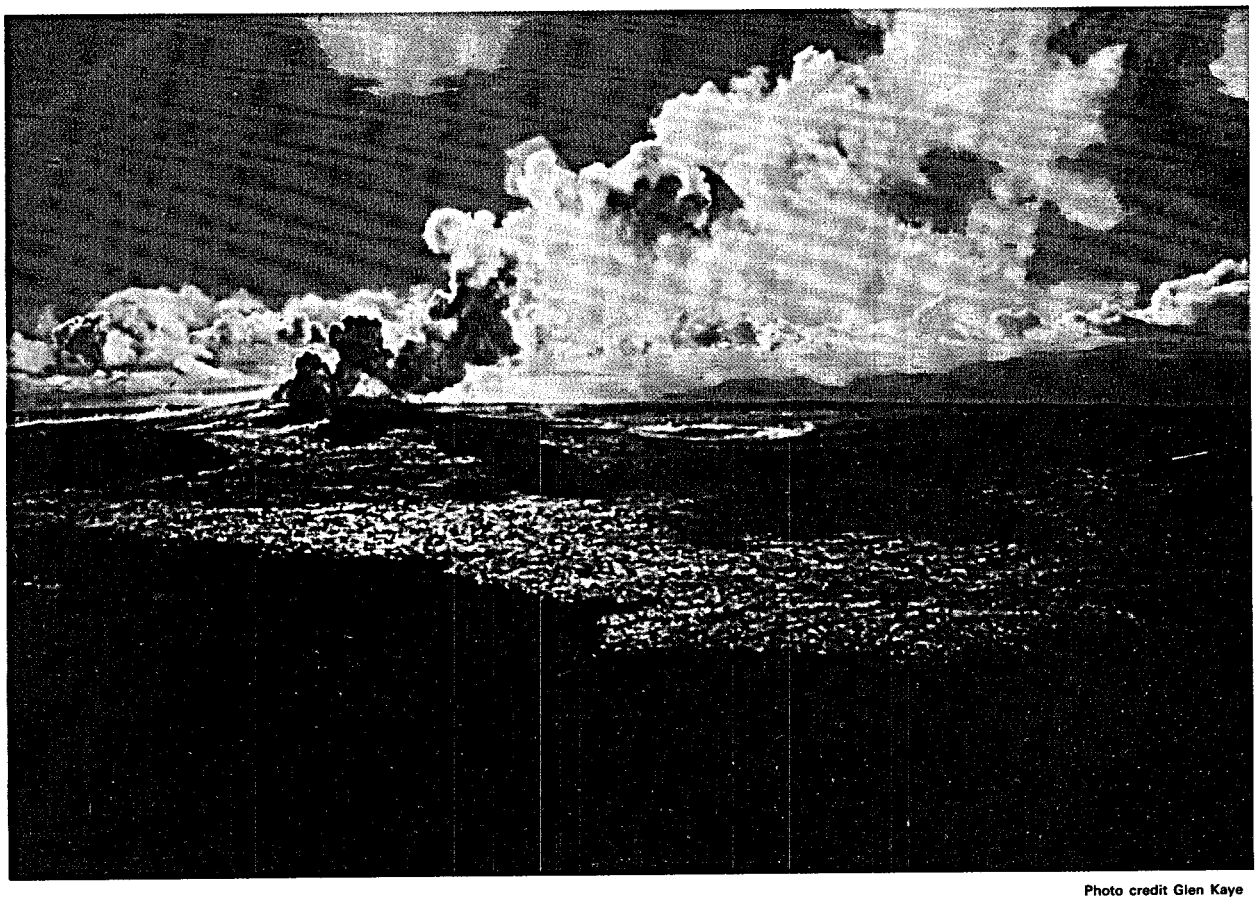


Photo credit Glen Kaye

A NOVELTY BECOMES RESOURCE

MASTER

GEOTHERMAL RESOURCES COUNCIL

Release for Announcement in
Energy Research Abstracts

DISCLAIMER

This report was prepared as an account of work sponsored by an agency of the United States Government. Neither the United States Government nor any agency Thereof, nor any of their employees, makes any warranty, express or implied, or assumes any legal liability or responsibility for the accuracy, completeness, or usefulness of any information, apparatus, product, or process disclosed, or represents that its use would not infringe privately owned rights. Reference herein to any specific commercial product, process, or service by trade name, trademark, manufacturer, or otherwise does not necessarily constitute or imply its endorsement, recommendation, or favoring by the United States Government or any agency thereof. The views and opinions of authors expressed herein do not necessarily state or reflect those of the United States Government or any agency thereof.

DISCLAIMER

Portions of this document may be illegible in electronic image products. Images are produced from the best available original document.

CONF-780708--P2

GEOTHERMAL ENERGY: A NOVELTY BECOMES RESOURCE

Transactions

Volume 2 Section 2

Geothermal Resources Council

Annual Meeting

25-27 July 1978

Hilo, Hawaii

Release for Announcement in
Energy Research Abstracts

GEOTHERMAL RESOURCES COUNCIL • P.O. BOX 98 • DAVIS, CALIFORNIA 95616

© GEOTHERMAL RESOURCES COUNCIL
1978

TABLE OF CONTENTS

Section 1

Introduction . . . . . *ix*

Program Committee . . . . . *xi*

Addoms, J. F., B. Breindel and C. M. Gracey: WELLSITE VERIFICATION TESTING OF AN ADVANCED GEOTHERMAL PRIMARY HEAT EXCHANGER (APEX) 1

Allen, C. A., T. W. Lawford and D. H. Van Haaften: LIQUID-FLUIDIZED-BED HEAT EXCHANGERS FOR A 50-MW PLANT. 5

Anderson, Lennart A. and Gordon R. Johnson: SOME OBSERVATIONS OF THE SELF-POTENTIAL EFFECT IN GEOTHERMAL AREAS IN HAWAII AND NEVADA 9

Anglin, Richard L., Jr.: LOCAL GOVERNMENT MANAGEMENT OF GEOTHERMAL RESOURCES. 13

Arnold, Charles, Jr., Joseph A. Coquat and Leonard E. Baker: EVALUATION OF SEALS FOR A GEOTHERMAL LOGGING TOOL 17

Atkinson, David J.: GEOTHERMAL DEVELOPMENT IN RENO. 21

Austin, John C.: A LOW TEMPERATURE GEOTHERMAL SPACE HEATING DEMONSTRATION PROJECT 23

Bannerman, J. K., Neil Davis and R. M. Wolke: GEOTHERMAL DRILLING FLUIDS SYSTEMS. 27

Barkman, Dr. James H.: THE LEARNING CURVE CONCEPT APPLIED TO THE DEVELOPMENT OF A HYDROTHERMAL RESOURCE 31

Basoeki, Ir. Moh., Vincent T. Radja: RECENT DEVELOPMENT OF 30 MW KAMOJANG GEOTHERMAL POWER PROJECT, WEST JAVA, INDONESIA 35

Beauchamp, Ellen L.: ENVIRONMENTAL RESPONSE TO NON-ELECTRIC GEOTHERMAL ENERGY: AN ATTITUDINAL ASSESSMENT 39

Beland, John M., John R. Ferebauer, John M. McGee, Stanley P. Szczepanowski: U.S. FOREST SERVICE CONSIDERATIONS FOR GEOTHERMAL LEASING IN THE ISLAND PARK AREA 43

Benoit, Walter R.: THE USE OF SHALLOW AND DEEP TEMPERATURE GRADIENTS IN GEOTHERMAL EXPLORATION IN NORTHWESTERN NEVADA USING THE DESERT PEAK THERMAL ANOMALY AS A MODEL 45

Bickmore, David K. and Kenneth W. Bull: FEDERAL GEOTHERMAL LEASING PROGRAM, 1974-78 47

Black, Alan D., James G. Wilson, Sidney J. Green and Jeddy D. Nixon: DEVELOPMENT OF IMPROVED ROTARY SEALS FOR DOWNHOLE MOTORS IN GEOTHERMAL APPLICATIONS. 51

Butler, David and Paul Larry Brown: AMBIENT GROUND-NOISE MEASUREMENTS AND EXPLORATION FOR GEOTHERMAL RESOURCES. 55

Butz, James R. and Glenn E. Coury: INTRODUCTION TO THE GEOTHERMAL WELL DESIGN HANDBOOK. 59

Campbell, Thomas A.: ANALYSIS OF GEOTHERMAL WELL PUMPING. 63

Cargill, Kirk and Robert D. Conover: CONCEPTS IN UNITIZATION OF FEDERAL GEOTHERMAL LEASES 67

Caton, Paul W.: TECHNIQUES FOR INTERPRETING AND IMPROVING Vp/Vs MEASUREMENTS WHEN ASSUMING A LAYERED GEOTHERMAL MODEL 71

Cerini, Donald J.: GEOTHERMAL ROTARY SEPARATOR FIELD TESTS. 75

Chapman, David S., Kevin T. Kilty and Charles W. Mase: TEMPERATURES AND THEIR DEPENDENCE ON GROUNDWATER FLOW IN SHALLOW GEOTHERMAL SYSTEMS 79

Chappell, Robert N., John L. Griffith, Wayne R. Knowles and Robert J. Schultz: THE MULTI-PURPOSE GEOTHERMAL TEST AND EXPERIMENTAL ACTIVITIES AT RAFT RIVER, IDAHO. 83

Charles, Robert W.: EXPERIMENTAL ALTERATION OF A GRANODIORITE IN A CIRCULATION SYSTEM 87

Chaturvedi, Lokesh, Conrad G. Keyes, Jr., Chandler A. Swanberg and Yash P. Gupta: POTENTIAL FOR GEOTHERMAL DESALINATION IN NEW MEXICO 91

Chen, Bill H. and Eugene M. Grabbe: PLANNING FOR GEOTHERMAL DEVELOPMENT IN HAWAII 95

Chen, Bill H., Deane H. Kihara, Paul C. Yuen and Patrick K. Takahashi: WELL TEST RESULTS FROM HGP-A. 99

Chen, H. K., J. R. Counsil and H. J. Ramey, Jr.: EXPERIMENTAL STEAM-WATER RELATIVE PERMEABILITY CURVES 103

Colp, John L. and Reginald T. Okamura: DRILLING INTO MOLTEN ROCK AT KILAUEA IKI 105

Combs, Jim and Dave Jarzabek: SEISMIC WAVE ATTENUATION ANOMALIES IN THE EAST MESA GEOTHERMAL FIELD, IMPERIAL VALLEY, CALIFORNIA: PRELIMINARY RESULTS 109

Conn, Andrew F. and Robert P. Radtke: EVALUATION OF CAVITATING JETS FOR INCREASED GEOTHERMAL DRILLING RATES 113

Corwin, Robert F., Sergio Diaz C. and Jorge Rodriguez B.: SELF-POTENTIAL SURVEY AT THE CERRO PRIETO GEOTHERMAL FIELD, BAJA CALIFORNIA, MEXICO 115

Coulter, George W.: A PRELIMINARY APPRECIATION OF EFFECTS ON AQUATIC ENVIRONMENTS OF GEOTHERMAL POWER DEVELOPMENT IN NEW ZEALAND 119

Cox, Malcolm E.: THE LAMBASA AREA GEOTHERMAL INVESTIGATION, FIJI 121

Crow, Neil B. and Paul W. Kasameyer: MONITORING NATURAL SUBSIDENCE AND SEISMICITY IN THE IMPERIAL VALLEY AS A BASIS FOR EVALUATING POTENTIAL IMPACTS OF GEOTHERMAL PRODUCTION 125

Culver, Gordon Gene and Gordon M. Reistad: TESTING AND MODELING OF DOWNHOLE HEAT EXCHANGERS IN SHALLOW GEOTHERMAL SYSTEMS 129

D'Alessio, Gregory J. and Robert Hartley: EPA POLLUTION CONTROL GUIDANCE FOR THE GEOTHERMAL INDUSTRY 133

Danesh, A., C. Ehlig-Economides and H. J. Ramey, Jr.: THE EFFECT OF TEMPERATURE LEVEL ON ABSOLUTE PERMEABILITY OF UNCONSOLIDATED SILICA AND STAINLESS STEEL 137

Defferding, Leo J. and Ron A. Walter: DISPOSAL OF LIQUID EFFLUENTS FROM GEOTHERMAL INSTALLATIONS 141

Dellechaie, F.: A GEOLOGICAL AND HYDRO-GEOCHEMICAL STUDY OF THE LA GRANDE AREA, UNION COUNTY, OREGON 145

Dennis, Bert R. and Hugh D. Murphy: BOREHOLE TEMPERATURE SURVEY ANALYSIS HOT DRY ROCK GEOTHERMAL RESERVOIR 149

Dhillon, H. and A. El-Sawy: AN APPROACH TO RISK ANALYSIS FOR GOVERNMENT-SPONSORED DEMONSTRATION PROJECTS 153

Dondanville, Richard F.: GEOLOGIC CHARACTERISTICS OF THE VALLES CALDERA GEOTHERMAL SYSTEM, NEW MEXICO 157

Donovan, L. E., J. L. Griffith, R. J. Schultz and P. M. Wright: DIRECT APPLICATIONS OF GEOTHERMAL ENERGY TECHNICAL ASSISTANCE PROGRAM 161

Donovan, L. E.: GEOTHERMAL - A VIABLE AND ECONOMIC COMFORT HEATING SYSTEM CHOICE 163

Downs, W. F., H. L. Barnes and J. D. Rimstidt: FIELD SCALING TESTS ON GEOTHERMAL BRINES 165

Edmunds, Stahrl W.: INSTITUTIONAL POLICY AND PLANNING ISSUES IN GEOTHERMAL DEVELOPMENT - THE CASE OF IMPERIAL COUNTY 167

Ehara, Sachio and Kozo Yuhara: SEISMIC NOISE MEASUREMENTS AT SOME GEOTHERMAL AREAS IN JAPAN 171

Eilers, L. H., L. K. Moran, E. B. Nelson, L. B. Spangle, B. E. Simpson and J. F. Williams: DEVELOPMENT OF GEOTHERMAL WELL COMPLETION SYSTEMS - I 173

Elders, W. A., J. R. Hoagland and E. R. Olson: HYDROTHERMAL MINERALOGY AND ISOTOPIC GEOCHEMISTRY IN THE CERRO PRIETO GEOTHERMAL FIELD, MEXICO. III. PRACTICAL APPLICATIONS 177

Ershaghi, I., E. L. Dougherty, H. Ucok and F. Ghassemi: PROBLEMS IN ESTIMATION OF SALINITY PROFILE IN LIQUID DOMINATED GEOTHERMAL SYSTEMS 181

Fan, Pow-foong: MINERAL ASSEMBLAGES OF HYDROTHERMAL ALTERATIONS OF BASALTS FROM HAWAII 185

Fassbender, Linda L., Clarence H. Bloomster and A. Henry Schilling: FEASIBILITY OF POTENTIAL GEOTHERMAL ENERGY APPLICATIONS FOR RIVERSIDE, CALIFORNIA 189

Fisher, Leonard A., Allan R. Black and Sam F. Fogleman: TOTAL ENERGY RECOVERY SYSTEM FOR AGRIBUSINESS: LAKE COUNTY STUDY 193

Frangos, W., G. W. Hohmann and G. R. Jiracek: THREE-DIMENSIONAL ROVING DIPOLE INTERPRETATION 195

Furumoto, Augustine S.: THE RELATIONSHIP OF A GEOTHERMAL RESERVOIR TO THE GEOLOGICAL STRUCTURE OF THE EAST RIFT OF KILAUEA VOLCANO, HAWAII 199

Garg, S. K.: PRESSURE TRANSIENT ANALYSIS FOR TWO-PHASE GEOTHERMAL RESERVOIRS 203

Godare, Bill: GEOTHERMAL WELLHEADS - THE HEART OF GEOTHERMAL PRODUCTION SYSTEMS 207

Goff, Fraser E. and Julie M. Donnelly: THE INFLUENCE OF P_{CO_2}, SALINITY, AND BEDROCK TYPE ON THE Na-K-Ca GEOTHERMOMETER AS APPLIED IN THE CLEAR LAKE GEOTHERMAL REGION, CALIFORNIA 211

Goldsmith, Martin: COOLING WATER REQUIREMENTS FOR GEOTHERMAL POWER PLANTS AND WATER AVAILABILITY IN THE IMPERIAL VALLEY 215

Goldstein, N. E., E. Mozley, T. D. Gamble and H. F. Morrison: MAGNETOTELLURIC INVESTIGATIONS AT MT. HOOD, OREGON 219

Goldstein, Steven, Ranvir Trehan, A. El-Sawy and J. Leigh: A COMPARATIVE ANALYSIS OF ENERGY COSTING METHODOLOGIES 223

Grijalva, Ramon L.: THE FOSSIL FUEL/GEOTHERMAL HYBRID CYCLE APPLIED TO MARGINALLY USEFUL LIQUID DOMINATED HYDROTHERMAL RESOURCES 227

Grim, Paul J., Clayton R. Nichols, Phillip M. Wright, George W. Berry and James Swanson: STATE MAPS OF LOW-TEMPERATURE GEOTHERMAL RESOURCES 223

Gudiksen, P. H., M. C. Axelrod, D. L. Ermak, K. C. Lamson and R. A. Nyholm: AIR QUALITY ASSESSMENT STUDIES OF GEOTHERMAL DEVELOPMENT IN THE IMPERIAL VALLEY 235

Gulati, M. S., S. C. Lipman and C. J. Strobel: TRITIUM TRACER SURVEY AT THE GEYSERS 237

Gunaji, N. N., Lokesh Chaturvedi, E. Thode, Leo LaFrance, C. Swanberg and A. Walvekar: A GEOTHERMAL FIELD NEAR NEW MEXICO STATE UNIVERSITY AND ITS POTENTIAL AS CAMPUS ENERGY SUPPLIER 241

Gustavson, Thomas C, and M. M. McGraw: POTENTIAL ENVIRONMENTAL CONCERNS ASSOCIATED WITH THE DEVELOPMENT OF GEOPRESSURED-GEOTHERMAL RESOURCES OF THE UNITED STATES GULF COAST 245

Gutschick, Vincent and Kenneth Rea: ENVIRONMENTAL ASSESSMENT OF DISSOLVED GASES IN LASL'S HOT DRY ROCK GEOTHERMAL SOURCE DEMONSTRATION PROJECT 249

Hankins, B. E., R. E. Chavanne, R. A. Ham, O. C. Karkalits and J. I. Palermo: CHEMICAL ANALYSIS OF WATER FROM THE WORLD'S FIRST GEOPRESSURED-GEOTHERMAL WELL 253

Hanson, Jonathan M. and Paul W. Kasameyer: PREDICTING PRODUCTION TEMPERATURE USING TRACER METHODS 257

Harrar, J. E., L. E. Lorensen, C. H. Otto, Jr., S. B. Deutscher and G. E. Tardiff: EFFECTS OF ORGANIC ADDITIVES ON THE FORMATION OF SOLIDS FROM HYPERSALINE GEOTHERMAL BRINE 259

Hayashi, Masao, Toshimitsu Mimura and Tatsuo Yamasaki: GEOLOGICAL SETTING OF REINJECTION WELLS IN THE OTAKE AND THE HATCHOBARU GEOTHERMAL FIELD, JAPAN 263

Hendrickson, Robert R., Sidney J. Green, Arfon H. Jones and Richard W. Winzenried: FULL-SCALE LABORATORY TESTING OF EXPERIMENTAL GEOTHERMAL ROCK BITS 267

Hendron, R. H.: HOT DRY ROCK ENERGY EXTRACTION OPERATIONS 271

Hill, James H.: THE LASL HOT DRY ROCK GEOTHERMAL ENERGY DEVELOPMENT PROJECT 275

Hirasuna, A. R., C. A. Stephens and G. R. Veal: IMPORTANT CONCLUSIONS BASED ON RESULTS OF GEOTHERMAL CASING PACKER SEAL ELASTOMERS TESTING 279

Hoagland, James R. and Wilfred A. Elders: HYDROTHERMAL MINERALOGY AND ISOTOPIC GEOCHEMISTRY IN THE CERRO PRIETO GEOTHERMAL FIELD, MEXICO. I. HYDROTHERMAL MINERAL ZONATION 283

Hohmann, Gerald W., Richard C. Fox and Luiz Rijo: TOPOGRAPHIC EFFECT IN RESISTIVITY SURVEYS 287

Horne, Roland N. and Henry J. Ramey, Jr.: STEAM/WATER RELATIVE PERMEABILITIES FROM PRODUCTION DATA 291

Hsieh, Chih-Hang and Henry J. Ramey, Jr.: AN INSPECTION OF EXPERIMENTAL DATA ON VAPOR PRESSURE LOWERING IN POROUS MEDIA 295

Hsu, Y. C., Y-M Lu, F. D. Ju, and K. C. Dhingra: ENGINEERING METHODS FOR PREDICTING PRODUCTIVITY AND LONGEVITY OF HOT-DRY-ROCK GEOTHERMAL RESERVOIR IN THE PRESENCE OF THERMAL CRACKS 297

Hunsbedt, Anstein and Paul Kruger: ENERGY EXTRACTION EXPERIMENTS IN THE SGP RESERVOIR MODEL 299

Ibrahim, Abdelwahid: DEPENDENCE OF VELOCITY AND RESISTIVITY OF VOLCANIC ROCKS ON TEMPERATURE AND POROSITY 303

Ingvarsson, I. J. and W. W. Madsen: DETERMINATION OF THE 5MW DESIGN CASE FOR POWER PRODUCTION AT RAFT RIVER 305

Ingvarsson, I. J. and S. E. Turner: WORKING FLUID AND CYCLE SELECTION CRITERIA FOR BINARY GEOTHERMAL POWER PLANT 309

Isherwood, William F. and Timothy J. MacGillvray: EVALUATION OF WILDCAT GEOTHERMAL PROSPECTS ON FEDERAL LANDS 313

Iyer, H. M., David H. Oppenheimer and Tim Hitchcock: TELESEISMIC P-DELAYS AT THE GEYSERS-CLEAR LAKE, CALIFORNIA GEOTHERMAL REGION 317

Jacobs, Harold R., D. Scott Cook and Robert F. Boehm: COMPARISON OF DIRECT CONTACT BINARY POWER PLANTS FOR GEOTHERMAL APPLICATION USING MULTIPLE CYCLES 321

Section 1

Jacobson, W. O.: OPERATIONAL HISTORY OF THE GEOTHERMAL LOOP EXPERIMENTAL FACILITY AT THE SALTON SEA KGRA 325

Jenkins, C. B.: NEW CONCEPT IN GEOTHERMAL STEAM PRICING 327

Jessop, Alan M.: GEOTHERMAL ENERGY FROM SEDIMENTARY FORMATIONS OF WESTERN CANADA 331

Jiracek, George R. and Michael T. Gerety: COMPARISON OF SURFACE AND DOWNHOLE RESISTIVITY MAPPING OF GEOTHERMAL RESERVOIRS IN NEW MEXICO 335

Johnson, Wayne: AN IMPROVED METHOD OF FLASHING AND SHOCKING GEOTHERMAL WELLS 337

Jorda, R. M.: THE EFFECTS OF CORROSION AND SCALE DEPOSITS ON THE CAPACITY OF WATER REINJECTION WELLS IN LIQUID DOMINATED GEOTHERMAL SYSTEMS 341

Joyce, Larry and Roger A. Fontes: AIR QUALITY AS THE LIMITING FACTOR ON DEVELOPMENT OF THE GEYSERS GEOTHERMAL RESOURCES 345

Karkalits, O. C. and B. E. Hankins: CHEMICAL ANALYSIS OF DISSOLVED NATURAL GAS IN WATER FROM THE WORLD'S FIRST GEOPRESSURED GEOTHERMAL WELL 351

Karlsson, Thorbjorn: CASING DESIGN FOR HIGH TEMPERATURE GEOTHERMAL WELLS 355

Kasameyer, Paul W. and Leland W. Younker: NATURAL FLUID-FLOW PATTERNS IN THE SALTON SEA GEOTHERMAL FIELD 359

Kauahikaua, James and Douglas Klein: RESULTS OF ELECTRIC SURVEY IN THE AREA OF HAWAII GEOTHERMAL TEST WELL HGP-A 363

Kennelly, James R. and Carl H. Geary: BINARY CYCLE EXPANDER FOR GEOTHERMAL POWER GENERATION 367

Kharaka, Yousif K., Patrick M. Brown and William W. Carothers: CHEMISTRY OF WATERS IN THE GEOPRESSRUED ZONE FROM COASTAL LOUISIANA -- IMPLICATIONS FOR THE GEOTHERMAL DEVELOPMENT 371

Section 2

Kroopnick, Peter M., L. S. Lau, R. W. Buddemeier and Donald Thomas: GEOCHEMISTRY OF A HAWAII GEOTHERMAL WELL: HGP-A 375

Kruger, Paul and Vasel Roberts: UTILITY ESTIMATES OF GEOTHERMAL ELECTRICITY GENERATING CAPACITY 379

Kruger, Paul: RADON IN GEOTHERMAL RESERVOIR ENGINEERING 383

Kunze, Jay F. and Klane F. Forsgren: THE ECONOMICS OF THE HEAT PUMP AS A DEVICE TO ASSIST IN GEOTHERMAL DISTRICT SPACE HEATING. 387

Kunze, J. F. and S. G. Spencer: ENVIRONMENTAL NECESSITY AND SUFFICIENCY: THE CASE OF THE RAFT RIVER PROJECT. 391

Larson, Tod C.: ECONOMIC FEASIBILITY MODEL FOR DIRECT HEAT APPLICATIONS OF GEOTHERMAL ENERGY. 395

Leigh, J. G. and J. N. Gupta: GELCOM: A GEOTHERMAL ELECTRIC LEVELIZED COST MODEL 399

Li, Charles T., D. P. Alzheimer, W. A. Wilcox, G. L. Roberts and W. F. Riemath: REMOVAL OF HYDROGEN SULFIDE FROM GEOTHERMAL STEAM 403

Lowell, R. P., C. H. Chen and J. K. Fulford: ON TRANSIENT TEMPERATURE INVERSIONS IN GEOTHERMAL BOREHOLES 407

Maurer, William C., John C. Rowley and Clifton Carwile: ADVANCED TURBODRILLS FOR GEOTHERMAL WELLS 411

McCright, R. D., R. E. Garrison and F. E. Locke: CORROSION TESTING IN A MULTIPLE-STAGE FLASH SYSTEM 415

McDonald, William J., Larry J. Remont and Clifton Carwile: IMPROVED GEOTHERMAL DRILLING FLUIDS. 419

McEuen, Robert B.: THERMAL WATERS OF BULGARIA: PRESENT USE AND PROBABLE ORIGIN 423

McNamara, Jack and Don Elmer: GEOTHERMAL RESOURCE DEVELOPMENT AND WILDERNESS PRESERVATION IN OREGON & CALIFORNIA 427

McNamara, Jack: THE REGULATORY PROCESS CONFRONTING GEOTHERMAL DEVELOPMENT IN CALIFORNIA: CAN WE BURN THE PAPER MOUNTAIN? 431

Meidav, Mae Z.: METHODOLOGY OF SOCIOECONOMIC IMPACT ASSESSMENTS OF GEOTHERMAL ENERGY DEVELOPMENT 433

Metzger, S. W.: GEOTHERMAL ENERGY DIRECT APPLICATIONS MARKET-ESTIMATOR MODEL 437

Michel, John W.: HEAT TRANSFER CONSIDERATION IN UTILIZING GEOTHERMAL ENERGY 441

Michels, Dr. Donald E.: CO_2 IN GEOTHERMAL STEAM: A RAPID, PRECISE, AND ACCURATE FIELD ASSAY TECHNIQUE 445

Miller, F. G., H. Cinco, H. J. Ramey, Jr. and F. Kucuk: RESERVOIR ENGINEERING ASPECTS OF FLUID RECHARGE AND HEAT TRANSFER IN GEOTHERMAL RESERVOIRS. 449

Miller, J. D. and R. W. Snyder: DYNAMIC SIMULATION OF THE RAFT RIVER GEOTHERMAL ELECTRIC PLANT AND ITS SUPPLY SYSTEM. 453

Miller, L. G., S. M. Prestwich and R. W. Gould: DRILLING AND DIRECTIONAL DRILLING A MODERATE-TEMPERATURE GEOTHERMAL RESOURCE 455

Miller, Richard J.: ENHANCED RECOVERY RESERVOIR ENGINEERING ASPECTS OF GEOTHERMAL DEVELOPMENT. 457

Miller, R. L.: RESULTS OF SHORT-TERM CORROSION EVALUATION TESTS AT RAFT RIVER. 461

Moench, A. F. and W. N. Herkelrath: THE EFFECT OF VAPOR-PRESSURE LOWERING UPON PRESSURE DRAWDOWN AND BUILDUP IN GEOTHERMAL STEAM WELLS 465

Morrison, Robert D.: UTILIZATION OF GEOTHERMAL COOLING WATERS FOR WASTE CONTAINMENT. 469

Morse, John G. and Lewis D. Thorson: RESERVOIR ENGINEERING STUDY OF A PORTION OF THE SALTON SEA GEOTHERMAL FIELD. 471

Nash, W. P., Charles Turley, James Petersen and F. H. Brown: VOLCANISM AND THE REGIONAL ASSESSMENT OF GEOTHERMAL POTENTIAL IN WEST-CENTRAL UTAH 475

Naughton, John J. and Donald Thomas: HELIUM IN FUMAROLE AND WELL GASES AS AN INDEX OF LONG-TERM GEOTHERMAL POTENTIAL 479

Nehring, Nancy L. and Alfred H. Truesdell: HYDROCARBON GASES IN SOME VOLCANIC AND GEOTHERMAL SYSTEMS 483

Netherton, Raymond and Lawrence B. Owen: APPARATUS FOR THE FIELD EVALUATION OF GEOTHERMAL EFFLUENT INJECTION 487

Nevin, Andrew E., J. T. Crandall, J. G. Souther and J. Stauder: MEAGER CREEK GEOTHERMAL SYSTEM, BRITISH COLUMBIA, PART I: EXPLORATION AND RESEARCH PROGRAM. 491

Newsom, M. M., J. A. St. Clair, H. M. Stoller and S. G. Varnado: CONTINUOUS CHAIN DRILL BIT DEVELOPMENTS 495

Nichols, K. E., J. L. Lobach and J. W. Hunt: TURBINE TESTING IN DIRECT CONTACT BINARY LOOP 499

Nicholson, Dr. Robert W.: DRILLING FLUID FORMATION DAMAGE IN GEOTHERMAL WELLS. 503

O'Daly, William L. and Gennaro Morelli: A CONTROL SYSTEM FOR STEAM GATHERING AT THE GEYSERS. 507

Oden, Hillary A., Timothy J. MacGillvray and John Lohrenz: FEDERAL GEOTHERMAL LEASE BIDDING. 509

Olson, E. R. and W. A. Elders: HYDROTHERMAL MINERALOGY AND ISOTOPIC GEOCHEMISTRY IN THE CERRO PRIETO GEOTHERMAL FIELD, MEXICO. II. ISOTOPIC GEOCHEMISTRY 513

Pearl, Richard Howard, Michael J. Galloway and Jay D. Dick: THE PAGOSA SPRINGS PROJECT -- THE FIRST PERMITTED GEOTHERMAL WELLS IN COLORADO 517

Phelps, David W. and Peter R. Buseck: NATURAL CONCENTRATIONS OF Hg IN THE YELLOWSTONE AND COSO GEOTHERMAL FIELDS 521

Phelps, Paul L. Don L. Ermak, Lynn R. Anspaugh, Calvin D. Jackson and Lowell A. Miller: PRELIMINARY ENVIRONMENTAL ASSESSMENTS OF KNOWN GEOTHERMAL RESOURCE AREAS IN THE UNITED STATES. 523

Pimentel, Kenneth D., Robert R. Ireland and Gary A. Tompkins: CHEMICAL FINGERPRINTS TO ASSESS THE EFFECTS OF GEOTHERMAL DEVELOPMENT ON WATER QUALITY IN IMPERIAL VALLEY 527

Pines, H. S., W. L. Pope, M. A. Green, P. A. Doyle, L. F. Silvester, R. L. Fulton: THE THERMODYNAMIC AND COST BENEFITS OF A FLOATING COOLING GEOTHERMAL BINARY CYCLE POWER PLANT AT HEBER, CALIFORNIA 531

Polito, Joseph: A SIMULATOR FOR SENSITIVITY ANALYSIS OF GEOTHERMAL WELL COST -- PROGRESS REPORT 537

Pope, W. L., H. S. Pines, L. F. Silvester, P. A. Doyle, R. L. Fulton and M. A. Green: OPTIMIZATIONS OF GEOTHERMAL CYCLE SHELL AND TUBE EXCHANGERS OF VARIOUS CONFIGURATIONS WITH VARIABLE FLUID PROPERTIES AND SITE SPECIFIC FOULING 539

Potter, Robert W. II: VISCOSITY OF GEOTHERMAL BRINES 543

Pritchard, James I. and George P. Zebal: HONEY LAKE KGRA GEOPHYSICAL SURVEY AND DRILLING TESTS 545

Quillin, Bob and Jim Combs: MICROEARTHQUAKE SURVEY OF THE RADIUM SPRINGS KGRA, SOUTH-CENTRAL NEW MEXICO 547

Quong, R., F. Schoepflin, N. D. Stout, G. E. Tardiff and F. R. McLain: PROCESSING OF GEOTHERMAL BRINE EFFLUENTS FOR INJECTION 551

Ramey, Henry J., Jr.: HAND COMPUTER PROGRAM FOR JAMES' LIP PRESSURE STEAM FLOW RATE 555

Ratigan, Joe L. and Ulf E. Lindblom: THE SINGLE-HOLE CONCEPT OF HEAT EXTRACTION FROM HOT DRY ROCK MASSES 559

Ridley, Albert P. and James V. Vantine: GEOLOGIC EXPLORATION METHODS FOR SITING POWER PLANTS AND OTHER STRUCTURES IN LANDSLIDE AND HYDROTHERMALLY ALTERED TERRAIN AT THE GEYSERS, CALIFORNIA 563

Rimstidt, J. D. and H. L. Barnes: EXPERIMENTS FOR RAPID ASSESSMENT OF THE SCALING PROPERTIES OF GEOTHERMAL FLUIDS 567

Riney, T. D., J. W. Pritchett and S. K. Garg: SALTON SEA GEOTHERMAL RESERVOIR SIMULATIONS 571

Rivera-R., Dr. Jesus: APPLICATION OF TYPE CURVE PROCEDURES FOR THE ANALYSIS OF PRODUCTION DATA FROM GEOTHERMAL WELLS 575

Robertson, David E., Jonathan S. Fruchter, J. Donald Ludwick, Connie L. Wilkerson, Eric A. Crecelius and John C. Evans: CHEMICAL CHARACTERIZATION OF GASES AND VOLATILE HEAVY METALS IN GEOTHERMAL EFFLUENTS 579

Rodzianko, Paul: THE PRIVATE SECTOR IN HYDROTHERMAL RESOURCE DEVELOPMENT 583

Rudisill, Jacob M.: A CASE HISTORY: THE COMPLETION OF A SHALLOW, OVER-PRESSURED GEOTHERMAL WELL 587

Schmitt, R. C., L. T. Cole and J. H. Oates: FLUIDIZED BED LOW-TEMPERATURE GEOTHERMAL DRYING 591

Shore, Greg A.: MEAGER CREEK GEOTHERMAL SYSTEM, BRITISH COLUMBIA, PART III: RESISTIVITY METHODS AND RESULTS 593

Siegel, B. Z. and S. M. Siegel: THE HAWAII GEOTHERMAL PROJECT: AN AEROMETRIC STUDY OF MERCURY AND SULFUR EMISSIONS 597

Snyder, Robert E.: GEOTHERMAL WELL COMPLETIONS: STATE OF THE ART 601

Souto, Jose M.: OAHU GEOTHERMAL EXPLORATION 605

Stanley, N. E., D. L. Siegel and W. D. Gertsch: SOIL COOLING FOR GEOTHERMAL ELECTRIC POWER PLANTS IN THE WESTERN UNTITED STATES: THE RAFT RIVER EXPERIMENT 609

Stoller, H. M. and J. L. Colp: MAGMA AS A GEOTHERMAL RESOURCE - A SUMMARY 613

Stone, Reid T., Henry L. Cullins and Max D. Crittenden: THE ROLE OF THE U.S. GEOLOGICAL SURVEY IN THE FEDERAL GEOTHERMAL LEASING PROGRAM 617

Summers, David A. and Ahmed A. El-Saie: PROGRESS IN THE WATER JET ASSISTED DRILLING OF ROCK 623

Suter, Glenn W. II: GEOTHERMAL DEVELOPMENT AND WILDLIFE BEHAVIOR 627

Swajian, Arthur, Gary L. Morris and Kenneth D. Pimentel: WATER QUALITY MANAGEMENT FOR IMPERIAL VALLEY GEOTHERMAL DEVELOPMENT 631

Swanberg, Chandler A. and Shari Alexander: THE USE OF THE RANDOM GROUNDWATER DATA FROM WATSTORE IN GEOTHERMAL EXPLORATION: AN EXAMPLE FROM THE IMPERIAL VALLEY, CALIFORNIA 635

Swanson, C. R.: SAN DIEGO GAS & ELECTRIC COMPANY'S GEOTHERMAL PROGRAM 639

Takashima, Ronald T.: GEOTHERMAL ENERGY RESOURCES: EXPLORATION BUDGETS AND COSTS RECOVERY 643

Tansev, Erdal O. and Mel L. Wasserman: MODELING THE HEBER GEOTHERMAL RESERVOIR 645

Tewhey, John D., Marjorie A. Chan, Paul W. Kasameyer and Lawrence B. Owen: DEVELOPMENT OF INJECTION CRITERIA FOR GEOTHERMAL RESOURCES 649

Thomas, Donald and Peter M. Kroopnick: ISOTOPES AND GASES IN A HAWAIIAN GEOTHERMAL SYSTEM: HGP-A 653

Tleimat, B. W. and A. D. K. Laird: INVESTIGATION OF HEAT TRANSFER COEFFICIENTS OF WORKING FLUIDS IN GEOTHERMAL POWER CYCLES 655

Tsang, Chin Fu, Gudmundur Bodvarsson, Marcelo J. Lippmann and Jesus Rivera R.: A STUDY OF ALTERNATIVE REINJECTION SCHEMES FOR THE CERRO PRIETO GEOTHERMAL FIELD, BAJA CALIFORNIA, MEXICO 659

Turner, Thomas A. and Dr. R. W. Rex: A PRACTICAL HYDROGEN SULFIDE ABATEMENT PROCESS FOR AIR DRILLING AND VENTING GEOTHERMAL STEAM WELLS 663

Urban, T. C., W. H. Diment and Manuel Nathenson: EAST MESA GEOTHERMAL ANOMALY, IMPERIAL COUNTY, CALIFORNIA: SIGNIFICANCE OF TEMPERATURES IN A DEEP DRILL HOLE NEAR THERMAL EQUILIBRIUM 667

Ushijima, Keisuke and Kazuo Ushijima: COMPUTER PROGRAM FOR CALCULATING THEORETICAL CURVES AND ITS APPLICATION TO VES DATA IN GEOTHERMAL AREAS 671

Varnado, S. G. and H. M. Stoller: GEOTHERMAL DRILLING AND COMPLETION TECHNOLOGY DEVELOPMENT 675

Veneruso, A. F. and H. M. Stoller: HIGH TEMPERATURE INSTRUMENTATION FOR GEOTHERMAL APPLICATIONS 679

Verity, Robert V. and Carl E. Fisher: PUMPING EXPERIENCE IN GEOTHERMAL WELLS AT EAST MESA 683

Vesely, Don: MUD SOLIDS CONTROL FOR MINIMUM LIQUID DISCHARGE DEMONSTRATED ON WYOMING WELL -- A POSSIBLE APPLICATION FOR GEOTHERMAL DRILLING 687

Vetter, O. J., D. A. Campbell and M. J. Walker: GEOTHERMAL FLUID INVESTIGATIONS AT REPUBLIC'S EAST MESA TEST SITE 689

Vetter, O., E. Woodruff, J. Watson and D. Shannon: SAMPLING IN GEOTHERMAL OPERATIONS - PHILOSOPHY AND REALITY 693

Wannamaker, Philip E., William R. Sill and Stanley H. Ward: MAGNETOTELLURIC OBSERVATIONS AT THE ROOSEVELT HOT SPRINGS KGRA AND MINERAL MTS, UTAH. 697

Warren, Nick: THE CHARACTERIZATION OF CRACK STRUCTURE CONTROLLING PERMEABILITY USING VELOCITY-PRESSURE DATA 701

Wassenaar, Johan A.: BUSBAR ECONOMICS OF LIQUID-DOMINATED GEOTHERMAL POWER. 703

Weiss, Richard: GROUND WATER MONITORING METHODOLOGY FOR GEOTHERMAL DEVELOPMENT. 709

West, Richard C. and James I. Pritchard: COMBINED ELECTROMAGNETIC AND GALVANIC (d.c.) ELECTRICAL RESISTIVITY SOUNDINGS 713

Wiegand, Jeffery W. and Craig Cummings: STATUS REPORT - GEOTHERMAL OPERATIONS RESEARCH PROJECT FOR CALIFORNIA AND HAWAII. 717

Williams, R. E.: GEOTHERMAL DRILLING IN HOT GRANITIC ROCK 721

Williams, Ralph E.: THE UTILIZATION OF HOT DRY ROCK - A SCENARIO. 725

Williams, Ralph E.: WELL PENETRATION AND STIMULATION. 729

Williamson, K. H. and E. P. Wright: ST. LUCIA GEOTHERMAL PROJECT. 731

Wonn, J. W.: ACOUSTIC SENSOR DEVELOPMENT FOR GEOTHERMAL BOREHOLE TELEVIEWER 735

Wright, Phillip M., Duncan Foley, Clayton R. Nichols and Paul J. Grim: WESTERN STATES COOPERATIVE DIRECT HEAT GEOTHERMAL PROGRAM OF DOE 739

Young, Chi-Yuh and Ronald W. Ward: 2-D INVERSION OF SEISMIC ATTENUATION OBSERVATIONS IN COSO HOT SPRINGS, KGRA 743

Zablocki, Charles J.: STREAMING POTENTIALS RESULTING FROM THE DESCENT OF METEORIC WATER -- A POSSIBLE SOURCE MECHANISM FOR KILAUEAN SELF-POTENTIAL ANOMALIES. 747

GEOCHEMISTRY OF A HAWAII GEOTHERMAL WELL: HGP-A

Peter M. Kroopnick — Hawaii Institute of Geophysics, Univ. of Hawaii

L. S. Lau — Water Resources Research Center, Univ. of Hawaii

R. W. Buddemeier — Hawaii Institute of Geophysics, Univ. of Hawaii

Donald Thomas — Hawaii Institute of Geophysics, Univ. of Hawaii

Extensive sampling and analysis have been carried out on the Hawaii Geothermal Project well-A (HGP-A) over a period of 12 months beginning in July 1976. Samples of the following types have been taken: downhole samples taken with a Klyne thief sampler, steam-condensate samples taken at the well head with a double cyclone separator and effluent water samples taken at the outlet of the steam silencer. Water quality analyses have included the following: Na^+, K^+, Ca^{++}, Mg^{++}, Cl^-, $S^=$, SiO_2, alkalinity and pH. Age dating of the well waters was done by ^3H analysis and ^{14}C analysis of CO_2 in the discharge gases.

Results. The results of the water quality analysis made on downhole water samples are summarized in Table 1; included in Table 1 is also the statistical profile of the data. The salient features of the data obtained are as follows:

Salinity and Chloride. Values for both parameters were low (Table 1) in comparison with those for open ocean water (33.4‰ and 17,000 mg/ℓ respectively) and were relatively free of variation with depth as illustrated by the chloride profile (Fig. 1).

pH. Downhole pH varied between 3 and 5 for the 6 sets of samples tested. The Feb. 14, 1977 depth profile obtained shortly after the well was quenched represented the only set of samples with significantly higher pH values.

Silica. All measurements indicated abnormally high silica levels in HGP-A well water when compared with normal Hawaiian ground water (<80 mg/ℓ). Silica profiles showed little variation with depth but large variations were observed between sampling periods.

Major Cations Na, K, Ca, Mg. Cation concentrations show a moderate variation with depth and conditions of the well prior to sampling (Fig. 2). The observed increase in potassium concentrations taken at shallow depths on Feb. 14, 1977 is thought to be a real perturbation in that it was observed for all ions for which determinations were made.

Tritium. Three samples were collected for tritium analysis (weir box, 690m and 1575m). All showed < 0.2 tritium units of radioactivity thus the mean age of the water is in excess of approximately 30 years.

Continuous Flow Series HGP-A. Samples of well fluid were collected both at the well head through a cyclone separator and condenser, and at the steam silencer outlet. In order to compare these numbers with the downhole results they must be multiplied by the factor 1/f where f is the steam fraction (generally 0.70 for HGP-A).

Table 2 presents a summary of both downhole and steady state discharge water chemistry data. The Cl^-, SiO_2 and major ion concentrations all have a similar concentration vs. time profile (Figs. 3 and 4). Initial ion concentrations are seen to change abruptly after approximately 4 hours of flow which corresponds to the time necessary to clear one well bore volume of liquid. After the initial change a steady state ion concentration is approached after 2-4 days. Each successive flow of the well resulted in slightly higher concentrations of chloride and major cations (Fig. 5).

The present interpretation of the data obtained to the present is that there are several sources of water in the well: ocean water at shallow depth, 5-10%; meteoric water at deeper levels, 65%; hydrothermal fluids, 25%. The mixing of seawater and coal meteoric waters makes a geochemical estimate of downhole temperatures rather difficult but work is presently underway to resolve these problems.

TABLE 1. Summary of downhole chemical parameters

Parameter	Mean	Median	Standard deviation	Coefficient of variance
Conductivity	3670 μmhos/cm 3500	3100 μmhos/cm	2270 μmhos/cm 1360	62% 39
Salinity	2.8 ‰ 2.6	2.3 ‰	1.4 ‰ 1.0	51% 39
Chloride	1160 mg/ℓ 1040	925 mg/ℓ	810 mg/ℓ 465	69% 45
Silica	440 mg/ℓ	420 mg/ℓ	230 mg/ℓ	52%
Sulfide	135 mg/ℓ	100 mg/ℓ	96.4 mg/ℓ	71%
Sodium	830 mg/ℓ 730	600 mg/ℓ	460 mg/ℓ 270	55% 37
Potassium	135 mg/ℓ 123	123 mg/ℓ	56.0 mg/ℓ 46.4	42% 38
Calcium	84.2 mg/ℓ 53.8	40 mg/ℓ	120 mg/ℓ 49.5	142% 92
Magnesium	2.1 mg/ℓ 1.0	1.0 mg/ℓ	3.8 mg/ℓ 0.7	62% 69

Where two values appear, the upper value includes all samples while the lower values excludes February 1977 depth samples at 692 m (2270 ft).

H. I. G. Contributor No. 884

TABLE 2
HGP-A geochemical summary
(Concentrations in mg/ℓ of total discharge)

		Cl	Na	K	Ca	Mg	SiO_2	$S^{=}$	pH	Trit.	t* qtz	t** Na/K	t*** Na/K/Ca
DOWNHOLE													
Non-flowing (ave. of 5 profiles):	mean	1040	730	123	53.8	1.0	440	135	3	<.1	240°C	250(WE)	231
	σ	±465	±270	±46	±49.5	±.7	±230	±96				252(FT)	
2270' (02/14/77)		4720	2008	245	445	14.0	432	.66	3	-	240°C	211(WE) 210	210
Low flow (average) of 4 samples		1040	480	103	22.6	.25	710	-	2.5	-	286°C	287(WE) 294(FT)	248
WEIR BOX													
approximate steady-state (01/30/77)		780	390	68	24	.11	41	-	8.5	-	93°C	256(WE) 259(FT)	229

*Fournier and Rowe (1966): $t = 1311/[5.196 - \log(SiO_2)] - 273$; SiO_2 in ppm.

**White (1968), Ellis (1969): $t = 855.6/[.6269 + \log(Na/K)] - 273$; Na and K in moles.
Fournier and Truesdell (1973): $t = 777/[.4693 + \log(Na/K)] - 273$; Na and K in moles.

***Fournier and Truesdell (1973): $t = 1647/[\log(Na/K) + \frac{1}{3}\log(\sqrt{Ca}/Na) + 2.24] - 273$; Na, K, and Ca in moles.

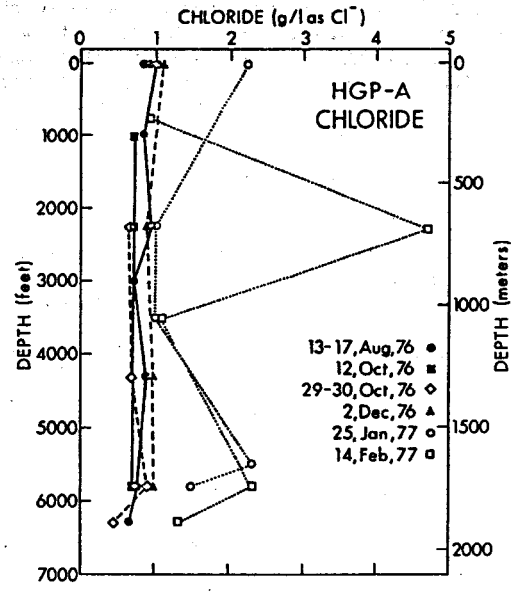


Figure 1. Downhole distribution of chloride for HGP-A.

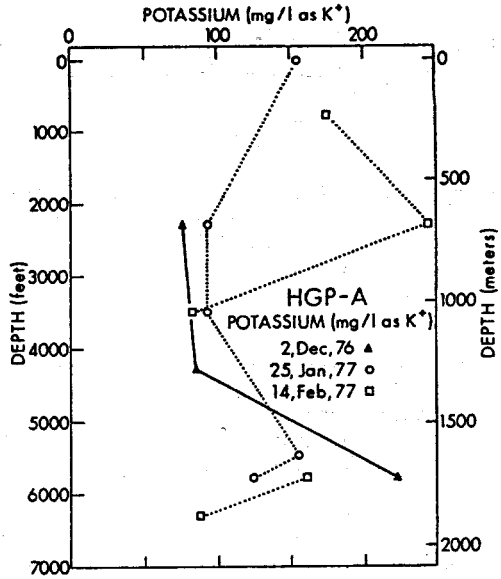


Figure 2. Downhole distribution of potassium for HGP-A.

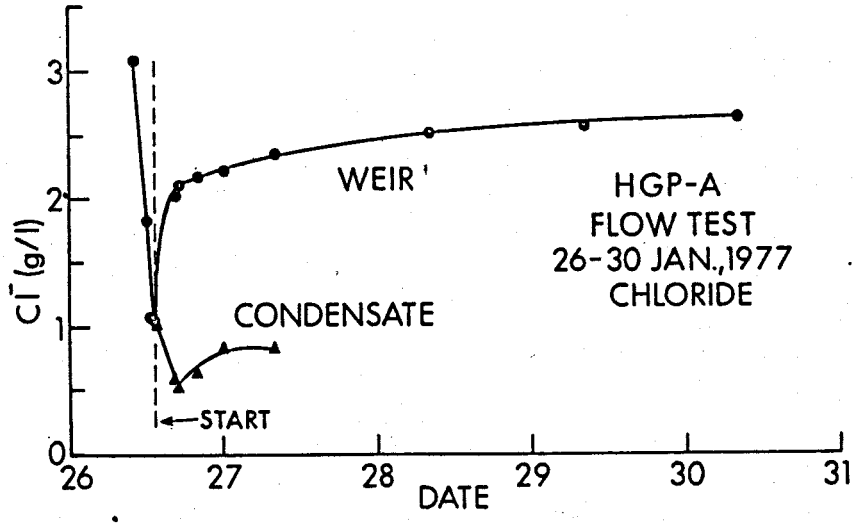


Figure 3. The approach of chloride to steady state for water samples collected at the weir and from the condenser.

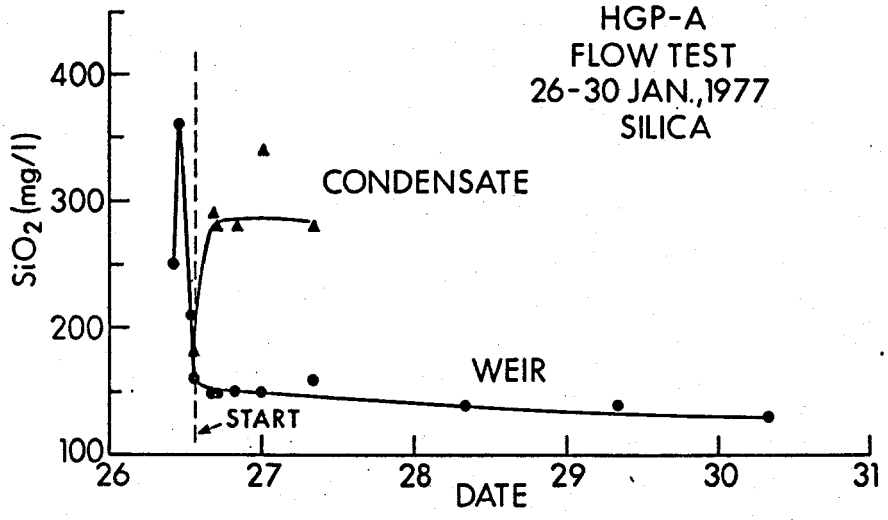


Figure 4. The approach of silica to steady state for water samples collected at the weir and from the condenser.

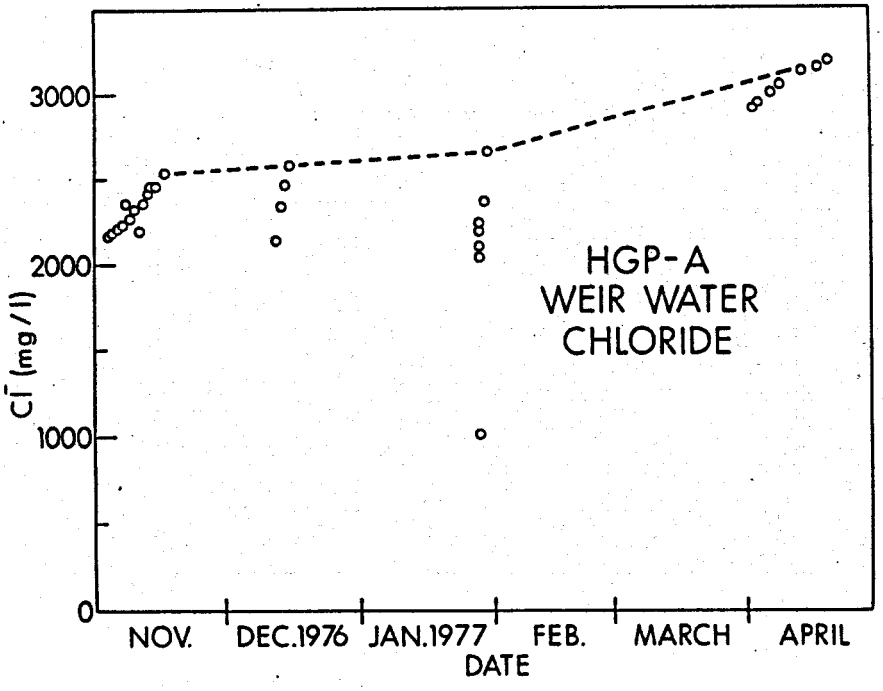


Figure 5. Chloride concentrations of samples collected from the weir and plotted versus the date of sampling. The steady rise after each well test suggests that the well has not reached equilibrium with the surrounding waters. To compare these results the reader must multiply them by (1-f) where f is the steam fraction of the discharge.

Geothermal Resources Council, TRANSACTIONS, Vol. 2 July 1978.

UTILITY ESTIMATES OF GEOTHERMAL ELECTRICITY GENERATING CAPACITY

Paul Kruger* and Vasel Roberts

Electric Power Research Institute
Palo Alto, California

ABSTRACT

Estimates of geothermal electric power generation capacity by the electric utility industry, obtained from both formal forecasts through the National Electric Reliability Council (NERC) and an informal survey conducted by EPRI in 1978, indicate a significant growth in reliance on geothermal resources compared to the estimates obtained a year ago. Data from the 10-year coordinated plan summaries of the Western Systems Coordinating Council for 1976 and 1977 show a 15%/a growth rate in geothermal power capacity over the 10-year periods, and in relation to the forecasted decline in total additions, it represents an increase of 20% in reliance on geothermal resources. The informal survey of more than 15 utilities showed a probable growth of geothermal power capacity to 7,475 MWe by 1995, at a mean growth rate of 16%/a. In comparison to the survey of 1977, the increase in announced capacity is more than 100%.

Estimates of the potential for producing electric power from indigenous U.S. geothermal resources are available from the electric utility industry in two forms: (1) formal forecasts of future year generating capacity filed with public utility commissions, and (2) informal estimates by individual utilities. An initial evaluation of these estimates was given by Kruger and Roberts (1977) based on data available in 1976 utility biennial forecasts and in the 1976 data for generating capacity compiled by the National Electric Reliability Council. The outlook indicated a moderate growth in geothermal electric energy generating capacity from the current value of 502 MW to about 2000 MW in 1985, a mean growth rate of about 14.2%/a compared to an expected growth rate of 5.3%/a for total electrical generating capacity over the same period.

A case for accelerated development of geothermal energy resources for electric power production is easy to make. The National Electric Reliability Council (NERC, 1977) has appraised the adequacy of future bulk power supply. From an analysis of generation reserve, the difference between installed generation capacity, and peak load demand, they indicated the possibility of inadequate generating capacity to serve the electric load in the United States as early as 1979. To meet future demand requirements, utilities have projected capacity installations of approximately 300,000 MW during the 1977-86 period as reported to the Federal Power Commission (FPC Order 383-4). Most of this additional capacity is either nuclear or coal-fired, with very little reliance on fluid fossil fuels. Thus, any delays in bringing the projected capacity installations on line, e.g., because of changes in environmental regulations for coal-fired units or difficulties in securing construction or operating licenses for nuclear units, will result in either inability to meet peak load demand or greater pressure to bring alternate energy-fuel units on line or both.

The potential for geothermal energy utilization for electric power production has been cited for more than a decade. A history of capacity forecasts was reviewed by Kruger and Roberts (1977), in which forecasts decreased from early values of more than 100,000 MWe to 2,078 MWe (NERC, 1976). However, based on the resource estimates of the U. S. Geological Survey (White and Williams, 1975) hydrothermal resources exist in the western and gulf coast states for a geothermal energy industry of more than 47,000 MWC. Utilization by the electric utilities appears to await increased assurance of economic conversion and resolution of existing regulatory and institutional uncertainties. Examination of the current history of capacity forecasts indicates that a minimum of 2,000 MW by 1985 has already been reached, based solely on the expectations for the established geothermal power station at The Geysers in northern California, and that a period of rapid growth of additional capacity may be near. However, forecasted capacity other than at The Geysers is conservatively small, reflecting the uncertainty of economic and

*Stanford University, consultant to EPRI

reliable electric energy conversion of geothermal resources other than this unique dry-steam resource.

The potential for geothermal energy utilization for electric power production can be estimated from data compiled by the National Electric Reliability Council for both contiguous U. S. electric generating capacity and planned capacity additions. Table 1 shows a comparison of the capacity data for the 10-year periods 1976-85 (NERC, 1976) and 1977-86 (NERC, 1977). All of the forecast geothermal capacity is from the western hydrothermal resources in regions served by the Western Systems Coordinating Council; none is yet forecast for the geopressured resources in the Gulf states. The comparison shows the expected decline in reliance on fluid fossil fuels and a growing reliance on nuclear power as well as a continuing major reliance on coal. The forecast of a steady mean growth rate in total generating capacity of about 4.5%/a from the actual total of 1975, coupled with the small but increasing percent of geothermal power, represents a moderate growth in reliance in geothermal resources to meet future requirements.

This growth in reliance is also seen in the 10-year coordinated plan summaries of the Western Systems Coordinating Council (WSCC, 1976 and 1977) from which the planned capacity additions for geothermal resources, compared to nuclear and total, are given in Table 2. The data reflect the decrease in total additional capacity forecast between the two summaries, and the greater reliance on nuclear power even though the additional capacity is forecast to decrease. The combination of a moderate increase in total geothermal capacity coupled to the decrease in total planned addition represents a 20% increase in planned reliance on geothermal energy between the two annual summaries. The mean growth rate for geothermal generating capacity is 14.8%/a from the 1977 summary, consistent with the 14.2%/a from the 1976 summary.

The second form of electric utility industry estimate of the growth of geothermal energy development is the informal survey made during the early part of 1978. The results of this survey of utilities are shown in Table 3. The values were obtained for three basic conditions:

TABLE 1

U. S. ELECTRIC GENERATING CAPACITY (GW, Contiguous U. S.)

	1975*		1976*		1976†		1985*		1985†		1986†	
	Act	(%)	Est	(%)	Act	(%)	Est	(%)	Est	(%)	Est	(%)
Coal	182.7	38.6	193.0	38.3	191.4	38.7	320.5	40.2	309.5	40.3	324.8	40.8
Oil	125.3	26.4	131.7	26.2	130.7	26.4	157.7	19.8	159.8	20.8	159.9	20.1
Natural Gas	61.3	12.9	61.9	12.3	60.3	12.2	48.0	6.0	46.7	6.1	45.8	5.8
Hydro	58.9	12.4	59.1	11.7	59.5	12.0	67.3	8.4	67.4	8.8	67.6	8.5
Nuclear	32.9	6.9	43.2	8.6	39.3	7.9	174.0	21.8	150.8	19.7	163.5	20.5
Geothermal (WSCC)	0.5	0.1	0.5	0.1	0.5	0.1	2.1	0.3	2.0	0.3	2.2	0.3
Other	12.4	2.6	13.9	2.8	13.1	2.6	28.4	3.6	31.0	4.0	32.5	4.1
TOTAL	474.0		503.3		494.8		798.0		767.2		796.3	
Growth Rate (%/a)			6.0		4.3		5.2		4.8		4.7	

* From NERC (1976)

† From NERC (1977)

(1) Announced - either publicly or through PUC-type biennial reports; (2) Probable - based on successful demonstration of technology for using liquid-dominated geothermal resources; and (3) Possible - based additionally on removal of institutional barriers and encouragement with governmental incentives. These informal estimates were compared to the values obtained in the 1977 survey and the growth rate for the estimate of the total installed capacity between the two surveys is as follows:

Growth Rate of Estimates (%/a) for Year

	1985	1990	1995	2000
Announced	71	119	116	114
Probable	5	66	71	68
Possible	18	80	81	66

These data show a doubling in the announced level of geothermal resource utilization and a significant growth in the potential for geothermal energy during the decade of the 1990's. Clearly the western electric utilities believe that with demonstration of the technology and public desire for this alternate energy source, geothermal resources energy could make a significant contribution to the electric power generation of the near future.

REFERENCES

P. Kruger and V. Roberts, Utility Industry Estimates of Geothermal Electricity Generating Capacity, Proceedings, Geothermal Resources Council Transactions, Vol. 1, May, 1977.

National Electric Reliability Council, Fossil and Nuclear Fuel for Electric Utility Generation, Requirements and Constraints 1976-1985, June, 1976.

National Electric Reliability Council, Fossil and Nuclear Fuel for Electric Utility Generation, Requirements and Constraints 1977-1986, August, 1977.

D. F. White and D. L. Williams, eds. Assessment of Geothermal Resources of the United States - 1975, U. S. Geological Survey Circular 726, June, 1975.

Western Systems Coordinating Council, Ten-Year Coordinated Plan Summary 1976-1985, May 1976.

Western Systems Coordinating Council, Ten-Year Coordinated Plan Summary 1977-1986, May, 1977.

TABLE 2

PLANNED CAPACITY ADDITIONS - WSCC 10-YEAR PLANS

	ADDED CAPACITY (MWe)					
	GEOTHERMAL		NUCLEAR		TOTAL	
	1976	1977	1976	1977	1976	1977
1976	0		2520		6135	
1977	0	0	206	1618	3075	3781
1978	271	161	80	0	6105	5453
1979	165	245	1170	80	5890	4944
1980	290	50	220	1390	4296	5561
1981	110	220	880	2130	5647	6229
1982	220	220	2740	1454	5768	3567
1983	190	270	4658	2130	9329	5196
1984	220	220	1270	4287	4904	7323
1985	110	110	5375	2500	7369	5939
1986		210		3049		5592
TOTAL	1576	1706	19119	18638	58518	53585
% TOTAL CAP	2.7	3.2	32.7	34.8		

TABLE 3

1978 EPRI SURVEY OF

ELECTRIC UTILITY FORECASTS OF GEOTHERMAL POWER CAPACITY

	Capacity (MW_e) by Year				
	1977 Actual	1985 Est	1990 Est	1995 Est	2000 Est
ARIZONA/NEW MEXICO	0				
Announced		50	50	50	50
Probable		150	250	450	450
Possible		250	450	800	1400
CALIFORNIA	502				
Announced		1969	2969	3569	3869
Probable		2409	4804	6423	7473
Possible		2969	6614	9123	10723
IDAHO/OREGON/WASH	0				
Announced		0	0	0	0
Probable		5	60	200	500
Possible		55	200	800	1500
NEVADA/UTAH	0				
Announced		55	55	55	55
Probable		110	320	430	430
Possible		110	320	430	540
GULF STATES	0				
Announced					
Probable					
Possible					
TOTAL	502				
Announced		2019	3019	3619	3919
Probable		2664	5414	7473	9023
Possible		3374	7664	11323	14723

Geothermal Resources Council, TRANSACTIONS, Vol. 2 July 1978

RADON IN GEOTHERMAL RESERVOIR ENGINEERING

Paul Kruger

Civil Engineering Department
Stanford University
Stanford, CA 94305

ABSTRACT

Radon transient analysis appears promising as a method complimentary to pressure transient analysis in the assessment of geothermal reservoirs. Measurement of radon is proving useful in two types of studies in geothermal reservoir engineering: (1) examining the structural properties of the reservoir as they affect the emanation of radon from rock to pore fluids, and (2) examining the flow properties of the reservoir as they affect radon migration. Several radon transient tests have been conducted to examine the relationship between radon concentration in wellhead condensate and changes in flow rate. The results indicate that details of reservoir structure and transport may be examined with radon as an internal reservoir tracer.

One factor in the slow growth rate of geothermal energy development is the difficulty in assessing geothermal reservoirs. Determination of geothermal reservoir properties should reduce markedly the risk associated with the construction of electric power plants in newly developed fields. Pressure transient analysis has been a valuable technique in obtaining reservoir information. Additional techniques are needed, and it appears that radon transient analysis may be of use in evaluating geothermal reservoirs.

Radon is the radioactive noble gas produced in nature from decay of radium dispersed in the earth's crust. The principal isotope of radon is 3.83-day ^{222}Rn resulting from alpha-particle emission from 1600-year ^{226}Ra, which in turn is produced in the natural uranium series originating with 4.5×10^9-year ^{238}U. Thus radon, as a natural constituent of geothermal fluids, can serve as an internal radioactive tracer in geothermal reservoirs. Since radon is produced essentially "forever" in the reservoir, but decays with its characteristic 3.83-day half life when separated from its radium parent radionuclide in the formation, it introduces a "time element" in geothermal reservoir tracer studies. This property of radon contrasts sharply with the stable gas components of geothermal fluids, such as CO_2, H_2S, and $\delta(^{18}O)$.

Radon concentration in geofluids depends on several reservoir parameters, primarily the concentration and distribution of radium in the reservoir formation, the conditions for emanation and diffusion into the pore fluids, and the transport properties of the convecting fluids from the emanation sites to the wellhead. These parameters, in turn, are related to different geologic factors. Radium is found rather uniformly distributed in sedimentary and igneous rocks at an average concentration of about 1 pg/g. Its distribution depends on the local thermodynamic and hydrochemical history of the formation. Since radium is a chemical homolog of the alkaline earth elements calcium, strontium, and barium, it can become redistributed with these elements in hydrothermal resources.

The emanation of radon in rock matrices depends on the chemical, mineral, structural, and thermodynamic properties of the rock. The recoil energy of ^{222}Rn on alpha decay of ^{226}Ra is 86 keV, sufficient to migrate about 1 μm in rock. The emanation from the rock is thus strongly dependent on surface area exposed, porosity, and composition of the cementing materials in the rock, as noted by Andrews and Wood (1972). It is also dependent on the pressure, temperature, and density of the pore fluid in the formation. The transport of radon depends on its solubility in the convecting fluid and the hydrodynamic properties of the reservoir, such as permeability-thickness, reservoir pressure gradients, and flow rate.

Two general types of information may be obtained with radon as an internal reservoir tracer. Under steady flow conditions, changes in reservoir properties will result in changes in radon concentration in the produced geofluids. And under

steady emanation conditions, changes in flow regime will also result in changes in radon concentration. A discussion of some of the types of information that can be obtained from radon measurements was given by Kruger, Warren, and Honeyman (1977). The challenge of successfully applying radon transient analysis to geothermal reservoir engineering rests with the ability to show the relationships between changes in reservoir or flow properties and changes in radon concentration. Sufficient data are needed to separate the changes due to each affect.

Several studies have been reported which examine the methods of using radon measurements in geothermal reservoir engineering. The development of wellhead sampling, radon separation, and measurement methods was described by Stoker and Kruger (1975). Their results for several types of geothermal resources in several locations showed that radon concentrations varied significantly, not only between vapor-dominated and liquid-dominated geothermal resources, but also between different wells in a single reservoir, and even in a single well as a function of time. These data indicated not only the local conditions affecting the absolute concentration of radon, but also the pulsing nature of the production of radon gas (and possibly other non-condensible gases, such as CO_2) over short time periods.

A series of radon transient tests with rapid changes in flow rate have been carried out during the past two years to examine the parameters affecting radon transport in geothermal reservoirs. The sites, test conditions, and gross observations are given in Table I. Linear and radial flow models, such as described by Stoker and Kruger (1975) considered the relationship between radon concentration at the wellhead and flow rate in the reservoir to be affected by the two sets of parameters; the distribution of radium in the reservoir and the transport conditions. The radium might be: (1) hydrothermally-deposited close to the wellbore, (2) dissolved in a boiling liquid deep in the reservoir, and (3) uniformly deposited along the transport pathway. The pathway might contain a steam saturation gradient in the reservoir ranging from all liquid to superheated steam. The transport conditions might be: (1) flow from a producing well in a field without interference from nearby wells, (2) flow from a well in a producing field interconnected to nearby wells, and (3) flow from a well in a newly producing field.

Table I shows some of the variations of field test conditions that have been tested. The initial study of the dependence of radon concentration on flow rate in a producing dry-steam well was reported by Kruger, Stoker, and Umaña(1977). The results showed a radon concentration transient following an abrupt decrease in flow rate in which the radon concentration decreased proportionally, with an apparent "decay constant" of about 12±4 days, indicating that the radon was not coming from radium deposited around the wellbore and supporting the idea of a boiling water table deep in the reservoir.

The second test, in the Larderello fields in Italy, was a two-week test with a rapid decrease in flow rate for one week and a rapid return to full flow. The radon concentration followed these changes proportionally in a time short compared to the half-life of radon. The results also support the model of radon not coming from radium deposited around the wellbore and supporting the idea of a boiling water table close to the wells.

The next two tests, described by Warren and Kruger (1978), broadened the range of application. The first examines the role of interference in radon transient analysis and the second examines the early production history of a new, high-productivity steam well. The last test in Table I is a radon transient in a hot water well. From the short 2-hour tests at two flow rates, the lack of change in radon concentration supports the model of Stoker and Kruger (1975) of a large uniform deposit of radium in the reservoir in which the radon concentration is not a strong function of flow rate. Additional transient tests are being planned to continue the development of radon transient analysis. To improve on evaluation of constant emanation of radon in these studies, laboratory-controlled tests are in progress to measure the emanation of radon from rock as a function of temperature, pressure, and pore fluid phase, as well as flow rate.

REFERENCES

Andrews, J.N. and D.F. Wood, Mechanisms of Radon Release in Rock Matrices and Entry into Groundwaters, Inst. Mining and Metallurgy Trans/B 81, No. 792 (1972).

Kruger, P., A. K. Stoker, and A. Umaña, Radon in Geothermal Engineering, Geothermics 5, 13-19 (1977).

Kruger, P., G.J. Warren, and B.D. Honeyman, Radon as an Internal Tracer in Geothermal Reservoirs, Proceedings, Third International Conference on Nuclear Methods in Environmental and Energy Research (ANS/ERDA), U. of Missouri, Columbia (1977) in press.

Stoker, A. K. and P. Kruger, Radon in Geothermal Reservoirs, Proceedings, Second United Nations Symposium on the Development and Use of Geothermal Resources, San Francisco, CA (1975).

Warren, G. J. and P. Kruger, Radon in Vapor-Dominated Geothermal Reservoirs, Technical Report SGP-TR-22 (1978) in preparation.

TABLE I

SUMMARY OF RADON TRANSIENT FLOW TESTS IN HYDROTHERMAL RESERVOIRS

SITE	CONDITIONS	OBSERVATIONS
Geysers, Calif.	Rapid change in flow rate in one production well in a shut-in producing field.	Transient proportional change in [Rn] with a "decay-constant" $\sim$ 12±4 days.
Larderello, Italy	Two rapid changes in flow rate in one production well in an isolated section of a producing field.	Transient proportional change in [Rn] with a "decay-constant" $\sim$ 0.5±0.5 days
Geysers, Calif.	Two rapid changes in flow rate in one well and no changes in a nearby well in a partially shut-in field of 20 wells.	No change in [Rn] in either well with ΔQ in one.
Geysers, Calif.	Two rapid changes in flow rate in one non-producing well in a new field.	Transient [Rn] build-up during constant Q and change in [Rn] with ΔQ.
Puna, Hawaii	Short-term tests in HGP-A well at two flow rates.	No change in [Rn] over the two short test periods.

THE ECONOMICS OF THE HEAT PUMP AS A DEVICE TO ASSIST IN GEOTHERMAL DISTRICT SPACE HEATING

Jay F. Kunze and Klane F. Forsgren

Jay F. Kunze and Klane F. Forsgren
Energy Services Division
Forsgren, Perkins and Associates, P.A.
Rexburg, Idaho 83440

Can heat pumps economically assist in geothermal space and water heating? If so, common cooler waters can be developed in addition to the rare hot resources which are now exploited. Though a lack of data prevents us from assessing actual reserves, it can be assumed that a mathematical distribution similar to a Poisson distribution applies. The curve would peak somewhere near the temperature of normal ground water (20° C), as shown in Figure 1. The curve, does not incorporate normal, near-surface, run-off water that resides in the ground only for brief periods (a year or so) and never has the opportunity to be geothermally heated. If such transient waters were included, the curve would be peaked at an even lower temperature, enclosing a much greater amount of water suitable for heat pump applications. At any rate, there is clearly an enormous energy potential if heat-pump assistance is practical.

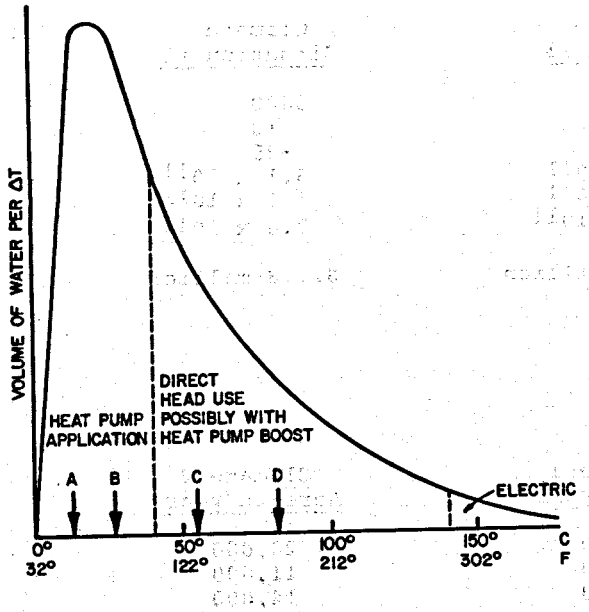


Figure 1 - A probable distribution for geothermal ground water.

The analysis summarized below considers source water of four temperatures: 55° F, 80° F, 130° F and 180° F, i.e. A, B, C and D shown in Figure 1. Case A represents a typical groundwater heat-pump application of the type recently popularized (1) for which a number of package heat pumps are available. This application has been quite successful for both heating and cooling some large buildings, particularly in climates that experience extremely cold winters when the coefficient of performance (COP) of an "air-cooled" heat pump drops to near unity. The typical COP of a "water-cooled" heat pump operating on 55° F water is 3.5, if it is assumed that 10° F is extracted from the water.

Case B represents the coolest waters normally considered geothermal. At 80° F, the water is too cool to be used directly for space heating, yet it is too warm to be used as domestic water. If homes and buildings are to use heat pumps and this water, in general, two water circuits will be necessary. A heat pump operating at this temperature and extracting 25° F will typically have a COP of 4.5.

Case C at 130° F considers the coolest waters practical for direct geothermal use, without heat-pump boosting. The direct use extracts 20° F from the water. There may still be an advantage, however, to providing a heat-pump boost under those circumstances. With heat-pump boost to extract 50° F from the water, a coefficient of performance of 5.5 might be expected.

Case D at 180° F represents a traditional direct use of geothermal energy at an ideal temperature for space heating and water heating. Typically, 50° F can be easily extracted from the water. Waters in this temperature range have been successfully used in district space heating systems in Iceland and Boise, Idaho for years. The current economics of building such a system into an existing city has been studied (2).

To evaluate the economics of these four resources, two different climates were compared. The first is an 8400° F.-day situation (#1) with an ASHRAE design temperature of -11° F., corresponding to cities with a climate similar to Idaho Falls. The second situation is 5600° F.-day (#2) with an ASHRAE design temperature of +3° F., corresponding to the climate in Boise, Idaho. However, for Situation #1, we recommend design water supply rates to adequately supply the needs at +15° F., using supplemental heat for colder conditions, which consume 5% of the annual heating load. For Situation #2, a +25° F. design load for the water supply system has been shown to be the economical optimum (2), for which supplemental heat supplies 5% of the annual requirements. For this analysis we have also assumed that all of the normal domestic water heating load is also supplied by the ground water heat source.

Reference #2 stressed the economics that required a large district heating system if a main pipeline was to be used economically, particularly a pipeline to be installed in existing streets. In new subdivisions, pipeline economics can be considerably more favorable, making smaller-sized systems economically practical. However, for the cases shown below, we have chosen a district system of homes and businesses equivalent to 7500 average homes, approximately the size of a city of 20,000 population.

This represents half of the city of Idaho Falls (Situation #1), 1/6 of the city of Boise (Situation #2). These homes were assumed to have a net average heat load of 600 Btu/hr °F temperature difference, where "net" refers to the actual heat loss minus the sensible (internally generated) heat. The main pipelines for such a section of a city will cost about $2 million, installed.

For comparison, a city of 20,000 people in Idaho consumes about 12,000 acre-ft. per year of domestic water. Hence, the water supply needs for space heating exceed the domestic needs if a typical ground water space heating pump is to be used. However, it should be noted that the domestic use peaks in the summer, while the space heating needs peak in the winter, making a synergistic solution possible.

Capital costs of the above cases are based on assumptions of well depth and productivity. These can vary substantially, depending on the geohydrology. For purposes of comparison, however, a geothermal gradient of 2 1/3 times the "world average" was assumed, probably characteristic of the likely situations throughout the west. Well productivity was assumed to worsen with depth, and larger pumping heads were required, not because of lower ambient water levels, but because the well would

	Climate Situation #1	Climate Situation #2
Total Heating °F	8400	5600
ASHRAE Design Temperature °F.	-11	+3
"Geothermal" System Design Temp.°F	+15	+25
Total Yearly Space Heating Needs(Btm)	9.1×10^{11}	6.1×10^{11}
Yearly Hot Water Needs	1.5×10^{11}	1.5×10^{11}
Total "Geothermal" Heat Market	10.6×10^{11}	7.6×10^{11}
Gross Revenues at Competitive Price of $3/M Btu	$3.18 million	$2.28 million

The water use requirements annually for each of the cases is as follows:

		Climate 1 Acre-ft/year	Climate 2 Acre-ft/year
a)	10° T Heat Pump	39,000	28,000
b)	25° T Heat Pump	16,000	11,000
c)	20° T Geothermal	20,000	14,000
c-1)	50° T Geothermal with Heat Pump Boost	7,800	5,500
d)	50° T Geothermal	7,800	5,500

be pumped to get the highest reasonable productivity. The following table shows the assumptions for each case and the capital cost of each.

Case	Well Depth ft.	Avg.Prod. per well Gal/Min	Climate #1 No. of Prod. Wells	Total Pumping Head including disposal	Avg.Prod. Well + Pump Cost	Climate #1 Total supply system cost including $2 million for main Pipelines	Climate #2 Total supply system cost including $2 million for main Pipelines
a	400	2000	19	300'	$50K	$3,140,000	$3,020,000
b	800	1500	10	400'	90	3,080,000	2,907,000
c	1500	1000	19	500'	180	7,130,000	6,549,000
c-1	1500	1000	8	500'	180	4,160,000	3,890,000
d	2500	700	11	700'	300	6,950,000	6,500,000

*For disposal of the used fluid, 20% of the production well costs was assumed for cases "a" and "b", 50% for "c", "c-1" and "d".

Annual electric power requirement for each of these cases is as follows. It is assumed that the cost of electricity is 3 cents/kwh.

Case	Climate #1 Pumping Million Kwh	Climate #1 Heat Pump Million Kwh	Climate #1 Total Cost Million $	Climate #2 Pumping Million Kwh	Climate #2 Heat Pump Million Kwh	Climate #2 Total Cost Million $
a	1.6	88.7	3.14	11.5	63.6	2.25
b	8.6	69.0	2.33	6.2	49.5	1.67
c	13.3	0	.40	9.6	0	.29
c-1	7.5	56.5	1.92	5.3	40.5	1.37
d	7.5	0	.23	5.3	0	.16

Conclusions

The comparison of the five different "geothermal" heating cases must be made with an understanding of the economic criteria upon which the organization (company) that supplies the geothermal water must work. A municipal system that enjoys low borrowing rates will be less affected by high capital costs than would a capitalized system. For the latter, a "pay back" guideline of three years may be considered typical and appropriate. With these assumptions, the following conclusions can be drawn relative to the costs of conventional oil and gas heating systems having fuel costs of $3/M Btu (the equivalent of about $450/hour).

Case A - Heat pumps using 55° F ground water would cost as much to operate as an oil or gas system. The initial installed cost by the home owner is about $500 more per home, and the water-supply system would add about $50/year, amortized, if the supply system were common with the regular domestic water supply. If a separate set of lines were needed, the system is not now cost competitive. The disposal of the continual high flow rates during winter does represent a problem for sewage treatment, and separate discharge lines may be the least costly solution. The application is pollution free at the user facility, giving it a definite advantage over fossil-fuel heating.

Case B - A system using 80° F groundwater heat pumps, requiring separate supply and disposal circuits for the domestic water system would save 25% in operating cost. But amortization of the capital cost exceeds this saving by $50/year per home, similar to Case A. However, the relative cleanliness, convenience, and compactness represent advantages well worth the extra cost.

Case C - Geothermal water of 130° F has negligible operating cost, and the savings are easily greater than the amortized capital cost. Home-owner equipment investment is $500 less than for heat pump.

Case C-1 - Using 130° F geothermal water with a heat-pump boost to extract more

heat from the water is more expensive than Case C, the direct use. However, the heat pump will cool the water to 80° F, virtually eliminatig any problem of thermal pollution if disposal is to be into a stream. This intangible advantage may, in certain cases, translate to a less expensive overall system than the direct use without heat-pump boost. Because of the substantially lower water supply requirements, the main pipeline system could accomodate significant expansion to serve 2 to 3 times as many homes and businesses.

Case D - The direct use of 180° F geothermal water has virtually no operating cost. For Climate #1 (8400° F-days), investment amortization is easily covered by the savings. In the case of Climate #2 (5600° F-days), the overall costs are equivalent to gas and oil. The homeowner investment if $500 less for the geothermal system, and cleanliness, convenience and compactness are further advantages.

Note that the conclusions are based on a $3/M Btu net cost of fossil-fuel heating. These current costs are expected to excalate faster than will the cost of electricity to drive heat pumps. Thus, the heat-pump cases should show improved economical competitiveness in the future.

A general conclusion to be drawn is that pumping costs are an insignificant part of the total (less than 20%). Hence, wells should be pumped to their fullest capability for reasonable pump capital costs.

Since every one of the five cases showed a combination of attractive economics and convenience, the test drilling for geothermal water is a sound investment. Regardless of the water temperature discovered, the typical situation should lead to a "geothermal" heating system that is attractive if implemented on a large enough scale. We have made no mention of maintenance and operating-labor cost comparisions for the five cases, for we feel these will be comparable, and will represent only an approximately 10% addition to the overall costs quoted above. If heat-pump applications are required, these do offer the added advantage of being able to air condition in the summer.

Finally we note that in certain areas of the country neither fuel oil or natural gas can be obtained in adequate supplies for newly constructed facilities. Any of the five cases above is significantly more attractive than electric heat or an air-to-air heat pump for climates at least as severe as approximately 5000°F-days annual heating needs.

****

References

(1) "Ground Water Heat Pumps - Home Heating and Cooling From Your Own Well", Popular Science, Feb. 1978, p.78.

(2) J.F. Kunze, L.E. Donovan, J.L. Griffith, "The Size Effect for District Space Heating in Boise, Idaho", Transaction of FRC, Vol. 1, May 1977. p.179.

ENVIRONMENTAL NECESSITY AND SUFFICIENCY: THE CASE OF THE RAFT RIVER PROJECT

J. F. Kunze and S. G. Spencer

EG&G Idaho, Inc.
Idaho Falls, Idaho

Long before it was drilled, the Raft River geothermal reservoir in southern Idaho was correctly characterized by geothermometry as a moderate-temperature resource. Three deep-hole wells have since been drilled into the paleozoic quartz-monzanite basement, reaching the predicted 150°C (300°F) temperatures well before encountering the poorly-fractured basement. Described below is the environmental program that began prior to drilling and accompanied the development of a complete well field for a 5-MW(e) [40-MW(th)] pilot plant.

Initial Considerations

A primary concern was to involve all organizations having an interest in the area's environment. Figure 1 shows the matrix of organizations whose involvement and help was solicited. The names with asterisks are those organizations which received funding to participate, in return for specific data and evaluations of the existing environment.

The major environmental concerns initially addressed were as follows:

1. The area is a fragile desert environment which once was a rich grazing area, a high steppe-grass country, prior to its being overgrazed in the latter part of the 19th century. Precipitation on the valley floor averages 25 cm (10 in.) per year.

2. Sensitive species could be disturbed by noise or habitat encroachment during drilling and construction.

3. Historical materials and artifacts could be destroyed. The area was traversed by the old Oregon-California trail.

4. With injection of the geothermal fluids being a planned necessity because of the huge quantities that must be flowed (42 L/sec/net-MW-output, or 680 gpm), would there be:

i) selective subsidence if the injected fluids are not of full quantity or do not mix with the producing reservoir?

ii) possible seismic activity from changes in reservoir pressures or fault lubrication?

5. Could the near-surface domestic aquifer be contaminated either during drilling or later during production and injection?

6. Could well testing, construction activities, or cooling-tower operation cause atmospheric contamination?

	AIR	WATER	PHYSIOGRAPHY	BIOLOGICAL	HUMAN	INTEGRATED PROGRAM
IDAHO NATIONAL ENGINEERING LAB	X	X	X	X	X	X
ERDA - IDAHO OPERATIONS	X					X
U.S. EPA		X				X
U.S. FISH AND WILDLIFE				X		
U.S. SOIL CONSERVATION SERVICE			X			
NOAA	X					
U.S. BUREAU OF LAND MANAGEMENT				X		X
U.S. GEOLOGICAL SURVEY		X	X			
U.S. BUREAU OF RECLAMATION		X				
ID DEPT OF WATER RESOURCES		X				
ID BUREAU OF MINES AND GEOLOGY		X				
ID DEPT OF FISH AND GAME				X		
ID DEPT OF HEALTH AND WELFARE	X	X				X
BATTELLE HUMAN AFFAIRS*					X	
BATTELLE NORTHWEST		X				
U OF UTAH RESEARCH INSTITUTE*	X			X		X
U OF UTAH*		X	X	X		
IDAHO STATE U*				X	X	
U OF IDAHO*		X		X		
BRIGHAM YOUNG U*				X		
U OF CALIFORNIA - BERKELEY*			X			
COLORADO SCHOOL OF MINES*			X			
UTAH STATE U*		X	X	X		
PRIVATE CONSULTANTS*		X	X	X		X
SERVICE COMPANIES*	X	X				

Fig. 1 Primary Participants in Raft River Environmental Program

The Fragile Ecosystem

The baseline assessments of the biota were conducted by three universities -- University of Utah, Idaho State University, and Brigham Young University. The significant aspects that can be

labeled fragile were:

1. The ferruginous hawk nesting grounds. Though the species is not officially threatened or endangered, the Raft River Valley is one of its few habitats. Figure 2 shows the nesting sites, with suggested 1-mile radius exclusion areas.

2. Sage grouse strutting grounds and brood-rearing areas. This species' environment is being encroached upon throughout the West.

The recommendations were made to prohibit drilling and construction during nesting periods. These recommendations are inadequate as a permanent solution--instead, an evaluation of the disturbance-effects patterns has been planned during the small pilot-plant programs, before major geothermal development begins.

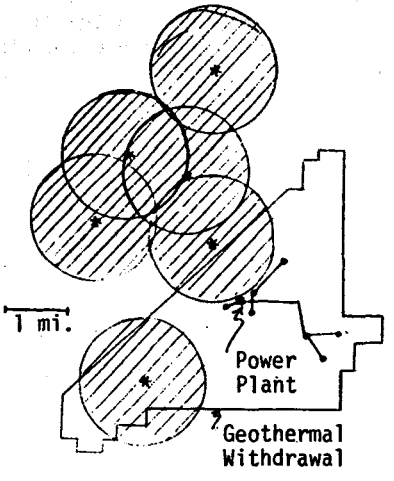


Fig. 2 Ferruginous Hawk Nests and Buffer Zones

Seismics

The Colorado School of Mines, under contract during 1974, conducted a study of the natural microseismic activity in the valley. During the entire 90 days of the study, only seven events with S-P times of less than 2.0 sec (corresponding to epicentral distances of less than 17 km) were detected. The scarcity of events and the low magnitude of their force seem to indicate that the area is more closely related to the aseismic Snake River Plain than to the active Basin and Range Province. Though naturally aseismic, the valley could become active as a result of long-term production and injection of the geothermal resource. Therefore, monitoring of microseismic activity is continuing, with four stations operating in the valley.

Subsidence

When benchmarks were releveled by the USGS in 1974, it became apparent that significant elevation changes had occurred in the northern part of the valley. Two types of movement were suggested; regional movements, probably as a result of tectonism, and a cone of subsidence of more than 0.8 m (2.6 ft) in an area of groundwater decline. The USGS line has been extended to include a grid around the production-injection field. No subsidence has been detected to date, although geothermal fluids have been produced and reservoir pressures have declined. Extensometers are being installed at various depths in the near-surface and geothermal aquifers to differentiate among: 1) subsidence that may result from production of the geothermal resource; 2) that which results from pressure declines in upper aquifers hydraulically connected to the geothermal resource; and 3) that which results from normal groundwater withdrawal for irrigation.

Water Quality Monitoring

Because of the major dependence on water for irrigation and domestic purposes in the area, the possible contamination of these supplies has been of prime concern. Both the surface and groundwaters have been sampled frequently during the past four years. Several irrigation wells show the influence of natural leakage from the geothermal resource (see Table 1). Because injection may alter or enhance this natural communication, a series of monitor wells has been drilled to depths of from 150 to 460 m.

TABLE 1

	RRGE-1	RRGE-3	Typical Irrigation Well*	Raft River
Depth, m, (ft)	1521 (4989)	1790 (5840)	110 (360)	--
T(°C)	147	149	29	18
pH	Avg. 7.2	6.3 to 7.5	7.7	8.4
Conductivity	3373	9530	4400	1060
Ca	53.5	193	92	104
K	31.3	97.2	19.6	9
Li	1.5	3.1	1.7	0.04
Na	445	1185	777	92
Cl^-	776	2170	1257	220
F^-	6.3	4.6	5.1	.72
HCO^-_3	63.9	44.4	131	229

* Near geothermal wells

Air Quality

Geothermal power plants at the Geysers in California have at times faced stiff opposition from environmentalists claiming that air quality standards had been violated. The primary concern was H_2S; secondarily, water vapor was a concern

(in essence it would be an "enrichment" to the arid climate of that region). Because of the poor image regarding air quality attached to ideas of geothermal development, a very thorough baseline study was begun at Raft River shortly after the first well "came in."

Both high-volume and low-volume air samplers were installed near the site and 15 miles to the north of Malta, the only nearby town. A complete meteorological system was installed, and pollution-monitoring cameras were mounted, aimed principally toward Pocatello (80 miles to the northeast) and the Salt Lake Valley (80 miles to the southeast).

The air samplers picked up significant quantities of phosphates (from local farming operations) and of sulphates (identified as those characteristic of the smeltering operations in the Salt Lake Valley). Pollution monitoring showed very significant ingress over the Strevell Pass from Salt Lake, with minor (1/4 as much) ingress from the Pocatello area.

Injection of most of the used geothermal fluid at Raft River is intended, except for that to be used beneficially for agriculture and aquaculture. Furthermore, H_2S has never exceeded 0.15 ppm in any of the deep wells. These factors alone would indicate that the extensive air-quality monitoring program was technically unessential. But when one deals with a preconceived negative image of geothermal development and air quality, it is politically essential to establish a thorough baseline for comparison at a later time.

Today's Concerns

Most of the initial concerns listed above have been adequately addressed and evaluated well in advance of developing a geothermal area in the valley. However, there remain two concerns which were not appropriately recognized until the wells were drilled and certain reservoir evaluation results were available:

1. Operation of the production and injection wells may well affect the near-surface aquifer. It is not certain that these effects will be detrimental, however.

2. Water consumption from wet cooling towers in a moderate-temperature geothermal power plant is three to five times greater, per unit net electric output power, than for fossil or nuclear power plants.

Better evaluation of the vertical connections in the aquifers, of the natural convective flows among strata, and of the chemistry of the various strata is the major data requirement for the current phase of the environmental program. Presently, the near-surface aquifer does not appear to be much purer than the geothermal aquifer. There seem to be connections between these aquifers, which implies that consumptive use of any water affects the inventory of the domestic and agriculture water resources in the valley.

Conclusions

The Raft River environmental program was designed to address the concerns associated with geothermal development. As development progressed, and more data became available, more emphasis was placed on particular concerns. The program is continually being modified to reflect these changes. The baseline-characterization studies represent an investment of $400,000. The environmental report preparation represents an additional $100,000. Routine monitoring of the parameters that may be affected by geothermal development is costing $150,000 per year. Is this excessive for a $15 million pilot plant development? Certainly we would hope to learn from the early pilot programs what environmental parameters are sensitive to geothermal development, and which are not, so that costs can be reduced. Geothermal developments tend to involve small quantities of power, with small environmental impact. Environmental study costs should be adjusted according to the potential impact.

This work was sponsored by the U.S. Department of Energy.

Geothermal Resources Council, TRANSACTIONS, Vol. 2 July 1978

ECONOMIC FEASIBILITY MODEL FOR DIRECT HEAT APPLICATIONS OF GEOTHERMAL ENERGY

Tod C. Larson

Science Applications, Inc.
La Jolla, California 92038

ABSTRACT

An Economic Feasibility Model (GEYSER) to determine the viability of direct heat applications of geothermal energy is described. The Price of the Product or the Return on Investment can be determined given the required economic parameters. Variables can be adjusted to perform sensitivity analysis, the key economic variables can be highlighted, and the range of profitability can be forecasted.

Work performed under the auspices of the U.S. Department of Energy, Contract No. ET-78-C-03-1529.

A model has been developed which evaluates the economic feasibility of direct heat applications of geothermal energy. The model, named GEYSER (Geothermal Energy Yearly Statements of Expenses and Revenues), is a generic model encompassing a wide range of investment possibilities and concerns a potential investor would have regarding the development of a new product, such as the rate of inflation, the future costs of alternative energy sources, and the present and future market demand for his product.

The GEYSER model will enable the potential investor to evaluate an investment possibility by using known information and ranges of projections for uncertain data, along with his own perceptions of the risks involved, to determine the viability of a potential geothermal operation. Many of the direct heat applications involve existing technologies which can be utilized to lower potential risks. Some direct heat uses, including space heating, industrial and agribusiness applications, are being presented at this conference.

This economic feasibility model is designed to provide two major functions:

1) to project the range of prices of a product developed with a geothermal resource, and

2) to project the range of return on investment for the venture.

These projections are based upon assumptions which form the basis of the model input. The investor with the highest degree of certainty regarding these assumptions will perceive a lower degree of risk.

The price and return on investment is calculated by projecting the income statements of the venture over the life of the investment. (An income statement is a standard accounting tool which displays income and expenses for the year.) The time series of expected income statements can also serve as a guide to measure and monitor the success of the investment. The project managers will be able to compare the actual income statements with the projected income statements to determine where cost projections differ.

The model has two forms of outputs: one assumes total revenues and forecasts the return on investment; the other works in reverse, assuming a return on investment and forecasting total revenues. Tables 1 and 2 display the income statement and "reverse income statement" formats, by which the investments are analyzed.

Unlike electric power plants which have long lead-times before development, most direct heat applications can be developed and put into operation in a short time, usually less than a year. Therefore, the current competing market prices and the projections of near-term and long-term future market prices are of critical concern. The following discussion shows how the economic feasibility model can be used to help evaluate present and future markets.

A. Present Markets

Given the variables listed below, the economic feasibility model is used to estimate the price of, and the return on investments for, the product. The model can be divided into two components.

Since geothermal energy will replace a portion of the energy cost to the operation, if the component data are available, a series of income statements can be generated for the energy costs and assumptions separately. In this way, it would be as if the energy producer functioned independently of plant production.

If desired, all components can be included in the overall income statement projections, as shown below. Many of the inputs to the model are optional. By using the inputs listed below, an algorithm is utilized, which calculates the expected revenues from the project and thus, the price of the product. Conversely, if the price of the product and the level of output are assumed, the return on investment can be calculated.

Using these inputs, the potential investor can generate a price for his product in constant dollars for comparison with the alternative price of the product, i.e., the alternative price of energy in the market, in the region at that point in time.

B. Projected Markets

Markets do not remain stable over time as witnessed by the increasing costs of oil, uranium and most other products. Inflation plays a major role in many investment decisions and must always be considered a variable. In addition, many prices increase as a result of increased demand. If a geothermal product is produced in a region which currently has adequate supplies, the price and return on investment will decrease for all producers in that region. Energy costs are very responsible to increases in demand (decreases in supply). The less dependent geothermal energy is on these fluctuations, the more viable and desirable it is. One of geothermal energy's potentially attractive attributes is that it

INPUT PARAMETERS FOR ECONOMIC FEASIBILITY MODEL

		Assumptions for Example
1.	Life of Investment	20 years
2.	Units of Output (Production Rate)	$176,360/yr. Total Revenue (TR)
3.	Price Per Unit of Output	
4.	Capital Costs	$967,879 (1978)
5.	Operating Costs (Fixed)	$39,541
6.	Operating Costs (Variable)	0
7.	Rent and/or Royalties	5% of TR
8.	Depreciation Method	Double Declining Balance
	a. Straight Lined	
	b. Declining Balance	
	c. Sum of Years Digits	
9.	Percent of Debt (% Equity)	50% debt
10.	Interest Rate	8%
11.	Discount Rate	8%
12.	Tax Rates	
	a. Federal	48%
	b. State	9%
	c. Property (Ad Valorem)	3% TR
13.	Depletion Allowance	None
14.	Intangible Drilling Cost Expensing	70%
15.	Drilling Costs	$300,000
16.	Investment Tax Credits	10%
17.	Return on Investment (Reverse Income Statement)	15%
18.	Exploration and Development Times	0
19.	Specific Tax Benefits or Subsidies	
	a. As Percent of Capital Costs	0
	b. As Percent of Taxes	0
	c. Per Unit of Output	0
20.	Price of Energy (Additional or Alternative)	0

is a capital intensive investment, which is not subject to fuel price increases. Once the well is drilled and the pipes, exchangers, etc., installed, the energy source, in many cases, has very little additional cost. Operating and maintenance costs may increase, but in most cases, this is a small component of the overall cost. Therefore, it is advisable to evaluate the geothermal prospect with regard to the specific alternative energy sources available to the investor (gas, electric, fuel oil, etc.) to obtain projections of future supply and demand for these components and their corresponding costs and assumptions. The feasibility model is generic, in that assumptions for the alternatives can be substituted and a direct comparison of the costs performed.

The two effects which will influence future costs and which can be reflected in the income statements are included in the model. They are:

1) Cost Escalation Factors
   a. operating and maintenance costs
   b. additional capital cost
   c. energy (product prices)
   d. learning curve effects
2) Inflation Factors.

The income statements displayed do not include cost escalation or inflation factors. The line items in the income statement can be adjusted to account for forecasted rates. Several indexes are available, such as the Consumer Price Index, which can help evaluate this impact on a product's economic feasibility.

Tables 1 and 2 illustrate sample outputs in constant 1978 dollars for a direct heat application. The assumptions are based upon cost and economic information from the *Total Energy Recovery System for Agribusiness* (International Engineering Company, Inc., May 1977), as well as drilling cost assumptions for a hypothetical site. The example is designed to illustrate the output of the model, rather than advocate the input assumptions to the model. The assumptions used in this presentation are not validated with any particular site in mind, but serve as an example.

This example illustrates the benefits which would accrue to a small developer operating the resource as a primary investment. Unlike a large corporation or conglomerate, the small developer cannot take advantage of early expensing of intangibles and investment tax credits in the immediate year. (This is shown in the income statements.) The expensing of intangible drilling costs can only be utilized until the net income before taxes is zero, because the deduction cannot be greater than total revenues. In addition, the small developer is unable to use the investment tax credit until the seventh year of operation. A large company would be able to efficiently use these tax advantages by utilizing them in conjunction with other investments, and thus receive a higher return on investment.

Table 1 forecasts the income statements in constant dollars. To determine the return on investment, the actual cash flow of the operation must be considered. The incomestatements allow for the calculation of tax expenses. Net income on the income-statements is zero during the first 6 years of production, nevertheless there is still a positive net cash flow. Depreciation is an accounting method used to determine taxes it reflects the recovery of capital but is not included in the calculation of the true cash flow. The cash flow is calculated by substituting the actual expenses such as the amortized loan payment for the paper expenses such as depreciation, expensing of intangibles and depletion. The cash flow and the net present value of the cash flow with an 8% discount rate is displayed for each year in the table. The internal rate of return of the cash flow is 11%.

At this point the investor might ask what conditions would be necessary to get a 15% return on his investment. How much would he have to raise the price of the product to satisfy this requirement? The model then goes through an iterative process whereby the price required for a 15% return is calculated. Table 2 displays the corresponding income statements in a reverse format. In this case total revenues increased to $199,000 per year indicating that a 12.8% increase in the price of the product would be necessary for a 15% Internal Rate of Return.

The investor, at this point, must look at the market for his products and determine future demand and cost and price escalations. The Total Energy Recovery System investment produces several products in a synergistic cascading system. The market for each of these products must be analyzed to determine the worth of each component of the investment. A finer breakdown of the capital costs and a review of market demands might indicate the net benefit of each component, as well as highlight any inefficiencies in the system.

In summary, the GEYSER model has been developed to analyze the economic feasibility of potential users of geothermal energy. The model allows for many applications using as few inputs as necessary for a simplified analysis of investment possibilities. The model can be modified to accommodate specific additions for further analysis.

TABLE 1. PROJECTED INCOME STATEMENTS (1978 DOLLARS*)

INCOME STATEMENTS AND CASH FLOW	YEARS																			
	1	2	3	4	5	6	7	8	9	10	11	12	13	14	15	16	17	18	19	20
TOTAL REVENUES	$176,360	176,360	176,360	176,360	176,360	176,360	176,360	176,360	176,360	176,360	176,360	176,360	176,360	176,360	176,360	176,360	176,360	176,360	176,360	176,360
ROYALTIES (RENT)	8,818	8,818	8,818	8,818	8,818	8,818	8,818	8,818	8,818	8,818	8,818	8,818	8,818	8,818	8,818	8,818	8,818	8,818	8,818	8,818
OPERATING & MAINTENANCE	39,541	39,541	39,541	39,541	39,541	39,541	39,541	39,541	39,541	39,541	39,541	39,541	39,541	39,541	39,541	39,541	39,541	39,541	39,541	39,541
ENERGY EXPENSE	0	0	0	0	0	0	0	0	0	0	0	0	0	0	0	0	0	0	0	0
DEPRECIATION (DOUBLE DECLINING BALANCE)	69,960	62,964	56,667	51,000	45,901	41,310	37,180	33,462	30,115	27,107	27,104	27,104	27,104	27,104	27,104	27,104	27,104	27,104	27,104	27,104
EXPENSING INTANGIBLE DRILLING COSTS ($244,944)	14,035	21,876	29,087	35,741	41,906	47,647	1,631	0	0	0	0	0	0	0	0	0	0	0	0	0
INTEREST ON DEBT	38,715	37,868	36,955	35,968	34,902	33,752	32,509	31,166	29,716	28,151	26,460	24,633	22,660	20,530	18,229	15,687	13,061	10,162	7,033	3,652
DEPLETION ALLOWANCE	0	0	0	0	0	0	0	0	0	0	0	0	0	0	0	0	0	0	0	0
PROPERTY TAX & INS.	5,291	5,291	5,291	5,291	5,291	5,291	5,291	5,291	5,291	5,291	5,291	5,291	5,291	5,291	5,291	5,291	5,291	5,291	5,291	5,291
NET INCOME BEFORE TAXES	0	0	0	0	0	0	51,390	58,082	62,878	67,455	69,147	70,973	72,945	75,076	77,377	79,919	82,545	85,443	88,572	91,954
STATE TAXES	0	0	0	0	0	0	4,625	5,226	5,658	6,070	6,223	6,387	6,564	6,756	6,963	7,192	7,429	7,690	7,971	8,276
FEDERAL TAXES	0	0	0	0	0	0	22,447	25,369	27,465	29,464	30,203	31,000	31,862	32,793	33,797	34,908	36,054	37,321	38,688	40,165
INVESTMENT TAX CREDIT	0	0	0	0	0	0	22,447	25,369	27,465	21,507	0	0	0	0	0	0	0	0	0	0
NET INCOME	0	0	0	0	0	0	24,317	27,484	29,753	31,920	32,720	33,584	34,517	35,525	36,614	37,817	39,059	40,432	41,912	43,512
CASH FLOW	73,420	73,420	73,420	73,420	73,420	73,420	73,284	68,430	67,975	63,211	36,582	35,620	34,580	33,458	32,246	30,937	29,523	27,997	26,347	24,566
NET PRESENT VALUE OF CASH FLOWS @ 8%	67,981	62,945	58,283	53,965	49,968	46,267	42,760	36,971	34,004	29,279	15,680	14,146	12,715	11,392	10,165	9,030	7,979	7,006	6,105	5,270

TABLE 2. REVERSE INCOME STATEMENTS (1978 DOLLARS*)

REVERSE INCOME STATEMENTS AND CASH FLOW	YEARS																			
	1	2	3	4	5	6	7	8	9	10	11	12	13	14	15	16	17	18	19	20
CASH FLOW	94,248	94,248	94,248	94,248	90,962	88,183	86,194	53,547	51,118	48,933	48,042	42,080	46,041	44,919	43,707	42,398	40,984	39,467	37,808	36,027
NET INCOME	0	0	0	0	17,278	31,887	34,281	36,560	38,741	40,704	41,504	42,368	43,302	44,310	45,399	46,574	47,844	49,216	50,687	52,297
INVESTMENT TAX CREDIT	0	0	0	0	15,949	29,434	30,110	0	0	0	0	0	0	0	0	0	0	0	0	0
FEDERAL TAXES	0	0	0	0	0	0	1,534	33,747	36,761	37,573	38,311	39,109	39,971	40,901	41,906	42,992	44,164	45,430	46,797	48,274
STATE TAXES	0	0	0	0	3,286	6,064	6,520	6,953	7,368	7,741	7,893	8,068	8,235	8,427	8,634	8,858	9,099	9,360	9,642	9,946
NET INCOME BEFORE TAXES	0	0	0	0	36,514	67,387	72,446	77,261	81,871	86,019	87,710	89,536	91,508	93,639	95,940	98,425	101,109	104,007	107,137	110,518
PROPERTY TAX & INSURANCE	5,970	5,970	5,970	5,970	5,970	5,970	5,970	5,970	5,970	5,970	5,970	5,970	5,970	5,970	5,970	5,970	5,970	5,970	5,970	5,970
DEPLETION ALLOWANCE	0	0	0	0	0	0	0	0	0	0	0	0	0	0	0	0	0	0	0	0
INTEREST ON DEBT	38,715	37,869	36,955	35,968	34,902	33,751	32,508	31,166	29,716	28,150	26,459	24,632	22,660	20,529	18,229	15,744	13,060	10,162	7,032	3,661
EXPENSING OF INTANGIBLES	36,878	43,839	50,318	56,368	25,527	0	0	0	0	0	0	0	0	0	0	0	0	0	0	0
DEPRECIATION	67,945	61,830	56,265	51,201	46,593	42,399	38,583	35,111	31,961	29,369	29,369	29,369	29,369	29,369	29,369	29,369	29,369	29,369	29,369	29,369
ENERGY EXPENSE	0	0	0	0	0	0	0	0	0	0	0	0	0	0	0	0	0	0	0	0
OPERATING & MAINTENANCE	39,541	39,541	39,541	39,541	39,541	39,541	39,541	39,541	39,541	39,541	39,541	39,541	39,541	39,541	39,541	39,541	39,541	39,541	39,541	39,541
ROYALTIES (RENT)	9,950	9,950	9,950	9,950	9,950	9,950	9,950	9,950	9,950	9,950	9,950	9,950	9,950	9,950	9,950	9,950	9,950	9,950	9,950	9,950
TOTAL REVENUES	199,000	199,000	199,000	199,000	199,000	199,000	199,000	199,000	199,000	199,000	199,000	199,000	199,000	199,000	199,000	199,000	199,000	199,000	199,000	199,000

* (1976 Dollars with 8% inflation per year)

Tod C. Larson

GELCOM: A GEOTHERMAL ELECTRIC LEVELIZED COST MODEL[1]

J. G. Leigh and J. N. Gupta

The MITRE Corporation, METREK Division
McLean, Virginia 22101

ABSTRACT

The model described in this paper is designed to project the costs of electricity generated from liquid-dominated hydrothermal geothermal resources. It exists in the form of an interactive computer program called GELCOM, written in FORTRAN IV. This paper provides an analytic explanation of the methodology.

This work was performed for the purpose of conducting site-specific analyses of the likely economic competitiveness of geothermal energy.[2] These analyses are being published separately. The model has also been used as a reference point in comparing and analyzing other methods of projecting geothermal energy costs.

GELCOM consists of an engineering cost estimating model and a levelized busbar cost model, as shown in figure 1. The field owner and operator ("Producer") and the conversion and generating plant owner and operator ("Utility") are treated as separate financial entities with different capital structures and subject to different tax and other regulations.

The engineering cost estimating model starts from resource characteristics data (such as temperature, salinity, well flow rate, depth, and rock hardness), and estimates the capital and operating costs for the production field and electrical generating plant. These estimates are made by interpolating between, or extrapolating from, twelve generic geothermal plant designs for different resource temperatures, salinities and conversion cycles. Well costs are estimated separately, from resource depth and rock hardness. The interactive nature of the program allows the program generated parameters to be overriden by the user, if desired.

The capital and operating costs are used as inputs to the levelized busbar cost model. This part of the program also requires financial data (debt/equity ratio, cost of money, tax rates, etc.). The algorithm used is based upon one which is standard in METREK, with certain extensions which have been found necessary to cope with factors specific to geothermal energy (e.g., capital reinvestment in replacement of production wells, injection wells and production plant).

Inflation and escalation are specifically taken account of in these calculations. The levelized busbar cost is computed as the cost in mills/kWh whose present value over the life of the project exactly equals the present value of all cost streams associated with the project (including return on equity). GELCOM includes the option of levelizing the imputed revenue stream obtained from energy production with or without accounting for inflation, i.e. in either constant or current dollars.

The program is designed to easily estimate the effects on busbar costs of reductions in the capital and O&M costs of components (perhaps achieved through RD&D or through experience), with different reductions being applicable for plants coming on-line in different years. It can also perform sensitivity analyses for the cost of electricity for varying resource and plant parameters. Fiscal incentives, such as depletion allowance, investment tax credit, and expensing intangible drilling costs are explicitly included in the program and may be used to evaluate the impact of these incentives on electricity costs. Figure 2 shows a flow chart for the program logic.

Figure 3 illustrates part of a typical program output, for, in this case, the geothermal prospect at Heber, California. The output starts by giving the field name, and the plant cycle, size and on-line date, followed by the physical field parameters and well flow rates and costs, indicating whether these were obtained from operator input or through the internal (default) program algorithms. Next, financial data are given for the Producer and the Utility.

[1]Work performed under the auspices of the U.S. Energy Research and Development Administration, Contract No. EG-77-C-01-4014.

[2]"Site-Specific Analysis of Geothermal Development--Scenarios and Requirements", R. K. Trehan, A. Cohen, J. N. Gupta, W. E. Jacobsen, J. G. Leigh, S. True, The MITRE Corporation, METREK Division, MTR-7586, Volume II, in process.

Then the estimated capital and operating costs for the plant, obtained from the engineering cost estimating model are displayed. The capital cost basis includes interest during construction. These cost estimates are for current (1977) technology. Finally, the levelized busbar costs or revenue requirements for this plant are given; the Producer costs are converted to mills/kWh of electrical output for convenience.

The next section of the output takes into account certain R&D advances postulated to be available when the plant design is finalized. The revenue requirements impact of each R&D advance is shown separately, then the revenue requirements impact for all advances together are shown. Finally, a sensitivity analysis is performed for the factors shown. Subsequent pages of the printout (not reproduced here) show similar information for subsequent plants on-line at this site.

The GELCOM data files currently contain characteristics of twenty-four geothermal (hydrothermal) prospect areas. Figure 4 illustrates estimated levelized costs of electricity (using current technology) from these prospects, including ranges of uncertainty due to resource temperature and plant reliability. The costs of likely competing energy sources are shown, computed using the same levelized busbar cost methodology.

A descriptive guide and users' manual for GELCOM has been prepared and is available in limited quantities.[3]

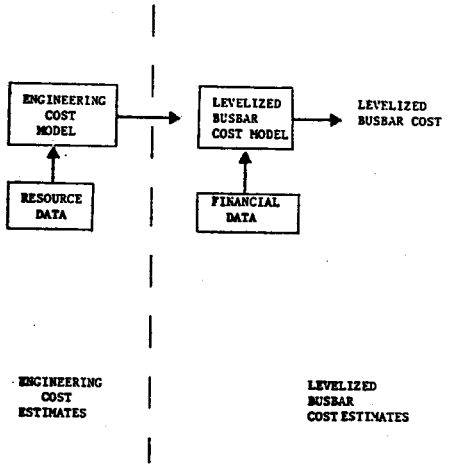
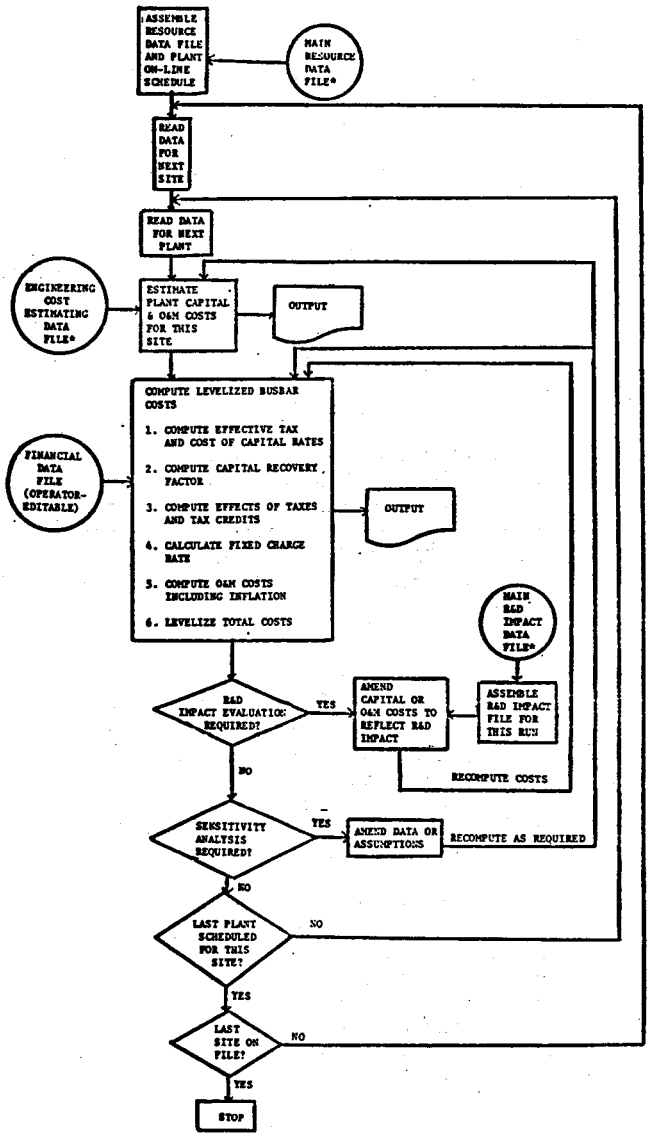


FIGURE 1

STRUCTURE OF GELCOM



*THESE FILES SHOULD NOT BE ALTERED BY THE OPERATOR.

FIGURE 2: LOGIC FLOW FOR GELCOM

[3] "GELCOM: A Geothermal Levelized Busbar Cost Model - Description and Users' Guide", J. N. Gupta, J. G. Leigh, The MITRE Corporation, M78-17, March, 1978.

FIGURE 3

EXAMPLE OF OUTPUT

```
                    HEBER , CALIFORNIA
                    BINARY SYSTEM , 50 MW ELECTRIC PLANT
                    FIRST PLANT ON LINE DATE : 1983

TEMPERATURE IN CENTIGRADE DEGREES (BEST ESTIMATE) : 190
WELL DEPTH IN METERS :                              1500
BRINE SALINITY :      LOW
OVERLYING ROCK TYPE : SOFT
THE WELL FLOW RATE IS NOT SPECIFIED ; THE DEFAULT FLOW RATE USED (KGM./HR.) =  266270
SPECIFIED COST PER PRODUCTION WELL ($) :   600000.0
SPECIFIED COST PER INJECTION WELL ($) :    600000.0

          PRODUCER FINANCIAL DATA                                UTILITY FINANCIAL DATA

DEBT  FRACTION :                              0.30     DEBT FRACTION :                              0.50
ANNUAL INTEREST RATE ON DEBT (FRACTION) :     0.08     ANNUAL INTEREST RATE ON DEBT (FRACTION) :    0.08
REQUIRED RATE OF RETURN ON EQUITY (FRACTION) : 0.20    REQUIRED RATE OF RETURN ON EQUITY (FRACTION) : 0.12
PROPERTY TAX RATE (FRACTION) :                0.01     PROPERTY TAX RATE (FRACTION) :               0.01
REVENUE TAX RATE OR ROYALTY (FRACTION) :      0.10     REVENUE TAX RATE OR ROYALTY (FRACTION) :     0.0
EFFECTIVE TOTAL INCOME TAX RATE (FRACTION) :  0.50     EFFECTIVE TOTAL INCOME TAX RATE (FRACTION) : 0.50
EFFECTIVE INVESTMENT TAX CREDIT  (FRACTION) : 0.04     EFFECTIVE INVESTMENT TAX CREDIT  (FRACTION) : 0.04
ESCALATION FACTOR FOR O&M COSTS :             0.05     ESCALATION FACTOR FOR O&M COSTS :            0.05
ESCALATION FACTOR FOR ENERGY COSTS :          0.0      ESCALATION FACTOR FOR ENERGY COSTS :         0.0
ESCALATION FACTOR FOR CAPITAL COSTS :         0.05     ESCALATION FACTOR FOR CAPITAL COSTS :        0.05
LIFE SPAN OF PRODUCTION WELLS (YEARS) :      10.00     LIFE SPAN OF UTILITY PLANT (YEARS) :        30.00
LIFE SPAN OF INJECTION WELLS (YEARS) :       10.00     ULTIMATE CAPACITY FACTOR :                   0.80
LIFE SPAN OF PRODUCER PLANT (YEARS) :        20.00     START UP COST MULTIPLIER :                   1.038
START UP COST MULTIPLIER :                    1.081

* NUMBER OF WELLS , CAPITAL COSTBASIS AND O&M COSTS , AND REVENUE REQUIREMENTS WITHOUT ANY R&D IMPACTS *

          CAPITAL COSTBASIS (1977 $)                             O&M COSTS (1977 $M/YR.)

 16 PRODUCTION WELLS :          11.556          PRODUCER
  7 INJECTION WELLS :            5.056               GENERAL :                    0.409
PRODUCER PLANT EXCLUDING WELLS :  7.284               WELL :                       0.138
REPLACEMENT PRODUCTION WELLS :    9.869               DEEP WELL PUMP :             0.721
REPLACEMENT INJECTION WELLS :     4.310               SPENT BRINE TREATMENT :      0.0
REPLACEMENT PLANT :               3.214               CHEMICAL & MECHANICAL CLEANING : 0.0
TOTAL FOR PRODUCTION FIELD :                 41.296   TOTAL :                                   1.268
GENERATING PLANT :                           35.785   UTILITY
TOTAL :                                      77.081        GENERAL :                    1.288
                                                           CHEMICAL & MECHANICAL CLEANING : 0.0
                                                           TOTAL :                                   1.288

** REVENUE REQUIREMENTS **

PRODUCER :  39.684 MILLS/KWHR
UTILITY :   18.813 MILLS/KWHR
  TOTAL :   58.497 MILLS/KWHR
```

FIGURE 3

EXAMPLE OF OUTPUT (CONTINUED)

```
                    HEBER , CALIFORNIA
                    (CONTINUED)

* R&D IMPACTS FOR PLANT NO. 1 - ON LINE DATE : 1983 *

R&D COMPONENT                                                  ANTICIPATED CHANGE (%)   CHANGE IN REVENUE REQUIREMENTS (MILLS/KWHR)
NUMBER OF PRODUCTION WELLS                                          -22.00                  -4.6978
CAPITAL COST PER PRODUCTION WELL                                     -5.00                  -0.9395
CAPITAL COST PER INJECTION WELL                                      -5.00                  -0.4110
CAPITAL COST OF PROCESS MECHANICAL (UTILITY)                        -50.00                  -1.1125
CAPITAL COST OF CONDENSER & HEAT REJECTION EQUIPMENT                -20.00                  -1.0635
PRODUCER DEEP WELL PUMP O&M COST FACTOR (BINARY SYSTEM , TEMP <260 C)  -33.00               -1.1564

** REVENUE REQUIREMENTS WITH ALL THE R&D IMPACTS INCLUDED. **

PRODUCER :  30.614 MILLS/KWHR
UTILITY :   16.637 MILLS/KWHR
  TOTAL :   47.251 MILLS/KWHR *

* SENSITIVITY OF COST OF ELECTRICITY (FROM PLANT NO. 1 , R&D IMPACTS INCLUDED) *

RESOURCE & OPERATING PARAMETERS                                                    MILLS/KWHR
HIGH RESOURCE TEMPERATURE ESTIMATE (225 DEGREES CENTIGRADE)                          36.450
LOW RESOURCE TEMPERATURE ESTIMATE (150 DEGREES CENTIGRADE)                           86.188
HIGH CAPACITY FACTOR VALUE :  0.85                                                   44.471
LOW CAPACITY FACTOR VALUE  :  0.60                                                   63.001
EXPENSING OF INTANGIBLE DRILLING COSTS ( 70.0% OF WELL COSTS EXPENSED)               44.051
DEPLETION ALLOWANCE ( 22.0% OF GROSS INCOME)                                         41.237
INVESTMENT TAX CREDIT ( 26.2% GROSS, 15.0% EFFECTIVE)                                44.776
```

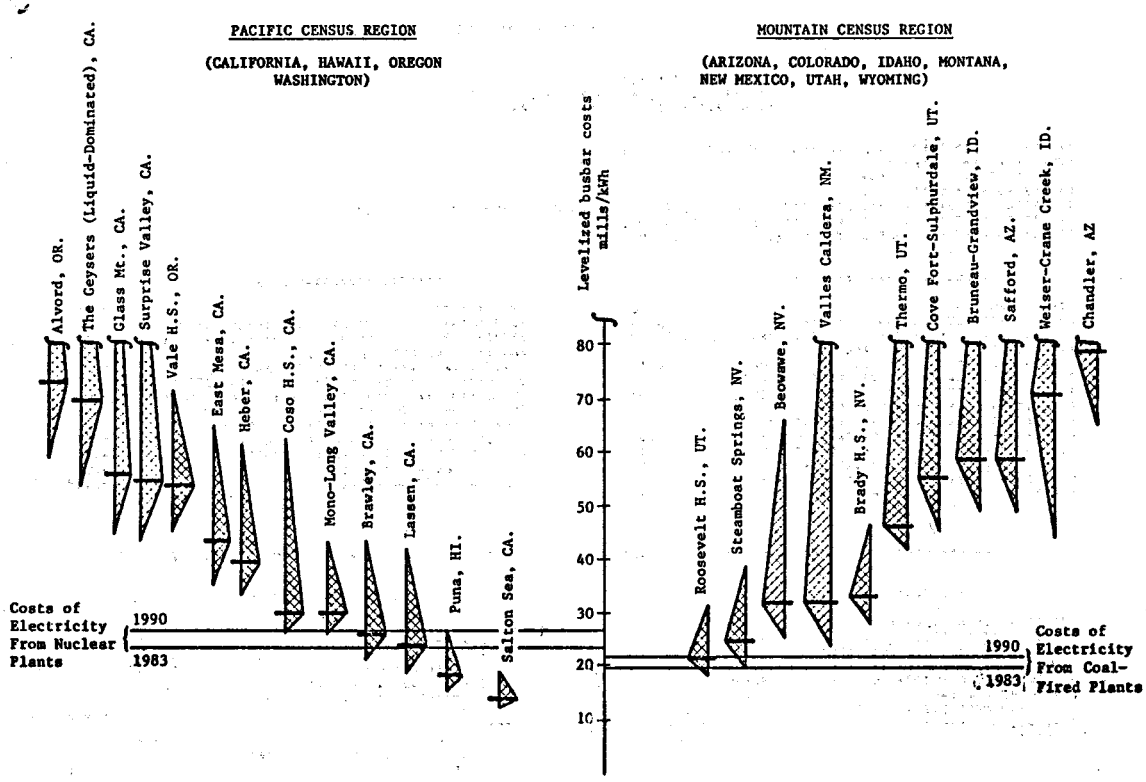


FIGURE 4: RANGES OF PROJECTED COSTS OF ELECTRICITY FROM HYDROTHERMAL LIQUID DOMINATED PROSPECTS (WITHOUT RD&D ADVANCES)

REMOVAL OF HYDROGEN SULFIDE FROM GEOTHERMAL STEAM

Charles T. Li, DP Alzheimer, WA Wilcox
GL Roberts, WF Riemath

BATTELLE, PACIFIC NORTHWEST LABORATORIES
Richland, Washington 99352

I. INTRODUCTION

Development of many geothermal energy sources is hindered because geothermal fluids contain impurities. Hydrogen sulfide (H_2S) is present in steam from most geothermal sources. The direct use of geothermal steam for power generation may therefore be both corrosive to the power generation-transmission equipment and offensive to the environment. Concentrations of H_2S as high as 1,600 ppm have been reported at the Geysers.(1) However, the concentration of H_2S in geothermal steam usually ranges from 60 to 1,000 ppm.

The H_2S problem in using geothermal steam for power generation has been illustrated by Bowen(2) in the following situation. A power plant with a capacity of 1,000 MWe requires 430 million pounds of steam per day. If the concentration of H_2S in the steam is 225 ppm (the average H_2S concentration in steam produced at the Geysers) a total of 48.4 tons of H_2S per day is carried by the steam to the surface. If 30 percent of H_2S is returned to the reservoir with steam condensate the total H_2S released to the atmosphere would be 33.9 tons per day. An H_2S release of this magnitude could lead to atmospheric concentrations such that corrosion of power generation and transmission equipment could occur as well as environmental impacts.

Since early 1976, Pacific Northwest Laboratories (PNL) under sponsorship of DOE (then ERDA) has been developing processes to remove H_2S from geothermal steam. The following criteria were established for such removal processes:

- They should be applicable at the upstream of power generation equipment to reduce H_2S corrosion problems.
- They should cause minimum degradation of steam quality.
- They should produce useful or environmentally innocuous byproducts.
- They should be inexpensive and simple to operate.

II. H_2S REMOVAL PROCESSES

Of the processes potentially capable of meeting the above criteria, two have been extensively investigated at PNL: sorption (both physical and chemical) of H_2S by solid sorbents, and oxidation of H_2S in presence of oxygen and catalysts.

1. Removal of H_2S by Solid Sorbents

Various sorbents, secured from catalyst manufacturers or prepared in our laboratory, have been investigated. These were first subjected to screening tests to evaluate their reactivities to H_2S. Tests were carried out in a simple gas uptake measurement apparatus; the gas used was a mixture of air and H_2S. A typical gas uptake curve for zinc oxide, a chemical sorbent, is shown on Figure 1. Two curves, one for fresh sorbent and one for regenerated sorbent, are shown. Spent zinc oxide was regenerated by heating it in an oven at 800°C for 10 hours. A drastic decrease in the reactivity of the sorbent was found upon reuse, as illustrated by the lower curve in Figure 1.

Sorbents selected by the gas uptake tests were further evaluated under simulated geothermal conditions in a bench scale gas sorption testing unit. The schematic of the testing unit is shown in Figure 2. The sorbent was placed in the sorption column where it removed H_2S from the simulated geothermal steam. Concentrations of the H_2S in inlet and outlet streams were monitored. Typical breakthrough curves (H_2S concentration versus time) for zinc oxide and a synthetic carbonaceous sorbent are shown in Figures 3 and 4, respectively. The

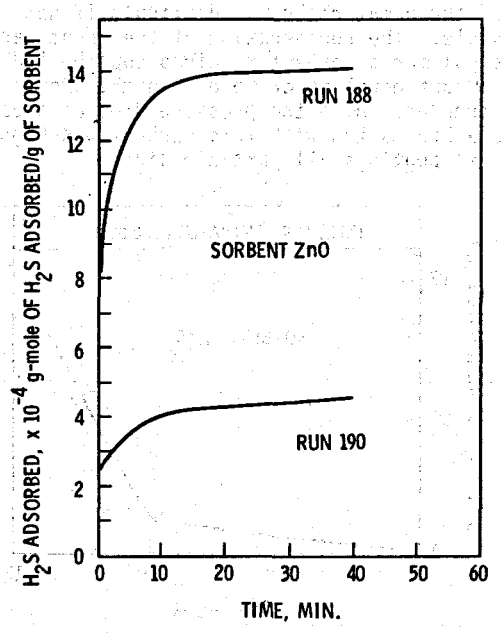


FIGURE 1. Gas Uptake Curves for ZnO

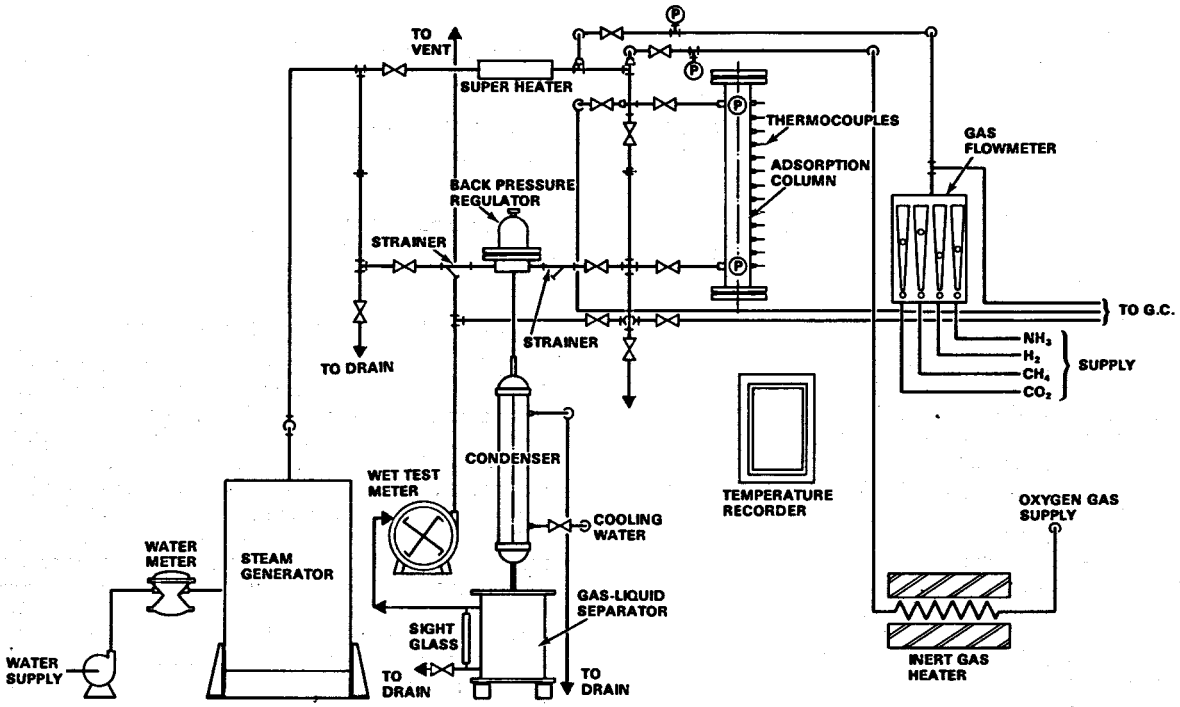


FIGURE 2. Flowchart for Removal of H_2S from Geothermal Steam Experiments

physical and chemical properties of the synthetic carbonaceous sorbent, as described by the manufacturer, were intermediate between those of activated carbon and a polymeric sorbent.

These experiments showed that, based only on their abilities to remove H_2S from steam, solid sorbents are promising materials for use in a geothermal treating process. However, the regeneration of these materials was difficult if not impossible. The regeneration of the spent carbonaceous polymeric sorbent required superheated steam in an amount equal to or more than the amount of steam treated. Also the pressure drop of steam across a bed packed with this sorbent was high due to the sorbent's small particle size.

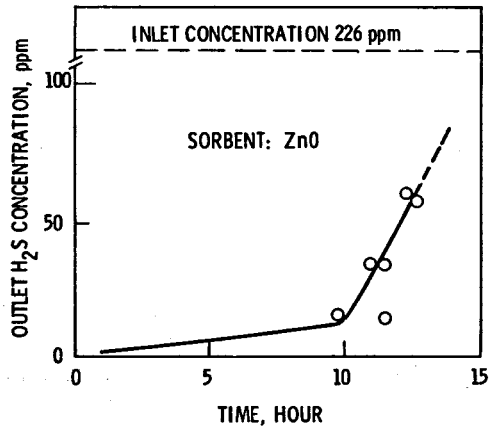


FIGURE 3. Breakthrough Curve for ZnO

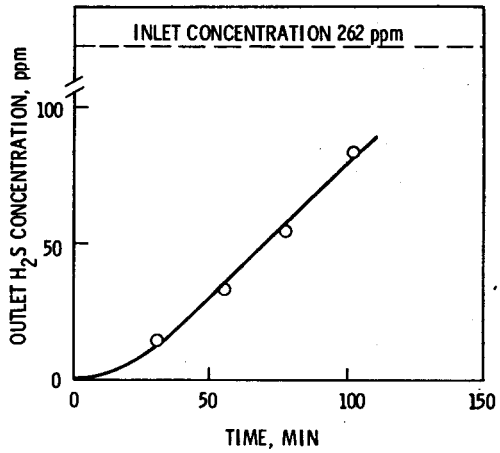


FIGURE 4. Breakthrough Curve for Polymeric Sorbent

The spent zinc oxide was regenerated by the oxidation of ZnS (the product of the steam treating process) with oxygen (or air) to form ZnO and SO_2. Thermodynamics of the oxidation of ZnS showed that regeneration at low temperatures was favorable for sulfate formations, while regeneration at high temperatures was favorable for oxide formation. Temperatures higher than 1100°C would be required for the predominant formation of zinc oxide. However, when the spent ZnO was regenerated at 700°C the surface area of the sorbent decreased to less than five percent of the original surface area. It was believed that the decrease of the surface area was one of the reasons for a severe decrease in the activity of the sorbent.

From the above work, we conclude that the regeneration of zinc oxide and the carbonaceous polymeric sorbent is either technically too difficult or economically too expensive for practical application.

2. Removal of H_2S by Catalytic Oxidation

The basic reaction of the oxidation of H_2S to elemental sulfur and water is shown in the following equation:

$$H_2S + \tfrac{1}{2}O_2 \rightarrow H_2O + S$$

Thermodynamic calculations indicate that the above oxidation reaction can proceed even under typical geothermal steam conditions. Based on typical geothermal steam conditions (225 ppm of H_2S) and with the stoichiometric amount of oxygen supply, more than 99.99 percent of H_2S can be theoretically removed from the steam. However, in order to enhance the reaction rate and to accomplish a complete (or near complete) removal of H_2S within a reasonable residence time a catalyst is required. Catalytic oxidation to remove H_2S from gas streams is an old process.[3,4,5,6] For example, use of the iron box and activated carbon box processes to remove H_2S from natural gas, manufactured gas and coke-oven gas were commercially practical in the old days. However, application of such processes to remove H_2S from geothermal steam containing more than 99 percent of water vapor has not been practiced.

RUN NO.		124	125	126	127	128	129	130	131
CATALYST		6	6	7	8	8	8	8	8*
WT. OF CAT. gm		80	80	80	80	80	80	80	79.8
BED VOLUMEN, Cm^3		128.8	184.0	114.1	143.5	164.9	131.7	181.0	122.5
STEAM RATE, $gm/cm^2/min$		20.2	20.5	20.5	20.6	20.8	21.0	21.0	20.8
SPACE VELOCITY, /min		184.6	130.9	211.1	168.9	148.4	186.8	136.3	184.4
RESIDENCE TIME, SEC		0.325	0.459	0.284	0.355	0.404	0.322	0.440	0.325
AIR RATE, ml/min		90	90	90	90	90	90	90	90
OXYGEN STOICHIOMETRIC		1.59	1.62	1.57	1.71	1.49	1.47	1.63	1.55
		H_2S CONCENTRATION ppm							
INLET		197.9	205.2	199.4	181.8	207.1	207.8	186.8	198.8
OUTLET H_2S CONCENTRATION vs. TIME	1 HR	0.6	0.6	1.0	1.3	1.5	0.7	0.9	1.0
	2	1.0	1.1	1.2	2.0	2.2	1.0	1.1	1.5
	3	1.3	1.5	1.8	2.6	3.3	1.2	1.5	2.0
	4	1.8	1.8	2.0	3.9	4.3	1.5	1.9	2.3
	5	2.2	2.0	2.6	4.9	7.5	1.8	2.2	2.5
	6	2.6	2.3	3.2	6.1	12.4	2.0	2.8	2.8
	7	3.1	8.2	3.9	6.8	16.5	2.2	3.2	
	8	3.8	8.2	4.6	7.5	20.3	2.4	7.5	
	9	4.0	12.7	6.6	8.3	24.2	2.5	12.2	
	10	4.9	16.5	9.5		28.1	2.8	16.9	
	11	8.2					3.0		
	12	8.8					7.2		
	13	6.3					12.3		
BREAKTHROUGH TIME, HR		–	–	–	–	8.5	–	8.2	
AVERAGE OUTLET, ppm		3.26	3.99	2.98	4.4	11.8	2.68	3.96	1.27
OUTLET OXYGEN CONC., ppm		67.5	62.4	64.7	62.2	62.9	47.6	67.5	61.9
% H_2S REMOVED		98.4	98.1	98.5	97.5	94.3	98.7	97.8	99.4
% SULFUR RECOVERY		61.9	79.8	77.9	80.3	87.99	64.62	89.51	69.39
*REGENERATED CARBON									

TABLE 1. Summary of Data for Catalyst Evaluation Test

In our laboratory, activated carbon was found to be an effective catalyst for H_2S oxidation in steam. Laboratory tests of the catalytic oxidation process were performed using the same equipment shown in Figure 2. The tests proved that the process using activated carbon as a catalyst indeed has the capability to remove H_2S from a simulated geothermal steam (steam + H_2S) as predicted by thermodynamic calculations. The process removed H_2S in the simulated geothermal steam from 200 ppm to less than 20 ppm most of the time. The process worked well as long as the temperature of steam being treated was kept above its saturation temperature and below about 235°C. The wet steam apparently caused the blinding of active catalyst sites and, as a result, the catalyst activity decreased markedly. To avoid this effect it was found necessary to maintain the steam in a superheated condition. When the process was operated above 235°C the entrainment of sulfur from the catalyst by the treated steam became significant. Typical data from laboratory experiments are shown in Table 1. It can be seen that in some cases times for breakthrough are longer than 13 hours. Here, the breakthrough time was defined as the time for the outlet H_2S concentration to reach 10 percent of that of the inlet stream.

Regeneration of the spent catalyst could be done by solvent extraction or distillation. Solvent for extraction could be either carbon sulfide (CS_2) or aqueous ammonium sulfide ($(NH_4)_2S$). The result of laboratory experiments showed that the activity of the regenerated catalyst obtained from the CS_2 extraction process was comparable to that of the fresh catalyst (see Run 131 in Table 1).

III. CONCEPTUAL PROCESS DESIGN

A conceptual process diagram is shown in Figure 5. Basically the process utilizes multiple reactors in a series. A three-reactor system will be used here for explanatory purposes. In Figure 5-a reactors 1 and 2 are "on-line" while reactor 3 is being regenerated. Geothermal steam passes through reactors 1 and 2 to remove H_2S and the treated steam exits for power generation. In Figure 5-b reactors 2 and 3 are "on-line" while reactor 1 is being regenerated. Figure 5-c shows that reactors 3 and 1 are "on-line" and reactor 2 is being regenerated. With this operating sequence the capacity of the catalyst can be fully utilized while maintaining a high H_2S removal efficiency. Solvent (CS_2 or $(NH_4)_2S$) with different sulfur concentrations is stored in three (or more) tanks. The spent catalyst is first extracted with solvent having the highest sulfur content stored in Tank I. The effluent is pumped to an evaporator where elemental sulfur is recovered. The energy required for solvent evaporation is supplied either from the exhaust of a turbine power generator or from a low grade geothermal steam or brine. The spent catalyst is then extracted with solvents having lower sulfur concentration stored in Tank II. The effluent of the extraction is stored in Tank I. The final extraction is done by pure solvent stored in Tank III and the effluent of the extraction is stored in Tank II. Solvent vapor from the evaporation is recovered in a condenser and goes to a surge tank and finally is pumped to Tank III.

IV. ADVANTAGES AND PROBLEMS

Major potential advantages of the catalytic oxidation process are:

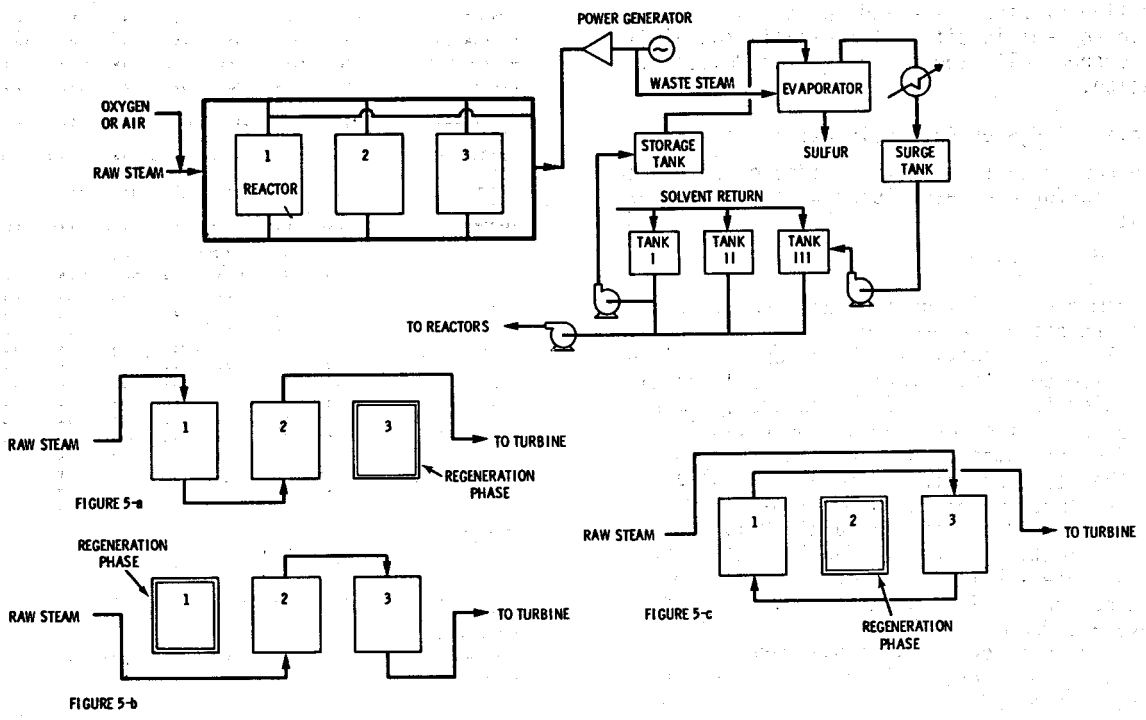


FIGURE 5. Conceptual Process Design

1. The catalyst, activated carbon, is readily available and relatively cheap.

2. Oxygen required in the process can be supplied as either air or pure oxygen.

3. The catalyst, activated carbon, can be easily regenerated and re-used.

4. Elemental sulfur is directly recovered from the catalyst regeneration process.

5. Energy required for the regeneration of catalyst is available at the geothermal power plant site.

Potential problems we foresee, before the catalytic oxidation process can be commercialized, are:

1. The pressure drop of steam across the catalyst bed: since the allowable sacrifice of the quality of steam is limited, the amount of catalyst to accomplish the required H_2S removal is very critical. Minimization of the pressure drop within the constraint of effective H_2S removal must be carefully studied.

2. Development of H_2S removal process for saturated geothermal steam: most geothermal steam is obtained from the flashing of hot geothermal water. Processes which can be operated at the steam saturation temperature would be most desirable.

3. Improvement of catalyst regeneration processes: CS_2 can be used for catalyst regeneration. However, CS_2 itself is a hazardous potential pollutant. A process of zero pollutant discharge must be developed.

4. The effect of trace amounts of heavy metals in geothermal steam to the activity of catalyst: we have learned that the presence of other non-condensable gas, such as CH_4, H_2, CO_2, and NH_3, does not interfere with the oxidation process. However, effects of trace amounts of vapor of heavy metals, such as mercury and arsenic, are unknown.

With these problems in mind PNL continues to work toward the development of this new catalytic oxidation process for removal of H_2S from geothermal steam.

REFERENCES

1. Pacific Gas and Electric Company, "The Geysers Power Plant, Unit 15, Environmental Data Statement," March 1974.

2. Bowen, R. G., "Environmental Impact of Geothermal Development," Geothermal Energy Resources, Production, Stimulation, Ed. by P. Kruger & C. Otte, Stanford University Press, Stanford, California 1973.

3. Kohl, A. L., and Reisenfeld, F. C. Gas Purification, McGraw-Hill Book Co., Inc., Chapter 8, 1960.

4. Giller, F., and Winkler, F., U.S. Patent 2, 168,933.

5. Lander, C. H., Sinnatt, F. S., King, J. G., and Bakes, W. E., British Patent 337.348.

6. Anon, Oil Gas J., 50(4), 59 (1951).

ON TRANSIENT TEMPERATURE INVERSIONS IN GEOTHERMAL BOREHOLES

R.P. Lowell, C.H. Chen, and J.K. Fulford

School of Geophysical Sciences, Georgia Institute of Technology
Atlanta, Georgia 30332

Introduction

Normally, the temperature increases with depth in the earth's crust. In geothermal areas, however, temperature profiles often show a rapid increase with depth over the first few hundred meters followed by a nearly isothermal region; and in many cases, there exist temperature inversions, regions in which the temperature decreases with depth. Healy (1971) has observed temperature inversions from the El Tatio geothermal area in Northern Chile, and Bodvarsson and Palmason (1964) have shown some examples of temperature inversions in Iceland. Bodvarsson (1973) has discussed several possible causes for such temperature inversions and has derived some simple models to show the diagnostic value of such inversions with regard to the structural and flow characteristics of geothermal systems.

There is one class of temperature inversion which has not been discussed by Bodvarsson (1973). This involves transient temperature inversions due to drilling disturbances. Very often in drilling a geothermal well, drilling fluid is lost from the wellbore into the adjacent rock formation. Since the drilling fluid is typically much cooler than the rock, injection of the drilling fluid will cool the rock. Temperature logs taken shortly after the injection of drilling fluid will show a region containing a temperature decrease with depth. After drilling ceases, the borehole will gradually return to equilibrium, and the artificially induced temperature inversion will disappear. An example of such a case is given in Figure 1.

The purpose of this paper is to give some simple models for the generation of temperature inversions which may result from the injection of drilling fluid into a formation and the subsequent relaxation of such inversions after drilling ceases.

Injection of Fluid Into Thin, Horizontal Fractures

Often in geothermal areas, the bulk permeability of the rock formations is quite low, and the permeability is due principally to narrow fractures. A good example of this is the Hengill geothermal area in Iceland where there appears to be just a few narrow, widely-spaced, nearly

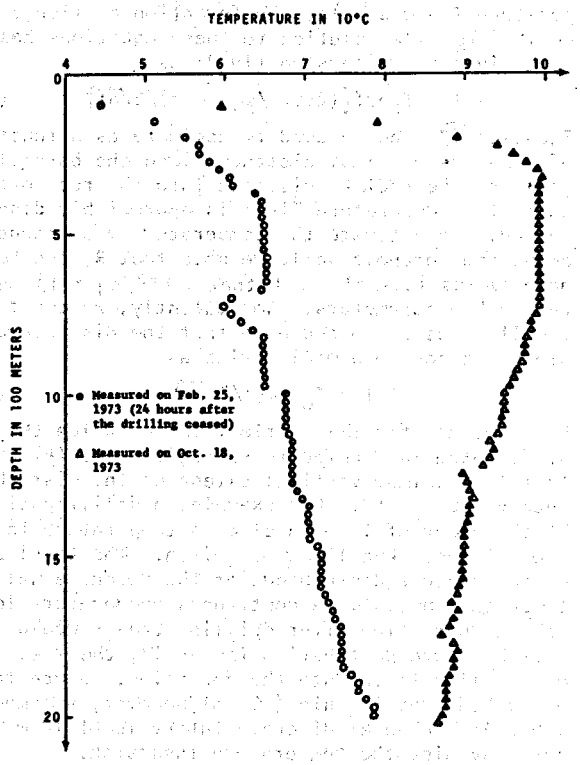


Figure 1 Temperature data from borehole MG-16 in the Reykir geothermal area, Iceland

horizontal contacts which act as fluid conductors (Bodvarsson, 1970).

It is useful to model the temperature inversion which would result from the loss of drilling fluid into a thin fracture. To consider this problem in an approximate way, we will neglect the usual drilling disturbance associated with energy dissipation due to drilling and fluid circulation through the drill stem and annulus. We will treat the disturbance simply as a result of drilling fluid being injected into the formation at a given flow rate and temperature. The mathematical formulation of the problem is then similar to that involved in thermal reinjection wells (Bodvarsson, 1972). Let r be the radial distance from the borehole, and z be the coordinate perpendicular to the fracture, which is located at $z = 0$. Neglecting heat conduction in the rock in

radial direction, the pertinent heat transfer equation for the rock is

$$a\partial^2T/\partial z^2 = \partial T/\partial t \qquad (1)$$

where a is the thermal diffusivity and T the temperature of the rock. The heat transfer by the fluid in the fracture is considered to be a boundary condition at z = 0. This condition takes the form

$$sq\partial T/\partial r = 4\pi r\lambda \partial T/\partial z\Big|_{z=0} \qquad (2)$$

where s is the specific heat, q the mass flow rate of the fluid, and λ the thermal conductivity of the rock. Let the fluid enter the formation at temperature T = 0 and let the formation at time t = 0 be at $T=T_o$. The solution to these equations has been given by Bodvarsson (1972) as

$$T = T_o\mathrm{erf}\left[(2\pi\lambda r^2/sq + z)/2\sqrt{at}\right] \qquad (3)$$

Equation (3) can be used to estimate as a function of time the vertical distance along the borehole wall and the radial distance into the rock over which the temperature field is appreciably disturbed. To estimate the temperature disturbance along the borehole wall, we note that R, the borehole radius is small such that $2\pi\lambda R^2/sq \simeq 10^{-5}$m for reasonable parameters. Consequently, we can take the limit as $r \to o$ and note that the disturbance along the borehole wall varies as

$$T = T_o\mathrm{erf}(z/2\sqrt{at}) \qquad (4)$$

Since we may fix the ratio T/T_o, at which the disturbance is assumed to be negligible, (4) shows that the maximum vertical extent of the disturbance varies as $t^{\frac{1}{2}}$. For example, a drilling time of the order of 1 month gives a temperature inversion of less than 10 meters width. The total zone of temperature disturbance at the borehole wall is twice this amount. A continuous temperature log made a short time after drilling ceases would show a temperature pertubation indicating the loss of drilling fluid into the formation. Since the perturbed zone is thin (~20 m),however, a temperature log taken at discrete intervals of 10 m or more may miss the temperature inversion.

Relaxation of the Drilling Disturbance

After drilling ceases, the borehole tends to return to equilibrium. For the situation in which the temperature perturbation has been due to the circulation of drilling fluid through the drill stem annulus and the heat generated by the drill stem and drill bit, there have been approximate calculations of the time required for the borehole to equilibrate. Bullard (1947) has shown that the time required for a return to within 1% of equilibrium is a factor of 10 or more longer than the time after which the drill bit passed a given depth. There have been no calculations of the relaxation of a drilling disturbance in the situation where drilling fluid has been lost to the formation.

To estimate the time required for the dissipation of the temperature disturbance due to drilling fluid loss into a thin fracture, we consider the cooling of an infinite region in which the initial condition is given by equation (3) with $t = t_o$, where t_o is the drilling time. Analytical solution of the conduction equation with this initial condition is somewhat tedious (Chen (1975) gives an approximate analytical treatment); consequently, we approximated the initial condition on a discrete finite difference grid and solved the heat conduction equation using finite differences. As an example, we let $t_o = 10^6$ sec. The time for the temperature to return to within 1% of equilibrium at the point of maximum temperature disturbance was approximately 2.2×10^7 sec., more than a factor of 20 larger than the drilling time. This is of roughly the same order as the time estimated by Bullard (1947) for the relaxation of a drilling disturbance in the absence of fluid losses.

Large Scale Fluid Losses

Fluid losses during drilling do not always take place by flow in thin fractures. In some cases, fluid is lost into thick, permeable formations. For example, the zone of anomalous temperatures in the borehole in Figure 1 is approximately 200 m thick. This region of anomalous temperature is known from drilling records to be a zone in which more than 40 kg/sec was lost into the formation. The large width of the temperature inversion precludes the possibility that the fluid losses took place in a thin fracture; but what is more striking is the rapid relaxation of the temperature disturbance. Figure 1 shows that the temperature inversion has disappeared within 8 months after drilling ceased. Such rapid relaxation, over such a thick zone, could not have been due to thermal conduction. The temperature disturbance must have been removed by convective processes.

In order the consider this problem quantitatively, we consider first the problem of fluid loss into the permeable formation. Since the flow rate is so great, we consider heat transport in the permeable formation as a purely convective phenomenon. Following Bodvarsson (1972) we write heat transport equation as:

$$\partial T/\partial t + (s/\rho c)\vec{q}\cdot\nabla T = 0 \qquad (5)$$

where ρc is the heat capacity of the rock and the other terms are as previously defined. The solution to (5) in cylindrical coordinates gives a temperature field which is translated radially into the solid. The radius r of the advance of the front is (Bodvarsson, 1972)

$$r = \sqrt{sM/\pi\rho ch} \qquad (6)$$

where M = qt, q being the mass rate of drilling fluid loss and t the time. h is the thickness of the formation. For the present example, $t \simeq 3 \times 10^6$ sec, q ≃ 40 kg/sec, h ≃ 200 m. This gives r ≃ 15 m. This is probably an underestimate of r, since it is not likely that the fluid is lost uniformly over the 200 m thickness of the formation.

We will assume that the borehole returns to equilibrium as a result of horizontal sheet flow in the permeable layer. Once the cold temperature front resulting from the drilling fluid loss passes the borehole wall, equilibrium is restored. The borehole temperature data show that less than 8 months or approximately 2.4×10^7 sec was required

for equilibrium to be attained. The minimum velocity required in the formation is therefore given by

$$v \leq (\rho c/\rho_f s)x/t \qquad (7)$$

where x is the horizontal distance between the temperature front and the borehole wall. Inserting $x = 15$ m and $t = 2.4 \times 10^7$ sec, and $\rho c/\rho_f s = 0.9$ gives $v = 5.6 \times 10^{-7}$ m/sec. which is a rather reasonable velocity. For example, assume that the flow is driven by a pressure gradient mainly of convective origin of $-\partial P/\partial x = 10^3 Nt/m^3$. Applying Darcy's law

$$\rho v = -K/\nu \, \partial P/\partial x \qquad (8)$$

where K is the permeability and ν the kinematic viscosity; $\nu = 0.3 \times 10^{-6} m^2/s$ gives $K \simeq 0.18$ Darcy. This is a rather high but not unrealistic permeability for a single permeable layer. If this layer gives rise to the main horizontal permeability over the upper 2000 m of the thermal reservoir, the bulk horizontal permeability is roughly $(0.18) \times (200/2000) \simeq 0.02$ Darcy, which is in line with gross scale horizontal permeability estimated for the Reykjavik temperature area by Palmason (1967).

Conclusions

In most cases borehole temperature data is taken in order to estimate equilibrium subsurface temperatures. Either equilibrium data is used or techniques are applied to non-equilibrium data in order to estimate equilibrium temperatures. Anomalous data are often discarded. In some cases, however, anomalous temperature data may be of significant diagnostic value. The above example of a transient temperature inversion due to drilling fluid penetrating a permeable rock formation is a case in point. It may be possible to determine the permeability of formations or to isolate thin zones of high permeability on the basis of observed temperature inversions in boreholes. It is clear that in the example discussed here, that the data is much too sketchy to permit more than a very crude estimate of the flow rate and formation permeability. The data discussed above serve primarily as an example of how transient temperature inversions may be utilized to obtain information about the permeability structure of geothermal reservoirs. It would be useful to take frequent logs as the borehole returns to equilibrium. This would enable one to make a much more accurate treatment of the problem.

Acknowledgments

The senior author thanks Dr. Jens Tomasson of the National Energy Authority, Reykjavik, Iceland for making the borehole data available and for useful discussions regarding borehole data. The senior author also thanks the Georgia Tech Foundation for travel support for the trip to Iceland which made these discussions possible. This research has been supported in part by the U.S. Geological Survey, Department of the Interior, under USGS Grant No. 14-08-001-G-365 and in part by the National Science Foundation, Division of Ocean Sciences under NSF Grant No. OCE-76-81876.

Bibliography

Bodvarsson, G., 1970, An estimate of the natural heat resources in a thermal area in Iceland; Proceedings of the 1st United States Symposium on the Development and Utilization of geothermal resources, Pisa, 1970, in: Geothermics, Spec. Issue 2, Vol. 2, part 2, pp. 1289-1293.

Bodvarsson, G., 1972, Thermal problems in the siting of reinjection wells, Geothermics, 1, 63-66.

Bodvarsson, G., 1973, Temperature inversions in geothermal systems, Geoexploration, 11, 141-149.

Bodvarsson, G. and G. Palmason, 1964, Exploration of subsurface temperature in Iceland, In: Proceedings U.N. Conference New Sources of Energy, Rome, 1961, United Nations, New York, 2, 91-98.

Bullard, E.C., 1947, The time necessary for a borehole to attain temperature equilibrium, Monthly Notices Roy. Astron. Soc. Geophysics Suppl., 5, 127-130.

Chen, C.H., 1975, Temperature disturbance in a geothermal borehole system, M.S. Thesis, Georgia Institute of Technology, Atlanta, Ga., 49 pp.

Healy, J., 1971, Geological report on wells 1-5, El Tatio, Internal Report. In: Survey for Geothermal Development in Northern Chile, UNDP Geothermal Project in Chile, Santiago, 34 pp.

Dup

Geothermal Resources Council, TRANSACTIONS, Vol. 2 July 1978

ADVANCED TURBODRILLS FOR GEOTHERMAL WELLS

William C. Maurer, John C. Rowley, Clifton Carwile

Maurer Engineering Inc. - Houston, TX
Los Alamos Scientific Laboratory - Los Alamos, NM
Department of Energy - Washington, D.C.

ABSTRACT

Maurer Engineering Inc. is continuing the development of a new high-temperature, 350°C advanced turbodrill for use in drilling geothermal wells. Existing downhole drilling motors are temperature limited because of elastomeric degradation at elevated temperature. The new turbodrill contains high-torque turbine blades and improved seals which allow higher bit pressure drops. This new geothermal turbodrill which is designed for improved directional drilling offers economic alternatives for completing geothermal wells. The advanced turbodrill will be tested in the Los Alamos Scientific Laboratory's hot dry rock geothermal wells.

INTRODUCTION

The purpose of downhole drill motors is to provide the power needed to rotate drill bits at the bottom of the boreholes. Drill motors are especially advantageous for 1) wells where drill pipe wear, fatigue, and twist-offs occur, 2) directional drilling in wells where direction and trajectory control are required to attain a preselected target, and 3) starting wells that are spudded in volcanic rock or alluvium containing large boulders.

BACKGROUND

First tested in the 1920's, drilling motors did not find widespread application until the 1950's, when turbodrill use began in the Soviet Union, [1, 2]. By the early 1960's, about 85% of the Soviet's oil and gas wells were drilled with turbodrills. Their usage has decreased to approximately 70 percent since rotary drilling is now being used in most Soviet wells deeper than 12,000 feet.

Drill motors are currently used in the United States primarily for directional drilling. Current motor seals typically limit bit pressure drops to less than 300 psi, which is inadequate for good bottomhole cleaning of cuttings. Commercial downhole motors operate at speeds of 300 to 1000 rpm, whereas roller-cone bits operate most effectively at speeds of 50 to 150 rpm. The bit bearings tend to fail in 5 to 15 hours at these high motor speeds thereby seriously limiting the application of drilling motors.

A review of the various types of downhole motors, i.e., turbines [3, 4], positive displacement [5, 6], and electric drills [7, 8], indicated that a turbodrill would be the most practical to upgrade for high-temperature because of the all-metal turbine blades.

GEOTHERMAL APPLICATIONS

Soviet geothermal drilling has not been reported in detail [9], but it is likely that turbodrills have been utilized in the geothermal drilling program in the Soviet Union since that is their principal mode of drilling. Directional geothermal wells have been drilled with turbodrills in the extensions of the Hachimantai field in Japan [10]. The Philippine geothermal development by Union Oil of California has also indicated [11] a program of multiple wells from individual locations.

Directional drilling with downhole motors has been used to control geothermal well blowouts in the extensively developed Lardarello, Italy [12] and Wairakei, New Zealand [13] fields.

Directional drilling has been used in The Geysers, CA geothermal field to drill multiple wells from a single pad. One drilling contractor [14] indicated that about 15 wells have been successfully completed at The Geysers by that technique. It was also indicated that several essentially vertical wells have been provided with multiple side-tracked completions at The Geysers.

The DOE-funded Raft River, ID geothermal project [15], conducted by the Idaho National Engineering Laboratory, has effectively utilized a downhole motor to drill two directional holes from the bottom of a vertical geothermal well, Figure 1. This three-legged completion enhanced the productively of the well three to five fold in this fracture-controlled formation. This technique, which increased the total well cost by only 20 to 30 percent, will undoubtedly be more widely applied in future geothermal drilling programs. Consideration is being given to using the new geothermal turbodrills in future Raft River wells.

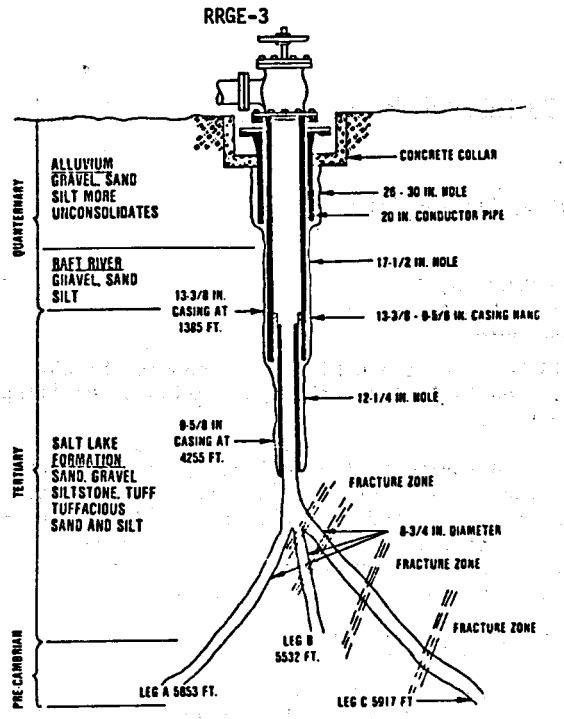


Figure 1 RAFT RIVER GEOTHERMAL WELL

The initial experimental approach to a hot dry rock geothermal project [16, 17] funded by DOE and conducted by the Los Alamos Scientific Laboratory (LASL), is based on the concept shown in Figure 2. The first borehole drilled into hot 200 to 300°C rock was hydraulically fractured and the second well was then directionally drilled to intersect the fracture.

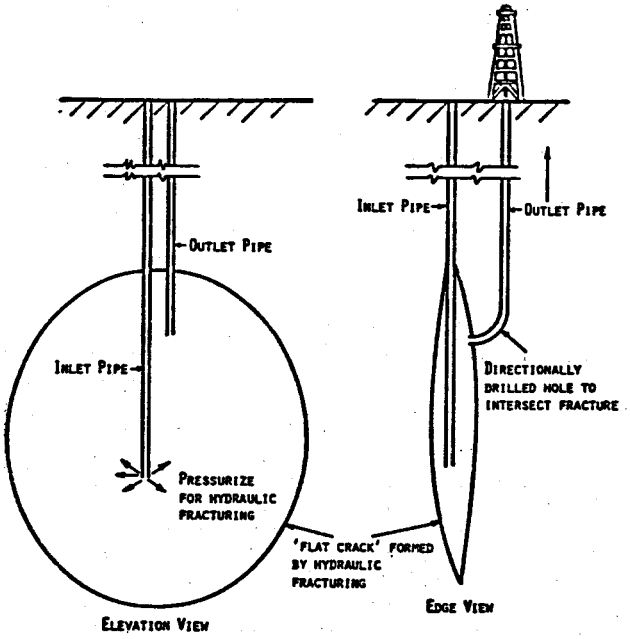


Figure 2 LASL HOT DRY ROCK WELLS

Directional drilling hard, hot granite has proven to be slow and expensive. Several approaches have been taken to improve the situation. The Dyna-Drill Division of Sii has provided an experimental unit, Figure 3, with a coolant flow hole in the rotor. This modification should provide better cooling by the drilling fluid and enhance the life of this drill motor at 200°C. For higher temperature service, the design of the turbodrill discussed in this report was initiated.

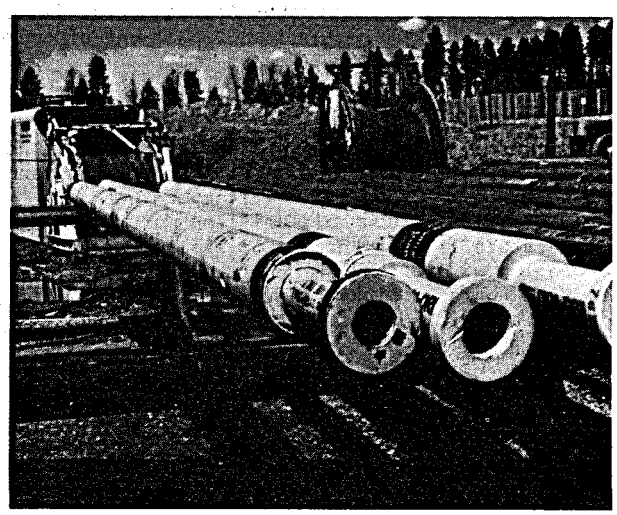


Figure 3 DYNA-DRILLS WITH HOLLOW ROTORS

HYDRAULIC DRILL MOTORS

There are two basic types of downhole hydraulic powered drill motors; positive-displacement and turbines. Positive-displacement motors have the distinct operational advantage that the rotary speed is directly proportional to the pump flow rate and flow rate gives a direct measure of the rotary speed. Volumetric efficiency decreases as motor torque increases because the increased pressure drop across the motor increases the leakage.

The torque delivered by a positive-displacement motor is directly proportional to the pressure drop across the motor. The rig mud pressure guage can therefore be used to monitor the bit torque.

Four types of positive-displacement motor concepts (Moineau, vane, piston, and gear) have been proposed for drill motors; but of these, only the Moineau type (Dyna-Drill) has been widely used for geothermal drilling. The Dyna-Drill is powered by an eccentric steel shaft rotating in a rubber stator. Dyna-Drill motors are limited to maximum operating temperatures of about 180°C primarily by the rubber stator. Attempts to increase the temperature capabilities using higher temperature elastomers have been of limited success because of their unfavorable fabrica-

tion properties and high costs.

TURBODRILLS

Turbodrills utilize axial flow turbine blade sections to apply torque to the drill bit. The torque developed by a turbodrill is maximum when the turbodrill stalls and decreases to zero as the rotary speed is increased to the runaway speed. Turbine torque can be increased by increasing the number of turbine stages, the fluid flow rate, or the exit angle of the turbine blades. Existing turbodrills deliver maximum power output at speeds of 500 to 1000 rpm. This high speed is excessive for roller bits and results in short bit bearing life.

ADVANCED GEOTHERMAL TURBODRILL DESIGN AND DEVELOPMENT

Existing turbodrills are limited to maximum operating temperatures of about 180°C due to the use of elastomeric thrust and radial bearings. Because of bearing limitations, these turbodrills are usually operated at bit loads of only 20,000 to 25,000 pounds, whereas many bits drill most effectively at bit loads of 40,000 to 60,000 pounds. This reduced bit load greatly reduces drilling rate, especially in the hard rocks encountered in many geothermal wells. These turbodrills do not deliver sufficient torque for optimum use of tricone drill bits; consequently, the bits drill at reduced speeds. Inadequate seals in existing drill motors, result in reduced bit hydraulics and reduced drilling rates.

Due to the temperature limitations of existing downhole motors, two advanced turbodrills are being designed for use in higher temperature wells:

- Directional Turbodrill - This turbodrill utilizes water to cool and lubricate the bearings and is designed to operate in hot geothermal wells at temperatures up to 350°C.
- Straight Hole Turbodrill - This turbodrill contains a sealed lubrication system which allows the bearings to operate in lubricant. The unit is applicable to both oil field and geothermal drilling.

The design specifications for these two turbodrills are given below:

GEOTHERMAL TURBODRILLS - SUMMARY SPECIFICATIONS

Parameter	Directional	Straight Hole
Rotary Speed:		
With Roller Bits	100-200 rpm	100-200 rpm
With Diamond Bits	400-800 rpm	400-800 rpm
Diameter:	7-3/4 inch	7-3/4 inch
Length:	21 feet	25 feet
Power Output:		
At 150 rpm	36 hp	65 hp
At 800 rpm	123 hp	222 hp
Flow Rate:	400 gal/min	400 gal/min
Temperature Limitations:	350°C	200°C
Bearing Life:	50 hours	100-200 hours

DIRECTIONAL TURBODRILL

A flow constrictor at the bottom of the high temperature directional turbodrill, Figure 4, allows approximately 10 percent of the drilling fluid to flow through the roller bearings to cool and lubricate them. The remaining fluid flows through the bit nozzles to remove the rock cuttings from the hole bottom.

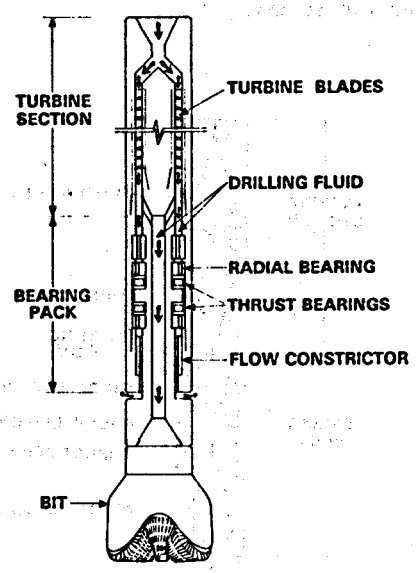


Figure 4 ADVANCED DIRECTIONAL TURBODRILL

The new turbodrills utilize advanced turbine blades which deliver 4 to 5 times more torque than the blades used in existing turbodrills. This allows the new turbodrills to be shorter and to deliver 100 percent more power than existing motors of comparable diameter. These turbodrills can be operated at rotary speeds of 100 to 200 rpm with high-torque roller bits and at 400 to 800 rpm with low-torque diamond bits.

A separate bearing pack is used to facilite turbodrill maintenance in the field. The bearing pack utilizes high-thrust roller bearings made of M50 tool steel. These bearings operate effectively at temperatures up to 600°C thereby overcoming a major temperature limitation of existing motors. These roller bearings have 10 to 80 times the life of the ball and rubber friction bearings used in existing motors.

Roller bearings are also used to accommodate the high radial loads in the turbodrills. These high loads are produced as the turbodrills are deflected in directional holes.

STRAIGHT HOLE TURBODRILL

The straight hole turbodrill, Figure 5, is designed to operate in abrasive drilling mud. The bearings are sealed in lubricant which is pressurized by the mud acting on top of a floating piston. Improved high-pressure rotary seals allow bit pressure drops of 300 to 800 psi across

diamond bits and 500 to 1000 psi across roller bits. This compares to only 200 to 500 psi with existing motors. These higher pressure drops should significantly increase drilling rates.

Although this turbodrill is currently designed for moderate temperature drilling (200°C), it is suited for drilling the shallower portions of geothermal wells, where drilling muds are required to prevent lost circulation into porous or fractured formations.

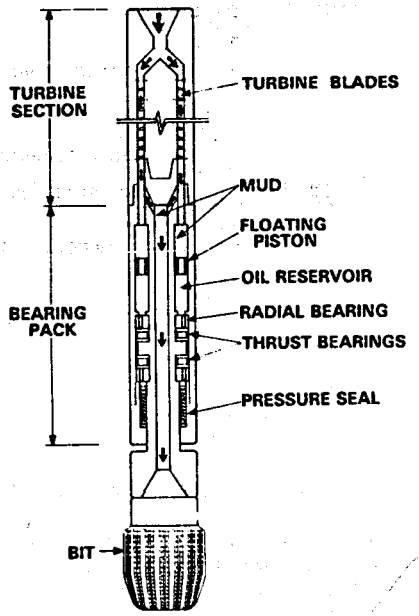


Figure 5 ADVANCED STRAIGHT-HOLE TURBODRILL

The temperature gradient in geothermal wells varies with hole depth; consequently, only the bottom portions of most geothermal wells are hot enough to necessitate the use of the directional geothermal turbodrill. When drilling with abrasive drilling mud, the straight hole turbodrill is preferred and should be used as long as possible before switching to the geothermal turbodrill.

CONCLUSIONS

Drilling motors have found rather widespread application for directional drilling of geothermal wells. An advanced high temperature turbodrill is being developed which will allow the drilling of several wells from a single location. The motivation for development of the advanced turbodrill was the directional drilling requirements in hot, hard granite for the LASL hot dry rock geothermal project. However, additional applications to other geothermal energy development projects can be expected.

ACKNOWLEDGEMENTS

The authors wish to express their appreciation to the individuals in the drilling and geothermal energy development industries who contributed to the survey of the usage of drill motors in geothermal wells. The authors also wish to thank J. W. Neudecker, LASL, for his valuable contributions to this turbodrill design effort.

REFERENCES

1. Thacker, J. H. and Postlewaite, W. R., "Turbodrills-Past and Present," The Drilling Contractor (December, 1956).
2. Salnikov, I. S., "Soviets Relying on Turbodrill to Help Meet Future Production Quota," J. Petr. Tech. (March, 1959).
3. Brun, A., "Turbodrill Solves Tough, Costly Operating Problems," World Oil (August 1, 1969).
4. Gatlin, C., Petroleum Engineering - Drilling and Well Completion, Prentice Hall, 1960 pp. 132-134.
5. McCollum, J. D., "Positive Displacement Downhole Motor for More Effective Directional and Straight Hole Drilling," Trans. Pet. Div. of ASME (September, 1966).
6. Garrison, E. P., "Downhole Motors Should Get Wider Use for Straight-Hole Drilling," The Drilling Contractor (March - April, 1976).
7. Delacour, J., "Electrodrilling in the U.S.S.R.," J. Petr. Tech. (September, 1963).
8. Kuhne, G., "New German Electrodrill Passes Important Tests," Petr. Eng. (February, 1964).
9. McNitt, J., Personal Communication, United Nations, Energy Section, Center for Natural Resources, Energy and Transportation.
10. Axtell, L. H., Ed., "Geothermal Energy Utilization in Japan," Geothermal Energy Magazine, 3, No. 2, 5-24 (1975).
11. Pyle, Del, Personal Communication, Union Oil Company of California.
12. Ugo, E., et al., "Control of a Geothermal Field After Damage to the Production Casing," to be published.
13. Byron, L. G., "Wild Steam Well Controlled by Directional Drilling," World Oil, 154, No. 5, 154-156 (1962).
14. Glass, W. A., "A 1977 Drilling Methods at The Geysers," Transactions Geothermal Resources Council Annual Meeting, May 9-11, 1977, pp 103-105.
15. Kunze, J. F. and Witherspoon, P. A., "Energy Extraction and Reservoir Management of a Moderate Temperature Hydrothermal System," Proceedings, Am. Nuclear Society, Energy and Mineral Resource Recovery Conference, April 12-14, 1977, pp 68-76.
16. R. A. Pettitt, "Los Alamos Hot Dry Rock Geothermal Energy Projects," Geothermal Resource Council, Transactions 1, pp 241-242, May 1977.
17. LASL Hot Dry Rock Project Staff, "Hot Dry Rock Geothermal Energy Development Project - Annual Report FY'77," Los Alamos Scientific Lab. Report LA-7109-PR (Feb., 1978).

Geothermal Resources Council, TRANSACTIONS, Vol. 2 July 1978

CORROSION TESTING IN A MULTIPLE-STAGE FLASH SYSTEM

R. D. McCright, R. E. Garrison and F. E. Locke

UNIVERSITY OF CALIFORNIA
LAWRENCE LIVERMORE LABORATORY

ABSTRACT

Corrosion rate results from a 720-hour exposure period to geothermal brine acidified to pH4 are discussed in this paper. The corrosion tests were performed in a four-stage flash system so that results obtained at different temperatures could be compared. Carbon steel and alternate construction materials were used as test specimens. Results indicate that carbon steel corrodes excessively (more than 50 mils/year) at temperatures above 150°C. Alternate construction materials (alloy steels) may be utilized under these conditions.

Work performed under the auspices of the Department of Energy, Contract No. W-7405-Eng-48.

One of the major concerns of acidification to control scale in geothermal power plants is the expected increase in corrosion rate of the plant construction materials. Therefore, the Lawrence Livermore Laboratory (LLL) has initiated a program for measuring the corrosion rate and evaluating other aspects of materials performance in acidified geothermal brines. The principal material of interest is carbon steel, of course, but alternate construction materials include alloy steels with chrominum and molybdenum as the alloy additions. Further, in the most severe conditions highly corrosion resistant alloys may have to be used as cladding or liners or for construction of limited size but high performance items such as valve trim.

In order to evaluate the performance of a wide variety of candidate materials under operating conditions, a four-stage flash system was construction at the LLL Field Test Site in the Imperial Valley. The system was designed to accomodate corrosion test specimens of two kinds: 1) direct exposure flat coupons for weight loss determinations, and 2) cylindrical electrodes for electrochemical determination of the corrosion rate by the linear polarization resistance technique (LPR). The LLL four-stage flash system replicates the San Diego Gas and Electric Co. Geothermal Loop Experimental Facility (GLEF). Both installations have been supplied with geothermal brine from Magmamax Well No. 1.

A schematic diagram showing the location of corrosion specimens in the LLL four-stage flash system is shown in Figure 1. Racks containing the direct exposure coupons were installed in the second, third, and fourth stage flash units. The nominal operating temperatures and pressures in these units were: second stage, 150°C and 50 psig; third stage, 125°C and 15 psig; fourth stage 110°C and 3 psig. Racks were located in the top (steam phase) and bottom (brine phase) of the second and third stage units and in the brine phase of the fourth stage unit. Thus, corrosion weight loss data were obtained at five locations in the system.

The individual corrosion coupons were nominally two inches by one inch. Thickness varied from about 1/16 to 1/8 inch according to the available stock of the alloy. The coupons were glass bead blasted (25-80 μm particles) and bolted onto a carbon steel support bar. Care was taken to electrically insulate the test coupon from the bar by means of Teflon washers and sleeves. The bars, each holding four to six specimens, were fixed to a steel ring which rested inside the flash unit. Overall dimension of the test rack was 13 inch diameter ring by 16 inch height.

The electrochemical specimens were placed in four locations in the system, as indicated in Figure 1. Specimens were exposed to untreated brine at 210°C (Station A), acidified brine at 210°C (Station B), acidified brine at 150°C (Station C), and acidified brine at 125°C (Station D). Three identical specimens of each alloy tested were mounted in probe holders manufactured by Petrolite Corporation. Briefly, the principle of corrosion measurement by the LPR technique is to apply a small potential difference (10 mV) between a pair of the three electrodes (reference and test) and measure the current which flows between another pair (test and auxiliary). This technique was described in our previous paper.[1]

The corrosion test period occurred during December 1977, January 1978 and February 1978. The test schedule is indicated in Table 1. The emphasis of the test procedure was to simulate real operating conditions. Therefore, during the

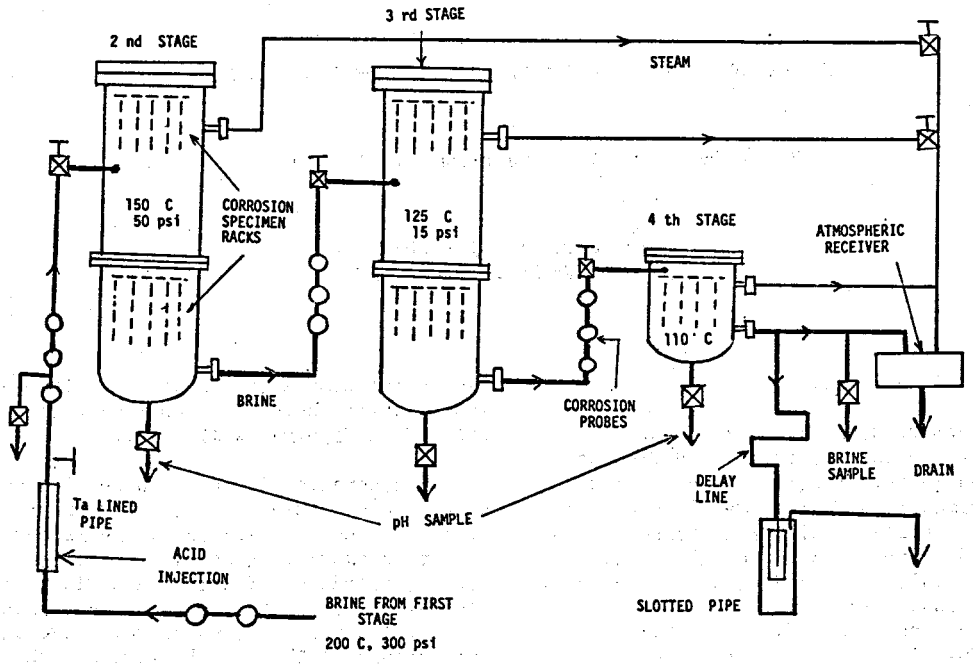


Figure 1 - Schematic of Four-Stage Flash System Showing Location of Corrosion Probes (LPR Technique) and Corrosion Test Racks.

first 36 hours of exposure, the system was operated with unmodified brine as would probably be the case in plant start-up. The test was interrupted because of the Christmas holidays. Also, short interruptions occurred because of planned or inadvertent shut-downs for maintenance. During the shut-down for the holidays, the corrosion specimens were removed from the flash tanks and stored in a dry atmosphere.

Table 1 - Schedule of Corrosion Tests in Flash Tank System

December 1977:

Segment I of Corrosion Test
36 hours of unmodified brine (pH 5.8)
196 hours of acidified brine (pH 4)

January-February 1978:

Segment II of Corrosion Test
4 hours of unmodified brine (pH 5.8)
530 hours of acidified brine (pH 4)

Acidification of the brine was accomplished by adding 1.5 N HCl as shown in Figure 1. The pH of the acidified brine was monitored hourly throughout the duration of the exposure test. Samples were drawn from four locations in the system as shown in Figure 1. The pH was determined on a Beckman Select-Mate pH Meter which was calibrated frequently against standard buffer solutions. The pH varied during the course of the run, due to a number of factors. The most important of these factors was variation in the incoming brine chemistry. Variation in the pH from the desired value of pH could be compensated by adjustment of the acid flow rate.

The corrosion penetration rate was calculated from the weight loss of the specimens. The conventional way to express corrosion rates is in mils/year (mpy). The data, shown in Table 2, were obtained from the formula:

$$mpy = 534\ w/DAt$$

where w is the weight loss in milligrams, D is the density of the alloy in grams/cm^3, A is the specimen area in in^2 and t is the exposure time in hours.

The results in Table 2 are the average obtained from three replicate specimens placed in the five locations indicated in Figure 1. Precision between the individual results was within 20%. The results indicate that the corrosion rates generally decrease as the temperature decreases. The worst case occurs in the steam phase at 150°C.

The alloy steels performed significantly better than the carbon steels at all locations. Surprisingly, the alloy containing only 0.5% molybdenum performed nearly as well as the alloys with higher chromium and molybdenum contents. The carbon, silicon, manganese and other minor constituent composition varied from one alloy steel to another so that we cannot properly ascribe

the improvement solely to the major elements. However, molybdenum additions to stainless steel are beneficial in chloride environments and under reducing conditions. On the other hand, chronium additions improve performance of steel and stainless steel in oxidizing environments. In this sense the two elements are complementary.

Although corrosion rates of 30-50 mpy for carbon steel (the pipe steel in the GLEF is ASTM A106 Grade B) are not catastrophic, plant acidification over a long period of time may require choosing other construction materials. Corrosion rates determined by linear polarization resistance (LPR) agreed generally with weight loss measurements after the LPR probes had been exposed to the brine for at least four days. The LPR probes showed much higher rates for shorter times. The chief advantage of the LPR technique is the much shorter time required to obtain information.

Table 2 - Corrosion Penetration Rates of Carbon and Alloy Steels as Determined by the Weight Loss Technique. Brine acidified to pH 4.

CORROSION PENETRATION RATES

(mils/year)

	CARBON STEELS		ALLOY STEELS				
	AISI 1009	ASTM A106B	1/2 Mo	1 Cr 1/2 Mo	2 1/4 Cr 1 Mo	5 1/2 Cr 1 Mo	9 Cr 1 Mo
2nd Stage Top Steam, 150°C	31	51	8	19	17	9	7
2nd Stage Bottom Brine, 150°C	27	38	16	17	13	11	10
3rd Stage Top Steam, 125°C	16	15	6	7	4	5	3
3rd Stage Bottom Brine, 125°C	15	15	8	8	7	6	6
4th Stage Brine, 110°C	24	16	4	5	4	4	4

Reference:

1. J. E. Harrar, R. D. McCright and A. Goldberg, Materials Evaluation for Geothermal Applications: Plant Materials. Transactions Geothermal Resources Council, May 1977, p. 129.

IMPROVED GEOTHERMAL DRILLING FLUIDS

William J. McDonald, Larry J. Remont, Clifton Carwile*

Maurer Engineering Incorporated, Houston, Texas
*Department of Energy, Washington, D.C.

Most constituents of drilling fluids start degenerating slowly at temperatures above 150°C. The rate of degeneration increases with temperature but mud properties can be maintained up to about 200°C by the replacement of degraded components. Breakdown is rapid above that temperature and there is no existing drilling fluid which retains its required rheological and filtration control properties above 250°C.

Although it is expensive, mud properties can be maintained by replacement and surface cooling as long as circulation is uninterrupted. However, shut-downs for trips, logging, completion and equipment repair operations allow borehole temperatures to rise as shown in Figure 1. The mud degrades and drilling related problems occur.

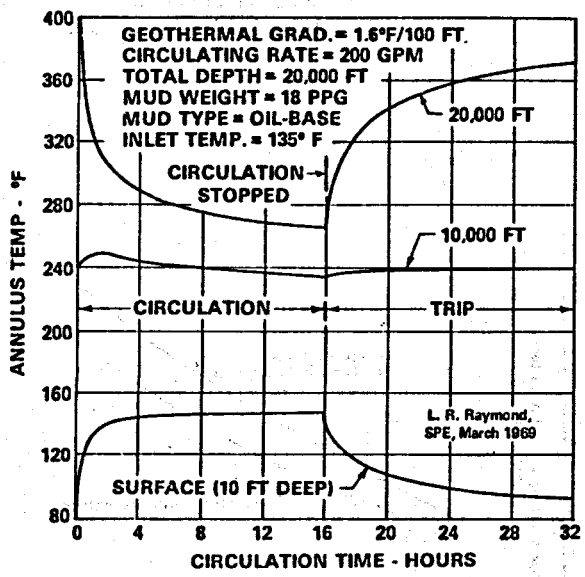


Figure 1 - Simulated Borehole Temperatures (Raymond, 1969)

Geothermal Conditions Affect Muds

Geothermal reservoirs often encounter two common trouble-some conditions: 1) high temperatures and 2) feed in of saline waters and acid gases. These conditions destroy the drilling fluid and create the basic problems shown in Table 1.

TABLE I

GEOTHERMAL DRILLING FLUID PROBLEMS

- Mud Solidification
- Lost Circulation
- Corrosion/Erosion

The consequence of these problems can be serious. Stuck pipe and twist-offs can occur or pipe replacement may be required; lost circulation can slow drilling or cause a blow-out; poor filtration control can damage potential producing formations.

The rheological problems arise because the clay colloids flocculate at high temperature giving rise to high shear strength and gel strength. A typical curve for gel strength is shown in Figure 2. Thinners such as lignosulfonates are virtually useless at temperatures above 200°C. The flocculation of the clay also makes it difficult to control filtration rates. Filtration control agents, such as carboxy methyl cellulose, also start to degrade rapidly at 150°C. The higher the proportion of solids in the mud, particularly the clay fraction, the more sensitive the mud becomes to high temperature flocculation. The presence of salts, even in small quantities, causes further sharp increases in shear and gel strengths.

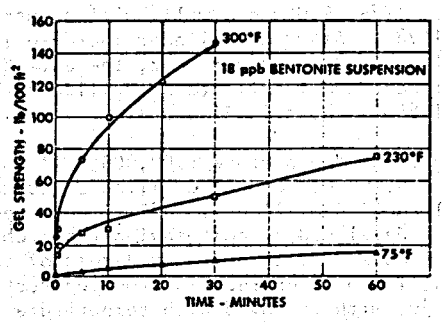


Figure 2 - Effects of Time and Temperature on Gel Strength (Raymond, 1969)

Problems become increasingly severe with mud weight. The barite itself greatly increases the solids content of the mud, making rheological control much more difficult. In order to remove drilled solids without removing the barite, expensive mud solids separation equipment such as centrifuges are necessary. Only a small fraction of the mud stream can be processed by this equipment. Watering back is also very expensive because of additions of barite required to restore the density. If the mud becomes contaminated, for example, by a salt water flow, the resulting high gel strengths, or thick filter cakes on permeable strata, may cause the drill pipe to stick, which will entail an expensive fishing job, or even loss of the well.

Oil muds are more stable, and some of them withstand temperatures up to about 250°C (475°F), but oil muds are not considered suitable for geothermal drilling because contamination of the aquifer by oil would decrease productivity. Furthermore, most operators are hesitant to use oil muds because of the possibility of environmental damage resulting from spills, separator discharges, or blowouts.

Savings Are Possible

Total drilling fluid costs are estimated to be approximately $210,000 per well. Direct costs of drilling fluid materials and fluid handling equipment accounts for approximately 10% or $70,000 of the 1976 average $700,000 cost of drilling and completing a geothermal well. Indirect costs relating to drilling mud adds an additional 20% or $140,000 per well. These indirect costs include problems such as stuck pipe, pipe failures due to corrosion, time lost due to loss of circulation, slow drilling from poor solids control, borehole stability and other problems which are the result of poor geothermal drilling fluids and poor engineering.

Fifty-six (56) geothermal wells were drilled in 1976 in the U. S. bringing the total number of wells in the U. S. to approximately 450 (Withan and Reed, 1976). In order to achieve the anticipated power level of 3,000 Megawatts (MWe) on line by 1985, 2,000 new wells will be needed (Glass, 1978). Assuming a linear increase in number of wells drilled per year, the estimated number of geothermal wells to be drilled between now and 1985 is shown in Figure 3.

Escalating the average $700,000 well cost at 7%, the estimated cost of drilling a geothermal well will be $1.2 million by 1985 without new technology developed by cost saving research. Shown in Figure 4 is the estimated cost of geothermal wells based on reducing the indirect mud costs by 50% with improved high temperature muds. At an estimated drilling rate of 500 wells/year (Figure 3) and a cost of $1.2 MM/well, the cost of drilling and completing geothermal wells will be approximately $600 MM annually by 1985.

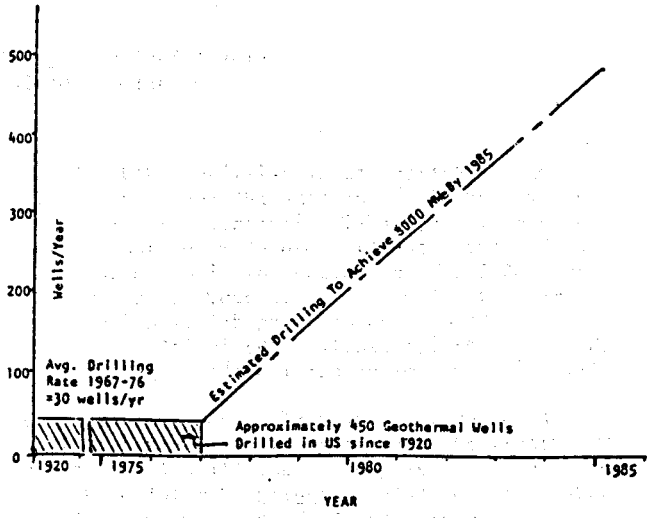


Figure 3 - Estimated Geothermal Production Drilling To Achieve 3000 MWe by 1985

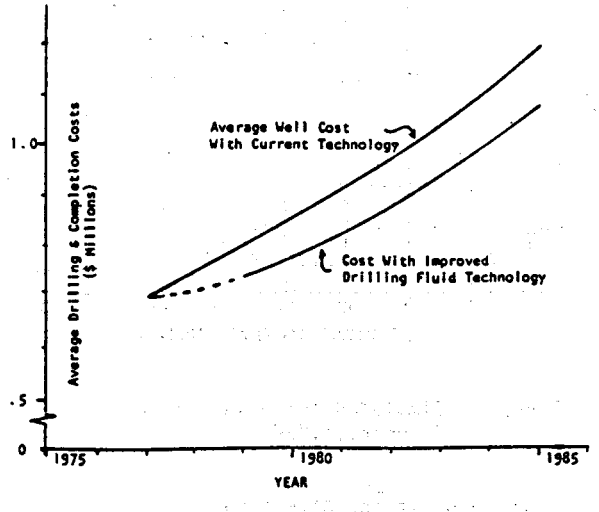


Figure 4 - Estimated Average Geothermal Well Drilling and Completion Cost

Improvements do not necessarily mean less expensive materials or equipment. Therefore, reduction in direct costs by use of better mud materials, procedures, and equipment is not anticipated; however, the improvements should not add significantly to present direct costs.

Indirect costs will be reduced as a consequence of improved geothermal muds. As indicated previously, these indirect costs presently account for an estimated 20% of the cost of drilling and completing a well. A saving of at least half of this amount should be possible with better geothermal muds and mud engineering. These improvements can be implemented over the next several years for an anticipated saving of $120,000/well by 1985.

TABLE II

ESTIMATED DRILLING ANNUAL GEOTHERMAL AND COMPLETION COSTS

	No. Wells	Present Muds $MM	Improved Muds $MM	Annual Savings $MM	Cumulative Savings $MM
'78	50	37.5	35.1	2.4	2.4
'79	75	60	55.1	4.9	7.3
'80	125	107	97.1	9.9	17.2
'81	200	183	166	17	34
'82	275	269	243	28	60
'83	350	366	330	36	96
'84	425	476	429	47	143
'85	500	600	540	60	203

Improving Geothermal Muds

A three phase approach has been taken to improving geothermal drilling fluids:

- Phase I - EVALUATION OF COMMERCIALLY AVAILABLE GEOTHERMAL MUDS
- Phase II - DEVELOPMENT OF IMPROVED GEOTHERMAL MUDS
- Phase III - APPLICATION AND UTILIZATION OF IMPROVED GEOTHERMAL DRILLING FLUID TECHNOLOGY

Phase I

The best high temperature drilling fluids that could be formulated from commercially available materials were obtained from five of the largest mud companies for evaluation (Remont et al, 1977). These included samples of 9 and 18 lb/gal water muds and 18 lb/gal oil muds. Dynamic tests were run at 175°C and static tests were run at 230°C and 260°C on all of the muds. Static tests were also run on some of the oil muds at 290°C.

Tests indicate that most of the water muds had high viscosity, high filtration rates, and poor corrosivity characteristics at temperatures above 175°C. The water muds gelled severely when exposed to elevated temperatures. Although the oil muds performed better than the water muds at high temperatures, problems were encountered with viscosity at temperatures above 230°C and with filtration control at temperatures above 260°C. As would be expected the corrosivity characteristics of the oil muds were much better than those of the water muds.

Phase II

An improved geothermal drilling fluid (HTM-1) was developed for drilling into hydrothermal reservoirs in Phase II. The mud can be prepared with conventional equipment from materials which are commercially available. Selling price of the unweighted mud, estimated at $13.00/bbl, is about the same as that of unweighted muds sold by major mud suppliers for use at high temperatures. The mud has excellent properties when prepared at room temperature and retains many of these properties even after static exposure at 260°C. Composition of mud HTM-1 is given in Table III.

TABLE III

HIGH TEMPERATURE MUD COMPOSITION

Water	1.0 bbl
Sepiolite	15 lb
Bentonite	5 lb
Brown Coal	20 lb
Sodium Polyacrylate	2-1/2 lb
Sodium Hydroxide	2 lb

Figure 5 shows a comparison of the filtrate of mud HTM-1 at 175°C - 500 psi with that of the five commercial muds tested in Phase I. Mud HTM-1 had better filtration control after being exposed to 260°C for 24 hours than any of the muds submitted by the major mud suppliers. Table IV shows the comparative cost of mud HTM-1 and the commercial muds.

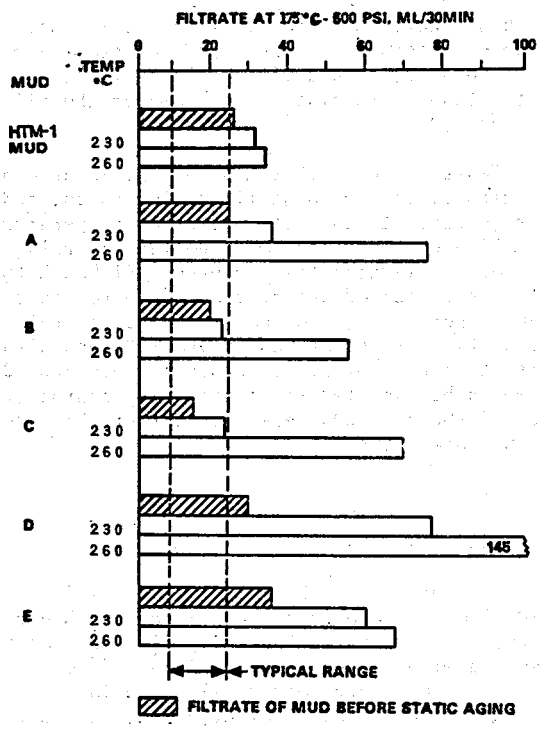


Figure 5 - Filtrate of Unweighted Water Muds Static Aged 24 Hours at the Indicated Temperatures

TABLE IV

COST OF GEOTHERMAL MUDS

Mud	Mud Type	Cost, $/bbl
HTM-1	Sepiolite/Brown Coal Sodium Polyacrylate	$13.00
A	Bentonite/CMC Mod. Lignite	12.05
B	Bentonite/Polymer Mod. Lignite	24.00
C	Bentonite/Lignite	12.61
D	Bentonite/Lignite Lignosulfonate	14.35
E	Sepiolite/Polymer	8.10

Phase III

The objective of Phase III, now in progress, is to increase application and utilization of improvements in geothermal drilling fluid technology accomplished through the support and efforts of DOE/DGE. The work is divided into six major task:

1) Coordinate Present Geothermal Mud Program
2) Develop a Comprehensive Geothermal Drilling Fluids Program
3) Critique Drilling Fluid Systems Used on Government Funded Geothermal Wells
4) Develop Generalized Drilling Fluid Well Plans
5) Technology Transfer
6) Laboratory Testing of Potential Mud Additives

Technology Transfer Meetings held in Norman, Oklahoma, and in Houston, Texas, have resulted in improved communications between DOE/DGE investigators and industry personnel. A generalized procedure for choosing the correct drilling fluid to use in a specific area has been developed. Additional laboratory tests conducted in Phase III have shown that many of the thermally stable commercial resins when added in small concentrations cause geothermal muds to solidify at high temperatures. Coal samples from various mines were the most promising materials tested. None of the coal samples tested were as effective as the brown coal evaluated in Phase II.

CONCLUSIONS

Improved geothermal drilling fluids will reduce well costs 10% and reduce the cost of power-on-line 3 to 5%. One new mud system to accomplish this has been developed and will be field tested soon. Laboratory work is continuing for further improvements. Also, a concerted effort is underway to assure application and utilization of the best available geothermal drilling fluid technology.

ACKNOWLEDGEMENT

The authors gratefully acknowledge the financial support and technical assistance of the Department of Energy, Division of Geothermal Energy and of Sandia Laboratories. Special acknowledgment is due also to many individuals who contributed ideas and suggestions and the following companies for their support and interest in the test program:

IMCO Services
Magcobar Division of Dresser Industries
Milchem, Incorporated
NL Baroid Petroleum Services
Oil Base Incorporated

REFERENCES

Fisher, P. W. & Pyle, D. E., "Corrosion-Erosion Control of Tubulars in Geothermal Drilling," API Meeting, October 25, 1977, Bakersfield, CA.

Glass, W. A., Geothermal Drilling Techniques & Problems & Forecast, Trans. IADC/CAODC Drilling Technology Conf., Houston, TX., March 6-9, 1978.

Hiller, H. K., "Rheological Measurements On Clay Suspensions and Drilling Fluids At High Temperatures and Pressures," Jour. Pet. Tech., July 1963.

Milligan, D. J., and D. J. Weintritt, "Filtration of Drilling Fluids at Temperatures Above 300°F," API Paper No. 926-6-F, 1961.

Raymond, L. J., "Temperature Distribution in a Circulating Drilling Fluid," Jour. Petr. Tech., March 1969.

Remont, L. J., W. A. Rehm, W. J. McDonald, and W. C. Maurer, "Evaluation of Commercially Available Drilling Fluids," prepared for Sandia Laboratories, 1977.

Weintritt, D. J., and R. G. Hughes, Jr., "Factors Involved in High-Temperature Drilling Fluids," Jour. Petr. Tech., June 1965.

Withan, R. and M. Ree, "Geothermal Wells in the United States," U.S.G.S. Compilation, May 1976.

THERMAL WATERS OF BULGARIA: PRESENT USE AND PROBABLE ORIGIN

Robert B. McEuen

Woodward-Clyde Consultants, San Francisco, California
San Diego State University, San Diego, California

ABSTRACT

Bulgaria is a country that is presently undergoing crustal shortening. It is also a country that has many geothermal manifestations. To date, most geothermal studies have dealt with areas undergoing crustal extension.

Moderate temperature resources may be expected in compressional areas that, like Bulgaria, have virtually no indication of recent igneous activity. For such areas, the most likely heat source is recently faulted radiogenic rocks similar to the granite so prevalent in the Balkan and Rila Mountains of Bulgaria. As compressional areas tend also to be areas of mountain building, their moderate temperature resources find ready application in space heating. In Bulgaria, present usage is primarily balneological and horticultural; however, direct heat is used to process linen, and antibiotics are being produced from algae grown in carefully monitored ponds filled with geothermal fluid.

As in other geothermal regimes, in Bulgaria there is a direct correlation between regional seismicity and geothermal resources potential. Trace element analysis of groundwater has been highly developed in Bulgaria as an exploration aid in the search for subterranean mineralized thermal waters.

INTRODUCTION

In 1976, I participated in an exchange under the terms of the Memorandum of Understanding between the Bulgarian Academy of Sciences (BAN) and the National Academy of Sciences of the U.S.A. Two extensive field trips were taken during my stay in Bulgaria. The first encompassed the high seismicity geothermal areas of southwestern Bulgaria; the second, the geothermal and petroleum provinces of northeastern Bulgaria. I have indicated on the geologic map shown in Figure 1 the approximate route traveled during these field excursions.

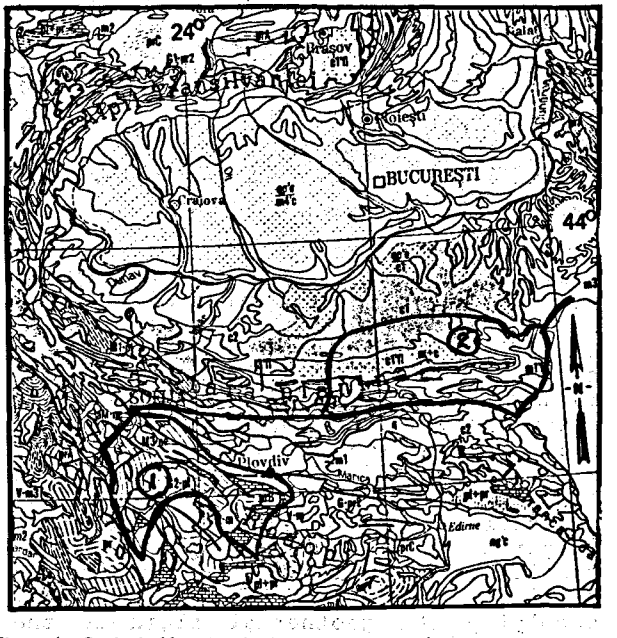


Figure 1. Geologic Map showing excursion routes (Bundesanstalt fur Bodenforschung/ UNESCO, 1971)

LOW TEMPERATURE GEOTHERMAL FLUID UTILIZATION IN BULGARIA

Thermal Waters of Southwestern Bulgaria

Most of the extensive and unusual applications of geothermal fluid in Bulgaria are to be found in western and southwestern Bulgaria. This area is identified as area 1 Figure 1.

Certainly the most unusual application in this area is the experimental antibiotic plant, which utilizes fluids obtained directly from a geothermal well to supply both the nutrients and the temperature conducive to the accelerated growth of algae. This algae is harvested and used in the production of antibiotics. This pilot plant, shown in Plate 1, is located a short distance from Sofia in one of the few areas within Bulgaria actually displaying "volcanic" rock. The small volcanic feature, at the base of which are located the wells, is characterized by an extensive travertine deposit.

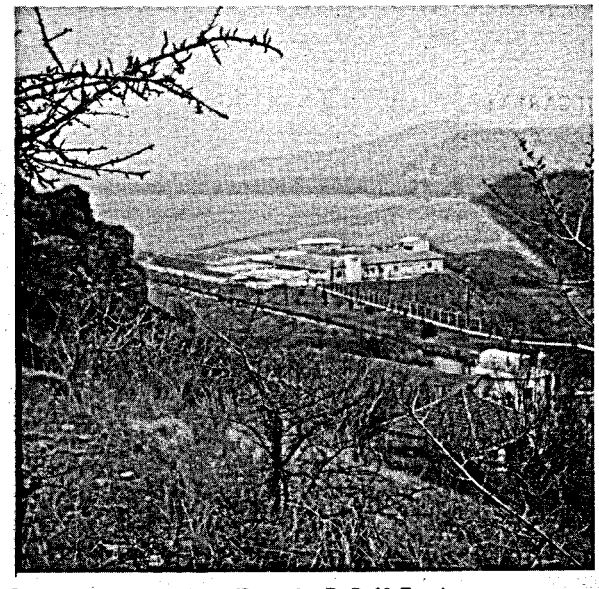


Plate 1. Antibiotic plant. (Photo by R. B. McEuen)

Further to the south in the Rhodope Mountains at the town of Velingrad, there are 7Ø mineral springs of elevated temperature. Most are used for balneological purposes; however, it is here that geothermal fluid is also used to heat a soccer field, which remains green throughout the year (Plate 2). In this same general area, geothermal waters are used in the processing of linen. Other applications for geothermal fluid in southwestern Bulgaria include extensive greenhouse facilities and trout rearing ponds (Plates 3 and 4). In Plate 3, the well supplying the geothermal fluid to the greenhouse facility is in the fenced area in the foreground. The greenhouse complex can be seen in the center left portion of the photograph.

Thermal Waters of Northeastern Bulgaria

The thermal waters of northeastern Bulgaria (area 2 of Figure 1) tend to be cooler than those found in the more mountainous areas of southwestern Bulgaria. Along the Black Sea coast, thermal water is encountered not only at the famous spas (Pomorie, Zlatni, Pyassatsi, and Drouzhba) but also when on drilling in the petroliferrous regions of the northern coast. The taking of geothermal gradient logs is a standard part of Bulgarian petroleum exploration programs. The deep geothermal aquifers encountered in this area may be fed by up-dip migration of thermal water from a thicker sequence of sediments that underlies the Black Sea.



Plate 3. Large geothermally heated greenhouse, western Bulgaria (Photo by R. B. McEuen)

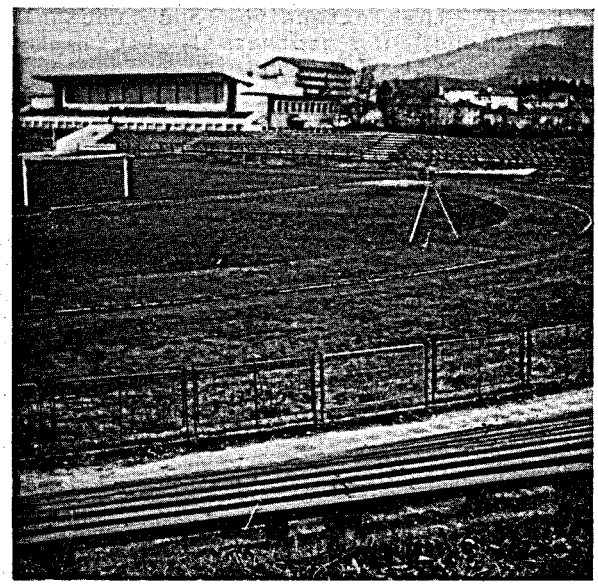


Plate 2. Geothermally heated soccer field, Velingrad, Bulgaria (Photo by R. B. McEuen)

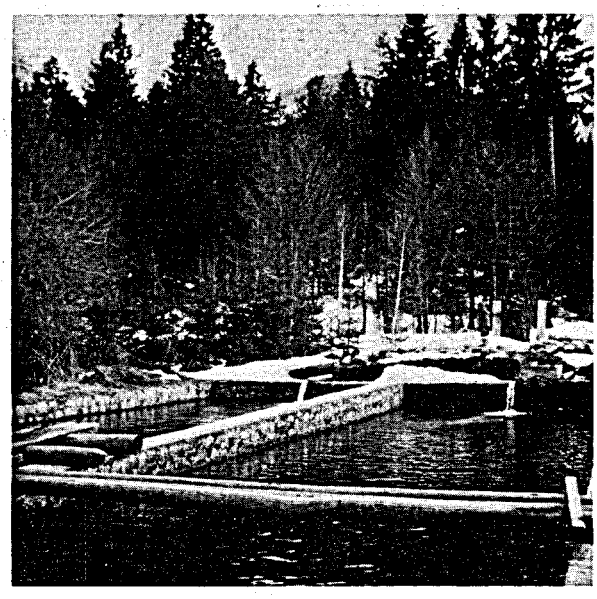


Plate 4. Geothermally heated trout rearing ponds southwestern Bulgaria (Photo by R. B. McEuen)

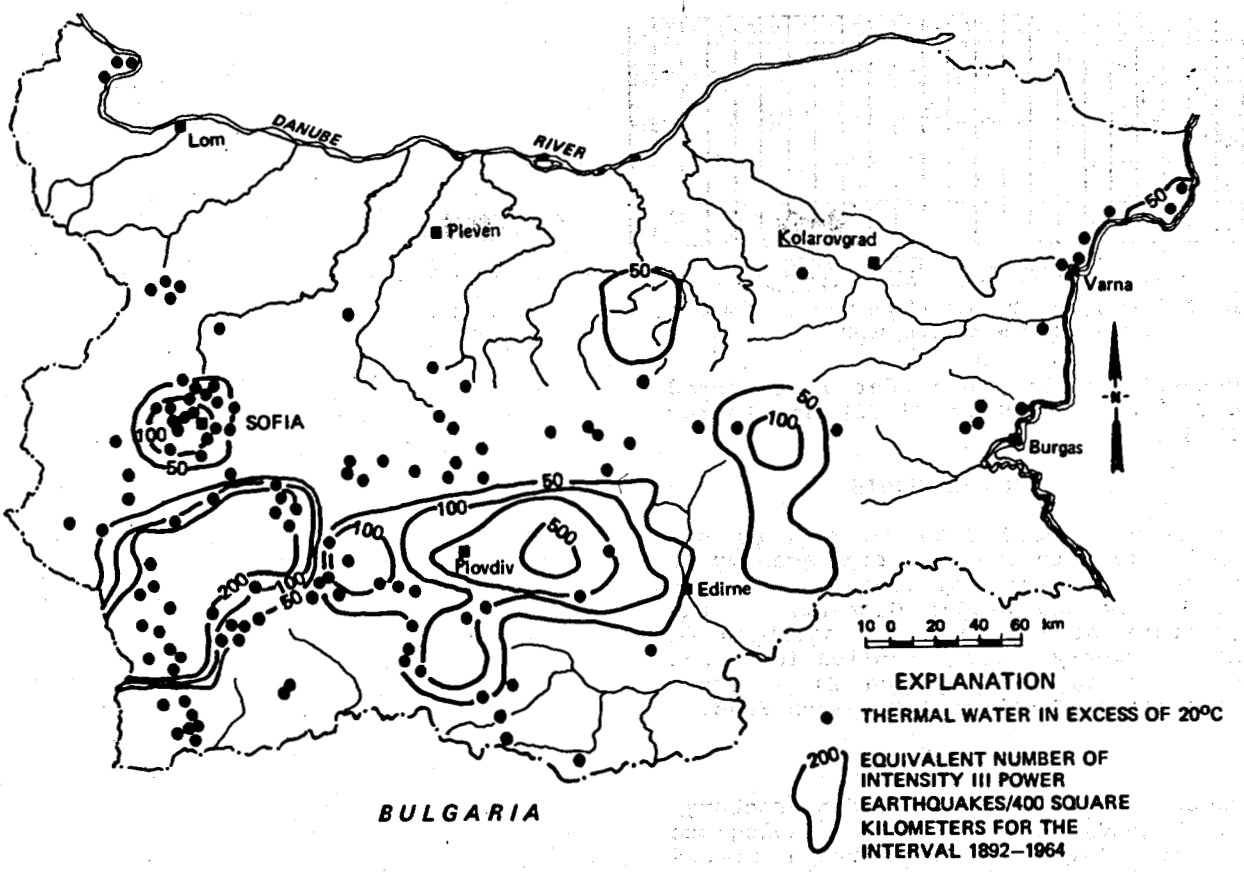


Figure 2. Spatial coincidence of thermal waters and seismicity (from Petrov, 1970 and BAN)

SPACIAL COINCIDENCE OF GEOTHERMAL MANIFESTATIONS AND EARTHQUAKES IN BULGARIA

Figure 2 shows the distribution and character of Bulgarian thermal springs, and areas of highest seismicity, as derived from the locations of historical seismic events. The circular symbol used in Figure 2 depicts the location of thermal waters having temperature in excess of 20° centigrade. The seismicity contours are in terms of equivalent number of intensity III power earthquakes/400 square kilometers for the interval 1892-1964. There is a marked correlation between the areas of hotter springs and the areas of higher seismicity.

TECTONIC SETTING

If one examines the 1-km depth temperature map (Čermák and others, 1975) for the Black Sea region, one is immediately struck by the generally high temperature values and the distinct east-west trend to the thermal anomalies. Although the tectonic picture is far from simple, these linear thermal anomalies roughly coincide with the region within which crustal shortening is occurring as a result of the junction between the Eurasian plate to the north and the African and Arabian plates to the south (McKenzie, 1972). Rates of compression along this zone approaching 3 cm per year have been estimated. Deep focus earthquakes, prevalent thrust faulting, and the sinuous nature of the Transylvanian Alps-Balkan mountain complex further attest to compressive forces in this region. These forces have brought to the surface large granitic plutons whose faulted margins provide an environment favorable for generation of low temperature geothermal fluid.

CHEMICAL VARIABILITY OF BULGARIAN THERMAL WATERS

Figure 3, taken directly from Petrov and others (1970) shows the variability of the trace element concentrations in five differing Bulgarian geothermal fluids. Fingerprinting the fluids geochemically is thought to provide an indication of the source rock in which the fluid has become heated. Such fingerprints seem to be more useful for target delineation than ionic ratio geothermometry due to problems introduced by the mixing of these typically low concentration thermal waters with groundwater. For

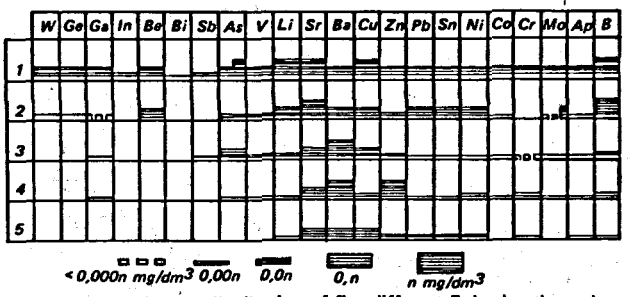


Figure 3. Trace element distribution of five different Bulgarian thermal waters (from Petrov and others, 1970)

further details the reader is directed to Petrov and others (1970) and Petrov (1963).

ACKNOWLEDGMENTS

The author would like to express his appreciation to the Bulgarian Academy of Sciences and, in particular, to Peter St. Petrov and Stojan Gasharov of the Institute of Geology. Preparation of this summary for publication was supported in part by San Diego State University's Geothermal Research Fund.

REFERENCES

Bundesanstalt fur Bodenforschung/ UNESCO, 1971, Carte Geologique Internationale de l'Europe et des Regions Riveraines de la Mediterranee, 1:5,000,000, Eastern Sheet.

Čermák, Vladimir, E.A., and Stegena, L., 1975, Geothermal mapping in Central and Eastern Europe: Proceedings of Second United Nations Symposium on the Development and Use of Geothermal Resources, v. 1, p. 47-57.

McKenzie, D., 1972, Active tectonics of the Mediterranean region: Geophysical Journal of the Royal Astronomical Society, v. 30, no. 2, p. 109-185.

Petrov, P.St., 1963, Certain criteria for mineral water prospecting: Association Internationale des Hydrogeologues Reunion de Belgrade, 1963, Belgrade.

Petrov, P.St., and others, 1970, Hydrologic studies of the mineral waters of Bulgaria: Technika, 1970, 196 p.

"GEOTHERMAL RESOURCE DEVELOPMENT AND WILDERNESS PRESERVATION IN OREGON & CALIFORNIA"

Jack McNamara

U. S. C. LAW CENTER

Don Elmer

DEPARTMENT OF ENERGY

Mr. McNamara's work performed under NSF Grant No. AER 75-09194 and D.O.E. Contract No. E-76-S-03-0113 (#29).

I. INTRODUCTION:

Preservation of "wilderness" values and the areas of the federal lands containing them began in 1924, when the Forest Service set aside part of the Gila National Forest in New Mexico in order to protect its distinctive "primitive" character. Forty years later, Congress, in the Wilderness Act of 1964, designated fifty-four units comprising some nine (9) million acres as the National Wilderness Preservation System (NWPS). All of these lands were located within National Forests, National Parks or Fish and Wildlife Refuges. Those agencies were also directed to inventory their domains for other wilderness areas and nominate same to Congress.

The Federal Land Policy and Management Act of 1976 extended this effort to the 500 million acres of public lands managed by the Bureau of Land Management. Their initial "inventory" got under way last year.

In addition, Congress itself creates additional, "instant" wilderness areas by statute. Pending legislation, e.g., would create such areas on 900,000 acres in Montana and nearly 100 million acres in Alaska.

In many areas of Oregon and California, wilderness study and evaluation has precluded even passive exploration for geothermal resources. This paper attempts to identify the precise areas of perceived conflict between geothermal development and wilderness study and evaluation and suggests a possible resolution.

II. THE FOREST SERVICE WILDERNESS PRESERVATION PROGRAM:

(a) 1964 Wilderness Act and R.A.R.E.:

This agency was the primary target of the 1964 legislation. The bulk of the existing NWPS lies within national forests. Shortly after the enactment of that statute, the Service began a "Roadless Area Review and Evaluation (R.A.R.E.)." More than eight years later, 274 wilderness study areas containing an additional 12.3 million acres were finally selected for inclusion in the NWPS. These from an initial R.A.R.E. inventory of 1449 areas totally 56 million acres.

The latter equalled almost one-third of the total National Forest areas. The Service could not satisfy the Sierra Club and other groups with even this effort, however. The "rejected" areas were therefore examined again during the Service's land use planning effort for each particular unit within its system. These planning efforts were conducted in a piecemeal fashion under existing Service policy since the early part of this century. Their planning efforts were queen Congressional sanction in the Multiple Use-Sustained Yield Act of 1960. Pressure by conservationist and environmental groups then brought about the Forest and Rangeland Renewable Resources Planning Act of 1974, which mandated such land use plans (LUP's) and the National Forest Management Act of 1976, which required extensive public participation in the planning process.

Simultaneous with this wave of legislative mandates, the Sierra Club demanded that many areas not included within the original, 56 million acre R.A.R.E. inventory be added to that list. Thus the process of wilderness review became an open-ended one, with no target appearing as a possible closing date for "final" decision.

From the standpoint of geothermal development, this was an unpalatable situation. Though a legislative compromise in the 1964 Act resulted in the inclusion of a clause allowing mining locations and mineral leases within wilderness areas until the end of 1983, that language did not, on its face, extend to geothermal resources. Thus a protracted court fight would be necessary, with exploration no doubt barred pending its outcome. In addition, areas being studied for possible wilderness status were even more strongly pro-

tected — by the statute, service regulations and court rulings, and closed to surface use altogether.

(b) R.A.R.E. II:

The situation got worse, from geothermal's point of view, when the Service initiated another full-blown, formal wilderness review in 1977 — the so-called R.A.R.E. II. Service Chief John McGuire characterized it as "an acceleration of the roadless portion of the Forest Service land management planning process." For geothermal, however, it constituted yet another legal and institutional roadblock. Adding areas identified by the Sierra Club and others, the Service came up with a new "initial inventory of 1,920 areas encompassing 65.7 million acres." These were published in the Federal Register on November 18, 1977.

(c) R.A.R.E. II Impact on California/Oregon:

Maps produced by the Service for California and Oregon showed that "wilderness study areas" practically blanketed many forests within the two states. Moreover, several of these areas to be "evaluated" were believed high in geothermal potential. A whopping 6,122,182 acres in California alone were under "review" and therefore closed to geothermal exploration, save by aircraft. Included were: over one million acres in the prized Inyo National Forest; 220,000 acres in the Lassen National Forest; 213,000 acres of the Mendocino National Forest; 200,000 acres in the Modoc National Forest; and 83,000 in the Plumas National Forest.

Oregon is the site of nearly 3 million acres of "R.A.R.E. II" inventory. Included are: 255,000 acres in the Deschutes National Forest; nearly 90,000 acres in the Fremont National Forest; 140,500 acres in the Willamette National Forest; and 203,000 acres in the highly-regarded Mount Hood National Forest.

Amidst much pressure from other federal agencies and the geothermal industry, Forest Service officials in all of the above named areas have been pushing ahead with the preparation of Environmental Impact Statements in order to allow geothermal leasing. Statements covering Inyo, Deschutes, Willamette, Fremont and Mount Hood are either out or will be some time this year. Their emergence will be a Phyrric victory, however, if the inclusion of R.A.R.E. II areas within their boundaries results in designation of all such lands as fit for "no surface occupancy" leases only. Such was the case in the EIS prepared for the geothermal lease sale in the Santa National Forest of New Mexico last year. Fully 12,000 of that areas's 30,000 acres were so restricted due to wilderness study and not a single bid was received on that acreage. Unless a parcel is situated among previously-leased private, state or other Federal land, thus allowing exploration through slant drilling, a "no surface occupancy" lease is virtually useless.

(d) What Can The Geothermal Community Do?

The Service will be making its determinations this year. A Draft EIS outlining the reasons for its choices is now being circulated. The geothermal community must inform itself and present testimony on key areas of interest in Oregon and California. The Service has stated that the "evaluation phase" of R.A.R.E. II shall give "particular emphasis" to "factors related to energy and mineral resources . . .". The mining and oil and gas industries have given strong imput to the Service, particularly in Forests located in the so-called "Overthrust Belt." The Department of Energy formally noted the negative impact of wilderness designation on domestic oil and gas production. It also mentioned coal and uranium, but not a word was heard concerning geothermal resources. In California and Oregon in particular very little non-conservationist input has been given by anyone in government or industry. Since resource assessment and exploration within study areas is not allowed, all minerals start off at a disadvantage in the Service's policy trade-offs. For geothermal resources, that disadvantage is becoming a bottomless pit.

III. BLM WILDERNESS INVENTORY:

The 1976 Land Policy and Management Act officially gave BLM wilderness inventorying and planning responsibilities for the first time. The impact of this inventory may not affect geothermal resource development as much as the Forest Service's program, however.

Though BLM controls over 470 million acres in the western states, nearly 300 million acres are in Alaska. Like the Service BLM began designating what it called "primitive areas" before being ordered to do so by Congress. Between 1969 and the enactment of the 1976 statute, eight areas totalling 170,000 acres were so classified. This is for less than the 12 million plus acres of Service land set aside for Wilderness Preservation. In part, it owes to the differing nature of the two agencies land holdings.

BLM's are much more likely to be part of a mixed land ownership pattern. When they are contained in large blocks, moreover, it is usually in semi-arid locales. Both of these characteristics should lessen the impact of any "wilderness study" tags put on potential geothermal areas. On BLM land, a "no surface occupancy" lease for study areas would therefore probably allow resource assessment to take place from contiguous parcels.

IV. CONGRESSIONAL "INSTANT WILDERNESS" LEGISLATION:

The two most notable recent developments in this arena are the 900,000 acre Absaroka-Beartooth proposal in Montana and the so-called "D-2" Alaskan lands legislation (HR. 39 (Udall)). The first has already been enacted. The second is the subject of much controversy. The sheer size of the wilderness withdrawal (over 100 million acres) gives pause, particularly when almost no resource assessment has yet taken place and rich oil and gas finds are located nearby. A pending amendment would allow deep hole and passive mineral exploration for a few years, with final wilderness designation postponed until that time. The geothermal industry should support this amendment. Unfortunately, the original Wilderness Act had an even stronger assessment requirement, directing the Forest Service, Park Service and Fish & Wildlife Service to enlist Bureau of Mines and the U.S. Geological Survey to identify "mineral resource values" on "a planned, recurring basis." To the author's knowledge such assessment, if it took place at all, was minimal.

"THE REGULATORY PROCESS CONFRONTING GEOTHERMAL DEVELOPMENT IN CALIFORNIA: CAN WE BURN THE PAPER MOUNTAIN?"

Jack McNamara

JM ENERGY CONSULTANTS, INC.

I. Introduction:

Geothermal developers have long complained of the seemingly needless red tape that they must undergo in California. Mary Jadiker of the Lake County Energy Council dubbed the sum of these requirements the "Paper Mountain". This paper examines California's regulatory requirements and proposed reforms recently suggested by the State Geothermal Resources Task Force and the State Energy Commission.

II. Present Regulatory Requirements and Proposed Reforms:

(A) WELL DRILLING REGULATION:

(1) "Conditional Use Permits": All of the promising geothermal areas in California lie within counties which have not yet adopted any pervasive planning or zoning guidelines for geothermal development. These entities, which are very powerful throughout California, require application for a "conditional use permit" for each individual well. Though a shopping center or housing tract developer faces the same requirement, the county officials involved are more familiar with the impacts of such projects. Their knowledge of natural resource operations is, by contrast, quite limited and the final outcome of any geothermal exploration project is not forseeable at the time of application. These projects, moreover, tend to cluster in traditionally unpopulated areas, where staff and budget support to respond to them are usually lacking.

The State Task Force recommended that the state fund geothermal planning efforts in the counties containing the most promising areas. The author thinks that any such legislation should set a one-year time limit on these efforts, rather than the nonbinding two year limit presently under consideration.

(2) Environmental Reporting Requirements: Each well permit application requires either an Environmental Impact Report (EIR) or a "negative declaration" (that no EIR is necessary). In many instances, the EIR, which is usually prepared by an outside consultant due to inadequate county staffs, attempts to analyze the impacts that will occur if the proposed exploratory well(s) discover a commercial resource and power plants are then constructed. Nondevelopment forces argue that such an effort is necessary. Developers characterize it as an exercise in speculation and a waste of time and money, since most explored areas are eventually dropped. In Lake County Energy Council v. County of Lake, the California District Court of Appeals has adopted the developer view.

The aforementioned county planning proposal would allow creation of a master land use blueprint and the use of "limited scope" EIR's thereafter. Both the State Task Force and the Federal Council on Environmental Quality have also proposed the joint preparation of impact statements by federal, state and local agencies. USGS and Imperial County have done just that for Magma's pilot plant at East Mesa and similar joint efforts are contemplated by the State Energy Commission, The Geysers counties, and the Federal Bureau of Land Management.

(3) State Drilling Permit: The State Division of Oil and Gas (D.O.G.) issues a drilling permit for all wells on private and state land and does so rather expenditiously. D.O.G. also designates "geothermal resources areas", an act which at present has no significance under CEQA.

The State Task Force recommended that these latter designations be accompanied by a full-field EIR and that CEQA be amended to allow exemption of further wells drilled therein from environmental reporting requirements. This suggestion has been translated into pending legislation but with significant differences from the original Task Force proposal. In some form, whether it involve D.O.G. or the Energy Commission (via pre-screening of potential plant sites), the State should speed up its environmental analysis of potential geothermal areas. This would at once spur county planning activity and, on occasion, supplant it.

(4) Air Quality Regulation: Local Air Pollution Control Districts (A.P.C.D.'s) require two permits prior to well drilling — an "authority to construct" and a "permit to operate". Since wells account for roughly 10% of H_2S emissions, these permits are rather quickly acquired.

(5) Sump Regulation: No less than five state agencies are involved in the regulation of drilling sumps or mudpits. The Division of Oil and Gas and Department of Fish and Game rely on the "waste discharge permit" issued by the relevant Regional Water Quality Control Board (R.W.Q.C.B.). Unfortunately, the counties administer the requirements of the State Solid Waste Management Board (SSWMB) and the State Department of Health (D.O.H.).

The Task Force recommended that both Solid Waste and Health exempt geothermal wells from their requirements and the former has done so. Legislation is necessary, however, to remove county enforcement of those state requirements. The Technical Advisory Committee (T.A.C.) of the State Geothermal Resources Board has drafted suggested statutory language, and it should be enacted.

(6) Energy Commission Well Permit Authority: The Commission considered exercising siting authority over geothermal wells.

The Task Force recommended that this be left to the counties and a recent Opinion of the State Attorney General held that the Commission lacked jurisdiction in this area. Commissioners Reed and Pasternak and the Commission's geothermal staff have also recommended against Commission well permitting as a policy matter.

(B) POWER-PLANT SITING:

(1) Background: The Warren-Alquist Act gave the State Energy Commission rather broad jurisdiction over power plant siting. It also contained several procedural advantages for geothermal plants over other facilities.

(2) Energy Commission Policy: Until the end of 1977, however, the Commission had done nothing to translate this legislative preference for geothermal into preferential regulatory action. The Task Force rejected the idea of delegating siting authority back to the counties and the P.U.C. however, and instead, recommended that the Commission shorten its geothermal siting process to nine months (half the statutory duration) for geothermal. Commission Staff then prepared an option paper recommending a 12 month process, and Commissioners Reed and Pasternak (the Commission's Geothermal Policy Committee) did likewise. Actual regulations were recently adopted, embodying a 12-month process, though there is a longer pre-screening process available at the option of the applicant.

(3) Local Power Plant Regulation: In response to a 1971 State Supreme Court decision (Orange Co. A.P.C.D. v. P.U.C.), the legislature enacted the Warren-Alquist Act, which gives the Energy Commission broad jurisdiction and pre-emptive powers over other state, local and regional agencies. The statute was a compromise, however. The Commission must make specific findings if its siting decision differs from e.g., an A.P.C.D.. These are, of course challengable in court. Given the heated controversy over H_2S in The Geysers, it is likely that such a challenge will be mounted to Commission approval of any plant in Lake County. In the alternative, the Commission might acquiesce in A.P.C.D. or other local agency refusal to permit certain plants at The Geysers. To avoid this slowdown, air quality data in the area must be sharply upgraded. Either G.R.I.P.S. or the Commission must be funded by D.O.E. and the state to obtain this information as quickly as possible.

(C) COORDINATION:

The actions of many federal, state and local agencies and their contractors have often worked at cross-purposes in California. To prevent a recurrence, the State Task Force recommended that a beefed up Geothermal Resources Board (adding the Commission and three public members) coordinate, monitor and mediate the myriad of geothermal-impacting activities. The Board's Technical Advisory Committee has set up a working liason with the relevant federal agencies and also serves as a forum to resolve difficulties among state and local entities. In addition, Board Chairperson Priscilla Grew and Energy Commissioner C. Suzanne Reed meet jointly with top federal officials in order to "steer" their activities into the most productive channels from the state perspective.

Geothermal Resources Council, TRANSACTIONS, Vol. 2 July 1978

METHODOLOGY OF SOCIOECONOMIC IMPACT ASSESSMENTS OF GEOTHERMAL ENERGY DEVELOPMENT

Mae Z. Meidav

Kendall Associates
San Francisco, California

Introduction

Socioeconomic impact assessment is a new field of investigation covering several traditional fields of sociology, economics, and political science. The goal of these assessment studies is to evaluate and predict the effects of the large-scale public or private development programs. Such studies, as mandated by the National Environmental Protection Act, (NEPA) have been required in the filing of State and federal environmental impact reports to assess both the positive and negative effects of a program, and to identify sensitive areas of impact on population, on economics, and on the quality of life.

The concern with the "environment" has become a key preoccupation: research, and legislation are focused on the ecosystem and problems resulting from technological advancement. General social concern with the environment has become a factor in social policy and the resulting legislation. Socioeconomic impact assessment is related to questions of resource conservation, resource development, environmental preservation or alteration, social progress, and distribution of benefits. It is thus a very direct application of diverse methodologies converging from several fields but now required for an integrated assessment. Currently, social assessment and prediction excercise is being used in such areas as: highway planning; community development; water resource development; nuclear, hydro and thermal power plant siting; drill siting; and for other new land uses.

Conditions of Appropriate Response To Proposed Projects

Recent government directives, legislative acts, and analytical reports list of a number of desirable impacts of new projects. These can be identified as:

1. Efficiency, or growth, in material development, maintaining a solid base of economic sufficiency, as a result of the project;
2. Causation of equitable distribution of resources, and economic opportunity for different segments of the population.
3. Contribution to the achievement of certain larger social goals.

In general, the problems of assessment are similar to classical analytical inquiry coupled with public policy formulations. The following are required in both:

1. An adequate description of ambient conditions.
2. Proper analysis of all possible impacts.
3. Presentation of all reasonable alternatives for the proposed action.

But problems arise when an attempt is made to compare essentially non-comparable entities such as:

1. The cost of the project.
2. The social desirability of the proposed project.
3. Impacts in areas of overlapping jurisdiction.
4. Impacts over different segments of time.

Procedures

One early model of socioeconomic procedures was formulated for the U.S.Army based upon an interpretation of NEPA (Vlachos, 1975). These were:

1. Definition of the problem or the proposed project.
2. Identification of communities impacted by any given project.
3. Profiling of communities in terms of baseline social and economic data.
4. Projection of possible impacts over selected time period.
5. Projection of a community model without the project over the same period.
6. Assessment of net community changes due to the project with comparison of alternative versions of the project.
7. Evaluation of various impacts in terms of benefits and liabilities for different communities, groups, sectors, and interests.

Another set of procedures was formulated for the U. S. Bureau of Reclamation (Fitzsimmons et al, 1975). These were based on the evaluation of five categories of social and economic effects:

1. Social effects at the individual and family level.
2. Social factors as perceived by of groups and communities.
3. Area socioeconomic effects.
4. Contributions to regional viability.
5. Relationship to the national good, and national preparedness for emergency.

Other procedural models are generated by various government agencies through RFP's on socioeconomic impact assessments. These projects provide direct

g. Model construction and analysis.

2. Selection of impacts for analysis on the basis of determination of:

   a. Extent (number of people affected).

   b. Intensity (seriousness or extent of impact).

   c. Duration.

   d. Irreversibility.

   e. Magnitude and severity.

   f. Political sensitivity.

3. Measurement of impacts by means of:

   a. Surveys (including small sample surveys).

   b. Informant interviews.

   c. Ethnographic studies.

   d. Census and other data banks.

   e. Documents and other records.

Socioeconomic Impacts Of Geothermal Energy Development

Impacts which are likely to be perceived as having the greatest positive consequences include:

1. Decreasing rate of depletion of oil and gas, because of substitution by geothermal energy.

2. Reduction in the amount of imported energy.

3. Development of industries that use geothermal electricity, heat, or minerals in geothermal regions.

4. Increase in government income.

5. Reduction of inflation rate due to lower energy cost.

6. Improvement in GNP.

Impacts which are likely to be perceived as having greatest negative consequences, in decreasing rank order, were ranked as follows:

1. Increased possibility of seismicity and land subsidence due to geothermal fluid extraction.

2. Increased noise level, especially during drilling and development.

3. Diminished water and air quality near geothermal installations.

4. Relocation of local population in order to accommodate geothermal installations.

5. Use of recreation, park, and wilderness areas for geothermal installations.

6. Use of agricultural and forest lands for development of geothermal installations.

Socio-Political Realities

Socio-political considerations are a reality that confronts any evaluator of socioeconomic impact assessments, regardless of the nature of the individual project. Socio-political forces which enable an individual or group to influence or be influenced by others, take on added importance because of the ultimate effects of these projects. Moreover, when a technology assessment team is required to judge concensus and public response it may pre-empt the role of elected representatives.

The evaluation of projects necessitates studying the diverse commitments the various publics have vis-a-vis the project and the impacted area. There are likely to be differential, if not conflicting interests on the part of multiple publics in relationship to these projects. Thus, methods of impact assessment that encompass this diversity have to be utilized.

The impossibility of separating facts from values in decision making is well known. It is independent of the type of methods used. Thus, the role of the evaluator must be known, since it is of vital importance for the results. Account need be taken of the evaluator's biases and interests in the policy addressed. Questions must be answered such as:

1. Is the evaluator an advocate of, protagonist for, or a neutral party to the impact assessment?

2. Is the evaluator a member of an "in house" or "outside" team?

3. How is the role of the evaluator perceived by:

   The various agencies involved?

   The various publics, and by the evaluator himself?

4. What circumstances; e.g. size of project and type of project, play a part in shaping the role of the evaluator? (see Vlachos, 1975:10)

Only relatively few of the operating variables can be identified. Moreover, they cannot be controlled throughout the forecast period. The complexity and dynamic nature of the systems which constitute the subject matter of socioeconomic studies at times totally obliterate the most carefully designed and executed study.

Conclusions

The systems which constitute the subject matter of socioeconomic impact assessments are complex, dynamic and interactive. Not only do they engulf feedback loops within their own dimensions, they also interact with the very technological change to which they are responding. The systems effect a degree of control and regulation over the technological innovation, generating an iterative loop with a counter-intuitive outcome.

There is insufficient knowledge for predicting the interaction of complex variables in the eco-system, or for predicting future, ecological consequences of many present-day developments and implementation of plans. The required environmental impact statements for proposed developments may not address the specific issues which could politicize an interest group or entire sector, because it may not reflect the crux of a given environmental problem, particular to the selected strategy and locale.

In general, environmental decision makers and planners operate in a world of variable uncertainty. They deal with problems which frequently seem of immediate importance (e.g., air pollution, health hazards) but face an unpredictable public. These projects have reasonably predictable effects, and involve direct costs reflected in estimates which are only accurate if

input into policy planning. Methodology in the RFP's is well defined with contract funds usually an order of magnitude higher than those allocated to that portion in EIR's and EIS's.

Sources of Data

Socioeconomic impact assessment studies rely upon data gathered from both primary and secondary sources. Primary data are drawn from field studies based on a research design specific to the problem area, community studies, various techniques of survey research. The secondary data is drawn from the voluminous data banks compiled by government agencies and private organizations. These sources require appropriate computer data retrieval programs and knowledge of the accessibility process.

Types of data sets which are compiled in an assessment study can be grouped according to the following categories:

1. Basic demographic characteristics, including population size, density, and distribution; growth trends, births, deaths, migration, marriages, divorces, infant mortality
2. Descriptive social characteristics of a population, including age, sex, race, nativity, ethnicity, occupation, education, income.
3. Employment data and economic indicators, including distribution across primary, secondary and tertiary sectors of the economy.
4. Housing data, including number of units, average value, rents, age, distribution, condition, vacancy rate.
5. Agricultural, industrial and commercial data.
6. Land use data, including incorporated and unincorporated areas, special districts, protective services, utilities, percentage land under cultivation, in residential development, and in industrial development.
7. School district data.
8. Social services data, including churches, health services, parks and recreational facilities.

Methodological Approaches

A wide range of methodological approaches is available. Given sufficient time and support, one can carry out a well-designed investigation utilizing techniques of scientific inquiry which focus ultimately on public policy issues. These projects, for the most part, are usually managed under less-than-ideal circumstances for scientific inquiry: tight deadlines, limited budgets, progress reports, and interim technical reports, are all part of the constraints in carrying out such projects. We can, however, identify basic features of the assessment studies: investigative design, identification of impacts, prediction, evaluation of options, and recommendations.

Methodological approaches include among others the following frameworks:

1. Community impact assessment framework, which is a process of assessing the effects and impacts of proposed interventions at the neighborhood scale, in contrast to a planning bias that gives precedence to larger community interests.
2. Quality of life and social indicators framework, in which factors are categorized under demography, economy, social structure, public services and social well-being and collective responses are identified
3. General systems framework, which requires an understanding of the inputs and ouputs of community socioeconomic systems for both the baseline condition and the likely change in the community, should the development occur.
4. Inductive modeling or grounded theory construction, based on a systematic review of a broad range of previous studies in order to generate a set of theoretical concepts and empirical generalizations.
5. Cost-benefit analysis which assesses project impacts in monetary terms as the aggregated value to each member of the nation, region or community.
6. Regionally based cost-benefit analysis which identifies more precisely who benefits from, and who pays for the cost of development.
7. Macro-level and micro-level of analyses with broad indicators of economic, social and environmental conditions.

Other methodological approaches include ethnographic field studies, survey research, individual well-being framework, and a social-psychological framework. Much of the current work in socioeconomic impact assessment is eclectic. Moreover, it has not been a critical issue whether a particular framework is identified, although implicit assumptions related to selected paradigms determine the results of the studies.

Investigative design components of socioeconomic impact studies are outlined as follows (Finsterbusch, 1977):

1. Selection of evaluation criteria.
2. Conceptual framework.
3. Measures for variables.
4. Sources of data; and means of obtaining them.
5. Information sought.
6. Analytical techniques to be employed.
7. Organization and selection of research team.

Investigative operational components for identification, selection and measurement of impacts are categorized as follows (Finsterbusch, 1977):

1. Identification of impacts by means of:
   a. Relevance Tree (scanning device for impact across broad areas).
   b. Literature survey.
   c. Delphi interviewing.
   d. Iterative interviewing.
   e. Contextual analysis.
   f. Contigency trees: systematic mapping of higher order impacts.

the project is completed on time with a minimum of delay. A project which makes eminently good technical sense could generate determined, fiercely emotional opposition. Most serious of all, opposition may surface at times during the life cycle of a project which are unpredictable. In practice, government and private decision makers and environment planners must estimate not only the environmental impact of a proposed project (physical, biotic, social, economic, legal) but the impact anticipated by others, and their reaction to that anticipation. Frustrating though this may be, the situation is worsened by the fact that this anticipation is usually based upon partial or distorted information. It is to the latter deficiency that socioeconomic impact assessments are addressed.

ACKNOWLEDGEMENTS

I wish to thank Tsvi Meidav for his constructive critique of this paper.

REFERENCES

Finsterbusch, Kurt. "The Potential Role of Social Impact Assessments in Instituting Public Policies," in Kurt Finsterbusch and C. P. Wolf, eds., Methodology of Social Impact Assessment. Stroudsburg, Pa.: Dowden, Hutchinson & Ross, Inc., 1977, pp. 2-12.

Finsterbusch, Kurt, and C. P. Wolf, eds., Methodology of Social Impact Assessment. Stroudsburg, Pa.: Dowden, Hutchinson & Ross, Inc., 1977

Fitzsimmons, Stephen J., Lorrie I. Stuart and Peter C. Wolff. A Guide to the Preparation of the Social Well Being Account Social Assessment Manual. Bureau of Reclamation, U.S. Department of the Interior, Contract No. 14-06-D-7342(5), July 1975.

Futures Group, A Technology Assessment of Geothermal Energy Resource Development. prepared for National Science Foundation, Contract C-836, April 1975.

Geonomics, Inc. Socioeconomic Impact Assessment of Geothermal Energy Development in the Imperial Valley, California. Electric Power Research Institute, Palo Alto, March 1976.

Geonomics, Inc. Socioeconomic Impact Assessment of Geothermal Energy Development on the Island of San Miguel, Azores, Portugal. Institute of Geoscience, San Miguel, April 1977.

Geonomics, Inc. Direct Heat Applications in the Geysers/Clear Lake Region: Geotechnical, Environmental, Socioeconomic, and Engineering Assessments and Agribusiness Applications, ERDA, August 1977.

United States Department of the Interior, Bureau of Reclamation, Amarillo, Texas, Request for Proposal, NO 50-V0958, Seward Feasibility Investigation, 1977.

United States Environmental Protection Agency, Cincinnati, Ohio, Request for Proposal No. CI 77-0175 Development of an approach for estimating and ranking socioeconomic effects of alternative water quality management strategies, 1977.

United State Nuclear Regulatory Commission, Request for Proposal No. RS-RES-78-192, Entitled "Post Licensing Studies of the Socioeconomic Impacts of Nuclear Power Station Siting", April 1978.

Vlachos, Evan et al, Social Impact Assessment: An Overview. U. S. Army Engineer Institute for Water Resources. IWR Paper 75-P7, December 1975.

Wolf, C. P. "Social Impact Assessment: The State of the Art," in Daniel H. Carson, ed., Man-Environment Interactions, Part I. Stroudsburg, Pa.: Dowden, Hutchinson & Ross, Inc., 1974 pp. 1-44.

Geothermal Resources Council, TRANSACTIONS, Vol. 2 July 1978

GEOTHERMAL ENERGY DIRECT APPLICATIONS MARKET-ESTIMATOR MODEL

S. W. Metzger

Idaho National Engineering Laboratory
Idaho Falls, Idaho 83401

DETAILED SUMMARY

Model Introduction

The subject model, which can best be described as a marketing economics tool, was conceived on the premise that a "quick and dirty" estimation technique often provides an acceptable degree of perception into the basic character of a market. This rather superficial calibration of a market could be considered in lieu of the data a more expensive, in-depth investigation would produce. The value of this market-estimator model will be dependent, however, upon the resources available to the researcher. Moreover, the model's value will be contingent upon the desired quality of data upon which a decision, either preliminary or final, will be based. The model is ideal for those situations which depict limited study resources and permit "order-of-magnitude" assessments. It is hypothesized by the author that most market decisions within, or without the geothermal community, are formulated with less than complete and accurate data which are obtained through less than optimum resource means.

Model Description and Use

The model is designed to accommodate data which have been reduced to specific direct applications of geothermal energy at specific sites. Through the use of weighted averages, however (and this will be discussed later), multiple-site application data can be transformed to fit the model input requirements.

The model is comprised of ten variables, each of which is characterized by a range of values, or class limits, corresponding to assigned factors. As the model employs a simplified "expected value" mathematical approach, the factors are treated in a multiplicative manner. Selecting for each of the model's ten variables that most optimum class-limit constraint (reflecting the theoretical maximum factor for that particular variable), and multiplying the respective factors covering the ten variables together, one would obtain a theoretical maximum of 15.4. On the other hand, if one selected a rather dismal geothermal energy scenario, and extrapolated as appropriate outside the class limits, selecting only non-zero values, the result would closely approach zero.

To use the model, an analyst would multiply the amount of energy "direct applications" would consume by the factor selected for each of the ten variables. Naturally, the given variables can be applied with greater ease where the area is small and the scenario is rather well defined. The multiplication of the ten selected variables by a given energy consumption, as described above, will yield a result that could vary from a fraction of one percent of the given energy amount, up to, as previously discussed, 15.4 times that energy amount. The degree of geothermal energy direct applications (GEDA) favorableness is directly proportional to the magnitude of the numerical result. A value relative to unity (i.e., the same value as the original energy consumption) could be interpreted as the feasible techno-economic market share that GEDA could enjoy. Consequently, any value greater than unity could indicate that geothermal energy could economically support all the feasible direct applications associated with a particular site and its market area. It should be noted that a composite factor greater than 1.0 does not imply that more energy is required relative to the original energy consumption amount. A result in excess of 1.0 would indicate the relative degree of confidence that GEDA can theoretically penetrate the energy application(s) being evaluated. As the result approaches 15.4, the confidence level indicating geothermal energy viability increases proportionately.

It would be a rare opportunity indeed that was evaluated by the model at several factors above unity. For example, to attain an extremely positive GEDA evaluation - one approaching the theoretical maximum value of 15.4 - one must encounter such anomalies as high-enthalpy resources at very shallow depths (a condition contrary to geothermal gradient expectations), very low salinity (a condition contrary to high-temperature resource characteristics), and extremely high alternate energy costs (substantially higher than the $3.00/mm Btu level).

If one were attempting to assess the GEDA potential for an area as large and diverse as a state, the data would have to be disaggregated, basically on a KGRA breakdown basis. Although the procedure is more rigorous than would be the case for a specific site assessment, the required energy consumption and energy cost information can usually be obtained for any geographical area in question.

Using these data in conjunction with geothermal resource data, weighted averages would be calculated for each geothermal application scheme. This would transform the data into a manageable format, which would then be compatible with the model's input requirements.

Upon experimenting with the model, one would soon detect the high degree of sensitivity built into the more critical variables - such as the one assessing the distance from production wells to the end-use location. Principles of economy of scale versus marginal utility come into play and effect definite trade-offs among the variables. It is the essence of these trade-offs which the model has attempted to capture in a representative mix of GEDA scenarios. The model can, in fact, be easily utilized to perform sensitivity analyses by simply modifying the input value for any one variable while controlling the remaining variables.

While the model's structure is most easily adapted to assess the potential of a specific GEDA candidate site, it is possible to evaluate the potential of different market segments. Where the GEDA potential (in terms of the actual or predicted energy consumption) cannot be readily obtained for a market, the following weights are suggested:

Market Sector	Direct Applications Weight
Agricultural	.30
Commercial	.60
Industrial	.20
Residential	.80

To arrive at a solution using these weights, the total (i.e., including electric applications) actual or predicted energy consumption for each market sector is reduced to GEDA potential by applying the weights respectively. Following this step, the model manipulation procedures are the same as previously discussed. The transportation application, a significant non-electric energy consumer, has been disregarded for GEDA purposes.

Model Limitations

Obviously, the most serious limitation of a modeling technique as general as this is the difficulty of using the model to "fine tune" the model input and output to accommodate a very complex evaluation. Such a model constitutes only a first approximation of a GEDA market. The numerical result is more an indication of economic viability than an absolute quantitative evaluation. Therefore, in terms of the categorical "generality" limitation, other limitations are implicitly associated with the model. For example, such important considerations as detailed resource characterization, well-casing design, pipe friction losses, pumping load, wellhead pressures, injection pressures, amortization costs and periods, dry holes, scaling and corrosion propensity, are not specifically addressed in the model. However, the model's variable constraint limits were selected with many of the foregoing kinds of economic limits under consideration. Also not reflected in the model are intangibles like legal, social, and institutional forces. Even if a researcher had unlimited resources, this kind of influence is difficult, if not impossible, to quantify. If an analyst desired such detail in a model, then he would have to forego the simplicity offered by the subject model and resort to one of the more complex models familiar to the geothermal community. At the other extreme, if the analyst enjoys the benefits of relatively complete data, the likelihood of his needing any model for other than a data-handling purpose is small indeed.

Certain economic credits associated with geothermal energy-cascading applications have not been specifically addressed. However, many of these applications are generally reflected in the class limits selected for the model's alternate-energy cost variable. In this same vein, it is very difficult to evaluate the non-thermal or consumptive benefits of fluid applications like irrigation, soil warming, and fish farming.

Insofar as interpretation of the model's results is concerned, given a theoretical maximum result of 15.4, it would be hazardous to infer that geothermal energy is actually superior to an alternate energy form by a factor of 15.4. In this same connection, as a result of the normative economic conditions upon which the model's variable-constraint class limits were based, it is quite possible that the actual data for a particular site in question could perturb the model values in such a way that the net output is grossly impaired. If this becomes the case, it would be a simple matter to custom-tailor the constraint values to arrive at a more realistic result.

GEOTHERMAL ENERGY DIRECT APPLICATIONS

Model Independent Variables

1. Number of production wells
2. Weighted average distance from resource to fluid end-use point
3. Weighted average production-well depth
4. Weighted average production-well life
5. Spent-fluid discharge method
6. Weighted average fluid quality
7. Total production fluid flow
8. Environmental criticality index
9. Geothermal power plant option (if applicable)
10. Weighted average alternate energy cost

Independent Variable Constraints with Estimator Factors

	Variable	Constraint				Factor*
1.	Number of Wells				1	1.25
		>	1	≤	3	1.00
		>	3	≤	5	0.80
		>	5	≤	10	0.40
				>	10	0.10
2.	Distance (mi)	≥	0	<	0.5	1.25
		>	0.5	≤	1	1.00
		>	1	≤	2	0.75
		>	2	≤	5	0.20
				>	5	0.05
3.	Well Depth (ft)			≤	1,000	1.50
		>	1,000	≤	2,000	1.00
		>	2,000	≤	4,000	0.80
		>	4,000	≤	10,000	0.55
				>	10,000	0.25
4.	Well Life (yr)			≤	3	0.15
		>	3	≤	5	0.50
		>	5	≤	12	0.75
		>	12	≤	20	1.00
				>	20	1.25
5.	Spent Fluid Discharge					
	Injection					0.70
	Other					1.25

	Variable	Constraint			Factor*
6.	Fluid Quality ($\frac{TDS}{ppm}$)		≤	500	1.25
		> 500	≤	1,000	1.00
		> 1,000	≤	2,000	0.80
		> 2,000	≤	4,000	0.70
		> 4,000	≤	10,000	0.50
		> 10,000	≤	20,000	0.25
			>	20,000	0.15
7.	Production Flow (lb/hr)		≤	25,000	0.10
		> 25,000	≤	100,000	0.25
		> 100,000	≤	400,000	0.70
		> 400,000	≤	1,000,000	1.00
			>	1,000,000	1.25
8.	Environmental Index			Uncritical	1.00
				Moderately critical	0.75
				Very critical	0.50
9.	Geothermal Power			Inapplicable	1.00
				Applicable	1.50
10.	Alternate Energy Cost ($/mm Btu)		≤	0.50	0.05
		> 0.50	≤	1.00	0.50
		> 1.00	≤	2.00	1.00
		> 2.00	≤	3.00	1.20
		> 3.00	≤	5.00	1.40
		> 5.00	≤	7.00	1.60
			>	7.00	1.80

*Where required, simple linear interpolation is used between class limits; extrapolation outside class limits can be handled in much the same manner.

MODEL USE EXAMPLE

Scenario: Town A wishes to investigate the economic prospects of a district heating system that would be capable of carrying an annual load of 50 billion Btu.

	Variable	Input	Factor*
1.	Number of production wells	4	0.90
2.	Weighted average distance from resource to fluid end-use point (mi)		
	2 wells @ 0.5 = 1.0		
	1 well @ 1.0 = 1.0		
	1 well @ 3.0 = 3.0		
TOTAL	4 5.0		
	5 ÷ 4 = 1.25	1.25	0.94
3.	Weighted average production-well depth (ft)		
	1 well @ 950 = 950		
	2 wells @ 2,200 = 4,400		
	1 well @ 3,000 = 3,000		
TOTAL	4 8,350		
	8,350 ÷ 4 = 2,088	2,088	0.99
4.	Weighted average production-well life (yr)		
	1 well @ 15 = 15		
	3 wells @ 20 = 60		
TOTAL	4 75		
	75 ÷ 4 = 19	19	0.97
5.	Spent-fluid discharge method	other	1.25
6.	Weighted average fluid quality (ppm TDS)		
	1 well @ 750 = 750		
	2 wells @ 1,000 = 2,000		
	1 well @ 1,500 = 1,500		
TOTAL	4 4,250		
	4,250 ÷ 4 = 1,063	1,063	0.99
7.	Total production fluid flow (lb/hr)		
	1 well @ 200,000		
	2 wells @ 175,000		
	1 well @ 250,000		
	800,000	800,000	0.90
8.	Environmental criticality index	Nearly Uncritical	0.95
9.	Geothermal power plant option	Inapplicable	1.00

	Variable	Input	Factor*
10.	Weighted average alternate energy cost ($/mm Btu)		

Local Energy	Cost ($/mm Btu)	% Local Use (i.e., GEDA Potential)	Result	
Natural Gas	2.50	60	1.50	
Fuel Oil	1.60	25	0.40	
Electricity	7.00	15	1.05	
			2.95	1.19

Analysis of Results

The net factor resulting from the foregoing variable inputs is 1.02 When applied to the 50 billion Btu energy quantity, the result is 51 billion Btu. As previously explained, this result does not imply that additional energy is required relative to the original 50 billion Btu design load. Any composite factor greater than 1.0 indicates the relative degree of confidence that GEDA can theoretically penetrate the energy application(s) being evaluated. The preliminary conclusion with respect to the example is that the GEDA proposition under review appears to be economically viable.

*Where required, simple linear interpolation is used between class limits; extrapolation outside class limits can be handled in much the same manner.

HEAT TRANSFER CONSIDERATION IN UTILIZING GEOTHERMAL ENERGY*

John W. Michel

Energy Division
Oak Ridge National Laboratory
Oak Ridge, Tennessee 37830

ABSTRACT

Although some forms of geothermal energy will require the application of high temperature technology, most involve only low temperatures. This paper emphasizes the importance of efficient, low cost heat exchangers in the use of low temperature sources and in the waste heat rejection systems of power generation cycles. Results of recent heat transfer development work at ORNL show that for the working fluids which are attractive for use in these cycles the condensation heat transfer effectiveness can be improved by a factor of from 3 to 7 by the use of fluted tubes and condensate drain-off skirts. Data are presented for condensation of six fluorocarbons, isobutane, and ammonia on a variety of tube surfaces. These results are being applied to the design of a 40-tube heat exchanger to be tested in a geothermal energy test facility.

*Research sponsored by the Division of Geothermal Energy, U.S. Department of Energy, under contract W-7405-eng-26 with the Union Carbide Corporation.

INTRODUCTION

While the utilization of any thermal energy source requires the application of general heat transfer principles, the use of geothermal energy can often involve many unique heat transfer considerations. Although some of the applications essentially make use of existing technology, many require adaptations to new working fluids and conversion cycles. Some of the applications involve high temperatures as in the use of the magma form of geothermal energy. Most, however, are concerned with the use of lower temperature sources such as the geothermal brines or geopressured fluids. It is this lower temperature applications that will be emphasized in this paper.

In the lower temperature applications, heat transfer considerations become of increasing economical and technological significance due to typically low conversion efficiencies and small size installations. One impact of the low cycle efficiency is that the amount of rejected heat from a Rankine cycle increases exponentially as cycle efficiency decreases. Typical geothermal conversion cycles reject up to nine times more heat than a modern coal-based cycle. Thus, in some cases, the heat rejection system may be the most costly system in a power plant operating at low cycle efficiency.

GEOTHERMAL SOURCES

As a basis for discussing the related heat transfer problems, it is important to define the nature of the available geothermal energy resources. Geothermal energy sources are available in many forms covering a wide range of temperatures as summarized in Table 1.

Table 1. Geothermal energy sources

Type	Temperature range	Estimated fraction of available resource
Hydrothermal		
Steam dominated	220–250°C	½%
Water dominated	<150–360°C	10%
Hot dry rock	130–>400°C	30%
Geopressured	150–200°C	20%[a]
Magmas	700–1200°C	40%

[a]Not including dissolved methane.

In addition to the variation in temperature noted in Table 1, some resources (e.g., hydrothermal) vary in composition (total dissolved solids and gases) from reservoir to reservoir and sometimes from time to time. Most brines are corrosive to many construction materials and have a strong propensity to form scale deposits, especially on heat transfer surfaces. Finally, most of the resources are remote from potential industrial, commercial, and residential users.

GEOTHERMAL APPLICATIONS

While the use of geothermal energy has found and should continue to find wide application for direct heat use in residential/commercial as well as industrial applications, the following discussion will be limited to its use in power conversion cycles. Although there are several types of power conversion cycles in use or under development (i.e., flash, total flow, binary, dual, hybrid, etc.), the binary cycle is receiving

perhaps the most interest.

As shown by Milora and Tester[1] for a given temperature of a geothermal heat source, there is probably an optimum working fluid. They show, for example, that R-115 is an attractive working fluid for a low temperature (∿150°C) source; i.e., is capable of capturing a larger fraction of the available energy, while R-22 is correspondingly superior for a 250°C heat source. It should be recognized that this analysis is based on thermodynamic considerations and when economic and safety factors are applied the optimum fluid for a particular temperature may change.

Working Fluid Evaporators

One of the main problems associated with the operation of a binary cycle using moderate to high temperature geothermal brines is that of scale formation on the evaporator heat transfer surface. Several schemes are under development to overcome this problem: (1) use of a hybrid cycle where steam flashed from a brine is used as the heat source for the working fluid evaporator, (2) use of a fluidized sand bed with brine to keep the evaporator surface scoured clean, and (3) use of a direct-contact evaporator where a hydrocarbon such as isobutane is dispersed and bubbled through the brine.

Working Fluid Condensers

As mentioned above, the heat rejection systems for power cycles of relatively low efficiency can be the most costly component of the system. Investigations are in progress at ORNL to improve the condensation heat transfer effectiveness for a variety of candidate working fluids for geothermal power cycles. These fluids, mainly hydrocarbons and fluorocarbons, have typically poor heat transfer properties as compared to water.

Based on the extensive test program with a variety of vertical fluted (Gregorig) tubes at ORNL as part of the OSW Seawater Desalting Project, it was anticipated that high condensation coefficients for working fluids like hydrocarbons could also be obtained. The principle of operation of the Gregorig-type surface is that surface tension effects of the liquid condensate film on the curved surface act to force the liquid into the troughs, thus maintaining a thin film on the crests while the liquid drains down the troughs. Condensation heat transfer experiments have been performed for several fluorocarbons and isobutane using the tubes shown in Fig. 1. Typical data is shown in Fig. 2 for R-113. On this correlation, Tubes F and E show significant improvement over the smooth tube performance and Tube F-7 shows even more enhancement indicating that R-113 does tend to flood the rills of a fluted tube.

Figure 3 illustrates the difference in condensation performance resulting from the differences in fluid properties with data shown for R-11, R-22, R-113, R-114, R-115, R-600a (isobutane), and R-717 (ammonia). Refrigerants 11 and 22 give the best performance but are below that for ammonia.

Work is now in progress to apply these results to the design of a heat exchanger to be tested at the DOE East Mesa Geothermal Test Facility. The design of this isobutane condenser makes use of rubber drain-off tube sheets fitted to aluminum fluted tubes (Tube F). The shell side (isobutane) is also designed to handle noncondensables by vapor sweeping across the tank bank in successively smaller flow areas to the purge point.

SUMMARY AND CONCLUSIONS

In the utilization of geothermal energy for power production, waste heat rejection is often the most important subsystem from an economic standpoint. For many of the applications, working fluids of poor heat transfer characteristics are employed which further complicate the situation. Use of vertical fluted tubes for condensation of these fluids has been shown to provide significant improvement in heat transfer over smooth tubes. The application of condensate drain-off skirts has been shown to provide additional benefits, especially for fluorocarbon and hydrocarbon working fluids.

REFERENCES

1. S. L. Milora and J. W. Tester, *Geothermal Energy as a source of Electric Power – Thermodynamic and Economic Design Criteria*, The MIT Press, Cambridge, Massachusetts, 1976.

ORNL PHOTO 6109-78

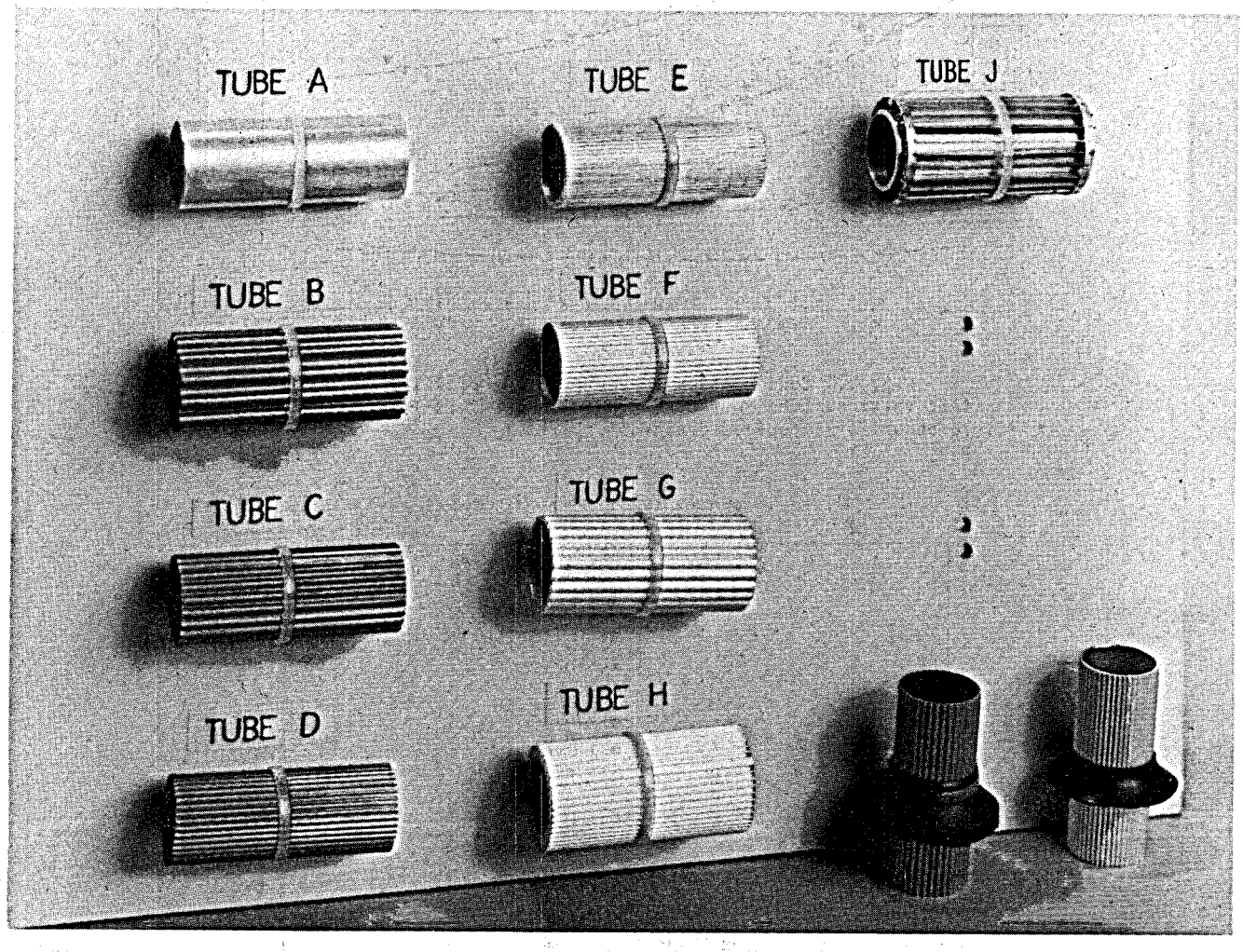


Fig. 1. Examples of experimental fluted tubes.

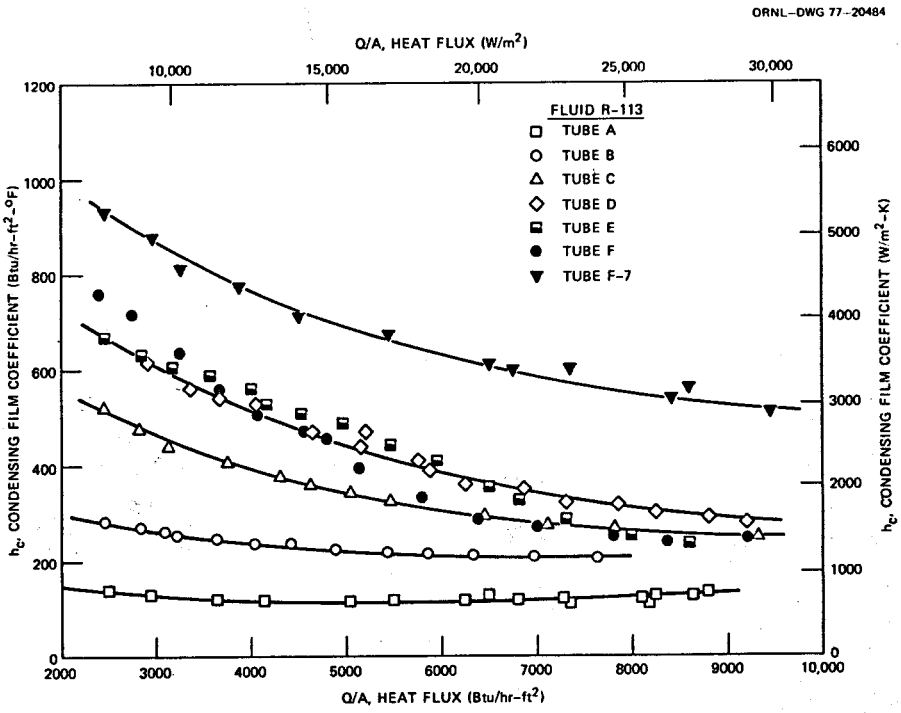


Fig. 2. Condensation characteristics of R-113 on various 4-ft vertical tube surfaces. (Note Tube F-7 is Tube F with seven uniformly spaced drain-off skirts.)

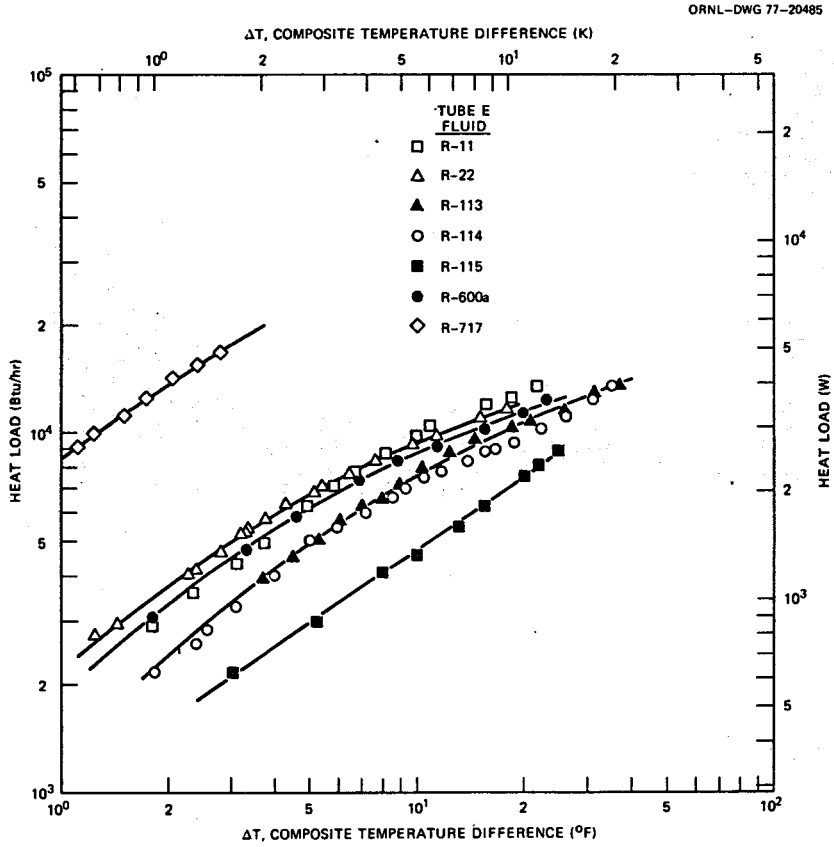


Fig. 3. Comparison of condensation characteristics of various working fluids.

CO_2 IN GEOTHERMAL STEAM
A RAPID, PRECISE, AND ACCURATE FIELD ASSAY TECHNIQUE

Dr. Donald E. Michels

Republic Geothermal, Inc.

ABSTRACT

A system for sampling and measuring noncondensable gases in steam has been devised for field use, giving results for CO_2 and non-CO_2 fractions as weight percent in steam. Six to eight determinations can be made per hour with a precision better than ±0.04 of the measured value, providing a way to examine short-period patterns in gas contents as well as finding concentrations needed for engineering design.

In this assay-type method condensate and noncondensable are collected together in a calibrated syringe at a precisely measured pressure and at ice water temperature. Henry's law is applied to compute the portion of the total gas which is dissolved in the condensate.

Hardware is designed around 1/8" O.D. stainless steel tubing which solves in a simple way sampling problems that otherwise tend to give serious inaccuracies. Several additional advantages flowing from the use of small-diameter tubing make the system especially serviceable in the field.

INTRODUCTION:

Henry's law describes the solubility of gases in water, providing a basis for measuring the concentration of those gases in geothermal steam. The method described here is convenient for low-pressure steamlines leading out of separators. There, a sample can be extracted from the line through a small diameter stainless steel tubing and condensed while maintaining association between the condensate and the noncondensables. By equilibrating a known volume of the mixture in both thermal and chemical senses one can set up a condition to which Henry's law applies and then calculate the % CO_2, etc.

Measurements of gas volume, condensate volume, and pressure are used to calculate the noncondensable concentration in the original steam. These measures are simplified by using a syringe for collecting and equilibrating the sample and using a manometer to measure pressure. Knowledge of the absolute pressure at the time of collection is needed for the calculations; for precise work it should be known within about 1cm of Hg. Since necessary measurements are made at the time of sampling there is no requirement to remove samples from the field. Calculations can be made in the field as well.

Collection and equilibration of a sample takes 7 to 10 minutes. For CO_2 mixed with other gases two samples must be taken to make one determination. One of these is collected into a NaOH solution to convert CO_2 to an ionic form. Syringes used for collection and equilibration of samples can be used also to transport them for further study, as, for example, if separate measures of noncondensables other than CO_2 are desired, perhaps by GC or MS.

The method is especially practical for steam which contains less than 5% noncondensables. Mixed noncondensable gases in which CO_2 is a major constituent are readily quantified separately, in the field, as CO_2 and non-CO_2 fractions. Precision of the method is better than ±0.04 of the measured value.

The high precision of the method and the relatively fast real-time results (6 to 8 determination per hour) make the method useful for studying subtle behaviors of geothermal wells. The method should be applied with caution if CO_2 concentration in the steam is smaller than about 0.3 weight % yet is still the most prominent noncondensable.

METHOD

Principles

Gas solubility in water is remarkably linear with respect to pressure. Such is true even for CO_2 if pH is less than 4.0 which corresponds to a CO_2 partial pressure of 0.1 atmosphere or more. Gas solubilities are strongly dependent on temperature, but collection in a bath of ice water can eliminate that complication.

It is intended in this method to collect the noncondensable gases and equilibrate them with the condensate at ice temperature so that a well-defined solubility coefficient applies. The steamline pressure is used to drive the sample into the syringe and hold it during equilibration. Thus, the absolute pressure of the steamline is the correct value to use for the calculations. By collecting the sample in a calibrated syringe, equipped so as to limit the extension of the plunger, both the liquid volume and the volume of the undissolved (excess) gas can be measured. The collected noncondensable gases and especially CO_2, are present in both liquid and gaseous compartments of the syringe. The amounts in each compartment are calculated separately and the results summed to complete the analysis.

If CO_2 is present two gas collections must be made. One, when the syringe holds a few ml of NaOH solution, enough to totally solubilize the CO_2. In this second collection there is no partial pressure of CO_2. This step provides for both a direct measure of non-CO_2 noncondensables and a means to accurately estimate the CO_2 partial pressure in the other sample.

Hardware

The major parts of the setup shown in fig. 1 are: (1) a small-diameter metal tubing to extract a representative sample from the steamline and assure that it remains representative. The tubing also serves as a cooling coil, (2) ice and water bath for temperature equilibration, (3) a calibrated syringe to measure gas and liquid volumes, and (4) a manometer to measure steamline pressure. As a practical measure, one needs also a sensitive means to detect when a solubility equilibrium has been reached.

The sampler design assures that several important functions are served.

The small-diameter tubing is used as a probe to go deep into the steamline in order to avoid problems of condensate on the pipe walls. Additionally its small diameter assures the continued integrity of the steam sample during condensation by maintaining the noncondensables in intimate association with their respective volumes of condensate. The small diameter tubing allows the surface tension of the condensate to maintain a droplet of water entirely across the tubing diameter, trapping a bubble of noncondensable in front of it early in the condensation stage. This arrangement of small-scale bubble and liquid drop persists until the sample emerges in the syringe. These essential effects are absent in tubing larger than about 1/8 inch I.D.

Most of the length of the stainless steel tubing is arranged into 2 coiled portions so that condensation (high heat load operation) is well separated from where the temperature equilibration takes place (low heat load operation). Length of the stainless steel tubing is chosen so that the flow rate through it is made small by viscous relationships to the fluid. In this way the flow

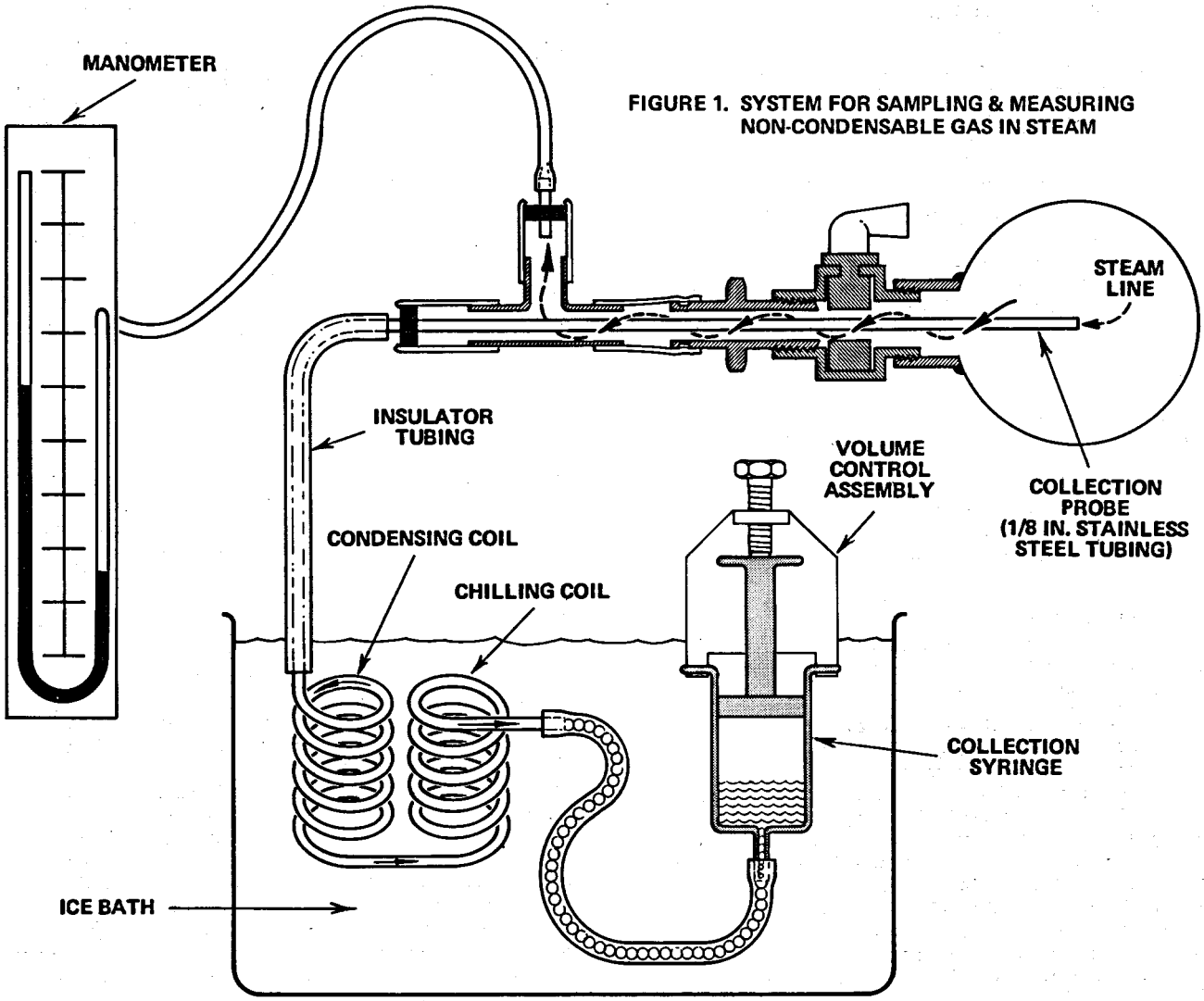


FIGURE 1. SYSTEM FOR SAMPLING & MEASURING NON-CONDENSABLE GAS IN STEAM

rate is kept low and smooth without valves. Thermal equilibration occurs inside the tubing, rather than inside the syringe.

A flexible transparent/translucent tubing connects the stainless steel tubing with the syringe, providing a window for monitoring the progress of fluid into the syringe. Equilibrium is judged to exist when bubbles no longer leave the stainless steel tubing while the syringe is being shaken in the ice bath.

The syringe has the attribute of possessing essentially zero volume at the start of the sample collection. After a stable flow is established through the tubing and the tubing is well flushed the collapsed syringe can be connected to the flexible tubing without interrupting flow and without introducing air into the syringe. Subsequently, the steamline pressure, transmitted through the sample as it is being collected, moves the plunger of the syringe until a mechanical stop arrests the plunger at a desired total volume. Fluid continues to enter the syringe until equilibration is achieved with both the steamline pressure and the gas solubility. The dissolution of CO_2 is moderately slow at ice temperature, thus, it speeds things up to shake the syringe during the pressurization stage.

The absolute pressure inside the syringe is required for calculations. This has been obtained by combining a manometer reading made at the time of sampling, with a barometric pressure obtained from a nearby airport. The manometer must be arranged so that neither the volume of the syringe nor its contents are disturbed by the shifting of fluids in the manometer. Thus, it is practical to connect the manometer separately, yet nearby the place where the sampling probe enters the steamline. Since streaming velocities inside steamlines are fairly high some aerodynamic effects cause differences between the pressure existing on the probe end of the sampler and on the manometer. These factors must be worked out for each case in order to accurately assess the pressure inside the syringe.

Calculations

Two sample collections, one with and one without NaOH in the syringe, yield the 5 items of data required for the calculations:

$$V_{L_1},\ V_{G_1},\ V_{L_2},\ V_{G_2},\ P_{T_1}$$

V and P refer to volume and pressure, L and G refer to liquid and gaseous phase, and 1 and 2 refer to the collections, specifically, 2 refers to that one involving NaOH. The subscript T on the pressure refers to the total absolute pressure inside the syringe at the time equilibrium is reached, that is, it is the sum of barometer and manometer indications, the latter adjusted for aerodynamic influences associated with the connections to the steamline.

$$\%CO_2 = K P_{T_1} \underbrace{\left(\frac{V_{G_1}}{V_{L_1}}\right)\left(1+\frac{M_C\ V_{L_1}}{V_{G_1}}\right)\left[1-\underbrace{\left(\frac{V_{G_2}}{V_{G_1}}\right)\left(\frac{V_{L_1}}{V_{L_2}-V_{NaOH}}\right)\left(1+\frac{M_N\ V_{L_2}}{V_{G_2}}\right)}_{F_1}\right]}_{F_2}$$

Where the terms are as defined above with the additions that constant K = .00256 involves the formula weight for CO_2, gas constant, temperature, and fluid density appropriate for pressure measured in cmHg, volumes in ml, and density in grams per ml. The term V_{NaOH} presumes that in the second collection NaOH is added before-hand as a water solution.

The equation above has been arranged so that the special significances of some portions are easier to see.

F_1 represents the fraction of P_{T_1}, which is due to non-CO_2 gases. The factor M_N suggests nitrogen in the case at hand, in the presumption that nitrogen dominates the non-CO_2 suite, a presumption that would be assessed independently.

F_2 represents the virtual pressure fraction for CO_2. The mathematics treats the dissolved CO_2 as if it were added to the gas phase compartment; this virtual pressure fraction is larger for larger V_{L_1} and generally exceeds the value 1.

The non-CO_2 fraction of the noncondensable gas is given by

$$\text{non-}CO_2\text{ fraction} = \frac{F_1}{F_1+F_2}$$

RESULTS:

This method has been applied to wells of Republic's development at East Mesa. Besides seeking the CO_2 content for use in engineering design, we also were interested in identifying trends.

Figure 2 shows an absence of trends in well FS between 4 and 8 hours after turn-on. Later measurements show that the concentration of CO_2 in well FS remained in that same narrow range throughout the 500-hour test period.

Figure 3 shows the trend observed for well SE. The change of concentration toward an asymptote suggests a contribution from unequal portions of the reservoir and their approach to a steady state situation. The decrease in CO_2 content in the first few hours after turn-on can be interpreted in various ways. One is that it is a consequence of cross-flow phenomena that occurred upon shut-in after a previous test.

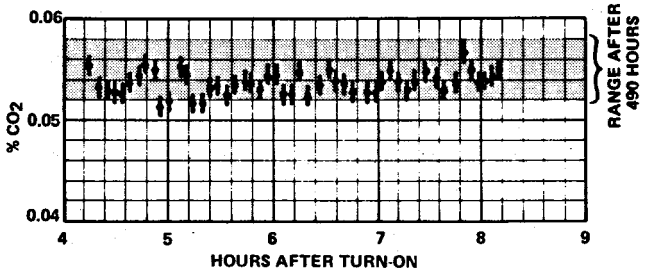


FIGURE 2. CO_2 IN TOTAL FLOW WELL FS

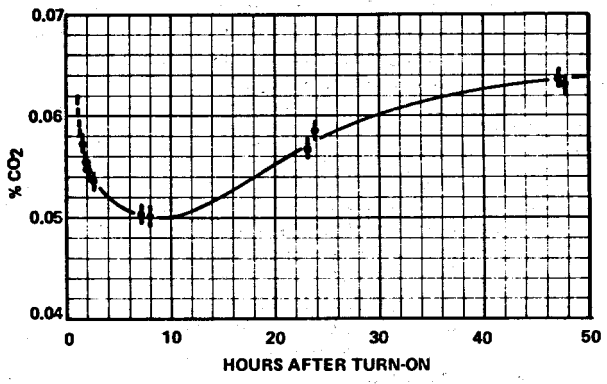


Figure 3. CO_2 IN TOTAL FLOW WELL SE

SUMMARY

A precise and rapid field method for measuring noncondensable gases in geothermal steam has been developed and used. The method is based on Henry's law and involves a direct measure of gas volumes, yielding a nondestructive assay-type analysis. The hardware that was developed in order to apply the Henry's law principle avoids two problems that are at risk in any sampling for noncondensables: (1) using a probe to withdraw the steam sample from deep within a steamline to avoid its being affected by condensate that might exist on the walls and (2) preventing a separation of condensate and noncondensable in a condensing coil that can lead to wrong proportions being introduced into the collection vessel. Calculations for the CO_2 and non-CO_2 components of the steam depend on five quantities measured in the field plus a barometric reading. The sample need not be removed from the field so requirements for transport and preservation are avoided. However, the sample is captured in a way convenient for removal from the field in case additional study is desired, and then the same material would be involved in both studies. The method can be used to study variations over time of noncondensable gases during production, leading to insight about reservoir conditions as well as providing data for engineering design.

Geothermal Resources Council, TRANSACTIONS, Vol. 2 July 1978

RESERVOIR ENGINEERING ASPECTS OF FLUID RECHARGE AND HEAT TRANSFER IN GEOTHERMAL RESERVOIRS

F. G. MILLER, H. CINCO, H.J. RAMEY, JR., and F. KUCUK

STANFORD UNIVERSITY, STANFORD, CA. 94305

ABSTRACT

Natural recharge of fluid filled geothermal reservoirs is shown to be important in the development of these reservoirs and in increasing geothermal energy reserves. Research contributions on methods for calculating water influx and heat transfer in petroleum reservoirs are discussed. The need to forecast the performance of geothermal fluid reservoirs subject to water influx is emphasized.

INTRODUCTION

Encroaching fluids are heat-carrying media which extend the economic lives of reservoirs and increase energy recoveries.

The concept of "natural recharge" may vary from one scientific discipline to another. From a geological point of view, natural recharge is important even if it is a "slow" process. From the reservoir engineering standpoint, natural recharge is important only if the amount of fluid encroaching into the reservoir during its commercially productive life is "substantial."

Water influx theory as applied to petroleum reservoirs has been developed extensively over a period of almost 50 years. In contrast to calculations for petroleum reservoirs, calculations for geothermal fluid reservoirs must include heat transfer effects as well as determinations of cumulative influx volumes. Thus, pertinent equations for geothermal fluid reservoirs are material-and-energy balance equations.

In the present study information is disseminated to the geothermal community on water influx theory developed by petroleum reservoir engineers. Material and energy balances relating to fluid influx into geothermal reservoirs also are discussed.

DEVELOPMENT OF WATER INFLUX THEORY

Although reservoir engineers have been concerned with water influx in geothermal fluid reservoirs for many years, little has been done to calculate this influx in terms of reservoir pressures and temperatures, rock and fluid properties, and geothermal fluid production rates. When influx waters enter these reservoirs they may undergo temperature changes. If these waters are cool compared to the reservoir fluids, their temperature increases as a result of heat transfer by both conduction and convection.

One of the first major contributions to water influx theory is a paper by Hurst (1943). He presented a model to calculate the cumulative water influx in a petroleum reservoir. He considered a reservoir associated with an aquifer of infinite radial extent, both being initially at the same pressure. At time zero the pressure is dropped instantaneously at the petroleum reservoir-aquifer interface and maintained constant. The solution for this problem is expressed in terms of a function G, related to the cumulative volume of water that has crossed the reservoir boundary in a given time.

The water influx research that probably has been most widely applied is reported in a paper by van Everdingen and Hurst (1949). They studied linear and circular oil reservoir-aquifer systems, but dealt mainly with circular systems of constant thickness, giving rise to plane radial flow in the direction of influx. They considered the aquifers adjacent to oil reservoirs to be either of finite or of infinite extent measured radially outward from the oil reservoir. van Everdingen-Hurst solutions fall into two categories. In the first of these the fluid pressure at time zero at the oil reservoir-aquifer boundary is dropped instantaneously from its original value to some lower value and thereafter maintained indefinitely at the lower value. The cumulative water influx at this boundary is calculated as a function of time for both finite and infinite aquifers. In the second category, influx water crosses the oil reservoir-aquifer boundary beginning at time zero and enters the reservoir at a constant rate indefinitely. The resulting drop in pressure at the oil reservoir-aquifer boundary is calculated as a function of time.

Figure 1 (Craft and Hawkins, 1969) is a typical family of curves representing some of the constant pressure case results of van Everdingen and Hurst. Dimensionless cumulative influx is symbolized Q_D, the ratio of aquifer radius to oil reservoir radius by R_e/R_w, and dimensionless time by t_D. Cumulative influx is given by: $W_e = B \cdot \Delta p \cdot Q(t_D)$, in which B is the water influx constant.

The concept of superposition is applied to actual situations in which the pressure changes with time at the oil reservoir-aquifer boundary.

Miller (1962) studied linear oil reservoir-aquifer systems considering constant pressure and constant rate cases similar to those of van Everdingen and Hurst's (1949) circular systems. For his constant-rate finite-aquifer cases he specified no-flow outer boundary for the aquifer. Miller's curves can be applied similarly to the van Everdingen-Hurst curves.

Barham and Nabor (1964) used Miller's equations and simplified his method of graphing dimensionless pressure and dimensionless cumulative influx as functions of time. They also extended Miller's analyses to include constant-rate finite aquifer cases in which the outer boundary of the aquifer is maintained at a constant pressure.

Chatas (1966) analyzed water influx in spherical petroleum reservoirs. He analyzed his systems with respect to the same constant pressure and constant rate cases as van Everdingen and Hurst (1949).

Recently Kucuk (1977) developed a water influx theory for elliptical oil reservoir-aquifer systems. He gave attention to both constant pressure and constant rate cases, and investigated elliptical systems having various ratios of the lengths of major axis a to minor axis b. The effect of these ratios on cumulative influx is examined in detail. If a/b approaches unity, Kucuk's systems become equivalent to the circular systems of van Everdingen and Hurst (1949). If a/b approaches infinity, the linear systems of Miller (1962) and of Nabor and Barham (1964) result. Thus, Kucuk's work covers an array of reservoir-aquifer configurations from linear through elliptical to circular.

Most models for water influx calculations require a knowledge of the average reservoir pressure history because pressure is handled as an independent variable. In some cases it is possible to forecast rates of production of reservoir fluids. In these cases average reservoir pressure becomes the unknown variable. Hurst (1958) solved this problem for reservoirs containing either gas-saturated oils or under-saturated oils. He developed solutions for linear and radial water influx considering the reservoir as a compressible system.

In 1971, Fetkovich presented important information about water influx from a finite aquifer. He used the concept of pseudo-steady flow to simplify his calculations. The water influx problem was solved by using a rate equation and a material balance equation without requiring the application of superposition. It was shown that this approach produces solutions accurate enough for practical purposes. Moreover, it can be applied to aquifers of any geometry.

Whiting and Ramey (1969) were concerned in their research with the development of appropriate equations and techniques to facilitate estimates of reserves and future productivity of geothermal fluid reservoirs. Their resulting equations are useful for estimating initial reservoir conditions, for matching past performance, and for predicting future performance of reservoirs for which their assumptions are realistic. They developed a material and energy balance equation which includes a water influx term. The Whiting-Ramey reservoir model is shown here as Fig. 2.

DEVELOPMENT OF HEAT TRANSFER THEORY FOR HOT FLUID INJECTION PROCESSES

Reservoirs containing high viscosity oils are sometimes practically impossible to produce using conventional production methods. Much research has been done on the recovery of heavy crude oils through injection of hot fluids into reservoirs. Petroleum engineering literature offers a large number of models to simulate such thermal recovery processes. Two of these are discussed here because they appear to be useful in the calculation of heat transfer in geothermal reservoirs.

Lauwerier (1955) presented an analytical solution to calculate the temperature distribution created by hot fluid injection into a horizontal, rock stratum filled with cool fluid. He considers that heat is transferred by convection in the direction of flow. At the same time he assumes temperature equilibrium vertically in the stratum. Heat transferred between the injection interval and the overlying and underlying rock is considered to be by conduction. He specifies that the hot fluid be injected at a constant rate and at a fixed temperature. His solution gives the temperature distribution within the injection interval as a function of time.

In 1959 Marx and Langenheim presented a method for estimating thermal invasion rates and cumulative heated areas for heat injection in a horizontal oil-bearing stratum of constant thickness. They specify a constant rate of hot fluid injection at a fixed temperature. They further assume a constant temperature for the heated area and that heat lost to the overlying and underlying strata is transferred by conduction. An important feature of their model is that no restrictions are imposed on the shape of the expanding heated area. Ramey (1959) extended their research to include variable heat injection rates.

In 1964 Ramey showed that vertical heat losses for both the Lauwerier and Marx-Langenheim models are the same when expressed as a fraction of the total heat injected into the oil reservoir. This finding indicates that two systems with different temperature distributions lose the same quantity of heat to adjacent strata. Ramey graphed the "fraction of total heat injected lost to adjacent strata, W_o*" as a function of $\log_{10} t_D$ for different heat injection models. Dimensionless time $t_D=(4Dt)/h^2$ in which D = thermal diffusivity, t = time, and h = formation thickness. His curve for either the Lauwerier or Marx-Langenheim model is shown here as Fig. 3.

DETERMINATION OF BOUNDARIES OF GEOTHERMAL FLUID RESERVOIRS

Natural underground fluid reservoirs, whether groundwater for water supply, petroleum, or geothermal-fluid have some form of physical boundaries. Geologic boundaries can be faults, permeability pinchouts, unconformities, downstructure water in the case of oil reservoirs, aquifer outcrops at the ground surface, or one of a number of other possible "seals" to confine the reservoir fluid to the reservoir.

If these reservoirs are developed for commercial purposes they also have economic boundaries. Estimates of oil reserves are based, for example, on the production performance of wells that can be drilled and produced economically. Oil-bearing rocks are generally considered as "nonproductive" if the permeability of the rock is so low that commercial production is not possible. Vast quantities of natural gas exist in the United States in deep natural underground reservoirs. At today's prices, these reservoirs cannot be developed commercially. Thus, this store of gas can be thought of only as a resource which may or may not represent reserves at some time in the future. The gas reservoir depths therefore are economic limits.

Reservoir fluid temperatures can represent an economic limit for geothermal reservoirs. Hot fluids produced for non-electrical uses can be recovered commercially from reservoirs at lower temperatures than fluids produced for electrical uses. The equipment necessary to transport the former fluids to their ultimate points of use as fluids is generally far less expensive than the equipment, mainly power plants, needed to convert the heat energy of produced reservoir fluids to electrical energy.

If the reservoir fluid decreases in temperature in directions away from the producing wells, its temperature may drop to an economic cut-off value. Water influx then becomes a case of relatively cool water moving into a relatively hot reservoir. The moving cool water gains heat by convection from the reservoir rock and fluids and by conduction from impermeable rocks sealing off the reservoir. As this process continues, the economic cut-off temperature limit moves in the direction of the moving influx water and the productive region of the reservoir shrinks. Additional energy is made available, however, by the influx water as it becomes heated. The overall reserves of the reservoir are thereby increased. A problem involving these phenomena is solved in the next section.

EXAMPLE OF APPLICATION

A geothermal reservoir subject to cold fluid recharge has been produced for 1 year. Assuming that the temperature difference between the cold zone and the reservoir is $30^{\circ}F$, calculate (a) the position of both the fluid and temperature fronts in the reservoir, (b) the amount of heat gained by the cold fluid by heat conduction from underlying and overlying strata, and (c) the heat transferred from rock to cold fluid at the cut-off temperature.

Data - average macroscopic velocity of cold fluid, $V_w = 0.03$ ft/day; porosity, $\phi = 0.2$; reservoir thickness, $h = 300$ ft; volumetric heat capacity of rock, $\rho_r c_r = 35$ Btu/ft^3-$^{\circ}$F; volumetric heat capacity of water, $\rho_w c_w = 68$ Btu/ft^3-$^{\circ}$F; thermal diffusivity of overlying and underlying strata $D = 0.96$ ft^2/day.

Solution - a unit width of aquifer-reservoir interface is considered. The volumetric heat capacity of the reservoir rock and fluid system is defined by: $\rho_1 c_1 = \phi\rho_w c_w + (1-\phi)\rho_r c_r = 0.2 \times 68 + (1-0.2)\ 35 = 41.6$ Btu/ft-$^{\circ}$F.

Applying the Lauwerier model and letting $X_T=0$ when $t=0$, the position of the thermal front at time t is given by:

$$X_T = V_T t = \left[\frac{\rho_w c_w V_w}{\rho_1 c_1}\right] t = \left[\frac{68 \times 0.03}{41.6}\right] 365$$

$$= 17.9 \text{ ft.}$$

The location of the recharge-fluid front at the same time t is given by:

$$X_W = (V_W t/\phi) = \frac{0.03 \times 365}{0.2} = 54.75 \text{ ft}$$

The W^* function presented by Ramey (1964) is used to determine the heat transferred by conduction to the cool fluid from overlying and underlying strata. Dimensionless time for Fig. 3 is given by:

$$t_D = \frac{4Dt}{h^2} = \frac{4 \times 0.96 \times 365}{(300)^2} = 0.0155$$

From Fig. 3, $W_o^* = 0.1$, and then:

heat gained by cool fluid $= V_w h \rho_w c_w \cdot \Delta T\ W_o^*\ t$

$$= 0.03 \times 300 \times 68 \times 30 \times 0.1 \times 365$$

$$= 6.7 \times 10^5 \text{ Btu/ft}$$

Finally, the heat transferred from rock to fluid in the reservoir, above the cut-off temperature, is given by:

$$(X_W - X_T) h \phi \rho_w c_w\ \Delta T = (54.75-19.9) \times 300 \times 0.2$$

$$\times 68 \times 30 = 4.51 \times 10^6 \text{ Btu/ft}$$

Although a constant rate of influx of fluid at a fixed temperature is considered in this example, a more general problem can be solved by use of the superposition principle.

CONCLUDING STATEMENT

This study discloses that a wealth of knowledge has been developed by reservoir engineers on the theory of water influx in petroleum reservoirs. Water influx has received attention also, however, by groundwater hydrologists and by geologists. Less is known about heat transfer in underground

reservoirs than is known about water influx.

The petroleum industry has done extensive research also on hot fluid injection processes, generally steam or hot water injection. These processes stimulate oil recovery and improve oil recovery efficiencies.

Petroleum research results can be drawn upon by geothermal fluid reservoir engineers to study the effects of encroaching cool waters on energy recoveries from geothermal reservoirs. The Lauwerier and Marx-Langenheim models are readily adaptable, for example, to such studies.

The Lauwerier analysis made in the present paper of a simple model of a geothermal fluid reservoir indicates the true significance of cool water encroachment. The results accentuate the fact that the reserves of the reservoir are energy reserves contained in the reservoir fluid, in the reservoir rock matrix, and in the rocks adjacent to the reservoir from which heat is transferred by conduction.

This study should be recognized as an initial phase of a research effort to develop water influx or fluid recharge theory for geothermal reservoirs. More sophisticated reservoir models than those analyzed here should be designed to generate better data to facilitate forecasts of production performance.

Field evidence of the effects of fluid recharge in energy reserves should be sought. If such evidence can be developed, it should be used to support, if possible, the research results gained from studies of models.

References

Hurst, W.: "Water Influx into a Reservoir and Its Application to the Equation of Volumetric Balance," Trans. AIME (1943), 151, 57-72.

van Everdingen, A.F., and Hurst, W.: "The Application of the Laplace Transformation to Flow Problems in Reservoirs," Trans. AIME (Dec. 1949), 305-324.

Craft, B.C., and Hawkins, M.F.: Applied Petroleum Reservoir Engineering, New Jersey: Englewood Cliffs (1959).

Lauwerier, H.A.: "The Transport of Heat in an Oil Layer Caused by the Injection of Hot Fluid," Appl. Sci. Res. (1955), 5, 145-150.

Hurst, W.: "The Simplification of the Material Balance Formulas by the Laplace Transformation," Trans. AIME (1958), 213, 292-303.

Marx, J.W., and Langenheim, R.H.: "Reservoir Heating by Hot Fluid Injection," Trans. AIME (1959), 216, 312-315.

Ramey, H.J., Jr.: Discussion of the above mentioned paper by Marx and Langenheim, Trans. AIME (1959), 216, 364-365.

Miller, F.G.: "Theory of Unsteady-State Influx of Water in Linear Reservoirs," J. Inst. Pet. (Nov. 1962), 48, No. 467, 365-379.

Nabor, G.W., and Barham, R.H.: "Linear Aquifer Behavior," Trans. AIME (1964), 231, 561-563.

Ramey, H.J., Jr.: "How to Calculate Heat Transmission in Hot Fluid Injection," Pet. Engr. (1964), 110-114.

Chatas, A.T.: "Unsteady Spherical Flow in Petroleum Reservoirs," Trans. AIME (1966), 237, 102-114.

Whiting, R.L., and Ramey, H.J., Jr.: "Application of Material and Energy Balances to Geothermal Steam Production," J. Pet. Tech. (1969), 893-900.

Fetkovich, M.J.: "A Simplified Approach to Water Influx Calculations--Finite Aquifer Systems," J. Pet. Tech. (1971), 814-828.

Kucuk, F.: "Transient Flow in Elliptical Systems," Ph.D. Dissertation, Stanford University (1978).

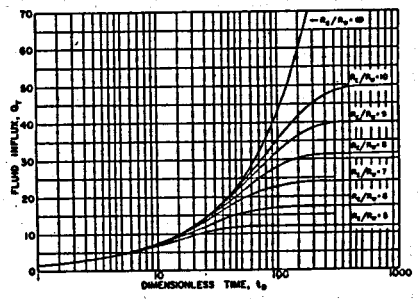


Fig. 1: Limited Aquifer Values of $Q(t_D)$ as a Function of t_D for Various Values of R_E/R_W

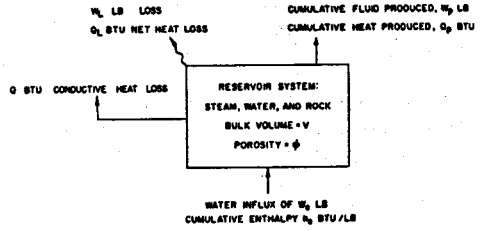


Fig. 2.: Schematic Diagram of Reservoir Model (after Whiting and Ramey, 1969)

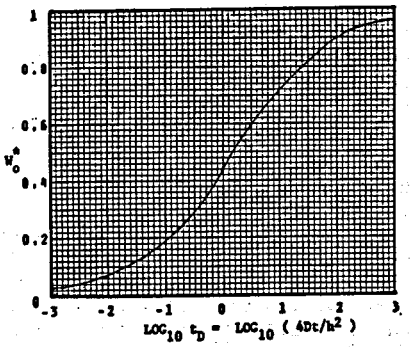


Fig. 3: Vertical Heat Loss vs Time Obtained from the Lauwerier Reservoir Model (after Ramey, 1964)

DYNAMIC SIMULATION OF THE RAFT RIVER GEOTHERMAL ELECTRIC PLANT AND ITS SUPPLY SYSTEM

J. D. Miller and R. W. Snyder

EG&G IDAHO, INCORPORATED
IDAHO FALLS, IDAHO

ABSTRACT

Thermal and acoustic simulations of the Raft River binary cycle plant have been developed and used to develop controls and operating procedures and to define plant performance. The thermal-hydraulic simulation describes the behavior of the geothermal, isobutane and coolant loops during startup, shutdown and power range operation. A separate simulation has been used to study acoustic effects in the geothermal loop.

The arrangement of the Raft River Geothermal Electric Plant is described in the paper by Ingvarsson et al along with the procedure used to optimize the configuration.

The lumped parameter thermal model used in the dynamic analysis represents the physical components of the three loops in terms of mass and energy conservation equations, thermodynamic and transport properties, resistance and heat transfer correlations and valve, pump and turbine operating characteristics. Standard controllers are incorporated and plant boundary and operating conditions are varied as required.

This model is implemented on the Time And Frequency (TAF) "problem solver" code and the INEL CDC computer. In addition to the customary transient computation mode, the simulation provides direct determination of steady state conditions and furnishes an evaluation of the dynamic characteristics of the linearized system. The latter features provide economical methods for mapping static or quasi-static operation and for generating data for controls design.

Control elements were incorporated in the plant and the thermal model based on operational requirements as follows:

a) Boiler feed valves (one for each of the dual boilers) control the flow of preheated liquid isobutane to the boilers and maintain liquid levels as the vapor flow rate varies.

b) Turbine bypass and throttle valves permit independent plant and turbine startup and shutdown.

c) Geothermal fluid recirculation control permits independent plant and supply system operation and allows for a controlled (50°F/hr) plant heatup. This is accomplished by bypassing a portion of the hot geothermal supply around the plant and by replacing it with an equal flow of cold plant exit fluid.

While the plant will usually be operated in the base load mode, the active control elements required for the operational considerations discussed above provide the capability for load following operation. Simulation studies were conducted to determine the best load control configuration. Turbine torque is controlled by using the throttle valves. A separate mechanism for controlling boiler pressures is required; both turbine bypass and geothermal fluid recirculation were studied. Static and dynamic performance characteristics were determined and the turbine bypass selected because of its speed of response and simplicity and because it minimizes fluctuation in operating parameters. Implementation of this control scheme is accomplished by driving both throttling and bypass valves, in opposite directions, from the load controller.

The thermal model was used extensively for detailed controller design, for definition of turbine design requirements, for parametric studies on the effects of ambient conditions, tube fouling and heat transfer variation, for malfunction studies and for the development of startup and power range operation procedures. The most significant of the operational constraints encountered throughout all these studies was the prevention of flashing in the boiler feed valves, with the attendant loss of control. Since the preheaters supply fluid very close to the boiler saturation enthalpy, cycle management and the provision of a preheater bypass flow is generally necessary to keep the fluid entering the feed valves cold enough to prevent flashing.

An acoustic simulation of the geothermal supply system was developed because of the water hammer hazard resulting from the large piping lengths and the low working stresses of the asbestos-cement pipelines. The Continuous System Modeling Program (CSMP) code was selected because its time delay capability provides a better approximation of the acoustic wave phenomena in the various pipe lengths. Supply and

injection wells and gaseous accumulators were simulated with lumped parameter models. Flow changes due to accumulators and pressure changes due to lumped line friction and to valves, gravity head and pumps were introduced at the ends of the frictionless lines.

The system controls include manual adjustments of individual well flows and closed loop control of injection pump inlet pressures to prevent lowering pressure below the outgassing level. In addition, a dump to a holding pond is provided at the plant exit to prevent thermal gradient damage to the asbestos-cement pipe in the event of an emergency plant bypass which would otherwise replace 150°F plant exit flow with 290°F plant supply flow.

The acoustic simulation has been used to determine valve stroking rate and gas accumulator sizing requirements, design the injection pressure controllers and develop operating procedures.

Plant and supply system dynamic simulation has proved to be a valuable tool in designing controls, evaluating static performance over the range of ambient and operating conditions and developing normal and upset operating procedures.

The analysis has lead to the selection of a load-following control using the turbine inlet and bypass valves to provide fast response with minimum disturbance of plant operation. It has provided approaches, to be confirmed during initial startup operation, for the prevention of flashing in the boiler feed valves.

DRILLING AND DIRECTIONAL DRILLING A MODERATE-TEMPERATURE GEOTHERMAL RESOURCE

L. G. Miller, S. M. Prestwich, and R. W. Gould

EG&G IDAHO, INC.
IDAHO NATIONAL ENGINEERING LABORATORY
Idaho Falls, Idaho 83401

INTRODUCTION

The high cost of geothermal well drilling has caused great concern in the geothermal community, because of the direct relationship of well cost to power-on-line costs. The utilization of large quantities of moderate-temperature geothermal fluids (300°F, or 150°C) for electric power production at the Raft River, Idaho Geothermal Project creates even larger concerns about well costs. Various techniques were used during the exploration and drilling of the present wells, to improve resource detection and well production. These techniques will be utilized in all future drilling at Raft River.

Some resources have been overlooked because of the use of standard drilling methods. Each type resource will require unique techniques for detection and enhancement. The lower the temperature of the resource, the more difficult it will be to detect. Dry steam and high-temperature water-dominated resources are rare anomolies. Moderate-temperature resources, however, should be quite abundant throughout the West. It is necessary to detect such resources, enhance the production or injection capabilities of each well, and at the same time increase well lifetimes in order to keep moderate-temperature resources competitive with other forms of energy.

Three production and two injection wells have been drilled in the Raft River Valley, with an additional production and an injection well to be completed in the summer of 1978. This paper describes the techniques used in the drilling and testing of these high-fluid-volume wells.

Exploratory Drilling

During the exploratory phase, only the surface casing was run and cemented; if no resource was found, the cost invested in the dry well would then have been as small as practical. Below the casing, the well was drilled with water, rather than mud. This prevented the plugging of permeable producing zones and fractures and kept the fluid column as light as possible, so that geothermal water could enter the hole. Air or foam would lighten the column even more, but these measures have not been necessary at Raft River. Water drilling may not be a necessity with very high-temperature resources, but is the only recommended method for medium temperatures and lower artesian pressures. Care must be exercised in the use of water drilling.

After drilling and locating the resource, the well can, in many cases, be completed by cooling with injected cold water and by cementing in the production casing. This control method did not work at Raft River. A very permeable zone between 1600 and 2400 ft (490 to 730 m) accepted the hot water from the reservoir and all injected cold water. The well could not be "killed" with this method. An alternate method, that of filling the lower portion of the hole with sand, was very successful and resulted in effective control prior to casing the well during well completion. Sand was then drilled out to complete the well.

Cost again became a major factor for design of RRGE-3. Two major areas of well cost are casing and cementing. Casing calculations determined that over a 30-year production period, a 1000-gallon-per-minute well, with 9-5/8 in. (24.45 cm) production casing, would be more economical (including the cost of pump operation and the increased pressure drop in the casing) than a well with 13-3/8-in. (34 cm) production casing. The length of the production casing was reduced by hanging it from the bottom of the surface casing (at 1200 ft); thereby lowering the total well cost. Utilizing a Basch-Ross liner hanger with circulating ports allowed crews to squeeze cement from the top of the hung production string in the event of remedial cementing. This reduced the very costly perforating squeeze cementing and saved more than 50%. The use of this technique has been considered acceptable by the State for such moderate-temperature (low-pressure) wells.

Also because of costs, much time and planning have been devoted to cementing techniques. Perlite and silica cements have been used, and stage cementing tried--all with less than desirable results. We are still attempting to find a cement and technique which will be effective for Raft River hole conditions. This year, two different cements are to be used in the wells, so that the application and long-term retrogression of two cements can be compared.

Multiple-Leg Wells

Well RRGE-3 became an experiment in well stimulation to reduce well costs by directionally drilling open-hole legs through the production zone below the casing. This increased production for a minor increase in well cost. The first leg was drilled westwardly to a depth of 5853 G.L., with disappointing production results. Analysis showed an apparent lack of producing fractures, so the decision was made to drill two additional legs, in hopes of encountering production fractures. Leg B was drilled northeastwardly to a depth of 4432 ft (1351 m); Leg C, northwesterly to a depth of 5917 ft (1803.5 m). Production increased by 500% with the completion of the third leg.

Although we were unable to prove what would happen in a homogeneous producing layer, our calculations for the Raft River reservoir imply that an extra leg that gets as far away as 400 ft (122 m) will increase the cost 20%, while increasing production 50%.

A second multiple-leg production well, RRGP-5, will be drilled this June. Injection Well RRGI-4 will be deepened and completed as a multiple-leg production well in October.

Where formations are tight, or where formation plugging is a problem, producing well life time and well operating pressures can be improved by using multiple-leg wells. Formation plugging in wells with two phase then is apparently most likely to occur near the well bore. By directionally drilling multiple legs, penetrating the injection zone, the rate of plugging should be proportionately reduced.

Geothermal Resources Council, TRANSACTIONS, Vol. 2 July 1978

ENHANCED RECOVERY RESERVOIR ENGINEERING ASPECTS OF GEOTHERMAL DEVELOPMENT

Richard J. Miller

PACIFIC RESOURCES MANAGEMENT, INC.

Abstract

The recovery of heat resources is the primary purpose of geothermal development. The production of primary reservoir fluids however, may recover only a very small percentage of reservoir heat. The adoption of effective enhanced recovery methods will be necessary if efficient use is to be made of existing geothermal resources. This summary paper outlines the reservoir engineering aspects of both primary fluid recovery and enhanced recovery methods.

The Nature of Geothermal Resources

Geothermal resource development has similarities to fluid-hydrocarbon development. Both resources employ similar exploration methods and require the drilling of wells for the production of fluids for conversion to useful forms of energy. Both resources are produced by fluids flowing through a porous media.

There are also several very important differences between geothermal and fluid hydrocarbon resources. Fluid hydrocarbon can be transported by a variety of means to wherever it is desired to use them. Geothermal resources must be used virtually on the production site because their energy value is lost in transit. Geothermal resources rely on physical properties which can disipate whereas hydrocarbon resources owe their value to chemical process.

In geothermal reservoirs the primary resource is heat. While it is necessary to have some fluid, such as water, in the reservoir to serve as a means of carrying the heat resources to a point of use the heat resource could exist alone without the fluid carrier and still be valuable as an energy resource. The fluid, on the otherhand, could exist alone and have value but not as an energy resource. The importance of this point is shown by (a) the significant experiments being conducted to tap the resources of hot dry rocks through water injection, and (b) the use of binary cycle plants for conversion to heat energy to electrical energy.

Purpose of Reservoir Engineering

Acceptance of the concept of reservoir heat being the primary resource and of reservoir fluids serving solely as heat transfer mediums requires that geothermal reservoir engineering consist of two interconnected parts:

(a) Determination of reservoir fluid reserves, production potential, reserve life, and recovery mechanism efficiency.
(b) Determination of reservoir heat reserves and optimum production methods for maximum recovery of those reserves.

The purpose of these determinations are to provide the basis for economic evaluation of geothermal exploitation projects. Without an adequate and thorough reservoir assessment knowledgable economic decisions cannot be made.

Evaluation of Reservoir Fluids

The key to evaluation of geothermal reservoirs is early determination of the nature of the reservoir and the production mechanism. Geothermal reservoirs can occur as one of three types:

(a) Vapor-dominated Geothermal fluids exist solely in the vapor phase.
(b) Liquid-dominated Geothermal fluids exist solely in the liquid phase with no vapor phase.
(c) A combination liquid-vapor system. A liquid reservoir is overlain by a

vapor-phase "cap", sustained by vaporisation of water deeper in the reservoir or source rocks.

Martin (1) has discussed how the nature of the reservoir thermodynamic conditions, and subsequent production can effect the recovery efficiency of the reservoir fluid particularly in liquid-dominated reservoirs. It is necessary therefore that early reservoir engineering evaluation determine the thermodynamic system that exists in the reservoir. Once the reservoir system is determined, the potential reserves can be determined. Several methods have been shown to be effective as evaluation procedures.

Volumetric assessment is the only approach available in early development stages. Because of the reliance on factors such as field areal extent, thickness, and porosity which are difficult to determine, the approach can be error-prone particularly in shattered igneous or metamorphic reservoirs.

Ramey and Whiting (2) have shown that the materials balance methods of petroleum engineering can be coupled with an energy balance to produce a means of determining reserves and future production from liquid reservoirs. The accuracy of the method increases with the length of time the reservoir has been in production. A modification of the equations can be made to adapt the approach to vapor-dominated systems.

Reservoirs with a reasonable period of production history can be evaluated using decline curves. Production rate vs time, production rate vs pressure, and cumulative production vs reservoir pressure (vapor reservoirs) can be used to determine future production and reserves.

These methods of reservoir assessment, when combined with reservoir pressure and geologic analysis can be used to determine the potential for natural and/or artificial recharge of the reservoir fluids. This is the essential objective of reservoir evaluation in terms of the primary resource, reservoir heat.

The materials balance equation contains a factor which describes fluid recharge from an acquifer. This factor can be calculated but it is more easily determined graphically as experience in petroleum engineering shows. This determination of recharge potential requires a lengthy period of production before existing appraisal methods can be used with any certainty.

Determination of Heat Reserves and Recovery Potential

Primary Heat Recovery

With an accurate geologic assessment of reservoir volume the original heat in the reservoir can be determined. This original heat in place (OHIP) is calculated as in (a) from readily obtainable data.

$$OHIP = 43850\,\Delta T\,(C_R P_R (1-S_F) + C_F P_F (S_F)) \quad (a)$$

On this basis the Geysers reservoir can be shown to contain about 3.7×10^8 BTU/acre.ft. or the equivalent of the chemical energy of 63000 Bbls/acre.ft. of crude oil. Depending on the nature of the reservoir rock the largest percentage of reservoir heat will be contained in the rock rather than in the fluids. Even with a high fluid recovery efficiency the vast majority of heat will be left in the reservoir. The reservoir heat recovered from produced fluids can be determined from the enthalpy of the produced fluids. Ultimate heat recovery can be determined by extrapolating the enthalpy of the produced fluid over the producing life of the fluid reserves. The result is the recovery efficiency of reservoir heat for primary fluid recovery.

Enhanced Heat Recovery

Increasing heat recovery requires the use of enhanced recovery methods. The most practical method is reinjection of condensed produced fluids. Assuming a large but finite reservoir with only fracture porosity and injection of cold condensed fluid equal to production rates (mass rates) the overwhelming heat content of the reservoir rock compared with that of the injected fluid would cause the water temperature to be increased to the temperature of the reservoir. This is done by a transfer of heat from the rock to the water, as the water moves from the injection well to the producing well.

Several important reservoir engineering problems must be considered in this process. The configuration of injection wells and injection rates must be determined so that a uniform cool water front is maintained to prevent the by-passing of hot primary reservoir fluids. The points of injection

must be selected to:

(a) Take advantage of existing natural influx of reservoir fluids and/or heat
(b) Be in communication with producing wells.

Whitherspoon et.al(3) has shown the effect of bottom zone injection in porous media. In fractured reservoirs injection in the bottom of the reservoir may be the most efficient method. The number of wells and the most efficient injection rates will depend on an accurate determination of the local heat flows within the reservoir rock.

In fractured, massive rock reservoir heat would be transferred to the injected water across a "heating surface" formed by the fracture walls. Maintenance of a stable temperature front would require that the rate of fluid injection be a function of the rate at which heat is conducted from the interior of the rock to the "heating surface." When so balanced the temperature front will only advance as the amount of heat in the rock declines thereby causing a decline in reservoir temperature. Because of the massive amounts of heat contained in such rocks the process of cooling could take an extremely long time during which period reservoir heat would be recovered through production of the reheated injected water.

Because of the increase in the amount of "heating surface" recovery of reservoir heat and the advance of the temperature front in porous media could occur more quickly. However, Witherspoon et.al (4) have found that under certain experimental conditions of sand thickness, heat and fluid flow the advance of a cold water temperature front could require over 100 years to travel 2400'. On a strictly technical basis this could mean that the life of a geothermal field could be extended from the current 30-40 years to 100-110 years.

It is of course theoretically possible to consider the removal of a very large percentage of reservoir heat with reduction of the reservoir temperature to near the temperature of the injected fluid. The limitation on this is economic. It may not be economically feasible to attempt high percentage recovery of reservoir heat. This is also part of the reservoir engineering requirement.

Conclusion

In conclusion, the production of the primary fluids from geothermal reservoirs will recover only a small fraction of the real resource, geothermal heat. Reservoir engineering methods are available to define and evaluate the enhanced recovery of heat through fluid injection. The use of these procedures as part of an accurate appraisal of geothermal energy potential.

Symbols

$\Delta T = T_R - T_w$
T_R = Reservoir Temperature
T_w = Working Temperature
C_R = Heat Capacity or Specific Heat of Rock
C_f = Specific Heat of Reservoir Fluid
P_R = Density of Reservoir Rock
P_f = Density of Reservoir Fluid
S_f = Reservoir Fluid Saturation as % of Total Reservoir Volume

References

(1) Martin, J.C., "Analysis of Internal Steam Drive in Geothermal Reservoirs", Journal of Petroleum Technology, Dec. '75.
(2) Whiting, Robert L. and Ramey, Henery J.: "Application of Material and Energy Balances to Geothermal Steam Production," Journal of Petroleum Technology, July, '69.
(3) Witherspoon, Paul A. et.al, "Analysis of Response of Geothermal Reservoirs under Injection and Production Procedures," SPE California Regional, April, '77.
(4) Witherspoon, Paul A. et. al, "Production and Reinjection in Geothermal Wells," Geothermal Resources Council, Transactions, Vol. 1, May, '77.
(5) McNitt, J.R., "Origin of Steam in Geothermal Reservoirs", SPE Annual Meeting, Oct., '77.
(6) Garg, S.K. and Pritchett, J.W. "On Pressure-Work, Viscous Dissipation and the Energy Balance Relation for Geothermal Reservoirs," Advances in Water Resources, Vol. 1, '77.

RESULTS OF SHORT-TERM CORROSION EVALUATION TESTS AT RAFT RIVER

R. L. Miller

Idaho National Engineering Laboratory
Idaho Falls, Idaho 83401

ABSTRACT

Four categories of short-term materials evaluations tests were conducted in geothermal fluid from well No. 1 of the Raft River Geothermal Experiment to obtain corrosion data relevant to the design of the Raft River Pilot Power Plant. The test programs are described and testing philosophies are discussed. The results of the tests are described and conclusions and recommendations are made for each type of material.

INTRODUCTION

The Geothermal Project at the Idaho National Engineering Laboratory (INEL) of the Department of Energy has identified materials selection as a major problem in geothermal plant design and fabrication. The tests reported here were undertaken primarily to evaluate the performance of selected candidate materials in the Raft River geothermal fluids.

This document is a report of exploratory and short-term evaluation tests conducted at the Raft River geothermal test facility. The tests were conducted under conditions close to those at the wellhead, i.e., at 150 psig and a temperature of about 270°F. Flow rates were maintained and at about 5 ft/sec. These tests consisted of:

1. A screening test designed to evaluate a number of alloy systems that have proven worthwhile in seawater and desalination applications. This test ran for 11 weeks.

2. Two short-term evaluation tests to study materials that passed the screening tests and to examine some additional materials for potential use. Samples were exposed for 5, 10, and 15 weeks according to the planned interval testing sequence.

3. A tube-to-tubesheet test designed to study galvanic and crevice corrosion in typical tubesheet and tube material combinations. These tests were limited to 3 and 5 weeks of exposure.

4. An examination of tubes, tubesheets and floating ends from a heat exchanger after a fouling test, for possible corrosion attack. These materials were examined after about 12 weeks of exposure.

The results of these tests are reported, and conclusions and recommendations are made for each type of material.

The environment used in these tests was geothermal fluid from well No. 1 (RRGE-1) of the INEL Geothermal Project at Raft River, Idaho. The suspended solids content of this fluid is of the order of 1 to 3 mg/kg of fluid. The dissolved solids content of this water is given in Table I with similar data for geothermal fluids from the other producing wells of the Raft River Geothermal Project.

Comparison of these data with Great Salt Lake or ocean water chemistry data to determine a possible origin does not suggest a direct relationship. The origin, flow direction, age and other geological parameters for the Raft River geothermal fluids is still unknown. However, these aspects of the Raft River geochemistry are under investigation and will be reported by others at a later date.

TABLE I

COMPARISON OF RAFT RIVER GEOTHERMAL FLUIDS

Species	Concentration		
	RRGE 1	RRGE 2	RRGE 3
Na^+	445	416	1185
K^+	31.3	33.4	97.2
Li^+	1.48	1.21	3.1
Mg^{+2}	2.35	0.58	0.60
Ca^{+2}	53.5	35.3	193
Sr^{+2}	1.56	1.03	6.7
F^-	6.32	8.32	4.55
Cl^-	776	708	2170
Br^-	<1.5	<1.5	<1.5
I^-	0.036	0.028	-
HCO_3^-	63.9	41.3	44.4
SO_4^{-2}	60.2	54.1	53.3
S^{-2}	0.1	0.256	-
SiO_2	114	126	151
Total Dissolved Solids	1560	1270	4130

Note: Concentrations are given in mg of dissolved species/kg of fluid.

OVERALL CONCLUSIONS AND RECOMMENDATIONS

The results of the foregoing tests have been definitive with respect to some alloys and nebulous for others. The following results, conclusions and recommendations are grouped according to generic classes of alloys.

Alluminum Alloys. The results of the screening tests were definitive with respect to the 1100, 5052, and 6061 aluminum alloys. These materials are un-acceptable for use in contact with the hot geothermal fluid.

Aluminum and its alloys depend on the stability of adherent oxide films of corrosion resistance. Raft River geothermal fluid is reducing, Eh = +105 mV. While this potential is too small to result in reduction of the oxide it may be large enough, at the temperature and pH of the hot fluid, to retard or prevent repair of damaged oxide sites. In any event, the corrosion rate is much too large for further consideration of these materials in the hot geothermal fluid.

Brasses and Bronzes. These materials gave acceptably low corrosion rates in the hot geothermal fluid. There appears to be a decreasing tendency toward dealloying with increasing copper content.

Admiralty brass has been selected as tube material for the boiler and preheaters. Aluminum bronze has been selected as tubesheet material because of its good weldability and low corrosion rate.

The most unfavorable data from the brass and bronze tests concern aluminum bronze containing 4-5% nickel. This material corroded at a rate about four times that of a similar, but nickel-free, material. The observed corrosion rate of the aluminum-nickel bronze was unacceptable and this alloy cannot be recommended for service in hot geothermal fluid environments. The reason for the accelerated rate of corrosion on this material appears to be a relatively selective attack on the nickel by sulfides in the geothermal fluid.

Copper-Nickel Alloys. This group includes Monel 400, 70Cu/30Ni, and 90Cu/10Ni alloys. As a group these alloys perform very well in seawater applications. In the geothermal fluid from RRGE-1, however, their performance was very poor. Large areas of corrosion were observed, surrounded by "mesas" of less corroded metal.

The corrosion behavior of these alloys has precluded their use in hot geothermal fluids containing even small amounts of sulfides.

Plain Carbon Steels. Pitting, crevice, and general corrosion in the plain carbon steels was too great for these materials to be viable candidates for thin structural members in direct contact with hot geothermal fluids. The gray cast iron showed some pitting and crevice corrosion but very little general corrosion.

Plain carbon steel and gray cast iron can be recommended for hot geothermal fluids service in thick structural members such as valves, fittings and pump parts if care is taken to monitor their condition.

Low-Alloy Steels. Pitting and crevice corrosion in these materials was sufficiently severe to preclude their use in some applications where they are frequently specified. These materials will be tested in a cooling tower environment to determine their applicability in aerated, cooled, and concentrated geothermal fluid treated with chromate and zinc to control corrosion.

Martensitic Stainless Steels. AISI 410 and AISI 440A stainless steels were the only two grades of martensitic stainless steels tested. The depth of corrosion was as much as 0.22 mm (0.008 in.) in 109 days. The typical use of these alloys is in pump shafts where crevices in bearings and seals are characteristic. Because of the severe corrosion in the test coupons, the use of these, or similar, alloys in any application involving hot geothermal fluid is not recommended.

Austenitic Stainless Steels. Several grades of austenitic stainless steel have been tested. These are AISI types 304 and 316 and the Allegheny-Ludlum alloys 6X and 216. The stability of these materials in the geothermal fluid varies according to the chromium, nickel and molybdenum content of the steel. The molybdenum-containing steels were somewhat more resistant to corrosion than was AISI 304 stainless steel.

The 304 stainless steel showed pitting and crevice corrosion to the extent that the use of this material is direct contact with the hot geothermal fluid is not recommended. The flat AISI 316 stainless steel coupons were superior to the AISI 304 stainless steel coupons; however, the AISI 316 stainless steel tubes in the tube-to-tubesheet test showed definite pitting. AISI 316 stainless steel is not recommended until longer-term tests show this material to be stable in the hot geothermal fluid.

Both alloys 6X and 216 were significantly better than the AISI 304 stainless steel and somewhat superior to the AISI 316 stainless steel. Except for some minor pitting, the corrosion in these alloys appeared to be of the order of the surface roughness of the coupons. The use of Allegheny-Ludlum 6X

and 216 alloys is recommended where their mechanical properties can be used to advantage.

Ferritic Stainless Steels. Ferritic stainless steels are usually more difficult to fabricate and less corrosion-resistant than the austenitic materials. Two grades of ferritic stainless steel were tested: Allegheny-Ludlum alloys 29-4 and 29-4-2. These materials showed outstanding resistance to corrosion in the RRGE-1 geothermal fluid environment. These materials are recommended for use where their mechanical properties can be used to advantage.

Nickel-Base Alloys. Hastelloy G and Inconel 625 were the two nickel-base alloys tested in the RRGE-1 geothermal fluid. Hastelloy G showed some minor pitting in both the flat coupon tests and the tube-to-tubesheet test. This is a wear-resistant alloy and where this property is required, the use of Hastelloy G is recommended.

Inconel 625 gave outstanding performance in all tests. The use of this material in contact with the geothermal fluid is recommended if its mechanical and physical properties are adequate.

Cobalt-Base Alloys. Haynes 6B, the only cobalt-base alloy used in the foregoing test, gave very good performance. This is wear-resistant material and its use in contact with the geothermal fluid is recommended where this property is required.

Titanium. ASTM B 265, Grades 2 and 12, titanium were used in several tests. This material has given outstanding performance in all tests and its use is highly recommended. One precautionary note should be made. Crevice corrosion of the metal is possible in other metal-to-metal joints or in contact with TFE at temperatures above about 149°C (300°F). Since the Raft River geothermal fluids are tending toward this temperature in the hotter wells, care should be taken in selecting titanium without further testing.

THE EFFECT OF VAPOR-PRESSURE LOWERING UPON PRESSURE DRAWDOWN AND BUILDUP IN GEOTHERMAL STEAM WELLS

A. F. Moench and W. N. Herkelrath

U.S. Geological Survey
Water Resources Division
345 Middlefield Road
Menlo Park, CA 94025

ABSTRACT

The equilibrium vapor pressure of liquid water in an unsaturated porous medium is less than the steam-table value. This phenomenon is incorporated into a finite-difference model for the production of steam in vapor-dominated geothermal reservoirs. In the model the steam is assumed to be produced by boiling of immobile liquid water in the vapor-dominated zone. Assuming radial symmetry, plots of pressure buildup and drawdown are obtained both with and without vapor-pressure-lowering. The results show that whereas pressure drawdown is virtually unchanged, the pressure buildup curve is significantly different when the vapor-pressure lowering effect is included. The pressure plateau predicted by the model without vapor-pressure lowering is eliminated, and the response is similar to that expected for noncondensable gas.

INTRODUCTION

As conceptualized by White, Muffler, and Truesdell (1971), vapor-dominated geothermal systems contain liquid water and steam together in a porous or fractured rock matrix. The liquid phase is believed to be held within the smallest pores and crevices by surface tension and adsorption.

As is commonly observed in soil systems (e.g., Westcot and Wierenga, 1974), the equilibrium vapor pressure of water in a porous medium decreases as the liquid saturation decreases. This "vapor-pressure-lowering" effect has been observed at elevated temperature for porous silica beads (Nonaka and Ishizaki, 1977) and in an artificial sandstone (Chicoine, and others, 1977).

Moench and Atkinson (1977) presented computed drawdown and recovery curves for geothermal steam wells with an immobile vaporizing liquid phase. In such a system vaporization of the liquid during steam production results in drying around the wellbore and the creation of a zone of superheated steam which increases in volume in direct proportion to production time. The purpose of this paper is to demonstrate the effect of a hypothetical vapor-pressure lowering upon pressure drawdown and buildup and upon the liquid-water saturation distribution in a system under production.

APPROACH

The method of analysis involves the use of a finite-difference model for the radial flow of steam in the presence of an immobile vaporizing or condensing liquid phase. The model is adapted from the one-dimensional, two-phase model of Moench (1976). Results are generated for realistic physical parameters, and are presented in terms of standard dimensionless pressure-squared and time groupings. The analysis assumes an initially constant temperature and pressure in the aquifer and an initially uniform distribution of liquid-water which partially fills the void space. It is also assumed that the steam and liquid water in the reservoir are in local thermal equilibrium with the reservoir rocks, and that temperature changes occur only as a result of vaporization and condensation. In the example which follows permeability, porosity, and well discharge are constant.

In this study a functional relationship between vapor pressure and liquid-water saturation was needed. Measurements of vapor pressure and liquid saturation in the rocks forming vapor-dominated geothermal systems have not been made. However, in order to illustrate the possible effects of vapor-pressure lowering, the following empirical expression was used (Herkelrath):

$$P_v = P_o \exp(-CS^{-4}), \qquad (1)$$

in which C is a constant. As shown in figure 1, there is reasonable agreement between the relative vapor pressure calculated from equation 1 and measurements of vapor pressure in a fine sand at room temperature (Westcot and Wierenga, 1974). There is evidence that the relative vapor-pressure-versus-saturation curve is not highly temperature sensitive (Nonaka and Ishizaki, 1977). Therefore, as a first approximation, C was assumed to be independent of temperature.

RESULTS

Figure 2 is a comparison of computed dimensionless pressure drawdown at the bottom of the production well with and without vapor-pressure lowering. Also shown is the drawdown curve for a

noncondensable gas (superheated steam). Values of the parameters used and definition of the dimensionless groups are given in tables 1 and 2.

As shown in figure 2, the pressure falls more rapidly when the vapor-pressure-lowering effect is taken into account. As pointed out by Moench and Atkinson (1977), the curves are displaced from the noncondensable gas curve because the vaporization process increases the apparent compressibility of the steam.

Figure 3 shows computed dimensionless pressure buildup using the dimensionless Horner time group. Without vapor-pressure lowering the response is similar to that presented by Moench and Atkinson (1977); there is an anomalous plateau in the pressure buildup caused by condensation near the well. With vapor-pressure lowering, the pressure plateau is shifted to very early times, and the response is similar to that for noncondensable gas. The shift in the plateau is a result of the fact that when vapor pressure lowering is included in the model, condensation begins immediately after shut-in.

Figure 4 illustrates the liquid water saturation distribution at shut-in time. With vapor-pressure lowering there is more liquid water present in the reservoir near the wellbore, and less liquid farther away. Because in this study temperature is only a function of the amount of vaporization or condensation which occurs at a given location, there is correspondingly less temperature reduction in the vicinity of the wellbore.

CONCLUSIONS

Including a vapor-pressure-lowering effect in the model increased the rate of pressure drawdown at the wellbore only slightly. On the other hand, the effect upon pressure buildup was to virtually eliminate the pressure plateau that exists in the model without vapor-pressure lowering. The result is a nearly linear buildup curve similar to that expected for a noncondensable gas. This may explain why pressure buildup data from geothermal steam wells do not commonly exhibit a pressure plateau.

Putting vapor-pressure lowering into the model changed the liquid saturation, and as a consequence, the temperature distribution in the reservoir. Complete drying near the wellbore did not occur, resulting in increased boiling (and greater temperature reduction) farther from the well.

Table 1.--Notation

P_D	dimensionless pressure squared $= \frac{\pi k h M_w}{q \mu Z_i R T} (P_i^2 - P^2)$	t_D	dimensionless time $= \frac{kt}{\phi \mu \kappa r_w^2}$
r_D	dimensionless distance $= \frac{r}{r_w}$	S	liquid-water saturation (percent of void space)
r	radial distance	S_i	initial liquid-water saturation
r_w	well radius	t	time
q	production rate	t_o	production time
P	pressure	Δt	time since shut-in
P_i	initial pressure	μ	steam viscosity
P_v	vapor pressure	Z_i	initial compressibility factor
P_o	saturated vapor pressure for flat surface interface at prevailing temperature.	R	gas constant
k	permeability	T	temperature
h	reservoir thickness	ϕ	porosity
M_w	molecular weight water	κ	steam compressibility

Table 2.--Values of Parameters Used

P_i	30×10^6 dynes/cm^2
k	7×10^{-8} cm^2
h	714 cm
q	2.78×10^4 g/s
ϕ	0.10
T	507 ^oK
S_i	0.10
ρ_s	2.3 gm/cm^3
c_{ps}	9.6×10^6 dyne-cm/(gm^oC)
r_w	20 cm
t_o	3.5×10^3 S
C	5.2×10^{-7}

NOTE: Values of remaining parameters are the known properties of water at the prevailing temperature and pressure.

REFERENCES

Chicoine, S.D., Strobel, C.J., and Ramey, H.J.,Jr., 1977, Vapor pressure lowering in two-phase geothermal systems: Paper 6767 presented at the 52nd Annual Fall Technical Conference of the Society of Petroleum Engineers of AIME, Denver, Colo., Oct. 9-12.

Herkelrath, W.N., 1977, The "heat-pipe" effect in vapor-dominated geothermal systems: Proceedings of the 3rd Workshop on Geothermal Reservoir Engineering, Stanford University, Stanford, Calif., Dec. 14-16.

Moench, A.F., 1976, Simulation of steam transport in vapor-dominated geothermal reservoirs: U.S. Geol. Survey Open-File Report 76-607, 43 p.

Moench, A.F., and Atkinson, P.G., 1977, Transient pressure analysis in geothermal steam reservoirs with an immobile vaporizing liquid phase--summary report: Proceedings of the 3rd Workshop on Geothermal Reservoir Engineering, Stanford University, Stanford, Calif., Dec. 14-16.

Nonaka, A., and Ishizaki, E., 1977, Stepwise multi-layer adsorption of water vapor on silica at temperatures from 130 to 150^oC: Jour. of Colloid and Interface Sci., v. 62, p. 381-388.

Westcott, D.W., and Wierenga, P.J., 1974, Transfer of heat by conduction and vapor movement in a closed soil system: Soil Sci. Soc. Amer. Proc., v. 38, p. 9-14.

White, D.E., Muffler, L.J.P., and Truesdell, A.H., 1971, Vapor-dominated hydrothermal systems compared with hot-water systems: Econ. Geology, v. 66, p. 75-97.

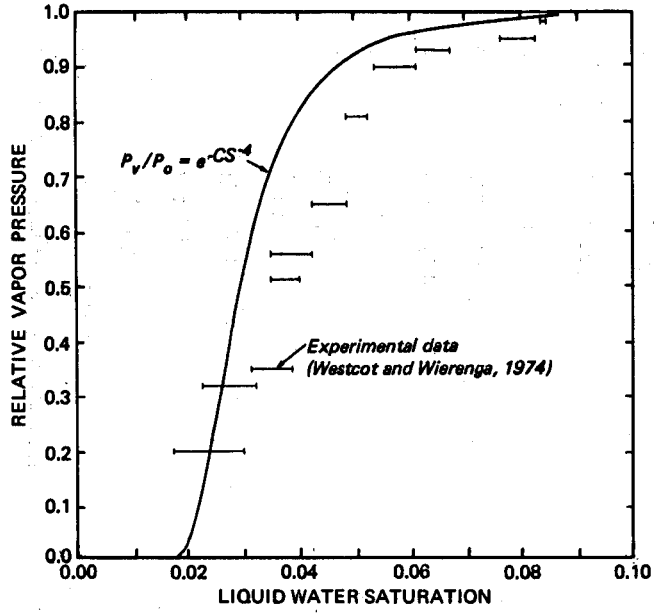


FIGURE 1. – Dependence of relative vapor pressure upon liquid saturation in a find sand.

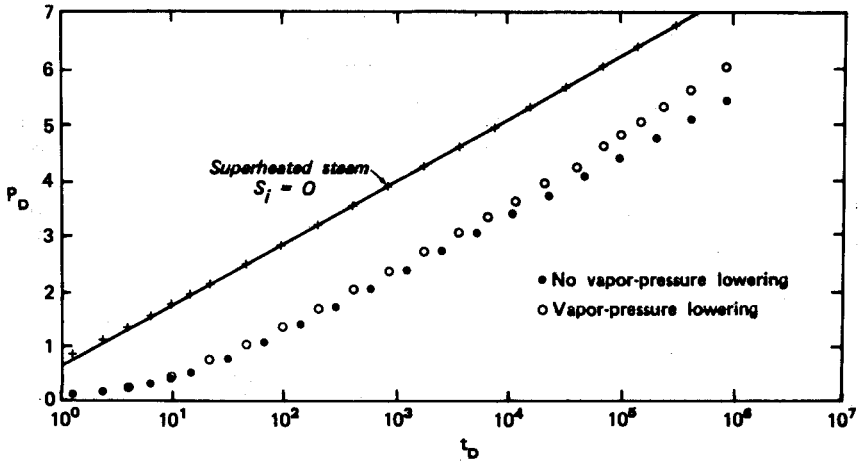


FIGURE 2. – Pressure drawdown versus time showing the influence of vapor-pressure lowering. Drawdown for superheated steam shown for comparison.

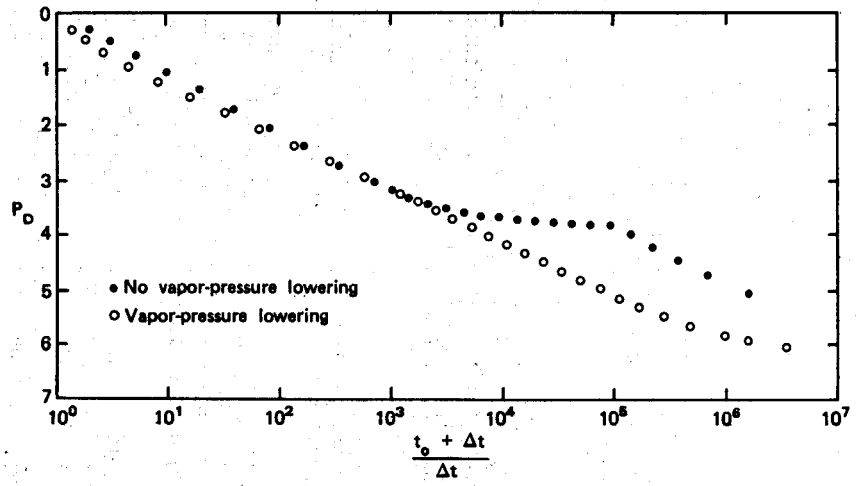


FIGURE 3. – Pressure buildup showing influence of vapor-pressure lowering.

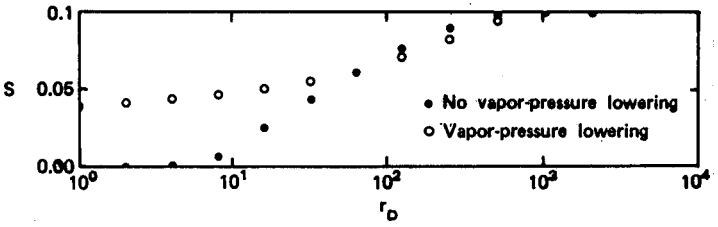


FIGURE 4. – Liquid water saturation distribution with and without vapor-pressure lowering at shut-in time.

Geothermal Resources Council, TRANSACTIONS, Vol. 2 July 1978

UTILIZATION OF GEOTHERMAL COOLING WATERS FOR WASTE CONTAINMENT

Robert D. Morrison

SCS ENGINEERS
LONG BEACH, CALIFORNIA 90807

ABSTRACT

Geothermal power production utilizing a binary conversion process requires a substantial quantity of water for the cooling of the secondary or working fluid. Once this cooling water has left the condenser in such a system, it requires some form of process to lower its temperature. Several process alternatives are available: an evaporative dry cooling tower, a wet cooling tower, or a cooling lake. In those operations where a cooling lake is utilized or where large amounts of makeup water are stored, certain design parameters can be easily integrated into this cooling loop for the purpose of isolating geothermal or associated wastes. The necessary physical conditions and benefits of this arrangement are the subject of this paper.

An integral component of either a binary or a hot dry rock energy conversion process is the large amount of water required. Water consumption in such energy generation facilities has been conservatively estimated at seven litres of water per kilowatt hour produced (U.S. Federal Energy Administration 1977).

In addition to this water demand, future geothermal plants may rely heavily upon the use of their otherwise waste heat by nearby industries in order to lower the cost of energy conversion. These industries will in turn require water for their various processes. The integration of these process waters and geothermal cooling water in a beneficial arrangement could provide a substantial economic contribution to any such multi-purpose installation.

Waters required for a binary energy conversion system may be cooled using one of three alternatives: a dry evaporation tower, a wet evaporation tower, or a cooling lake (Resource Planning Associates 1977). Figure 1 illustrates the typical arrangement of these choices and their sequence in the cooling cycle. In those instances in which a cooling lake is utilized, several adaptations can be incorporated into the loop to contain waste products generated by either the geothermal or associated activities. Success of this procedure is predicated upon a number of physical conditions:

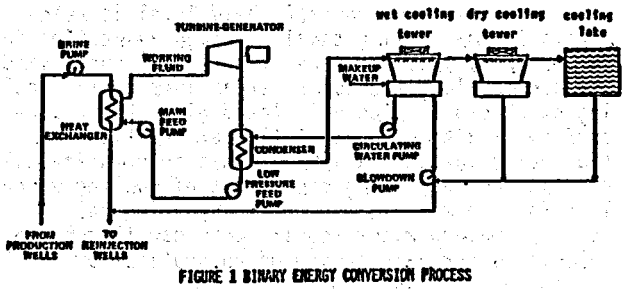


FIGURE 1 BINARY ENERGY CONVERSION PROCESS

- a large volume of cooling water
- a shallow, impermeable geologic boundary
- isotropic and homogeneous sediments underlying the canal
- available land.

When these four conditions are met, the cooling lake can be restructured into a canal. By redesigning this segment of the cooling cycle, a natural system can be realized for isolating any wastes placed into a disposal pond within the loop.

Figure 2 illustrates the configuration of this proposed design.

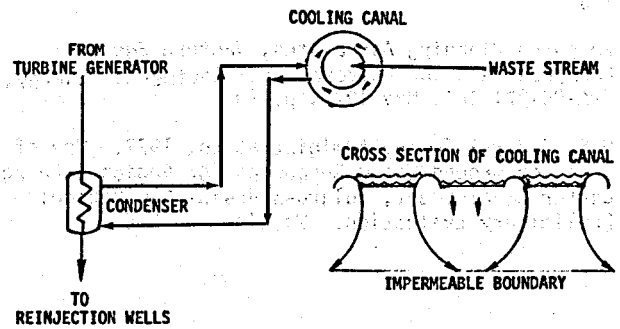


FIGURE 2 COOLING CANAL/DISPOSAL CONFIGURATION

This simplified version of the system demonstrates how the cooling waters would flow around the disposal area and thence to the condenser to complete

the cooling cycle. The cross section in Figure 2 illustrates how the cooling canal could be utilized for isolating the waste lagoon hydrologically.

This wastewater disposal technique relies upon controlled leakage of waters in the cooling canal to a level where the subsurface soils are saturated to the underlying geologic boundary. The process by which this hydrologic mound is realized is illustrated in the cross section of the cooling canal in Figure 2. The arrows shown infiltrating from the ponds indicate the means by which the hydrologic boundary conditions on the perimeter of the waste pond can isolate the wastes in the disposal pond.

When detailed subsurface conditions are known and a controlled hydrostatic head level is maintained in the cooling canal, seepage velocities in the disposal lagoon can be essentially immobilized. Velocities along the outer streamlines of the cooling canal can also be calculated given known subsurface conditions, especially permeability (Polubarinova-Kochina 1962). This information will provide data regarding the amount of cooling water lost for the maintenance of the hydrological mounds. Makeup water requirements can thereby be calculated for maintenance of an equilibrium within the cooling loop.

The inclusion of this simple extension of the cooling loop in a binary process can provide an attractive economic incentive, especially in a situation where energy production is marginally possible. Trade-offs between geothermal energy production activities with other processes must be pursued if this resource is to provide a substantial alternative energy source.

References

Polubarinova-Kochina, P. Y., 1962. Theory of Groundwater Movement. Translated by R. J. M. DeWiest. Princeton University Press, Princeton, N.J.

Resource Planning Associates, Western Energy Resources and the Enivornmental Geothermal Energy, EPA-PB-271 561, May 1977, p. 60.

U.S. Federal Energy Administration, 1977. Use of Brackish Ground Water Resources for Regional Energy Center Development, Tularosa Basin, New Mexico: Preliminary Evaluation. Washington, D.C.

RESERVOIR ENGINEERING STUDY OF A PORTION OF THE SALTON SEA GEOTHERMAL FIELD

John G. Morse and Lewis D. Thorson

LAWRENCE LIVERMORE LABORATORY
LIVERMORE, CALIFORNIA 94550

ABSTRACT

A well testing program is being conducted in the Salton Sea Geothermal Field in the vicinity of the Geothermal Loop Experimental Facility. Six well tests have been conducted as of January 15, 1978. Equipment has been developed and modified for use in the corrosive hot temperature brine environment. A computer program using superposition of analytic solutions is being developed to assist in analyzing the data. Initial results indicate that the reservoir has horizontal permeabilities of 100 to 500 md while vertical permeabilities across the shale layers are from 0.1 to 1.0 md.

Work performed under the auspices of the U.S. Department of Energy, Contract No. W-7405-Eng-48.

A series of well tests are being conducted on wells in the vicinity of the Geothermal Loop Experimental Facility (GLEF) located in the Salton Sea Geothermal Field, Calipatria, California. These tests involve monitoring the pressure transient responses of observation wells due to production and injection of geothermal brine. An additional series of tests involve the direct measurement of pressure transients in the injection and production wells. The objective of the well testing program is to measure flow parameters of the geothermal reservoir. Flow parameters of interest in this study are the horizontal and vertical permeability, injectivity of injection well and location of possible barrier or recharge boundaries. These tests are being conducted with the consent and invaluable cooperation of Magma Power Company and San Diego Gas and Electric Company. Well testing was begun in June of 1977. Six tests have been conducted as of January 15, 1978. Analysis of pressure transients observed during well tests requires reasonably optimal production, injection, start-up and shut-in conditions. Uncertainty in the computed reservoir parameters is directly related to how "optimal" test conditions are. To obtain "optimal" test conditions at the GLEF site would have required a complete restructuring of the operating plan for the GLEF which was not a feasibile approach. The approach presently being used is to coordinate the tests to coincide with the operating plans of the GLEF and obtain the best available data. Despite the somewhat less than optimal testing conditions completed tests have produced some useful data. Wells involved in the study are shown in Figure 1.

The testing period through January 15, 1978, has provided invaluable field experience in conducting well tests in the highly corrosive environment of the Salton Sea Geothermal Field (SSGF). The first five tests have demonstrated the feasibility of and developed methods for the conduct of well interference tests in this hostile environment. Existing well field pressure monitoring equipment was modified for use in the SSGF. The Hewlett Packard quartz pressure transducer was modified to prevent failure of the cable head assembly. This involved the injection of a hot temperature stable grease into the cable head to isolate the electrical connections.[1] The modified

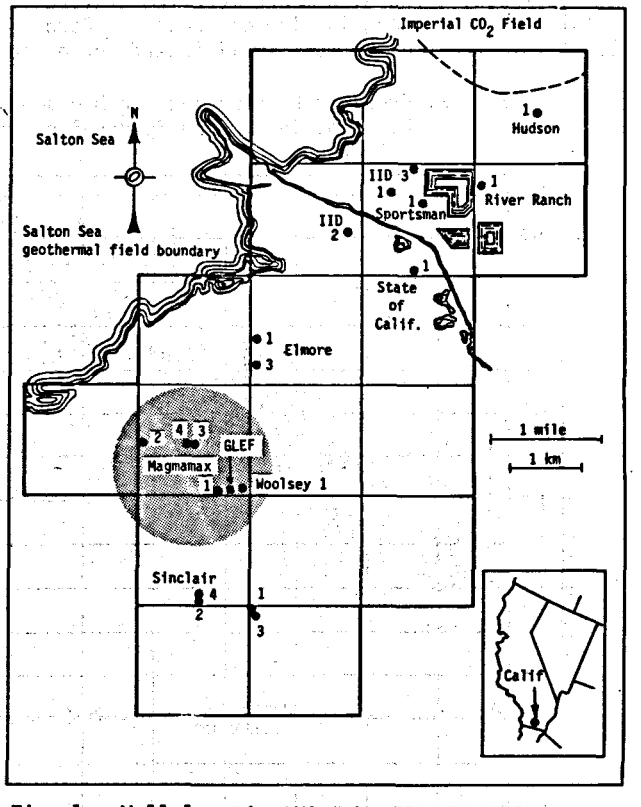


Fig. 1. Well locations in the SSGF. Wells in shaded area are presently used in support of the Geothermal Loop Experimental Facility, GLEF.

instrument package operated for two months in Magmamax #4 without failure. Other researchers have experienced failure in much less corrosive brines with unmodified cable head assemblies in two days to a week.[2]

The Sperry-Sun downhole chamber pressure monitoring system was used successfully at shallow depths in Magmamax #1 and Magmamax #4. The lubricator/packer assembly was modified to permit the use of a safety line in addition to the stainless steel tubing for support of the chamber. No chambers were lost in the wells and no tubing failure was experienced during the tests. Attempts to use the Sperry Sun chambers at depth in the SSGF wells has met with repeated failure of the tubing. The tubing fabricated from Fe-26Cr-1M_o commonly used with the Sperry Sun equipment was found to be unusable in the SSGF wells. Corrosion tests are presently being conducted on two tubing materials for use with the Sperry Sun equipment: Hasteloy C-276 and Incoloy 825. The tubing samples are being tested at a depth of 2400 ft. and temperature of 260°C in Magmamax #4. Initial results are very promising. A series of production tests is planned for April and May of 1978 using the Hasteloy C-276 tubing at reservoir depth.

In addition to the HP-Gauge and the Sperry-Sun equipment, two Paro-Scientific, Inc., quartz pressure transducers have been acquired and modified for use in the well testing program. These transducers have the same (.01 psi) accuracy as the Hewlett-Packard gauge, but are more temperature stable. With the acquisition of these two Paro-Scientific transducers multi-well interference and production tests can be conducted. During the rest of 1978, multiwell interference tests will be conducted using the wells involved in support of the GLEF and also wells Elmore #3 and Sinclair #3. Data from these tests should improve estimates of reservoir parameters for this portion of the SSGF.

Analysis of data from the planned tests and tests already completed presents several problems. Tests to date have shown significant diurnal noise in observation wells. This noise ranges from 0.3 to 3.0 psi in overall amplitude and is present regardless of the measuring device used. The gas filled Sperry Sun system tended to have high peaks in the noise due to heating of the tubing but the same basic noise was present when using the Hewlett-Packard quartz gauge. The basic signal noise appears to be related to the heating and cooling of the well head and/or the amount of CO_2 in the well column. In Figure 2, a composite pressure fluctuation plot obtained in Magmamax #4 is shown. The first portion of the plot was obtained with Sperry-Sun equipment. The second portion with the Hewlett-Packard quartz gauge. The pressures were measured at shallow depths and the pressure scale shows only the relative change in pressure.

Smoothing the data was accomplished by performing a 24-hour moving average on either side of each data point. Results of this technique are shown in Figure 3.

The analysis of the smoothed data from Magmamax #4 is a more complex problem than smoothing it. A brief description of the problems involved in analyzing data from Magmamamx #4 should help to

Fig. 2. Pressure Fluctuations In Magmamax #4 From 7/12/77 to 9/27/77. Data Obtained Using Sperry-Sun and Hewlett-Packard Equipment.

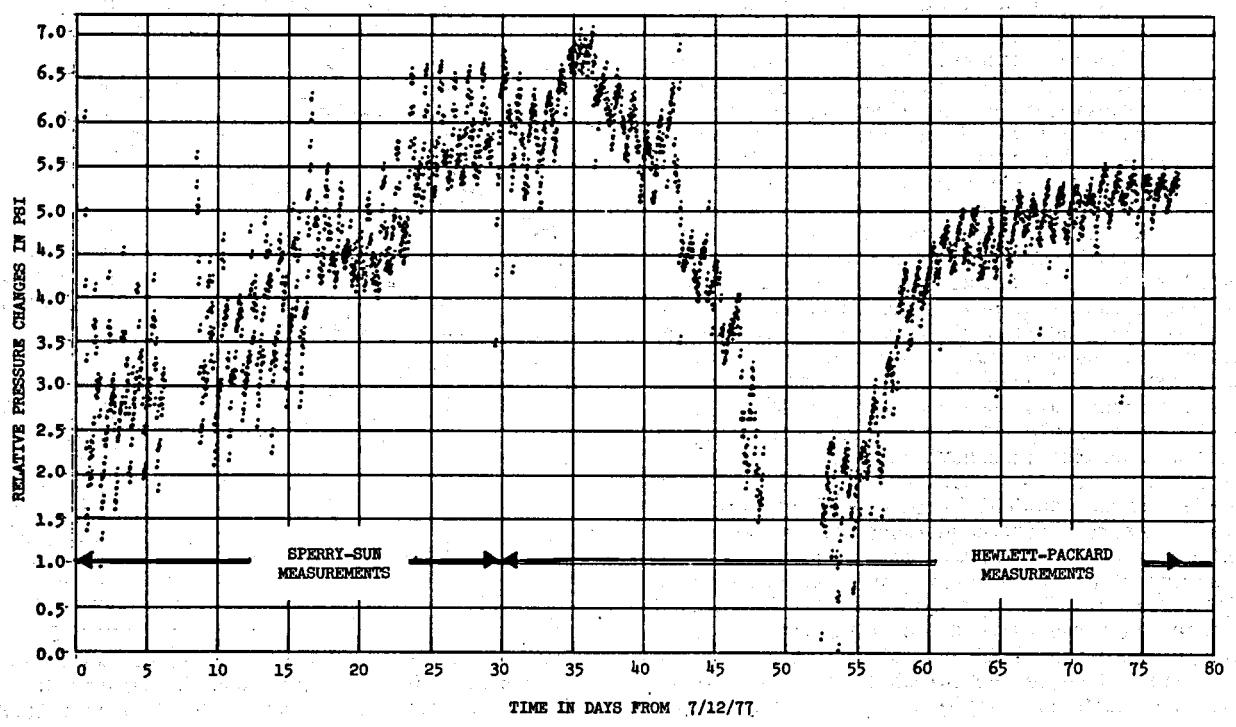
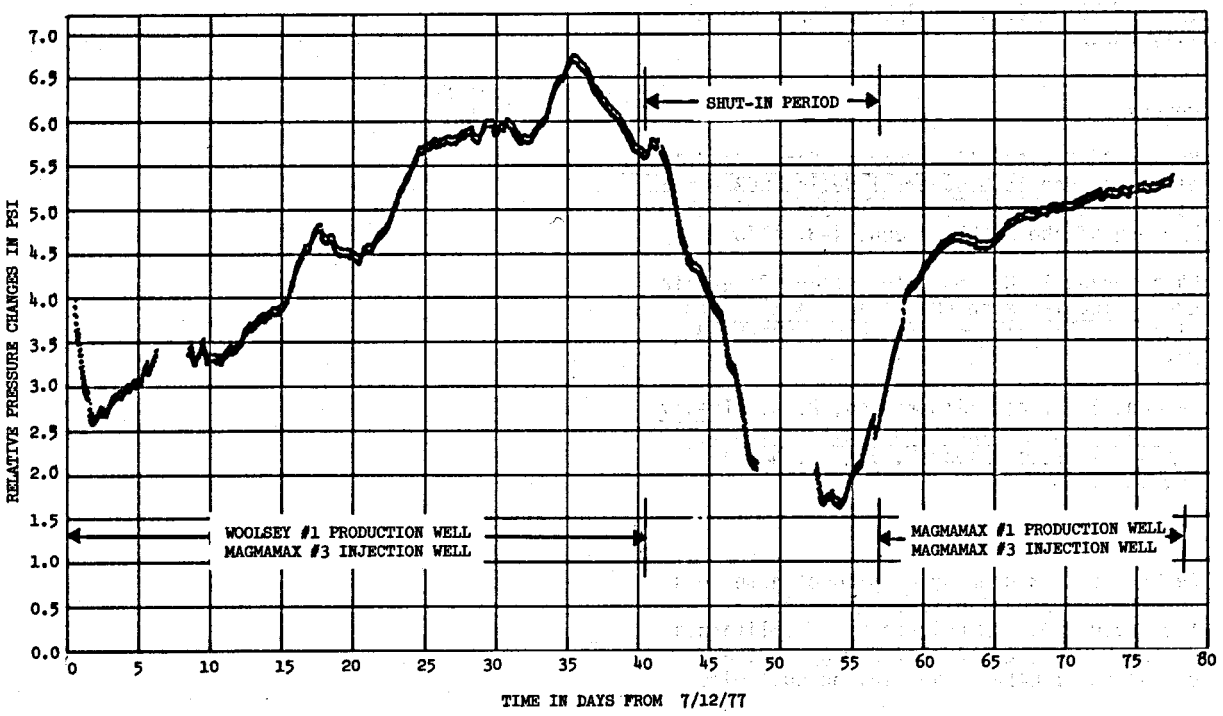


Fig. 3. Plot Of Smoothed Data From Magmamax #4 From 7/12/77 to 9/27/77. Data Smoothed Using 24 Hour Moving Average Around Each Data Point.



illustrate the complexities of data analysis in the SSGF. Magmamax #4 is located 50 ft. from the injection well, Magmamax #3. The bottom of the perforations in Magmamax #4 are 200 ft. above the top of the perforations in Magmamax #3. Separating the perforated intervals in the two wells is a series of thick shales. The over-pressure at injection depth in Magmamax #3 is 300 to 400 psi. At shut-in, the observed pressure fall-off in Magmamax #4 was 4.0 to 5.0 psi. Using the solution technique for a confined two aquifer system, developed by Neuman, S. P. and Witherspoon, P. A.,[3] an approximate value for vertical permeability across the shale layers of 0.1 to 1.0 millidarcies is obtained. A more refined analysis of the vertical permeability using the data from Magmamax #4 is not possible. Pressure response in Magmamax #4 was affected not only by the injection well but also by the production wells which could produce a 1.0 to 2.0 psi rise in Magmamax #4 at shut-in. Analysis is further hampered by the fact that production and injection flow rates vary considerably over the period of time data was collected at Magmamax #4.

Production, injection, and observation wells in the vicinity of the GLEF are perforated at varying depths which adds an additional complication to analysis of the well test data. Woolsey #1 was the production well until the shut-in period on August 22, 1977, see Figure 3. This well is produced from zones common to both the injection well (Magmamax #3) and the observation well (Magmamax #4). From start up on September 7, 1977, Magmamax #1 was the production well, (see Figure 3). Magmamax #1 produces all of its flow from the same zone as the observation well.

To adequately analyze well test data such as that obtained from Magmamax #4, we are developing a computer based solution technique. The program uses superposition of solutions to analyze pressure transients produced by complex flow histories from multiple wells. The code is sufficiently general to allow the use of analytic solutions such as for partially penetrating wells and multiple leaky aquifers. Use of the different analytic solutions will assist in taking into account the complex well field geometries.

The code is modular in structure making additions and modifications particularly easy. The capability of real time as well as hard copy graphical output is built-in and plays an important role in data analysis. The code operates with teletype interaction allowing a user maximum flexibility in fitting the data.

Application of this program to data obtained from the well tests should provide the most accurate estimates of reservoir parameters obtainable given the field conditions under which the tests are conducted.

This work is being carried out as part of the Lawrence Livermore Laboratory industrial support program which provides technological support for the joint Magma Power-San Diego Gas and Electric Company-DOE 10 mw Geothermal Loop Experimental Facility (GLEF).

References

1. Morse, J. G., Adapting Coaxial Cable Head Assemblies for Use in Geothermal Wells, UCRL-80152, Paper to be Presented at the 85th National Meeting of the AIChE on June 4-8, 1978.

2. Narasimhan, T. N. and Witherspoon, Reservoir Evaluation Tests on RRGE 1 and RRGE 2 Raft River Geothermal Project, Idaho, LBL-5958 May, 1977.

3. Neuman, S. P. and Witherspoon, P. A., Theory of Flow in a Confined Two Aquifer System, Water Resources Research, Vol. 5, No. 4, August, 1969.

Reference to a company or product name does not imply approval or recommendation of the product by the University of California or the U.S. Department of Energy to the exclusion of others that may be suitable.

"Work performed under the auspices of the U.S. Department of Energy by the Lawrence Livermore Laboratory under contract number W-7405-ENG-48."

Volcanism and the regional assessment of geothermal potential in west-central Utah

W. P. Nash, Charles Turley, James Petersen and F. H. Brown

Dept. of Geology and Geophysics, Univ. of Utah, SLC, UT 84112

Introduction. Late-Tertiary and Quaternary volcanism is common along the eastern margin of the Basin and Range Province in west-central Utah. The areal distribution, lithology, magnitude, and age of these volcanic systems, in conjunction with water chemistry data, can be used as criteria for the exploration for and assessment of geothermal resources on a regional scale.

Geologic Setting. West-central Utah is situated along the eastern margin of the Basin and Range Province and is characterized by episodic volcanism over the past 30 million years. The area of this study extends westward from the Wasatch Fault system and is dominated by the north-south structural trend of the Basin and Range Province. The whole region has a generally high heat flow, a thin crust and is seismically active. Several young volcanic centers are distributed along a north-south trend, and four Known Geothermal Resource Areas, Thermo, Roosevelt Hot Springs, Cove Fort, and Crater Springs, are contained within the area of study (Fig. 1).

Lithology. The region contains basalt and rhyolite lavas, the bimodal association characteristic of the Basin and Range Province in the late Cenozoic. Lithologic types are identified in figure 1. The prevalent model for the bimodal association is that in an area of high regional conductive heat flow, mantle derived basalts impart additional heat convectively which is sufficient to cause partial fusion in the lower crust, thus producing silicic magmas. As opposed to basalts, these silicic magmas may have substantial residence times in the upper crust. Accordingly, rhyolitic systems are an attractive initial target for geothermal exploration in the western interior of the United States. Usually the two rock types are associated in space and time, however, basaltic volcanism contemporaneous with rhyolite is absent in the Thomas Range and Honeycomb Hills.

Age relationships. The ages of volcanism over the past 10 m.y. are given in figure 1. Quaternary centers extend from Roosevelt Hot Springs K.G.R.A. in the south to Crater Springs K.G.R.A. to the north. The most recent activity has been in the Black Rock Desert where all the volcanism has taken place within the last one million years, and the latest eruption took place less than 1,000 years ago. The area contains White Mountain, the youngest rhyolite dated in Utah (0.4 m.y.).

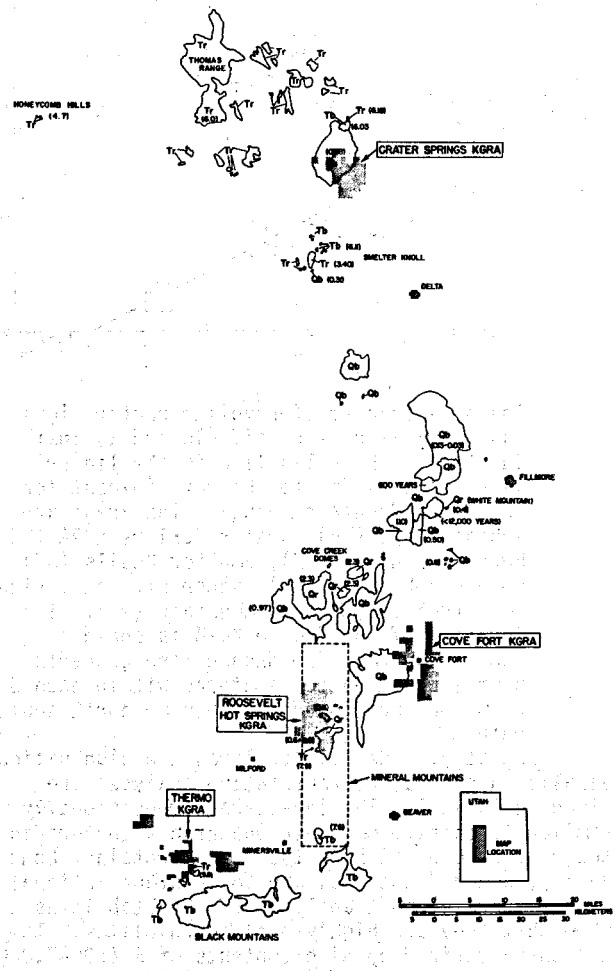


Fig. 1. Distribution of late Tertiary and Quaternary volcanic rocks in west-central Utah. Ages are shown in millions of years. Qb = Quaternary basalt, Qr = Quaternary rhyolite, Tb = Tertiary basalt, Tr = Tertiary rhyolite. K.G.R.A. administrative units are shown as shaded areas.

In terms of silicic volcanism, the pattern that emerges is eruption of rhyolite initially in the south at Thermo K.G.R.A. and Roosevelt K.G.R.A. around 10 and 8 m.y., respectively. Voluminous rhyolite was erupted to the north in the Thomas Range 6 m.y. ago. At 4.7 m.y. a small amount of rhyolite was erupted in the northwest to form the Honeycomb Hills. Subsequent rhyolitic volcanism shifted progressively southward to Smelter Knolls (3.4 m.y.), Cove Creek domes (2.3 m.y.), and Roosevelt (0.8-0.5 m.y.). The youngest rhyolite, White Mountain (0.4 m.y.) was erupted approximately 40 km northeast of the Cove Creek domes. With the exception of the single, small rhyolite dome of White Mountain, rhyolite centers younger than 8 m.y. show a regular distribution with respect to age and geographic locality (Fig. 2).

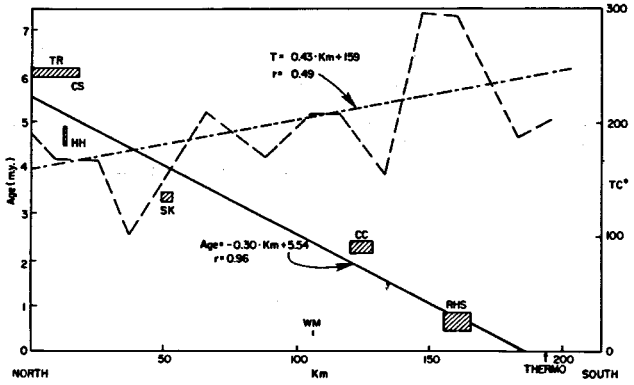


Fig. 2 Age of volcanism of rhyolite centers less than 8 million years old plotted against latitude. The solid line is the linear least squares fit to the data (except for the White Mountain point). The areas are Thomas Range (TR), Crater Springs KGRA (CS), Honeycomb Hills (HH), Smelter Knolls (SK), Cove Creek domes (CC), Roosevelt Hot Springs KGRA (RHS), and White Mountain (WM). The location of the Thermo KGRA is shown at about 190 km. The dashed line connects highest Na-K-Ca temperatures within each 5 km window projected to the same north-south path.

Chemistry. The silicic lavas are high silica, alkalic rhyolites; representative analyses are given in Table 1. The lavas are compositionally similar to those from other Quaternary centers in the western U.S. such as the Coso Mountains, Long Valley, Jemez Mountains, and Yellowstone National Park. Trace element analyses of the Utah lavas show that they are highly evolved rhyolites. They are characterized by high contents of F (500-7,800 ppm), Be (7-14 ppm), Nb (47-84 ppm), and Rb (335-808 ppm). This suggests that these lavas are derived from highly evolved magmas which probably have had significant residence times in the crust to allow extreme compositions to develop.

Regional exploration criteria. The data on age of volcanism, magnitude, and lithology combined with water chemistry (Parry and Cleary, 1978) provide some potentially useful information with regard to exploration for concealed geothermal resources. The criteria chosen here for delineating geothermal potential are 1) the location of rhyolite centers together with a measure of their size, 2) the location of all volcanic rocks younger than one million years, and 3) the location of waters which yield last wall-rock equilibration temperatures in excess of 200° using the Na-K-Ca thermometer (Fournier and Truesdell, 1973). These data are shown in figure 3.

Roosevelt Hot Springs, a proven geothermal resource has all three indicators (Lipman et al., 1978, Evans and Nash, 1978). Other volcanic centers typically have two indicators. Thermo K.G.R.A., Honeycomb Hills and the Thomas Range lack evidence of young volcanic activity. Crater Springs K.G.R.A., Smelter Knolls, and the Cove Creek domes lack evidence of hot water at depth.

Table 1. Chemical analyses of representative silicic lavas from west-central Utah

	1	2	3	4	5	6	7	8
SiO_2	76.89	74.61	76.69	63.51	73.06	75.33	76.52	76.45
TiO_2	0.23	0.05	0.19	n.d.	0.17	0.04	0.12	0.08
Al_2O_3	11.88	12.54	12.03	11.04	13.38	12.52	12.29	12.79
Fe_2O_3	0.87	0.05	0.84	0.25	0.41	0.33	0.31	0.30
FeO	0.18	1.00	0.10	0.43	1.29	0.82	0.46	0.29
MnO	0.06	0.04	0.04	0.03	0.16	0.07	0.05	0.10
MgO	0.21	0.10	0.09	0.05	0.58	0.27	0.08	0.12
CaO	0.49	0.64	0.74	11.08	1.12	0.47	0.64	0.40
Na_2O	3.01	3.85	3.26	3.63	4.34	3.99	3.80	4.39
K_2O	5.66	4.61	5.03	3.99	4.49	4.61	5.24	4.53
P_2O_5	0.06	n.d.	n.d.	0.03	0.09	0.04	0.02	0.06
CO_2	0.09	0.06	0.03	0.10	0.05	0.08	n.d.	n.d.
F	0.05	0.71	0.23	7.97	0.39	0.09	0.16	0.44
H_2O^+	0.09	1.50	0.47	0.10	0.09	0.82	0.12	0.10
H_2O^-	-	0.34	0.04	0.04	n.d.	0.10	0.06	n.d.
Sum	99.77	100.10	99.78	102.25	99.71	99.58	99.87	100.25
-O=F	0.02	0.30	0.10	3.36	0.23	0.05	0.07	0.19
Total	99.75	99.80	99.68	98.89	99.48	99.53	99.80	100.06
(ppm)								
Li	43	102	69	201	63	-	50	109
Be	7	12	11	11	9	-	6	12
Zn	25	55	30	20	65	-	40	45
Nb	50	45	85	50	35	-	25	35
Zr	165	110	100	50	115	-	100	90
Y	45	175	55	120	80	-	15	20
Sr	35	5	5	200	30	-	35	n.d.
Rb	335	460	405	810	285	-	195	340
Th	50	50	50	25	35	-	25	35
Pb	35	30	35	40	40	-	35	35
Ba	60	5	n.d.	n.d.	25	-	200	n.d.

1. Crater Springs K.G.R.A., CSV-12
2. Smelter Knoll, SK-75
3. Thomas Range, TR-79
4. Honeycomb Hills, HH-40
5. White Mountain, WM-3
6. Thermo K.G.R.A., BMV-2
7. Roosevelt K.G.R.A., MR-3A
8. Roosevelt K.G.R.A., MR-75-20

- = not determined
n.d. = not detected

Cove Fort K.G.R.A. has no silicic volcanism associated with it which has been dated at less than 17 m.y. in age, although silicic bodies are present to the southwest which warrant investigation.

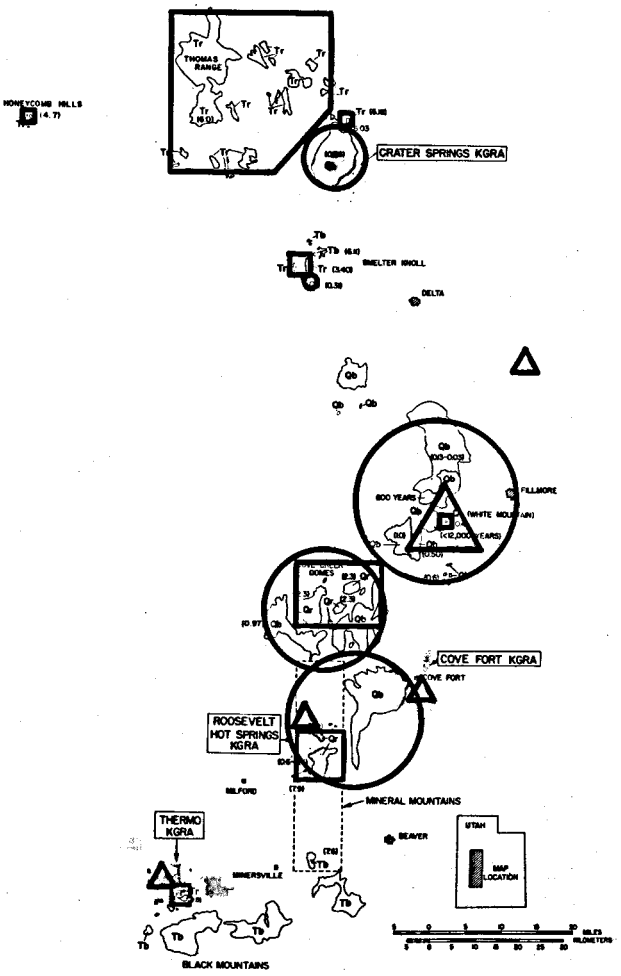


Fig. 3 Summary of exploration criteria. Rectangle = rhyolite, circles = volcanism less than 1 million years ago, triangles = Na-K-Ca temperatures greater than 200°C. The size of the symbols are adjusted to contain the areal extent of the volcanic fields or water samples, and thus provide some relative measure of the magnitude of each system.

One area other than Roosevelt with all three indicators is the Black Rock Desert. This region has the youngest basalt and rhyolite of the entire area together with calculated water temperatures in excess of 200°C. Only one rhyolite dome is present in the volcanic field (Fig. 4), however, very recent basalt is abundant. The southern portion of the area contains thermal springs and a Holocene tufa field which is growing with active springs at its north and south ends. Faulting is very recent (less than 600 years in some cases) and is aligned in a north-south direction. It appears that the locus of volcanism has been controlled by this structural trend for at least 0.6 m.y., and possibly for the last one million years. In spite of the small volume of rhyolite, the region represents an attractive area for detailed exploration for concealed heat sources.

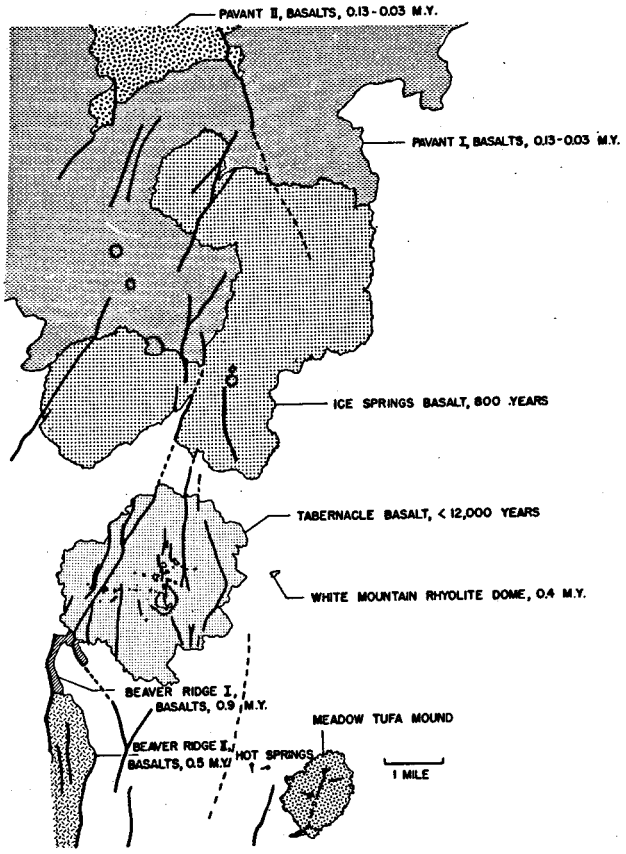


Fig. 4 Quaternary basalt flows in the vicinity of the White Mountain rhyolite dome, Black Rock Desert. Basalt ages are from Hoover (1974).

References

Evans, S. H., Jr. and Nash, W. P., 1978, Quaternary rhyolite from the Mineral Mountains, Utah U.S.A. (in press).

Fournier, R. O., and Truesdell, A. H., 1973, An empirical Na-K-Ca geothermometer for natural waters: Geochim. Cosmochim. Acta, 37, 1255-1276.

Hoover, J. D., 1974, Periodic Quaternary volcanism in the Black Rock Desert, Utah: Brigham Young Univ. Geol. Studies, 21, 3-72.

Lipman, P., Rowley, P., Mehnert, H., Evans, S., Nash, W., and Brown, F., 1978, Pleistocene rhyolite of the Mineral Mountains, Utah - geothermal and archeological significance: Jour. Research U.S. Geol. Survey, 6, 133-147.

Parry, W. T. and Cleary, M., 1978, Na-K-Ca and SiO_2 temperature estimates for Utah spring and well waters: Final Vol. 78-1, U.S. Geol. Survey Grant 14-08-0001-G-341, 51 p.

This work was supported by U.S. Geological Survey, Grant No. 14-08-0001-G-343.

HELIUM IN FUMAROLE AND WELL GASES AS AN INDEX OF LONG-TERM GEOTHERMAL POTENTIAL

John J. Naughton and Donald Thomas

Chemistry Department and Hawaii Institute of Geophysics,
University of Hawaii,
Honolulu, Hawaii 96822

ABSTRACT

We have used fumaroles and degassing vents around Kilauea volcano as models of producing geothermal areas. Excess helium has been found in gases from fumaroles characterized by long-term activity, and is absent in gases from short-lived hot spots, from dry vents or fissures formed by recent activity, and from old degassed lava lakes. From this it is inferred that the absence of helium in gases from geothermal areas would indicate that they receive heat from a limited magma body, and would be expected to yield extractable heat for only a comparatively short period. The geothermal well at Puna, Hawaii, has given positive helium indications.

Work performed under support from grants from the Hawaii Natural Energy Institute and the National Science Foundation, Grant EAR73-00201-A02.

One factor that must be of concern in the economic development of geothermal areas is the expected longevity of the sources as viable heat producers. Fumaroles and hot springs frequently are found as surface manifestations of such regions. Also fumaroles are generally associated with volcanoes. Kilauea volcano on the island of Hawaii has several of these in various stages of activity. Some have been continuously active throughout historic times and others appear and disappear sporadically depending on conditions from prior or impending eruptions. Isolated, crusted-over lava lakes and hot spots also exist. We have used these areas as models for various types of geothermal activity, and have investigated the changes of the composition of emitted gases with time. Here we will attempt to show the potential of helium as a gaseous indicator of geothermal potential.

Helium is present in the gases issuing from many fumaroles [1] and hot springs [2], and the isotopic composition

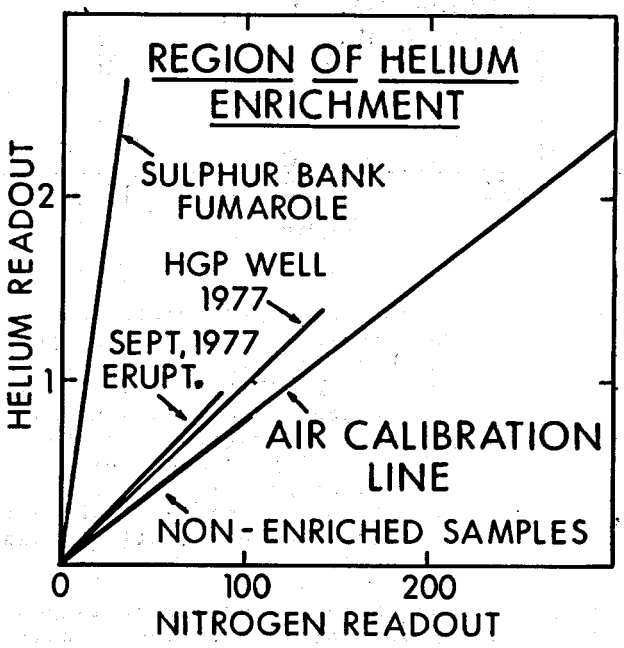


Fig. 1. Helium-nitrogen plot for standard air and for geothermal gases. Instrumental integrator readouts for each gas are in arbitrary units.

($^3He/^4He$ ratio) indicates that such gases tap sources deep within the crust of the earth, or even within the mantle [3][4]. The ready emission of this gas might be expected since its easy diffusion through hot silicates has long been known and studied. The concentration found in geothermal gases is low and requires special equipment for detection, but in some cases it can exceed the concentration in air by about two orders of magnitude.

We have sampled fumarolic and volcanic gases using various evacuated and pump-through devices, but generally we have favored collection into evacuated tubes which contain activated silica gel. This adsorbs certain of the gases and quenches the high temperature composition [5]. Also it prevents reaction between

H. I. G. Contributor No. 885

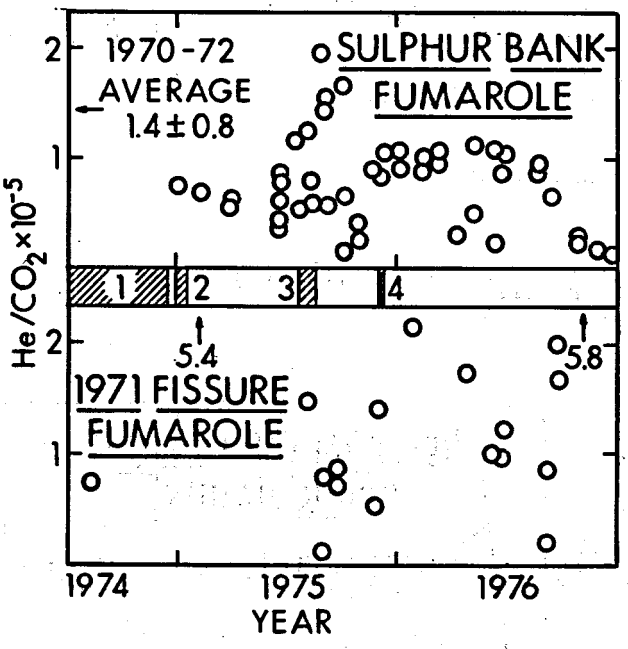


Fig. 2. Change of He/CO_2 ratios as a function of time for Sulphur Bank and 1971 Fissure fumaroles. Activity of neighboring volcanic complexes noted by numbered region in center. 1. Activity at Mauna Ulu (decreasing). 2. Kau eruption. 3. Mauna Loa eruption. 4. Earthquake. Small Kilauea eruption.

components which may occur during long-time holding at room temperature. Analyses of the collected gases has been carried out using gas chromatography with conventional thermal conductivity detectors [5]. For the analysis of helium in recent work we have used a small, very sensitive helium mass spectrometer (a "leak detector"). Each analysis is compared with that of an air standard in which the helium content is known and constant (5.24 ppm). A complete quantitative analysis of a geothermal gas also can be made with this equipment.

An indication of the presence of helium in excess of the content in air is sufficient for the purpose of this work. This can be made graphically by a plot of the instrumental readouts for helium and nitrogen (Fig. 1). A series of determinations are made on each sample to give a meaningful average. These plot as points on a straight line as the sample pressure is lowered by consumption in the analyses. The reference air sample is run, and is followed by the geothermal gas sample. An excess of helium is revealed by the position of the He vs. N_2 plot lines with reference to a similar plot obtained for the air standard (Fig. 1). Some data plots of recent collections are shown on this figure by way of illustration.

To study time related trends at a single fumarole we also have determined the complete gaseous composition, in some cases over a period of several years. From these data helium-to-carbon dioxide ratios can be calculated (Fig. 2). These are believed to be of greater geochemical significance than the analytical content of He in the total gas mixture since there is evidence that CO_2, like He, has its source deep in the magma column [6]. In addition it is a major component of almost all geothermal gases, and, in our experience, varies by only about 1% over a long period from a long-lived fumarole. Also it is little influenced by air infilteration or other meteoric imput as would be the case for the other major geothermal gaseous components (H_2O, O_2 and N_2). Thus it makes a good internal reference standard with which to compare other components such as helium. We have sought to relate this He/CO_2 ratio to the activity of the associated volcanic complex, but thus far have found no very certain correlation (Fig. 2). This type of study must, however, be systematically continued over long periods for such interrelations to be unambiguously detected.

From the He-N_2 plots, helium enrichment has been noted in the gases from the following sources: (1) Sulphur Bank, a solfotaric fumarole situated on an older Kilauea caldera rift to the northeast of the present caldera, which has been active continuously throughout historic times. This fumarole yields a varying flow of helium with an average concentration about two orders of magnitude greater than that found in air. Also it has a $^3He/^4He$ isotopic ratio greater than any other thus far found from a terrestrial source [4]. (2) The fissure produced by the August 1971 eruption on the floor of Kilauea caldera contains fumaroles that continue to yield helium in relatively high concentration. Fluctuations in the He/CO_2 ratio with time (Fig. 2) are evident for these first two high helium fumarolic areas, and these may be connected with eruption events at Kilauea, but many more closely spaced sample analyses are needed over a long period to definitely pin down on such correlation. (3) The fissure produced by the July 1974 eruption across the floor of Kilauea caldera at first showed a slight enrichment in helium, but this dropped off within a few months despite the continuous emission of hot gases.

It has become analogous to a typical "hot spot" in its behavior, and the excess of helium seems to have disappeared.

On the other hand we have found no evident enrichment of helium in the gases collected under the following conditions which might be expected to produce geothermally associated material: (1) Soil gases extracted from the thin soil cover near an erupting volcanic vent (Mauna Ulu); (2) gases from old lava tubes in a hot steaming area (a "hot spot" near prehistoric Kalalua crater); (3) gases from a very hot (~700°C) fissure near the vent at Mauna Ulu (which died out after a few weeks); (4) gases collected from deep within dry fissures into which lava from recent eruptions had withdrawn (May 1973 rift); (5) gases from a non-producing exploratory well drilled near the summit of Kilauea (Keller's well); (6) gases from fumaroles at the edge of Halemaumau crater; (7) and gases from a hole recently drilled by the U. S. Geological Survey through the thick crust of the old Kilauea Iki lava lake (formed 1959-60). We note then that helium seems to be absent in gases emitted from short lived "hot spots" or "rootless" regions, and these would be expected to yield extractable heat for only a relatively short period.

Finally we may conclude from the results obtained thus far that helium seems to be found only in gases from fissures and fumaroles which have a history of long-term, vigorous and continuous activity. Consequently, we may deduce that the continuous presence of excess helium in the gases being emitted from vents or wells in a possible geothermal area is a good indicator of the long-term potential of such a region as a viable geothermal source. Such excess helium has been detected in the gas from the Hawaiian Geothermal Project (HGP) well at Puna, Hawaii.

REFERENCES

[1] Naughton, J. J., J. H. Lee, D. Keeling, J. B. Finlayson and G. Dority, Helium flux from the earth's mantle as estimated from Hawaiian fumarolic degassing. Science, 180, 55-57 (1973).

[2] Roberts, A. A., I. Friedman, T. J. Donovan and E. H. Denton, Helium survey, a possible technique for locating geothermal reservoirs. Geophys. Res. Let., 2, 209-210 (1975).

[3] Mamyrin, B. A., I. N. Tolstikhin, G. S. Anufriev and I. L. Kamanskiy, Anomalous isotopic composition of helium in volcanic gases. Dokl. Akad. Nauk. S.S.S.R., 184, 1197-1199 (1969).

[4] Craig, H. and J. E. Lupton, Primordial neon, helium, and hydrogen in oceanic basalts. Earth Planet. Sci. Let., 31, 369-385 (1976).

[5] Naughton, J. J., E. F. Heald and I. L. Barnes, The chemistry of volcanic gases. 1. Collection and analysis of equilibrium mixtures by gas chromatography. J. Geophys. Res., 68, 539-544 (1963).

[6] Moore, J. G., J. N. Batchelder and C. G. Cunningham, CO_2-filled vesicles in mid-ocean basalt. J. Volcanol. Geotherm. Res., 2, 309-327 (1977).

Geothermal Resources Council, TRANSACTIONS, Vol. 2 July 1978

HYDROCARBON GASES IN SOME VOLCANIC AND GEOTHERMAL SYSTEMS

Nancy L. Nehring and Alfred H. Truesdell

U.S. GEOLOGICAL SURVEY, MENLO PARK, CALIFORNIA 94025

Introduction. The analysis of hydrocarbon gases in volcanic and geothermal systems has traditionally been limited to methane and occasionally ethane. Stoiber, et al. (1971) analyzed three gas samples from a fumarole on Santiaquitio Volcano, Guatemala and identified a wide range of organic compounds including aliphatic and aromatic hydrocarbons, aldehydes, ketones, alcohols, halogenated hydrocarbons, and sulfur compounds. Gunter (1978) analyzed several samples from Yellowstone National Park for the C-1 to C-4 hydrocarbons. The normal alkanes, isobutane, ethene, and propene were identified. The present work reports on the analysis of C-1 to C-6 hydrocarbons, including normal and branched alkanes, alkenes, and cyclic compounds, from a variety of volcanic and geothermal systems.

Method. Samples were collected in evacuated bottles containing NaOH using a procedure similar to that described by Giggenbach (1975). After analysis of residual gases (in headspace over NaOH), a 1-10 cc aliquot was taken in a gas-tight syringe and analyzed on a Hewlett-Packard 5700A gas chromatograph equipped with a flame ionization detector. Dual columns 6' by 1/8" were packed with Porapak Q and helium carrier gas was used at 60 psi inlet pressure. Each analysis was temperature programmed as follows: 30°C for 2 min, 8° per min to 150°C, and held at 150°C for 16 min. Representative chromatograms are shown in Figs. 1 to 4, and their peaks are identified in table 1. Identification of the gases was based on retention time and confirmed on representative samples by GC-MS using a Perkin-Elmer 990 gas chromatograph coupled through a membrane separator to a Bell and Howell 21-491 mass spectrometer. A 6-foot Porapak Q column was used with a helium flow of 20 ml/min. The analysis was temperature programmed as given above. The membrane separator was held at 20°C until the water was eluted, then held at 0° for the remainder of the analysis.

Discussion. Samples were obtained from several volcanic and geothermal systems. These systems were arranged in four groups on the basis of the gas analyses:

1. Fumaroles from the active volcanoes of Kilauea, Hawaii; St. Augustine, Alaska; and Mount Hood, Oregon.
2. Hot springs and fumaroles associated with igneous or crystalline rocks represented by samples from Steamboat Springs, Nevada and Lassen National Volcanic Park, Calif.
3. Steam and hot water wells associated with sedimentary rocks at Cerro Prieto, Mexico; Larderello, Italy; and The Geysers, Calif.
4. Systems such as Yellowstone National Park, Wyoming in mixed igneous and sedimentary terrane.

Gases from fumaroles in recent lava flows at Kilauea and St. Augustine are probably of volcanic origin with no contribution from sedimentary or organic sources (Fig. 1A and 1B). These samples are characterized by a generally low content of hydrocarbons; only the C-1 to C-4 normal alkanes and the corresponding alkenes are present. The difference in the size of the peaks between different chromatograms is likely due to dilution of the samples by varying amounts of carbon dioxide or by near-surface atmospheric contamination. A sample from a crater fumarole at Mount Hood, Oregon, produced a similar chromatogram (Fig. 1C), although Mount Hood last erupted in the 1700's and the fumaroles are now well below boiling.

Methane is though to be one of the gases originally present in a degassing magma (Ellis, 1957). The other hydrocarbon gases are in reasonable ratios to have been formed by the pyrolysis of methane (Gordon, 1948).

Distribution of gases from igneous and crystalline rock areas related to past volcanism such as Steamboat Springs, Nevada, and Lassen Volcanic National Park, Calif. (Figs. 2A and 2B) show a strong resemblance to the volcanic gases. Methane concentrations are higher, often constituting 1 percent or more of the total gases. A triplet identified as 1-butene, n-butane, 2-butene is characteristic of these samples and also appears in the Kilauea chromatogram. C-5 and C-6 hydrocarbons are generally present in small amounts.

The increased methane may be generated from the reaction of carbon dioxide with hydrogen in the presence of liquid water (Hulston, 1964). Sediments may contribute small amounts of methane

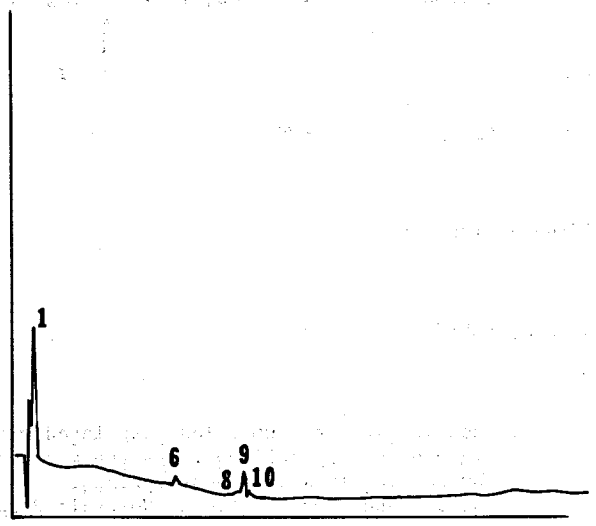


Fig. 1a KILAUEA, HAWAII

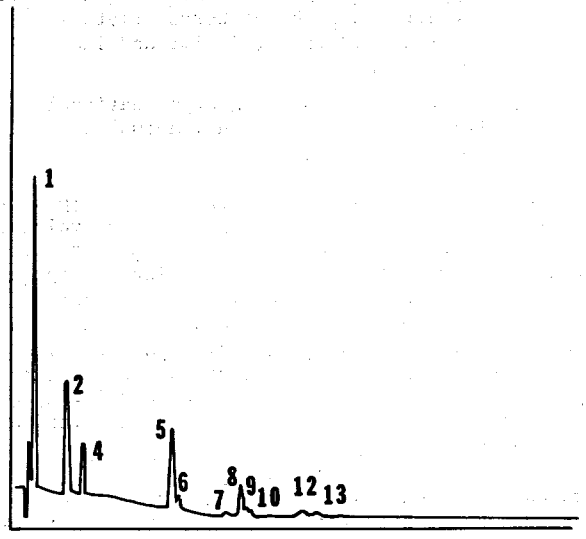


Fig. 1b ST. AUGUSTINE, ALASKA

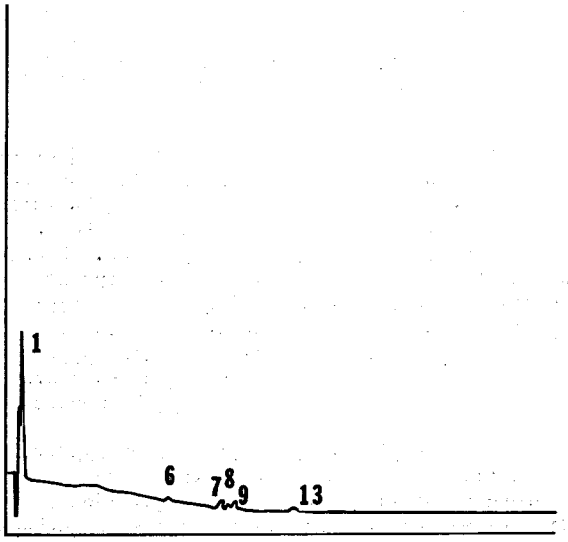


Fig. 1c MT HOOD, OREGON

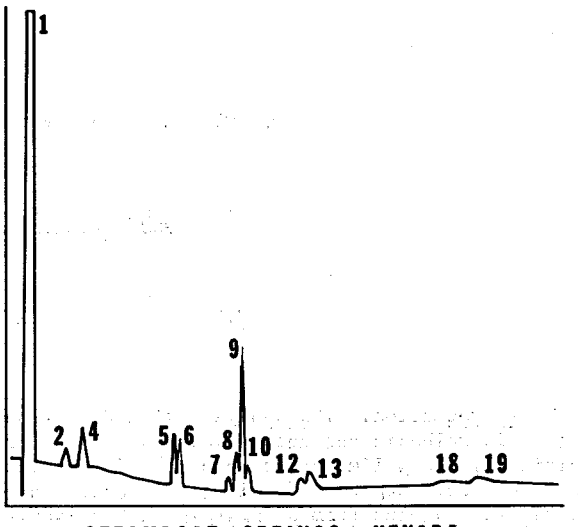


Fig. 2a STEAMBOAT SPRINGS, NEVADA

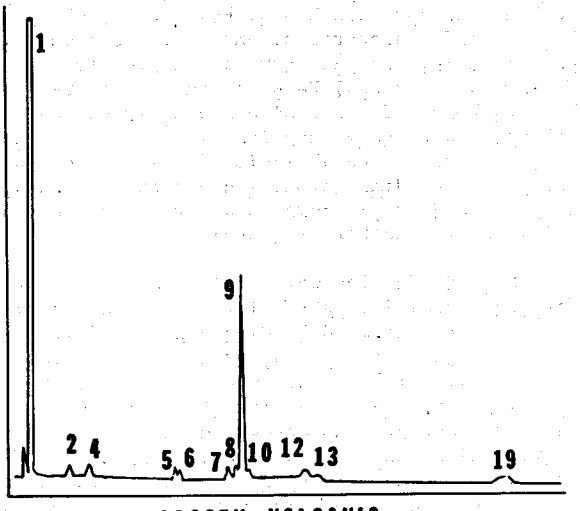


Fig. 2b LASSEN VOLCANIC NATIONAL PARK, CALIFORNIA

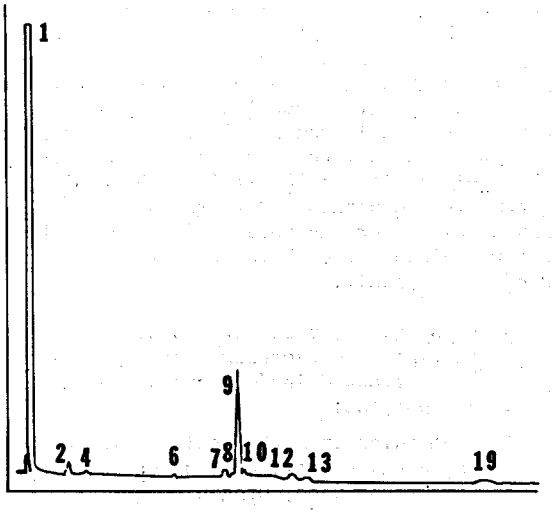


Fig. 2c MORGAN SPRINGS, CALIFORNIA

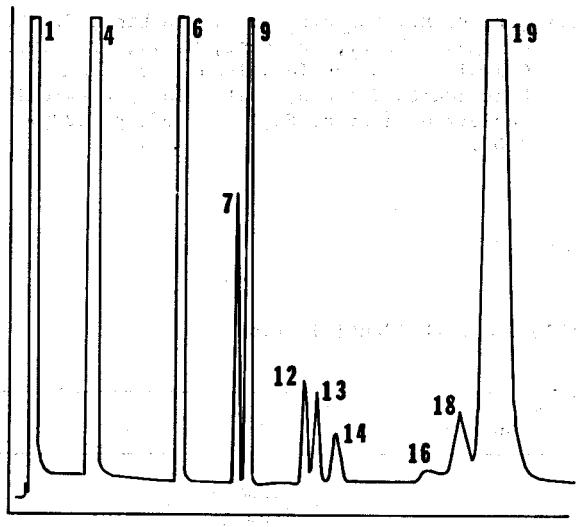


Fig. 3a CERRO PRIETO, MEXICO

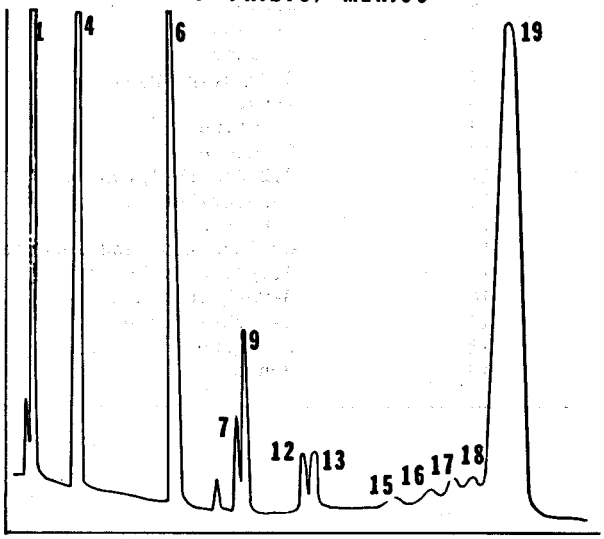


Fig. 3b LARDERELLO, ITALY

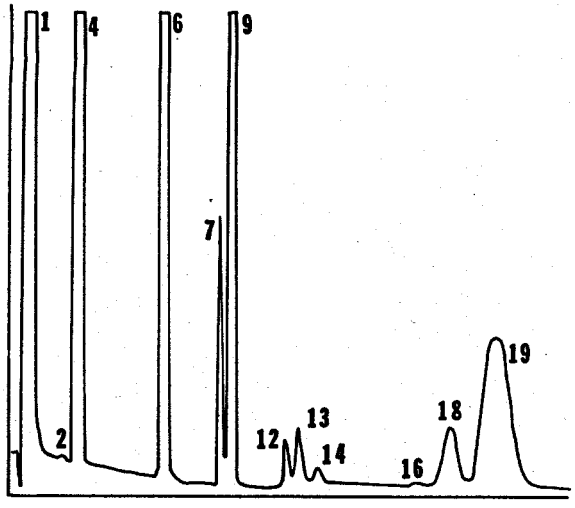
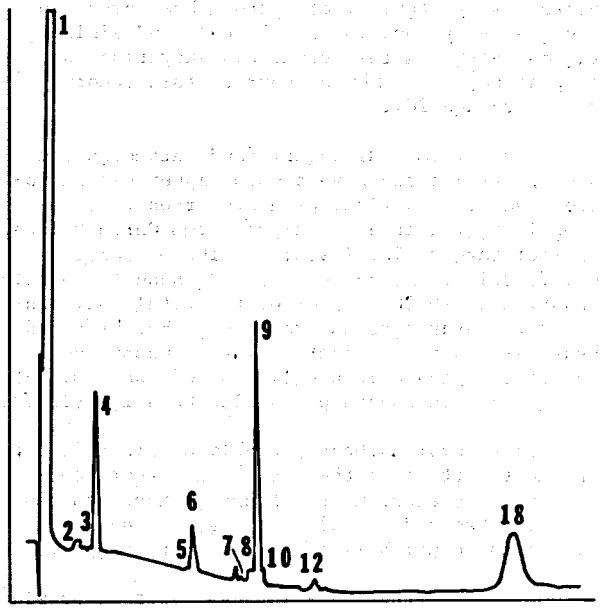
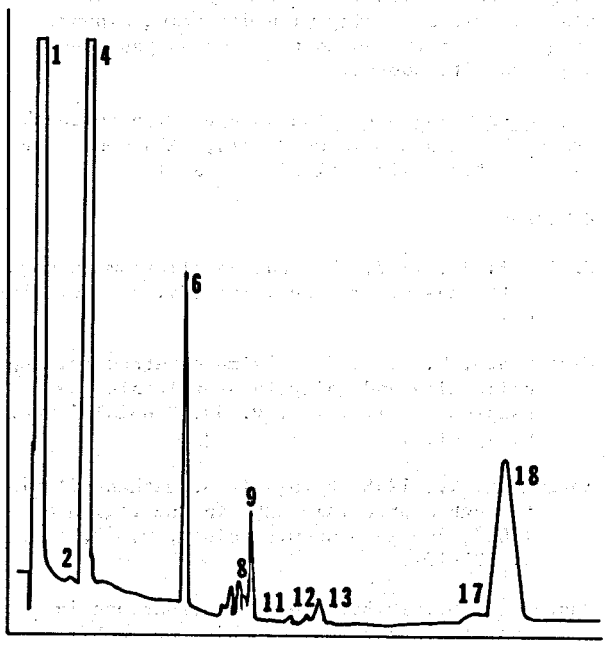


Fig. 3c THE GEYSERS, CALIFORNIA



YELLOWSTONE NATIONAL PARK, WYOMING

Fig. 4a



YELLOWSTONE NATIONAL PARK, WYOMING

Fig. 4b

and also account for the presence of the C-5 and C-6 hydrocarbons. The proximity of the acid hot springs and fumaroles in Lassen National Volcanic Park and the high-chloride springs at Morgan Hot Springs suggests that they belong to a single geothermal system. That hydrocarbon gases from the two areas show identical peaks and similar ratios (although the actual concentrations are less at Morgan) adds support to this theory (Figs. 2B and 2C).

Gases from sedimentary (and metamorphosed sedimentary) areas have a much higher concentration and wider variety of hydrocarbons. This type is represented by samples from Cerro Prieto, Mexico; Larderello, Italy; and The Geysers, Calif. (Figs. 3A, 3B and 3C). Methane frequently constitutes 10-30 percent of the total gas. Unsaturated hydrocarbons are absent, but branched hydrocarbons are present in large amount and variety. Benzene is usually one of the dominant peaks, and cyclopentane has also been identified.

These hydrocarbons probably originated, for the most part, from the breakdown of more complex organic substances. Magmatic heat sources are hypothesized for all these areas and may make minor contributions to the hydrocarbons.

Mixing of the preceding gas types is possible and evident in samples from Yellowstone National Park, Wyoming. Comparison of Fig. 4A with 4B shows an increase in both the number of hydrocarbons and the amount of the normal hydrocarbons and benzene. Apparently, a gas of igneous origin is mixing with differing amounts of a sedimentary gas as the igneous gas moves away from its source.

Acknowledgment. The authors with to thank Frank Church and Dave DesMarais, NASA-Ames, for mass spectrometric analysis of samples.

References

Ellis, A. J., 1957, Chemical equilibrium in magmatic gases, Am. Jour. Sci., v. 255, p. 416-431.

Giggenbach, W. F., 1975, A simple method for the collection and analysis of volcanic gas samples, Bull. Volc., v. 39, Special issue, p. 132-145.

Gordon, A. S., 1948, Pyrolysis of methane flowing through a procelain tube in the region of 1000°, American Chem. Society, v. 70, p. 395-401.

Gunter, B. D., 1978, C_1 - C_4 hydrocarbons in hydrothermal gases, Geochim. Cosmochim. Acta, v. 42, p. 137-139.

Hulstan, J. R., 1964, Isotope geology in the hydrothermal areas of New Zealand, Proc. of the U. N. Conf. on New Sources of Energy, Rome 1961, v. 2, part 1., p. 259-263.

Stoiber, R. E., Leggett, D. C., Jenkins, T. F., Murrmann, R. P., and Rose, W. I., Jr., 1971, Organic compounds in volcanic gas from Santiaquito Volcano, Guatemala, Geological Society of America Bull., v. 87, p. 2299-2302.

Table 1. Peak identification

Number	Name
1	Methane
2	Ethene
3	Ethyne
4	Ethane
5	Propene
6	Propane
7	2-Methylpropane
8	1-Butene
9	n-Butane
10	2-Butene
11	2,2-Dimethylpropane
12	2-Methylbutane
13	n-Pentane
14	Cyclopentane and 2-Pentene
15	2,2-Dimethylbutane
16	3-Methylpentane
17	2-Methylpentane
18	n-Hexane
19	Benzene

Geothermal Resources Council, TRANSACTIONS, Vol. 2 July 1978

Dup

APPARATUS FOR THE FIELD EVALUATION OF GEOTHERMAL EFFLUENT INJECTION

Raymond Netherton and Lawrence B. Owen

Lawrence Livermore Laboratory
Livermore, California

Abstract

Methods for evaluating subsurface disposal systems, based on data derived from membrane filtration tests and core flooding experiments, have been described in the literature. Utilizing these techniques, we have developed and successfully tested equipment for evaluation of injectability of any geothermal effluent including hypersaline brine from the Salton Sea Geothermal Field (SSGF).

Work performed under the auspices of the U. S. Dept. of Energy, Contract No. W-7405-Eng.-48.

Reference to a company or product name does not imply approval or recommendation of the product by the University of Calif. or the U. S. Dept. of Energy to the exclusion of others that may be suitable.

Introduction

Direct injection of low temperature effluents into porous media may not be feasible at many geothermal fields because of high suspended solids loading and resultant plugging of primary porosity in the reservoir. If effluents are supersaturated with respect to silica, calcite or other phases, scaling of the injection line or completion interval may also limit injection. Various pre-injection clarification techniques including settling, chemical pretreatment, reaction clarification and pressure filtration utilizing packed columns or precoat additives are currently being evaluated for use at the SSGF by Magma Power Company and Lawrence Livermore Laboratory. We are supporting these activities with filtration and core flooding tests to establish the relative injectability of effluents. Results of our preliminary analyses are reported elsewhere.[1-2]

Filter tests are useful in establishing the size distribution of suspended solids, the scaling potential of brine at the sand face, and in developing estimates of the useful lifetime of injection wells.[3-4] Tests are simple to execute, inexpensive, and are an efficient means of rapidly comparing injectivity of different effluents. Filter tests can also be used subsequently as a quality control monitor during full-scale operation of disposal systems[5]. Injection estimates derived from filter data generally pertain only to problems caused by particulate plugging or scaling, and estimates of injection well performance tend to be conservative because membrane filters with 0.45 μm pre size are normally used.

Core flooding experiments provide a means of studying the effects of brine-rock interaction on injection.[6-12] Changes in core matrix properties resulting from particle invasion, chemical alteration, dissolution, precipitation, or authigenic mineralization can be resolved during subsequent analyses with the scanning electron microscope. While representative core samples from the injection interval are most desirable for testing they are not always available. Standard cores, matched with respect to reservoir rock composition, texture, porosity and permeability are often chosen for study. Subsurface disposal is assumed to be viable if 2 to 12 thousand pore volumes of effluent can be flowed through a core (typically 2.54 cm diameter and 10.16 cm long) at a representative flow rate with negligible permeability decline.

Apparatus

A schematic diagram of the prototype system for filtration and core flooding is shown in Figure 1. The system has the following capabilities:

a) Filter tests
b) Core tests with unfiltered brine
c) Core tests with filtered brine
d) In-line backwashing of membrane filters
e) Pumping capability for testing non-pressurized effluents
f) Brine-resistant flow monitor

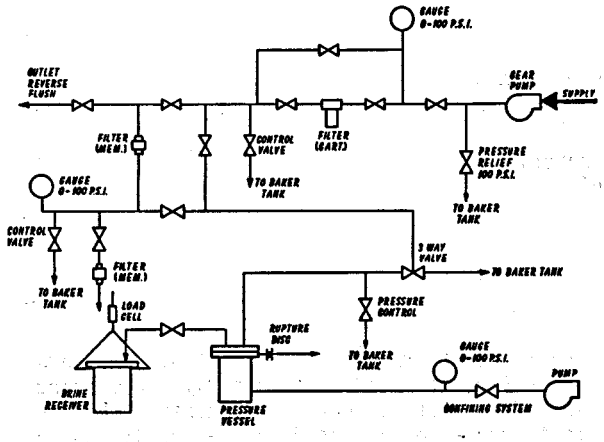


Figure 1. Filtration and Core Flooding Apparatus

The system was designed to minimize temperature flucuations and residence time as a means of controlling precipitation of extraneous solids during experiments. Temperature control was effected by insulating all piping and by-passing the total inlet brine flow to the system via pressure control valves located adjacent to the membrane filter and core pressure vessel. Corrosion-resistant 316 stainless steel tubing and valves with Teflon inserts were used exclusively to prevent formation of corrosion products that might bias test results. The brass covers of the cartridge filter housings were nickel-plated for the same reason. A pump was provided to permit testing non-pressurized effluents. We found that Oberdorfer model no. 2136 (10 GPM, 100 PSI) gear pumps with W88 gears and Teflon packing operate reliably for sustained periods at temperatures up to 100°C.

Filter Tests

Membrane filters are provided for particle size determinations, measurement of suspended solid concentration and for evaluation of injection well performance utilizing test procedures and analytical models developed by Barkman and Davidson.[3] For the latter application, 0.4 μm Nuclepore 47mm polycarbonate membrane filters, mounted in Nuclepore in-line holders, are operated at 50 PSI pressure differential for 60 minutes. Either membrane or fiber-wound cartridge filters are available as prefilters to establish minimum clarification criteria for successful operation of core samples. Manifolding is provided to permit in-line backwashing of membrane filters with hot brine clarified by flow through cartridge filters. During filter tests, input brine temperature is obtained with a calibrated thermocouple mounted on the respective filter input line.

Core Tests

The core flooding apparatus was modified after a design suggested by Piwinskii and Netherton. Core samples 2.54 cm in diameter by up to 15.24 cm in length are jacketed with TYGON tubing and emersed in an oil-filled 316 stainless steel pressure vessel. The vessel is rated to 5000 PSI and oil pressure is applied via a pump. In the original design, the vessel cover was fabricated from 1020 carbon steel. We found that these covers corroded rapidly on exposure to either brine or to the humid atmosphere at the test site. We subsequently replaced the covers with units fabricated from Ti-6Al-4V alloy, a material that has been shown to be compatible with SSGF brine at temperatures to 200°C.[14]

A schmatic diagram of the pressure vessel is shown in Figure 2. Oil temperature is automatically maintained with $\pm 2^{o}$C of the desired temperature by a heating tape, wrapped around the pressure vessel, and its associated power supply and thermostat control. Core temperature is monitored via an oil-filled orifice tube that penetrates into the oil-filled portion of the pressure vessel. Input brine temperature is monitored with a calibrated thermocouple located on the pressure vessel input line.

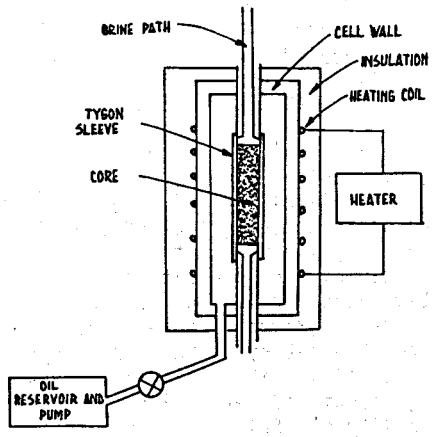


Figure 2. Schematic Detail of the Pressure Vessel

Each core sample is fitted with perforated inserts as shown in Figure 3. The inserts provide support and also simulated the completion interval in the injection well. Post run analysis of the inserts provides data on downhole slot or perforation plugging. Prior to a run, cores are evacuated for 30 minutes with a vacuum pump connected directly to the output line of the pressure vessel. This procedure insures rapid saturation of the core and eliminates possible brine-rock interactions that might occur if cores are saturated in salt solutions prior to exposure to geothermal brine.

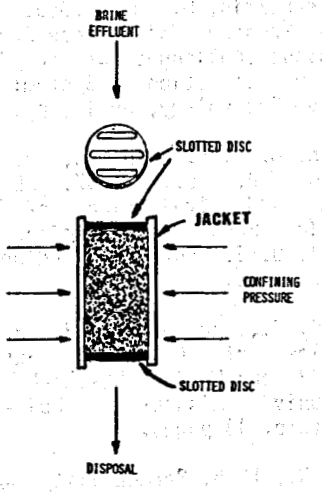


Figure 3. Schematic Detail of the Core Mount

Flow Monitoring

We designed a brine-tolerant flow monitoring system to avoid potential scaling problems that might influence the accuracy of conventional flow meters. Brine effluents from either cores or filters are stored in a container suspended from a load cell. The load cell output is continuously read with a digital voltmeter. Prior to runs, linear calibration curves are obtained by transferring known volumes of brine to the storage container and recording the corresponding load cell response. A schematic of the system and a typical calibration curve are shown in Figures 4 and 5, respectively.

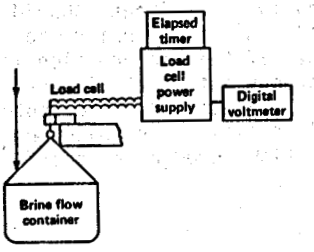


Figure 4. Flow Monitoring Equipment

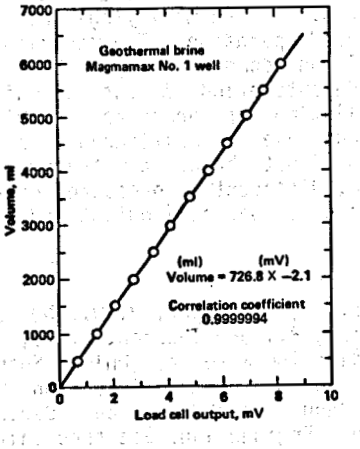


Figure 5. Typical Load Cell Volume Calibration

Testing Procedure

In establishing the relative injectability of various effluents, we first measure the concentration of suspended solids and particle size distributions with membrane filters. Water quality ratios and the effect of filter cake formation on injection well performance are then established after the method of Barkman and Davidson. We then began core tests initially utilizing either 0.45μm membrane or 1.0μm cartridge-type prefilters. Subsequently, other filters are substituted to establish core response to different concentrations and size distributions of suspended particulates. These tests are useful in establishing the minimum clarification requirements for injection.

It should be emphasized that the chemical stability of effluent should be known as a function of time prior to filter or core tests. If this information is unavailable, erroneous interpretation of test data may result because of the potential for additional precipitation following filtration or flow through a short length of core.

Conclusions

The prototype system works extremely well, but requires constant attention by an operator for data collection and periodic pressure adjustments; variations in input brine temperature, flowrate and pressure cause flucations in differential and confining pressures. We are modifying the system for unattended operation. The modifications which should be completed by early summer 1978 include automation of data acquisition and installation of pressure regulators. Data readout via a multichannel recorder will include input brine temperature, core temperature, differential pressure, confining pressure, load cell output and time.

References

1. Owen, L. B., Kasameyer, P. W., Nether-Netherton, R., and Thorson, L. D., 1977, Predicting the Rate by Which Suspended Solids Plug Geothermal Injection Wells: Third Annual Workshop on Geothermal Reservoir Engineering, Stanford University.

2. Tewhey, J., Chan, M., and Owen, L. B., 1978, Development of Injection Criteria for Geothermal Resrouces: Submitted Proc. Geothermal Resources Council Annual Meeting.

3. Barkman, J. H. and Davidson, D. H. (1972), Measuring Water Quality and Predicting Well Impairment: Jour. Petroleum Technology, pg. 865-873.

4. Johnston, K. H., and Castagno, J. L., 1964, Evaluation by Filter Methods of the Quality of Waters Injected in Waterfloods: U. S. Bureau of Mines Rpt. 6426, 14 pages.

5. Doscher, T. M. and Weber, L., 1957, The Use of the Membrane Filter in Determining Quality of Water for Subsurface Injection: Drilling and Production Practice, (API), pg. 169-179.

6. Keelan, D. K. and Koepf, E. H., 1977, The Role of Cores and Core Analysis in Evaluation of Formation Damage: Jour. Petroleum Technology, May, pg. 482-490.

7. Farley, J. T. and Redline, D. G., 1968, Evaluation of Flood Water Quality in the West Montalvo Field: Journ. Petroleum Technology, July, pg. 683-687.

8. McCune, C. C., 1977, On-Site Testing to Define Injection-Water Quality Requirements: Jour. Petroleum Technology, Jan pg. 17-24.

9. Jordan, C. A., Edmondson, T. A., and Jeffries-Harris, M. J., 1969, The Bay Marchand Pressure Maintenance Project-Unique Challenges of an Off-Shore Sea-Water Injection System: Jour. Petroleum Technology, April, pg. 389-396.

10. Champlin, J. B. F., Thomas, R. D. and Brownlow, A. D., 1967, Laboratory Testing and Evaluation of Porous Permeable Rock for Nuclear Waste Disposal: U. S. Bureau of Mines Rept. 6926, 32 pages.

11. Curry, R. B., and Beasley, R. P., 1960, The Flow of Colloidal Suspensions Through Porous Media: Research Bulletin 741, Univ. Missouri, College of Agriculture, 43 pages.

12. Mungan, N., 1965, Permeability Reduction Through Changes in pH and Salinity: Jour. Petroleum Technology, Dec. pages 1449-1453.

13. Piwinskii, A. J. and Netherton, R., 1978, An Experimental Investigation of the Permeability of Kayenta Sandstone to Hypersaline Brine in the Temperature Interval 70-90 C at 10.3 MPa Confining Pressure: Univ. Calif. UCRL-52382.

14. Austin, A. L., Lundberg, A. W., Owen, L. B. and Tardiff, G. E., 1977, The LLL Geothermal Energy Program Status Report, January 1976-January 1977, UCRL-50046-76.

MEAGER CREEK GEOTHERMAL SYSTEM, BRITISH COLUMBIA, PART I: EXPLORATION AND RESEARCH PROGRAM

Andrew E. Nevin[1], J.T. Crandall[1], J.G. Souther[2], and J. Stauder[3]

[1] Nevin Sadlier-Brown Goodbrand Ltd., [2] Geological Survey of Canada,
[3] British Columbia Hydro and Power Authority: all Vancouver, B.C.

Abstract

The Meager Creek geothermal area, 150 km north of Vancouver, B.C., centres on a large intermediate Cenozoic volcano. The reservoir systems feeding two independent hot springs on opposite flanks have been partially defined by geologic mapping (Read), resistivity (Shore), shallow drilling, and other operations. Interim conclusions bearing on current exploration are that the targets are water-dominated reservoirs at depths of 1000-2000 m in volcanic feeder pipes or nearby open fractures; that natural diffusion from these takes place slowly through weakly permeable fractured quartz diorite "basement"; and that the waters re-equilibrate with low temperature minerals and lose their geochemical memories in transit. The current program leans heavily on a newly developed pole-pole resistivity method (Shore), and is aimed at developing targets for 2000-metre exploratory drill holes.

Introduction. Independent investigations of the geothermal potential of the Meager Creek area were started in 1973 by the British Columbia Hydro and Power Authority and by the federal Department of Energy Mines and Resources (EMR). B.C. Hydro's goals are the commercial development of steam. The B.C. Geothermal Resources Act of 1973 provides B.C. Hydro, a Crown Corporation, with the right to extract geothermal energy (Nevin and Stauder,1976). EMR is charged with geological mapping, pure geophysical research, and Canada-wide assessments of geothermal resource potential as outlined by Jessop (1975). Souther (1976) describes a Cordilleran program and (1978) a current synthesis of Canadian projects.

Initial selection of the Meager Creek area was made on the weight of its large Cenozoic central volcano of intermediate composition flanked by hot spring systems. These are the Pebble Creek hot spring to the northeast, a dilute sodium bicarbonate brine flowing at 100 litres per minute, and the Meager Creek hot spring to the south, a dilute sodium chloride brine flowing at 500-1000 lpm. Maximum temperatures recorded in both are about 60°C.

The Meager Creek area is located about 150 km north of Vancouver, at latitude 50° 34'N and longitude 123° 23' W. It is 70 km from two 230 kV and one 500 kV power lines through which B.C. Hydro transmits power to the Vancouver load centre.

Geographic features which affect exploration methods include extremely high relief (see map), heavy and commercially valuable timber at elevations up to about 4000 feet (1200 m); only scattered outcrops, except between tree line at 5000 feet (1500 m) and the irregular lower edge of the permanent snowfield at about 6500 feet (2000 m); and no road access until 1977.

Recent Work. Four commercially important operations have been conducted since the report by Nevin and Stauder(1976). The first of these was geologic mapping by Read(1977; and this volume) at a scale of 1:10,000, under contract from EMR. Read's work provides not only certain geological and spatial factors acting on control of reservoirs, but also a distinct sense of the evolution of the volcanic edifice.

Hammerstrom and Brown (1977), also under contract from EMR, have shown that trace elements in both the Meager Creek and Pebble Creek hot springs have re-equilibrated at temperatures of 60-80°C, and offer no clues as to the 'upstream' thermal history. The waters are in equilibrium with the observed alteration assemblage kaolinite-laumontite-calcite-chalcedony.

Dipole-dipole resistivity surveys have outlined the southern or Meager Creek reservoir. The northern or Pebble Creek reservoir has been reconnoitered, first by a self-potential survey, and in 1977 by a new computer-controlled multiple electrode pole-pole resistivity method which is described by Shore (this volume). The fourth increment of commercially important information consists of three additional research wells drilled to depths of 60 to 90 m on the south reservoir. The hottest of these had a bottomhole gradient of 37°C per 100 m.

EMR continues to sponsor various surveys in the region, particularly aimed at the deep geophysics of the crust. In 1977 four 200-m holes were drilled, one at the edge of the Meager Creek area. All returned geothermal gradients of about double the crustal norm (J.F. Lewis, in preparation.)

Interim Conclusions. The map shows the extent of the geothermal reservoirs and anomalous areas known to date. Our interim conclusions, to be used to guide continued exploratory work, have evolved from work reported by Read (this volume) and Shore

(this volume), and other data.

1. The major part of the rock underlying the valley floors is fractured Cretaceous quartz diorite, with some younger intrusives and septa of phyllite and metavolcanic rock. In the main it is only weakly permeable. Diffusion of hot water from the presumed sources--open and high temperature reservoirs--takes place slowly with attendant chemical re-equilibration and substantial heat loss.

2. As in much of the Pacific Northwest, the rock and overburden are saturated with water to within a few metres of the surface. Temperature gradients in shallow wells have to be interpreted subjectively and cautiously, since the effects of the hydrologic system on the thermal regime cannot be isolated in the early exploratory stages. Heat flow values are subject to large errors unless the circumstances are unusally well controlled.

3. The geophysical anomalies considered important are generally at interpreted depths of 1000 m or more beneath the surface. Since the ground water column extends to the surface, the interpreted reservoirs are likely to exist at hydrostatic pressure of 100 atmospheres or more, which is inconsistent with a vapour-dominated system, as described and defined by White, Muffler, and Truesdell (1971). The commercial target is a water-dominated system.

4. The south or Meager Creek reservoir, as it is presently known, is a tabular body which occupies about 5 sq. km and dips gently to the north under the volcanic edifice. The leading hypothesis is that it consists of a slow discharge plume from a presumably permeable feeder pipe for the southermost volcanics, as noted by Nevin Sadlier-Brown Goodbrand Ltd. (1975), and Lewis and Souther (1978).

5. The north or Pebble Creek reservoir (see map) is a conduit of unknown configuration subjacent to the Pebble Creek hot spring and has been extended about 8 km along the Lillooet River by various geophysical means: dipole-dipole resistivity surveys using X spacings of 300 m to n = 4; self-potential traverses; and deep pole-pole resistivity surveys. The shallow anomalies (1000 m or less) are not yet controlled by shallow drilling and their thermal nature has not been confirmed. The geophysical environment is subject to considerable "noise" from conductive river gravels, deposits of glacial outwash clays, and minor disseminated pyrite. The deep pole-pole anomaly defines a geologically valid resistivity low, but may derive in part from a septum of pyritic and graphitic(?) phyllite. While the thermal nature of the geophysical extension to the northern reservoir is not yet confirmed, we do have some insight into structural and thermal controls: A strong system of regional faults parallels the Lillooet valley and probably slices through many of the overburden-covered rock units in the valley floor. The latest eruptions (Read, this volume) came from the vicinity of the northern part of this reservoir less than 2500 years B.P.

Current Program. The exploration effort is putting considerable weight on the multiple pole-pole resistivity method. Development of the method evolved (Shore, this volume) from the desire for a deeper ratio of penetration versus electrode spread under conditions of extreme topography and forest cover. The speed of data acquisition and the information on anisotropic resistivity properties are important added benefits.

Deep drilling is currently in the preliminary planning stages. We can anticipate that much of the exploratory drilling will be conducted in quartz diorite. We can also expect a low rate of penetration from conventional oil field or geothermal drilling tools. The owner would sustain high footage costs and would assume all risks for delays and unexpected events. The present oil and gas boom in the Canadian prairies, and the remoteness of Meager Creek from such fields, would lead to problems in obtaining a rig for this unorthodox job. However, a large diamond drill, generally used for metal exploration and geotechnical work, would be ideally suited for geothermal drilling at Meager Creek if properly equipped with a reinforced tower, special draw works, and the appropriate blowout preventor or rotating head. It would have a high and predictable penetration rate, a lower footage cost, and much lower risk factors, some of which would be assumed by the contractor. Thus the slim hole is under serious consideration for the first several 2000 m exploratory wells.

References Cited

Hammerstrom, L.T., and Brown, T.H., 1977, The geochemistry of thermal waters from the Mount Meager hot springs area, B.C.: Geol. Surv. of Canada, Open File Report, 34 pp.

Jessop, A.M., 1975, Energy R & D program statement, Task V: Exploit renewable energy resources, Program 4: Geothermal energy: EMR, Earth Physics Branch, Geothermal Series No.4, Ottawa, 6 pp.

Lewis, John F., in preparation, Report of drilling near Mt. Meager and Mt. Cayley volcanic centres 1977: EMR, Earth Physics Branch.

Lewis, T.J., and Souther, J.G., 1978, Meager Mt. B.C. -A possible geothermal energy resource: EMR, Earth Physics Branch, Geothermal Series No. 9, Ottawa, 17 pp.

Nevin, Andrew E., and Stauder, J.; 1976, Canada, -Early Stages of Geothermal Investigation in British Columbia: Second UN Symposium on the Development and Use of Geothermal Resources, San Francisoco, Proc, pp. 1161-1165.

Nevin Sadlier-Brown Goodbrand Ltd., 1975, Report on Detailed Geothermal Investigation at Meager Creek (unpubl) to B.C. Hydro and Power Authority, 18 pp.

Read, Peter B., 1977, Meager Creek volcanic complex, southwestern British Columbia: Geol.

Surv. Canada, Rept. Activities, Part A, Paper 77-1A, pp. 277-281.

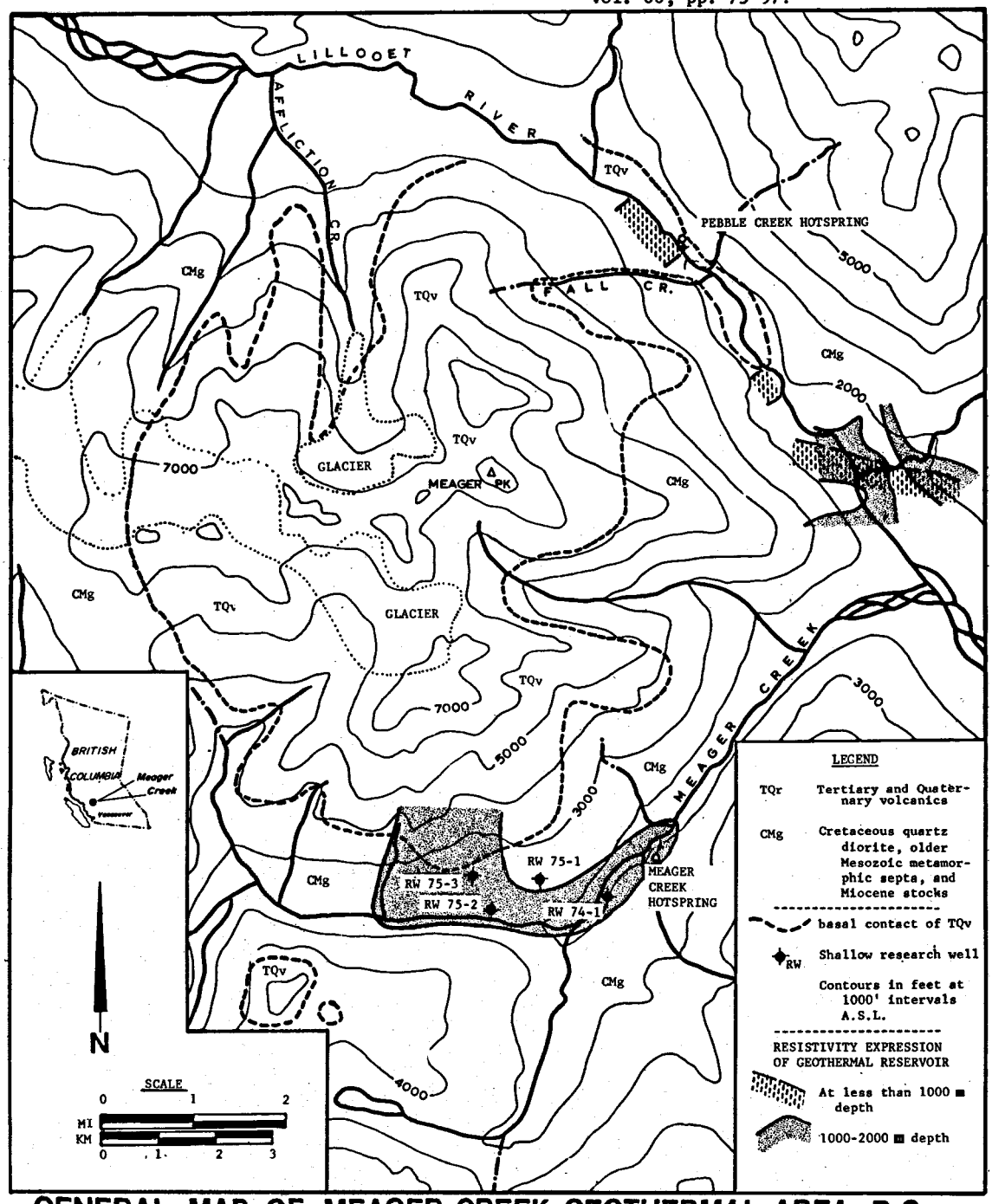
Read, Peter B., 1978, Meager Creek geothermal system, British Columbia, Part II: Geology: this volume.

Shore, Greg A., 1978, Meager Creek geothermal system, Part III: Resistivity methods and results: this volume.

Souther, J.G., 1976, Geothermal potential of western Canada; Second UN Symposium on the Development and Use of Geothermal Resources, San Francisco, Proc., pp. 259-267.

Souther, J.G., 1978, Canadian Geothermal Research Program; Amer. Assoc. Petrol. Geol., Circum-Pacific Energy & Minerals Resources Conference, Honolulu.

White, D.E., Muffler, L.J.P., and Truesdell, A.H., 1971, Vapor-dominated hydrothermal systems compared with hot-water systems: Econ. Geol., vol. 66, pp. 75-97.



GENERAL MAP OF MEAGER CREEK GEOTHERMAL AREA, B.C.

Geothermal Resources Council, TRANSACTIONS, Vol. 2 July 1978

CONTINUOUS CHAIN DRILL BIT DEVELOPMENTS

M. M. Newsom
J. A. St. Clair
H. M. Stoller
S. G. Varnado

SANDIA LABORATORIES
ALBUQUERQUE, NM 87185

ABSTRACT

Under DOE's Geothermal Well Technology Program, the Continuous Chain Drill Bit, in which fresh cutting surfaces are cycled into place without removing the bit from the hole, is under development by Sandia Laboratories. Fixed head bit testing has optimized cutting surface diamond patterns, developed adequate bit hydraulics, and solved the apex problem thru application of Stratapax® cutters in the bit nose. Prototype chain drill testing has demonstrated structural integrity, identified some hydraulic erosion and cycling mechanism problems, and confirmed superior drilling rate and lifetime performance to commercial diamond bits when drilling hard abrasive rock.

Work performed under the auspices of the U.S. Department of Energy, Contract No. AT(29-1)-789 for the Division of Geothermal Energy.

CONCEPT

A continuous Chain Drill Bit prototype is shown in Figure 1. The cutting structure consists of natural and synthetic (Stratapax®*) diamonds set in a tungsten carbide matrix. The four Stratapax® cut the center of the hole. The cutting structure is attached to links of a continuous chain. Five links constitute the cutting surface. There are sufficient links to replace the cutting surface 15 times before making a trip.

Drilling fluid pressure is used to cycle the chain downhole. To cycle, the bit is pulled off the bottom and the mud pumps are turned off. The pressure drop activates a spring, piston and pawl mechanism. The spring drives the piston to a reset position which engages the pawl in the chain. The rise in pressure from the restart of the mud pumps drives the piston, pawl and chain to a new drilling position, thus exposing five new cutting links.

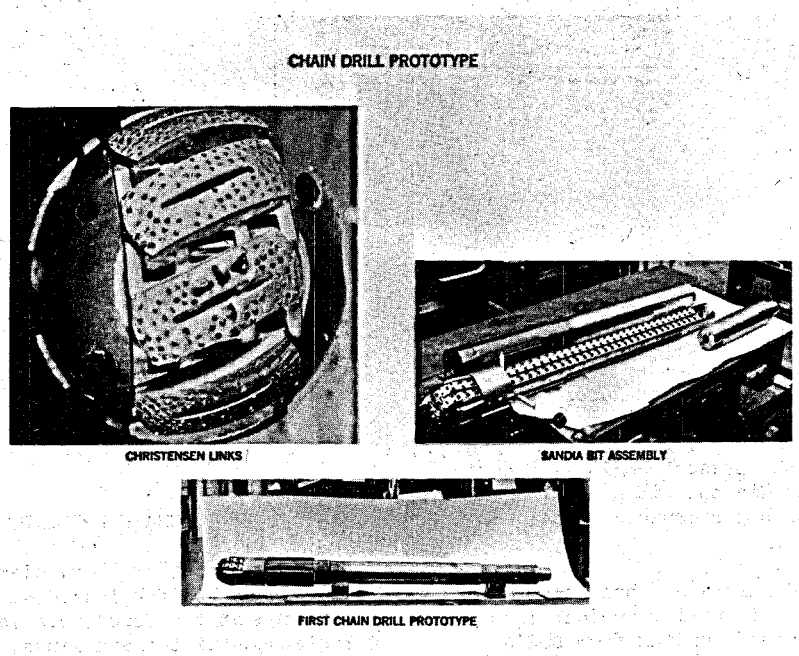


Fig. 1

*Trade name of General Electric Company

Drilling is done by a combination of bit load and rotation as in conventional rotary drilling

FIXED HEAD BIT DEVELOPMENT PROGRAM

The cutting structure design and bit hydraulics evolved in the fixed head bit development program, Figure 2. Ten fixed head bits that

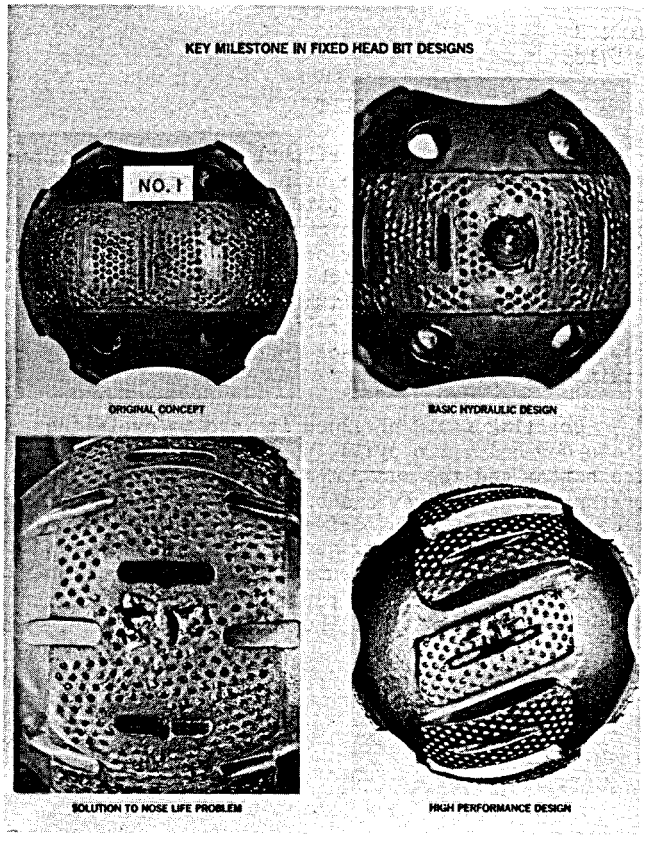


Fig. 2

employed eight different diamond configurations were built by Christensen, Inc. to Sandia's specifications. These fixed head bits were tested at the Reed/Terra Tek Drilling Research Laboratory. Christensen provided consulting services on the eighth fixed head bit design. This design has been incorporated into the present chain link design. A conventional hard rock diamond bit provided comparative rate and lifetime performance data.

*Development of improved Stratapax^{R} bonding procedures and optimization of cutting surface rake angle was accomplished under funding from DOE's Division of Oil, Gas, Shale and In Situ Technology.

The final cutting structure design employs several unique design features:

1. Stratapax^{R} are used in the nose of the bit.* This eliminated the nose area as the life limiting factor and increased the instantaneous penetration rate for a fixed bit load.

2. A modular hydraulics design was incorporated which significantly improved bit cooling and cleaning. An increase in drilling life while drilling with a higher bit load resulted.

3. A lighter-than-normal balanced diamond set was incorporated. Uniform wear rate and a load of 120 pounds per diamond (equivalent to 15,000 pounds maximum bit load) were the design criteria. This resulted in fewer diamonds per square inch (compared to conventional bits) which increased penetration rate for a given bit load with little loss in bit life.

Test results of the fixed head bits are summarized in Figure 3.

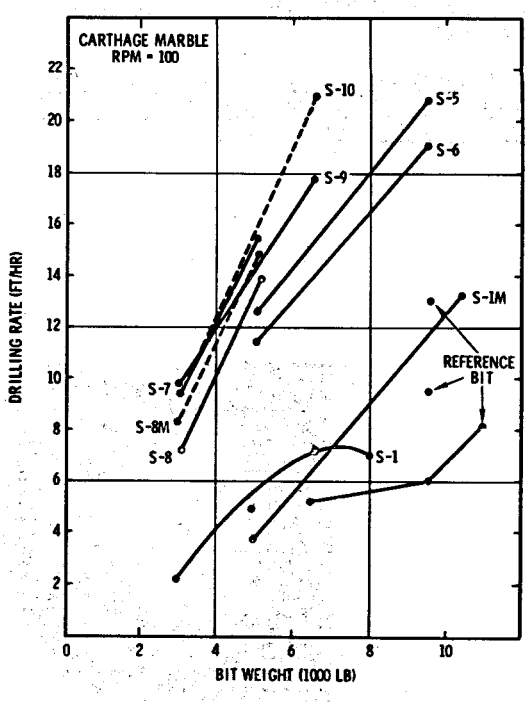


Fig. 3

CHAIN DRILL PROTOTYPE

A prototype 4 3/4 in. diameter chain drill was designed and fabricated at Sandia. This bit was tested at the Reed/Terra Tek DRL utilizing Christensen-built chain links. Chain links of an alternate design have been built by NL Hycalog and are being prepared for evaluation.

Testing of the prototype was done at room temperature and atmospheric pressure in Sierra White Granite at 100 rpm. Bit loads were varied to maintain a 4 ft/hr penetration rate. Testing was terminated when the required bit load exceeded 15,000 pounds.

The prototype bit was tested in September 1977. The footage drilled versus bit load for all tests is shown in Figure 4.

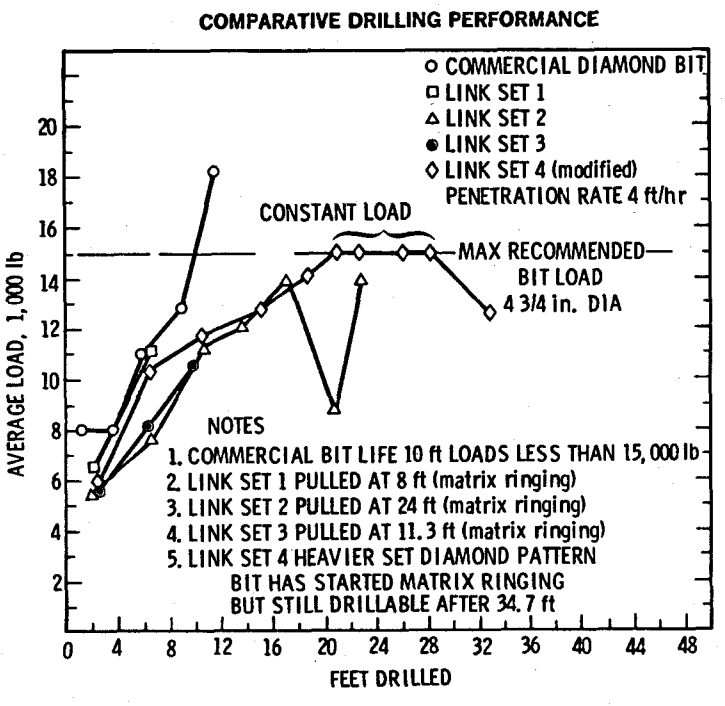


Fig. 4

The diamond cutting surfaces for links No. 1, 2, and 3 were specified to be identically set. Insufficient diamond coverage in Link Set No. 1 and No. 3, however, resulted in early ringing of the matrix causing reduced drilling performance. Link Set No. 2 performed best of the first three link sets, but ringing also terminated this test. Additional diamonds were added to Link Set No. 4. Performance of these cutting surfaces was outstanding.

Some fluid erosion problems were noted but these can be easily corrected with harder materials and increased openings of the fluid entry holes. The chain cycling mechanism was overly sensitive to fluctuations in drilling fluid pressure. Current emphasis is directed at improving the reliability of the mechanism. Overall, the chain bits out drilled the control bit by about a factor of two on the average with generally lighter bit loads.

ECONOMIC COMPARISONS

Using the depth versus time data generated in the prototype drilling test series, minimum cost per foot calculations have been made. A summary of these calculations is presented in Figure 5 which shows footage cost savings relative to a conventional bit versus starting depth.

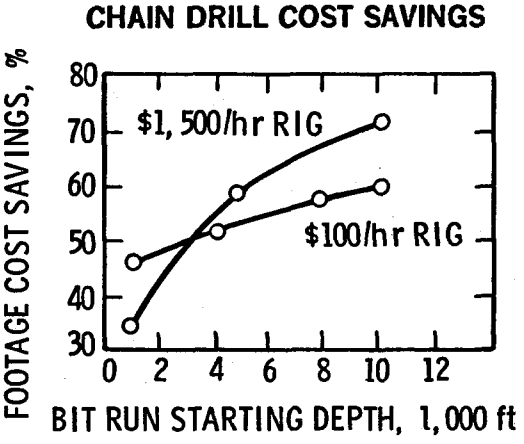


Fig. 5

The chain drill offers appreciable cost savings on all conditions considered.

CONCLUSIONS

1. The chain drill structural design has been proven adequate in laboratory testing.
2. The diamond set chain links have achieved notable penetration rates and lifetimes.
3. Fluid erosion is not considered a problem.
4. The chain cycling mechanism has been demonstrated but improved performance is needed.
5. Based on laboratory data, economics of the system appear attractive.

The cutting structural design has features that could improve conventional diamond bits, such as:

1. Stratapax in the nose area of the bit.
2. Modular hydraulic design.
3. Minimum diamond set pattern to obtain increased rilling rates and uniform wear rates.

TURBINE TESTING IN DIRECT CONTACT BINARY LOOP

K. E. Nichols, J. L. Lobach, J. W. Hunt

Barber-Nichols Engineering Co.
6325 W. 55th Avenue
Arvada, CO 80002

ABSTRACT

The turbine power loop test program successfully demonstrated the production of electricity from a geothermal source using isobutane in a direct contact heat exchanger. The tests were completed at the East Mesa Component Test Facility utilizing brine from well Mesa 6-2.

The turbo-generator unit consists of an axial flow, partial admission turbine, a gearbox, and a 60 KW 3600 rpm KATO generator. These components, along with controls and safety features, were mounted on a common skid.

The turbine was calibrated on pure isobutane at subcritical and supercritical turbine inlet conditions. The IC_4 was heated using a conventional tube and shell heat exchanger. An endurance run of 500 hours was then completed using an existing direct contact heat exchanger loop designed and operated by DSS Engineers of Ft. Lauderdale, Florida. At the conclusion of this testing, the turbine, connecting pipes, and a portion of the direct contact heat exchanger were disassembled and inspected for evidence of scaling or erosion in the test hardware. The only scale deposition noted was in the turbine nozzles and blading. The remainder of the loop was in good condition and gave no evidence of distress which would prevent continued operation of the test loop. The scale formed on the nozzles and blading was shown to be primarily silicate by analysis. It was felt that liquid brine carryover was occurring. A demister component was added between the DCHX and the turbine and a subsequent 105 hour run showed insignificant scaling in the turbine.

DISCUSSION

The turbo-generator was designed to operate with either of two direct contact heat exchanger (DCHX) systems. One system is a subcritical IC_4 DCHX loop designed and built by DSS Engineers (Ref. 1) and the other is a supercritical IC_4 DCHX loop by Occidental Research Corp. (Ref. 2).

Based on discussions with DSS and Occidental, the system operating parameters were established to be as shown in the following table. The anticipated water vapor fraction was calculated assuming saturated water vapor and real gas properties at the discharge of the DCHX. Turbine available energy was calculated based on an isentropic expansion of the mixture. Turbine design conditions were then determined for the respective cycles.

TABLE 1

	Occidental	DSS
Isobutane, lb/hr	2000	2650
Water vapor, lb/hr	49	32
Total vapor, lb/hr	2049	2682
DCHX pres., psia	600	315
Max. temp., °F	300	220
Condensing temp., °F	110	110
Condenser pres., psia	84.5	84.5
Turbine head, Btu/lb	38.7	23.4

The turbine selected for this application is a partial admission impulse design incorporating a single rotor and a nozzle block with two nozzle geometries; One nozzle configuration for the supercritical cycle and the other nozzle configuration for the subcritical cycle. The proper nozzle configuration is achieved by removing and rotating the nozzle block so that the inlet of the selected nozzles lines up with the inlet piping.

The detailed turbine design parameters are shown in Table II. The nozzle throat and exit areas were calculated using the gas properties for isobutane presented in "Fluid Thermodynamic Properties for Light Petroleum Systems" by Kenneth E. Starling (Ref. 3).

A double reduction Barber-Nichols gearbox (GR=6.05) was used in the power equipment module. Lubrication was provided by an internal driven lube pump, and oil temperature was controlled by a water cooled heat exchanger mounted on the gearbox housing. A mechanical seal on the high speed shaft was used to contain the isobutane in the turbine exhaust housing.

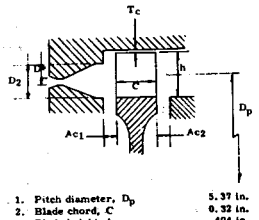
The generator was a standard 60 KW KATO 3Ø synchronous machine. The generator power

package used a speed control consisting of a Woodward governor, an SCR power controller and a load bank consisting of two electric space heaters. The governor was an electronic unit with isochronous capability that measured shaft speed and provided a voltage output that increased or decreased as the speed attempted to move from the set point. The output voltage from the governor was used to modulate a power controller which adjusted the load on the generator by controlling power fed to the parasitic load bank. The speed set point on the governor could be changed allowing turbine performance to be measured over a speed range. This variable speed feature allowed the one turbine design to meet the different energy levels of the subcritical and supercritical cycles.

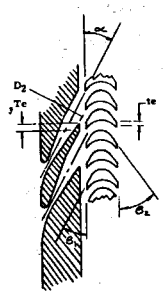
TABLE II

TURBINE DESIGN PARAMETERS FOR

DIRECT CONTACT POWER LOOP TURBINE



1.	Pitch diameter, D_p	5.37 in.
2.	Blade chord, C	0.32 in.
3.	Blade height, h	.404 in.
4.	No. of blades, Z	102
5.	Blade entrance angle, β_1	32°
6.	Blade exit angle, β_2	32°
7.	No. of nozzles, N	*
8.	Trailing rotor edge width, te	.010 in.
9.	Throat diameter, D^*	*
10.	Exit diameter, D_2	*
11.	Nozzle area ratio, Ar	*
12.	Nozzle angle, α	*
13.	Edge thickness between nozzles, Te	*
14.	Arc of admission, ϵ_n	*
15.	Tip clearance, T_c	.015 in.
16.	Axial clearance between nozzle & wheel, A_{c1}	.020 in.
17.	Axial clearance between wheel & exhaust, A_{c2}	.030 in.
18.	Arc of exhaust, $\epsilon_{exh.}$	*
19.	Design pressure ratio, $PR_{des.}$	*



*NOZZLE DESIGN PARAMETERS

		Sub.	Super.
7.	No. -nozzles	2	1
9.	Throat dia.	.229 in	.199 in
10.	Exit dia.	.286 in	.337 in
11.	Area ratio	1.587	2.87
12.	Angle	18°	18°
13.	Edge thk.	.010 max	N/A
14.	Admission	45°	26.1°
18.	Exhaust	55°	55°
19.	Pres. ratio	3.79	7.21

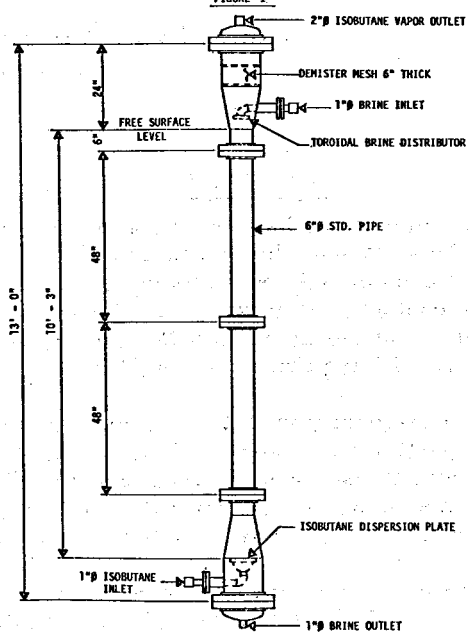
The DSS test loop consisted of the following major components: a direct contact heat exchanger that is a combination preheater and boiler, an isobutane separator, a stripping column, a condenser, a hotwell, an IC_4 feed pump and brine pump. The preheater and boiler were combined into one single column having an overall height of about 13 feet. The distance between the isobutane distributor at the bottom and the brine distributor at the top was 10' 4". The straight section of the column was 9' in length with an inside diameter of 6". A sketch of the DCHX is shown in Figure 1.

TEST RESULTS

During the endurance test the direct contact heat exchanger maintained the same level of

DIRECT CONTACT HEAT EXCHANGER

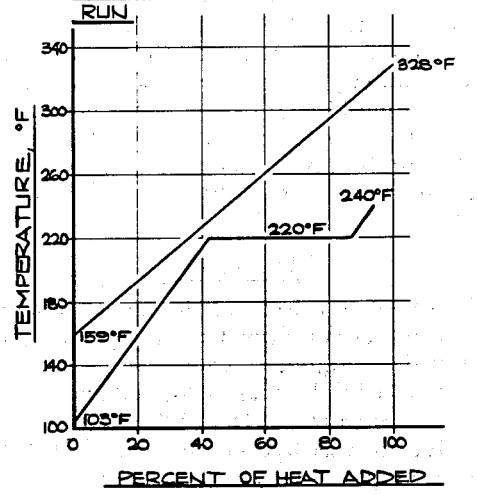
FIGURE 1



heat transfer performance throughout the 500 hours. The capacity to transfer heat was not effected in any way by the geothermal brine. Figure 2 shows a typical plot of temperature vs. percent of heat added to the isobutane during the endurance run. Any variations in the DCHX heat transfer performance were caused

FIGURE 2

TYPICAL PLOT OF TEMPERATURE PERCENT OF HEAT ADDED FOR THE DCHX DURING THE ENDURANCE RUN



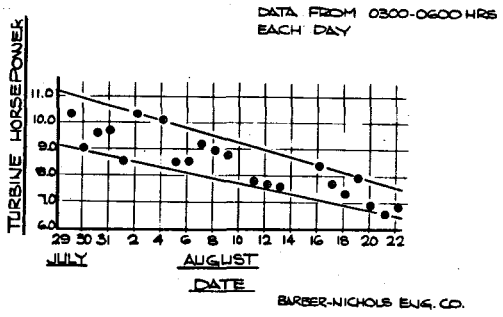
BARBER-NICHOLS ENG. CO.

by variations in incoming brine temperature, brine flow rate and isobutane flow rate.

Scaling properties of the brine did effect the performance of the turbine. Figure 3 illustrates the effect of scaling on turbine horsepower as a function of time. The data from 0300 hrs. to 0600 hrs. each day was used because the maximum turbine output occurred between these hours more often that at any other time of day. The turbine horsepower changed from an average value of 10.25 hp to 7 hp. The scatter in the data was caused by a number of factors. They included variations in inlet brine temperature which changed the amount of superheat and effected fluid wetness, variations in atmospheric conditions which effected the condenser cooling water temperature and sludge accumulation in the condenser cooling water tubes both of which raised the turbine exhaust pressure, and the scale deposition on the turbine nozzles and rotor.

FIGURE 3

500 HOUR ENDURANCE RUN



The scale formation that occurred in the nozzles and rotor was analyzed. The principal constituent was determined to be silica. There is evidence that liquid brine carryover from the DCHX was occurring and that this brine was then flashing in the expansion area of the turbine nozzle. A demister component to trap this liquid upstream of the turbine has been installed. Test results with the demister will be available by the 1978 Annual Meeting time.

ISOBUTANE LOSS RATES

Brine samples were taken from the outlet of the DCHX in order to measure the concentration of isobutane in the brine and to estimate the isobutane loss. The brine samples were taken from a tee located directly below the DCHX outlet. The line was purged several times before connecting the sample cylinder in order to ensure that a proper sample would be taken. The sample bomb was oriented vertically to ensure a full liquid sample and avoid trapping vapor. The brine samples were then cooled and analyzed by the chemistry laboratory at the East Mesa Test Facility.

The analysis for isobutane was made with a Perkin-Elmer model 910 gas chromatograph. Prior to injecting the sample into the gas chromatograph, the brine samples were flashed into a second cylinder which had been evacuated to a vacuum of 26.5 inches hg. For the initial sample the pressure rise in the evacuated cylinder was 11.5 inches hg when the brine sample was allowed to flash into it. This pressure rise was due to the dissolved gases and water vapor pressure of the brine sample. The brine remaining in the sample cylinder was analyzed with the gas chromatograph and the IC_4 level was approximately 1 ppm. The evacuated cylinder into which the brine was flashed contained only gas. The gas mixture in this cylinder was determined to have water vapor, isobutane, CO_2, and trace quantities of other gases. Of the 11.5 inches of hg total pressure it was estimated that 1 inch hg was water vapor, 9.1 inches CO_2, and 1.4 inches isobutane vapor. This volume of gas plus the 1 ppm residual in the flashed brine translates into 110 ppm.

The test results reported by LBL are shown in Table III. The last column in this table is the percent of equilibrium solubility of isobutane in the brine. This is based on isobutane solubility data reported by the University of Utah (Ref. 4). The equilibrium solubility was taken for a brine having a salinity of 0% by weight TDS which is the closest to the actual TDS of well Mesa 6-2 of 0.41% by weight.

TABLE III

MEASUREMENT OF ISOBUTANE CONCENTRATIONS AT THE BRINE OUTLET OF DIRECT CONTACT HEAT EXCHANGERS

Date	Sampling Conditions Temp. °F	Pressure, PSIG	Observed Isobutane Concentration PPM	Percent Equilibrium Solubility*
July 25	150	293	110.0	29.3%
Aug. 9	157 F	297	1600	445. %
Aug. 10	154 F	305	940	256. %
Aug. 19	163	306	120.0	33.6%
Aug. 20	157	295	103.0	28.7%
Aug. 21	156	300	49.0	13.3%
Aug. 23	Not Recorded		50.0	
Aug. 24	164	300	80.6	23.2%
Aug. 24	167	315	89.2	25.0%

The results of August 9 and 10 were an order of magnitude higher than the other tests. The reason for these higher values are speculative. The remaining tests average 87 ppm or about 25% of equilibrium solubility. This is felt to be the most accurate estimate of IC_4 levels as the sampling and analytic techniques improved. These levels were measured at the outlet of the DCHX with no attempt to strip the spent brine.

CONCLUSIONS AND RECOMMENDATIONS

1) Stable long term operation of the DCHX coupled with the turbine was achieved in the test program.
2) Tests indicated possible liquid carryover as evidenced by high nozzle discharge coefficients measured during the testing.
3) Laboratory measurement of isobutane carryover in the brine effluent from the DCHX averaged 87 ppm isobutane fraction in the latter stages of the endurance run. This quantity amounts to 25% of the equilibrium solubility expected for the brine from well Mesa 6-2.
4) No decrease in heat transfer performance was noted in the DCHX nor was any scale formation found from the injected brine. Scale deposition was noted in the turbine nozzles, particularly in the area of the supersonic expansion cone.

Based on these results, additional tests are being performed with a demister vessel located between the heat exchanger loop and the turbine. The effect of liquid mist carryover on on nozzle discharge coefficient and scaling will be evaluated.

ACKNOWLEDGMENTS

Support for this work has been provided by the Department of Energy through Lawrence Berkeley Laboratories, Berkeley, CA.

REFERENCES

1) E. F. Walh, F. Boucher; SAN/1076-1; "Theory and Practice of Near Critical Pressure Direct Contact Heat Exchanger"; Occidental Research Corp.
2) W. B. Surratt, G. K. Hart; ORO 4893-1; "Study and Testing of Direct Contact Heat Exchangers for Geothermal Brines", 1977; DSS Engineers, Inc.
3) K. E. Starling, "Fluid Thermodynamic Properties for Light Petroleum Systems"; Gulf Publishing Co., 1973.
4) H. R. Jacobs, R. F. Boehm, A.C. Hansen, "Application of Direct Contact Heat Exchangers to Geothermal Power Production Cycles. Project Review, December, 1974 - May, 1977"; Mechanical Engineering Dept., University of Utah, Salt Lake City.

Geothermal Resources Council, TRANSACTIONS, Vol. 2 July 1978

DRILLING FLUID FORMATION DAMAGE IN GEOTHERMAL WELLS

Dr. Robert W. Nicholson

Republic Geothermal, Inc.

ABSTRACT

Matrix type hot water reservoirs are highly susceptible to near well bore permeability impairment due to drilling fluid filtrate and particle invasion. The drilling fluids must be properly formulated to allow an efficient drilling operation and yet neither interact with the formation and in-situ fluids nor permanently plug the formation. Examination of the unique factors in matrix type geothermal reservoirs leads to steps which can be taken to alleviate formation damage problems during drilling.

Highly productive wells are critical to the economic viability of hot water dominated reservoirs. Severe formation damage near the well bore by the drilling fluids can significantly reduce well productivity when production is primarily from matrix flow. Avoiding serious damage during the drilling operation is far more economical than trying to restore the damaged well bore. Generally, drilling fluids and drilling techniques are used which yield the most economic drilling operation, however, drilling cannot be considered successful if the resulting well is severely impaired. Proper design of the drilling fluid and implementation of good drilling procedures can limit the damage during drilling operations.

The basic factors unique to matrix type hot water reservoirs which make them susceptible to drilling fluid damage are:

A. Highly permeable formations which are usually normally pressured.
B. Formation fluids which contain many different solutes.
C. Temperatures usually in excess of 300°F.

Drilling fluids are formulated from a liquid phase containing dissolved solids and a solid phase which provides viscosity and fluid loss control. Since most hot water matrix type reservoirs are normally pressured (0.433 psi/ft) the pressure exerted by the mud (drilling fluid) column will be greater than the formation. This is desirable to keep the well from flowing and the formation from caving while drilling. However, this differential pressure forces particles and filtrate into the formation.

The basic concept of filtration and the development of a filter cake on the well bore is depicted in Fig. 1. As virgin formation is exposed by the drill bit, mud particles and filtrate rapidly enter the pores and plugging begins. With time, particles consolidate to form an inner filter cake (Fig.1.b) and eventually a dynamically stable (during mud flow) outer mud cake (Fig. 1.c) develops and the filtration rate reaches a constant minimum.

Thus, after drilling has been completed, the formation near the well bore contains drilling mud particles and filtrate. If reverse flow during production does not remove all the invaded liquid and solids, the pores will remain plugged and the well productivity will be greatly reduced.

Severe damage due to mud filtrate was suspected in a well near Westmorland in the Imperial Valley. Permeability measurements made on plugs from cores cut in the production zone showed this to be the case. Fig.2 illustrates the severity of mud filtrate damage even though particles above 0.45 microns in the filtrate had been removed. Reverse flow did not restore the permeability and there appears to be a permanent 20% reduction in permeability. A number of such tests were conducted and in many cases much more severe damage occurred and some cores did not recover any permeability on reverse flow.

The liquid phase which contains solutes must be compatible with the formation and formation fluids. Clay minerals contained in the matrix may be sensitive to certain ionic atmospheres and may disaggregate, or swell, when exposed to the liquid phase of the drilling fluid. Figs. 3 and 4 illustrate core tests from the same well as in Fig. 2. It is apparent that ionic concentrations on these particular cores greatly effects the permeability. Additionally, the formation fluids may contain anions or cations, which in contact with anions or cations from the liquid phase of the drilling fluid, may cause insoluble precipitates. Some formation fluids in the Imperial Valley contain free barium. Sulphates in the make-up water of the drilling fluid, or chemical additives, may cause a very insoluble precipitate, barium sulphate, to be formed in the pore channels causing permeability reduction.

Clay solids are used in making up drilling fluids to increase the viscosity for hole stability and to suspend the drilled cuttings. These solids

also form the filter cake to reduce filtrate invasion. The high temperatures encountered in geothermal drilling greatly effect montmorillonite type clays which have historically been used for oil and gas drilling. However, increased temperature causes suspensions of montmorillonite to form very high gel strengths (measurement of force needed to initiate flow). A reasonable gel strength is necessary to suspend cuttings when fluid circulation stops during connections and when pulling the drill string for a bit change. However, excessive gel strengths cause very high surge pressures from the well bore to the formation when the drill string is run in the hole. Also, after the fluid has been quiescent, very high pressures must be used to initiate flow if the gel strength is very high. These high pressures cause deeper invasion and a deep damaged zone around the well bore.

Fig. 5 illustrates the high temperature gelation tendency of montmorillonite clay suspensions[1]. Dramatic increases occur above 250°F with concentrations above 18 pounds per barrel (typical concentrations used in actual drilling vary from 15 to 24 ppb). Also, gel strengths continue to increase with prolonged exposure at high temperatures as shown in Fig. 6 and actual solidification will occur. Calcium montmorillonites can form a low grade cement in the 300°F temperature range. The montmorillonitic particles which have invaded the matrix near the well bore will continue to consolidate with time. After cessation of drilling the formation near the well bore, cooled during drilling operations, will increase to its original temperature further enhancing the solidification of the invaded particles.

Experience with two wells drilled successively in the Imperial Valley illustrate the severity of productivity damage due to montmorillonite solidification. The mud systems were very similar, both containing high concentrations of montmorillonite. The first well was flowed extensively almost immediately after drilling stopped and has been a fairly productive well. The second well was flowed for a very short period of time and shut-in due to restrictions by the water control regulations. This well was tested several months later and had very low productivity, however the first short flow indicated a highly productive well. Several attempts were made to increase the productivity, none were successful. X-ray diffraction analysis of core material showed no montmorillonite but much illite and amorphous clays. After a hydrochloric-hydroflouric acid treatment a large amount of fines came out of the well. An analysis of these fines showed high percents of montmorillonite and amorphous clays and no illite. It was concluded that initial flow was not long enough, or early enough, to remove the drilling particles and filtrate before solidification which severely damaged the near well bore permeability.

For drilling operations in a matrix type hot water reservoir, the following general steps should be taken to help reduce formation damage:

A. Use drilling fluid materials which do not have adverse high temperature properties.
B. Analyze the formation solids and fluids to formulate the liquid phase to be compatible with both.
C. Coordinate the mud properties and drilling techniques to reduce the well bore to formation pressure differential.
D. Flow sufficient volumes from the well as soon as possible after drilling to remove invaded particles and filtrate.

Very encouraging developments[2,3] in high temperature drilling fluids have been made recently and field experience with these have been quite favorable. Sepiolite clays have replaced montmorillonite. These clay suspensions build reasonable viscosity and do not form excessive gel strengths at high temperatures. Also, these fluids are not very susceptible to contaminants. Usually a polymer, such as sodium polyacrylate is added to increase viscosity and help reduce filtrate loss. Adequate filtration control is still a problem with many of the sepiolite formulations.

Formulation of the drilling fluid liquid phase to be compatible with formation solids and liquids can be done where such data are available However, for exploratory drilling no data exists and an inhibitive type system should be used such as potassium chloride. Reducing the invasion with low differential pressures also helps reduce the depth of any plugging due to noncompatibility.

Drilling practices in the production zone should be employed to limit the differential pressures into the formation. Circulation rates and mud properties (viscosity and yield point) should be coordinated to produce a low annulus pressure loss and still clean the hole properly. Gel strengths and yield points should be used to estimate a maximum speed of running the pipe in the hole to help reduce high pressure surges. Mud weights should be kept as low as possible utilizing all mud cleaning equipment available.

As discussed above, once a well has been completed, early flow of sufficient quantities of formation fluid will help remove filtrate and particles from the well bore and formation, reducing the possible time and temperature reactions which may cause plugging. Monitoring the produced fluids and solids can indicate when all the drilling fluids have been removed which can be removed by reverse flow.

1. Annis, Max R., "High-Temperature Flow Properties of Water-Base Drilling Fluids", SPE preprint 1698, 1967.

2. Carney, L.L. and Meyer, R.L., "A New Approach to High Temperature Drilling Fluids", SPE preprint 6025, 1976.

3. Bannerman, J.K. and Davis, N., "Sepiolite Muds Used for Hot Wells, Deep Drilling", Oil and Gas J., Feb. 27, 1978.

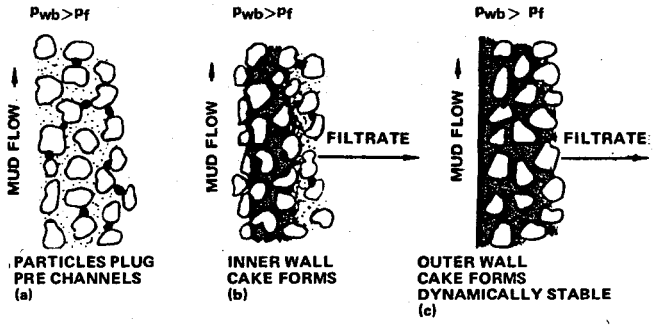


FIGURE 1. STAGES OF FILTRATION AND WALL CAKE BUILDUP ON THE WELLBORE

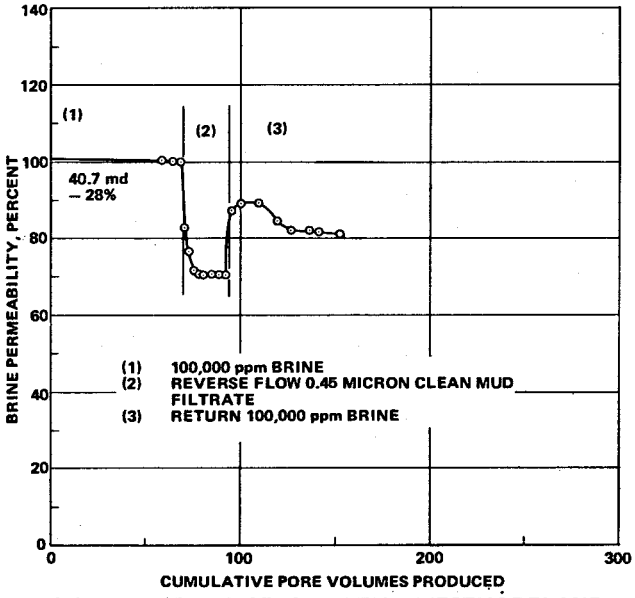


FIGURE 2. FLUID SENSITIVITY – WESTMORELAND CORE PLUG

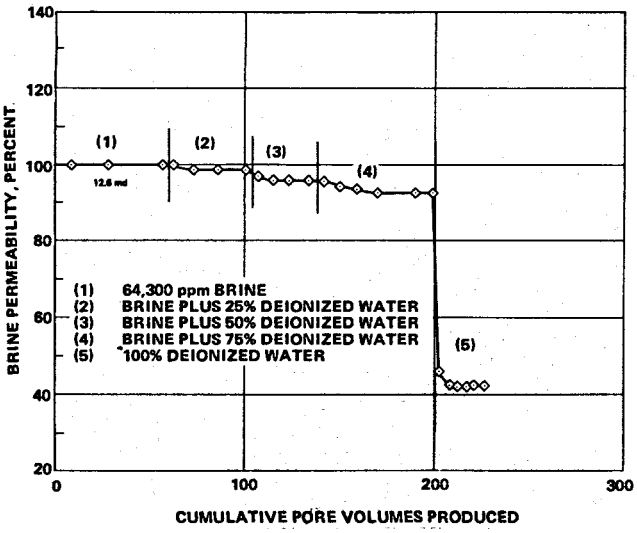


FIGURE 3. FLUID SENSITIVITY–WESTMORELAND CORE PLUG

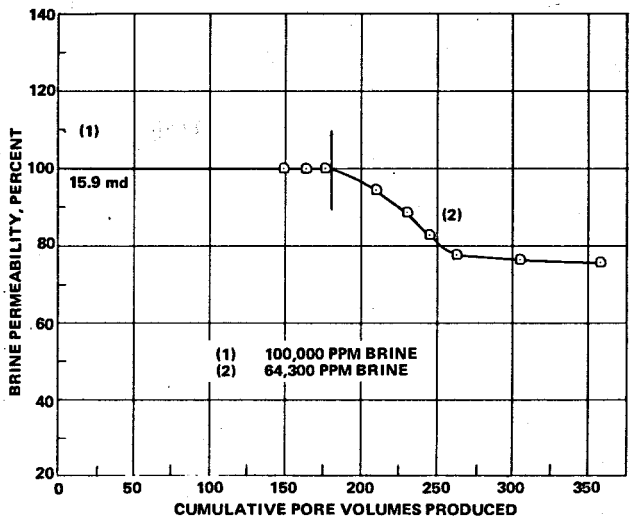


FIGURE 4. FLUID SENSITIVITY – WESTMORELAND CORE PLUG

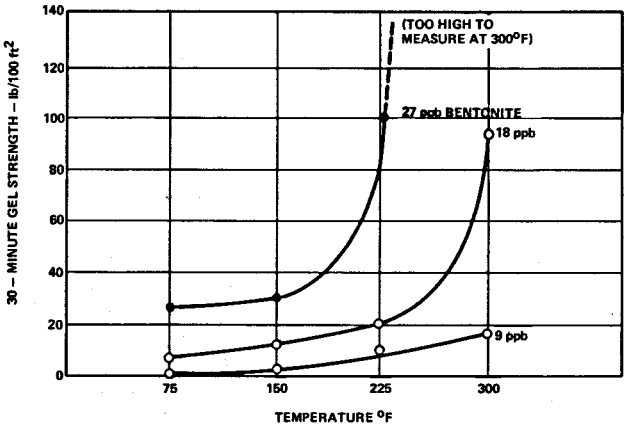


FIGURE 5. EFFECTS OF TEMPERATURE AND BENTONITE CONCENTRATION ON 30 MIN. GEL STRENGTH (FROM REF. 1)

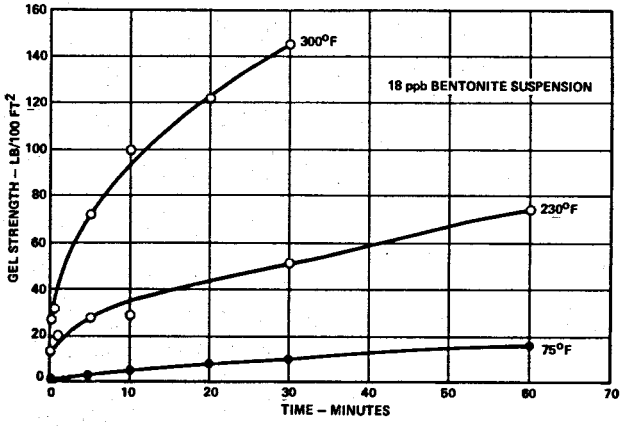


FIGURE 6. EFFECTS OF TIME AND TEMPERATURE ON GEL STRENGTH (FROM REF. 1)

A CONTROL SYSTEM FOR STEAM GATHERING AT THE GEYSERS

William L. O'Daly

Thermogenics, Inc.
A Subsidiary of
Hughes Aircraft Company
Culver City, California 90230

Gennaro Morelli

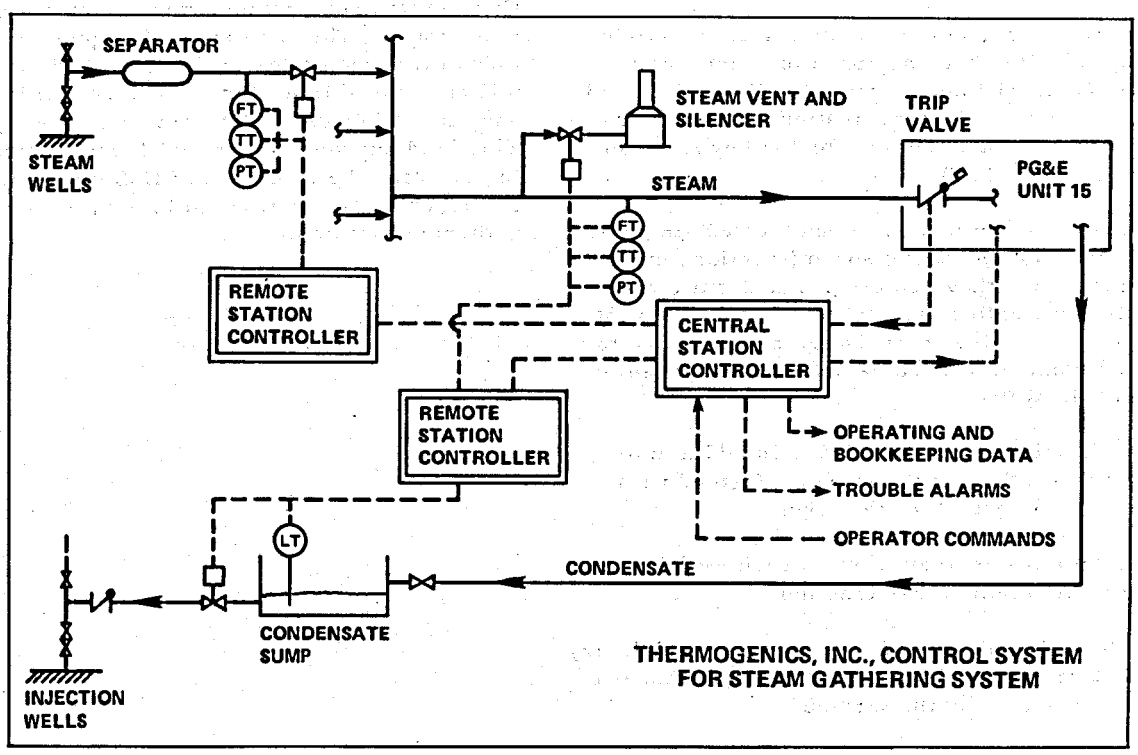
Daniel, Mann, Johnson, & Mendenhall
3250 Wilshire Boulevard
Los Angeles, California 90010

Steam gathering and delivery to the new Pacific Gas & Electric Company (PG&E) Unit 15 at The Geysers will be controlled by an automatic computerized system.

Thermogenics, Inc., lease owner and operator, and the consulting firm of Daniel, Mann, Johnson, & Mendenhall (DMJM) initiated the development of a controlled steam venting system in response to Northern Sonoma County Air Pollution Control District (APCD) requirements for reduction of total H_2S emissions. Approval by the APCD of a construction permit was contingent upon the installation of a gathering system that could rapidly reduce emergency steam venting during air quality episode alerts.

Total reservoir steam venting usually occurs because of unscheduled power plant outages. At existing plants, this venting continues unabated until the gathering system can be turned down. The steam wells are manually shut in if the power plant is to remain out of service for an extended time. Manual shutdown of existing steam fields can take several hours.

The Northern Sonoma County APCD requirement for the Thermogenics steam field specifies capability of reducing unabated steam venting by 60 percent within one hour. As of this writing, the California Air Resources Board is close to approving rules that would require reducing H_2S emissions resulting from "stacking" (venting) 90 percent within 15 minutes. Commitment of funds by Thermogenics, Inc., to design and construct a gathering system that would comply with the APCD venting requirements afforded a basis for justifying additional funds for a completely automatic system.



Automatic control systems added about 15 percent to the investment cost of the gathering system. Approximately 50 percent of that increase was required simply to control emissions. The addition of controllers and computers has converted a remote manually operated system into an automatic system and established a control center for operation of future steam reservoirs. The savings to be realized in operating manpower alone has been determined to be cost-effective.

The simplified flow diagram presented above shows the major components of the Thermogenics steam gathering system. There are nine steam wells connected by pipeline with PG&E Unit 15. A condensate line from Unit 15 returns water to a collection sump. The sump delivers the condensate to injection wells by pipeline. Powered control valves are located at each well, at the condensate sump exit, and at the steam manifold venting system.

Remote station controllers are installed near the control valves, and a central station controller is located in an operator's control room. The central station controller is composed of a cathode ray tube (CRT) terminal and a central processor unit (CPU). The steam gathering system is designed to be monitored and operated from the control room. No operator will be required to perform programmed functions. The preprogrammed computer will control the steam venting and every other operating function desired.

The operator can, however, modify set points to correspond with changing operating conditions. The computer will accept plain English words and common symbols. Communication with the computer is through a standard tabletop keyboard and a video screen (CRT).

Control valves can be opened and closed singly or simultaneously and at any speed (fractions of a second) because they are electro-hydraulic and computer-controlled. Except for emergency venting, however, valve controls are programmed to open and close only at rates safe for the preservation of the wells.

Routine functions and operations, in addition to emergency venting, that can be performed with the automated control system are:

1. Control of the steam flow at each well for optimal steam rate extraction
2. Automatic balancing of the system for delivery of steam at the flow, pressure, and temperature required by the turbine
3. Accelerated plant startups and shutdowns
4. Continuous data collection on well production and well status
5. Centralized operation and control of both the newly installed and future Thermogenics steam gathering systems
6. Periodic data printout as programmed or on operator command
7. Data acquisition during well testing

The above capabilities result in the following advantages:

1. Reduced H_2S emissions
2. Reduced number of operating personnel
3. Steam conservation resulting from faster and more accurate operations
4. Fast response to the steam turbine needs
5. Well status records showing trends in anticipation of the need for new wells
6. Central control of several steam fields
7. Reduced maintenance costs because of fewer discrete instruments

Government requirements for abatement of H_2S emissions at The Geysers will require relatively large investments for equipment. More efficient utilization of this equipment can be realized by adopting it for automatic control of operations. This bold approach taken by Thermogenics, Inc., in accepting the challenge of H_2S emissions abatement sets a new trend in operation of steam gathering systems.

FEDERAL GEOTHERMAL LEASE BIDDING

by Hillary A. Oden, Timothy J. Mac Gillvray, and John Lohrenz

U.S. Geological Survey
Reston, Virginia, Menlo Park, California, and Denver, Colorado

Abstract

We examined the four-year bonus bidding history for Federal geothermal leases compared with the longer history of bidding for Federal offshore oil and gas leases. Differences and similarities were found, the more interesting of the latter were: (1) the standard deviation of bids for a lease appeared to be about the same for both types of leases, and (2) the fraction of money left on the table was almost exactly the same. These similarities arose even though offshore oil and gas lease bids were orders of magnitude higher than geothermal bids.

Introduction

Federal geothermal leases have been offered by sealed bonus bids, highest bid winning, since 1974. In four years from 1974 through 1977 that leases were offered, 262 received one or more bids. The average number of bids received per lease and highest bid per lease and per acre had been decreasing until 1977 when all increased (Table 1).

Table 1

Summary of Federal Geothermal Lease Bidding
by Year

	1974	1975	1976	1977	1974-1977
No. of leases offered	80	181	188	118	567
No. of leases receiving bids	50	82	70	60	262
For leases receiving bids					
Avg. no. of bids/lease	2.48	1.61	1.36	1.92	1.78
Avg. highest bid/acre	$138.02	$24.78	$8.56	$28.47	$40.03
Avg. highest bid/lease	$220,472.00	$52,105.00	$15,383.00	$50,952.00	$74,161.00

We compared the bids for these 262 geothermal leases which received one or more bids with the statistical properties of sealed bonus bids, highest bid winning, for Federal offshore oil and gas sales starting in 1954. One difference between Federal offshore oil and gas leases and geothermal leases is that the former have commanded much higher bids. During 1976 when the average highest bid for geothermal leases was $8.56/acre, 246 offshore oil and gas leases were issued with an average high bid of $1,759/acre - more than 200 times the "price" for geothermal leases. That difference gave impetus to this study. We were interested in which statistical patterns of bids were the same in spite of the huge difference in the magnitude of bids. Also, we wanted to know which patterns changed.

Lognormality of Bids

Statistical tests have shown that Federal offshore oil and gas lease bids can be considered lognormally distributed (1,3). We tested these geothermal lease bids for lognormality using the Kolmogorov-Smirnov one-sample test (6). None of the leases failed the test at a level at which 10 per cent could have failed and we still would not have concluded non-lognormality. We concluded that Federal geothermal lease bids were lognormally distributed.

Occurrence of Low, Noise Bids

Dougherty and Lohrenz (2) defined an algorithm for detecting low, noise bids, i.e., bids so low and far removed from other bids as to be deemed "irregular".

About 2 percent of Federal offshore oil and gas bids in their study were low, noise bids.

Using the same algorithm, only one low, noise Federal geothermal lease bid (out of 466 received) was found. Towne bid $1.25/acre for a lease in the January 22, 1974, sale when the two other bidders bid $61.36 and $478.36/acre. Obviously, low, noise bids have not been important in any geothermal lease sale as they have been for offshore oil and gas lease sales.

Standard Deviation of the Bids

The standard deviation of the logs of the bids is a measure of the disagreement between bidders bidding. The greater the disagreement, the higher the standard deviation. The pooled standard deviation for all 262 geothermal leases was 1.12. This means that overall, 68 percent of bids were within $e^{+1.12}(=3.07)$ and $e^{-1.12}(=0.326)$ times the statistical mean bid. This pooled standard deviation compared with a value of 1.04 for 2,428 Federal offshore oil and gas leases and 1.09 for 1,178 of those bids for which the individual bid variances could be considered homogeneous. Thus, there is remarkable agreement in the standard deviation exhibited by Federal geothermal and offshore oil and gas lease bidders bidding.

We also tested the geothermal lease bids for homogeneity of variances. If homogeneity exists, that means that the amount of disagreement between bidders does not appear to vary statistically from lease to lease. If the disagreement fluctuates widely, variances are heterogeneous and there is no statistical meaning to the pooled standard deviation. We used Bartlett's chi-square test (6) on all leases having six or more bids where directly applicable. A larger test statistic than obtained would be obtained 71 percent of the time given homogeneity of variances; therefore, we concluded that Federal geothermal lease bids have been homogeneous in variances. Federal offshore oil and gas lease bids did not display this broad homogeneity of variances (3).

Money Left on the Table

The sum of highest bids for these 262 geothermal leases was $19.4 million of which $8.9 million was left on the table, i.e., exceeded the next highest bid. Thus, 46 percent of bonuses paid was left on the table. For 2,636 Federal offshore oil and gas leases receiving bids from 1954 through 1975, $7.5 billion of $15.9 billion is bonuses was left on the table. The numbers are orders of magnitude larger, but the per cent of Federal offshore oil and gas lease bonus money left on the table is 47 percent, in almost exact agreement with geothermal bids.

Federal Pre-sale Estimates Compared to Bids

The Federal Government estimated the value of each geothermal lease offered prior to bidding. Starting in 1968, this has been done for offshore oil and gas leases also.

[1] Including all leases receiving bids, a larger statistic would be obtained 12 percent of the time. Including leases with five or less bids biases the test toward rejecting homogeneity when it exists, however.

One way of assessing how these pre-sale estimates compare to the subsequent bids is counting how many bids of all bids received are below the pre-sale estimate for the lease. The more bids received below the pre-sale estimate, the more aggressive the estimates are compared to bids; the less, the more conservative. Six percent of geothermal lease bids were below the estimate; 31 percent of offshore oil and gas lease bids were below pre-sale estimates for sales through 1976 (4).

Another comparison is the ratio of the sums of the pre-sale estimates to the mean of the bids for the leases. Since bids are lognormal, the applicable statistical mean is the geometric mean. For geothermal lease bids, the ratio of these two sums was 0.29; for offshore oil and gas bids it was 0.76 (4).

Federal geothermal lease pre-sale estimates appear to have been more conservative, compared to bids, than Federal offshore oil and gas pre-lease estimates. We state that assessment as a statistical fact only. Let no one make unwarranted judgements that the pre-sale estimates are too high or too low. We do not know whether the estimates were high, low, or perfect because we have no quantitative definition of what perfect pre-sale estimates would have been.

Comparison of Bids Among Bidders

Individual Federal offshore oil and gas lease bonus bidders have displayed widely varying aggressive/conservative bidding within a sale compared to competing bidders (4). How aggressive or conservative a bidder has been was assessed by computing the fraction of all other competing bids which were below the individual bidder's bids. The higher this fraction, the more aggressive the bidder compared to his competitors; The lower, the more conservative. A bidder whose fraction is 0.50 could be said to be unbiased compared to a "jury of his peers" bidding. Table 2 shows these fractions for all bidders bidding four or more times in the January 22, 1974, geothermal sale in which the largest number of bids were received. The same widely varying aggressive/conservative stances of individual bidders are displayed for these geothermal bids.

TABLE 2

Bias of Individual Bidder's Bids
Jan. 22, 1974, Geothermal Sale

Bidder	No. of Bids	Percent of Other Bids Below Bidder's Bids
Union/Thermal/Magma	5	87.5
Union Oil Co.	8	56.0
Signal	7	50.0
Thermogenics	4	47.1
Chevron	4	23.1

Solo and Joint Bids

Joint bids are those bids where more than one bidder "owns" a portion of a bid; for solo bids, 100 percent of the bid ownership belongs to one bidder. Fiftynine percent of Federal offshore oil and gas lease bonus bids through 1976 have been joint bids (5). A much smaller proportion, only four percent, of geothermal bids have been joint bids. More than half of these occurred in the January 22, 1974, sale. Joint bids have not been a significant factor in geothermal lease bidding as in offshore oil and gas lease bidding. This appears consistent with the hypothesis that the much higher bids for offshore oil and gas leases are an impetus for forming joint bidding groups.

Major Oil Company Bidding for Geothermal Leases

Some so-called major oil companies have bid on Federal geothermal leases. Amoco, British Petroleum, Chevron, Exxon, Gulf, Mobil, Shell, and Texaco have participated in 49 percent of all Federal offshore oil and gas lease bids through 1976 (5). Only 10 percent of geothermal bids had any of these major oil companies participating. These bids were highest only eight percent of the time. Therefore, the concentration of major oil companies in geothermal bidding is far less than in Federal offshore oil and gas lease bidding.

Summary

We have shown the following similarities and differences between Federal geothermal and offshore oil and gas lease bonus bids:

1. Both appear to have been lognormally distributed.
2. Low, noise bids appear never to have been a substantial factor for geothermal bids, whereas they have for offshore oil and gas bids.
3. There is a remarkable agreement between the standard deviation (which measures the amount of disagreement of bids between bidders for the same lease) for geothermal and offshore oil and gas leases. This is true even though offshore oil and gas lease bids averaged orders of magnitude larger. Geothermal bids exhibited homogeneity of variances.
4. There is also remarkable agreement between the fraction of money left on the table for these two kinds of lease bids. Of course, the amount of money left on the table for offshore oil and gas leases was orders of magnitude higher
5. Federal pre-sale estimates for geothermal leases have been somewhat more conservative than for offshore oil and gas leases.
6. Individual bidders appear to have displayed the same widely varying aggressive and conservative biases compared to competing bidders in a given geothermal sale than were evident in offshore oil and gas lease sales.
7. Joint bids and bids involving a major oil company have occurred far less frequently in geothermal lease bidding than in offshore oil and gas lease bidding.

Perhaps the most interesting of the above findings is that geothermal and offshore oil and gas bonus lease bidders have shown the same amount of disagreement between their bids on the same lease. Why? Does this mean the technical and economic uncertainties bidders have in deciding what to bid were the same? Or, is it a case of bidders explicitly or implicitly implementing different strategies so what we are really seeing is a disagreement in bidders' strategies? Have the bidders' differing strategies been the same for both kinds of leases? None of these questions can be answered from data, but do adduce interesting speculations about the process of bidding.

References

1. Brown, K. C., 1969, Bidding for offshore oil—Toward an optimal strategy: Dallas, Southern Methodist University Press, 76 p.
2. Dougherty, E. L., and Lohrenz, John, 1977, Statistical analyses of bids for Federal offshore leases: Jour. Petroleum Technology, v. 28, p. 1377-1390.
3. Dougherty, E. L. , and Lohrenz, John, 1977, Money left on the table in sealed, competitive bidding—Federal offshore oil and gas lease sales: Proc. Soc. Petroleum Engineers-Am. Inst. Mining, Metallurgical, and Petroleum Engineers Symposium on Petroleum Economic Evaluation (Dallas, Feb. 21-22), p. 291-300.
4. Dougherty, E. L., and Lohrenz, John, 1977, A study of the agressive/conservative patterns of bidders and pre-sale evaluation—Federal oil and gas lease sales: 52nd Fall Tech. Conf. Soc. Petroleum Engineers—Am. Inst. Mining, Metallurgical, and Petroleum Engineers (Denver, Oct. 9-12), preprint SPE 6807.
5. Dougherty, E. L., and Lohrenz, John, 1978, Statistical analyses of solo and joint bids for Federal offshore oil and gas leases: Soc. Petroleum Engineers Jour., v. 18, no. 2, p. 87-95.
6. Gibra, I. N., 1973, Probability and statistical inference for scientist and engineers: Englewood Cliffs, N. J., Prentice-Hall, 590 p.

NOTE: This report has not been edited for conformity with Geological Survey editorial standards.

Geothermal Resources Council, TRANSACTIONS, Vol. 2 July 1978

HYDROTHERMAL MINERALOGY AND ISOTOPIC GEOCHEMISTRY IN THE CERRO PRIETO GEOTHERMAL FIELD, MEXICO. II. ISOTOPIC GEOCHEMISTRY

E. R. Olson and W. A. Elders

Institute of Geophysics and Planetary Physics
University of California
Riverside, California 92521

ABSTRACT

Stable isotope measurements on borehole samples from Cerro Prieto provide estimates of temperature and water-rock ratios (W/R) in the geothermal system. Shales normally have lower W/R in some wells. The best samples for temperature calculations are hydrothermal vein minerals.

Our isotopic measurements have aided current exploration at Cerro Prieto. For example, no temperature log could be run deeper than 1800 meters in exploration well M92, but isotopic temperatures indicate only 200°C at 2500 meters. In addition isotopic temperatures and wide W/R ranges in wells M91 and M92 suggest that they lie at the probable margin of the productive field. In the center of the field light oxygen del values for the produced fluid appear to delineate extensive drawdown.

Similar studies could assist geothermal exploration elsewhere, and provide baseline information to monitor the effects of production.

Introduction

Active hydrothermal systems are valued as natural laboratories for the study of metamorphic and ore-forming processes (White, 1974). In particular, they afford an opportunity to test chemical and isotopic thermometers developed from theory or laboratory experiments (Truesdell, 1976; Clayton et al., 1968). It is now clear that isotopic measurements can also provide practical insights to geothermal systems themselves. The purpose of this second of three papers on our current work at the Cerro Prieto Geothermal Field, Mexico, is to demonstrate the utility of isotopic studies to geothermics.

Isotopic data can be used to determine the origin and degree of mixing of geothermal waters, to identify zones of boiling and steam loss, to delineate zones of extensive drawdown during production, to calculate subsurface temperatures, to distinguish lithologies or specific zones that have interacted with large volumes of water, and to characterize fluid circulation. Our isotopic data in conjunction with mineralogical studies provide information to guide exploration decisions and to improve reservoir models.

Temperature Estimates

Temperatures can be calculated from isotopic ratios because the partition of stable isotopes between two phases in equilibrium is a simple function of temperature such that [$\Delta = f(T^{-2})$] (Friedman and O'Neil, 1977). Figure 1 shows how the oxygen isotope difference or fractionation between calcite and water [$\Delta = \delta ct - \delta w$] varies with temperature. In order to calculate a temperature we need to measure the oxygen del values of both the geothermal fluid and calcite (or another mineral). The nominal precision of such temperature estimates is roughly ±1%, but the true uncertainty is usually limited by the nature of geothermal samples.

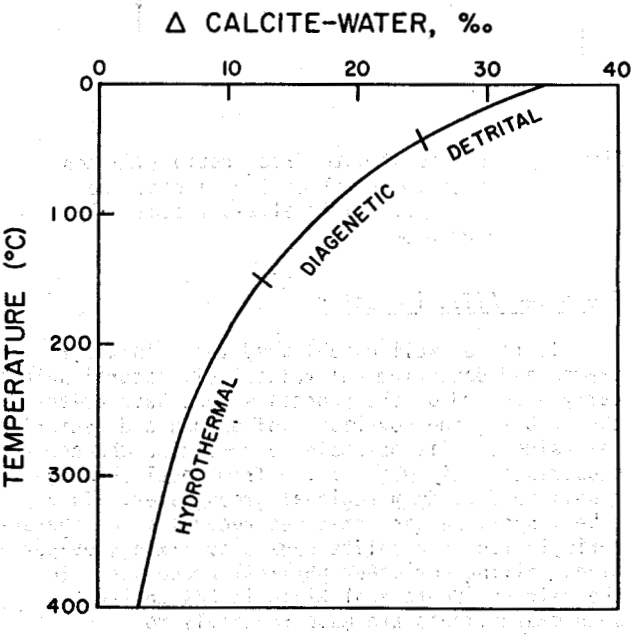


Figure 1. Oxygen isotope fractionation between calcite and water (after Friedman and O'Neil, 1977).

Water-Rock Ratios

The temperature effects shown in Figure 1 involve a redistribution of stable isotopes. Any shift in phases that have become lighter (e.g., calcite) must be balanced by those that have become heavier (water). From this atomic mass balance we can compute how much of one phase has interacted with the other to accomplish the measured effects. Two limiting cases are illustrated in Figure 2; in both, calcite and water have the same initial del values, δ_1 and δ_2 respectively, but their final del values differ greatly. If there is very little water in the system (W/R→0), the calcite is little affected and the only measurable shift is in the water del value. In the opposite case (W/R→∞), the only measurable effect is in the calcite del value. For either case, the ultimate fractionation (Δ) is the same. Therefore, if we can determine the shift of water and rock del values we can compute a minimum water-rock ratio for a geothermal system. In practice, this is most useful as a qualitative indicator of duration and rate of flow.

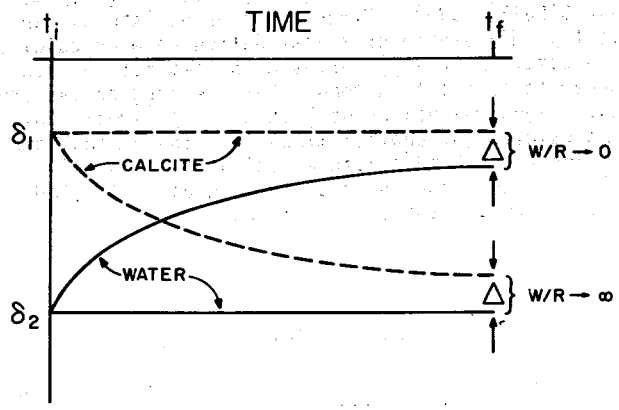


Figure 2. Effect of water/rock ratio (W/R) on oxygen del values for calcite and water during idealized isothermal exchange.

Processes Affecting Water

It is now well established that, in their oxygen and deuterium del values, all natural waters carry a record of the processes that have affected them. Using the covariance of oxygen and deuterium del values, it is possible to determine whether a subsurface fluid was derived from local surface runoff or from deep regional groundwater. In a like manner, we can sometimes recognize the characteristic isotopic shifts caused by mixing, evaporation, boiling, or other physical processes. In the Wairakei Geothermal Field in New Zealand, such measurements are made routinely to detect changes in the subsurface fluids (Ellis, 1976). Isotopic and chemical evidence have pointed to boiling as an important process in vapor-dominated hydrothermal systems such as those at Yellowstone and at The Geysers (White et al., 1971).

Applications to Cerro Prieto

We have found for almost all Salton Trough geothermal fields that the oxygen del value of calcite is not just a function of temperature because of great variations in water-rock ratios, even on a very local scale (Olson, 1977). For example, Figure 3 shows that del values for calcites from well M92 at Cerro Prieto between 2000 and 2200 meters depth have a range of almost 20 °/oo. Vein calcite is systematically the lightest, sandstone and siltstone are intermediate, and shale has the heaviest del values. Because of their low permeability, the shales have limited interaction with geothermal fluids and so preserve detrital/diagenetic del values (+20 °/oo). Vein calcite, on the other hand, is precipitated directly from hydrothermal fluids and is therefore in equilibrium with hot water. Similar ranges of del values are seen in other wells. We believe this range represents a spectrum of increasing W/R from shale to vein calcite. It follows, therefore, that temperature estimates based on vein minerals have the best chance of reflecting the reservoir conditions.

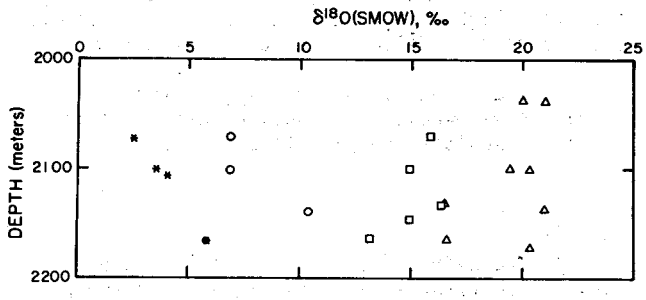


Figure 3. Oxygen del values for calcite hand-picked from M92 cuttings (*=vein calcite; O-sandstone, □=siltstone; Δ=shale).

Figure 4 shows isotopic temperatures for well M92 calculated from vein calcite del values. M92 is an exploration well drilled more than two kilometers southeast of the production field (see Elders et al., 1978, this volume, Fig. 1). There is a substantial uncertainty in these temperature estimates because fluids have not been sampled from it. We have, therefore, assumed a value of -8.0 °/oo for the fluid based on samples from the producing wells (see below). These estimates are important because although the well was completed to 2560 meters, for technical reasons

temperature logs could not be measured below 1800 meters. Although our temperatures are preliminary, they indicate that M92 lies near the probable limit of the production field. This inference is supported by the wide spread of del values in different rock types as seen in Figure 3. This spread is characteristic of wells on the margins of the Salton Sea Geothermal Field. Wells near the center should show a high isotope shift and a much narrower spread of del values indicating high temperatures and high water-rock ratios. This observation is an additional means of evaluating exploration wells. For example, it was partly on this basis that we inferred that another exploration well, M84, would be a good steam producer (Elders et al., 1978, this volume).

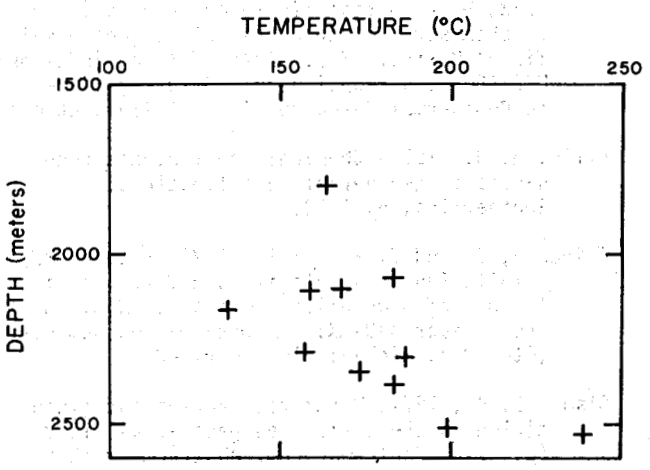


Figure 4. Isotopic temperatures calculated from oxygen del values for calcite in well M92 using δwater = -8.0 °/oo.

Comparison of M90 and M91

M90 and M91 are exploration wells drilled about 1.5 kilometers from the producing field (see Elders et al., 1978, this volume, Fig. 1). Oxygen isotope data for calcite in sandstone from these two wells are quite different (Fig. 5). In M90 all del values lie between 0 and -4, whereas those from M91, which mainly come from greater depth, range from 0 to +9 °/oo. The larger range of del values in M91 indicates that the well is in a zone of more limited fluid flow than is the case for M90.

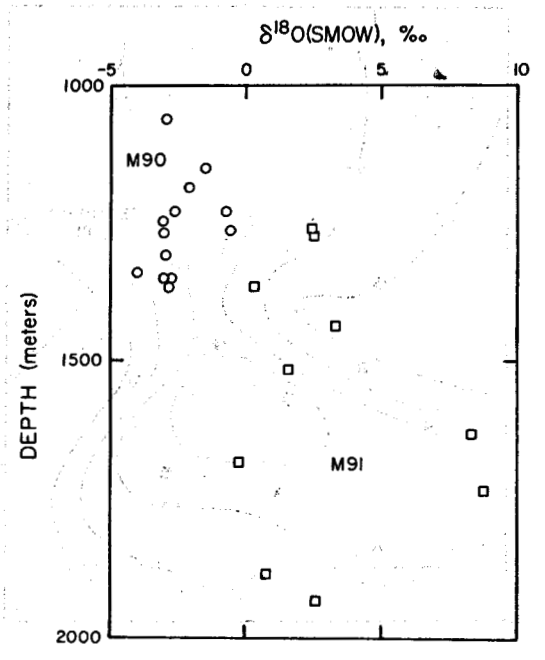


Figure 5. Oxygen isotope profiles for calcite in sandstone in M90 (O) and M91 (□).

Produced Fluids

The data of Figure 6 show a potential application of isotope geochemistry to field management. They are isopleths of oxygen del values for subsurface brines. They were calculated from measured values of fluids sampled in April 1977 in the production field assuming a mass ratio of steam to water of 20%. This calculation would be improved by using measured enthalpy and flow rates, but the values would change by less than 0.5 °/oo. There is clearly a zone of del values lighter than the apparent background value of -8.0 °/oo in the center of the producing field. Among the possible explanations are (1) the lighter water comes from a zone of already highly exchanged rock and therefore the water is less shifted by reaction with it; (2) it is controlled by equilibria with different minerals; or (3) production has caused a "drawdown" of lighter fluid. The third mechanism was proposed by Truesdell; it would also explain chemical zoning of these fluids (personal communication, 1978). To discriminate between these ideas further work using hydrogen isotope measurements of the fluids and oxygen isotope measurements of minerals is planned.

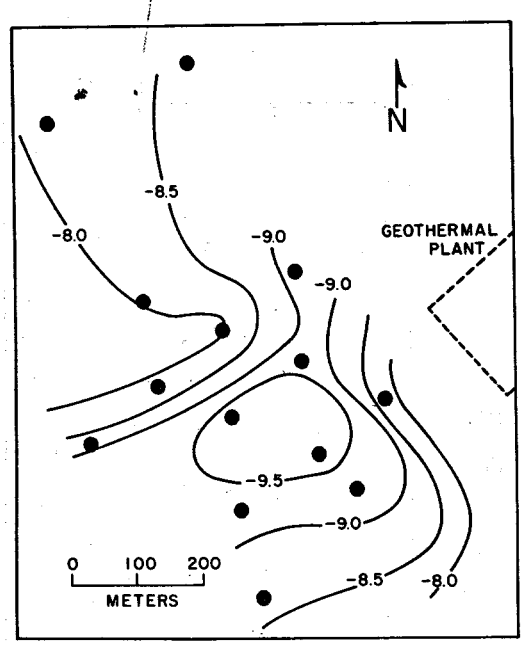


Figure 6. Oxygen del value isopleths (°/oo, relative to SMOW) for Cerro Prieto brines collected April 1977 by A. Truesdell, USGS.

Conclusions

Isotopic measurements on rocks and fluids can be used both to calculate temperatures and to characterize circulation in geothermal systems. Such data can be obtained inexpensively even during drilling. If the system being explored is of a type that is well understood, isotopic data can be used as an exploration tool. The isotopic values preserved in minerals reflect conditions before they are disturbed by drilling and production, and may provide a baseline for studies of the fluids once production is underway. We feel that these concepts which have proved so useful in the Cerro Prieto Geothermal Field could be applied to any hydrothermal system.

Acknowledgements

We are grateful for the capable assistance of L. Ansell, L. Armstrong, and G. Laurin in making the isotopic measurements that are the foundation of this paper. The rock samples were provided by our Mexican colleagues of the Comisión Federal de Electricidad. We enjoyed stimulating discussions with A. Truesdell, United States Geological Survey.

This work was supported for six months by the Division of Geothermal Energy of the Department of Energy, USA, subcontract no. 7100410.

References

Clayton, R. N., L. J. P. Muffler, and D. E. White, 1968, Oxygen isotope study of calcite and silicates of the River Ranch No. 1 well, Salton Sea geothermal field, California: Am. J. Sci., 266, 968-979.

Elders, W. A., E. R. Olson, J. R. Hoagland, C. E. Barker, P. D. Johnson, and P. Collier, 1977, A comprehensive study of samples from geothermal reservoirs: Petrology and light stable isotope geochemistry of wells M48, M84, M90, M91, M92 and Prian No. 1, in the Cerro Prieto geothermal field, Baja California, Mexico: UCR/IGPP contribution no. 77/37, 153 p.

Elders, W. A., J. R. Hoagland, and E. R. Olson, 1978, Hydrothermal mineralogy and isotopic geochemistry in the Cerro Prieto geothermal field, Mexico. III. Practical applications: UCR/IGPP contribution no. 78/10, submitted to Geothermal Resources Council Transactions.

Ellis, A. J., 1976, Chemical and isotopic techniques in geothermal investigations: Geothermics, 5, 3-12.

Friedman, I. and J. R. O'Neil, 1977, Chapter KK: Compilation of stable isotope fractionation factors of geochemical interest: U.S.G.S. Prof. Paper 440-KK: in Data of Geochemistry (6th ed.), Michael Fleischer, ed.

Olson, E. R., 1977, Water-rock ratios and fluid mixing in the Salton Sea geothermal field (abst.): Geol. Soc. Am. Abstracts with Programs, 9, 1119.

Truesdell, A. H., 1976, Summary of Section III: Geochemical techniques in exploration: Proceedings, Second U. N. Symposium on the Development and Use of Geothermal Resources, 1, liii-lxxix.

White, D. E., 1974, Diverse origins of hydrothermal ore fluids, Econ. Geol., 69, 954-973.

White, D. E., L. J. P. Muffler, and A. H. Truesdell, 1971, Vapor-dominated hydrothermal systems compared with hot-water systems: Econ. Geol., 66, 75-97.

UCR/IGPP contribution no. 78/9

THE PAGOSA SPRINGS PROJECT--THE FIRST PERMITTED GEOTHERMAL WELLS IN IN COLORADO

RICHARD HOWARD PEARL, MICHAEL J. GALLOWAY, AND JAY D. DICK

Colorado Geological Survey
Denver, Colorado

ABSTRACT

The geothermal resources at two areas in Colorado-Pagosa Springs and Glenwood Springs-are being explored and developed for direct application uses.

At the first site, Pagosa Springs, any thermal waters developed will primarily be used to heat a new high school complex. Geological, hydrogeological, geophysical, and geothermometer studies were done in the region to fully delineate the reservoir. It was determined that the reservoir encompasses some 4 sq. kilometers and may have a temperature of 125°C.

Before drilling commences it was necessary to apply for permits from the Colorado Oil and Gas Conservation Commission, Water Quality Control Commission, and Air Quality Control Commission. All permits have been issued. To test the aquifer and to determine what legal hydrological conditions the thermal waters are occurring under, a 2-3 day aquifer test will be run.

Work done under U.S. Department of Energy, Division of Geothermal Energy contract No. EG-77-S-07-1678.

INTRODUCTION

With funding from the U.S. Department of Energy/Division of Geothermal Energy (DOE/DGE) the Colorado Geological Survey in 1977 initiated a two year exploration and development program leading to the development of the geothermal resources for direct application uses at two locations in Colorado. This paper discusses efforts to date and problems encountered. It was the intention of DOE/DGE for this to be an exploration and drilling project to bring the geothermal resources "on-line" as quickly as possible, therefore the project was designed to be a development project and not a paper study.

In 1973 the Colorado Legislature passed the Geothermal Resources Act which provides for the exploration, development, and production of geothermal resources in the State. This law required the Colorado Oil and Gas Conservation Commission to promulgate rules and regulations to govern the drilling of geothermal wells. The wells to be drilled during this project are the first wells permited under this law. As a result of this being the first geothermal project in Colorado the various state regulatory agencies are having to set new procedures or modify existing procedures for this development.

SITE SELECTION

The geothermal areas in Colorado which have potential for development were delineated by Barrett and Pearl (1978). Based on geochemical modeling of estimated reservoir temperatures Pagosa Springs and Glenwood Springs were selected for further exploration efforts to determine if the resources could be developed. Primarily due to local interest, Pagosa Springs was selected as the first site of investigation, and in the fall of 1977 geological and geophysical investigations started. Local officials plan that any thermal fluids developed will be used to heat a new high school complex, to be built on the south side of town, and/or for other purposes.

HYDROLOGY

Pagosa Springs is located in southwestern Colorado on the San Juan River, some 60 miles east of Durango. The town is named for the hot springs which are located along the south bank of the river across from the downtown section. The springs issue from Cretaceous Mancos Shale at a temperature of 54°C (Barrett and Pearl, 1976). The measured discharge of the spring is approximately 265 gpm(17 l/sec). The thermal waters are a sodium sulfate-bicarbonate type with 3200 mg/l total dissolved solids. Geothermometer analysis shows that the reservoir temperature ranges from 75°C to 125°C. Hydrogeological mapping by Galloway has determined that the area surrounding Pagosa Springs is a regional groundwater discharge area.

GEOLOGY AND GEOPHYSICS

Pagosa Springs is located on the eastern side of the San Juan drainage basin, which is bounded on the east and north by the San Juan Mountains. These mountains consist primarily of Tertiary volcanic flows and volcano-clastic rocks. The Archuleta anticlinorium, one of four major tectonic provinces in southwestern Colorado and northwestern New Mexico

(Ryder, 1977), is the dominant structural feature in the Pagosa Springs area. The anticlinorium, which forms a structural divide between the Chama Basin on the east and the San Juan Basin on the west continues southward to the Nacimiento uplift in New Mexico (Ryder, 1977).

Surface geological mapping of the Pagosa Springs area has been done by Dunn (1964), Hail (1971), Steven and others (1974), and Wood and others (1948). The major stratigraphic units in the area are the Mancos Shale and the Dakota Sandstone, both of upper Cretaceous age. Overlying the Precambrian basement may be up to 396 meters (1,300 feet) of Meszoic sediments. Numerous north, northwest trending faults are found throughout the region. The major fault, with up to 91 meters (300 feet) of displacement, is the northern extension of the Jacimiento fault of New Mexico. This feature is located approximately 2.4 km (1.5 miles) west of town.

To fully evaluate the geothermal reservoir, detailed geophysical surveys were conducted by personnel from Geophysics Fund, Inc. of the Colorado School Mines. They ran dipole-dipole and dipole-bipole resistivity, vibro-seis surveys and soil mercury analysis. Interperation of the data shows that a resistivity anomaly of 15-30 ohm-meters (background of 300-400 ohm-meters) surrounds the hot springs. Measured resistivity levels at the spring were higher than values mesured on either side of the spring. The resistivity surveys indicate that the geothermal reservoir encompasses an area of approximately 4 sq. km. (43,000 sq. feet). Located in and around the downtown section of Pagosa Springs are some 20 existing hot water wells. Based on interpretation of drillers logs and talking with the well owners it was determined that the existing wells are completed in the top of the Dakota Sandstone. Even though water from these wells is generally as hot as water from the spring, it is believed that the Dakota Sandstone is a secondary reservoir and that the primary reservoir lies at a greater depth. Since there are no indications of a definite heat source, it is assumed that deep circulation in an area of slightly enhanced geothermal grandient is the driving mechanism for this thermal area. Assuming a geothermal gradient of at least 30°C/km, a minimum circulation depth of 2-3 km (6,000-10,000 feet) would be required to produce 60°C-80°C water. This depth requires that most of the water circulation takes place in fractures of the Precambrian basement.

The results of the soil mercury surveys are inconclusive, but the possibility exists that an anomaly may occur south of the hot springs. There are no surface traces of faulting in the Pagosa Springs area but vibro-seis surveys indicate there may be several minor faults present in the subsurface.

In addition, 6 heat flow holes were drilled to more fully delineate the extent of the reservoir. Preliminary measurements indicatate that the gradients may range from 65°C/km to 130°C/km.

INSTITUTIONAL ISSUES

As required by the Geothermal Resources Act of 1973 application was made to the Colorado Oil and Gas Conservation Commission for permission to drill one exploration/production well and two observation wells at Pagosa Springs. The Act also requires that the Oil and Gas Conservation Commission submit the permit application to the Colorado Division of Water Resources for an assessment of the impact of the geothermal development on adjacent water resources. A public hearing was held before the Oil and Gas Conservation Commission on March 20, 1978, and the permit application approved.

Permit applications were also filed with the Water Quality Control Division and Air Quality Control Division of the Colorado Department of Health. Federal and State laws prohibit the addition of any substance to surface waters which might degrade their quality or raise their natural temperature by more than 1°C. To meet these requirements all produced fluids will be cooled prior to disposal in the San Juan River. The permit applications were filed in January, 1978 and approved in late March, 1978.

FUTURE PLANS

At the time this paper was submitted all permit applications had been approved. Bids from drilling contractors have been received and were awaiting financial review prior to issuing drilling contracts.

Due to economic considerations it is desirable that the exploration/production test well be drilled as near the proposed school site as possible. Since no land was leased for this project by local officals drilling is limited to available municipal, county, or school district property. There are two projected drill sites at the proposed school complex and one near existing hot water wells in the downtown section. The new school site is located on the fringe of the resistivity anomaly and the downtown site is over 1200 meters (.75 miles) from the proposed school site. While this is a potential problem it is not felt to be serious.

An exploration/pumping well will be drilled during the spring of 1978 to a maximum depth of 2,000 feet. Straddle packer and/or drill stem tests will be performed prior to setting the casing. A 2-3 day aquifer test will be run after the well is completed. At the present time it is planned that two observation wells, 400 and 2,000 feet deep, will also be drilled. These wells will be used during the aquifer test.

After completion of drilling and testing, the well will be turned over to either Archuleta County, the City of Pagosa Springs, or the School District for use in the Pagosa Springs area. School District officials intend to use the water to heat a proposed high school. Other uses will depend on temperature and volume of water encountered in the drilling program.

PROBLEMS

One of the major problems encountered is in attaining, in a timely manner the necessary permits. This is a combination of bureaucratic delay and the fact that this is a new permitting process for the State. The proposed well is neither a groundwater well nor a high temperature geothermal production well and therefore does not fit into any single category.

Another problem, which could potentially have been much worse, is the availability of land. Because of ownership the drilling site is restricted to two pieces of land, one at the proposed school site and the other in the county courthouse parking lot, 200 meters north of the spring.

Escalating drilling costs is the third major problem encountered. Bids received for the drilling and completion of the three wells ranged from a low of $152,000 to a high of $500,000. Because of inflation and the high number of coal and uranium exploration projects in the Colorado- Wyoming area, drill rigs of the required depth capacity are scarce and very expensive. The high costs may require trimming the program to the bare essentials.

CONCLUSION

It is anticipated that by carrying this project through to completion that several important developments will have resulted. They are: 1, The respective state agencies will have become aware of some of the problems in regulating the development of geothermal resources; 2, Private companies and individuals will become aware of the time delays in getting the necessary permits; 3, Potential developers of low-temperature geothermal resources will become cognizant of the fact that many times the factor governing the location of the geothermal well is not the location of the resource but the land situation, especially where the resource is located either in or close to a community; and 4, A geothermal resource will be developed and put to beneficial direct application uses in a region where the natural energy supplies are declining.

REFERENCES

Barrett, J.K., and Pearl, R.H., 1976, Hydrogeological data of thermal springs and wells in Colorado: Colorado Geol. Survey Inf. Ser. 6, 124 p.

_____, 1978(In press), An appraisal of Colorado's geothermal resources: Colorado Colorado Geol. Survey Bull. 39.

Dunn, D.E., 1964, Evolution of the Chama Basin and Archuleta anticlinorium, eastern Archuleta County: Univ. of Texas, Dept. of Geology, PhD dissertation.

Hail, W.J., Jr., 1971, Geologic reconnaissance map of the Chris Mountain and Pagosa Spring quadrangle, Archuleta County, Colorado: U.S.Geol. Survey open-file report.

Steven, T.A., Lipman, P.W., Hail, W.J., Jr., Barker, Fred, and Luedke, R.G., 1974, Geologic map of the Durango qudrangle, southwestern Colorado: U.S. Geol. Survey Misc. Inv. Series Map I-764 scale 1:250,000

Ryder, R.T., 1977, Mineral resources of the Chama-southern San Juan Mountain wilderness study area, Mineral, Rio Grande, Archuleta, and Conejos Counties, Colorado: U.S. Geol. Survey open-file report 77-309, 21 p.

Wood, G.H., Kelly, V.C., and MacAlpine, A.J., 1948, Geology of the southern part of Archuleta County, Colorado: U.S. Geol. Survey Oil and Gas Inv. Prelim. Map OM-81

NATURAL CONCENTRATIONS OF Hg IN THE YELLOWSTONE AND COSO GEOTHERMAL FIELDS

David W. Phelps and Peter R. Buseck

Departments of Geology and Chemistry
Arizona State University
Tempe, Arizona 85281

Introduction

The association of Hg mineralization with geothermal activity is well-documented (White, 1967; Dickson and Tunnel, 1968). More recently, anomalous amounts of Hg have been discovered in geothermal areas that have no associated Hg mineralization (Koga and Noda, 1976; Matlick and Buseck, 1976; Robertson and others, 1977). New data from Yellowstone National Park and Coso Hot Springs, Inyo County, California, show anomalous concentrations of Hg in soils, rocks and hot spring deposits from these thermal regions.

Sampling and Analytical Technique

Soil samples were collected from the A soil horizon at a depth of 5-10 cm below the surface and immediately placed into sealed plastic bags. At the base camp the samples were air dried in a cool, protected location, sieved using an 80 mesh stainless steel sieve and the -80 fraction stored in tightly sealed glass vials. The rock and hot spring deposit samples were returned to the laboratory, manually crushed to a -80 mesh size and stored in tightly sealed glass vials.

Mercury analyses of soil samples were performed within 2 or 3 days after collection using a field portable Jerome Instrument Co. thin-gold film Hg detector. The instrument has an absolute sensitivity of 0.5 ppb Hg under field conditions. Details of the analytical procedure have been presented by McNerney and others (1972) and Matlick and Buseck (1976).

Results

Nearly 1,000 soil samples have been collected and analyzed for Hg from Yellowstone. Background concentration of Hg in soils from Yellowstone is 20 ppb and is comparable to background values for soils reported from other areas (Matlick and Buseck, 1976; Davies, 1976). As shown in figure 1, the background concentrations of Hg in soils from Yellowstone are independent of bedrock geology. Background levels are the same inside and outside the caldera.

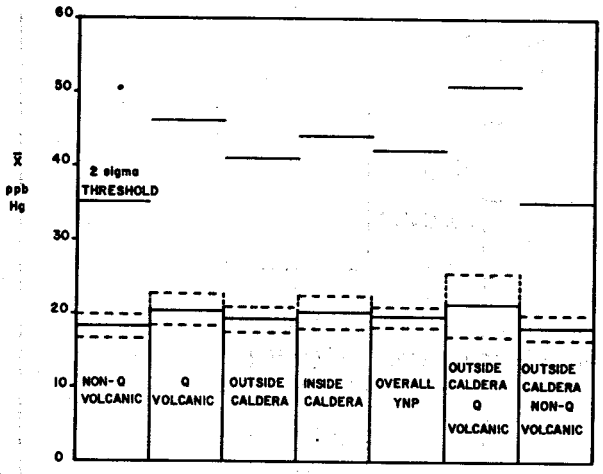


Figure 1 - Background Hg concentrations for soil samples from different geologic environments at Yellowstone. The 2 sigma threshold includes 95% of all the samples used to compute the background value. Dashed lines represent 2 standard deviations of the mean.

Anomalous amounts of Hg were found in soils from thermal areas (figure 2) in Yellowstone. Peak to background ratios of >1,000:1 were recorded in soils from several thermal basins. In the Norris and Upper Geyser Basins, the distribution of Hg in soils is erratic, showing little correlation with the presence of hot springs or geysers. However, in the Mud Volcano region the Hg concentrations in soils contour around areas of intense vent activity. Although the Mammoth Hot Springs have a much weaker Hg anomaly than any other major thermal basin that we studied at Yellowstone, anomalous concentrations of Hg (peak to background ratios up to 15:1) were detected in four of the 32 samples collected from the Mammoth area. In all cases at Yellowstone the Hg anomalies are narrow and extend outward from the thermal area for only a few hundred meters.

Fourteen volcanic rock and 14 hot spring deposit samples from Yellowstone have been analyzed for Hg. All but one of the fresh rhyolite and basalt samples contain less than 5 ppb Hg (one rhyolite contains 9 ppb Hg), whereas hydothermally altered rhyolites contain up to 730 ppb Hg. Sinter

samples show a wide range of Hg concentrations from a low of 9 ppb Hg to a high of 21,500+ ppb Hg. Travertine from the Mammoth Hot Springs and Soda Butte areas contains less than 20 ppb Hg. However, one travertine sample collected from the Upper Geyser Basin contains 3,600 ppb Hg. A plot of the Hg content of rock and hot spring deposit samples against the Hg content of soil samples collected from the same location reveals that the soil samples are enriched in Hg by factors ranging from 1.5:1 to 100:1 relative to the rock or hot spring deposit samples.

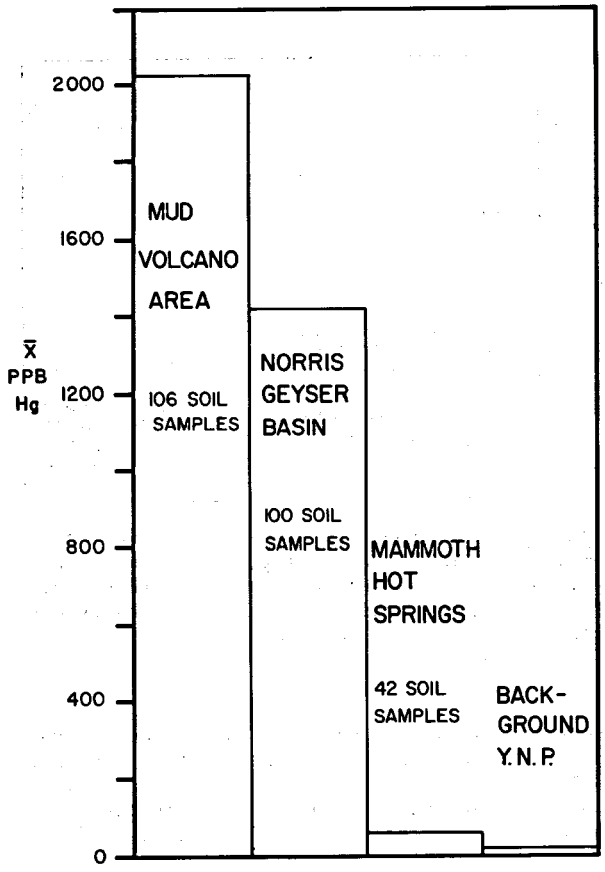


Figure 2 - Average Hg value of all soil samples collected from 3 thermal areas compared to the background Hg value of soil samples from Yellowstone.

Forty-nine soil samples have been collected and analyzed for Hg from the Coso Hot Springs region, California. The samples range in concentration from background levels of 15 ppb Hg to peak values to 3,600 ppb. Results from the Coso area show a broad, low-level anomaly (peak to background ratios of 2:1 to 3:1) over most of the region with a much stronger anomaly (peak to background ratios up to 100:1) superimposed on the broad anomaly. The broad, low-level anomaly roughly corresponds to the surface exposure of a young rhyolite dome field. The strong Hg anomaly at Coso correlates with an area of high heat flow (Combs, 1976) and present day geothermal activity.

Discussion

The results of our study show that natural background concentrations of Hg in rocks and soils from Yellowstone and Coso are quite low. However, near thermal areas the concentration of Hg in both rocks and soils is considerably higher than background levels. The preferential concentration of Hg in soil samples relative to rock samples from the same locality shows that soils are best suited for the detection of Hg anomalies associated with geothermal activity.

The magnitude and shape of the Hg anomalies varies from one geothermal area to another. At Coso The Hg anomaly is several kilometers across and extends well beyond the present limits of geothermal activity. Similar broad anomalies have been reported from Long Valley, California, and Summer Lake Oregon (Matlick and Buseck, 1976). The Hg anomalies at Yellowstone, however, are quite narrow and they are restricted to the immediate vicinities of the thermal features.

Although the association of Hg mineralization and geothermal activity has been known for some time, only recently has it been demonstrated that anomalous quantitities of Hg occur in unmineralized geothermal areas. The results of the present study plus those of other recent studies suggest that anomalous amounts of Hg may be a characteristic of geothermal activity whether or not Hg mineralization has occurred.

References Cited

Combs, J., 1976, The Coso Geothermal Project Technical Report #3: U.S. Energy Research and Development Administration, ERDA Prime Contract E(45-1)-1830, 24 pp.

Davies, B.E., 1976, Geoderma, V. 16, pp. 183-192.

Dickson, F. and Tunnel C., 1968, Ore deposits in the U.S. (Graton-Sales vol.) J.D. Ridge, ed., 1933-1937, V. 2, pp. 1673-1701.

Koga, A. and Noda, T., 1976, Proc. 2nd U.N. Geotherm. Symp., C. Pezzotti, ed., V. 1, pp. 761-766.

Matlick, J.S. and Buseck, P.R., 1976, Proc. 2nd U.N. Geotherm. Symp., C. Pezzotti, ed., V. 1, pp. 785-792.

McNerney, J.J., Buseck, P.R. and Hanson, J.C., 1972, Science, V. 178, pp. 611-612.

Robertson, D.E., Crecelius, E.A., Fruchter, J.S. and Ludwick, J.P., 1977, Science, V. 196, pp. 1094-1097.

White, D.E., 1976, Geochemistry of Hydrothermal Ore Deposits, H.L. Barnes, ed., pp. 575-631.

PRELIMINARY ENVIRONMENTAL ASSESSMENTS OF KNOWN GEOTHERMAL RESOURCE AREAS IN THE UNITED STATES

Paul L. Phelps, Don L. Ermak, Lynn R. Anspaugh*
Calvin D. Jackson and Lowell A. Miller

Lawrence Livermore Laboratory
San Francisco Operations Office, Department of Energy

SUMMARY

Utilization of geothermal resources in the United States is on the threshold of undergoing rapid expansion. The Department of Energy (DOE) is sponsoring a number of programs in support of developing the technology and resources related to achieving such an expansion. These include electrical power plant demonstration projects, resource development, environmental research and loan guarantees. In order to assure that any development of geothermal resources takes place in an environmentally acceptable fashion, the Office of Assistant Secretary for Environment, DOE, has recently implemented a program that focuses on the early identification of environmental assessment needs. This program is called the Geothermal Overview Project. It is now in place at several Known Geothermal Resource Areas (KGRAs). These include The Geysers-Calistoga, Mono-Long Valley, Roosevelt Hot Springs, Raft River and regions of the Texas-Louisiana gulf coast. In the future, programs at other high priority KGRAs will be implemented. These will include Hawaii, Coso Hot Springs, Northern Nevada and Oregon.

The basic purpose of the Geothermal Overview Project is to identify, summarize, and assess the environmental issues of the top priority KGRAs from among the approximately 40 KGRAs currently identified by the Division of Geothermal Energy, DOE, as having high possibilities for commercial development. The Geothermal Overview Project addresses issues pertaining to air quality, ecosystems quality, noise effects, geological effects, water quality, socioeconomic effects and health effects. For each KGRA the following functions are accomplished: (1) identification of key issues, (2) inventory of all available data, (3) analysis and assessment of available data, and (4) identification of what additional information is required for adequate assessments.

*Paul L. Phelps, Don L. Ermak, Lynn R. Anspaugh
Lawrence Livermore Laboratory
Livermore, California 94550
Calvin D. Jackson and Lowell A. Miller
San Francisco Operations Office
Department of Energy
1333 Broadway
Oakland, California 94612

Vital to the Overview approach is the free and open flow of information and the early involvement of all interested parties which include local, state, and federal agencies, electrical utilities, resource developers, universities, private and public groups. By involving all interested parties from the very outset, the Overview report will reflect a con ensus of these groups. Another aspect is to avoid redundency of efforts by clearly establishing the status of current and planned research, including environmental baseline measurements and effects studies. It is also clear that time and money do not permit environmental studies to be conducted simultaneously at a large number of KGRAs. The Overview Project does, however, permit selecting on a priority basis those areas having the most critical need for environmental assessments.

Implementation of the Overview Project has been done through subcontracts to a number of groups, with overall management responsibilities at the Lawrence Livermore Laboratory. Criteria for selection of a particular subcontractor mandated that they be located reasonably close to the KGRA; working relationships could be established with the various participants within the geothermal industry developing the resource; and appropriate involvement could be developed with the various government agencies responsible for the planning and regulating aspects. The various lead subcontractors currently in place are:

- Lawrence Livermore Laboratory: The Geysers-Calistoga, California (in cooperation with Sonoma, Lake, Mendocino, Napa Counties: GRIPS)
- University of California, Los Angeles: Mono-Long Valley, California
- University of Utah Research Institute: Roosevelt Hot Springs, Utah
- Idaho National Engineering Laboratory: Raft River, Idaho
- University of Texas-Austin, Louisiana State University, Gulf Region

Advisory committees were established for each KGRA. Membership was drawn from experts associated with the development or management of the various geothermal resources. The advisory committees were charged with identifying all appropriate participants, planning workshops and reviewing reports. Participation was typically represented by the following groups:

Federal Government: Geological Survey, Bureau of Land Management, Environmental Protection Agency, Fish and Wildlife Service, Forest Service, Department of Agriculture, Department of Energy

State Government: Air Resources Board, Energy Commission, Water Resources Board, Fish and Game Commission, Division of Oil and Gas, Land Commission, Railroad Commission, Department of Health, Public Utility Commission

Local Government: Planning Department, Public Works Commission, Air Pollution Control District, Multi-county regional groups, Agriculture Commission

Developers: Electrical utilities, resource developers (steam, hot water, suppliers, etc.)

Others: Universities, private environmental laboratories, national laboratories, environmental groups

A workshop approach has been used, since a goal of the Overview Project was to have input from all participants in the process of identifying key issues and priorities. These participants represent, in most cases, the best possible expertise available for each KGRA.

The workshops were designed to review current knowledge and ongoing or proposed environmental programs. Usually one day was required for such a review, with a second day spent in small groups to address specific issues and requirements. This approach has been very successful in surfacing information that could not be conveniently obtained by other methods. The specific subcontractor is responsible for evaluating all data and developing a comprehensive report. These reports have been made available to local, state, or federal agencies, utilities, developers, or public groups.

To date, the most complex study has been carried out for The Geysers-Calistoga KGRA in Northern California and will be used as an example for this paper. This was done in conjunction with the Geothermal Resources Impact Projection Study (GRIPS), a regional body consisting of the counties of Lake, Mendocino, Napa, and Sonoma. Other participants were the California State Energy Commission and the Department of Energy. Jointly sponsored workshops (Lawrence Livermore Laboratory and GRIPS) were held for issues relating to air quality, ecosystems quality, noise effects, and water quality. Yet to be held are workshops on socio-economic effects and health effects.

A number of environmental concerns were identified at The Geysers-Calistoga KGRA which either are currently impeding development or are expected to become significant in the future.[1] These concerns have been combined to form twenty-one issues, each dealing with a measurable impact on the environment. The issues were prioritized according to their potential for impeding geothermal development if not properly controlled or mitigated. Priorities were set in a quantitative manner by subjecting them to the following questions:

- Does this issue involve an impact which is currently affecting the region, and is it expected to occur in the future?
- Is the impact restricted to the geothermal development area or does it extend beyond these boundaries?
- Do regulating agencies consider this issue to be sufficiently serious to provide legal means for control?
- Is this issue currently an impediment to geothermal development, and is it expected to be an impediment in the future?

The most critical issue identified at the Geysers-Calistoga KGRA is related to the release of hydrogen sulfide from power plants, geothermal wells, and steam by-pass systems. Currently, the California air quality standard of 30 ppb is being exceeded a significant number of days each year. The Sonoma County Air Pollution Control District Office (APCD) has formally requested cancelling hydrogen sulfide variance permits for five power plants which will result in long-term shutdowns. Also, the Lake County APCD has requested the State Air Resources Board to require shutdown of old power plants as new ones come on-line.

The continued development of these resources requires the effective control of hydrogen sulfide emissions. Assuming that sufficient control is achieved to allow additional geothermal development, there is a need for methods of predicting the transport of hydrogen sulfide throughout the region. This capability has the potential for determining the source when a hydrogen sulfide episode occurs, for predicting the impacts of a specific power plant site, and for assessing the regional impacts of large-scale development.

The remaining issues, which potentially will have less impact, were ranked into three categories. The issues included in the first two categories are described below.

Category 1

A comprehensive regional basedline study of rare and endangered species is needed to identify the species inhabiting the region and to locate their habitats. This issue has already led to an intensive delay in at least one geothermal project and to inadvertent destruction of some rare plant populations.

Much of The Geysers region is characterized by steep slopes which are covered with an unstable mantle of badly decomposed rock. These mantles often move downslope as large sheets forming landslides. Within key development regions, the surficial geology should be mapped and potential hazards identified.

As development approaches more populated areas, there will be an increasing need for practical, effective silencing systems to reduce the noice from the free venting and drilling of steam wells.

Recent data suggests that an extensive hot-water dominated reservoir exists in the region northwest of the current development area. The potential for the development of this resource to degrade or deplete potable groundwater supplies and hot springs in the region needs to be evaluated.

Nearly all of the environmental impacts are highly dependent upon the location of the geothermal facilities due to the complex terrain of the region. A description of the future development is needed which identifies the air basins, water sheds, and counties where geothermal growth will occur.

Category 2

Under current operating practices essentially all pollutant emissions to the atmosphere occur through the cooling tower. After hydrogen sulfide, boron emissions are of primary concern. Of secondary importance are emissions of ammonia, mercury, arsenic, and sulfates. Further studies need to be conducted to determine the dispersion of these substances in the atmosphere, their possible accumulation in soils and on vegetation, and their potential effects on the local ecosystems.

Baseline data concerning the terrestrial and aquatic ecosystems of the region is needed to facilitate planning and siting of geothermal facilities, to conduct impact assessments and monitoring, and to effectively manage these renewable resources. The specific information sought is species composition, abundance, habitat location, and relationships between species.

The construction of geothermal facilities has a direct impact on the local ecosystems resulting in habitat loss for terrestrial species and stream alteration for aquatic species. An assessment of the magnitude of these effects from future development needs to be undertaken.

Development of the hot water resource may result in higher use of existing freshwater supplies by geothermal industries and waste disposal problems of spent geothermal water and cooling water blowdown. An assessment of these water management problems will be needed prior to development.

With geothermal development approaching more populated areas, there is the need to establish noise criteria for communities within The Geysers-Calistoga region. Impact studies for future geothermal sites should be made using existing noise propagation models to ensure these standards are met.

In the development of The Geysers there have been a number of accidental releases of steam condensate and drilling wastes. These areas should be monitored to determine the long-term effects of such accidents.

There are a variety of groups conducting environmental research and assessment activities in The Geysers region, and the data resulting from these efforts is often very difficult to locate. Consequently, a centralized information source is needed from which environmental data pertaining to the region can be obtained.

This has been a summary of the major environmental issues and information requirements needed to promote the development of geothermal energy at The Geysers-Calistoga KGRA. A more detailed description of the situation at The Geysers, the environmental issues, and the proposed research and assessment studies is presented in the Overview Report.[1]

(1) D. Ermak and P. Phelps, Eds., An Assessment of Environmental Issues and Requirements for the Geysers-Calistoga KGRA, Lawrence Livermore Laboratory, in preparation (1978). Currently available in draft form.

Acknowledgments

The authors wish to thank the many individuals from industry and government too numerous to recognize individually, but who made so many important contributions. We would especially like to acknowledge the cooperation from GRIPS: T. Cordill, J. Roberts, F. Tucker, L. Vollentine, M. Walters, and S. Rae. A special thanks, also, to team leaders N. Crow, L. Rosen, C. Molenkamp, P. Gudiksen, K. Pimentel, C. Hall from LLL, and P. Leitner, St. Mary's College.

Geothermal Resources Council, TRANSACTIONS, Vol. 2 July 1978

Dup

CHEMICAL FINGERPRINTS TO ASSESS THE EFFECTS OF GEOTHERMAL DEVELOPMENT ON WATER QUALITY IN IMPERIAL VALLEY

Kenneth D. Pimentel, Robert R. Ireland, and Gary A. Tompkins

University of California Lawrence Livermore Laboratory
Livermore, California 94550

ABSTRACT

A two-year baseline water quality study in Imperial Valley, together with newly available brine chemistry data, has led us to propose a minimum list of chemicals that should be measured in future monitoring programs to ensure that geothermal development does not adversely affect water quality.

INTRODUCTION

In 1975, the U.S. Department of Energy (DOE) requested Lawrence Livermore Laboratory (LLL) to plan and implement an integrated environmental baseline and assessment study in Imperial Valley, California in support of anticipated geothermal energy resource development. This study, the Imperial Valley Environmental Project (IVEP) [1], includes a water quality study that documents baseline chemical water quality in the major rivers of the Valley and in site-specific sampling networks in the Salton Sea, Brawley, Heber, and East Mesa Known Geothermal Resource Areas (KGRAs). Samples collected at 80 sites each month for 13 mos include public water supplies, domestic groundwater wells, agricultural irrigation and drainage systems, rivers, and the Salton Sea. Collected samples were analyzed for the following major and trace chemical constituents and physical parameters:

- Na,K,Ca,Mg,Cl,SO_4,CO_3,HCO_3,SiO_2,TDS,SC,pH,Temp.;
- Ag,As,B,Ba,Cd,Cr,Cs,Cu,F,Fe,Hg,Li,Mn,Mo,Ni,Pb,Rb, Se,Sr,V,Zn.

The purpose of this paper is to justify the list of chemicals we propose for continued monitoring in the IVEP Transfer Plan [2]. Developers are proposing plans to construct no less than six demonstration power plants in the Valley within the next 5 yr, affecting all four KGRAs. We suggested a minimum-cost program to assess the impacts that might occur if large-scale geothermal development takes place.

Work performed under the auspices of the U.S. Department of Energy by the University of California Lawrence Livermore Laboratory under contract number W-7405-ENG-48.

In this paper, we concentrate on the three beneficial uses of municipal and domestic water supply, agricultural water supply, and warm freshwater habitat. Our study has three main parts. First, data on the chemical composition of geothermal fluids are summarized. Second, a detailed case study of the pollution of an agricultural drain in the Salton Sea KGRA is presented. Finally, toxicity data on trace elements are used to suggest which elements should be included in a minimum-cost monitoring program for the future.

BRINE CHEMISTRY

Table 1A summarizes concentrations of important geothermal constituents in brines from wells in the Salton Sea, Brawley, Heber, and East Mesa KGRAs and in areas near Westmorland. The data were obtained from the Division of Oil and Gas, from published literature, and directly from developers. The data are arithmetic averages of all available data in each area, with the number of wells sampled in each area varying. We emphasize these data are intended to identify trends and overall differences among the resource areas, and not to gain a detailed understanding.

The table consists of four basic types of data: major constituents, trace elements, two important fingerprint ratios, and figures for recognizing patterns in major and trace constituents. The easiest way to analyze the relationships among major constituents is with the use of the Stiff diagram [3]. The Stiff diagram (Fig. 1) is a plot of eight major chemicals that characterize the water; cations are plotted on

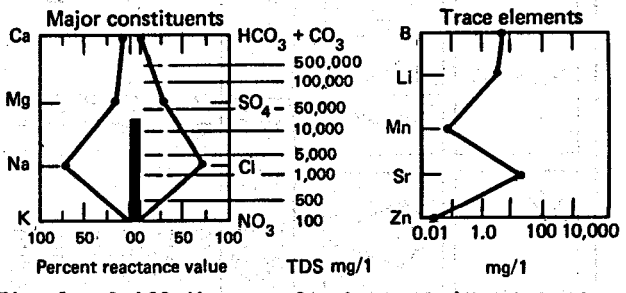


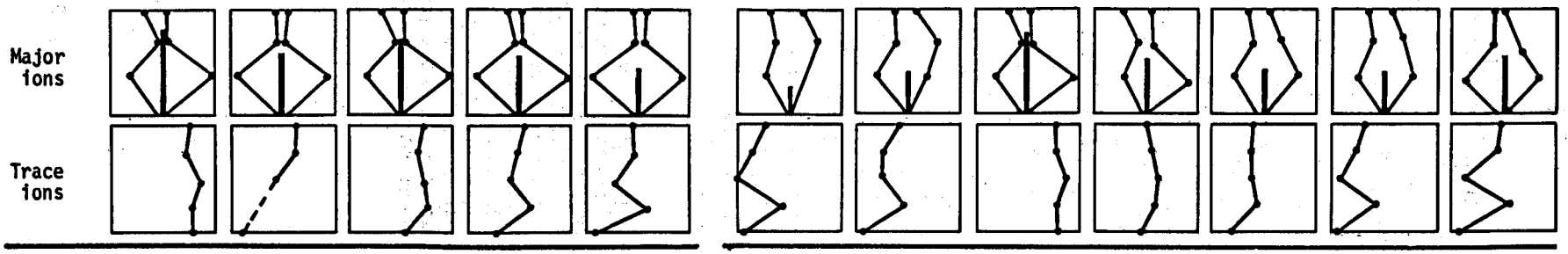
Fig. 1. Stiff diagram of major constituents and logarithmic diagram of trace elements used in Tables 1A and 1B.

Table 1A. Average concentrations in geothermal brines, mg/l.

Ion	Salton Sea	Westmorland	Brawley	Heber	East Mesa
Na	52000.	10000.	22000.	4200.	2600.
K	14000.	1400.	3800.	260.	190.
Ca	24000.	690.	8100.	880.	130.
Mg	106.	188.	34.	5.4	3.4
Cl	145000.	18000.	46000.	7900.	3900.
SO_4	84.	57.		99.	155.
CO_3	0.	130.	0.	3.3	33.
HCO_3	140.	2900.	49.	27.	490.
TDS	240000.	37000.	76000.	14000.	7600.
pH	5.2	7.5	6.1	6.5	7.3
As	11.		2.6	<0.1	0.16
B	350.	63.	140.	14.	5.4
Ba	433.		363.	3.8	2.2
Cu	4.	0.07	0.11	0.53	0.03
F	9.	2.24		1.6	2.0
Fe	2300.	0.3	65.	22.	2.2
Li	211.	48.	100.	9.5	6.3
Mn	1200.	2.8	190.	2.7	0.42
Ni	<4.				0.03
Pb	100.	3.6	1.1	1.9	0.09
Se					1.2
Sr	500.		340.	53.	38.
Zn	660.	0.04	14.	0.83	0.07
K/Na × 10	2.68	1.31	1.75	0.61	0.74
Cl/SO_4	1730.	316.		80.	25.

Table 1B. Average concentrations in water samples in Salton Sea KGRA, mg/l.

Vail4 Canal	Sump 120	Sinclair 4	Sump 116	Vail4A Drain	Alamo River	Salton Sea
168.	1080.	58442.	2470.	970.	607.	10600.
6.3	20.	14918.	247.	66.	15.	195.
93.	373.	26992.	2050.	437.	201.	850.
35.	187.	736.	385.	160.	120.	1200.
158.	989.	154590.	8540.	1870.	760.	14700.
357.	1990.	19.	1590.	1480.	960.	8100.
15.	<2.5		<2.5	<2.5	<2.5	63.
152.	338.	0.	380.	330.	205.	143.
928.	5030.	266560.	17700.	5970.	3000.	38600.
8.2	7.0	5.3	6.8	7.6	7.7	8.8
0.005	<0.005	10.	0.005	0.005	0.007	<0.01
0.25	1.1	332.	9.7	2.	0.76	6.8
0.09	0.097	1100.	0.54	0.093	0.12	0.07
<0.005	0.005	3.	0.075	0.007	0.014	0.08
0.5	0.57	14.	0.48	0.05	0.66	1.1
0.03	0.08	1240.	0.26	0.08	0.045	0.24
0.08	0.31	344.	14.3	1.24	0.23	3.2
0.01	0.30	1475.	47.	1.9	0.035	0.08
0.01	<0.01	<4.	0.31	<0.01	<0.01	<0.2
<0.01	0.01	60.	0.29	0.02	0.01	<0.1
<0.005	<0.005		<0.01	<0.005	<0.005	0.02
1.3	5.0	448.	38.	6.0	3.2	13.5
0.02	0.03	600.	7.8	0.12	0.02	0.03
0.38	0.19	2.55	1.0	0.68	0.25	0.18
0.44	0.50	8140.	5.36	1.26	0.79	1.82



the left and anions on the right as percent reactance. The solid bar in the center gives total dissolved solids (TDS) in mg/l on a logarithmic scale. All geothermal brines contain primarily NaCl with varying amounts of Ca. Potassium is high relative to surface water. Sulfate content is low and small amounts of carbonate and bicarbonate are usually present. Nitrate was omitted from the table because of its low content in brines. The main differences in the major constituents of brine are in the TDS and pH, and in the ratios of K/Na and Cl/SO_4, which are shown in the bottom two lines of Table 1A.

Important trace elements are shown in the diagrams at the bottom of Table 1A. Boron, Li, Mn, Sr, and Zn are among the more abundant trace elements in geothermal brines throughout the Valley. Barium and Fe are also relatively high, but are of less concern in monitoring applications.

VAIL 4A DRAIN CASE STUDY

In establishing monitoring networks in the Salton Sea KGRA, high concentrations of many chemicals were encountered in an agricultural drainage sump adjacent to the Sinclair 4 Geothermal Well evaporation ponds (see Fig. 2). High levels of chemicals in Sump 116 suggested that the large amounts of crystalline salts in the evaporation ponds was causing pollution. In studying the area, we found that salts were leaching from the ponds into the agricultural drainage tile system in the plot of land to the east of the ponds, the tile system empties into Sump 116, and the collected drainage in the sump is pumped periodically into Vail 4A Drain.

Figure 2 shows water sampling sites in this study. Chemical characteristics of water samples from these sites are given in Table 1B. Most of the data are arithmetic averages of analyses of five to seven samples taken in the spring, fall,

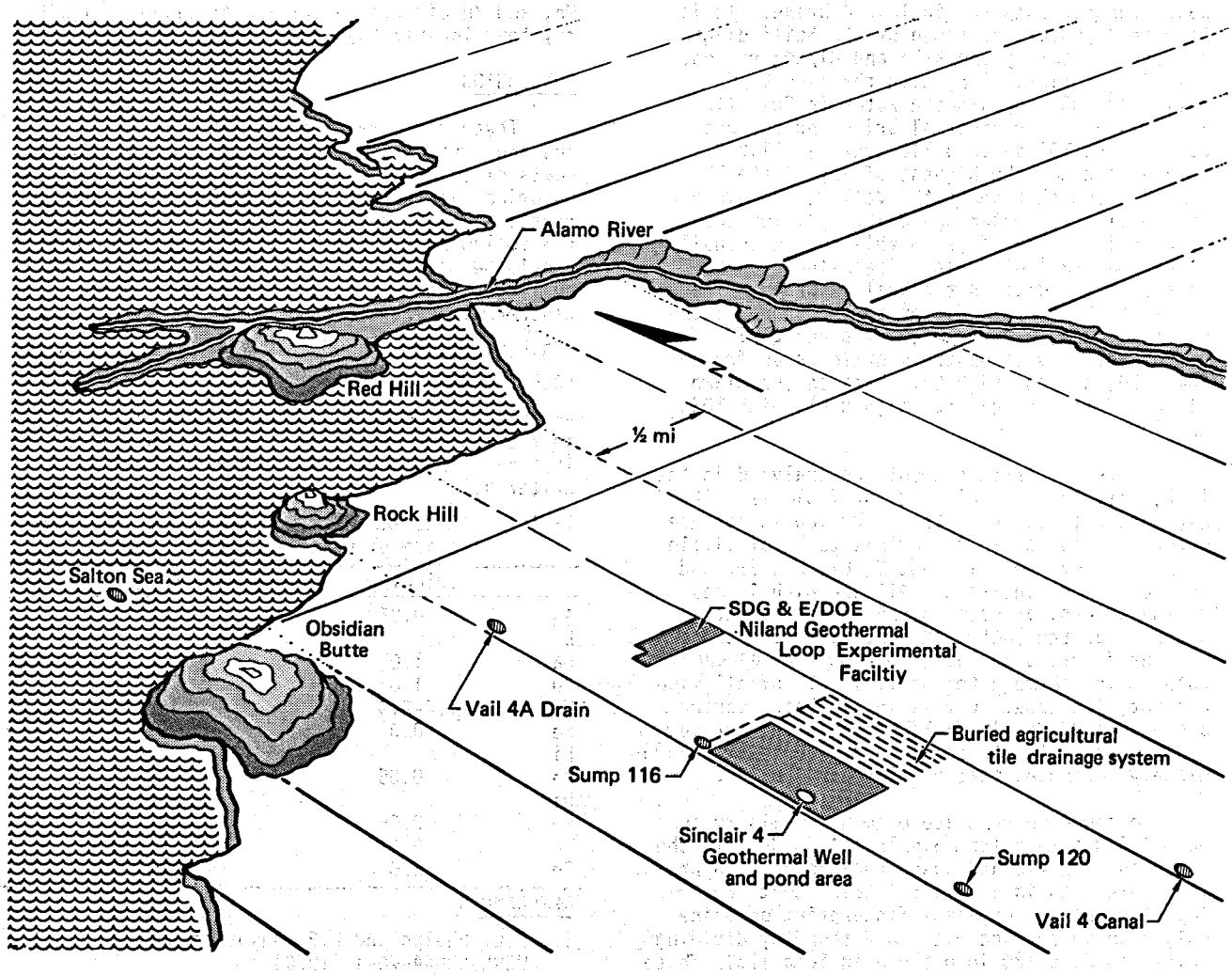


Fig. 2. Water sample sites near the Sinclair 4 Geothermal Well in the Salton Sea KGRA used in the Vail 4A Drain case study.

and winter of 1976. The data from the Sinclair 4 Well were obtained in 1967 [3]; however, developers involved in this study indicate that the 1967 analysis is representative of the brine chemistry since that time. The Salton Sea data are from a single sample taken offshore in December 1976.

The diagrams at the bottom of Table 1B provide a quick analysis of the data. The irrigation water entering the area in Vail 4 canal is quite hard, high in Ca, Mg, and Na, and dominated by SO_4. The pH is high, and both K/Na and Cl/SO_4 ratios are low. The irrigation water leaches out salts in the soil as it travels toward the buried tile drains, and becomes more enriched in NaCl than in other minerals as is evident from the Stiff diagram of Sump 120. Sinclair 4 brine is high in NaCl, as well as Ca and K, and very low in Mg and almost devoid of SO_4. The K/Na and Cl/SO_4 ratios are enormous relative to normal surface waters in the Valley.

The water in Sump 116 is similar in its major constituents to Sinclair 4 brine. It is high in K and Cl, as shown by the Stiff diagram and even better by the K/Na and Cl/SO_4 ratios. This fingerprint, along with the high Ca/Na ratio and TDS suggests the water in Sump 116 is a mixture of geothermal brine and surface water. The TDS in Sump 116 averaged 17,700 mg/l, which was the highest of any of the 18 sumps tested throughout the Valley; the average TDS in all sump water was 8,700 mg/l for the same period. The water in this sump eventually flows down Vail 4A Drain. Its effect can be seen from the data on the Vail 4A Drain. The key indicators, in addition to the shape of the Stiff diagram, are the high K/Na and Cl/SO_4 ratios relative to upstream drain water from Sump 120, and the high Ca. Data on the Alamo River and Salton Sea show high NaCl, high TDS, and low K.

Of the 21 trace elements we analyzed in the IVEP, only 13 were selected for Table 1B. The elements omitted are either very low in surface waters, or so low in the brines to be of little interest. Of those listed, B, Li, Mn, Sr, and Zn are of most interest. All are high in most of the brines, as seen in the trace element diagrams at the bottom of Table 1A. The trace element diagrams in Table 1B show that as canal water moves through the soil, levels of all five elements increase. Levels in Sinclair 4 brine are orders of magnitude higher than in upstream drain water. The trace element diagram of Sump 116 closely resembles that of Sinclair 4 brine.

We now compare trace element chemistry in Sump 120 upstream from Sinclair 4 ponds with the water in Sump 116 and downstream in Vail 4A Drain. Those elements in Sinclair 4 brine that are important as a geothermal fingerprint of brine pollution in surface water are found by dividing values in Sump 120 into those in Sump 116. These ratios show that Cu, Li, Mn, Pb, and Zn are good markers. Dividing trace quantities in Sump 120 into those in Vail 4A Drain downstream show which elements are persistent in surface water. In this case, only Li, Mn, and Zn remain high.

We included B and Sr in the trace element diagrams, because of their high levels in the brines and boron's toxicity in agriculture. However, as geothermal markers, they are not very useful. Note the relatively unchanging levels of boron and strontium in the trace element diagrams and in the data. Strontium has also not been shown to be a toxic element. Other elements that are high in Sinclair 4 brine are Ba, Fe, and Pb. However, they are inadequate as markers because they drop to ambient levels downstream in Vail 4A Drain because they tend to precipitate.

WATER QUALITY CRITERIA AND TOXICITIES

To evaluate the data presented in the above sections, the following table of recommended limits of trace elements for municipal and agricultural water is presented (Table 2). The maximum trace element levels for the third beneficial use of freshwater as aquatic habitat, is much more difficult to set. However, Ireland [5] found that in Imperial Valley waters, B, Cu, Li, Mn, and Zn might pose threats to Tilapia zillii fry that inhabit the drains.

CONCLUSION

These toxicity data, together with the drinking and irrigation water criteria and the known costs of chemical analyses, augment our findings on brine chemistry throughout the Valley and on constituents in the Vail 4A Drain. These suggest the following minimum lists of parameters that should be monitored in future programs for water quality management during the development of the geothermal resources in Imperial Valley:

- Na,K,Ca,Mg,Cl,SO_4, CO_3,HCO_3,TDS,SC,pH,Temperature;
- B,Li,Mn,Zn.

Arsenic, Se, Pb, and Ni should also be considered in the future because of their possible elevation in some brines above existing water quality criteria.

Table 2. Recommended maximum concentrations of trace elements in water [4].

	Drinking	Irrigation
As	0.05	2.0
B		2.0-10.0
Ba	1.0	
Cu	1.0	5.0
F	1.4-2.4	15.
Fe	0.3	20.
Li		2.5
Mn	0.05	10.
Ni		2.
Pb	0.05	10.
Se	0.01	0.020
Zn	5.0	10.

REFERENCES

1. P.L. Phelps and L.R. Anspaugh, UCLLL Rept. UCRL-50044-76-1 (1976).
2. L.R. Anspaugh, et al., UCLLL Rept. (in prep.).
3. Cal. Dept. Wtr. Res. Bull. #143-7 (1970).
4. Nat. Acad. Sci., Water Quality Criteria (1972).
5. R.R. Ireland, et al., UCLLL Rept. (in prep.).

Geothermal Resources Council, TRANSACTIONS, Vol. 2 July 1978

THE THERMODYNAMIC AND COST BENEFITS OF A FLOATING COOLING GEOTHERMAL BINARY CYCLE POWER PLANT AT HEBER, CALIFORNIA

H.S. Pines, W.L. Pope, M.A. Green, P.A. Doyle, L.F. Silvester, R.L. Fulton

Lawrence Berkeley Laboratory
University of California
Berkeley, California 94720

ABSTRACT

The application of the *floating cooling* concept to evaporative heat rejection systems is studied as a method of improving the performance of geothermal powerplants operating upon medium temperature hydrothermal resources. The LBL thermodynamic process computer code GEOTHM is used in the case study of a 50 MWe isobutane binary cycle power plant at Heber, California. It is shown that operating a fixed capacity plant in the floating cooling mode can generate significantly more electrical energy at a higher thermodynamic efficiency and reduced bus bar cost for approximately the same capital investment. Floating cooling is also shown to minimize the adverse influence on plant performance due to a declining resource temperature.

INTRODUCTION

The development of medium temperature hydrothermal resources for the production of electrical energy has not proceeded at the pace hoped for by the geothermal community. This predicament is certainly influenced by the lower thermodynamic efficiency inherent in these resources and the associated higher costs of the thermal-mechanical energy conversion. This paper will show that application of the *floating cooling concept* to *evaporative heat rejection systems* can significantly increase the energy available from medium temperature hydrothermal resources. A binary cycle power plant utilizing the floating cooling heat rejection method can generate significantly more electrical energy at a higher thermodynamic efficiency and reduced bus bar cost than the same plant operating in the convential fixed condensing temperature mode, for approximately the same capital investment.

The *floating cooling concept** as defined in this study refers to the off-design operation of an atmospheric cooled geothermal power plant rejecting heat to a forced-draft wet cooling tower. The cooling system always operates at full capacity in response to a naturally varying wet bulb *sink* temperature. The turbine back pressure (i.e. the condensing temperature) is periodically adjusted to generate the maximum available net power provided by the variable sink temperature. The net power output of the plant will *float* with the daily and seasonal wet bulb temperature fluctuations. A fixed cooling cycle, on the other hand, operates at a constant condensing temperature and delivers constant net power during the time of the year that the design wet bulb temperature is not exceeded.

The practical thermodynamic advantages of floating cooling for medium temperature geothermal energy systems are twofold:

(1) Floating cooling can significantly increase the net power production of plants located in regions where the climatology exhibits large daily and seasonal wet bulb temperature variations.

(2) The percentage increase in net power is greater at lower resource temperatures. Floating cooling systems will counteract the adverse influence on plant performance due to a declining resource temperature over time.

Recent economic studies[2,3] have shown that medium and low temperature hydrothermal resources below 180°C favor organic fluid binary cycles over flash steam systems. The thermodynamic properties of these organic fluids (much higher vapor pressures and lower specific volumes than steam at similar condensing temperatures) allow turbines to be constructed whose efficiencies are less sensitive to the floating cooling operating mode than are steam turbines. These organic fluid expanders can operate over the range of exhaust pressures experienced with varying wet bulb temperatures with minor variations in turbine efficiency. The design and cost of these machines for a floating cooling application are not radically different from machines built to operate at a fixed exhaust condition.

FLOATING COOLING IN THE IMPERIAL VALLEY - A CASE STUDY

The remainder of this report is devoted to com-

*This concept has recently been examined for low temperature resources by INEL.[1]

puter modelling of the thermodynamic and cost benefits derived for floating cooling when applied to commerical-size geothermal isobutane binary cycle power plants located at Heber, Ca. The resource and sink characteristics of the Heber site are typical of a number of medium temperature hydrothermal resources in California's Imperial Valley. Floating cooling is particularly suited to exploit the source and sink conditions characteristic of the Heber site for the following reasons:

(1) The local desert climate exhibits high maximum annual wet bulb temperatures over relatively few degree days and large daily and seasonal wet bulb temperature variations.

(2) The temperature of this resource (180°C) is best matched with an organic fluid binary cycle power plant.[2]

(3) As the reservoir is developed to a full generating capacity of say 200 MWe, the resource temperature is predicted to decline about 30°F over 25 years making the floating cooling binary cycle even more appropriate.

A FLOATING COOLING COMPUTER MODELLING SCENARIO USING PROGRAM GEOTHM

The computer model used in this study is the LBL-developed thermodynamic process computer code GEOTHM. The unique single-step optimization capability of the GEOTHM code is first employed in the design of a *minimum energy cost* 50 MWe net base load power plant. This is a fixed 1% wet bulb temperature design, i.e., the plant will deliver 50 MWe constant net power during the 99% of the year that the design wet bulb temperature is not exceeded. The program's off-design optimization routines then simulate the operation of the fixed capacity plant in the *floating cooling mode, during daily and seasonal* wet bulb temperature variations, to *maximize power production* throughout the year. The floating cooling plant will generate *more than* 50 MWe net power during 99% of the year. Assuming that surplus floating power can be sold at the same rate as the base load power, the cost of energy for the floating cooling plant will be computed to include the revenues derived from the surplus energy sales. The cost of energy for both the floating and fixed operating modes are then compared.

A) DESIGN AND OPTIMIZATION OF THE 50 MWe BASE LOAD PLANT

The binary cycle power plant modelled in this study is illustrated by the simplified schematic flow diagram, Figure 1. Brine downhole and reinjection pumps are not shown, but have been included in the model. In order to design and cost optimize this system, the GEOTHM equipment and cost models require that the user input reasonable equipment efficiency and cost data applicable to the particular plant to be modelled. The data for *this* paper was obtained from a comprehensive feasibility study for a fixed cooling 50 MWe isobutane binary cycle design at Heber performed by Holt/Procon for EPRI.[2] Equipment design data included turbine and pump efficiency ratings, and heat exchanger and condenser heat transfer coefficients. For Holt's assumed values of the six system state parameters listed in Figure 1, GEOTHM verified Holt's baseline design, i.e., his fluid mass flows, component sizes, and parasitic power calculations. Scaling factors built into GEOTHM's component costing routines were then adjusted so that component costs computed by GEOTHM were normalized to match Holt's vendor quotations. The brine cost ($/Btu) was normalized to Holt's for the same flow rate and primary heat exchanger duty. Direct and indirect cost factors were similarly scaled so that total plant and field capital cost, and cost of energy were in agreement. Finally, GEOTHM's non-linear optimization routines were used to design the plant to produce 50 MWe net power at minimum cost of energy for an 80°F 1% wet bulb temperature. GEOTHM adjusted the six optimizable cycle parameters to arrive at the minimum energy cost cycle illustrated on the T-Q plot in Figure 2, Case 1. The GEOTHM optimized design is in excellent agreement with Holt's. Case 1 cycle design information is summarized in column 1 of Table 1. It is important to note that Holt's 50 MWe (net) design did not include the approximately 5 MWe of brine production and injection pumping power, whereas Case 1 does.

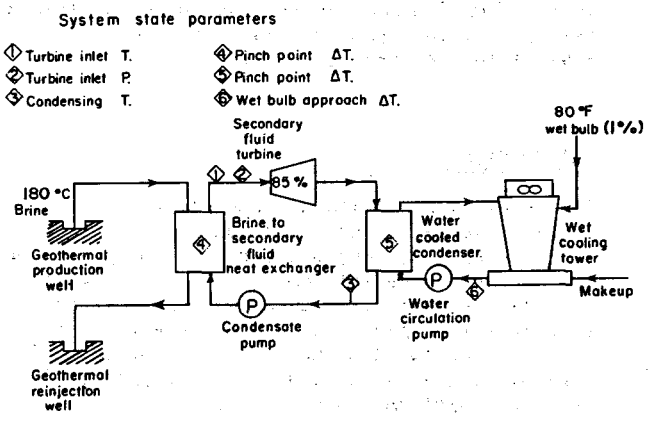


FIGURE 1 Simple geothermal binary cycle power plant schematic. The six system state parameters are optimized with program GEOTHM for a minimum energy cost design objective.

B) OFF-DESIGN FLOATING COOLING MODELLING

Once the plant has been designed, i.e. equipment sizes, costs, and fluid mass flows established at the GEOTHM minimum energy cost design, the off-design optimization routines can be invoked to *operate* the plant in the floating cooling mode. In addition to fixing the brine flow rate, the GEOTHM floating cooling model assumes that the

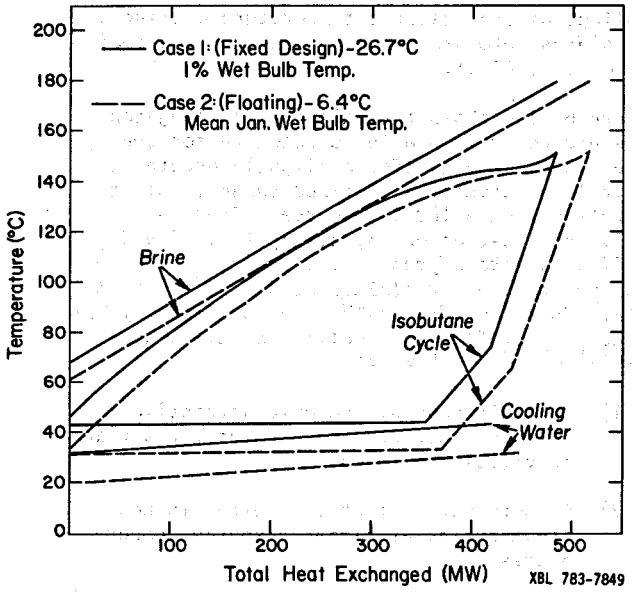


FIGURE 2 T-Q plots illustrating the adjusted floating cooling power plant operating conditions so that plant can generate maximum net power at the stated wet bulb temperatures. Note particularly the 10°C shifts in condensing and cooling water temperatures.

following six conditions will remain constant throughout the year: (1) turbine inlet temperature, (2) turbine inlet pressure, (3) heat exchanger area, (4) condenser area, (5) cooling tower packing area and, (6) cooling water flow rate. Coupling the six constraints with the six system state variables mathematically dictates a unique solution for the turbine back pressure at any given wet bulb temperature. The one-to-one relationship linking turbine back pressure with wet bulb temperature is plotted in Figure 3. The off-design turbine efficiency will vary with turbine back pressure according to the turbine performance model shown in Figure 3. In order to

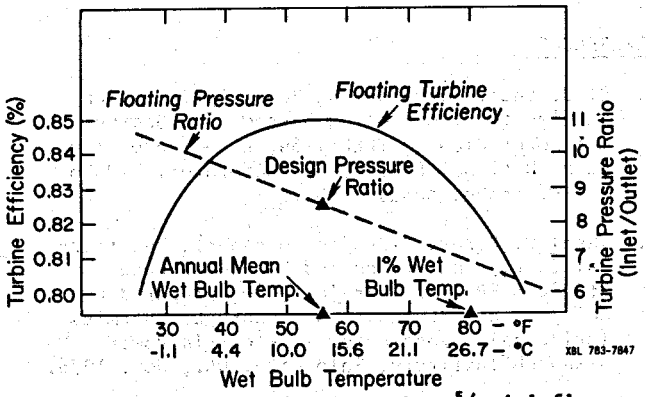


FIGURE 3 Turbine performance chart[5] (axial-flow organic fluid machine). Plots of turbine operating conditions (efficiency and pressure ratio) required by floating cooling wet bulb temperature variations. Peak efficiency design point corresponds to annual mean wet bulb temperature.

maximize the off-design production of floating power, the turbine has been designed to operate at its peak efficiency for a turbine back pressure corresponding to the *annual mean* wet bulb temperature.

The T-Q plot in Figure 2 shows how the cycle has adjusted to accomodate a seasonal shift in the wet bulb temperature. Case 2 represents the adjusted floating cooling thermodynamic operating condition of a plant experiencing the increased cooling potential afforded by the mean January wet bulb temperature (6.4°C) for Heber, Calif. Case 2 is a significant departure from the Case 1 fixed 1% wet bulb temperature (26.7°C) design for the following reasons:

(1) The isobutane condensing temperature and the cooling water inlet temperature are both about 10°C lower.

(2) The reduced condensing temperature, and consequently the reduced turbine back pressure, allows the turbine to extend its expansion process to produce more useful work. This plot shows the extended turbine expansion line, resulting in a 14 MWe (28%) increase in net power!

(3) The increase in available energy at the lower wet bulb temperature shows up as an increase in the heat transferred across the heat exchanger and condenser and as a decrease in the brine reinjection temperature.

(4) The greater heat transfer load imposed upon the constant area exchanger and condenser is compensated by an increase in the mean temperature difference across these devices.

C) SEASONAL FLOATING POWER OUTPUT FOR A HEBER POWER PLANT

The *monthly mean* net power generated by a floating cooling power plant for the 180°C Heber resource is computed using published monthly mean climatological data.[4] Figure 4 is a plot of the monthly mean floating net power output and monthly mean floating cycle efficiency (cycle efficiency ≡ Net Power/Total Heat In). These seasonally varying floating power and efficiency curves can be normalized to *average annual floating* values by integrating the area beneath each curve. Figure 4 shows that operation as a floating cooling plant can increase the output of a 50 MWe fixed cooling plant to 61 MWe average annual floating net power, a 22% increase, provided that the generator is designed to accommodate the largest anticipated floating power output (85 MWe gross). The average cycle efficiency is also improved from 10.9% to 12.1%.

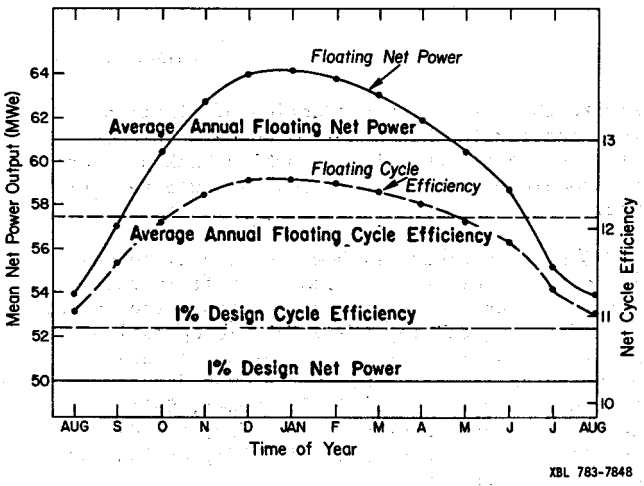


FIGURE 4 Seasonally varying *monthly mean* floating net power output and floating cycle efficiency for 50 MWe (1%) floating cooling power plant, 180°C resource temperature. The floating performance curves are normalized to *average annual floating* values for comparison with the fixed capacity plant design.

D) DECLINING RESOURCE TEMPERATURE SCENARIO

In order to illustrate the increasing benefits of floating cooling at lower resource temperatures, a modelling scenario for the development of the Heber resource has been devised. This scenario assumes that a 50 MWe net (1% wet bulb design) binary cycle power plant is to be constructed every 7 years for a total of 4 plants or 200 MWe net generating capacity. In compliance with reservoir engineering estimates of a declining resource temperature at Heber, these plants are designed to operate over their assumed 25 year lifetimes at different average resource temperatures: 180°C, 175°C, 170°C, and 165°C respectively. Each plant is designed for minimum cost of energy (assuming constant 1976 dollars).

Each plant is then modelled to float with the seasonally varying wet bulb temperature. The seasonal variation of the monthly mean floating net power for 50 MWe (1%) plants designed to operate at different average resource temperatures is shown in the 3-D isometric plot, Figure 5. As predicted, *the mean floating net power is seen to increase for plants designed to operate at lower resource temperatures.*

COST BENEFITS OF FLOATING COOLING

The results of these four power plant case studies are summarized in Table 1. Modification of a fixed capacity plant to operate in the floating cooling mode requires only a *minor increase* in the plant and field capital investments. Nevertheless, revenues derived from the sale of surplus floating power *substantially reduces* the cost of energy produced compared to same plant operated at fixed capacity. The bus bar cost of energy for each plant operating in both the fixed and floating modes is plotted in Figure 6. As the cost of energy increases with decreasing resource temperature, floating cooling is seen to mitigate this cost increase by as much as 14%. The increasing *thermodynamic benefits* of floating cooling, as the resource temperature declines, translates into *greater percentage energy cost reductions*, ΔCost.

Figure 6 also shows that floating cooling can generate power from a 167°C resource for the same cost of energy (for a slightly greater capital investment) as a fixed capacity plant operating from a 180°C resource. From an equivalent cost of energy standpoint, *floating cooling has the effect of increasing the Heber resource temperature (ΔT_{EQ}) by 12.8°C or about 23°F.* This *temperature-cost equivalence effect* suggests that floating cooling may allow geothermal binary cycles to:

1) Maintain general economic attractiveness to lower resource temperatures than previously believed.

2) Compete more effectively with flashed steam cycles at higher resource temperatures.

CONCLUSIONS

A computer modelling case study of the thermodynamic and cost benefits of a floating cooling geothermal binary cycle power plant at Heber, California has been described. The operation of a 50 MWe (net) fixed capacity plant in the floating cooling mode increases net power production by 22% and reduces the cost of energy by 12.5%, for approximately the same capital investment. Floating cooling can also minimize the adverse influence on plant performance due to the predicted temperature decline of the Heber resource.

The potential thermodynamic and cost benefits of the floating cooling operating mode should serve to stimulate the development of medium temperature hydrothermal resources in areas where the climatology exhibits large daily and seasonal temperature variations.

REFERENCES

1. C. J. Shaffer, "Floating Power Optimization Studies for the Cooling System of a Geothermal Power Plant," TREE-1164, EG&G Idaho, Inc., Idaho National Engineering Laboratory, Idaho Falls, Idaho, August, 1977.

2. Vasel W. Roberts (Project Manager), "Geothermal Energy Conversion and Economics-Case Studies: EPRI-301, Project 580, prepared by Holt/Procon, Ben Holt and Edward L. Ghormley (principal investigators), Electric Power Research Institute, Palo Alto, CA., Nov. 1976.

3. C. H. Bloomster and C. A. Knutsen, "The Economics of Geothermal Electricity Generation From Hydrothermal Resources," BNWL-1989, Battelle Pacific Northwest Labs., Richland, Washington.

4. Imperial Irrigation District, "Imperial Valley Annual Weather Summary 1977 - Monthly High, Low, and Mean Temperatures and Rainfall, 1914-1977," from Records of Watermaster.

5. Kenneth E. Nichols P.E., "How to Select Turbomachinery for your Application," Barber-Nichols Engineering Company, Arvada, Colorado.

ACKNOWLEDGMENT

We gratefully acknowledge the support of DOE/DGE for LBL Cycle studies and GEOTHM development.

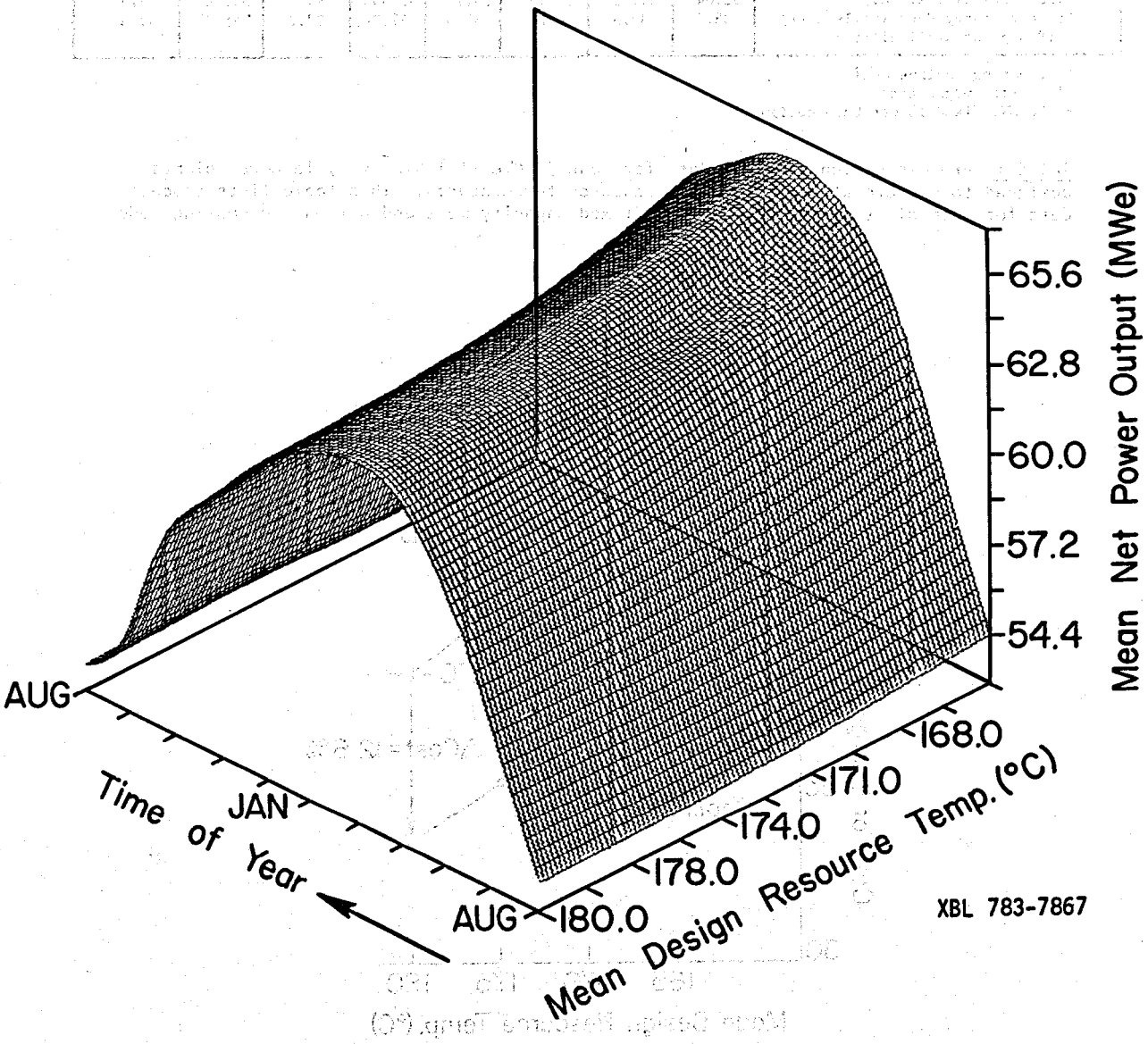


FIGURE 5 Seasonally varying monthly mean floating net power output for 50 MWe (1%) plants designed to operate at different average resource temperatures. The mean floating net power *increases* for plants designed to operate at lower resource temperatures.

PROCESS DESIGN PARAMETERS	MEAN DESIGN RESOURCE TEMPERATURE (°C)							
	180+	180*	175+	175*	170+	170*	165+	165*
Avg. Net Power (MWe)	50.0	61.0	50.0	61.2	50.0	61.7	50.0	62.4
Avg. Gross Power (MWe)	69.8	81.3	70.2	82.0	70.7	83.1	71.9	85.4
Avg. Cycle Efficiency (%)	10.9	12.1	10.7	12.0	10.4	11.7	9.9	11.1
Brine Flow Rate (kg/sec)	966	1009	1055	1095	1140	1189	1240	1267
Annual Fuel Requirement ($MWhrx10^3$)**	3462	3770	3520	3836	3622	3965	3803	4211
Brine Unit Cost ($/MWhr)**	1.99	1.99	2.13	2.13	2.24	2.24	2.31	2.26
Plant Capital Cost (M$)	31.04	32.35	31.65	33.18	32.95	34.42	34.46	36.79
Bus bar Energy Cost (Mills/kWhr) (85% plant availability)	38.3	33.5	40.4	35.3	42.9	37.2	45.7	39.3

* floating cooling design
** thermal megawatts
\+ 50 MWe fixed 1% wet bulb design

TABLE 1 Process design and cost data for four 50 MWe (1%) binary cycle power plants designed to operate at different mean resource temperatures. This table lists process data for each plant operating in both a fixed capacity mode and a floating cooling mode.

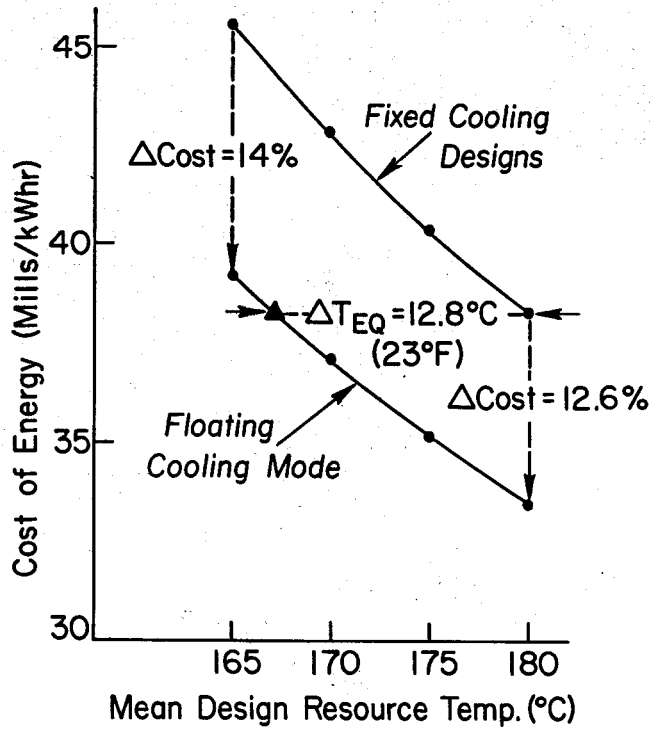


FIGURE 6 Bus bar cost of energy for 50 MWe (1%) plants operating in both fixed and floating modes for different mean design resource temperatures.

Geothermal Resources Council, TRANSACTIONS, Vol. 2 July 1978

Dup

A SIMULATOR FOR SENSITIVITY ANALYSIS OF GEOTHERMAL WELL COST--PROGRESS REPORT

Joseph Polito

Sandia Laboratories
Albuquerque, NM 87185

ABSTRACT

A computer based simulator for geothermal well costs is being developed by Sandia Laboratories. The purpose of the project is to provide an analysis tool with which to investigate the sensitivity of geothermal drilling costs to various technological improvements. Output from the simulator will provide information to aid the research manager in the allocation of resources to research projects. In its final form the simulator will accept models of rotary and novel drilling systems at the level of aggregation specified by the user. This paper presents an overview and progress report on the development of the simulator.

The manager of the Geothermal Well Technology Program at Sandia Laboratories has need of an analysis tool to rapidly assess the potential of proposed research projects. Questions which must frequently be answered are:

a) What are the relative merits of two or more competing proposals to improve rotary drilling technology?

b) Given that a research project has been selected, what drilling regimes yield its optimal performance; what are the consequences of its implementation on other aspects of drilling?

c) What are the relative merits of advanced drilling methods when compared to conventional methods?

These questions pose a dilemma for the research manager because of the wide variety of projects that must be considered and the various levels of aggregation implied by the three categories. A systematic comparison of alternatives is an essential part of the decision making process, but the effort required to construct a specific model for each of the situations described above is prohibitive.

A reasonable approach is to develop a general system that has the capability to address all of the above questions. The requirements for such a modeling framework are:

1) It must permit rapid construction of models that represent widely varying technology. This aspect is essential to providing timely analyses. In addition, it must be easy to vary the parameters and the structure of the model to study the effects of improvements to technology.

2) It must permit technology based models. Previous programs for predicting geothermal well cost have relied on historical and statistical data that are updated by appropriate escalation factors. This approach, while valid in other settings, is inadequate for the purpose of comparing technological alternatives. In particular, it provides little insight into the cost and performance of advanced methods needed for question (c).

3) It must permit the user to specify the level of aggregation. For example, question (b) may require a very detailed model of only a small portion of the drilling operation. Question (a) generally requires a less detailed model, but one that includes the entire drilling process. For question (c), a highly aggregated "first cut" model will be required initially to answer the "yes-no" type questions. In later analyses, more and more detail must be added to address tactical questions such as "how much?" and "what kind?"

In order to satisfy these requirements, a computer program is being developed which models drilling as a combined continuous/

discrete process in which some variables change discretely in time and others are governed by continuous equations. The program is an extension of the GASP IV simulation language with specialized input and additional logic. In particular, little or no programming is required by the user. Model specification is performed mainly by data input, and a flexible editing capability is provided so modifications of the model can be made easily and without the need for reprogramming.

A graphical representation of the system is first prepared by the user. A simple example of part of a rotary drilling model is shown in Figure 1. The half circle shapes are nodes, and arcs connect the nodes. The arcs are differentiated by numbers in squares. Three operations are shown: drilling, tripping out, and tripping in. The arcs and nodes represent the logical relations among operations.

In the example, the operation "drilling" terminates in one of three ways: The bit is worn, total depth (TD) is reached, or a predetermined time for running the bit elapses. The first of these to occur terminates drilling. In this case, each termination leads to node 2. On arc 2 the bit is tripped out. At node 3 the program will determine whether TD has been reached or if the well is to be cased and cemented at this point. If one of these, then control transfers to arc 3 or 4, respectively. If only a bit change is required, arc 5 will be taken, corresponding to tripping in a new bit. Tripping in leads to node 1 and drilling resumes.

After drawing the network, the user prepares data input which describes the network, the governing equations for each operation, and the logical relations for terminating and selecting operations. The computer will then simulate the system and compute the cost based upon the functions specified.

Within this framework the level of aggregation can be controlled by the modeler, conventional and unconventional methods can be represented with equal facility, and, with the edit features (not described herein) easy modification and parametric analysis can be performed.

Currently the program is in an experimental state. Simple models are being run to validate its output against classical "drilling equation" models. A detailed, technology-based network model for rotary drilling is being developed.

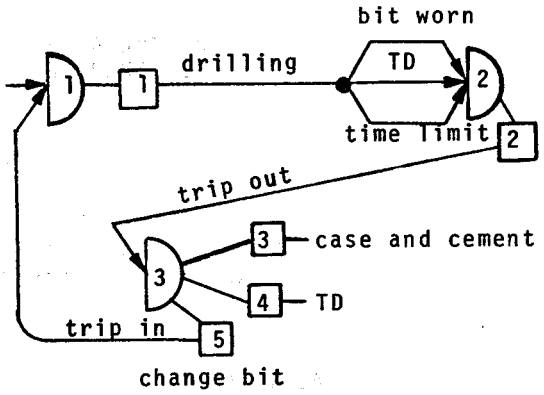


Figure 1. Simple Drilling Model

Geothermal Resources Council, TRANSACTIONS, Vol. 2 July 1978

Dup

OPTIMIZATIONS OF GEOTHERMAL CYCLE SHELL AND TUBE EXCHANGERS OF VARIOUS CONFIGURATIONS WITH VARIABLE FLUID PROPERTIES AND SITE SPECIFIC FOULING

W.L. Pope, H.S. Pines, L.F. Silvester, P. A. Doyle, R. L. Fulton & M. A. Green

Lawrence Berkeley Laboratory
University of California
Berkeley, California 94720

ABSTRACT

A new heat exchanger design program, SIZEHX, is described. This program allows single step multiparameter cost optimizations on single phase or supercritical exchanger arrays with variable properties and arbitrary fouling for a multitude of matrix configurations and fluids. SIZEHX uses a simplified form of Tinker's method for characterization of shell side performance; the Starling modified BWR equation for thermodynamic properties of hydrocarbons; and transport properties developed by NBS. The report will include results of four parameter cost optimizations on exchangers for specific geothermal applications. The relative mix of capital cost, pumping cost, and brine cost ($/Btu) are determined for geothermal exchangers illustrating the invariant nature of the optimal cost distribution for fixed unit costs.

INTRODUCTION

Little information exists concerning general strategies for the optimization of heat exchangers. A few simple cases have appeared[1,2,3] which have one or more of the following drawbacks: (1) solutions are based on constant properties, (2) wall and fouling resistances are ignored or treated as constant, and (3) shell side pressure drop is based on ideal, pure cross-flow, friction data. Leakage (or bypass) factors must be assumed apriori.

In geothermal applications, specifically supercritical binary power plants using light hydrocarbons as secondary fluids in a Rankine cycle, the forgoing exchanger optimization schemes are seriously limited. For example, on even the most easily exploited, moderate temperature, low salinity (<20,000 ppm TDS) resources (1) brine scaling rates can change as much as a factor of thirty over the temperature and velocity range of economic interest,[4] and (2) the working fluid specific heat, density, thermal conductivity, and viscosity can change by factors of about three or more in the primary heat exchanger. These result in a markedly nonlinear overall heat transfer coefficient distribution. Because the working fluid in most supercritical Rankine cycles operates just slightly above the critical pressure, assumptions of linearity in these properties between terminal conditions can lead to significant errors. In addition, more complex fluids; i.e., mixtures of light hydrocarbons are being seriously considered[4] as "solutions" to problems of reservoir temperature decline for binary cycle power plants.

On Heber brine, the fouling resistance dominates at the exchanger cold end, and thus can have a *decisive* influence on the brine injection temperature and therefore the cycle design energy cost and resource utilization efficiency. Increasing the "design fouling factor" increases the optimum injection temperature, and therefore it must be prudently "selected" to ensure economically feasible designs. Obviously, one needs site specific scaling data to make good system design decisions. In addition, because exchangers are traditionally purchased based on *customer* specified terminal temperatures and fouling factors, the geothermal customer needs efficient heat exchanger design aids. A problem in many cases is that suitable codes are proprietary. Another problem is which code to use. A *third* problem is that the optimum injection temperature depends also on exchanger cost and these costs are not very well known.

A common dilemma arises when the customer goes out for preliminary exchanger quotes. It is the rule rather than the exception to not only receive quotes at a variety of unit costs, but also a variety of configurations all for the same *specified* service, duty, terminal temperatures, and fouling factors! On detailed comparison of the various proposals, it is also not uncommon to find that the design velocities and pressure drops are all quite different leading to differences in subsequent operating costs. How is the choice to be made? How significant are the differences? Unfortunately, even if the significance of the differences are not known, the customer usually has only two choices - he must either (1) accept the low bid (which might be one with the greatest pumping power requirements, thus compromising the cycle net power) or (2) throw them all out and go back to the drawing board.

Recent geothermal research activities, then, have revived a multitude of interesting and complicated problems in the ostensibly well known area of heat exchanger design. Because the exchangers in geothermal binary cycles represent the order of 30% of the total capital cost, it is imperative

they be built with a minimum of over-design in both capital cost (area) and operating cost (pressure drop) while maximizing brine utilization efficiency. The problem then becomes a complex mix of trade-offs between several competing influences. Several optimizable parameters can be investigated to determine their sensitivity on the design objective. The purpose of this study is to explore some of the trade-offs in heat exchanger selection for geothermal binary cycle power plants.

THE GEOTHM/SIZEHX PROGRAM

We have developed a new heat exchanger design routine, SIZEHX (Ref. 5, Sec. 5) which can be used for exchanger conceptual design and optimization at an enhanced level of understanding. The SIZEHX code was developed to complement the GEOTHM[5] heat and mass balance routines and take advantage of GEOTHM's powerful multiparameter optimization[6] capabilities.

The SIZEHX code uses relatively complex computational algorithms with none of the previously mentioned simplifying assumptions with regard to constancy of properties and scaling. We have developed a practical cost optimization strategy which can be applied to geothermal exchangers to determine optimum terminal conditions, velocities, and design coefficients at the conceptual level prior to requesting exchanger quotes. Space does not permit a description of the SIZEHX code here; however, relatively complete documentation[5] is available.

COMPLETE CYCLE CHARACTERIZATION

Previous studies have shown[6] that to determine the overall optimum, or minimum energy cost, design for an assumed conversion process on an assumed resource, the complete geothermal plant and field must be characterized and optimized. However, to perform these complete cycle optimizations, one needs subsystem costs and overall design heat transfer coefficients as input. The design process, then, is iterative in nature, and at various points in time, the process designer must get updated heat exchanger and other subsystem quotes to be sure he is currently assuming realistic overall heat transfer coefficients and unit costs.

ISOLATING THE HEAT EXCHANGER FOR SUBSYSTEM OPTIMIZATION

For the purposes of this heat exchanger study, then, assume that preliminary overall process economic calculations have been done and that we can simply single out the primary heater of a supercritical isobutane binary cycle by fixing the resource temperature and working fluid states. We want to investigate in detail the effects of exchanger geometry, cost per unit area, and design fouling factor on total annual exchanger operating costs to establish design U's and optimum exit brine temperatures.

Specifically, we suggest that investigating the above effects on single tube pass exchangers assuming single segmental baffles will provide typical general performance for any well designed commercial exchanger.

We define as "optimum" an exchanger for which the following function has been minimized:

$$X_{TOT} = X_A + X_{Pi} + X_{Po} + X_{UF} \quad (\$/Btu) \quad (1)$$

where X_A is the heat exchanger total capital investment ($/Btu)

X_{Pi} is the cost of tube side pumping power ($/Btu)

X_{Po} is the cost of shell side pumping power ($/Btu)

X_{UF} is the utility fluid (brine) cost ($/Btu)

It is important to note here that we do not fix tube length, number of tubes, or velocities with SIZEHX. We specify tube diameter and mass rate, and the former are determined by zone heat balances and momentum balances over the exchanger length to satisfy the specified pressure drops.[5] These then are subsequently optimized along with the pinch point in accordance with the specified minimum total cost objective, Equation (1).

ASSUMPTIONS FOR THIS STUDY

For the purposes of this study, we have assumed the resource temperature is fixed at 455.37°K (360°F), the isobutane mass flow rate is known, and the inlet temperature and pressure and exit temperature are fixed at values established by Ben Holt.[4] These are:

$$T_{in} = 319.26°K \ (115°F)$$
$$P_{in} = 45.83 \text{ Bars } (650 \text{ psig}) \quad (2)$$
$$T_{out} = 422.04°K \ (300°F)$$

In this study, all cases have assumed a 4/2 series/parallel exchanger array with external plumbing cost and external plumbing pressure drop ignored. We have normalized the brine cost ($/Btu) to values recently established by Holt[4] for the same brine flow rate and exchanger duty. We also assume the same tube side design fouling factors established by Holt from tests conducted by San Diego Gas and Electric, SDGE,[7] on brine at the Heber Resource. For carbon steel tubes, Holt's design fouling factor was characterized by (Ref. 4, p. 29):

$$R_f = .0001 \ °F/Btu/hrft^2 \text{ for } 270°F<T_B<360°F$$
$$R_f = .0011 \quad " \quad " \quad 176°F<T_B<270°F \quad (3)$$
$$R_f = .0033 \quad " \quad " \quad 148°F<T_B<176°F$$

Any dependence of brine velocity on the design fouling factor was ignored herein, but SIZEHX could easily deal with this if it were factored in.

All cases assume 1.77 and 1.71 for the exchanger direct and indirect cost factors, and a fixed charge rate of 20% to establish the exchanger annual capital cost. For pumping power, we have assumed plant power at 35.2 mills/kwh[4] with pump adiabatic efficiencies of 80% and motor efficiencies of 95%. In order to investigate exchanger geometry with a minimum of constraints, we assume

tube and shell side pressure drops and brine flow rate "are material" and explore a variety of configurations and costs with the following as optimizable parameters:

1. The heat exchanger pinch point delta T (K°)
2. The tube side pressure drop (BARS)
3. The shell side pressure drop (BARS) (4)
4. The tube outside diameter (m)

All cases assume bare 16 gauge carbon steel tubes (no external surface). All cases assume an equilateral triangular tube matrix with a tube pitch to diameter ratio, s/d_o, equal to 1.25. The shell diameter to baffle spacing ratio, Ds/ℓ, is varied between:

$$1.0 \leq Ds/\ell \leq 5.0$$

and for reasonable corresponding baffle cut to diameter ratios, H/Ds, we adopt values suggested by A.P. Fraas (Ref. 8, p. 154).

RESULTS OF SIZEHX HEAT EXCHANGER OPTIMIZATIONS

Table 1 and Figures 1 and 2 are the results of our preliminary optimizations of primary heat exchangers for a supercritical isobutane binary cycle on a Heberlike resource.

Input values in Table 1 were selected to explore the effects of (1) shell side geometry and tube size, (2) exchanger cost per unit area and (3) tube side cleanliness. All cases except Case 6 assume Holt's design fouling factor. Cases 1, 2, and 3 cover a broad range of baffle cuts and spacings all at a fixed $6.00 per square foot and .75 in O.D. tube diameter. Cases 2, 4, and 5 explore a range of tube O.D.'s from the calculated optimum, 0.438 inch O.D., to 1.0 inch O.D. all for the same baffle cut and spacing ratios and cost per square foot. Cases 2, 7, and 8 illustrate the effect of increasing exchanger cost per square foot for fixed baffle cut and spacing ratio and tube O.D. Finally, cases 2 and 6 illustrate the influence of tube side fouling for the same fixed baffle cut and spacing ratio, tube diameter, and cost.

Table 1 shows that matrix geometry and tube O.D. have *virtually no effect* on the optimum brine exit temperature. This is determined by (1) brine cost, (2) capital cost, and (3) fouling factor alone for the assumed working fluid states. Another interesting point is that the optimum tube side and shell side pressure drops are virtually the same (cases 1,2,3) for the same tube diameter and cost per square foot *regardless* of baffle spacing ratios (for the Ds/ℓ and H/Ds pairs assumed here). The larger baffle spacings and cuts achieve higher overall heat transfer coefficients and fewer tubes through higher optimum brine velocities and simply result in shorter, more practical, shells. The total cost per Btu, X_{TOT}, decreases with increasing baffle spacing primarily by reducing the exchanger capital cost fraction, X_A/X_{TOT}.

In addition, as the cost per square foot increases (cases 2, 7, and 8), the optimum pinch point (mean delta T) and the tube side and shell side pressure drop increase obtaining higher economically justified design overall heat transfer coefficients and even fewer tubes through increased velocities, resulting in even shorter shells. As the cost per square foot increases, the capital cost fraction X_A/X_{TOT} increases, of course, but the optimum brine cost fraction X_{UF}/X_{TOT} decreases.

It should be pointed out, however, that although Case 1 (at $Ds/\ell = 1.0$) is shown as the lowest total (fouled) cost, this "design" might have to be thrown out for structural reasons - the shell inside diameter is about 45 inches here making the unsupported tube length to diameter ratio about 90/0.75 = 120. (The SIZEHX code currently performs no tube natural frequency calculations or other obviously important structural checks).

It should also be pointed out that our simplistic fixed unit cost assumption, dollars per square foot of *matrix surface*, can be misleading for significantly different numbers of tubes (drilling and rolling costs), significantly different lengths (baffle cost), and for significantly different shell diameters (shell cost).

For all the .75 inch O.D. tube, design fouling factor cases shown here, the number of tubes is between 1523 and 1674 and the shell diameters range from 45.7 in. diameter to 47.8 in. diameter (both relatively small ranges). For the .438 in. O.D. "optimum tube diameter" case, Case 4, however, the number of tubes is 6687 and the shell is about 55.5 in. O.D. For the 1.0 in. tube case, the number of tubes is 837 and the shell is 45.5 in. in diameter.

From the forgoing, then, the case with the most "optimistic" capital cost here is clearly Case 4 which is only of academic interest any way from the point of view of scale removal.

CONCLUSIONS

A new shell and tube heat exchanger design routine SIZEHX[5] has been used with simple cost assumptions to demonstrate the influence of matrix geometry, tube diameter, fouling, and cost per square foot on the optimum total annual cost, injection temperature, and brine velocities on supercritical geothermal exchangers optimized at a fixed brine cost.

The brine cost is found to dominate all other considerations in geothermal heat exchangers. A 2% reduction in X_{TOT} can achieve a $4 M savings over the life of each 50 MWe (net) geothermal binary power plant at 1976 brine costs in the primary exchanger/field subsystem alone.

The SIZEHX/GEOTHM[5] program has performed complex multiparameter optimizations believed to be impractical with previously documented codes. A *specified* design fouling factor was used in this work; however, SIZEHX is capable of determining the *optimum design fouling factor*, or optimum cleaning frequency, given the cleaning costs and the cost of plant-down time, assuming constant scaling rates.

ACKNOWLEDGMENT

We gratefully acknowledge the support of DOE/DGE for LBL Cycle studies and GEOTHM development, and H.J.M. Hanley for transport properties.

TABLE 1 SIZEHX Optimized Supercritical (1/1) Exchanger Designs (4/2 series/parallel arrays)

Sample Case	No. of Optim. Parameters	Assumed Input Values			- CALCULATED OPTIMUM RESULTS -													
					Optimizable Parameters				Δt Mean	U_{ol}	V_{brine} (max)	Tube length	Brine exit temp.	X_A/X_{TOT}	X_{pu}/X_{TOT}	X_{uf}/X_{TOT}	X_{TOT} X10^6	P/Q
		Ds/ℓ	H/Ds	$/ft^2	Δtpp (C°)	ΔPi (Bars)	ΔPo (Bars)	do (in.)	(C°)	(B/hrft^2°F)	(ft/sec)	(ft)	(°F)	(%)	(%)	(%)	($/Btu)	(%)
1	3	1.0	0.46	6.00	13.454	1.973	0.791	0.75 •	17.02	271.1	4.891	66.8	150.5	.093	.0180	.889	.632	.1105
2 Base-line	3	2.0	0.25	6.00	13.486	1.998	0.758	0.75 •	17.05	238.6	4.795	74.4	150.5	.104	.0176	.878	.640	.1092
3	3	5.0	0.16	6.00	13.46	1.991	0.796	0.75 •	17.03	202.1	4.637	85.0	150.6	.121	.0164	.862	.652	.1114
4	4	2.0	0.25	6.00	13.651	1.906	0.598	0.438	17.18	247.5	4.676	29.3	150.5	.100	.0156	.884	.635	.0961
5	3	2.0	0.25	6.00	13.443	1.967	0.803	1.00 *	17.01	223.5	4.745	115.	150.6	.111	.0178	.872	.645	.1111
6 "clean" ≠	3	2.0	0.25	6.00	9.598	2.305	0.865	0.75 *	13.12	315.2	5.052	80.9	139.6	.107	.0205	.873	.613	.1218
7	3	2.0	0.25	12.00	14.02	2.208	1.266	0.75 *	17.68	263.0	5.156	69.1	154.1	.166	.0218	.812	.703	.1486
8	3	2.0	0.25	18.00	16.27	2.224	1.272	0.75 •	20.04	273.6	5.379	59.3	161.8	.196	.0207	.783	.757	.1521

All above except Case 6 assume the step function fouling factor from Ref. 4 on tube side and zero fouling factor on shell side.
≠ Assumes .0001 °F/Btu/hr ft^2 fouling factor on tube side - virtually clean.
• Specified parameter for these runs.

XBL 783-7866

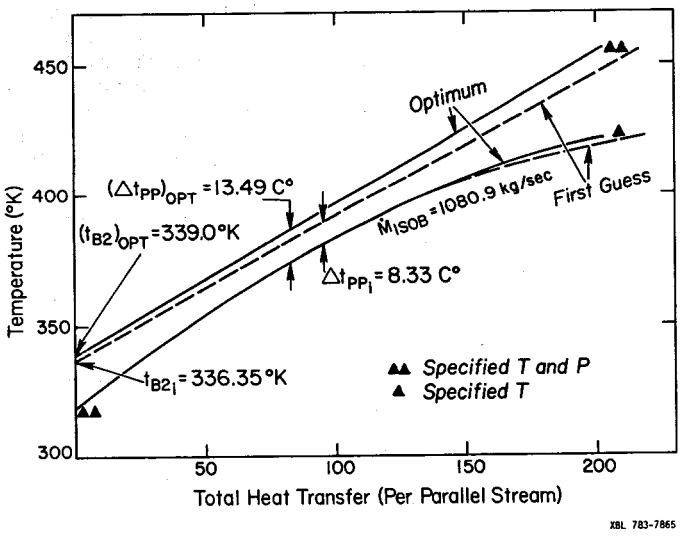


FIGURE 1 Typical T/Q plot (Case 2) illustrating change of brine temperature profile and pinch point shift in SIZEHX optimization.

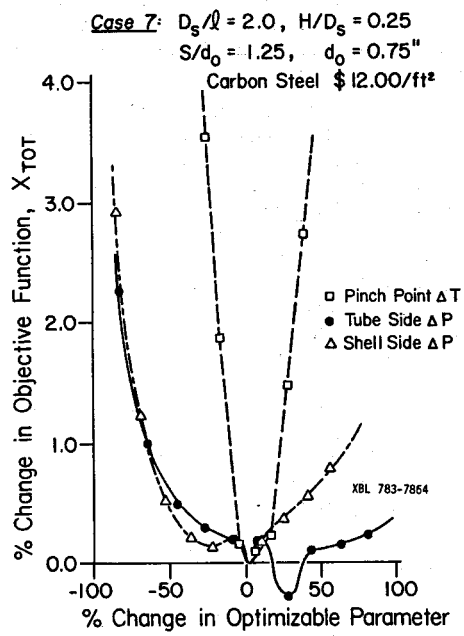


FIGURE 2 Typical sensitivity plot from 3 parameter optimization (Case 7). Note the strong influence of pinch point (brine cost) on the total cost, X_{TOT} ($/Btu).

REFERENCES

1. McAdams, W.H. Heat Transmission, 3rd Ed., Chap. 15, McGraw Hill, Inc., NY 1954
2. S.L. Milora and J.W. Tester, Geothermal Energy as a Source of Electric Power, Thermodynamic and Economic Design Criteria, Appen. B, The MIT Press, Cambridge, Mass. 1976
3. S.E. Turner and W.W. Madsen, "HEDCOR-A Heat Exchanger Cost and Design Optimization Routine" E.G.&G. Idaho, Inc., Idaho National Engineering Laboratory, Idaho Falls, Idaho, April 1977.
4. Vasel W. Roberts (Project Manager), "Geothermal Energy Conversion and Economics-Case Studies" EPRI-301, Project 580, prepared by Holt/Procon, Ben Holt and Edward L. Ghormley (principal investigators), Electric Power Research Institute, Palo Alto, CA, Nov. 1976.
5. M.A. Green, R.N. Healey, H.S. Pines, W.L. Pope, L.F. Silvester, and J.D. Williams, "GEOTHM-PART 1, A Users Manual for GEOTHM. (Computer Design and Simulation of Geothermal Energy Cycles.) LBL Publication-202, July 1977.
6. H.S. Pines and M.A. Green, "The Use of Program GEOTHM to Design and Optimize Geothermal Power Cycles." Presented at the Eleventh *Intersociety-Energy Conversion Engineering Conference*, Lake Tahoe, Nevada, September 12-17, 1976, LBL 4454, June 1976.
7. San Diego Gas & Electric Company, "Test and Evaluation of a Geothermal Heat Exchanger," EPRI Rept. 376, September 1975.
8. A.P. Fraas and M.N. Ozisk, Heat Exchanger Design, John Wiley and Sons, Inc., New York 1965.

VISCOSITY OF GEOTHERMAL BRINES

Robert W. Potter II

U.S. GEOLOGICAL SURVEY, MENLO PARK, CALIFORNIA 94025

One of the prerequisites of modeling the flow of fluid in a geothermal reservoir is knowledge of the viscosity of the fluid involved. Due to a general paucity of viscosity data for high-temperature brines, the general practice outside the petroleum industry has been to use some empirical correlation of the viscosity of pure water other than those formulated for the steam tables (Kasameyer et al., 1977; Gray et al., 1976; and Mercer et al., 1975). This paper suggests some alternative methods to model the viscosity of brines and describes a model which allows the limited data for brines to be extrapolated to conditions of interest in a geothermal reservoir.

Experimental data for the viscosity of solutions of NaCl+KCl, NaCl+Na_2SO_4, NaCl+$MgSO_4$ and NaCl, KCl, Na_2SO_4, $MgSO_4$, and seawater concentrates are available at temperatures up to 150°C and ambient pressure (Korosi and Fabuss, 1968). Figure 1 shows the change in viscosity of NaCl solutions as the molality (moles/kg water) is increased at a constant temperature of 150°C. As the salt content is increased there is a progressive difference in the viscosity of the solution compared to pure water, and even low molalities differences of several percent exist. For bines similar to those of the Salton Sea (4 molal), errors of 46 percent result at 150°C. The differences increase with temperature so that at reservoir temperatures of 250°C one could expect errors greater than 70 percent.

A theoretical corresponding state model for the bulk thermochemical properties of brines was developed in previous papers (Potter and Haas, 1977, 1978). Applying this model yields the following equations for the viscosity of a brine (μ):

$$\mu_b^n = \Sigma f_i \mu_i \text{ at a constant T, P} \qquad (1)$$

where μ_b is the viscosity of the brine, μ_i is the viscosity of the ith binary component (e.g. NaCl+ H O at the same ionic strength as that in brine and f_i is the mole fraction of the ith component. To test equation (1) values were calculated with this equation and compared to experimental data of Korosi and Fabuss (1968) for ternary salt solutions and seawater concentrates. These viscosity data have a stated precision of ±0.2% and can be reproduced by equation (1) to within ±0.4% (Table 1). Although equation (1) evidently can be used to calculate fairly precisely the viscosity of complex solutions, it has several limitations with respect to being applicable to geothermal systems.

The viscosity data are currently unavailable for many of the binary components of geothermal brines. However, most are minor components, and their effects on the total viscosity are small. The viscosity effects of minor components can be approximated by assuming that their effects are the same as those of a similar electrolyte for which data are available; for example, data can be used to estimate the contribution of KBr to the total viscosity. A more serious limitation is the total lack of data for temperatures greater than 150°C for the binary components. Unfortunately, equation (1) does not yield an extrapolative mathematical expression of viscosity as a function of temperature.

It was proposed by Potter and Haas (1977) that NaCl solutions could be used to model the thermochemical properties of geothermal fluids. They found that the enthalpy of the brine was predicted within 0.5% by a NaCl solution with the same equivalent molality as the geothermal fluid. The viscosity of seawater concentrates was calculated assuming that the viscosity of a NaCl solution with the same ionic strength was equal to that of the brine. The data of Korosi and Fabuss (1968) could be calculated to within ±0.5% (Table 1). Hence, it appears that the viscosity of NaCl solutions can be used to describe the viscosity of fluids. However, as in the case of the theoretical equation (1), the lack of viscosity data for NaCl solutions at temperatures greater than 200°C limits their practical use.

Ozbek et al. (1977) have produced an empirical correlation of the available experimental viscosities of NaCl solutions up to 150°C. Unfortunately, this correlation is not extrapolative. The form of the equation chosen and the overweighting of the data in the 20°-40°C range has produced an equation that describes the data very well at temperatures less than 50°C, but systematically varies from the data at higher temperatures. For example, the deviation of 40°C is ±1.4%, at 60°C ±1.6%, at 120°C ±3.9%, and at 150°C ±7.9%, with a strong tendency for the calculated viscosities at temperatures greater than 120°C to be greater than

the experimental. This behavior makes the extrapolation of the function to obtain reliable viscosities at higher temperatures dubious.

The petroleum industry has used a correlation contained in Matthews and Rossell (1967); however, these data are presented graphically up to 204°C (400°F) and are not readily extrapolative to higher temperatures. In addition, various other experimental workers have generated correlations of their data, but these are limited to temperatures less than 150°C.

For these reasons the following correlation method was developed. The viscosity of pure water and a given NaCl solution is the same only at different temperatures. However, we can compare the relationship between the temperature at which water has the same viscosity as the NaCl solution, the equivalent water temperature (t_w), with the temperature of the NaCl solution (t_b):

$$t_w = f_{(t_b)} \quad \text{at constant composition} \qquad (2)$$

If equation (2) is an extrapolative function, then the aforementioned difficulties can be overcome. To test this relationship, the data of Kestin contained in Ozbek et al. (1977) were used to generate values of t_w for NaCl solutions from 0 to 6 molal at t_b up to 150°C. Equation (2) was found to be a first-order equation (the correlation coefficient $r^2 = 0.9998$) and hence is readily extrapolative. Figure 2 shows a plot of the t_w versus t_b for 0 to 6 molal NaCl solutions. The following equation was derived to describe t_w as a function of t_b and composition (x=molality):

$$t_w = (0.001599x - 0.5628929x^2 + 0.0393889x^3) + (1.00 - 0.120946x + 0.0142110x^2 - 8.7747\times10^{-4}x^3)Tb \qquad (3)$$

Equation (3) describes the available experimental data for NaCl solution to ±1% and has a distinct advantage over previous correlations. Previous experience with such correlation methods (Potter and Haas, 1977, 1978) has shown that the ability to extrapolate the function beyond 325°C breaks down due to the onset of critical phenomena in water. Most modeling programs have built into them an equation for the viscosity of pure water (e.g., Gray et al., 1976). Equation (3) yields an equivalent water temperature which can be put directly into existing routines to yield the viscosity of the solution.

In summary, data for NaCl solutions can be used as a reliable model for the viscosity of geothermal brines. An empirical correlation method allows the existing data for the viscosity of NaCl solutions to be extrapolated to temperatures as high as 300° to 325°C. This correlation should suffice until viscosity data for NaCl up to these temperatures are available.

References

Gray, W. G., O'Neill, K., and Pinder, G. F., 1976, Simulation of heat transport in fractured, single-phase geothermal reservoirs: Proc. 2nd Workshop Geothermal Reservoir Engineering, p. 222-228.

Kasameyer, P., Thorson, L., and McKee, C., 1977, Modeling thermal and flow fronts for arbitrary well arrays, Geothermal Res. Council, Trans. vol. 1, p. 163-165.

Korosi, A., and Fabuss, B. M., 1968, Thermophysical properties of saline water: Office of Saline Water Progress Report No. 363, 53 p.

Matthews, C. S., and Rossell, D. G., 1967, Pressure buildup and flow tests in wells, monograph vol. 1, H. L. Doherty Series, Soc. of Pet. Eng.

Mercer, W. M., Pinder, G. F., and Donaldson, I. G., 1975, A Galerkin finite element analysis of the hydrothermal system at Wairakei, New Zealand, Jr. Geophys. Res., vol. 1975, p. 2608-2621.

Ozbek, H., Fair, J. A., and Phillips, S. L., 1977, Viscosity of aqueous sodium chloride solutions from 0-150°C: Lawrence Berkeley Laboratory Report # LBL-5931, 61 p.

Potter, R. W., II, and Haas, J. R., Jr., 1977, A model for the calculation of the bulk thermodynamic properties of geothermal fluids: Geothermal Res. Council, Trans. vol. 1, p. 243-244.

Potter, R. W., II, and Haas, J. L., Jr., 1978, Models for the calculation of the density and vapor pressure of geothermal brines: U.S. Geol. Survey Jr. Research, vol. 6, p. 247-257.

Table 1. Calculation of the dynamic viscosity (micro Pa S) of seawater at 150°C compared to the data of Korosi and Fabuss (1968).

	NaCl	KCl +KBr	$MgSO_4$ +$MgCl_2$	Solution
Molality	0.4772	0.0101	0.0646	--
μ_i	202.5	197.1	200.5	--
f_i	0.6722	0.0142	0.3136	--
μ_{calc}	--	--	--	201.8
μ_{obs}	--	--	--	201.5
$\mu_{equiv\ NaCl}$	--	--	--	201.1

Geothermal Resources Council, TRANSACTIONS, Vol. 2 July 1978

HONEY LAKE KGRA GEOPHYSICAL SURVEY AND DRILLING TESTS

James I. Pritchard and George P. Zebal

Electrodyne Surveys
P. O. Box 1522
Sparks, NV 89431

George P. Zebal and Assoc.
P. O. Box 1822
Newport Beach, CA 92663

An integrated geophysical survey of the Honey Lake, California KGRA was conducted by Electrodyne Surveys for GeoProducts Corporation of Oakland, CA to aid in the evaluation of the geothermal resource potential that exists in the vicinity of the Wendel Hot Springs. The study area covers approximately 24 square miles and is located along the northeast shores of Honey Lake on the western boundary of the Basin and Range physiographic province. The study area is bordered to the north and east by the Skedaddle and Amedee Mountains and to the northwest by Schaffer Mountain. These mountains are composed primarily of Pliocene andesite flows and layered pycoclastic rocks, and the valley basin is covered by Pleistocene to recent locustrine, aeolian sand and alluvial fan deposits (McFarlan et al, 1977).

Two faults, the Litchfield and Amedee Faults, are known to traverse through or near the prospect area. These faults are nearly conjugate, with the Litchfield Fault trending in an east southeast direction, and the Amedee Fault trending in nearly a north-south direction. Numerous tuffa deposits occur throughout the prospect with one set extending east from the southern extremity of Schaffer Mountain towards the Skedaddle Mountains and another set extending north-northwest from Wendel Hot Springs towards the peak of Schaffer Mountain. Numerous thermal springs occur in the vicinity of the Wendel Hot Springs and extend along a line of tuffa deposits that trend north-northeast. The surface water temperature of the Wendel Hot Springs is approximately 86°C and will soon by used to heat hydroponic facilities, which are being constructed near the hot springs.

The geophysical survey was divided into a reconnaissance and a detailing phase. Four types of geophysical methods were employed during the reconnaissance phase: gravity, ground magnetics, scalar AMT-MT (audio-magnetotelluric and magnetotelluric) soundings and tensor MT soundings. A total of 241 gravity stations were occupied by Lanton Surveys with ground magnetic measurements being made at the same time. Thirty-eight AMT-MT soundings were completed with data obtained with a two axis fluxgate magnetometer. Bandpass recordings were made at three frequency ranges, 0.02-0.08hz, 8-26hz and 100-1000hz and spectral analysis of the orthogonal electric and magnetic field components yielded scalar apparent resistivity values at specific frequencies. Four additional MT soundings were recorded utilizing a frequency range of 0.01 to 30hz and were subjected to tensor analysis by Terraphysics. The tensor apparent resistivity sounding curves were also matched to one dimensional models.

All four geophysical methods indicated that the study area was structurally more complicated than had been originally estimated. The gravity data suggests that the Litchfield Fault probably changes direction and trends to the southeast at least a mile further to the west then had been previously reported. Another fault was also postulated as extending south-southeast from Schaffer Mountain, through the Wendel and Amedee Hot Springs. The intersection of this fault with the Skedaddle Fault occurs at the Wendel Hot Springs. Therefore, there are three predominant directions along which major faulting trends within the valley: east, north-northeast and north-northwest.

Two areas of high apparent conductance and low gravity values were found to border an area of gravity high and low apparent conductance in the central portion of the northern half of T 29N, R15E. These three areas appeared to parallel the previously mentioned Schaffer Mountain fault. To better define the structural relationships and the volumetric extent of the possible geothermal reservoir in that region, a detailed electrical resistivity survey was conducted utilizing the Electro-Sonde Profiling technique (West and Pritchard, 1978). This technique combined

controlled-source electromagnetic soundings with audio and sub-audio end-on-end telluric profiles and galvanic soundings.

A total of 26 line miles of ESP profiles were completed from 4 overlapping source bipoles in the area north and west of the Wendel Hot Springs. Each source bipole was two miles in length and a set of modified Schlumberger soundings were accomplished from each source. In addition, 14 time domain, vertical magnetic and parallel electric field soundings were completed. At the time of the due date for these summaries, a complete analysis of the ESP profiles had not been completed, so a complete discussion of the results will have to wait until the G.R.C. meeting. From the results of this survey temperature gradient, sites will be picked as well as deep drilling test sites. The results from the deep test should be available by July 1978. Ultimately, both electric and nonelectric uses of the geothermal energy will be developed by GeoProducts in the Wendel Hot Springs area.

These geophysical survey results will also be used in choosing forty acres of GeoProduct's leased land, which will be given to a consortium of the Chico-Reno-Lassen Colleges to be used as a research site for non-electric usage of geothermal energy. The consortium plan to drill three holes, 1000, 2000, and 5000 foot drill holes, in the near future.

REFERENCES

McFarlan, J. M., Melton, W. J., Morse, M. T., and Cleary, C. R., 1977, Proposed Geothermal Leasing, Honey Lake Valley, EAR: U.S. Dept. Interior, BLM Report #1791.

West, R. C. and Pritchard, J. I., Combined electromagnetic and galvanic (d.c.) electrical resistivity soundings: presented at Geothermal Resource Council Meeting in Hilo, Hawaii, July 25-28.

MICROEARTHQUAKE SURVEY OF THE RADIUM SPRINGS KGRA, SOUTH-CENTRAL NEW MEXICO

Bob Quillin and Jim Combs

MICROGEOPHYSICS CORP.
GOLDEN, COLORADO

GEOTHERMAL SERVICES, INC.
SAN DIEGO, CALIFORNIA

ABSTRACT

For a nine-week period during September, October and November of 1975, seismicity was monitored in the area of Radium Springs Known Geothermal Resources Area (KGRA) located in South-central New Mexico in the Rio Grande Rift. The seismic array consisted of five, three-component seismograph stations with maximum station separation of less than 15 km. Two microearthquakes with coda-duration magnitudes of 0.0 were located and are apparently associated with surface mapped faults in the near proximity of the hot springs. By far the most abundant type of local seismic activity, hundreds of events per day, were nanoearthquakes of from 0.25 to 2.0 sec total duration corresponding to coda magnitudes of -3.2 to -1.1. These nanoearthquakes are caused by natural hydrofracturing associated with the local geothermal regime.

INTRODUCTION

The seismicity of any particular geographic region may have as its source a variety of wave generating phenomena, some of which are of geological origin and are therefore geophysically interesting. Other man-made sources such as well pumps, trains (Sanford et al., 1968), mine blasts, etc., may be scrutinized and discarded if they do not provide useful information. Of the sources which are of geological origin, there are still several mechanisms which may be associated with particular types of earthquakes. For example, large earthquakes, i.e., magnitude (M) $\geq$ 4.0, may be typically associated with active regional tectonics or perhaps violent volcanic activity (Dibble, 1969). As noted by Ward (1972), microeathquakes (M < 3) have been observed near many major geothermal areas around the world. Ward and Björnsson (1971) have shown that geothermal areas which are structurally related to fissure systems generally have microearthquake activity, whereas those areas that have few prominent fissures and seem only related to intrusions of silicic magma appear to have little or no microearthquake activity.

However, there are events, here termed nanoearthquakes (Combs and Hadley, 1977), which may be associated with both types of geothermal areas. Thermally induced differential expansion between fluid in isolated pores and enclosing minerals decreases effective pressure at the pore-mineral interface. With a sufficient increase in temperature, effective pressure becomes equal to the tensile strength, and the rock fractures. This type of mechanism is known as hydraulic fracturing and is inevitable in hot intrusive environments (Knapp and Knight, 1977). The number of events per day produced by this mechanism is a function of the size and age of the intrusion.

Other mechanisms for the generation of nanoearthquakes may be pore pressure in conjuction with local tectonic stress patterns. These nanoearthquakes are important in geothermal areas because they indicate potential free-circulation for geothermal fluids (Brown and Butler, 1977).

The objective of this microearthquake survey at the Radium Springs KGRA was to determine active fault zones in the area and their characteristics by the analysis of the associated seismicity.

GEOLOGICAL, GEOCHEMICAL, AND GEOPHYSICAL BACKGROUND OF THE RADIUM SPRINGS KGRA AND VICINITY

The Radium Springs KGRA is located in the Southern Rio Grande Rift in South-central New Mexico. The Rift is characterized by heat flow values $\geq$ 2.0 HFU (Reiter et al., 1975).

Radium Springs is located at the northern end of the Mesilla Basin (Fig.1), one of the southernmost grabens comprising the Rio Grande Rift (Seager, 1975). The springs issue at the base of a rhyolitic hill on the east boarder of the Rio Grande River lowland with reported temperatures of 76°C and 85°C (Summers,1965). Tests using the Na-K-Ca geothermometer indicated subsurface temperatures in excess of 200°C both at Radium Springs and at a nearby well (Fig. 1; Swanberg, 1975).

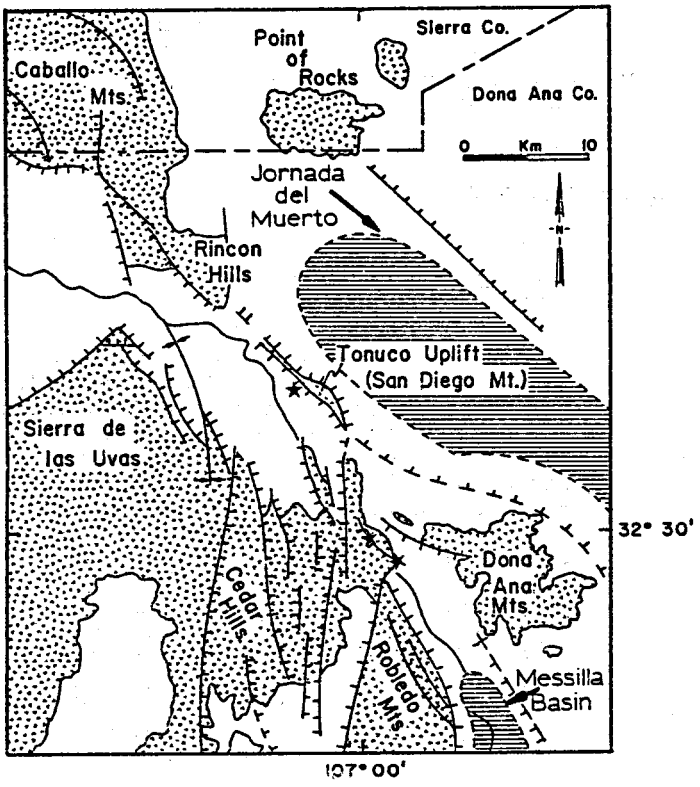


Fig. 1 Late Tertiary fault pattern in Radium Springs vicinity (Seager, 1975). Stars indicate locations of geothermometer temperatures in excess of 200°C (Swanberg, 1975) with middle one indicating Radium Springs while the other two are local water wells.

In one of the few published geophysical studies of the Radium Springs vicinity, Jiracek and Smith (1976) conducted a bipole-dipole resistivity survey covering an area of approximately 65 km^2 of the Southern Jornada del Muerto and Northern Mesilla Valley. This resistivity survey demonstrated that the Jornada del Muerto is structurally separated from the upper Mesilla Valley. However, the questions of the location of the subsurface reservoir for the thermal fluids and the associated heat source were not answered.

In a regional instrumental study, Sanford (1965) located two microearthquakes with magnitudes (M) of 2.8 and 2.9 approximately 7 km southwest of the Radium Springs KGRA. Another microearthquake (M = 2.9) was located approximately 15 km southwest of the KGRA. However, occurrences of geothermal resources are typically charaterized by a relatively high level of microearthquake activity. Assuming that perhaps events of smaller magnitude had possibly gone undetected, a five-station seismic array was deployed in the immediate vicinity of Radium Springs in order to further examine the geophysical characteristics of the Radium Springs geothermal area.

RECORDED SEISMICITY

Events coming from outside the array included events with S-P time intervals ranging from 3.0 to 8.0 sec, which correspond to epicentral

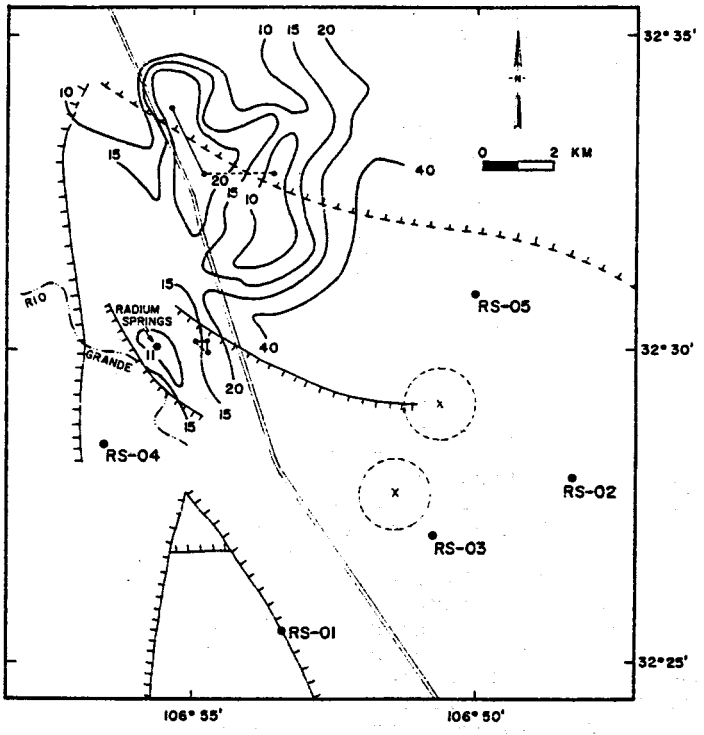


Fig. 2 Multi-information figure. Resistivity contour map of Jiracek and Smith (1976) in ohm-meters. Mapped and postulated faults of Seager (1975). Seismic station locations. Microearthquake epicenters with dashed circles indicating 1 km uncertainty.

distances of about 20 to 60 km, respectively. These events are probably associated with faulting or mine blasts in the San Diego and Caballo Mountains. Only the records of Sept. 29, 30 and Oct. 3 were examined in detail. Two miroearthquakes were located inside the seismic array. Using a layered crustral velocity model and the hypocentral location program HYPO71 (Lee and Lahr, 1975), epicenters were determined to approximately 1 km. The hypocentral locations (Fig. 2) of the microearthquakes are in close proximity to the stations registering the highest level of natural seismicity (RS-02 and RS-05) and appear to be on extensions of mapped or inferred faults. These microearthquakes have coda-duration magnitudes of approximately zero. Microearthquakes of this sort indicate active faulting which could provide permeable paths for fluid convection upward along the fault zone.

By far the most abundant type of events were nanoearthquakes from 0.25 to 2.0 sec total duration equivalent to coda-duration magnitudes of -3.2 to -1.1. Many of these events were obscured by low frequency noise of only slightly lower amplitude. By using a digital bandpass filter (20 to 40 Hz), the high frequency events could be separated from the lower frequency noise.

Another type of seismicity which was recorded were spiky sequences (Fig. 3) which typically lasted from a few minutes to almost 30 minutes. The events were only identified on station RS-05. Each pulse would typically be from one to three cycles in duration, with varying amplitudes. The predominant frequencies of these events were 25 to 40 Hz. Sequences of this type have been recorded and analyzed by Rinehart (1965; 1969) and Nicholls and Rinehart (1967) in a geophysical study of geyser action in Yellowstone National Park. They correlate these sequences with percolation of steam in underground fractures or cavities in the process of heating water which then erupts from the geyser.

With a sufficient increase in temperature, effective pore pressure becomes equal to the tensile strength, and the rock fractures (Knapp and Knight, 1977). In areas of unusually high geothermal gradients these thermally induced events may be generated at much shallower depths, and accordingly in rocks of lower tensile strengths. These induced events would be of very low magnitude and probably occur in swarm sequences such as the events described above.

SUMMARY

The seismicity of the Radium Springs KGRA, located in South-central New Mexico, has been studied using a maximum station separation less than 15 km. Several events per day were detected with S-P time intervals ranging from 3.0 to 8.0 sec, corresponding to epicentral distances of about 20 to 60 km. By far the most abundant types of seismic activity are nanoearthquakes of from 0.25 to 2.0 sec total duration, equivalent to coda magnitudes of -3.2 to -1.1. These nanoearthquakes are caused by natural hydrofracturing associated with the local geothermal regime. The highest numbers of these events were detected on stations

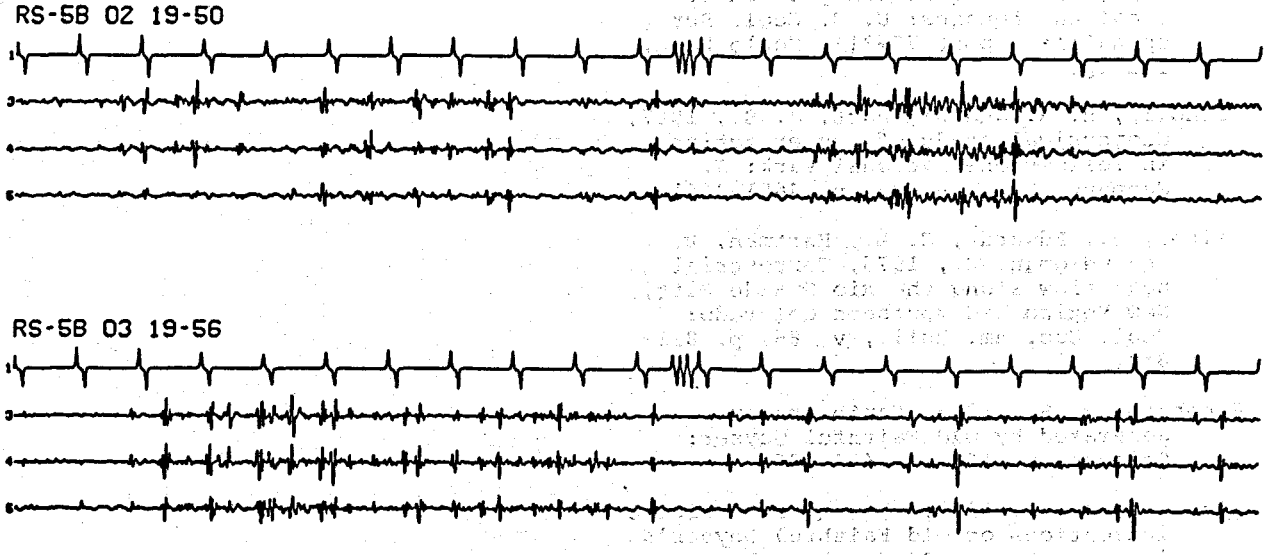


Fig. 3 Spiky Event Sequences

RS-02 and RS-05 (Fig. 2). Two microearthquakes of coda derived magnitude 0.0 were located in the near proximity of seismic stations RS-02 and RS-05 and appear to be associated with extensions of mapped faults (Fig. 2).

REFERENCES

Brown, P. L. and Butler, D., 1977, Earthquakes, geothermal systems and fracture production: Invited paper for: The 18th United States Symposium on Rock Mechanics, Keyston, Colorado.

Combs, J. and Hadley, D., 1977, Microearthquake investigation of the Mesa geothermal anomaly, Imperial Valley, California: Geophysics, v. 42, p. 17-33.

Dibble, R. R., 1969, Seismic power recordings during hydrothermal eruptions from Ruapehu Crater Lake in April 1968: J. Geophys. Res., v. 74, p. 6545-6551.

Jiracek, G. R. and Smith, C., 1976, Deep resistivity investigations at two known geothermal resource areas (KGRAS) in New Mexico: Radium Springs and Lightning Dock: New Mex. Geol. Soc., spec. pub. no. 6, p. 71-76.

Knapp, R. B. and Knight, J. E., 1977, Differential thermal expansion of pore fluids: fracture propagation and microearthquake production in hot pluton environments: J. Geophys. Res., v. 82, p. 2515-2522.

Lee, W. H. K. and Lahr, J. C., 1975, HYPO71 (Revised): a computer program for determining hypocenter, magnitude, and first motion pattern of local earthquakes: U. S. Geol. Surv. open-file report 75-311, Menlo Park, 112 pp.

Nicholls, H. R. and Rinehart, J. S., 1967, Geophysical study of geyser action in Yellowstone National Park: J. Geophys. Res., v. 72, p. 4651-4663.

Reiter, M., Edwards, C. L., Hartman, H. and Weidman, C., 1975, Terrestrial heat flow along the Rio Grande Rift, New Mexico and southern Colorado: Geol. Soc. Am. Bull., v. 86, p. 811-818.

Rinehart, J. S., 1965, Earth tremors generated by Old Faithful Geyser: Science, v. 150, p. 494-496.

Rinehart, J. S., 1969, Thermal and seismic indications of Old Faithful Geyser's inner workings: J. Geophys. Res., v. 74, p. 566-573.

Sanford, A. R., 1965, An instrumental study of New Mexico earthquakes: New Mex. State Bur. of Mines and Mineral Resources, cir. 78, 12 pp.

Sanford, A. R., Carapetian, A. G. and Long, L. T., 1968, High frequency microseisms from a known source: Bull. Seism. Soc. Am., v. 58, p. 325-338.

Seager, W. R., 1975, Cenozoic tectonic evolution of the Las Cruces area, New Mexico: New Mex. Geol. Soc., 26th Field Conf., p. 241-250.

Summers, W. K., 1965, A preliminary report on New Mexico's geothermal energy resources: New Mex. State Bur. of Mines and Mineral Resources, cir. 80, 41 pp.

Swanberg, C., 1975, Detection of geothermal components in groundwaters of Dona Ana County, southern Rio Grande Rift, New Mexico: New Mex. Geol. Soc., 26th Field Conf., Las Cruces Country, p. 175-180.

Ward, P. L., 1972, Microearthquakes: prospecting tool and possible hazard in the development of geothermal resources: Geothermics, v. 1, p. 3-12.

Ward, P. L. and Björnsson, S., 1971, Microearthquakes, swarms, and the geothermal areas of Iceland: J. Geophys. Res., v. 76, p. 3953-3982.

Geothermal Resources Council, TRANSACTIONS, Vol. 2 July 1978

PROCESSING OF GEOTHERMAL BRINE EFFLUENTS FOR INJECTION

R. Quong, F. Schoepflin,* N.D. Stout, G.E. Tardiff, & F.R. McLain

Lawrence Livermore Laboratory, University of California
*Bechtel Corporation

ABSTRACT

The handling of brine effluents for injection is a critical part of any geothermal conversion process. Brine effluents from the San Diego Gas & Electric/Department of Energy - Geothermal Loop Experimental Facility were characterized for particulate concentration and chemical composition. Bench scale tests were conducted with inorganic and organic coagulants as a means of enhancing the sedimentation process for separation and removal of suspended solids, principally amorphous silica. The effects of temperature, retention time, and pH on the precipitation of supersaturated silica, subsequent floc settling properties, and supernatant clarity were determined. A pilot sized clarifier with mixed media sand or precoat pressure filtration have been successfully tested as a means of producing injectable brine effluents. Preliminary cost estimates range in the vicinity of 20¢/1000 gallons.

Introduction

An important consideration in geothermal development projects is the handling and disposal of spent brine effluents. At The SDG&E/DOE Geothermal Loop Experimental Facility (GLEF) located in the Imperial Valley, California, spent brine is discharged from the 4-stage flash process and injected back into the formation via an injection well, Magmamax #3.

In the GLEF process, brine containing 20% total dissolved solids is flashed successively from a reservoir temperature of 300°C to the process exit temperature of 90°C. Evolution of the steam phase concentrates the brine by ~ 25%, while evolved CO_2 gas elevates the brine pH to ~ 5.5. All of these factors contribute to the production of a supersaturated brine in metal sulfides, carbonates, and amorphous silica. The solids that precipitate have reduced considerably the injectivity of the well. Extensive rework of the well has been required. (Nugent & Vick, 1977; SDG&E bimonthly reports, 1977).

Effluent Solids Characterization

The actual concentration and chemical composition of the particulates depend on the method of steam condensate disposal for a given brine (Table 1). In previous measurements suspended solids concentrations in brine effluents in combination with high pH condensate were found to be as high as 480 ppm (Quong, Bishop, and Hill, 1977). Prior to recombination, if the pH of the steam condensate is lowered to pH 5 from pH 6.7 in the first stage and as high as pH 9-10 in the 4th stage, the production of suspended solids can be significantly reduced (Table 1). However, brine effluents without condensate is now the preferred mode of operation. This best simulates large scale operation in which cooling water makeup becomes a critical requirement. Steam condensate would be the principal source of cooling water makeup. The main constituent in the brine effluent without condensate recombination is amorphous silica. Initially, silica concentration in Magmamax #1 brine is ~ 500 ppm. This drops to ~ 300 ppm after the flash process and transit time to the injection wellhead. Brine effluent collected at the injection wellhead and held at 90°C will continue to precipitate silica, reaching an equilibrium concentration of roughly 200 ppm in 2-3 hours. The necessary steps for effluent treatment become

TABLE 1

Chemical Composition, Concentration, & Mineralogy of Suspended Solids in Brine Effluent - GLEF Operation with Magmamax #1 Brine

Element[a]	w/o Condensate Combination (Conc., %)	With pH 5 Condensate Combination (Conc., %)
Si	40.5	14
S	0.2	5.7
Pb	0.14	40.0
K	0.2	0.7
Ca	0.65	1.9
Mn	0.06	-
Fe	4.0	4.6
Cu	0.15	3.3
Zn	0.15	-
Particulate Conc. ppm	178	25
Mineralogy[b]	amorphous silica	amorphous silica, galena

(a) by x-ray fluorescence analysis, R.W. Ryon (LLL)
(b) by x-ray diffraction analysis, M.A. Chan (LLL)

reasonably clear - namely separate and remove the particulates and produce a fluid that is not supersaturated in any species which would precipitate in the formation and impair injection longevity.

Coagulants and Coagulant Aids

An integral part of a process for removal of colloidal solids is the use of chemical coagulants. The role of these additives is to: 1) destabilize the colloids through neutralization of surface charge to allow particle agglomeration. 2) adsorb and attach onto colloidal particles. This bridging action is an important factor in particle destabilization and aggregation.

The most commonly used coagulants are inorganic: $FeCl_3$, $Fe_2(SO_4)_3$, MgO, and $Al_2(SO_4)_3$. Organic polymers or polyelectrolytes are also used with greater frequency and success. In general these compounds have been used or developed primarily for removal of turbidity and colloidal solids from ambient temperature, low salinity waters that are commonly encountered in municipal water and sewage systems. Their effectiveness in the higher temperature, high salinity Niland brines is virtually unknown.

As a result, commercially available inorganic and organic coagulants were tested individually and in combination at different concentrations, pH, and temperatures in GLEF effluent. Time was also a factor since silica precipitates continuously. Testing was conducted with conventional jar testing apparatus.

The data acquired to date can be summarized as follows:

- o In normal brine effluents (pH ~ 5.5, temp. 85°C) with or without chemical additives, agitation significantly aids coagulation and flocculation of effluent solids.
- o Temperature in the range of 40°C to 85°C does not benefit or impair the effectiveness of an additive.
- o At pH 5.5 without aging, supernatants remain supersaturated, and cloud with silica post precipitation. Coagulants have little effect on increasing the precipitation rate of dissolved silica.
- o Silica concentration declines rapidly to saturation levels by raising the brine pH to 5.9 (Table 2). Floc particles settle well, but supernatant clouds with hydroxide, $Fe(OH)_3$, post precipitation.

TABLE 2

Effect of NaOH Addition on Silica Concentration in Brine Effluent from the GLEF

NaOH added ppm	pH	SiO_2 concentration, ppm in supernatant @ 30 minutes
0	5.5	236
25	5.9	199
75	6.0	185
125	6.2	162

- o Silica concentration in brine effluents is rapidly reduced to below saturation by mixing with 1-2 weight % native sludge solids (Figure 1).

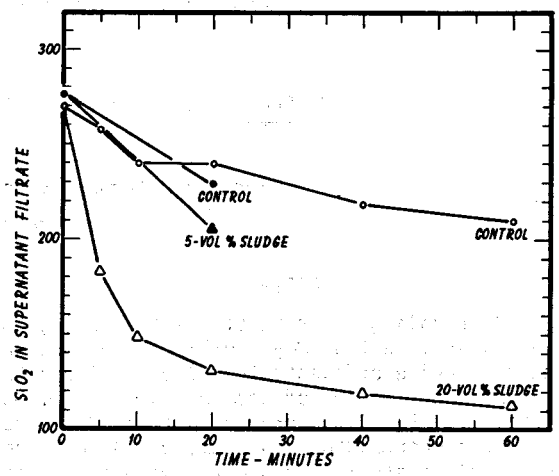


Figure 1. The effect of solids (sludge) contact with brine effluent on the precipitation rate of silica.

- o Inorganic coagulants are slightly beneficial. $Fe_2(SO_4)_3$ at ~ 100 ppm is the most effective of the inorganic additives. Significant improvement is achieved in sedimentation rate and supernatant clarity with combined sludge contact.
- o Cationic polymers are somewhat beneficial. Again effectiveness is significantly improved in combination with sludge contact. A range of 5-10 ppm of the polymer is necessary.
- o Anionic polymers (coagulant aids) in combination with sludge contact are highly effective flocculents. Flocs settle rapidly and supernatant clarity as low as 3 NTU's have been achieved. About 5 ppm is required at the start. Dosage should decrease with sludge recycle in a continuous process.

Pilot-Sized Clarifier

Brine effluent solids removal tests were conducted with an upflow, sludge blanket type clarifier (a settling tank modification shown in Figure 2). A rapid mix tank precedes the clarifier. At a test flow rate of 10 gal/min. residence time in the rapid mix tank is 5 minutes and in the clarifier 100 minutes. Upflow velocity in the quiescent zone is 0.38 gpm/ft^2.

The best clarifier performance to date produced overflow consisting of 44 ppm (15 NTU) residual solids with silica reduced to saturation. These data show that clarification alone is capable of removing at least 80% of the injectable solids contained in the effluent brine. The operating conditions of the test unit which produced this level of performance were 1) intimate contact of brine effluent (10 gpm) and sludge (1 gpm) in the rapid mix tank to precipitate supersaturated silica. 2) use of an anionic coagulant aid, M-580 (a hydrolyzed polyacrylamide,

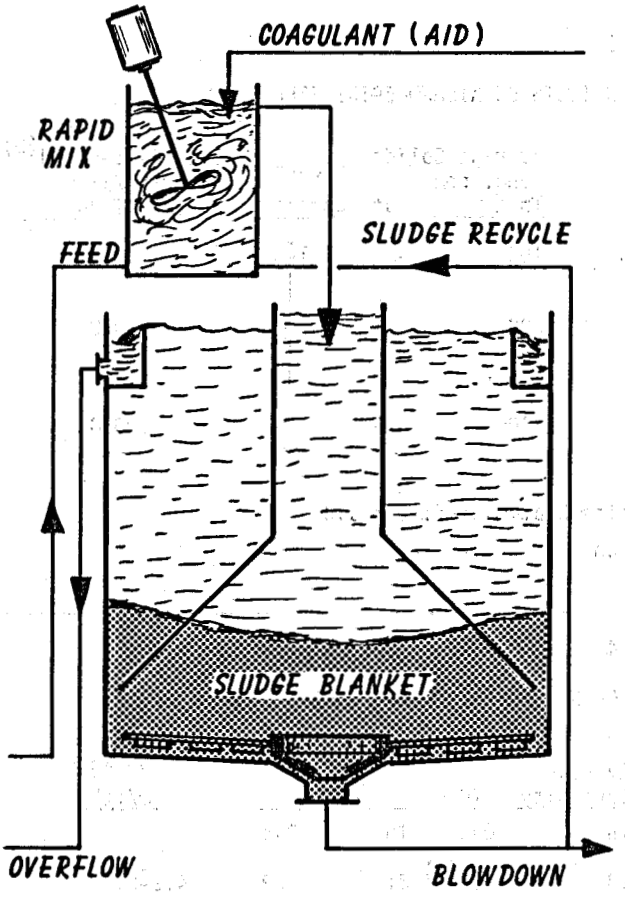


Figure 2. Schematic of Pilot Scale Clarifier Tested for Removal of Suspended Solids from Niland Brine Effluents

Calgon Corp.) at 3 ppm, added to the rapid mix tank. 3) a fully developed sludge blanket, ~ 24" thick and 6-10% by weight solids. and 4) a quiescent zone, with upflow rates of roughly 0.4 gpm/ft^2 for settling of residual flocs.

Precoat Pressure Filtration

A pilot sized precoat pressure filter consisting of wire wound elements precoated with commercial diatomaceous earth filter aid was tested as a means of final brine effluent clarification before injection. The tests on the 11 ft^2 unit were conducted at a flow rate of 0.9 gpm/ft^2 using brine from the clarifier. Two grades of filter aid were tested - a medium grade, with and without body feed; and a coarse grade without body feed. The tests were stopped when the pressure drop across the filter rose to 30 psi, the manufacturer's operating specifications. At constant flow rate, the length of the filtering cycle depends primarily on the solids content of the brine, which varied by as much as a factor of 3 in these tests. At all test conditions, the pressure filter was capable of producing filtrate containing less than 5 ppm (2 NTU) suspended solids > 1μm. Use of body feed did not significantly increase the filtering cycle time. The coarse filter aid was as efficient as the medium grade and in addition removed 41% more solids per unit weight of filter aid used.

Summary test results and comparative filter aid costs are given in Table 3. Mechanical operation of the pressure filter was straight forward. Backwash time was approximately 3-minutes for complete removal of the filter cake. The cake falls off in coherent pieces. Renewal of the filtering elements with precoat takes about the same amount of time -- 3 minutes.

Mixed Media Sand Filtration

A mixed media sand filter was also tested for effectiveness as the final clarification or polishing step for brine effluent. The media consisted of 18" of anthracite coal, 9" of silica sand, 3" of garnet sand, and 3" of garnet support, packed in a 20" diameter bed. We conducted the tests at 4.2 gpm/ft^2 using brine overflow from the clarifier. In all three test cycles on the same bed, average turbidities of the outflow brine were running 0.5-0.6 NTU (see Table 4), well within the limits of injectability. A core flooding test with Kayenta sandstone and output from the sand filter produced negligible decline in core permeability after passage of 2000 pore volumes (Tewhey, Chan, and Owen 1978).

In summary the tests demonstrate the technical feasibility of mixed media sand filters for polishing clarified brine effluents to well below acceptable solids levels for injection. The beds are relatively easy to operate, and are efficient. Projecting the filter size for 550 gpm of effluent, equivalent to one well flow, about 135 ft^2 (13' dia.) of bed area would be required.

Cost Estimate

A preliminary cost estimate for a brine effluent treatment and solids removal system based on the above process - i.e., clarifiers and sand filters gives total costs of 20¢/1000 gallons (Richardson, 1978) based on a 50MW facility producing 10 Mgd effluent. Assuming 100 lbs of Niland brine produces 1 kWh, then effluent plant costs are 1.7 mils/kWh. The costs vary by a few tenths of a mil depending on extent of chemical additive usage, operating pressures of the filters, and ultimate sludge moisture content.

TABLE 3

RESULTS OF PRECOAT PRESSURE FILTRATION TESTS ON NILAND BRINE EFFLUENTS

Test No.	Conditions[a]	Cycle Time to 30 psi ΔP Hrs.	Average Solids Conc. ppm In	Out	Flowrate gpm/ft^2	Cost Filter Aid[b] Mils/kWh/ppm Brine Solids
1	Precoat: JM Hyflo Super-Cel (medium grade)	4.0	108	< 5	1.1±0.2	.0054
2	Precoat: JM Hyflo Super-Cel Bodyfeed: 150 ppm	2.0	292	1	↓	.0078
3	Precoat: JM 545	2.2	340	< 5	↓	.0038

[a] Precoat layer: 0.2 lbs/ft^2 JM: Johns-Manville Celite Diatomite filter aid

[b] Filter aid cost: $7/100 lbs 100# brine ⟶ 1 kWh

TABLE 4

MIXED MEDIA SAND[a] FILTRATION OF NILAND BRINE EFFLUENTS

Cycle[b]	Cycle Duration hrs	ΔP Across Bed psi Initial	Final	Average Turbidity, NTU In	Out	Average Temp °C In	Out	Flow Rate gpm/ft^2
1	8.5	0.3	1.6	28	0.6[c]	81	79	4.2±0.4
2	23.0	0.3	46.6	33	0.5	81	79	↓
3	14.5	1.0	16.6	28	0.5	77	75	↓

[a] Mixed media: 18" anthracite coal
9" silica sand
3" garnet sand
3" garnet support

[b] Filter was backwashed with filtrate after each cycle

[c] 1 NTU ≅ 2-3 ppm suspended solids

Acknowledgement

The authors thank J.E. Harrar, S.B. Deutscher, C.H. Otto, and C.O. Pruneda for field analytical support, and F.E. Locke, and N.L. Rector for field engineering support.

References

Nugent, J.M. & L.R. Vick, Well Operations - Salton Sea Geothermal Field. Geothermal Resources Council Transactions 1, (1977), 233-234.

Quong, R., H.K. Bishop, J.H. Hill, Scale and Solids Deposition in the SDG&E/USERDA Geothermal Loop Experimental Facility at Niland Ca., Geothermal Resources Council Transactions 1, (1977), 249-250.

Richardson, G.H., National Technical Services, Inc., Consultant to Lawrence Livermore Laboratory, 1978.

San Diego Gas & Electric, Geothermal Loop Experimental Facility, Bimonthly Reports 1977, ERDA Contract No. E(04-3)-1137.

Tewhey, J.D., M.A. Chan, and L.B. Owen, Development of Injection Criteria for Geothermal Resources, to be published in Geothermal Resources Council Transactions 2, (1978).

"Work performed under the auspices of the U.S. Department of Energy by the Lawrence Livermore Laboratory under contract number W-7405-ENG-48."

HAND COMPUTER PROGRAM FOR JAMES' LIP PRESSURE STEAM FLOW RATE

HENRY J. RAMEY, JR.

PETROLEUM ENGINEERING DEPT., STANFORD UNIVERSITY, STANFORD, CA 94305

Programmable hand computers are rapidly becoming the engineer's slide rule of the future. Read-write recording programmable hand computers offer a capability not available through computer terminals. These hand computers will have a massive impact on engineering. There is currently a resistance on the part of both technologists and management to accept the role of the hand computer. Programming hand computers elevates the level of logic and computing ability of technologists. Problems will be solved without error that were previously avoided. Management hesitance to invest in hand computers because of obsolescence or duplication of large computer facilities should be reconsidered. One way to meet the current engineer shortage is by upgrading the capabilities of existing staff. The hand computer is one means to this end. The purpose of this report is to present a useful program which may be reprogrammed on other hand computers, the James' Lip pressure method for finding steam mixture flow rates.

An important geothermal fluid production problem is measuring the flow rates from wells in liquid-dominated steam reservoirs[1]. One such method is the James' Lip Pressure method[1]. In this method, a steam-liquid mixture is passed from a well head through a horizontal pipe of constant diameter, d inches, and exhausted to a muffler. The "lip" pressure is measured through a 1/4" hole drilled 1/4 inch from the end of the pipe. The liquid collected from the muffler is measured in a weir. The liquid height in H inches is recorded. From this information, it is desired to compute the following: (1) the liquid rate, W_L, kilo lbs/hr, (2) the total mass rate, W_t, kilo lbs/hr, (3) the mixture enthalpy, BTU/lb, and (4) the steam quality, mass fraction vapor.

A hand computer program capable of making the necessary computations is presented in Tables 1-3. This program is written in reverse polish logic for the HP-67/97 hand computers. The program description including equations is given in Table 1. The equations are sufficient for the program to be rewritten for other hand computers. The program runs in about 5 seconds, and is a useful aid for making flow rate calculations for liquid-dominated steam wells. The mixture enthalpy equation is a curve fit of graphical data presented by James. The User Instructions are presented in Table 2. The program commands are presented in Table 3.

Example Calculation

Given H = 3.5 inches
p = 5 psig
d = 6 inches

Answers W_L = 24.09 K lbs/hr
W_t = 81.70 K lbs/hr
h = 865.18 Btu/lb
x = 0.71 weight fraction
d^2p = 629.49 in^2-psia

Reference

James, R.: "Steam-Water Critical Flow Through Pipes," Proc. Inst. Mech. Engrs. (1962), 176, No. 26, p. 741.

TABLE 1. Program Description

Program Title GEOTHERMAL STEAM RATE BY JAMES' LIP PRESSURE
Name HENRY J. RAMEY JR. Date 11-10-76
Address PETROLEUM ENGINEERING DEPT., STANFORD UNIV.
City STANFORD State CA Zip Code 94305

Program Description, Equations, Variables, etc. PROGRAM CALCULATES: (1) WEIR LIQUID RATE, (2) STEAM-LIQUID MIXTURE ENTHALPY, (3) TOTAL MASS RATE, & (4) STEAM QUALITY BY RUSSELL JAMES LIP PRESSURE METHOD. EQUATIONS ARE:

WEIR LIQUID RATE: $W_L = 1.051(H)^{2.5}$

MIXTURE ENTHALPY: $y = (c-y) + b(\ln h) + a(\ln h)^2$

$$y = \left(\frac{8}{d}\right)^2 \left(\frac{W_L}{p^{0.96}}\right)$$

WHERE: $y \leq 4.78$: $c-y = 290.46$; $b = -75.157$; $a = 4.8158$; $700 < h \leq 1100$
$y > 4.78$: $c-y = 627.24$; $b = -178.76$; $a = 12.787$; $250 < h < 700$

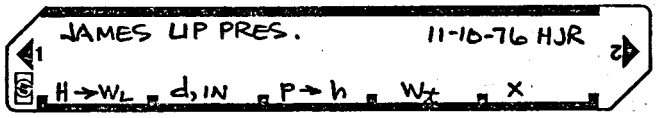
LIP PRESSURE: $W_t = 223.84 \dfrac{d^2 p^{.96}}{h^{1.102}}$

SYMBOLS: W_L = WEIR LIQ. RATE, K LBS/HR; h = MIXTURE ENTHALPY, BTU/LB
W_t = STM.+LIQ. RATE, K LBS/HR
p = LIP PRES., PSIA; x = STEAM QUALITY, MASS FRACTION
d = PIPE I.D., INCHES; H = LIQ. HT. IN WEIR, IN.

REFERENCE:
JAMES, R.: STEAM-WATER CRITICAL FLOW THROUGH PIPES, PROC. INST. MECH. ENGRS, VOL. 176, NO. 26, P. 741, 1962.

Operating Limits and Warnings ERROR IN ENTHALPY CALC. IS ± 2% AT MOST; FOR $h \leq 700$, ± 0.6%. RUN TIME ON HP-67 IS 5 SEC. NOTE: IF BAROMETRIC PRESSURE IS OTHER THAN 14.7, CORRECT PRESSURE SHOULD REPLACE 14.7 ON STEPS 021 TO 024.

TABLE 2. User Instructions



STEP	INSTRUCTIONS	INPUT DATA/UNITS	KEYS	OUTPUT DATA/UNITS
1.	ENTER PROGRAM			
2.	TO SEE MIXTURE ENTHALPY			
	ENTER LIQUID HEIGHT IN WEIR, IN.	H, IN.	A	W_L, KLB/HR
3.	ENTER PIPE DIAMETER, IN.	d, IN.	B	d^2, IN.^{2}
4.	ENTER LIP PRES., PSIG	P, IN.	C	h, btu/lb
5.	PRESS D TO SEE TOT. MASS RATE, W_t		D	W_t, KLB/HR
6.	PRESS E TO SEE STEAM QUALITY		E	x, MASS FR.
7.	ENTER NEW LIP PRES., GO TO 4			

Table 3 Russell James Lip Pressure Computer Program for HP 67/97

STEP	KEY ENTRY	KEY CODE	COMMENTS
001	*LBL A		
	ENT^		
003	2		
004	.		
005	5		
006	YX		
007	1		
008			
009	-		
010	0		
011	5		
012	1		
013	x		
014	STO1		
015	RTN		
016	*LBL B		
017	X2		
018	STO2		
019	RTN		
020	*LBL C		
021	ENT1		
022	1		
023	4		
024	.		
025	7		
026	+		
027	.		
028	5		
029	6		
030	YX		
031	RCL2		
032	x		
033	STO3		
034	RCL1		
035	+		
036	6		
037	4		
038	+		
039	1/X		
040	4		
041	.		
042	7		
043	6		
044	KEY?		
045	GTO1		
046	R↓		
047	CHS		
048	2		
049	5		
050	e		
051	.		
052	4		
053	8		
054	*		
055	STO6		
056	7		
057	5		

STEP	KEY ENTRY	KEY CODE	COMMENTS
057	.		
058	1		
059	5		
060	7		
061	CHS		
062	STO7		
063	4		
064	.		
065	8		
066	1		
067	6		
068	STO8		
069	*LBL 2		
070	RCL6		
071	x		
072	4		
073	x		
074	CHS		
075	RCL7		
076	X2		
077	+		
078	√x		
079	CHS		
080	RCL7		
081	-		
082	2		
083	÷		
084	RCL8		
085	÷		
086	e^		
087	STO9		
088	RTN		
089	*LBL 1		
090	R↓		
091	CHS		
092	6		
093	2		
094	7		
095	.		
096	2		
097	4		
098	+		
099	STO5		
100	1		
101	7		
102	8		
103	.		
104	7		
105	6		
106	CHS		
107	STO7		
108	1		
109	2		
110	.		
111	7		
112	x		
113	-		
114	1		
115	STO8		
116	STO2		
117	*LBL D		
118	1		
119	.		
120	1		
121	8		
122	2		
123	YX		
124	RCL3		
125	+		
126	1/X		
127	2		
128	2		
129	3		
130	.		
131	6		
132	4		
133	x		
134	STO0		
135	RTN		
136	*LBL E		
137	1		
138	ENT1		
139	RCL1		
140	RCL6		
141	+		
142	-		
143	RTN		
	R/S		

REGISTERS

0	1	2	3	4	5	6	7	8	9
W_t	W_L	d^2	$d^2p^{0.96}$	y		c	b	a	h
S0	S1	S2	S3	S4	S5	S6	S7	S8	S9

A $H \rightarrow W_L$ | B Enter d, in. | C $p \rightarrow h$ | D W_t | E x, fr. | I

THE SINGLE-HOLE CONCEPT OF HEAT EXTRACTION FROM HOT DRY ROCK MASSES

Joe L. Ratigan*
Ulf E. Lindblom**

*RE/SPEC Inc., Rapid City, SD
**Hagconsult ab, Götehorg, SWEDEN

INTRODUCTION

The warm water aquifer or steam geothermal capacity of the geological formations in Sweden is relatively low in comparison to many regions of North America. Regions with warm water aquifers are limited to southern Sweden and the Baltic Islands. For this reason, research investigations in Sweden have been recently concentrated on exploitation of geothermal energy by means of pumping water through a single drillhole drilled to a depth of approximately 3 to 4 km in the hot, dry rock regions of the Fennoscandian Shield. In the southern regions of Sweden, young sedimentary rock masses with relatively low thermal conductivity of thicknesses of approximately 2 km overlay the heat producing crystalline granitic rock masses. In this regard, the sedimentary formations act somewhat as insulators allowing the younger granites with high radioactive decay heat generation rates to reach high in situ temperatures.

The geothermal energy future of Sweden depends heavily on dry, hot rock extraction technology. The single drillhole concept for extracting geothermal energy possesses several advantages as a method of energy production, one of which is economical. The investigation of the concept is relatively inexpensive due to the low drilling costs for a single hole. Preliminary calculations have indicated that a single geothermal drillhole located in the Skåne or Gotland regions could potentially provide a productivity of several hundred kcal/s. The cost of this type of geothermal well, excluding surface equipment, is expected to be approximately $400,000 to $800,000.

The feasibility of the single drillhole concept of geothermal energy extraction can be examined in two manners, viz: (a) the full scale concept can be constructed in the regions of expected high productivity or (b) numerical modeling techniques can be developed and validated for modeling the concept, examining feasibility, and optimizing the engineering design aspects of the system. The purpose of this paper is to describe the modeling efforts which have been undertaken to analyze the single drillhole concept and future plans for validation of the numerical techniques.

HEAT EXTRACTION CONCEPT

The single drillhole concept (SDC) of geothermal heat extraction is graphically illustrated in Figure 1. This proposed concept is particular to the Skåne region of Sweden. As illustrated in the figure, a 44.4 cm hole is first drilled to the Precambrian granite, after which a 34.4 cm casing is cemented to the sedimentary rock surface. The "heat exchanger" portion of the drillhole is then created by drilling a 31 cm hole through the Precambrian granite to a depth of approximately 3.5 km. Water, nominally at a temperature of 20°C, is pumped through the outer annulus between the exit pipe and the cemented casing. After the water has experienced its heating cycle, it is returned to the earth's surface via a 8.8 cm insulated pipe. The thermal energy carried in the return water is subsequently extracted by means of a surface heat exchanger.

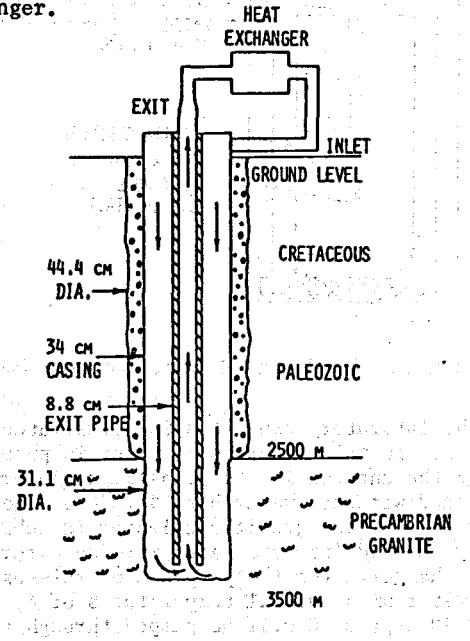


Figure 1. Single-Hole Heat Extraction Concept.

This concept of heat extraction from hot dry rock masses varies significantly from some of those under investigation in the United States (1)* in that the heat exchanger surface is a drillhole periphery rather than a thermally induced fracture.

*Numbers in parentheses refer to references at end of text.

The major difference between these two methods relates to the heat transfer surface area available for energy extraction. Obviously, the extraction concept utilizing the fracture can result in a significantly greater rock surface available to the water. However, the fracture method can be expected to have a shorter period of productivity. Intermediate to these two methods of heat extraction is the dual drillhole concept presently being exploited in France (2). In this system, two diverging holes are drilled from the surface to a water-producing sedimentary formation. One of the drillholes acts as the water inlet; the other, the water exit. The productivity of the dual drillhole concept to date has been greater than 600 kcal/s, which is sufficient to heat approximately 500 flats. This concept will also be analyzed in Sweden for the limited regions of applicability.

In an effort to analyze the SDC of geothermal extraction, a laboratory model is being constructed at Chalmers University of Technology, Geotechnical Division, Göteborg, Sweden. The experiment will be utilized to examine the feasibility of the concept of heat extraction and also to provide a situation for evaluating the capability of the finite element computer code discussed later.

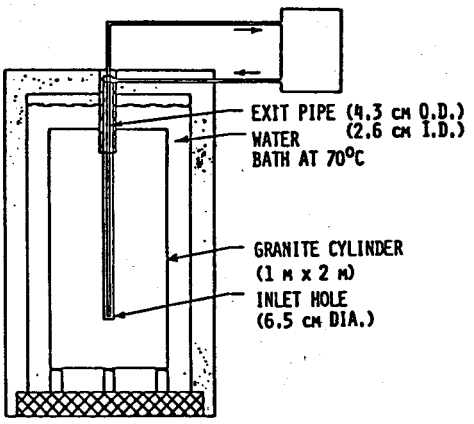


Figure 2. Geothermal Laboratory Experiment.

The laboratory apparatus is illustrated in Figure 2. In this experiment, water is pumped through the annulus in the granitic cylinder (contained within a water bath @ 70°C). The heat extracted from the granitic cylinder is subsequently removed from the water with an external heat exchanger. For the purposes of this experiment, water with initial temperatures of 6, 20, 30 and 40 degrees C will be pumped through the block at various flow rates. A double walled vacuum return pipe will be used for the water exit in order to minimize heat conduction losses from the exit water to the inlet water.

MODELING OF LABORATORY TEST

The field equations describing the heat transfer in the SDC are formulated under the following assumptions, viz:

- groundwater flow within the rock masses is negligible
- rock and water properties are temperature and direction independent
- flow within the drillhole is fully turbulent
- conductive heat loss from the exit water to the inlet water is negligible
- thermally induced flow is negligible

Estimates of the conductive heat loss through the exit pipe can be obtained by examining the magnitude of the Peclet number (ratio of convective to conductive heat transfer). As will be demonstrated later, the Peclet numbers arising in the analysis are sufficiently high to neglect the heat loss through the exit pipe. The resultant field equations subject to the above assumptions are:

ROCK

$$k_r \nabla^2 T_r + Q = \rho_r c_r \frac{\partial T_r}{\partial t} \qquad [1]$$

WATER

$$k_w \nabla^2 T_w + \rho_w c_w V_z \frac{\partial T_w}{\partial z} = \rho_w c_w \frac{\partial T_w}{\partial t} \qquad [2]$$

where T = temperature

t = time

Q = volumetric heat generation due to radioactive decay

ρ = density

c = heat capacity

k = thermal conductivity

and the subscripts w and r indicate water and rock, respectively. The coordinate system, boundary conditions and identification of regions of the model utilized in analyzing the laboratory experiment are illustrated in Figure 3. In modeling the laboratory experiment, the transient terms in Equations [1] and [2] are neglected. The inlet water temperature is fixed and conductive heat loss at the water exit location is neglected (3). The top and outside of the granite cylinder are subjected to a convective boundary condition given by Newton's Law of Cooling, while the lower surface of the cylinder is taken to be insulated. The value of the Peclet number referred to later is calculated as

$$\frac{\rho_w c_w V_z \ell}{k_w}$$

where ℓ = width of inlet annulus

The inlet, outlet and water bath temperatures will be referred to as T_I, T_O, and T_B, respectively.

In order to solve the field equations, a finite element code (SPECTROM-45) was developed. The code is similar to the finite difference program developed by Sorey (4).

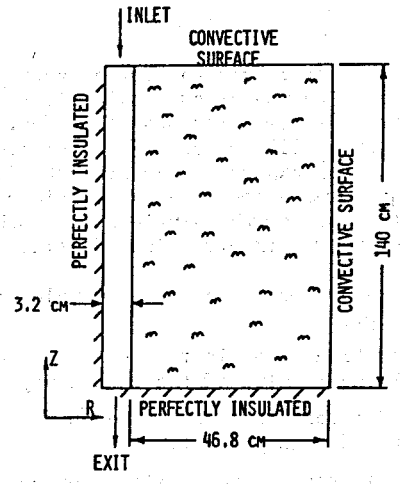


Figure 3. Model for Numerical Analysis of SDC.

The rock and water properties utilized in the modeling are shown in Table 1 and can be considered nominal values from the literature (cf. Reference (5)). The model was examined with two values of film coefficient (h) between the granite cylinder and the water bath, 5 and 500 $w/m^2-{}^oK$. The exit water temperatures for the aforementioned inlet water temperatures and various inlet annulus water velocities are presented in Table 2 for the case where $h = 500\ w/m^2 - {}^oK$. As expected, as the the water velocity increases, the water temperature rise decreases. However, the total energy extracted from the granite cylinder per unit area of the annulus ($\rho_w c_w V_z (T_0 - T_I)$) increases as the velocity increases. Obviously, if greater velocities were examined the energy extraction would eventually decrease with increasing velocity, since as the velocity approaches infinity, the temperature rise must approach zero. In other words:

$$\lim_{V\to\infty}\left[K_w\nabla^2 T_w + \rho_w c_w V_z \frac{\partial T_w}{\partial z} = 0\right] = \frac{\partial T_w}{\partial z} = 0$$

which implies

$$T_w(z) = \text{constant}$$

TABLE 1

LABORATORY MODEL THERMAL PROPERTIES

PROPERTY	WATER	GRANITE
K(W/M-^{o}K)	0.7	3.5
C(W-HR./KG-^{o}K)	1.2	0.2
(KG/M^3)	1000	2700

TABLE 2

LABORATORY MODEL EXIT WATER TEMPERATURES (^oC)

INLET WATER TEMPERATURE (^oC)	INLET FLOW RATE (CM/MIN.)			
	.25	2.5	25	250
6	70	61.3	20.1	8.1
20	70	63.2	31.1	21.6
30	70	64.9	38.7	31.6
40	70	65.9	47.4	41.7

For each film coefficient, all of the exit temperature results (for each velocity and inlet temperature) were analyzed in terms of the ratio of the energy extracted to the maximum possible energy extraction. The results of this analysis are presented in Figure 4 in terms of energy ratio as a function of the Peclet number for both values of film coefficient. It is interesting to note that the energy extraction ratio is independent of inlet water temperature for the range of conditions examined. The magnitude of the Peclet numbers resulting in this analysis clearly justifies the assumption of negligible conductive heat loss through the exit pipe.

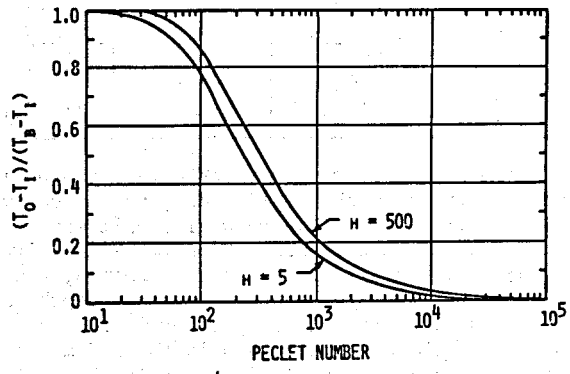


Figure 4. Energy Extraction from Laboratory Model.

During the summer of 1978, results of the laboratory test will become available. At that time, these results will be compared to the predictions of the finite element codes. Modifications to the code or finite element model will be made if discrepancies exist in the comparison.

MODELING OF THE SKÅNE CONCEPT

The proposed SDC of geothermal extraction for the Skåne region (see Figure 1) was also analyzed with the finite element code. The model employed was similar to that used for the modeling of the laboratory experiment (see Figure 3). The model has a radius of 1 km with a fixed temperature dictated by an assumed geothermal gradient. Three geothermal gradients were assumed in the analyses, viz:

Sediments - 20,40,60 ^{o}C/km

Granite - 30,60,90 ^{o}C/km.

The lowest values of geothermal gradient are representative of those reported in (6) and the higher values are utilized for comparison purposes. The lower boundary of the model was taken to be insulated and the upper boundary was given a convective boundary condition ($h = 5$ w/m^2 - ^{o}C). The inlet water was given a fixed temperature of 20°C and the conductive losses at the exit were assumed to be zero. The model encompassed a region from the earth's surface to a depth of 3.5 km and the heat generation in the granite was taken to be $4(10^{-5})$ w/m^3.

In this model, the transient terms of Equations *[1]* and *[2]* were not neglected. The transient term in Equation *[2]* is significant for a very short period of time (7) (less than a year), whereas the transient term in Equation *[1]* persists for a much greater time. The material properties utilized in this analyses are given in Table 3 and again, can be considered nominal from the literature.

TABLE 3

SKÅNE MODEL THERMAL PROPERTIES

PROPERTY	WATER	SEDIMENTS	GRANITE
K(W/M-^{o}K)	0.7	3.0	3.0
C(W-HR./KG-^{o}K)	1.2	0.2	0.2
ρ(KG/M^3)	1000	2400	2700
Q(W/M^3)	--	--	$4(10^{-5})$

Two inlet water flow rates were employed in the simulation of the field model, specifically 1.5 ℓ/s and 15 ℓ/s. The resulting exit water temperatures and well production rates are given in Table 4. In all of the cases examined, the increase of water temperature per unit depth was approximately 3 to 4 times greater in the granite portion of the drillhole than in the sedimentary portion. From this preliminary analysis, one could conclude that an extension of the drillhole in the granite could be advantageous. Similarly, a region with less sediments might provide greater well productivity. These situations will be examined later, once the finite-element code has been validated with the results of the laboratory experiment.

TABLE 4

HEAT EXTRACTION FROM SKÅNE MODEL

GEOTHERMAL GRADIENT* (^{o}C/KM)	EXIT TEMPERATURE (^{o}C)		EXTRACTION (kcal/s)	
	1.5 ℓ/s	15 ℓ/s	1.5 ℓ/s	15 ℓ/s
20/30	60	27	60	105
40/60	100	33	120	195
60/90	138	39	177	285

*Sediments/Granite

SUMMARY

The single drillhole concept of geothermal energy extraction possesses possibilities for utilization in several regions of Sweden. The relatively low drilling costs for a single hole in formations of expected high productivity have lead to the formulation of a systematic examination of the potential for the single hole geothermal well. The program involves four distinct steps:

- Laboratory modeling of the single drillhole concept.
- Validation of a finite element computer code with the results of the laboratory experiment.
- Field investigations in Sweden for sites of expected high productivity.
- Optimization of heat extraction and engineering design aspects of the concept utilizing the validated finite element code.

This program plan results in a relatively inexpensive method of establishing feasibility and well productivity. Several of the above steps have been completed to date. Work on the uncompleted steps will continue through 1978.

ACKNOWLEDGEMENT

The financial support provided by The National Swedish Board for Energy Source Development and RE/SPEC Inc. for certain portions of this work is gratefully acknowledged.

LIST OF REFERENCES

(1) J. Weertman, et. al., "Heat Extraction from Hot, Dry Rock Masses", Prepared for the National Science Foundation, Oct., 1976, NTIS No. PB-265116.

(2) La Geothermie En France, Bulletin Du B.R.G.M., Paris, 1975 (Second Series, Part 2).

(3) D. K. Gartling, "Some Comments on the Paper by Heinrich, Huyakorn, Zienkiewicz and Mitchell", Int. J. Num. Meth. Engrg. 12, 187-190 (1978).

(4) M. L. Sorey, "Numerical Modeling of Liquid Geothermal Systems", Ph.D. Dissertation, Univ. of Calif., Berkeley, 1975.

(5) H. Stille, A. Burgess and U. E. Lindblom, "Groundwater Movements Around a Repository, Phase 2, Technical Report 1, Geological and Geotechnical Conditions", Submitted to Kärnbränslesäkerhet, Stockholm, Sweden.

(6) U. E. Lindblom, "Geotermisk Energi", Stockholm, Sweden, (1975).

(7) H. D. Murphy and R. G. Lawton, "Downhole Measurements of Thermal Conductivity in Geothermal Reservoirs", Energy Technology Conference and Exhibition, Houston, Texas, Sept., 1977.

GEOLOGIC EXPLORATION METHODS FOR SITING POWER PLANTS AND OTHER STRUCTURES IN LANDSLIDE AND HYDROTHERMALLY ALTERED TERRAIN AT THE GEYSERS, CALIFORNIA

Albert P. Ridley
James V. Vantine

WOODWARD-CLYDE CONSULTANTS, SAN FRANCISCO, CALIFORNIA 94111
GEOTHERMAL DIVISION UNION OIL COMPANY OF CALIFORNIA, SANTA ROSA, CALIFORNIA

INTRODUCTION

The Geysers Geothermal Field is located in the Mayacmas Mountains about 25 miles north of Santa Rosa in Northern California (Figure 1). The bedrock in the region consists of mostly Jurassic and Cretaceous aged rock of the Franciscan assemblage. These include graywacke, greenstone, shale, chert and serpentinite that have undergone intense shearing and folding. Numerous Quaternary aged landslides blanket much of the steep terrain. Many areas are underlain by hydrothermally altered rock.

Assessment of foundation conditions should consider the presence of landslide deposits and hydrothermally altered rock in the steep terrain at The Geysers. Detailed geologic mapping of existing landslide deposits is important for siting of power plants, roads, steam wells, and other facilities. Geologic exploration methods should assess the suitability of the highly sheared rock for support of the planned developments and consider the unusual but potentially hazardous subsurface conditions brought about by heat including: hot groundwater, hot rock, argillic alteration and near surface steam.

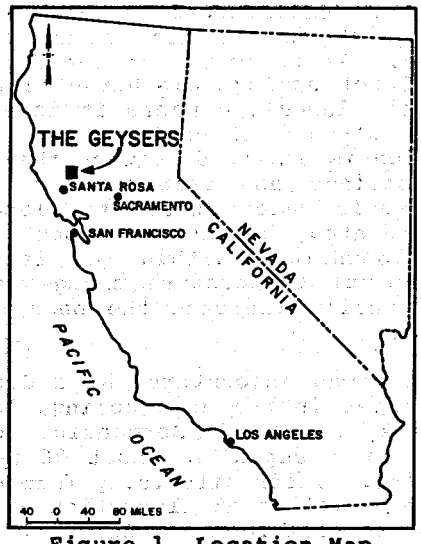


Figure 1 Location Map

AN EXAMPLE OF FOUNDATION EXPLORATION THE GEYSERS

METHODS OF STUDY

One of the more recent feasibility siting studies which utilized many of the modified exploration methods, which have been developed for use at The Geysers, was performed to evaluate potential candidate sites for a planned 5 megawatt power plant. The purpose was to utilize an unused resource of relatively low pressure steam. Review of published geologic maps showed the candidate sites to be within a large Quaternary aged landslide. In addition, hydrothermally altered and weak bedrock was present at the sites. The foundation exploration methods for this study required use of the usual methods such as: aerial photograph interpretation, detailed geologic mapping; with modification of methods such as: seismic refraction surveys, and shallow exploration drilling and trenching.

Aerial photograph interpretation was performed using stereo pairs of: black and white photographs at a scale of 1"=880'; color photographs at a scale of 1"=3000'. It indicated that the two candidate sites were located within a complex landslide (Figure 2). Bedrock contacts and vegetation differences, were clearly evident on the color and false color infrared photographs. Detailed geologic mapping using the 1"=880' black and white photographs and a 1"=100' topographic base map helped define the landslide limits.

Consideration of groundwater temperatures was useful in determining the landslide and bedrock conditions. Temperatures of springs were measured with a laboratory thermometer. The downhole temperature within the borings was measured with a potentiometer pyrometer with a range of -300°F to +400°F.

Six shallow seismic refraction traverses were performed across the mapped landslides to evaluate the subsurface landslide geometry. The survey was performed using a 12-channel refraction seismograph.

Explosive charges were used as energy sources in shallow holes (2 to 5 feet deep) at the ends of each line. Because of the warm ground the usual techniques had to be modified. The explosive charges were packed in ice to reduce the hazard of premature detonation due to high ground temperature. Areas of very hot ground and shallow steam were avoided entirely.

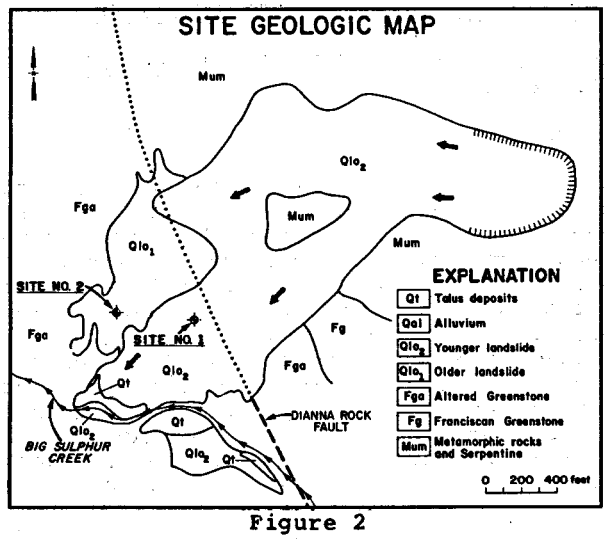


Figure 2

A number of exploration pits were excavated with a dozer-mounted backhoe to supplement the geologic mapping. The exploration pits were located in areas away from shallow steam vents. In hot moist ground often the pit could not be inspected until after a cooling off period. The geologic features exposed in the pits were logged at a scale of 1"=2'. Samples of materials were obtained from the pits for laboratory analysis.

A number of exploration borings were drilled using a CME 750 All-Terrain drill rig which was able to move about on the steep site because of its special balloon tires and 4-wheel drive design. Borings less than 45 feet in depth were drilled using an 8-inch diameter hollow-stem auger and conventional drive sampling methods. A deep boring, intended to penetrate the full depth of the landslide, was drilled using rotary wash-boring methods. In order to satisfy the requiresments of the California Division of Oil and Gas (CDOG), well casing was set in the deep rotary boring to reduce the potential for an uncontrollable steam blowout. Eight and one-half inch O.D. casing was cemented into place to a depth of 30 feet, 7 inch O.D. casing was set to 41 feet, and 5 1/2 inch O.D. casing was set to 72 feet. Return drilling fluid temperature was monitored continuously. A CDOG requirement was that the boring be sealed and abandoned if the temperature of the return drilling fluid exceeded 167°F. Upon completion, the deep rotary boring was backfilled and sealed with cement.

RESULTS OF STUDY

The aerial photographs indicated that the landslide materials are deeply eroded and dissected by stream tributaries. An unusual feature was a zone of hydrothermal alteration which was detected trending northeastward partially through and partially beneath the mapped landslide area. The limits of the landslide were determined by detailed field mapping.

A large area upslope was mapped to determine the bedrock units upslope and landslide debris source. A predominantly graywacke unit was mapped beneath the site area, an ultrabasic rock unit was mapped immediately upslope and a large greenstone unit was mapped farther upslope. At least two landslides of different age, aerial extent and rock debris composition were mapped. An older landslide composed of highly hydrothermally altered ultrabasic and serpentine debris lies northward (beneath site No. 2) and partially beneath a younger and larger landslide. The younger landslide is composed of relatively unaltered angular ultrabasic, serpentinite and greenstone debris (beneath site No. 1) as shown in Figure 2. Remnants of the younger landslide occur on the opposite side of Big Sulphur Creek and suggest that landslide debris once filled the creek channel to a depth of over 100 feet. Field mapping shows that about 40 feet of undisturbed stream terrace deposits rest on the toe of the younger landslide. As is common at The Geyers, a series of hot springs discharge along the base of the landslide where it is exposed in the stream channels. A close correlation is observed between the volume of the springs and rainfall, suggesting that meteoric water enters the landslide and is heated by hot bedrock as it migrates downslope within the landslide mass. Abrupt temperature changes within borings usually indicate the base of the landslide.

Groundwater was encountered at a depth of about 80 feet in the deep boring, located near site No. 1. Serpentine gravel extended to a depth of about 80 feet in that boring. Stiff silty clay formed as a result of hydrothermal alteration extended from 80 to 114 feet. Below 114 feet competent chert bedrock was encountered.

Return drilling fluid temperatures reached a maximum of 118°F at a depth of 117 feet in the deep boring. Borings near site No. 2 encountered a chaotic mixture of hydrothermally altered serpentine and ultrabasic rocks in a matrix of moist stiff clay extending to a depth of at least 45 feet.

In the vicinity of site No. 1 the seismic refraction survey showed a material with a P-wave velocity of 2280 to 3600 fps extended to an average depth of 80 feet, where it was underlain by material with a P-wave velocity of 6000 to 8300 fps. This is interpreted as the contact between the gravel and clay layers.

The slide plane between the older and younger landslide deposits was clearly exposed in one of the exploration pits. Samples of wood fragments from this slide plane were age dated by Carbon-14 methods in an effort to estimate the age of the younger landslide. The Carbon-14 age was determined to be less than 500 years, however, this is inconsistent with other data. The age is considered to be in error.

Geologic mapping and exploration pits showed that a 40 foot thick layer of undisturbed stream terrace deposits rest unconformably on the toe of the younger landslide. By comparison with dated stream terraces in the area, it is estimated that the stream terrace deposits are on the order of 800 to 5,000 years old. Comparison of geomorphic characteristics of the younger landslide with dated landslides in the area suggests that it is on the order of 13,000 years old.

Based upon the geologic studies it appears that the landslide materials beneath site No. 1 have not been active for approximately 800 to 5,000 years. In addition, there is no reported evidence of historical instability. Based upon the geologic studies and additional detailed soils engineering studies site No. 1 was selected as the most suitable candidate site for the proposed power plant.

CONCLUSIONS

Careful detailed geologic studies are needed in selection of sites within the hydrothermally altered bedrock and landslide terrain at The Geysers. Potential risks can be minimized by utilizing investigative techniques which are compatible with the hydrothermal environment which includes hot rock, hot water, and shallow steam. Care must be taken in interpretation of these investigative techniques in this unusual physical environment. Provided detailed geologic and geotechnical studies are performed which identify and assess the potential hazards, suitable sites for planned geothermal developments can be selected in the hydrothermally altered bedrock and landslide terrain at The Geysers.

ACKNOWLEDGEMENTS

The funding for the site studies were provided by the Pacific Gas and Electric Company and Magma Power Company. The authors gratefully acknowledge Pacific Gas and Electric Company, Magma Power Company, Union Geothermal Division of Union Oil Company of California, and Thermal Power Company, for their assistance and cooperation in preparation of this paper.

EXPERIMENTS FOR RAPID ASSESSMENT OF THE SCALING PROPERTIES OF GEOTHERMAL FLUIDS

J. D. Rimstidt and H. L. Barnes

Ore Deposits Research Section, 204 Deike Building
The Pennsylvania State University
University Park, Pennsylvania 16802

This research was supported by the U.S. Department of the Interior, Bureau of Mines, under contract #G1055140. Equipment field tests were performed at the Bureau of mines corrosion test facility at the Salton Sea Geothermal Field in the Imperial Valley, California.

Even though we are all aware that scaling is a major problem in many geothermal heat extraction systems, too often such systems are designed with only minimal regard for scale prevention. After construction, it is very costly to make major design changes which might alleviate the problem. However, there are some simple thermodynamic and kinetics principles that can be utilized in the basic design of these systems. In addition, it is useful to perform simple field tests on the geothermal fluid to determine its scaling characteristics under conditions similar to those expected in the heat extraction facility. We have designed two simple experimental methods which can be used at low cost to empirically test scaling behavior prior to the installation of expensive pilot or power plants. These experiments and related kinetic factors are considered here.

While in the reservoir, geothermal fluids contain dissolved minerals and gases in concentrations normally near equilibrium with the surrounding rocks. Because reservoirs have variable mineralogies, fluids produced even from different parts of a single reservoir may contain very different concentrations of solutes. When extracting heat from these geothermal fluids by cooling and/or flashing, supersaturation results. For examples, cooling alone may cause silica supersaturation or flashing may release CO_2, thus causing carbonate minerals to precipitate.

Where and when minerals precipitate after the heat extraction process depends upon both thermodynamic and kinetic parameters. While thermodynamic properties determine what could precipitate, kinetic factors determine where and when any precipitation takes place. The rate that any particular compound precipitates is determined by the degree of supersaturation, the temperature, and the $(\underline{A}/\underline{M})$ ratio of the system. The $(\underline{A}/\underline{M})$ ratio is the ratio of the relative surface area available for growth of the solid to the relative mass of water present in the system. In general, sulfides precipitate fastest, then carbonates and sulfates, and slowest are silica and silicates.

The quantitative effects of major kinetic variables have been evaluated for deposition of scale containing silica. Decreasing temperature causes a decrease in the precipitation rate as is illustrated by the dashed line for several degrees of supersaturation, S, in Figure 1. This

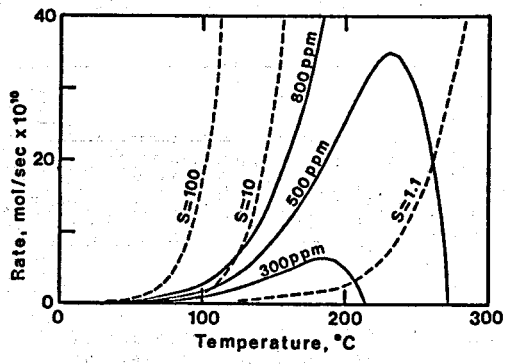


Figure 1. The rate of quartz precipitation as a function of temperature and degree of supersaturation (S) (shown by the dashed lines) and as a function of temperature and concentration (shown by the solid lines).

figure also shows that increasing the degree of supersaturation at a constant temperature causes an increase in the precipitation rate. Therefore, in a cooling solution, at a constant concentration of silica, these two effects compete. As the temperature decreases, the degree of supersaturation increases while the rate of precipitation at constant degree of supersaturation decreases. This means that the effective rate of precipitation passes through a maximum as shown for three representative silica concentrations by the solid lines in Figure 1. This leads to the important conclusion that if heat is removed quickly in order to pass through the thermal region of rapid precipitation in one step, then the silica can be quenched into solution because the precipitation

rate becomes negligible at lower temperatures.

The rate of precipitation is also directly proportional to the (A/M) ratio of the system. The surface areas of pipes, well casing, and walls of other components furnish substrates for growth of scale. Also solid particles, such as iron oxides, suspended in the solution often have relatively large, active surfaces which can grow, agglomerate, and eventually be incorporated into scales. This effect is especially important if the degree of supersaturation is great enough for the deposition of amorphous silica. Generally, the homogeneous nucleation rate of silica is affected by temperature, and degree of supersaturation in the same way as is the precipitation rate, although in heterogeneous systems epitaxial nucleation more often will dominate over homogeneous nucleation.

Where reactions in geothermal systems are very complex, as in typical multicomponent fluids, then the current state of understanding of hydrothermal chemistry may be inadequate to predict whether scaling may be important. For such situations, we have developed two types of simple experiments. In the first, a quenching experiment (Figure 2), we may observe which phases

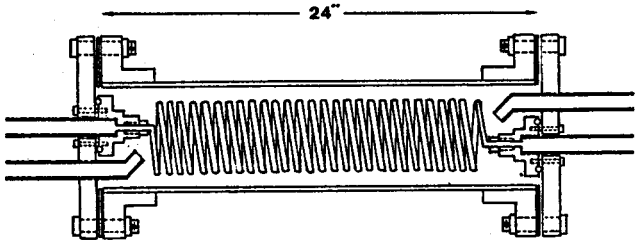


Figure 2. Schematic illustration of the quenching experiment. The geothermal fluid enters through the top left pipe, traverses the copper coil where it is cooled to the run temperature and exits through the pipe on the bottom right. The run temperature is controlled by mixing cool water with some of the geothermal water and circulating it through the heat jacket which surrounds the coil. The plumbing which controls the mixing and flow rates is now shown.

precipitate at various temperatures and whether it is possible to quench any of them into solution. It operates by quenching the fluid to various fixed temperatures by passing it through a copper coil immersed in water of a temperature fixed by mixing geothermal water with cool irrigation or domestic water. This method has been used on brines from Magmamax #1 (Salton Sea Geothermal Field, Imperial Valley, California). Shown in Figure 3 are the amounts of scale that

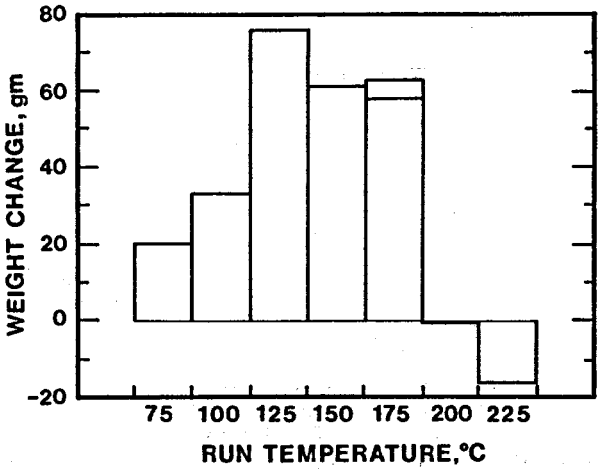


Figure 3. The amount of weight change of 25 foot sections of 1/4" copper tubing used in quenching experiments on Magmamax #1. Increases in weight represent the amount of scale deposited by flows of 1 gallon/min for 4 hours and decreses in weight were the result of dissolution of some of the copper. The experiment at 175° was run twice.

precipitated in segments of copper tube during tests at various temperatures. This scale was predominately aragonite and manganocalcite containing small crystals of galena, sphalerite, copper arsenides, and copper oxides.

The second type, a flashing experiment, causes the hot geothermal fluid to expand through an orifice and then traverse at constant temperature a length of copper tubing where scaling takes place (Figure 4). These experiments are

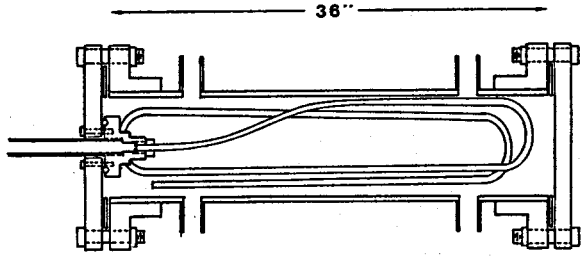


Figure 4. Schematic illustration of the flashing experiment. The geothermal fluid enters from the left, is expanded through an orifice mounted in the assembly on the left end-plate and then flows through a 10-foot length of 1/2" copper tubing which empties directly into the surrounding

heat jacket. The spent brine and steam leave the heat jacket through the ports at the top and bottom of the right end.

commonly run at constant flow rates of two gallons per minute. Both cooling and vapor loss occur, with the temperature and pressure drop being controlled by the orifice diameter. The amount of vapor released is determined by its accumulated volume in the upper part of the cylinder after the upper right port is closed. The vapor can be sampled at the top of the experiment to determine steam composition and the liquid can be sampled at a port in the bottom of the experiment to find its composition and the content of suspended solids. This method has also been tested on Magmamax #1 brines and resulted in small amounts of a hard, black scale being precipitated in the tube. Its texture and composition is quite different from that produced by the quenching experiments.

Effective use of these experiments to model scaling rates involves some further considerations. For example, because these methods involve only a small amount of fluid, a bypass line must be provided so the well can flow at a high enough rate to obtain a sample representative of fluids from production zones. These experiments can also be connected in series or in parallel to better duplicate a particular heat-extraction scheme. Because some precipitation reactions may be very slow relative to the flow rates in these experimental units, holding chambers can be inserted at appropriate places downstream in the system to retain the fluid at certain temperatures for appropriate lengths of time. Because the (A/M) ratio is an important parameter in the rate of precipitation and the pipe walls may furnish only a small area for deposition relative to the surface area of suspended solids, samples of suspended materials must be collected along the experimental flow path in order to determine their concentrations, compositions, surface areas and growth rates.

The scales from both experiments are treated similarly. The copper coil is removed after each run, dried and weighed. This weight, and the known flow rate, are used to calculate the amount of scale precipitated from each gallon of fluid under the conditions of the experiment. The coil is then cut into one foot sections which are weighed separately to determine the distribution of scale along the length of the tube. Scale samples are removed from representative sections and analysed. Bulk chemical analysis by emission spectroscopy gives a rough but quick indication of the composition. Scanning electron microscopy shows the crystal size and surface texture. The best method for identification of the crystalline phases present is x-ray diffraction but, if the scale contains x-ray-amorphous material, IR spectrophotometry can help identify it. These techniques are complemented by reflected light microscopy which can be used to identify sulfides and oxides which are at too low a concentration to be detected by x-ray diffraction. Reflected light microscopy also shows zoning and exsolution textures. Finally, the electron microprobe can be used to accurately determine the composition of individual phases.

The goal of this analytical scheme is to characterize the physical and chemical properties of the scales in order to identify the reactions involved and to be able to design fluid processing facilities that can ameliorate their effects. For example, if scaling cannot be prevented, then the choice of chemical or mechanical methods to clean the scale depends upon a knowledge of its mineralogy and texture. If a scale is predominately composed of particles that are cemented together by carbonate minerals, simple cleaning by dilute acids may remove it but, if the particles are cemented by iron oxides and silica, a more costly mechanical method may be necessary. Ideally, the information gained from the scale analysis should lead to methods which control the scale deposition process based on the specific chemical reactions which must be controlled. Furthermore, the textures and zoning patterns of the scales reflect the mechanism of the precipitation process. A small grain size implies a very high degree of supersaturation while cyclic zoning might indicate short term fluctuations between liquid and steam flow.

In conclusion, it is important to know the fluid chemistry and scaling properties of a geothermal fluid before trying to use it as a source of energy. Although some simple thermodynamic and kinetic principles offer a general guide to designing a useful heat extraction system, it is necessary for typical complex brines to evaluate the scaling properties of each fluid by observing it under conditions similar to those expected in the heat extraction process. From such data, we have been able to make progress toward understanding the scaling problem in the especially complex Salton Sea Geothermal Field. Clearly, a test program of this general type should be an initial step in the development of any geothermal area because it offers immediate information on the nature of the scaling problem so that rational decisions involving scale control can be made during the design of any geothermal system.

SALTON SEA GEOTHERMAL RESERVOIR SIMULATIONS*

T. D. Riney, J. W. Pritchett and S. K. Garg

Systems, Science and Software
P. O. Box 1620, La Jolla, California 92038

The Salton Sea Geothermal Field (SSGF) is a high salinity, high-temperature resource. The San Diego Gas & Electric Company has constructed a nominal 10 MWe Geothermal Loop Experimental Facility (GLEF) which will use brine produced from Magma Power Company's Woolsey No. 1 (W1) and Magmamax No. 1(M1) wells; the Magmamax No. 2 and No. 3 (M3) wells will be used for reinjection. Intermittant brine production/injection has been performed since May 1976, but no associated fluid flow data have been published. The Lawrence Livermore Laboratory (LLL), however, has correlated the data available from surface measurements and logs from various wells in the SSGF. We have used this limited data base and the MUSHRM simulator to synthesize a preproduction reservoir model for a portion of the SSGF which contains the GLEF site. The simulator is then applied to the model to examine reservoir performance under different assumptions to improve our understanding of the system and its potential for exploitation.

The main sequence reservoir rock in the SSGF is bedded sandstone with shale lenses and layers, overlain with a relatively impermeable shale bed (caprock), and is believed by the LLL investigators to be separated into "upper" and "lower" reservoirs by a relatively thick and continuous shale layer [Towse, 1975; Schroeder, 1976]. From studies of cores, cuttings and logs from wells drilled in the SSGF, Towse [1975] determined the approximate depths to the top of the upper reservoir and to the major shale break separating the upper and lower reservoirs. Since the geologic layers dip in a northwesterly direction essentially parallel to the Brawley Fault Zone, we selected the region covered by the finite difference mesh in Figure 1 for our study. A cross-section is constructed by projecting the data onto a vertical plane parallel to the surface trace of the Brawley Fault Zone (Figure 2). The interfaces between the geologic layers are taken to be planes dipping to the northwest which approximate the points depicted. The temperature-depth profiles measured in the geothermal wells [Palmer, 1975] have been projected to construct the approximate temperature contours shown in Figure 2. The GLEF production wells (W1, M1) are perforated almost entirely within the upper reservoir whereas the injection wells (M2, M3) are perforated mostly within the lower reservoir.

Whether or not the interfacial shale barrier prevents significant fluid exchange between two reservoirs will have a profound effect on their response to imposed production/injection conditions. In the absence of vertical permeability data, two limiting cases were analyzed.

1. Production from upper reservoir without injection, i.e., shale barrier prevents fluid injected into lower reservoir from entering upper reservoir.
2. Production and injection occur in upper reservoir, i.e., vertical fractures channel injected fluid into upper reservoir.

Schroeder [1976] analyzed the sparse data available from drillstem test records from M1 and W1 and concluded that the horizontal permeability of the reservoir sands in the upper reservoir shale/sand sequence exceeds 500 md. The sands comprise over 50 percent of the sequence and their porosity exceeds 0.3. For the upper reservoir sequence we assume the following properties: rock horizontal permeability = 500 md; grain density of rock = 2.65 g/cm^3; initial porosity of rock = 0.20; rock thermal conductivity = 2.1×10^5 ergs/sec-cm-°C; rock specific heat = 10^7 ergs/g-°C; brine salinity(s) = 0.25; irreducible liquid saturation = 0.3 and irreducible vapor saturation = 0.05. The latter two parameters define the relative permeabilities, in the case of two-phase flow, using the Corey formulation.

The 2D areal version of S^3's MUSHRM reservoir simulator is capable of treating the dipping and thickening upper reservoir if we consider the component of gravity along the direction of dip and vary the rock properties to offset variations in thickness. The Brawley and Red Hill faults are assumed to prevent any fluid flow across the side boundaries (Figure 1). The fluids produced by wells on opposite sides of the Brawley Fault appear to have a different origin, but there is no definite evidence that the Red Hill fault is a sealing fault.

Figure 2 shows that the temperature at the mid-plane of the upper reservoir is much less at the southeastern end (left, y = 0) than at the northwestern end (right, y = L). No pressure data are available. Using the S^3 brine equation-of-state (s = 0.25) and the temperature-depth profiles at the two ends, the corresponding mid-plane hydrostatic pressures are computed to be P(0) = 38.02 bars and P(L) = 85.07 bars. By considering the temperature variation and dip angle along the length of the reservoir (Figure 2), it is found that if there were no preproduction flow, the value of P(L) would need to be 88.24 bars. The lengthwise pressure

*Work performed under NSF Grant No. AER75-14492 A01.

drive, ΔP = 3.17 bars, apparently causes an influx of ~ 50°C groundwater from the southeast end (y=0) which would cool the upper reservoir if hot brine infusion from the lower reservoir were completely precluded by the shale barrier. A vertical permeability of 0.01 to 0.1 md would suffice for steady state convective transport across the shale barrier to swamp heat conduction, a value too small to affect reservoir response to exploitation.

These boundary conditions and reservoir properties were incorporated into MUSHRM and a series of calculations performed until a satisfactory match with the mid-plane preproduction temperatures in the upper reservoir was obtained. A 1D version was first applied to the dipping and thickening upper reservoir with the provision that for each zone there is infusion of 275°C brine (s = 0.25) at the rate required to obtain the corresponding projected mid-plane preproduction temperature. The total rates of 50°C groundwater (s = 0.25) influx and convective brine infusion are calculated to be $\dot{M}_0$ = 26.7 kg/sec and $\dot{M}_c$ = 294.8 kg/sec, respectively. These totals and the lengthwise variation of the influx rate were maintained, but the temperature of the brine and the lateral distribution of the influx rate were allowed to vary in a subsequent series of 2D areal calculations. A symmetric distribution with maximum at the center was found to best fit the lateral variation of the mid-plane temperatures measured in the wells. Having selected the lateral distribution influx rate, the calculation was then rerun with the with the temperature of the brine source reduced to 251°C in order to better match the mid-plane temperatures. The desired mid-plane temperatures for the well locations are satisfactorily matched by the steady-state temperature contours calculated with the preproduction model (Figure 3). The velocity plot, Figure 4, shows that the infusion of hot brine from the lower reservoir pushes a large part of the incoming cold groundwater to the edges of the upper reservoir, producing the lower temperatures there.

We make the conservative assumption that the infusion of hot brine from the lower reservoir remains at its preproduction value (M_c = 294.8 kg/sec) during exploitation of the upper reservoir. The hydrostatic pressure at the downstream end of the reservoir is maintained (P(L) = 85.07 bars); the production/injection rates are held constant during the course of a given calculation. When injection occurs, the injected brine is taken to be 50°C and to comprise 80 percent of the mass produced ($\dot{M}_I = 0.8\,\dot{M}_p$).

A production rate of $\dot{M}_p$ = 100 kg/sec is assumed appropriate for a net 10 MWe at the GLEF site. For convenience, this equivalence is used for higher rates, e.g., nominal 50 MWe means $\dot{M}_p$ = 500 kg/sec. Since the temperature of the produced brine declines with time, these nominal values of electrical power production become less meaningful.

A series of preliminary calculations using an approximate equation-of-state was performed to examine the sensitivity to the boundary condition assumed at the upstream (southeast) end of the reservoir. Above nominal 50 MWe (production only) to 250 MWe (with injection), the assumption of constant hydrostatic pressure requires increasing ground-water influx above the preproduction value. Constant ground-water flow ($\dot{M}_0$ = 26.7 kg/sec.) was selected as being a more realistic boundary condition since the available groundwater is limited primarily to leakage from irrigation canals supplied by the Colorado River.

Essentially steady-state pressure and velocity fields are soon established wherein the mass flow rate out of the downstream end of the reservoir ($\dot{M}_L$) plus the excess rate of production over injection must balance the mass rate of fluid entering the reservoir from the upstream groundwater and convection mass sources: $M_L + (M_p - M_I) = M_0 + M_c$ = 321.5 kg/sec. The following table gives the values of $\dot{M}_L$ for imposed production/injection rates of interest. For $\dot{M}_L < 0$, fluid is entering the downstream end of the upper reservoir and the time (t_r) required for this replacement fluid mass to equal the total preproduction fluid mass in the upper reservoir (3.05×10^{12} kg) is also given. Power production in excess of nominal 50 MWe (production only) to 250 MWe (with injection) requires a tremendous replinishment of hot brine from the downstream end.

Production Rates		Production Only ($\dot{M}_I$ = 0)		With Injection ($\dot{M}_I$ = 0.8 $\dot{M}_L$)	
Nominal MWe	$\dot{M}_p$ (kg/sec)	$\dot{M}_L$ (kg/sec)	t_r (yrs)	$\dot{M}_L$ (kg/sec)	t_r (yrs)
0	0	322	---	322	---
10	100	222	---	302	---
50	500	-179	542	222	---
250	2500	-2179	44	-179	542
325	3250	-2929	33	-329	295

Two nominal 50 MWe simulations treated the four-zone production/injection pattern shown in Figure 1. All production wells are located within the two computational zones containing W1 and M1, and all injection wells are in the zones containing M3 and M2. Figure 5 shows the time history of the bottomhole temperature of the brine produced from each of the two production zones. Results for both assumptions regarding the effectiveness of the shale barrier are presented. The proximity of the production zones to the injection zones causes a rapid decline of the temperature of the produced fluid when the injected fluid is assumed to enter the upper reservoir. Without injection, there is a reversal of the flow at the downstream boundary as anticipated by the table.

From the preproduction model it is apparent that the preferred production region of the upper reservoir is near its center; the injection zones should be either along the two edges of the reservoir or downstream to minimize potential cooling of the produced brine. Figure 6 depicts an improved (and symmetric) production/injection pattern used for a nominal 50 MWe simulation. Both production and injection areas are five times those used above and the intensity of exploitation (well spacing) is more realistic. Figure 7 shows the time history of the bottomhole temperature of the produced brine averaged over all the calculational zones in the production area for the case where it is assumed that the injected fluid enters the upper reservoir. The maximum and minimum brine temperature decline of only 2°C over the 30-40 year period is in sharp contrast to the result obtained with the result obtained with the simple four-zone pattern with injection. Flow at the downstream end of the reservoir

remains outward, in agreement with the table; no assumption on the availability of hot brine recharge is required (with injection).

Two additional simulations examined the response of the upper reservoir to nominal 250 MWe power production using a preferred production/injection pattern (Figure 6). Compared to the nominal 50 MWe simulations, the intensity of exploitation is one-third that employed when using the simple four-zone pattern and five-thirds that employed when using the improved pattern. Figure 8 shows the time history of the maximum, minimum and average bottom hole temperature of produced fluid for the case where all of the injected fluid is assumed to enter the upper reservoir. A 20°C decline of the averaged temperature is predicted over a 30-40 year period. There is a reversal of the flow at the downstream end required for this large scale exploitation of the upper reservoir even with injection. The case where no injected fluid is assumed to enter the upper reservoir results in an average temperature decline of only 3°C over a 30-40 year period. Attainment of this reservoir response, however, requires tremendous replinishment of hot brine at the northwest end.

Because of the limited data base, the simulations presented necessarily invoked a variety of hypotheses concerning geology, temperature and pressure, groundwater flow, convective flow, etc. and will likely require revision to include new information as the SSGF resource moves from the exploration and assessment stage of development to the exploitation and utilization stage. Only the upper reservoir of a portion of the SSGF was treated. This portion of the resource appears capable of supplying brine for a net 50 MWe demonstration plant with very little temperature decline over a 30-40 year design life. Uncertainties regarding boundary conditions and the effectiveness of the shale barrier between the upper and lower reservoir prevent an evaluation of the ability of the upper SSGF to sustain a 250 MWe plant. The capacity of the lower reservoir should also be considered in such an evaluation.

REFERENCES

Palmer, T.D. [1975], "Characteristics of Geothermal Wells Located in the Salton Sea Geothermal Field, Imperial County, California," Lawrence Livermore Laboratory Report, UCRL-51976.

Schroeder, R.C. [1976], "Reservoir Engineering Report for the Magma-SDG&E Geothermal Experimental Site Near the Salton Sea, California," Lawrence Livermore Laboratory Report, UCRL-5094.

Towse, D.F. [1975], "An estimate of the Geothermal Energy Resource in the Salton Trough, California and Mexico," Lawrence Livermore Laboratory Report, UCRL-51851.

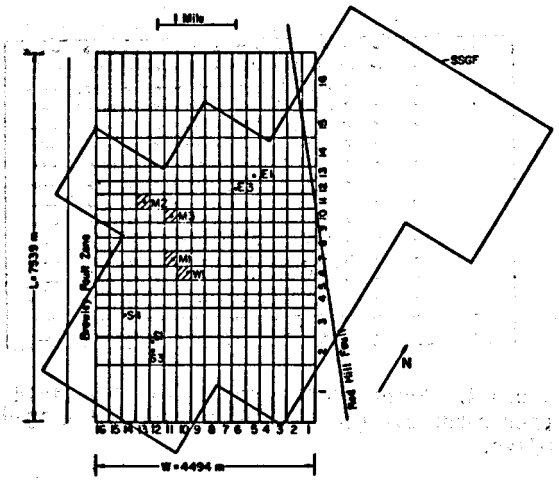


Figure 1. Portion of the SSGF chosen for simulation. Development wells within the region are also shown.

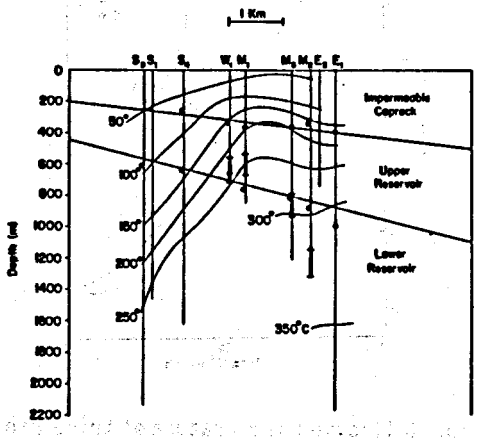


Figure 2. Vertical section and projected data from development wells. Points due to Towse [1975].

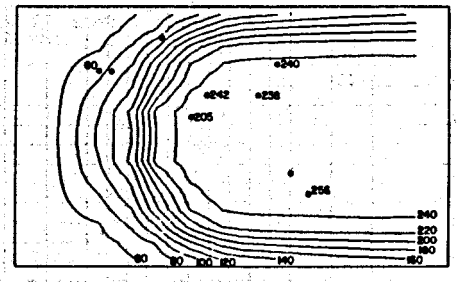


Figure 3. Preproduction model temperature contours (°C) compared with mid-plane temperatures measured at well locations.

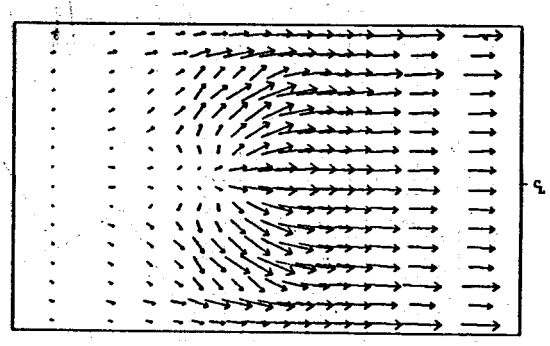


Figure 4. Preproduction model velocity field in upper reservoir (longest vector is 0.91 × 10-4 cm/sec.

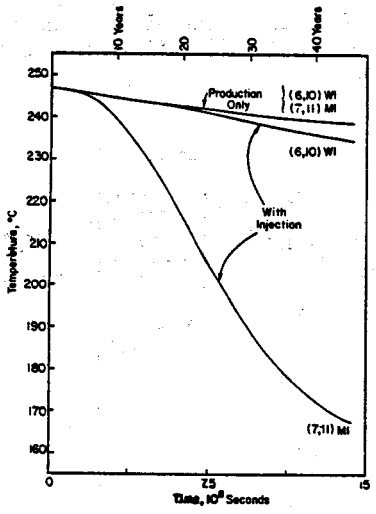


Figure 5. Wellbottom temperature of brine produced from upper reservoir (nominal 50 MWe, simple four zone pattern).

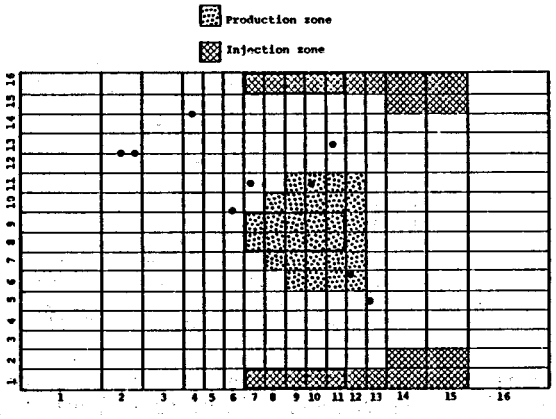


Figure 6. Improved production/injection patterns for exploitation of upper reservoir: nominal 50 MWe (heavily outlined areas) and nominal 250 MWe (total areas shown).

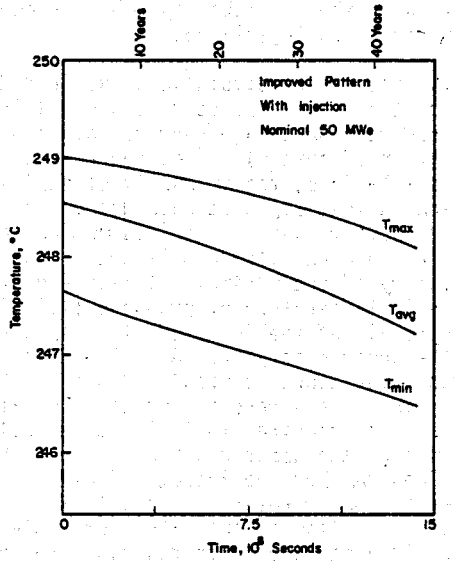


Figure 7. Wellbottom temperature range of brine produced from upper reservoir (nominal 50 MWe, improved pattern with injection).

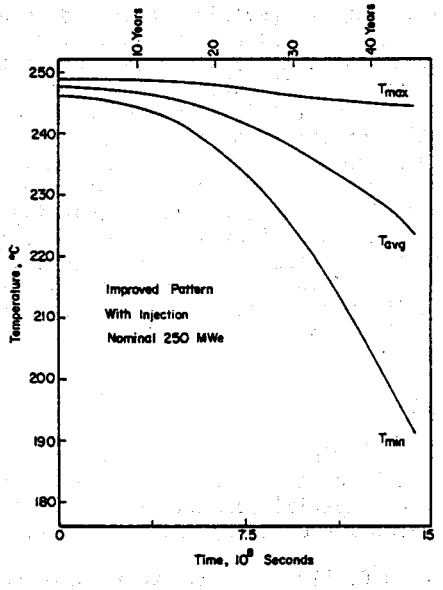


Figure 8. Wellbottom temperatures of brine produced from upper reservoir (nominal 250 MWe, improved pattern with injection).

Geothermal Resources Council, TRANSACTIONS, Vol. 2 July 1978

APPLICATION OF TYPE CURVE PROCEDURES FOR THE ANALYSIS OF PRODUCTION DATA FROM GEOTHERMAL WELLS

DR. JESUS RIVERA-R.

COMISION FEDERAL DE ELECTRICIDAD
COORDINADORA EJECUTIVA DE CERRO PRIETO

ABSTRACT

It has been already shown[1] that the decline-curve analysis approach can be successfully applied to geothermal wells. It was shown in Reference 1 that by plotting monthly production vs. time on either semilog or log-log paper together with the rate decline models given by Arps[3], it was possible to predict the future production of wells of the Cerro Prieto Geothermal Field.

This paper shows that production forecasting can also be performed by an entirely graphical procedure. The procedure is based on the use of a basic dimensionless graph which was developed by Fetrovich[2]. He found that rate decline models developed by Arps[3] could be placed on a single log-log type curve. The aim of this paper is to show how this graph was used to handle production data from some wells of the Cerro Prieto Geothermal Field. The results obtained from the graphical procedure agreed with those obtained from that procedure reported before[1].

INTRODUCTION

In spite of the fact that decline curves are one of the most extensively used forms of production data analysis employed in the evaluation of oil reservoirs, there are quite a few published papers on their application to geothermal reservoirs. The results obtained from the application of this type of data analysis to geothermal wells of Cerro Prieto show that the method deserves more serious consideration for application to other geothermal fields around the world.

As it is well known[1,2,3] the three types of declines are exponential, hyperbolic and harmonic. The easiest one to analyze by means of conventional methods[1,3] is the exponential decline, because the hyperbolic decline is difficult to analize either mathematically or graphically. This problem has been overcome with the application of the type curve procedure[2] used in this report. As it can be seen from Figs. 1 thru 4, the basic dimensionless graph provides the type of decline, and if this decline turns out to be hyperbolic, the exponent of the equation describing this type of decline can also be determined.

FUNDAMENTAL CONSIDERATIONS

Fetrovich[2] showed that the exponential decline is actually a longtime solution of the constant-pressure case[6]. He presented a dimensionless graph in wich the exponential, hyperbolic and harmonic decline models were brought together. This graph is the basis for the analysis presented in this paper. The basic equations for the analysis are[1,2,3] as for follows:

$$W(t) = W_i \cdot (1 + bD_i t)^{\frac{1}{b}} \quad \ldots (1)$$

Eq. (1) corresponds to a hyperbolic decline. If b=0, the exponential decline is obtained

$$W(t) = W_i \exp(-D_i t) \quad \ldots (2)$$

Finally, if b=1 from eq. (1) the harmonic decline is obtained

$$W(t) = W_i (1+D_i t)^{-1} \quad \ldots (3)$$

The decline models given by eqs. (1) thru (3) were plotted as a set of log-log type curves in terms of dimensionless mass flow rate, W_D, and dimensionless time, t_D. The dimensionless variables are defined as follows[2]:

$$W_D = \frac{W(t)}{W_i} \quad \ldots (4)$$

$$t_D = D_i t \quad \ldots (5)$$

APPLICATION OF TYPE-CURVE MATCHING TO CERRO PRIETO WELLS.

The type-curve matching is not new; it has been applied for several years in analyzing constant rate pressure tran

sient data in both oil and gas wells[7,8,9] the procedure is as follows:

The field data are graphed on a tracing paper sheet having exactly the same size log-log coordinates as the type-curve. Next the field data curve is positioned over the type-curve, moving it so that the axes are kept parallel until field data match uniquely any one of the decline curves.

The final step of this procedure is illustrated in Figs. 1 thru 4 showing different types of match. The dashed lines in these graphs correspond to real coordinate axes; meanwhile, those variables within the dashed squares are real variables. Field data are shown as circles. Dimensionless coordinated axes are shown as continuous lines as well as the basic decline curves.

The type-curve analysis was applied to 18 producing wells of Cerro Prieto. They exhibited the three types of decline. Figs. 1 and 2 correspond to wells A and B that showed a harmonic type of declination. Fig. 3 illustrates the behavior of a well with a hyperbolic decline. From this figure it is evident that the last two points fall apart from the general trend, it is because of severe scale problem within the producing casing string which reduced drastically the productivity of the well. Well A exhibited an exponential decline as is evident from Fig. 4. Sometimes it is not possible to obtain a unique match of all of the field data points with a single curve as is illustrated in Fig. 5. The behavior of this well is believed to be due to a slowly increasing scale build-up at either the casing producing string or at the slotted linner.

The main advantage of the procedure described in this paper is that production forecasting is made by extending the line drawn through the field data points according to the dimensionless curve from the basic type-curve that uniquely matched the data points. Future production rates corresponding to any time are read directly from the real axes. The application of decline curve procedures, both the one described in this paper and that used in Reference 1, to Cerro Prieto wells on a monthly basis during 1977, produced results that agreed within 6.8 per cent for both steam and total mixture production, between the rates predicted from the theory to the production rates actually measured in the field.

NOMENCLATURE

b = decline curve exponent

D_i = initial decline rate, t^{-1}

t = real time, (months for t_D)

t_D = dimensionless time, (eq. 5)

W_i = initial mass flow rate, ton.

W(t) = mass flows rate at time t; ton.

W_D = dimensionless mass flow rate, ton.

REFERENCES

1. Rivera, R.J.:"Decline Curve Analysis A Useful Reservoir Engineering Tool for Predicting the Performance of Geothermal Wells", Geothermal Resources Council, TRANSACTIONS, Vol. I (May, 1977), 257-259.

2. Fetrovich, M.J.:"Decline Curve Analysis Using Type Curve Analysis", Paper SPE 4629 presented at the 48th Annual Fall Meeting of the Society of Petroleum Engineers of AIME, Las Vegas, Nevada, Sept. 30-Oct. 3, 1973

3. Arps, J.J.:"Analysis of Decline Curves", Trans: AIME (1945) 160, 228 247.

4. Slider, H.C.:"A Simplified Method of Hyperbolic Decline Curve Analysis", Jour. Pet. Tech. (March, 1968) 235.

5. Gentry, R.W.:"Decline Curve Analysis" Jour. Pet. Tech. (January, 1972) 38.

6. van Everdingen, A.F. and Hurst, W: "The Application of the Laplace Transformation to Flow Problems in Reservoirs", Trans. AIME (1949),186 305-324.

7. Ramey, H.J.,Jr., Kumar, A. and Gulati M.S.:"Gas Well Test Analysis Under Water-Drive Conditions, Monogrpah American Gas Association (1973).

8. Agarwal, R., Al-Hussainy, R. and Ramey, H.J.,Jr.:"An Investigation of Wellbore Storage and Skin Effect in Unsteady Liquid Flow: I. Analytical Treatment", Soc. Pet. Eng. Jour. (Sept., 1970) 279.

9. Earlougher, R.C., Jr.:"Advances in Well Test Analysis", SPE Monograph Series Vol. 5., Society of Petroleum Engineers, Dallas, Texas (1977).

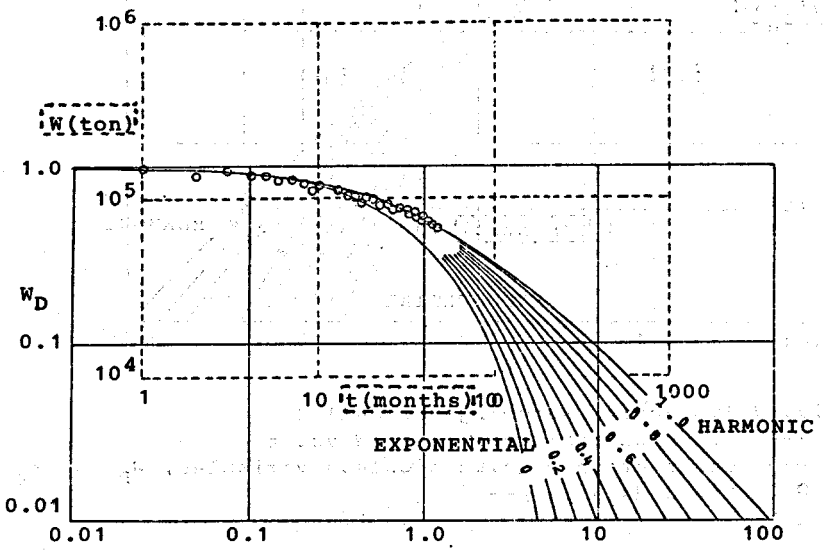


Fig. 1 Type-curve matching for well A
------ Graph on real variables, W vs. t
——— Basic graph on dimensionless variables, W_D vs. t_D
0 Field data points

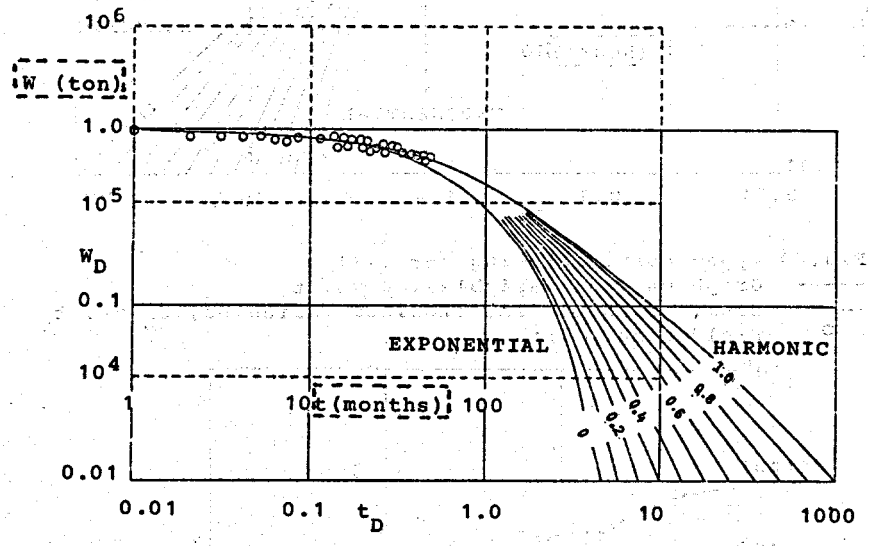


Fig.2 Type-curve matching for well B
---- Graph on real variables, W vs. t
——— Basic graph on dimensionless variables, W_D vs. t_D
o Field data points

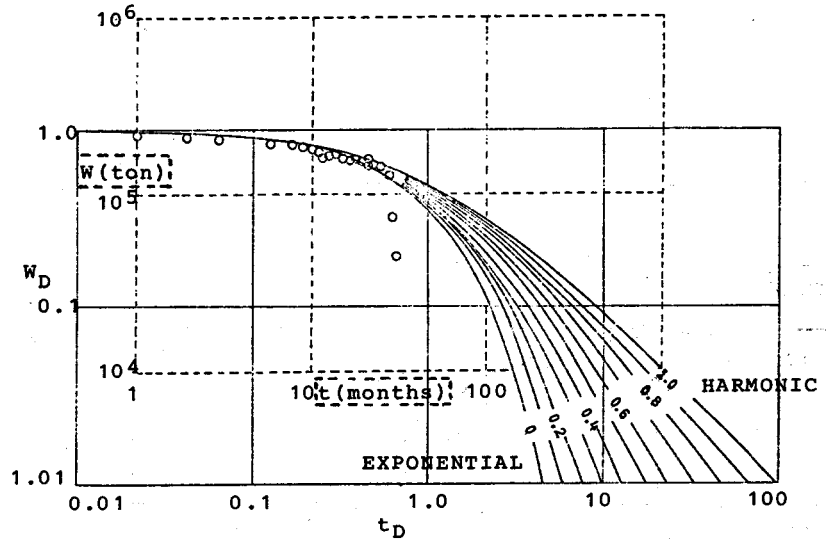


Fig. 3 Type-curve matching for well C
----- Graph on real variables, W vs. t
——— Basic graph on dimensionless variables, W_D vs. t_D
o Field data points

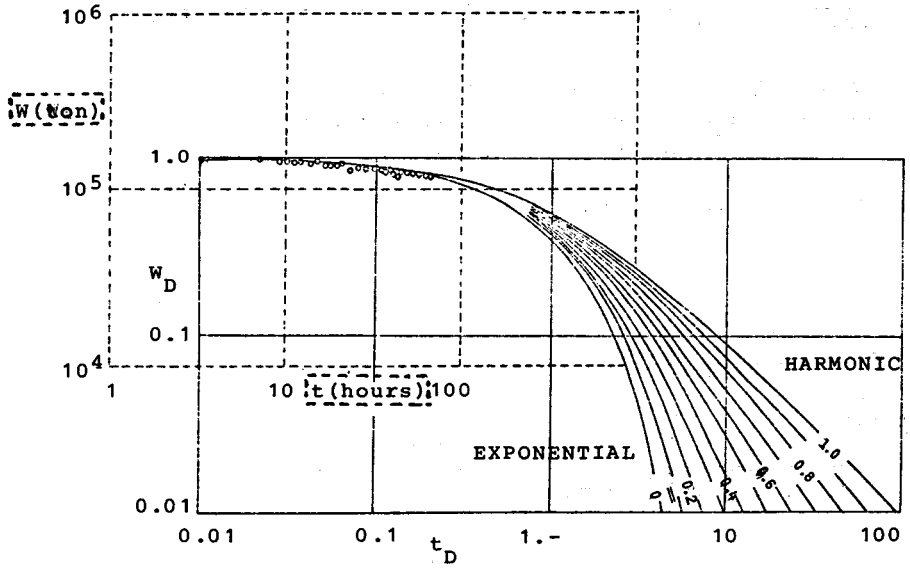


Fig. 4 Type- curve matching for well D
----- Graph on real variables, W vs. t
——— Basic graph on dimensionless variables, W_D vs. t_D
o Field data points.

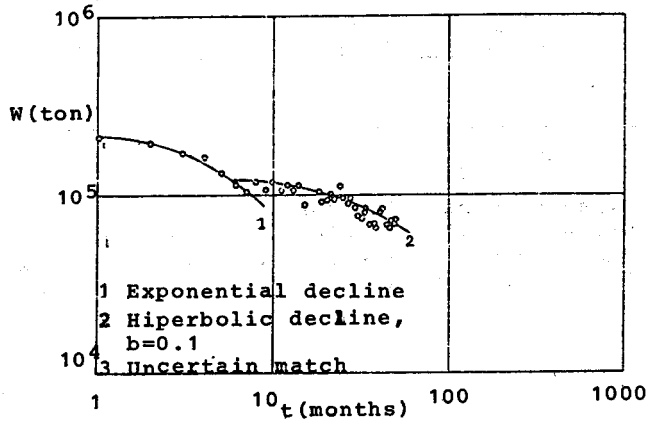


Fig. 5 Type-curve matching for well E.
o Field data points

CHEMICAL CHARACTERIZATION OF GASES AND VOLATILE HEAVY METALS IN GEOTHERMAL EFFLUENTS

David E. Robertson, Jonathan S. Fruchter,
J. Donald Ludwick, Connie L. Wilkerson,
Eric A. Crecelius and John C. Evans

Battelle
Pacific Northwest Laboratories
Richland, Washington 99352

The rapidly increasing number of successfully drilled geothermal production wells is a good indication that geothermal energy development may meet or exceed projected forecasts of its potential as a cheap, clean source of energy. However, geothermal energy is not without some environmental impact. Indeed, the very hot geothermal processes which create the steam or hot water used for energy production can also mobilize volatile and hot-water-leachable chemical constituents and bring them to the surface from great depths in the earth. Non-condensable gases such as hydrogen sulfide, ammonia, radon, carbon dioxide, methane, and other volatile elements such as mercury, boron, arsenic and selenium are vented to the air when geothermal resources are tapped. Thermal waters reaching the earth's surface contain very high concentrations of a wide variety of dissolved chemical constituents, some of which are toxic in relatively low concentrations (H_2S, NH_3, Hg, As, Cu, Zn, Se, Pb, Ag, Zn, Sb and Cd. It is essential that the effluents from each specific site be characterized to define and quantify the releases of undesirable materials.

During the past three years, under National Science Foundation (NSF) and Department of Energy (DOE) funding, our laboratory has been engaged in characterizing the above mentioned noxious gases and heavy metals released in effluents from two geothermal power plants and numerous test facilities. These areas include The Geysers, CA; Cerro Prieto, Baja CA; Raft River, Idaho; Tigre Lagoon, Louisiana; and the Imperial Valley, CA sites at Niland, East Mesa and Heber. This paper summarizes some of the results of our chemical characterizations of geothermal effluents.

To chemically characterize and quantify the geothermal gases and trace elements in geothermal well effluents, and to establish mass balances of these constituents entering and leaving the power plants, samples of incoming steam were condensed and the condensates and noncondensable gases were sampled. The power plant effluents consisting of cooling tower waters, cooling tower exhaust air, ejector off-gases, and brine waters were also collected for analyses.

When steam-brine separators were not available at the well-heads, a small portable separator was used to separate the steam from the brine phase (see Fig. 1).

HIGH PRESSURE STEAM-WATER SEPARATOR

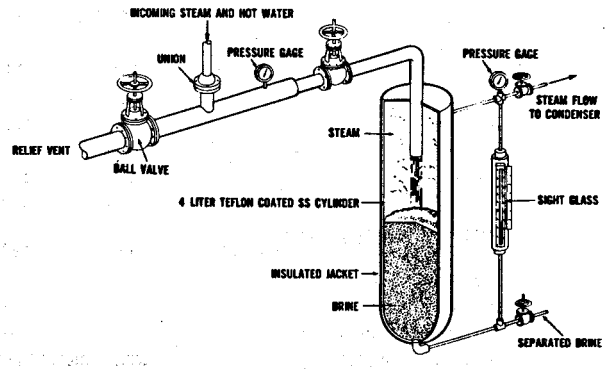


Figure 1

To condense the steam and separate the noncondensable gases a specially designed, non-metallic steam condenser was used (see Fig. 2.

NON-METALLIC STEAM CONDENSER

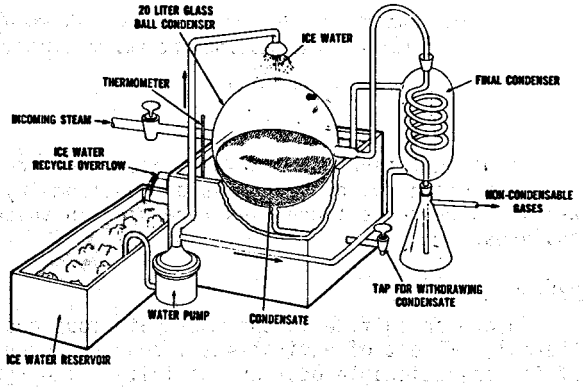


Figure 2

A number of difficult to preserve constituents and several chemical parameters were measured immediately after sampling in a mobile laboratory. These included H_2S, NH_3, F^-, dissolved S^{2-}, pH, oxidation-reduction potential (Eh), and various chemical forms of mercury. Samples of liquids and gas scrubber solutions were collected and preserved for laboratory analyses of a variety of other major and trace constituents.

CONCENTRATIONS OF VARIOUS CONSTITUENTS IN GEOTHERMAL NON-CONDENSABLE GASES, STEAM CONDENSATES AND BRINE

NON-CONDENSABLE GASES	THE GEYSERS[1]	RAFT RIVER[2]	VERMILION BAY[3]	EAST MESA[4]	EAST MESA[5]	NILAND[6]	NILAND[7]	HEBER[8]	CERRO PRIETO[9]
H_2S (ppm) VOL.	28,400 - 57,400	215	0.5 - 5	580 - 630	380	1390 - 1620	4670	--	15,000 - 20,000
Hg (µg/ℓ)	1.8 - 5.8	0.039	< 0.001	2.3 - 3.6	3.3	0.8 - 1.6	1.8	< 0.03	0.3 - 0.4
NH_3 (µg/ℓ)		--	130	108	--	45	--	--	17.8
Rn (pCi/ℓ)	3,820 - 27,800*	--	10 - 40	280 - 305	1095 - 1262	830 - 1150	535 - 644	3,200 - 4,300	--
As (µg/ℓ)	< 0.003	--	--	--	--	--	--	--	< 0.016
STEAM CONDENSATE									
H_2S (mg/ℓ)	49 - 225	0.66	--	2.8	0.09	5.5	9.5	--	36 - 71
NH_3 (mg/ℓ)	157 - 818	1.8	--	98	15.5	331	360	--	88 - 163
Hg (µg/ℓ)	2.8 - 10	0.13	--	14.4	1.45	2.20	3.12	3.9	3.8 - 5.4
B (mg/ℓ)	6.4 - 76	< 0.1	--	< 0.1	--	5.9	--	< 0.1	< 0.1
As (mg/ℓ)	0.0014 - 0.092	0.012	--	--	--	--	--	--	0.006
FLASHED BRINE									
NaCl (%)	--	0.13	10.4	1.77	--	16.5	--	--	2.27
H_2S (mg/ℓ)	--	0.1	--	0.33	0.07	--	--	--	0.16
NH_3 (mg/ℓ)	--	0.27	90	6.5	1.4	394	400	--	127
Hg (µg/ℓ)	--	0.022	0.007	0.003	< 0.001	0.020	0.11	0.44	0.049
B (mg/ℓ)	--	0.13	40	9.8	--	340	--	--	19
As (mg/ℓ)	--	0.028	0.045	--	--	--	10.0	--	0.50 - 2.3
RATIO: NONCONDENSABLES (ℓ) / STEAM (kg)	1.96 - 4.46	0.25	1.6**	17.7	4.54	8.8	9.27	--	9.7
BRINE FLOW (kg/hr)	--	--	--	10,600	--	109,000	--	7,500	1.58×10^6
STEAM FLOW (kg/hr)	--	--	--	860	--	13,600	--	--	7.37×10^5
TEMPERATURE (°C) (INCOMING)	--	--	--	151	--	165	204	161	--

1. UNITS 3, 4, 7, 8 AND 11 - SAMPLED OCTOBER 1975 AND MAY 1976
2. DOE WELL - SAMPLED SEPTEMBER 14, 1976
3. DOE GEOPRESSURED WELL NEAR DELCAMBE, LA - SAMPLED MAY 26, 1977
4. BLM WELL 6-2 - SAMPLED MARCH 30-31, 1977
5. REPUBLIC GEOTHERMAL WELL 38-30 - SAMPLED SEPTEMBER 7, 1977
6. WOOLSEY WELL - SAMPLED MAY 5, 1977
7. MAGMAMAX #1 WELL - SAMPLED SEPTEMBER 9, 1977
8. NOWLIN WELL - SAMPLED MARCH 2, 1977
9. MAIN STEAM HEADER - SAMPLED MAY 12, 1976

* RADON DATA FROM THE GEYSERS BY STOKER AND KRUGER, 1973 AND BY ANSPAUGH, et. al., 1977

** NO STEAM WAS PRODUCED. THIS IS THE RATIO OF NONCONDENSABLE GAS TO BRINE IN ℓ/kg

Table 1

Neutron activation analysis, atomic absorption spectrophotometry, plasma emission spectrometry and X-ray fluorescence techniques were used in these analyses.

Hydrogen Sulfide

Hydrogen sulfide is the most notorious geothermal effluent of environmental concern because of its objectionable odor and toxicity. The H_2S concentrations in non-condensable gases were extremely variable at the geothermal sites which were studied, and ranged from as high as 5.7% (by volume) at The Geysers Unit 11 to as low as 0.5ppm at the Tigre Lagoon, Louisiana geopressured well site. The Imperial Valley, California sites exhibited quite variable H_2S concentrations, and all sites were substantially lower in H_2S compared to the Cerro Prieto geothermal field located only about 30 km south of the California border. The non-condensable gas concentration in the steam phase at the Raft River, Idaho site was very low compared to all other areas, and the H_2S levels in the gas were only 215 ppm. The H_2S levels in the flashed brine at all hot water dominated sites was always very low, indicating that the vast majority of the H_2S follows the steam phase when superheated brines flash into steam as the pressure is lowered at the well heads.

Mercury

Because of its high vapor pressure, mercury is an extremely volatile element in geothermal fluids, and exists in elevated concentrations in the gas and steam phases. Mercury concentrations in non-condensable gases ranged from 0.03 µg/ℓ at Heber, California to 5.8 µg/ℓ at The Geysers Unit 3.

The mercury concentrations at most sites were 10^5 to 10^6 times higher than mercury levels in the ambient air. Mercury concentrations in the ejector off-gases at The Geysers and Cerro Prieto were considerably lower than in the non-condensable gases in the incoming steam. The ejector

off-gases are scrubbed by cooling tower water during the steam condensation in the power plants and some of the mercury is removed. Mercury levels in cooling tower exhaust air ranged from 0.18 to 1.3 ng/liter, compared to ambient air levels of approximately 0.001 to 0.010 ng per liter of air at most sites.

The dominant form of volatile mercury in all gaseous samples was elemental Hg^0 vapor. This was determined by using selective mercury vapor sorption traps, which were designed and tested to quantitatively separate and trap Hg^0 vapor, mercury chloride vapor, methyl mercury chloride vapor, and dimethylmercury vapor.

It was surprising to observe mercury occurring in the incoming noncondensable gases and in the ejector offgases as Hg^0 vapor when H_2S levels in these gases were so high, frequently ranging from 1.0 to 5.7 percent. Apparently, the elevated temperatures and reducing environment, together with the high vapor pressure of Hg^0 permit the mercury to exist unassociated with the high sulfide levels.

With the condenser systems used in this work, roughly one-third to one-half of the mercury condenses when the steam is condensed. The mercury concentrations in steam condensates ranged from 0.13 µg/ℓ at Raft River, Idaho to 14.4 µg/ℓ at the BLM East Mesa Well #6-2. These levels are about 100 to 10,000 times the mercury concentrations in uncontaminated fresh or ocean waters.

At the hot water dominated sites the mercury follows the steam phase during brine flashing, resulting in very low mercury concentrations in the flashed brine.

Mass balances of mercury entering the Cerro Prieto power plant and at several of The Geysers generating units have been made, based on measured mercury concentrations in incoming and outgoing effluents together with mass flow rate data supplied by the operators.

At Cerro Prieto an excellent mass balance for mercury was obtained. A total of 6.1 g of mercury pwer hour was measured entering the plant, and 6.8 g/hour was accounted for in the effluents leaving the plant. Most of the mercury leaves in the cooling tower exhaust, where 5.4 g/hour escapes to the atmosphere. About 0.6 g/hour is discharged to an evaporation pond with the separated brine.

At The Geysers Units 3, 7, 8 and 11, more mercury was measured entering the units than could be accounted for in the various effluents. The mercury influxes into Units, 3, 7, 8 and 11 amounted to 4.7, 3.9, 2.7 and 22.2 gms/hr respectively. Only 10 to 60 percent of the incoming mercury was accounted for in releases to the atmosphere, with the cooling tower exhaust air being the dominant pathway. Reinjection of excess condensate (cooling tower water) into the geothermal reservoir removed only a small fraction of the mercury. The mercury imbalances at The Geysers could very well be accounted for in the sludge that deposits in the bottom of the cooling towers and must be periodically disposed of in certified landfills. This sludge, which is composed primarily of sulfur from the oxidation of H_2S, contains 0.02 to 0.2 percent mercury. It is difficult to obtain quantitative estimates of the rate of formation of the sludge, but this appears to be an important scavenging mechanism for mercury at The Geysers.

Arsenic

The arsenic in geothermal effluents, unlike mercury, predominantly remains with the flashed brine and only a very small fraction follows the steam phase. Arsenic vapor was undetectable (less than 0.003 to 0.016 µg/liter) in the noncondensable gases. Arsenic concentrations in steam condensates ranged from 0.001 to 0.09 mg/liter. In the flashed brines the arsenic concentrations were much higher, and ranged from 0.028 mg/ℓ at Raft River, Idaho to 10 mg/ℓ in the high salinity brine at Niland, CA. The chemical forms of the arsenic in the condensates and brines are partitioned between inorganic As^{+3} and As^{+5}. The As^{+3} form is more prevalent in fresh condensate and brine exhibiting a reducing Eh, but as these waters become exposed to the atmosphere the As^{+3} gradually oxidizes to As^{+5}, the least toxic of the inorganic forms.

The arsenic mass balance at the Cerro Prieto power plant shows 4.4 grams per hour entering the power plant in the steam phase, while the vast majority of the arsenic, 2480 grams per hour, is discharged with the separated brine to a large evaporation pond. The arsenic going to the power plant is condensed and delivered to the cooling tower. At The Geysers power plants 6.3, 15 and 2.1 grams per hour of arsenic enter the power plants at Units 3, 8 and 11, respectively. Most of this arsenic is condensed and reinjected, but the cooling tower sludge could also be an important repository for arsenic deposition.

Boron

Boron concentrations in steam condensates at The Geysers ranged from 6.4 to 76 mg/ℓ. Cooling tower waters contained considerably higher boron levels because of the concentrating effect by evaporation of water in the cooling towers. At The Geysers power plants 2, 5.8, 11, 35, and 5.2 kg/hr of boron enter Units 3, 4, 7, 8 and 11 respectively. Most of this boron is reinjected. At the hot water dominated sites boron was found in the steam condensate only at Niland, at a concentration of 5.9 mg/ℓ. The boron concentrations in the flashed brine phases ranged from 0.13 mg/ℓ at Raft River, Idaho to 340 mg/ℓ in the highly saline Niland brine. At Cerro Prieto 30 kg/hr of boron is released with the flashed brine to the evaporation pond and less than 0.07 kg/hr goes to the power plant with the steam phase.

Ammonia

Ammonia is a ubiquitous constituent in geothermal effluents, and it is present in the noncondensable gas, steam condensate and brine. Ammonia concentrations in steam condensates ranged from as high as 818 mg/ℓ in several Geysers wells

supplying steam to Unit 11 to 1.8 mg/ℓ at Raft River. At Raft River and East Mesa the ammonia concentrations in the steam condensates were much higher compared to the flashed brine, but at Niland and Cerro Prieto the ammonia levels were about the same in the brine and condensate. At Cerro Prieto 92 kg/hr and 0.1 kg/hr of ammonia enter the power plant as condensable and non-condensable ammonia respectively, while 200 kg/hr are released to an evaporation pond with the flashed brine. Most of the ammonia leaving the power plant in steam condensate is released to the atmosphere from the cooling towers.

The ammonia flow into Units 3, 7 and 11 at The Geysers amounted to 94, 76 and 230 kg/hr, respectively. About 80% of this is volatilized to the atmosphere from the cooling towers.

Radon

Radon-222 gas was highly variable in the non-condensable gases from the various sites, ranging from 10 pCi/ℓ at the Tigre Lagoon geopressured site to 4,300 pCi/ℓ at Heber, CA. By comparison, the radon-222 concentrations measured by other investigators at The Geysers ranged from 3820 to 27,800 pCi/ℓ. The radon-222 follows the non-condensable gas phase and is essentially all released to the atmosphere.

Acknowledgments

This work was supported by Grant 75-14714 from the National Science Foundation - Research Applied to National Needs, and by the Department of Energy contract EY-76-C-06-1830.

Geothermal Resources Council, TRANSACTIONS, Vol. 2 July 1978

THE PRIVATE SECTOR IN HYDROTHERMAL RESOURCE DEVELOPMENT

Paul Rodzianko

Geothermal Energy Corporation
39 Broadway, New York, N. Y. 10006

Contrary to apparent popular belief, the private sector is very much alive as an active force in geothermal resource development for power generation. Its role as a much-needed alternative--and therefore as a deterrent--to ever-increasing government intervention and dominance in this field is only beginning to emerge. The formidable obstacles to the private development of a geothermal power industry are, in my opinion, no more insurmountable than the financial challenges encountered by the pioneers in the development of automobiles, television, airplanes, or natural gas. These obstacles, must, however, be examined from the viewpoints of both the purchaser of the power derived from this resource as well as of the resource company providing it. In particular, one major preconception appears to have led to the complicated impasse presently slowing the development of this important domestic energy resource.

For a highly-regulated utility to commit its own funds for the construction of a power generation facility, an exploration company must invest great amounts of front-end drilling and testing dollars to "prove" the reservoir. In order to generate a satisfactory rate of return on such an investment, the resource company is forced to look at 55MW units, not smaller ones, as the starting point for reservoir development. To date, however, no utility has been willing to finance and construct, at its own risk, a power plant on this basis.

The considerations outlined below will point out the need for the private sector to learn from past successful geothermal development experiences and thus minimize front-end field investment in anticipation of smaller initial unit sizes. Implicit in this approach is the recognition of the crucial need for reservoir operating experience particularly at the early stages of field development. Upon these beginnings can be built the firm financial foundation necessary for a thriving and sustained development in the geothermal industry.

CONSTRAINTS AND CONSIDERATIONS

1. Impact of field investment. A massive front-end investment in the ground will "up the ante" as regards the size of the initial power plant. A production company with 55MW worth of production wells completed will not accept a cash flow based on 10 or 20 MW. It will need revenues commensurate with the size of its resource investment. For every $10 million so invested by a production company, the utility must invest two to three times that amount ($20-$30 million) in the plant, thus magnifying the potential financial impact of reservoir risk. If substantial new transmission facilities are required, the amount of investment by the utility goes higher still.

2. Reservoir risk. By its charter and public mandate, a utility must attempt to eliminate any risk, including that of the geothermal reservoir, to which it could be exposed in a construction or financing program. All of the resource testing performed and up-front investment made by a production company cannot furnish the operating experience on which reliability under commercial operating conditions is ultimately assessed. Unless a supplier is willing to guarantee a supply of steam or resource over the useful life of the plant, the utility could lose its entire investment if the resource fails, thereby remaining limited in its ability to cooperate with the producer.

3. Base load reliability. Even if the threat of complete reservoir failure were eliminated, another utility concern arises regarding reliability. Given the nature of the resource, geothermal power plants are best suited for base load operation. Operating availability has been reported into the high 90% range for various units. If, as a result of operating difficulties, the plant is available for only 50% of the time at 80% of rated output or is down for prolonged periods, the utility in question will face a major load planning problem. The larger the units of initial size, the greater will be the dilemma of the utility load planners. For a relatively small utility, a 55 MW unit with uncertain performance characteristics may not warrant taking the risks involved. Obtaining large blocks of replacement base load power supplies on short notice with high costs will be a very real and unpleasant possibility. Furthermore, whenever possible, initial unit output should be matched to available excess capacity on

nearby existing transmission lines so as to eliminate the need for utility investment in whole new linkups prior to the establishment of resource reliability.

4. Resource utilization. The question of optimizing the match between available technology and long-term reservoir/resource characteristics is of major commercial importance as well. Not all resources discovered in this country will have ideal characteristics. Reservoirs with temperatures of 390°F, for instance, may, in the long-term, be most economically and efficiently developed utilizing binary cycle technology as opposed to flash systems. Without actual operating experience and testing of the reservoirs' performance characteristics, however, it is impossible to predict the adaptability, applicability, or reliability of any untried technology. The only way to obtain this kind of information is by drawing on the most closely-related proven technology available. Alternate technological approaches could then be tested on the operating model for incorporation into later units. In assessing reservoir risk, especially at the early stages of field development, it appears desirable to minimize any risks in above-ground facilities and to limit exposure solely to the below-ground reservoir risk. After the reservoir's performance characteristics have been sufficiently well-defined, subsequent and larger plants could be built on a truly optimized basis, realizing the full economies of scale.

5. Utility financing constraints. In addition to the foregoing, there is the question of utility financing capability. Many utilities are coping with ever-increasing construction budgets as a result of the spiraling costs and tight cash flows due to inflation and continuing regulatory constraints. A very small proportion of new building is done by means of internally-generated cash flows. A utility is caught between the need to borrow more to complete its construction programs and to minimize debt in order to retain its rating rather than face an increase in its cost of capital by borrowing too much. Should they add to that scenario the unscheduled, ex-budget demands of the producers for the utility to construct power plants on reservoirs when and if discovered, they will have a yet additional, purely financial, dilemma.

RECOMMENDATION

The solution to this complicated impasse between the developer and the utility consists of matching front-end field investment to smaller initial unit sizes and developing a capital base specifically designed to accept reservoir risk. These objectives can be implemented by the private sector in cooperation with the government rather than by the private sector's being subsidized by means of a demonstration program financed by the taxpayer.

The two largest fields in the world today started with extremely small generating plants. Units 1 and 2 at the Geysers are approximately 12MW each. In Italy, the average size is 11MW per unit with the initial unit having been 250 KW. In Japan, small initial units are the rule as well. A 55 MW starting point for reservoir development should not be considered a mandatory norm although it may be appropriate in some situations.

Starting small will minimize the risk to utilities, to financial institutions, to equity investors, and not least, to production companies. Deficiencies in resource evaluation, engineering design, and economic conditions can be compensated for much more readily on 10 to 20 MW unit sizes rather than with the $50 million investment packages necessary for a 55 MW plant. As much as possible, the element of risk needs to be minimized both for the financial backer as well as for the utility customer.

Although the logic dictating field development from small units appears compelling, several questions come to mind. These concern the relative inefficiencies of small plants, the unchanged nature of reservoir risk, and the characteristic conservatism of the equity investor. In response to these, I feel that it would be a mistake not to contemplate and, indeed, plan field development beyond the initial unit. Conversion inefficiencies of the smaller units can be reduced in the long run by proper integration into the expanding capacity of the field. Reservoir risk is not eliminated, merely tackled in more "bite-size" chunks. With these strategies in mind, the equity market for geothermal financing should become much more accessible and the development of this invaluable domestic energy resource should be accelerated.

TECHNIQUE FOR IMPLEMENTATION

To accomplish this objective, a new capital base must be developed. Resource companies, over their many decades in exploration activities, have evolved a capital structure which, while permitting exposure to "dry hole" risks, could not survive in a highly-regulated environment. On the other hand, utility companies are limited as to what investments and risks they can incorporate into their closely-scrutinized rate base. Some utilities and public entities still recollect write-offs from earlier, ill-fated geothermal drilling ventures. What is needed now is a new kind of company designed to accept reservoir risk and to accumulate operating experience first on small units, then on progressively larger ones. This entity would purchase the geothermal resource (generally at the well-head), own, finance and construct the power plant, and sell electricity to the utility. Its planning would be based on and coordinated with its client geothermal exploration companies. The schedules and objectives thus derived would be integrated into the load and financial planning requirements of the utilities. One potentially significant problem that this kind of cooperation resolve is the timing difference between an exploration company's development timetable based on lease anniversaries and

utility willingness or ability to commit funds for plant construction. While a utility is generally willing to purchase electricity, it is not always in a position to commit construction funding. As an option, the local utility could purchase the plants after a number of years of successful operation. The capital base accumulated in the meantime by the geothermal power plant company could then be reinvested in additional similar geothermal development ventures. An informative memorandum issued by the President of the Geothermal Resources Council (November 3, 1977) speaks of just such a company--part of a developing, separate power plant industry.

It is necessary to the purpose of this article to mention the government financial programs designed to assist the geothermal developer--the Geothermal Loan Guarantee Program (GLGP) and the Demonstration Plant Program (PON). The GLGP has many positive attributes, in particular the flexibility of its structure. It can serve, basically, as an insurance policy (paid for by the user) covering reservoir risk for up to 75% of the cost of a given project thereby reducing the need for initial risk capital of limited availability. The most the PON will provide is 50% by means of an outright grant at the expense of the taxpayer. The GLGP is applicable to any commercially-viable project brought before it--the PON favors one or two predefined project formats. The GLGP does not claim to solve the overall problem of reservoir assessment, whereas the PON implies that the information acquired on the demonstration reservoir will be valid for future discoveries. The GLGP does not specify unit size, the PON does, etc., etc. As noted above, the government is a potent force in the geothermal industry. A purely financial, flexible partnership appears both possible and beneficial with the GLGP to a degree impossible to conceive of under the PON. By recognizing the unique characteristics of each geothermal reservoir, the GLGP provides a broad-based opportunity for the rapid development of this resource with significantly less cost (if any at all) to the taxpayer.

Assuredly, the problem of reservoir risk is a crucial one. Nonetheless, it is reasonable to assert that the private sector working in partnership with the government, rather than through direct subsidization, will be successful in dealing with it. Let us look at plant sizes and front-end investments commensurate with acceptable financial risks and base our business strategy on the ever-growing involvement and dynamism of the private sector.

Geothermal Resources Council, TRANSACTIONS, Vol. 2 July 1978

A CASE HISTORY
THE COMPLETION OF A SHALLOW, OVER-PRESSURED GEOTHERMAL WELL

Jacob M. Rudisill

Thermal Power Company
San Francisco, California 94108

ABSTRACT

This paper presents a case history of the drilling and completion of a shallow over-pressured geothermal well, Utah State 72-16, situated in the Roosevelt Geothermal Field, Beaver County, Utah. The problems encountered and the techniques used in completing this well are reported to assist other operators in safely drilling and completing in such shallow, over-pressured resources. The tasks of greatest difficulty were 1) the running of the 9-5/8" production casing and 2) remedying the consequence of an indicated imperfect cementing of the 13-3/8" surface casing. Patience, cooling of the well, and carefully performed and evaluated cement jobs were the techniques employed which contributed to the successful completion of these tasks.

This paper presents a case history of the drilling and completion of a shallow over-pressured geothermal well, Utah State 72-16, situated in the Roosevelt Geothermal Field, Beaver County, Utah. The problems encountered and the techniques used in completing this well are reported to assist other operators in safely drilling and completing in such shallow, over-pressured resources. The tasks of greatest difficulty were 1) the running of the 9-5/8" production casing and 2) remedying the consequence of an indicated imperfect cementing of the 13-3/8" surface casing.

Utah State 72-16 was spudded October 22, 1976 in Section 16 of the Roosevelt Geothermal Field by Thermal Power Company, Operator for a joint account with O'Brien Resources Corporation. A 12¼" hole was drilled to 85 feet in coarse granite alluvium, and then opened to 26". Conductor casing of 20" diameter was cemented at 85 feet with 200 sacks of cement. A 20" Hydril blowout preventer (BOP) was flanged to the conductor and a 17½" bit was used to drill below the shoe of the 20" casing. Drilling penetrated unconsolidated gravel, granite fragments and a pebble conglomerate of silicified granite fragments, when at 312 feet the well began to flow. The Hydril was used to shut-in the well, which registered 25 psig surface pressure. Drilling proceeded past 312 feet with mud weighted to 13.5 pounds per gallon (ppg). An alluvium/granite interface at 425 feet was drilled without incident, but during a deviation survey at 514 feet, the well flowed again. Drilling was continued down to 585 feet using 14.5 ppg mud, although mud returns were reduced or cut to 13.6 ppg and heated as high as 186°F. It was decided to weight the mud to 15.2 ppg, run casing, and cement the hot, mud-cutting zones behind pipe.

The 13-3/8" surface casing was cemented at 580 feet with 400 sacks of cement with good returns to surface by 2345 hours on November 1, 1976. Within 3½ hours the annulus between the 20" and 13-3/8" casing commenced flowing water, which was stopped with the Hydril. Before the annulus could be cemented from the top, a new seep developed outside the 20" casing in the cellar bottom. Finally, cement was applied both down the annulus and in the cellar bottom and a cement bond log (CBL) and temperature log were run.

There are two (2) components of a cement bond log; the amplified casing bond portion (CB), and the variable density log (VDL). Both portions must be interpreted for a correct determination of the cement bond. Reading the CB portion of the log of the 13-3/8" surface casing alone, the bond could be interpreted as being excellent from surface to 100 feet, fair from 100 feet to 260 feet, and excellent below 260 feet. Interpreting the two (2) logs together, however, reveals that from 0 feet to 22 feet there is only a fair bond, from 22 feet to 270 feet a very poor bond, and from 270 feet to bottom a poor bond consisting of a cement sheath resting (not bonding) against the formation. This latter phenomenon is revealed by the

poor acoustical arrivals in the VDL log. Such arrivals are termed poor when the vertical lines of the VDL are relatively undisturbed. In the log of the 13-3/8" surface casing, only the sharp, evenly spaced signature of the casing collars is present, indicating that the cement sheath was incompletely bonded to the formation. Perforating and squeeze cementing behind the casing was not employed in these circumstances for several practical reasons. Drilling proceeded below the 13-3/8" surface casing with a readiness to make an immediate abandonment of the well if further adverse circumstances required it.

While drilling ahead with heavily salted water, the well kicked gas and some steam at 633 feet. After killing the well with 14.1 ppg mud, it was decided that further drilling would utilize mud to control the well's pressure. However, use of drilling mud had its own drawbacks because the high heat throughout the well caused the coagulation of barite and gel, making it very difficult to resume mud circulation after any interruption of drilling. Furthermore, the 14.1 ppg mud was constantly being cut in weight by additional heat and geothermal fluid entry. It was finally found that a mud weight of 15.2 ppg was required to prevent fluid entry and reduction of mud weight.

While weighting up the mud at 633 feet, the well was tested to determine if the well was sufficiently productive to merit completion. Testing was performed through the drilling stack and choke manifold, using the method of James. This technique was successfully employed at both 633 and 836 feet and proved insufficient productivity to complete the well at such depths.

On November 15, 1976, while drilling at 1245 feet, the drilling string torqued up and then spun free, accompanied by a loss of mud circulation. Some 300 barrels of lost circulation material (LCM), gel, and barite was pumped down with no returns. While building up a new supply of mud, the well was tested, and the readings of pressure and temperature indicated that a major hot water and steam flow had been encountered; the well was ready for completion. However, completion operations against the wellhead's pressure of 250 psig over hydrostatic presented tremendous problems. Even 15.2 ppg mud was being cut by the entry at 1245 feet, and the wellbore heat alone caused a significant decrease in density of mud statically resting in the wellbore. These problems with the mud, coupled with a reluctance to temporarily close a potentially productive zone with cement plugs, forced the used of "snubbing" equipment to remove the drilling string from the hole. This laborious operation alone required seven (7) days to set-up and perform.

The greatest problem threatening the safe completion of Utah State 72-16 however, was that of running the 9-5/8" production casing. Pressure control while running and cementing is important for a sound primary cement job. Even if a plug was set above the main zone at 1245 feet to isolate it, it was feared that the mud could be cut and heated by the upper zones, and a loss of pressure control occur. Additionally, should the casing be run successfully, the high temperatures at such shallow depths could cause the cement to flash set during its application, preventing a complete or satisfactory bond. Considerable time was devoted to analyzing these problems and their possible solution. However, on November 25, 1976, a stream of hot water and steam appeared approximately 25 feet southwest of the wellhead and commenced to flow steadily at about 15 gallons per minute. This event prompted the election to run and cement a string of production casing.

The effort to run 9-5/8" production casing commenced with the setting of a bridge plug at 1144 feet in the open-hole. The plug failed to seal off the pressure completely, as did a pill of 12% LCM dropped on it in an attempt to seal of possible leaks. Two (2) attempts were made to place a 75 lineal foot plug of cement on the plug; neither attempt succeeded. Despite these setbacks, however, much had been learned by now about how to deal with the well. Foremost of these lessons were the advantages gained by cooling the well with water before attempting operations with mud. The cooling promised savings of mud and rubber components of the BOP from the heat of the well. Accordingly, while mixing up heavy mud, the well was cooled by circulating water through open-ended drill pipe "hung" near the plug. When the 15.5 ppg mud was mixed, it was pumped into the well and displaced the water. The wellhead pressure was reduced to zero and remained safely so for several hours. This process of "cooling and killing" proved essential in the running and cementing of the 9-5/8" production casing.

On December 16, 1976 a slow (11 hour) process of washing and reaming wall cake down to the plug was started. Following this reaming, for 15½ hours the well was cooled by circulating water through the drill string, and up the annulus of the well. In rapid succession, the water was displaced with 16.3 ppg mud, the drilling string pulled out, and the rams of the Shaffer BOP's changed to handle casing. The 9-5/8" production casing string was

modified to use the "cool and kill" method to provide a good cement job. The string sequence was a float shoe, one (1) joint of pipe, a float collar, a second joint of pipe with a centralizer, a "stab-in" float collar, a third joint of pipe with a centralizer, and the remaining 24 joints of casing. The casing was run in three (3) hours and the shoe set at 1098 feet below Kelly Bushing. Immediately, the mud was displaced and water again circulated through the hole, this time flowing down through the casing and shoe and up the annulus between the casing and the wall of the hole. This cooling continued ∿ 20 hours, then the water was displaced with 16.4 ppg mud, and mud was circulated outside the 9-5/8" production casing for ½ hour to condition the hole. Next, open ended drill pipe was run to the 'stab-in" float collar and 15.5 ppg cement slurry with 40% silica flour was pumped through the annulus between casing and open hole. Over 100% excess cement was used so that cement returns, although cut by water at first, finally had the same weight as that cement entering the well. It is believed that careful selection and control of cement slurry weight was of special importance in the circumstances at Utah State 72-16. Upon completion of cementing, the drill pipe was backed out of the "stab-in" collar, the mud displaced out of the casing, and cool water circulated in the casing to prevent the flashing of cement outside the 9-5/8" production casing. Three (3) float valves provided triple insurance that the heavier cement would stay in place and remain undisturbed while setting up. The circulation of the water up the annulus between the drill pipe and casing was a critical cooling operation which continued for 22 hours after the cement was emplaced. For a final time the well was killed with 15.0 ppg mud and an expansion spool and master valve flanged onto the production casing on December 20, 1976.

The effectiveness of this elaborate procedure on the 9-5/8" production casing was immediately investigated with a CBL. Bonding was fair to good from 20 feet to 86 feet, and excellent to very good from 80 feet to 548 feet. This region shows excellent cement bonding to the 13-3/8" surface casing as evinced by the strong "formation arrivals" in the VDL. From 548 feet to 1098 feet, the cement bonding is very good as shown by both the low amplitude of the CB and the continuous formation arrivals in the VDL. Some micoannulus effect is shown by the moderate formation arrivals of the VDL (moderate meaning the first few arrival lines are generally undisturbed). However, a micoannulus does not generally cause a loss of hydraulic seal. In short, the majority of the 9-5/8" production casing CBL is of a textbook quality.

Utah State 72-16 was cleaned out, deepened 9 more feet to a total depth of 1254 feet and completed with two (2) wellhead gate valves on December 31, 1976. Still to be corrected, however, were the consequences of the poor 13-3/8" surface casing cement job, manifested by the constant 15 gpm of geothermal water flowing from the seep near the wellhead. Considerable analysis again preceded action. On February 7, 1977, a grouting program for the well was initiated. Two initial vertical drill holes to 65 feet, located about 10 feet from the wellhead, failed to take sealant and stop the seep. Consequently, efforts were then re-directed towards sealing off the 13-3/8" surface casing cement sheath at the shoe of the 20" surface casing. An angle hole (G-3) directed towards this target successfully found the seep conduit, but grouting with Geoseal proved ineffective and the hole was plugged and abandoned. A fourth angle hole suffered the same fate, and was abandoned. A fifth angle hole (G-5) intercepted the seep's conduit again, so effectively that the entire seep's flow would exit G-5. Attempts to cement (instead of grout) the seep from G-5 only caused the cement to exit the seep and not setup. This led to the final hole, G-6, which also intercepted the seep's conduit. Cement was pumped through G-6 while G-5 was allowed to flow. Cement appeared in both G-5 and the seep using a 3 to 1 mix of water and Portland Ideal, Type 1A cement. G-5 was gradually closed in while pumping down G-5 continued and the water-to-cement ratio was decreased markedly. As the slurry ratio was further decreased, pumping pressures began to build and the spring stopped flowing altogether. After two (2) hours of pumping a 0.75 to 1 slurry ratio at 70 psig, no further injection at that pressure was possible. This near classic "squeeze job", using 220 sacks of cement, stopped the seep and all gas flows in the well's cellar. The six (6) grout wells were capped and Utah State 72-16 was completed and ready for testing. On a 22-hour flow test in early April 1977, the well flowed from a reservoir of 468°F water at total mass flow rates up to approximately 1,300,000 pounds per hour. No surface seepages were found subsequent to this test. The well is presently shut-in awaiting further testing or production use. All wellbore data from Utah State 72-16 is now available to the public at the University of Utah Research Institute in Salt Lake City.

In conclusion, the history of Utah State 72-16 illustrates three (3) major requisites for dealing with a shallow,

over-pressured well. First, such a well poses problems unique to the well and its geologic setting. Solutions to these problems are probably not obvious. Considerable thought, discussion, and experimentation is required for the discovery of these problems' solutions. Patience, then is the first requirement for completing such wells, even though such patience can be quite expensive. Secondly, cooling of a shallow, over-pressured geothermal well is a valuable tool in completing such wells. Keeping the well cool (1) saves the mud from heat and fluid entry degradation, (2) aids in a proper primary cement job, and (3) prolongs the life of such surface equipment as rotating head rubbers and BOP rams. In general, cooling the well buys the operator increased safety and greater operational flexibility. Finally, wells like Utah State 72-16 require a good primary cement job on each casing string. This involves careful attention to sufficient cooling and cement slurry weight and cement volumes to insure a good cement sheath. The follow-up of a good cement job should include a definitive appraisal of the job before proceeding with the well.

In summary, patience, cooling, and carefully performed and evaluated primary cement jobs, are recommended in any efforts to complete shallow, over-pressured geothermal wells.

My appreciation and thanks are extended to Mr. Royce "Buddy" Bowden, formerly of Loffland Brothers, Inc. and now of Thermal, who devised the "cool and kill" technique which permitted the safe completion of Utah State 72-16; to other members of the geothermal operations staff of Thermal, and to O'Brien Resources Corporation and Amax Exploration, Inc. for permission to publish.

Geothermal Resources Council, TRANSACTIONS, Vol. 2 July 1978

FLUIDIZED BED LOW-TEMPERATURE GEOTHERMAL DRYING

R. C. Schmitt and L. T. Cole
IDAHO NATIONAL ENGINEERING LABORATORY
IDAHO FALLS, IDAHO 83401
and
J. H. Oates
J. R. SIMPLOT COMPANY
CALDWELL, IDAHO 83605

SUMMARY

EG&G Idaho, Inc., as part of its activities performed for the Department of Energy's Division of Geothermal Energy and under contract to DOE's Idaho Operations Office, is commencing a series of low-temperature geothermal drying experiments at the Raft River Geothermal Site. This paper will delineate the results from the initial test work, particularly as it pertains to the use of geothermal heat in drying operations on waste materials from potato processing operations.

The objectives of these experiments is to investigate the feasibility of using geothermal heat for waste material drying, recovery, and handling, food processing drying operations, or drying of agricultural materials. The experiment will initially investigate drying an activated sludge biomass slurry and drying waste potato solids from the J. R. Simplot Company potato processing plant located at Burley, Idaho. The J. R. Simplot Company is a participant in the experiment and other industry representatives have also been invited to participate. The biomass material is currently part of the treatment in Simplot's Burley, Idaho plant waste stream and poses problems of disposal. The material, when dewatered and processed, is expected to be a protein food suitable for animal and fish consumption. A companion experiment will involve feeding operations and diet studies using the dried materials at a commercial fish farm. The material will be partially dewatered by centrifuge at the Burley treatment plant prior to delivery to the Raft River experiment. The waste materials are expected to be received with a moisture content of 60 to 90%.

The dryer will be a fluidized bed system and the thermal energy for drying will come from geothermal water, with temperatures up to about 132°C (270°F), circulated through the tube side of heat exchange tube bundles. The bed around the tube bundles will be fluidized using air with a velocity of approximately 0.3 m/sec (1 ft/sec). Heat will be provided to the dryer from either one or two separate heat exchange bundles, each having a heat transfer area of 1.8 m^2 (19 ft^2). Each tube bundle is capable of supplying 38 kW (thermal), or enough heat to vaporize 53 liters of water. The material to be dried will be passed through a colloid mill for uniform particle sizing of about 1.27×10^{-6} meters, atomized with an atomizing nozzle, and injected as an atomized slurry into the heated bed. Air will be used for the atomizing nozzle, but the use of flashed geothermal water to produce steam for the atomizing nozzle will also be investigated. The atomized material will dry almost instantly as it comes in contact with the heated bed. The characteristic of the fluidized bed will be isothermal and stabilized at the boiling temperature of water. After a bed of dried material is formed, the fluidizing allows the product to exit the system in a granular or pelletized form by using an overflow tube as the level of the bed rises. A pictorial of the system is shown in Figure 1. The apparatus stands approximately 2.74 m (9 ft) tall and is made from a piece of 0.25 x 0.25 m (10 x 10 in.) square structural tubing. The heat exchanger bundles are bolted into the side of the dryer in two places, as shown. The system is undergoing installation and checkout at the time of this summary. Results from the biomass and potato waste work are to be complete for reporting at Hilo.

The experiment has the potential for stimulating a more widespread direct use of geothermal energy since there may be numerous applications for a system of this type in food processing operations, agriculture, and waste management. Grain, sugar beet pulp, alfalfa, and onion drying operations are a few examples. Also for example, the participating J. R. Simplot Company has an interest in the use of geothermal heat in an existing potato processing plant located near Caldwell, Idaho, where a geothermal well exists on the plant grounds. Additional work is expected to follow the first series of tests, using other materials and process conditions from other industry.

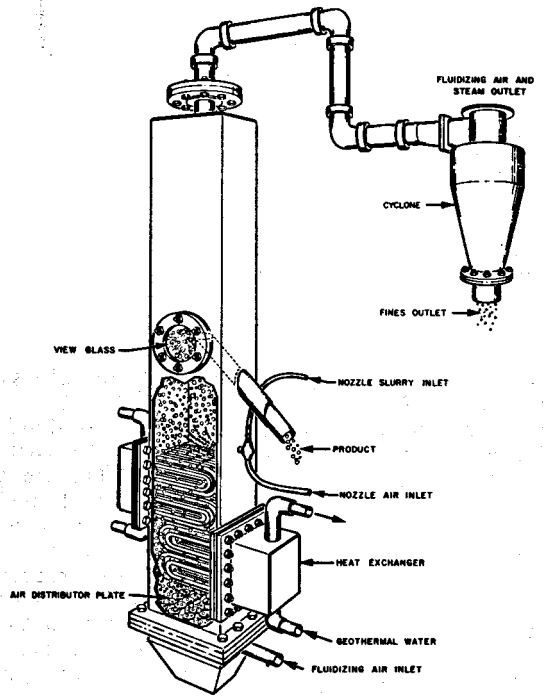


Fig. 1 Geothermal Dryer Assembly

Geothermal Resources Council, TRANSACTIONS, Vol. 2 July 1978

Meager Creek geothermal system, British Columbia, Part III: Resistivity Methods and Results

Greg A. Shore

Deep Grid Analysis (1977) Ltd., Vancouver, British Columbia

Abstract

Electrical resistivity survey has been the principal geophysical exploration tool applied at Meager Creek geothermal area, 150 km north of Vancouver, B.C. Dipole-dipole reconnaissance traverses have been successful in identifying areas of anomalous resistivity in the accessible valley areas around the volcanic complex. Extremely steep topography imposes severe spatial constraints on the layout of long-spacing arrays, and impedes anomaly examination and resolution. A multiple pole-pole array addressed by a computer-based scanning receiver is being employed to increase effective penetration within the limited operating space and to provide a multidirectional data base for anisotropy studies.

Introduction

The Meager Creek geothermal area is located 150 km north of Vancouver, British Columbia. Its main feature is a large central Cenoozoic volcano, flanked by two hot spring systems in the lower valleys (Nevin et al., and Read, this volume).

Nevin et al. (this volume) describe the present exploration context at Meager, and provide a general map relating geology, geophysically indicated reservoir areas and topography.

Most of the resistivity survey to date has been conducted over the quartz diorite basement in the valleys, with some operations on the north side conducted on the overlying Tertiary and Quaternary volcanics. Overburden is pervasive in all but the higher altitudes, and is relatively resistant except in the immediate vicinity of present and previous stream channels where resistivities as low as 2 to 10 ohm-metres may occur.

Two local factors severely impede dipole-dipole survey operation and data interpretation: (1) extreme topography forces alignment of long-spacing arrays along the valleys, the arrays often painstakingly installed on steep sidehill from helicopter pads hand-cleared from dense forest, and (2) a high frequency of horizontal resistivity mode changes and near-surface conductive patches which complicate array responses, a situation further impeded by the difficulty or impossibility of installation of parallel or perpendicular detail lines.

Dipole-dipole Resistivity

In 1974 dipole-dipole survey traverses using portable frequency domain IP equipment were operated along the valleys around the volcanic complex (Nevin Sadlier-Brown Goodbrand Ltd., 1974). A dipole spacing of 305 m (1000 feet) was used, with N = 1 to 4. Some 152 m dipole spacings were used to resolve shallow detail. These traverses were remarkable in that almost all areas presently being studied and detailed as resistivity anomalies were identified in or inferred from these original data, or can retrospectively be seen as indicated or suggested in the data.

Follow-up survey in 1975 resolved more fully the dimensions of the "south reservoir". A parallel line was successfully installed above the original discovery line, permitting some evaluation of the dimensions of the anomaly (fig. 1). Using much higher power (40 kva) time domain equipment and 610 m (2000 feet) dipoles with N = 1 to 8, the south reservoir boundaries were defined to the east and west, a resistive sub-bottom was identified, and a tabular, conductive reservoir

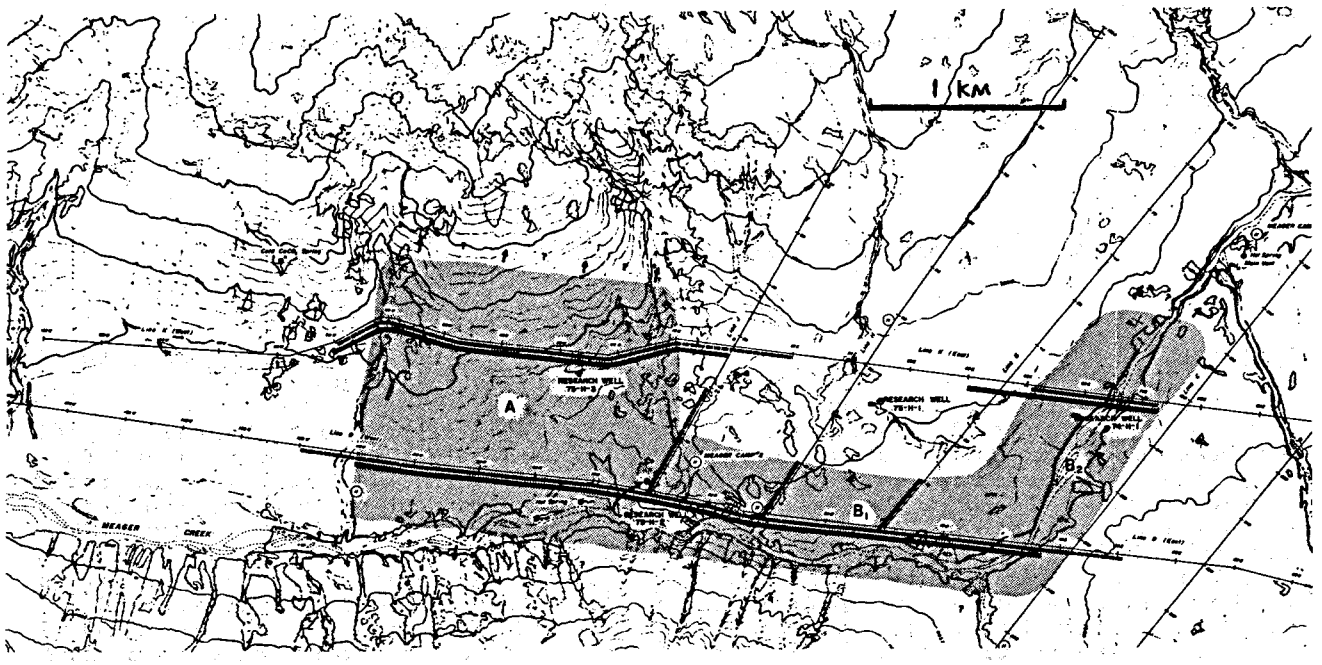


Fig. 1 Resistivity lines over south reservoir. Anomalous areas shaded.

indicated as dipping gently to the north, into the volcanic complex (Nevin Sadlier-Brown Goodbrand Ltd., 1975). Resistivities within the anomaly are estimated at a mode of about 25 to 30 ohm-metres, in background resistivities of 200 to 1200 ohm-metres.

The sloping bench over the south anomaly (fig. 1) is about the only place in the area where a parallel line can be offset, and was surveyed only with major difficulty. The larger array lengths (>6 km) stretched almost the entire length of the Meager valley.

Multiple Pole-pole Array

The multiple pole-pole array requires the same preparations as a simple pole-pole array: one current and one potential reference electrode, each placed remote from the survey grid and from each other. The active current electrode is free to set up anywhere on the grid, and the active potential "electrode" is actually up to 40 pre-installed electrodes wired to a central receiver point. For every current position, all forty potential positions are measured, data tested, apparent resistivity values and 3-dimensional plotting data calculated and stored. Each successive current electrode position provides an additional 40 measurements, each of a depth penetration and current orientation controlled by the relative positions of the pair of electrodes involved.

Fig. 2 shows the nominal plan plotting positions for data derived from two successive current electrode positionsin a 20 potential electrode array. Current flow direction is indicated by line orientation, and relative depth penetration by line length. Each set of 20 measurements requires less than five minutes operating time, once the electrodes are placed. (In extreme telluric disturbances, sample integration and software filtering may be continued as long as required to obtain adequately noise-cancelled readings.)

Penetration of the pole-pole array at Meager has not yet been confirmed by drilling, but in view of the DC signal and the resistive nature of the environment, it is thought that penetration approaches the theoretical maximum. Depending on operational practicalities (signal magnitude at receiver, available transmitter power) penetration of the pole-pole array may exceed that of dipole-dipole arrays by

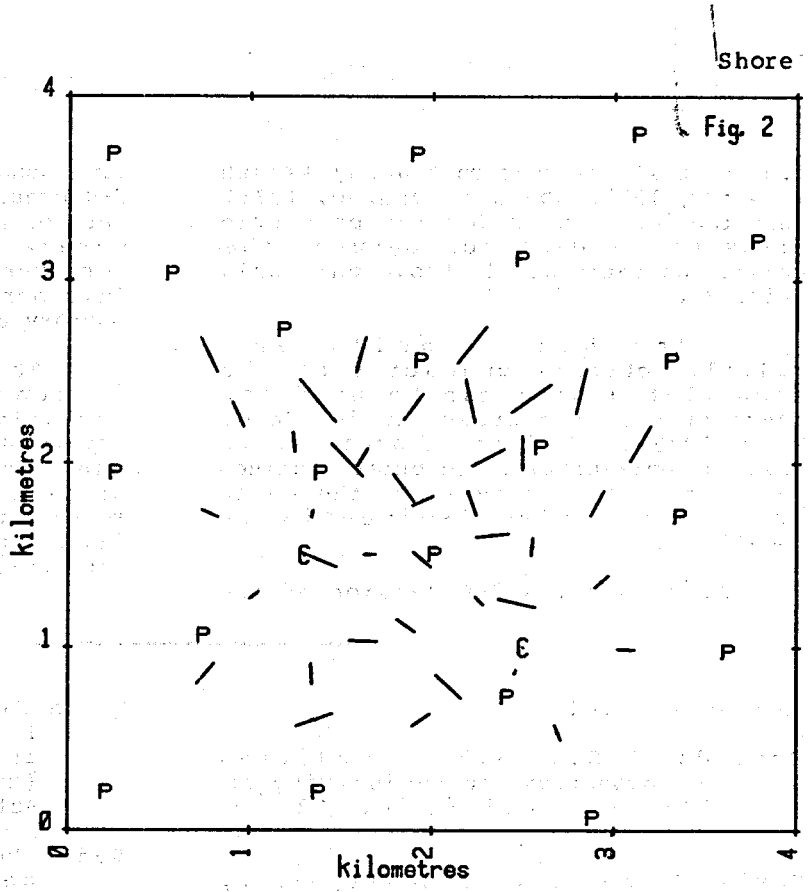


Fig. 2 Multiple pole-pole array using 20 potential (P) electrodes. Plan drawing shows nominal plotting position (1/2CP) for readings originating from two separate current (C) electrode positions. Lines show current orientation, with length proportional to effective penetration (L=1/10 Ze by horizontal scales).

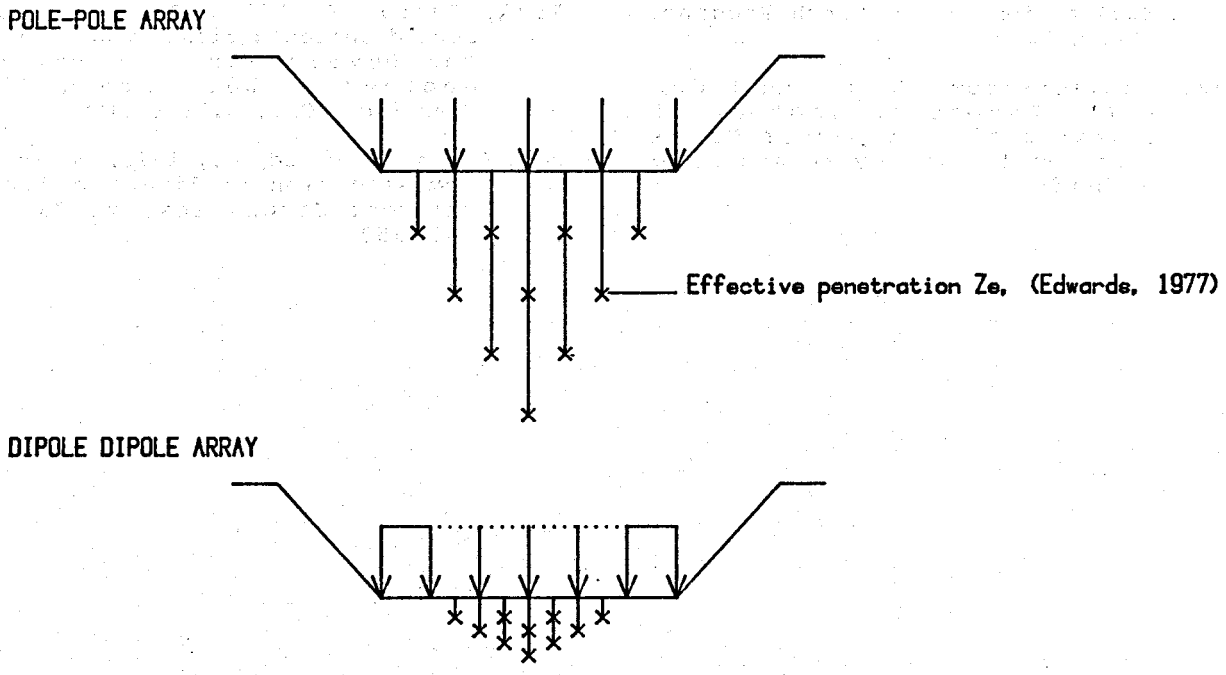


Fig. 3 Pseudosections comparing 2-D effective search in physically restrictive terrain.

four to six times per unit array length (Edwards, 1977, Roy and Apparao, 1971) when the length used for the pole-pole array is the distance between the on-grid operational electrode pair only (fig. 3).

The high density and multidirectional character of the accumulated data can be used for conventional anisotropy studies (e.g. Risk, 1975). Work is in progress to develop semi-automatic computer routines for statistical analysis of the data, toward objective 3-dimensional modelling.

At present, a 3-D version of the time-honored subjective examination of 2-D pseudosecctions is carried out using sets of plan and pseudosection drawings generated in the field using the receiver computer and an XY plotter. This permits a rapid availability of summary data to guide field operations.

The array design objective of increased vertical and lateral investigation in areas of extreme topography has been satisfactorily met; the interpretation opportunities provided by the dense data product represent a potentially powerful tool in dealing with complex exploration geometries.

References Cited

Edwards, L.S., 1977, A modified pseudosection for resistivity and IP: Geophysics, V. 42, p. 1020-1036

Nevin, Andrew E., Crandall, J.T., Souther, J.G., and Stauder, J., 1978, Meager Creek Geothermal System, British Columbia, Part I: Exploration and Research Program: this volume

Nevin Sadlier-Brown Goodbrand Ltd., 1974, Report on geothermal investigation at Meager Creek (unpubl) to B.C. Hydro and Power Authority

Nevin Sadlier-Brown Goodbrand Ltd., 1975, Report on detailed geothermal investigation at Meager Creek (unpubl) to B.C. Hydro and Power Authority, 18 pp.

Read, Peter B., 1978, Meager Creek geothermal system, British Columbia, Part II: Geology: this volume

Risk, George F, 1975, Proceedings, Second United Nations Symposium on the Development and Use of Geothermal Resources, San Francisco, Ca., p.1191-1198

Roy, A., and Apparao, A., 1971, Depth of investigation in direct current methods: Geophysics, v. 36, p. 943-959

THE HAWAII GEOTHERMAL PROJECT: AN AEROMETRIC STUDY OF MERCURY AND SULFUR EMISSIONS

B.Z. Siegel and S.M. Siegel

PACIFIC BIOMEDICAL RESEARCH CENTER AND DEPARTMENT OF BOTANY
UNIVERSITY OF HAWAII, HONOLULU 96822

ABSTRACT

Predrilling environmental baseline studies and extensive ongoing comparative aerometry in volcanic and rift areas have made it possible to characterize the University Experimental Geothermal Well (HGP-A) as a low-Hg, low-H_2S emitter and to account for high levels of Hg in the environs of HGP-A in terms of natural events and processes in Kilauea and the East Rift.

Work performed under National Science Foundation Research Grant GI-38319, Energy Research and Development Administration Research Grants E(04-3)-1093 and EY-76-C-03-1093, and by grants from the University of Hawaii's Environmental Center and Research and Training Revolving Fund.

The environmental program of the Hawaii Geothermal Project (HGP) was inaugurated in May 1975, coincident with final drill-site selection, and 7 months in advance of the December start of drilling operations. (Kamins, et al, 1976). Aerometric data collected from May to August, 1975, gave no indication of abnormal levels of H_2S or oxides of sulfur, nitrogen or carbon. These findings were not surprising, as the Kilauea East Rift was quiescent, and the closest readings carried only light and sporadic vehicular traffic in a rural setting. It was therefore somewhat surprising to find air Hg levels totalling 0.9 ± 0.4 $\mu g \cdot m^{-3}$ (by flameless atomic absorption spectrophotometry). This Hg consisted of Hg^0 vapor, trapped on gold foil and ionic species, presumably as halide salts (Siegel and Siegel, 1978). Similar total air values prevailed through June 1976, but when the well was first flashed, during July 1976, the ambient air Hg levels rose to 9.9 $\mu g \cdot m^{-3}$. Unfortunately there had been no opportunity to establish air levels during warm-up or pre-warmup phases or flow tests after drilling was completed in April 1976. Unknown to the HGP environmental staff, a long quiescent cone, Heiheiāhulu, located on the East Rift some 15 km SW of wellhead (HGP-A) had begun fuming in late spring of 1976. (Eaton, 1977). This site was shown to be an active source of Hg and H_2S. During the same period prior to flashing, air Hg levels at the Sulfur Banks fumerole area, 40 km WSW of HGP-A, reached nearly 50 $\mu g \cdot m^{-3}$.

It is virtually impossible to be familiar with the Island of Hawaii yet unaware of the proximity to HGP-A of a host of natural thermal sites. Nevertheless, a realistic assessment of the situation that yielded the high air Hg level when the well was flashed in July was only possible when the well was again scheduled for flashing after a nearly 2 month shutdown. On 31 October, prior to warmup, HGP-A ambient air yielded 16 $\mu g \cdot m^{-3}$ of Hg. During the warmup phase, 1-2 November, levels of 16-18 $\mu g \cdot m^{-3}$ were found, but on 3 November, after 4 hours flashing, the level had fallen to 7 $\mu g \cdot m^{-3}$, yet during the two weeks after the well was shutdown, values of 13-29 $\mu g \cdot m^{-3}$ were recorded.

The HGP-A baseline Hg level, varying around a mean of approximately 1 $\mu g \cdot m^{-3}$, is itself high, when compared with more representative air values of 0.003-0.030 $\mu g \cdot m^{-3}$ (McCarthy, 1970, Siegel and Siegel, 1975). This, taken together with other data that had accumulated by November 1976 suggested strongly that Hg measurements at HGP-A could not be interpreted without additional information about the activity status of the Kilauea system. This surmise was fully confirmed by (a) repeated direct measurement of Hg emission in steam condensate and (b) Hg aerometry before, during and after the Kalalua eruption of September 1977.

Expressed as emission, the steam plume releases as much as 10 $g \cdot 24\ hr^{-1}$ at well start-up but under stabilized flow conditions, approaches an asymptotic value of about $1g \cdot 24\ hr^{-1}$ (fig. 1). This may be compared with Environmental Protection Agency Emission Standards of 2300g or 1600g in 24 hr for coal-fired electric and incinerator facilities, respectively (EPA, 1976). A low Hg content of about 1 $\mu g \cdot \ell^{-1}$ is also characteristic of discharge waters (Kroopnick, et al, 1977).

The environmental impact of Kalalua eruption as reflected by Hg aerometry has been detailed elsewhere (Siegel and Siegel, 1978), but aspects of this study underscore the influence of natural process on the apparent quality of ambient air at HGP-A. (fig. 2 A and B).

Atmospheric Hg values about 1 km downwind from Kalalua crater and at the edge of Halemaumau Firepit in Kilauea are seen to rise to peak levels of 50-200 $\mu g \cdot m^{-3}$. The fumeroles (sulfur banks) followed, with an air maximum of slightly over 10 $\mu g \cdot m^{-3}$, and at HGP-A, which had been shut down for over 3 months, air Hg rose to about 5 $\mu g \cdot m^{-3}$ within two weeks following the onset of eruption activity. It is of interest to note in passing that the Heiheiahulu ambient exceeded 10 $\mu g \cdot m^{-3}$ on 30 July, some 6 weeks before the eruption began.

As noted the conspicuously high atmospheric baseline for Hg at HGP-A was not associated with high baseline values for other volcanic gases. This may be explained in part by the stability of Hg whether in elemental or oxidized form, allowing it to be transported long distances from source (Lockeretz 1974, Siegel and Siegel, 1978). An additional factor may be the presence of sulfur-free, Hg-rich natural emissions. A notable example is the Puhimau hot spot along the Chain-of-Craters Road in Hawaii Volcanoes National Park.

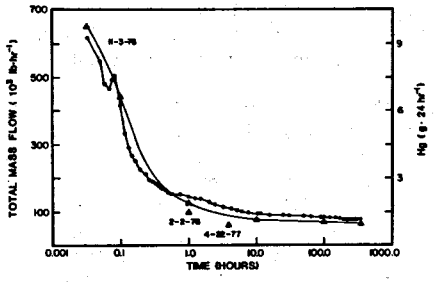


Fig.1 Rate of Hg emission from HGP-A in relation to mass flow. Solid circles (left ordinate) mass flow 11-3-76; solid triangles (right ordinate) Hg on 11-3-76; open triangles Hg on 4-22-76 and 2-2-78.

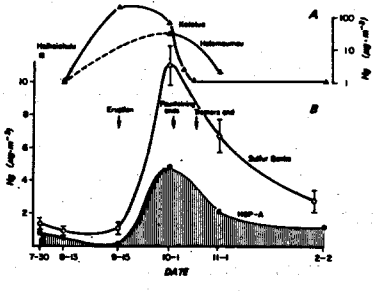


Fig. 2 Variation in atmospheric Hg during the course of the Sept 1977 eruption of Kalalua. Triangles-Kalalua and Halemaumau levels on graph A (right ordinate); circles and squares-levels at Heiheiahulu, Sulfur Banks and HGP-A on graph B (left ordinate). Standard errors are shown by vertical bars.

The site, approximately 40 km WSW of HGP-A appeared after a 1938 earthquake. More than 0.5 km^2 of surface is crusted and perforated with holes, remaining from decayed or partially decayed tree trunks. From these scores of holes nearly neutral Hg-rich steam and CO_2 are emitted but H_2S, SO_2 and SO_3 are consistently absent. At 2 m elevation above ground, Hg levels of 2-15 $\mu g \cdot m^{-3}$ were measured in 1976 and 1977.

Although the existence of H_2S and SO_2 sinks between fumerolic or volcanic sites and HGP-A cannot be overlooked as a possibility, we suggest that some of the emitted reduced forms of sulfur undergo oxidation to SO_3 (H_2SO_4) during transport. This idea is supported by reports of low pH and high sulfate in Hawaiian rainwater. (Eriksson, 1957), and the correlation of acid rains with volcanic activity (Kratky, et al 1974).

Unfortunately, little attention was given to H_2SO_4 during the earlier phases of the environmental program. In July and August, 1977, with HGP-A shut down, barium chloride/perchloric acid traps were deployed both around the wellhead and in natural fume areas of Kilauea, together with MSA and Bendix SO_2 detection tubes. At the wellhead and the nearest human habitation about 1 km to the West, levels of 250 $\mu g \cdot m^{-3}$ of H_2SO_4 were found without H_2S or SO_2. In contrast natural acid emissions ranged from 500-6,600 $\mu g \cdot m^{-3}$ and were accompanied by 3.5 to 5 ppm of SO_2, and by H_2S as well.

Although changes in well chemistry could not be ruled out at this early stage in development and reservoir assessment, necessitating continued surveillance for Hg and toxicants thus far absent such as As compounds, our principle concern became H_2S. At the wellhead during four trials when the well was flashed for at least one hr. the highest H_2S level found directly in the plume averaged somewhat more than 3 ppm. (fig 3A). Higher values, 5.5-7 ppm, were highly localized in low-lying steam over discharge waters during warmup and startup stages, but these fell off to the 3 ppm level as well. The wellhead and its environs fall below the occupational units for H_2S of 10 ppm for 8 hrs (Threshold Limit Value, State of Hawaii, 1977) and 20 ppm for 5 min.(Short-term Limit Value, State of Hawaii), although natural emission sites in the Hawaii Volcanoes National Park may be frequently in violation. The more general environmental effects of wellhead H_2S are a matter of distance (fig 3B). The air concentration decay of H_2S averaged for three steam flow tests shows a 3-fold reduction from wellhead to 30 m, and an overall reduction of about 10-fold (to < 30ppb H_2S) from wellhead to 100 m, both downwind. By comparison, the Sulfur Banks experimental sulfur well shows a higher output at source and steeper fall-off.

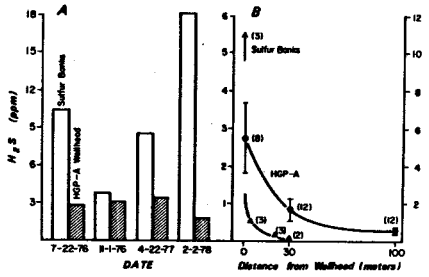


Fig. 3 Atmospheric H_2S levels. A compares the Sulfur Banks with HGP-A wellhead levels on four dates when well was flashed. B compares data for the fall-off in air H_2S with distance at the Sulfur Banks fumerole with data for HGP-A. Circles-HGP-A (left ordinate); Triangles-Sulfur Banks (right ordinate).

No detailed comparisons are needed to establish the fact that HGP-A is a remarkably clean geothermal source(Ellis, 1975, Sabadell and Axtmann, 1975, Siegel and Siegel, 1975), and is, hopefully, representative of the Kapoho Reservoir. The emissions chemistry is a matter of circumstance, but our ability to assess it accurately and realistically in its volcanic setting is a direct consequence of early, ie pre-drilling, baseline investigation, and the opportunity to carry out in-depth environmental chemistry on the natural thermal environments of Hawaii. A less comprehensive effort would have left the entire project vulnerable to the responses and reactions of the more sensitive environmentalists, and perhaps justly so.

The authors thank their students William Cade, Melvin Calvan, Pamela Lahne, Ann Larosa, Kapuanani Lee, Janet Phelan, and David Siegel for assistance in field and laboratory operations, and their colleagues Drs. Irving Breger, and Gordon Eaton, United States Geological Survey, and Dr. Gordon MacDonald, University of Hawaii, for their advice and encouragement.

REFERENCES

Kamins R, Chun M, Berger A, Bonk W, Siegel B, Siegel S, Speitel T, Lau S, Buddemaier R, Kroopnick, P and Hufen T. Environmental Baseline Study for Geothermal Development in Puna, Hawaii. Report to U.S. Energy Research and Development Administration. Hawaii Geothermal Project, University of Hawaii. September, 1976.

Siegel, S and Siegel, B. Water Air and Soil Pollut. In Press (1978).

Eaton, G. Personal Communication (1977).

McCarthy J, Meuschke L, Ficklin W, and Learned R. U.S. Geol. Survey Prof. Paper 713, 37 (1976).

Siegel S and Siegel B. Env. Sci Tech. 9, 473 (1975).

Environmental Protection Agency. National Emission Standards 121:0461 (1976).

Kroopnick, P, Buddemaier R, Thomas D, Lau S, Bills D, Siegel S, and Siegel B. Am. Geophys. Soc. Ann Mtg. Washington, May 30, 1977.

Siegel B and Siegel S. Env. Sci. Tech. In Press (1978).

Lockeretz W. Water Air and Soil Pollut. 3,17 (1974).

Ericksson E. Tellus IX, 4 (1957).

Kratky B, Fukunaga E, Hylin J and Nakano R. J. Env. Qual. 3, 138 (1974).

State of Hawaii. Hawaii Occupational Safety and Health Standards Act 57, 1972, Rev. Aug. 1977

Ellis, A. Amer. Sci 63, 510 (1975).

Sabadell J and Axtmann R. Env. Health. Perspect. 12,1 (1975).

GEOTHERMAL WELL COMPLETIONS: STATE OF THE ART

Robert E. Snyder

COMPLETION TECHNOLOGY COMPANY
HOUSTON, TEXAS

ABSTRACT

Present methods for completing steam and liquid dominated, dry rock, and geopressured geothermal wells are described by interpretive review of actual and proposed operations in The Geysers, Imperial Valley, the Valles Caldera, New Mexico project, and Louisiana-Texas geopressured zones. Limitations of technology and equipment that has been adapted from the petroleum industry to meet new and unique requirements of these downhole environments are objectively analyzed.*

Introduction

Geothermal wells present unique problems to completion engineers with backgrounds in the petroleum industry. The four basic types of development in the United States, steam and liquid dominated, dry rock and geopressured geothermal production, all produce water (or a form thereof) and heat. And all require high volume production, as heat recovery and profits are directly proportional to water flow. The producing "reservoirs" in each of these areas, however, are radically different, and the completion methods have very little in common.

The Geysers

Reservoir rocks in this area consist of dense, hard metamorphosed sediments that are competent enough to allow open hole completions. Natural, highly conductive fractures allow high volume flow of dry, superheated steam at 500°F (250°C) without need for stimulation by hydraulic fracturing or acidizing. After stabilization, steam is clean and there is no inflow of sand. The dry steam is non-corrosive.

The fractured rocks are highly sensitive to plugging by drilling mud and to contact with water, which condenses the steam and kills flow. Thus, the producing zone is drilled-in with air after cementing casing at a higher point. The reservoirs are substantially underpressured, containing typically 500 psi at 7,000 foot depths.

Wells are difficult to air drill because of abrasive rocks and high temperatures. Directional drilling is desireable but expensive. Since mud or completion fluids cannot be used and wells are not "killed", logging and evaluation techniques are limited by high temperatures. And well control from the time the drill string is pulled is less than desireable, with great reliance being placed on a single, large diameter valve. Large diameter casings can be weakened by improper drilling and wellhead operations, Fig. 1. Rubber type elastomers are very shortlived and are unreliable in seals and BOPs.

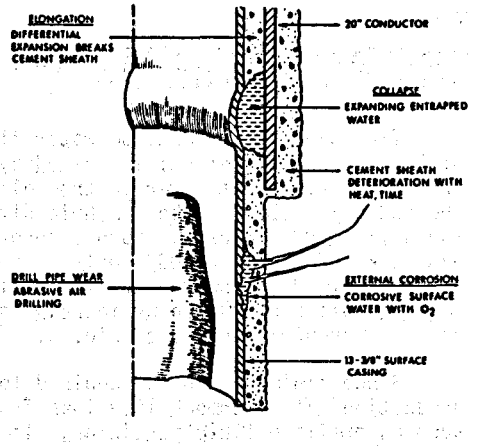


FIGURE 1

CASING PROBLEMS THAT CAN BE MORE SEVERE IN GEOTHERMAL WELLS DUE TO HIGH TEMPERATURES AND LARGE DIAMETER STRINGS COMMONLY USED.

Imperial Valley

Wells in this development are completed in very thick and prolific sandstones in a large Tertiary sedimentary basin. Maximum well depths are about 8,000 feet. Reservoir pressures are slightly less than hydrostatic and conventional drilling muds can be utilized. Drilling is relatively simple and directional wells can be completed from central locations to cut costs.

*Work performed under Sandia Contract 05-6199 sponsored by U.S. Department of Energy, Division of Geothermal Energy, 1978.

Wells are mechanically easy to complete. Circulating fluids temporarily control reservoir temperatures which can be moderate to very hot (350°F, 180°C to over 600°F, 310°C) to allow proper logging and use of packers, etc. for stimulations or treating. It is common practice to install very long sections of California-type liners in open hole below a section of plain liner that is cemented, Fig. 2.

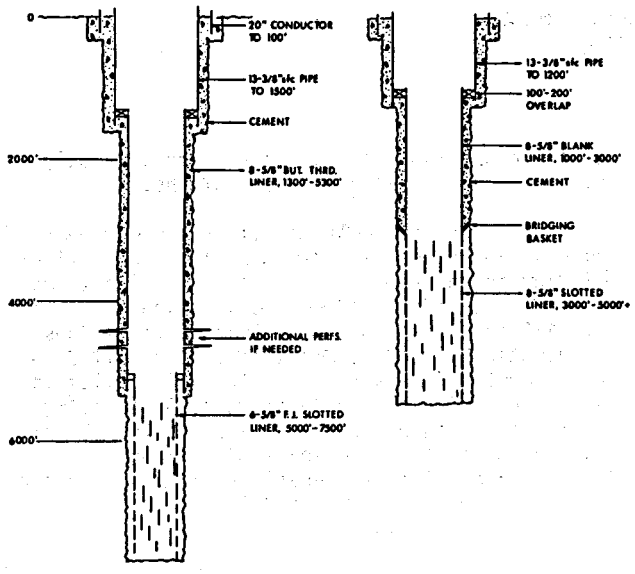


FIGURE 2

TYPICAL IMPERIAL VALLEY COMPLETIONS FOR TWO WELL DEPTHS. FULL CASING STRINGS OR TIE BACK CASING WOULD BE REQUIRED AS TUBING FOR INJECTION WELLS. LARGE DIAMETER SURFACE PIPE IS NEEDED FOR DOWNHOLE PUMPS.

The objective is maximum water flow with a small pressure differential created by the reduced density of hot water in the well. PIs of 250 bpd/psi at 200 psi bottom hole differential would yield 50,000 bwpd. Such a reservoir would have a kh of nearly 60,000 md ft, requiring 600 net feet of 100 md sand. Artificial lift systems improve well performance by increasing the bottom hole differential pressure, Fig. 3.

Since minimum skin is required for maximum production rate, permeability loss from damage such as drilling fluid particles, clay swelling, scaling across slots, or sand particle shifting cannot be tolerated. Such problems are becoming evident with increased development. Another major problem is injection well plugging by scale precipitates. Investigations are ongoing to find methods to either prevent particle dropout (Fig. 3) or filter out particles before reinjection.

Hot, dry rocks

The objective of this program, presently represented by the Valles Caldera project in New Mexico is to create a downhole heat exchanger in natural rock through which water can be pumped, to mine earth heat. Hydraulic fracturing techniques are required for volcanic type rocks in which fracture orientation can be controlled, or at lease defined, to allow well-well communication. This requirement parallels similar needs for improving reserve recoveries in low permeability petroleum reservoirs.

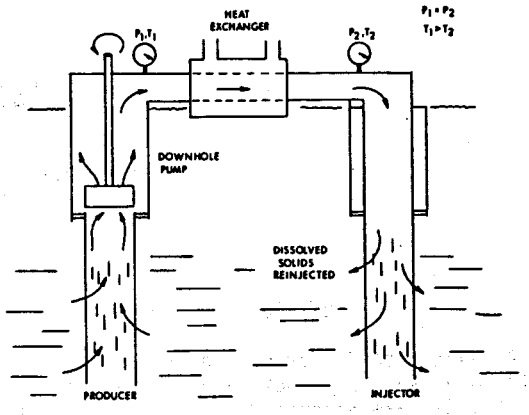


FIGURE 3

CLOSED, PRESSURIZED PRODUCING AND REINJECTION SYSTEM. DOWNHOLE PUMP ASSISTS NATURAL FLOW AND MAINTAINS WATER PRESSURE ABOVE THE FLASH POINT. SOLIDS ARE KEPT IN SOLUTION AND REINJECTED INTO THE PRODUCING RESERVOIR.

U. S. Gulf Coast Geopressured Geothermal Zone

This development is designated a geothermal project because the most obvious product is hot water. However the primary economic product is natural gas. These wells will be deep (up to 20,000 feet), hot (up to 400°F, 200°C), high pressured (up to 25,000 psi bottom hole), and expensive ($5 million). And there will be many drilling and completion problems. Geopressure (higher than hydrostatic) wells require multiple casing strings to control downhole zones with very steep pressure gradients. And hot water wells require large diameter tubing for highest flow, Fig. 4. The minimum requirement will likely be

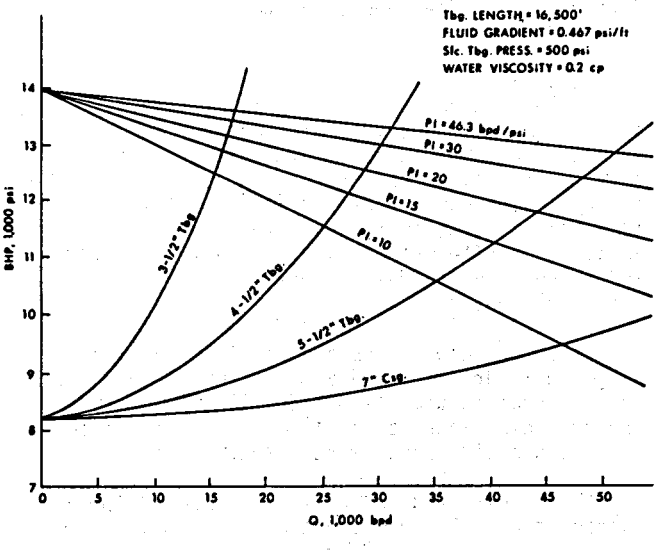


FIGURE 4

DATA BY R.M. JORDA

FLOW CAPACITIES FOR VARIOUS TUBING SIZES CONSIDERING FORMATION PI AND FRICTION LOSS IN NEW PIPE. NO METHANE BREAKOUT IN TUBING WAS ASSUMED. IN ACTUAL DESIGN THE BENEFIT OF TWO PHASE FLOW SHOULD BE CONSIDERED.

5-1/2 inch tubing, assuming no scale buildup.

Sand control may be required for reliable and productive completions and it will be difficult to install in high-density fluid environments (up to 18 ppg). Cementing is difficult as heavy slurries do not effectively displace thickened muds. High strength tubulars with corrosion and H_2S resistance may be required. Control of tubing movement with temperature change may be difficult, and reliable long-life seals between tubing and casing will be required.

If reinjection to the geopressured zone is proved to be a requirement for economic reservoir life, equipment to pressure brines to high surface injection pressure is presently not available and the power requirement would seriously cut already marginal net energy recovery.

References

1. Blair, A. G., Tester, J. W. and Mortensen, J. J., LASL Hot Dry Rock Geothermal Project, July 1, 1975-June 30, 1976, Progress Report LA-6525-PR, Los Alamos Scientific Laboratory, New Mexico.
2. Boyd, W. E., Completion Techniques for Geothermal - Geopressured Wells, Report for ERDA Contract E (40-1) - 5243, Center for Energy Studies, Univ. of Texas, 1977.
3. Chasteen, A. J., "Geothermal Energy on the Pacific Coast", 2nd UN Symp., San Francisco, May 1975, Vol. 2, pp. 1335-1337.
4. Cromling, J., "How Geothermal Wells are Drilled and Completed", World Oil, Dec. 1973, pp. 42-45.
5. Fertl, W. H. and Timko, D. J., How Downhole Temperatures, Pressures Affect Drilling, 10 part series reprinted from World Oil, Gulf Publishing Co., Houston, 1973.
6. Jones, P.H., "Geothermal and Hydrocarbon Regimes, Northern Gulf of Mexico Basin", Proceedings of First Geopressured Geothermal Energy Conference, Center for Energy Studies, Univ. of Texas, June 2-4, 1975.
7. Jorda, R. M., An Engineering Study of Water Reinjection for Geothermal Systems, Sandia Laboratories Contract 05-6199 Sponsored by DOE, Jan. 1978.
8. Kharaka, Y. R., Callender, E. and Wallace, R. H., Jr., "Geochemistry of Geopressured Geothermal Waters from the Frio Clay in the Gulf Coast Region of Texas", Geology, Vol. 5, April 1977, pp. 241-244.
9. Kruger, P. and Otte, C., Editors, Geothermal Energy Resources, Production, Stimulation, Stanford University Press, Stanford, CA, 346 pages, 1973.
10. Mathias, K., "The Mesa Geothermal Field - A Preliminary Evaluation of Five Geothermal Wells", UN Symp. (see Ref. 3), Vol. III, pp..1741-1748.
11. McGetchin, T.R., et al, Hot Dry Rock Geothermal Energy: Status of Exploration and Assessment, Report No. 1 of the HDR Assessment Panel, La-UR 77-1157, Los Alamos Scientific Laboratory, New Mexico.
12. Snyder, R. E., Geothermal Well Completions: An Overview of Existing Methods in Four Types of Developments, Sandia Laboratories Contract 05-6199 Sponsored by DOE, Jan. 1978.
13. Snyder, R. E., "How Steam is Produced and Handled at The Geysers", World Oil, June 1975, pp. 43-48.
14. Stuart, C. A., Geopressures, Proceedings of Second Symposium on Abnormal Subsurface Pressure, Louisiana State University, Jan. 30, 1970.
15. Suman, G. O., Jr., World Oil's Sand Control Handbook, Gulf Publishing Co., Houston, 1975.
16. Suman, G. O., Jr. and Ellis, R. C., World Oil's Cementing Handbook, Including Casing Handling Procedures, Gulf Publishing Co., Houston, 1977.
17. Geothermal Resource Investigations, East Mesa Test Site, Imperial Valley, California, Status Report, United States Dept. of the Interior, Bureau of Reclamation, April, 1977.

OAHU GEOTHERMAL EXPLORATION

José M. Souto

Colorado School of Mines
Golden, Colorado 80401

ABSTRACT

A geophysical reconnaissance of Oahu was carried out over two ancient calderas to evaluate geothermal potential. Electrical resistivity, microseismicity, and soil mercury surveys were carried out. The geothermal potential appears to be favorable in the Koolau caldera where high values of mercury in the soil are present along with low electrical resistivities.

Work performed under the auspices of the Office of Naval Research, Contract No. N00014-76-C-0750.

A combination of geothermal reconnaissance methods as used on Oahu, Hawaii, to determine the potential for the occurrence of geothermal energy. The presence of young volcanics and the position of Hawaii in the middle of the thin oceanic crustal plate are factors that favor the presence of a geothermal reservoir at commercial depths.

Earlier geophysical work has outlined two ancient magma chambers (Strange and others, 1965). These have distinct gravity and magnetic expressions which indicate the presence of dense material under calderas in the Waianae and Koolau ranges. Half of each caldera has been eroded away by the ocean.

The Honolulu series erupted in the vicinity of the Koolau caldera along parallel fissures oriented NE-SW. One lineation consists of Koko, Kalama, and Kapuo craters, which were last active 30 thousand years ago (Cox, 1966). A second lineation includes Diamond Head, Kaau, and Ulupau craters. This area was extensively studied with a variety of geothermal methods including electrical, seismic and geochemical surveys.

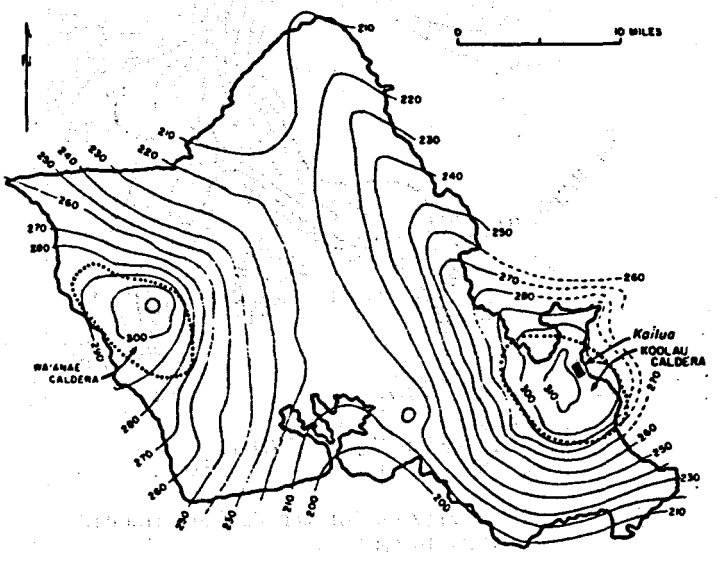


Fig. 1 Gravity map of Oahu after Strange and others, 1966 (MacDonald, 1970). Bouguer anomalies in milligals.

Deep electrical resistivity mapping is effective in locating low resistivity zones caused by temperatures. Keller (1975) proposes a variety of dipole mapping in which two intense dipole sources, oriented in mutually perpendicular directions, are used to energize the subsurface. The two orthogonal components of electric field are measured at distances ranging from 2 to 20 miles. Computer softwear has been developed for the artificial rotation of the sources, providing a variety of formats for presenting survey results. These include computations of minimum resistivity, average resistivity, conductance, and anisotropy.

In the Koolau caldera, electrical resistivity mapping was carried out using an intense DC source powered by a 50 KW generator, which was able to carry the signal through the strong cultural noise. Two perpendicular sources transmitted alternatively allowing four resistivity measurements for each receiver station occupied. Minimum and average resistivities calculated indicate a zone of low resistivity extending southward from Kailua

to Waimanalo, and higher values around Olomana Peak (Figure 2).

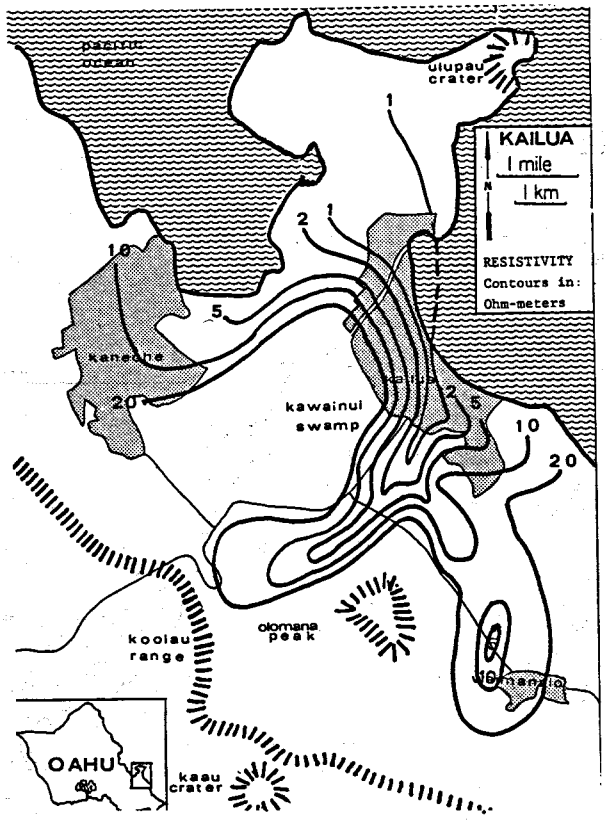


Fig. 2 Reisitivity map of the Koolau caldera. Contours in Ωm.

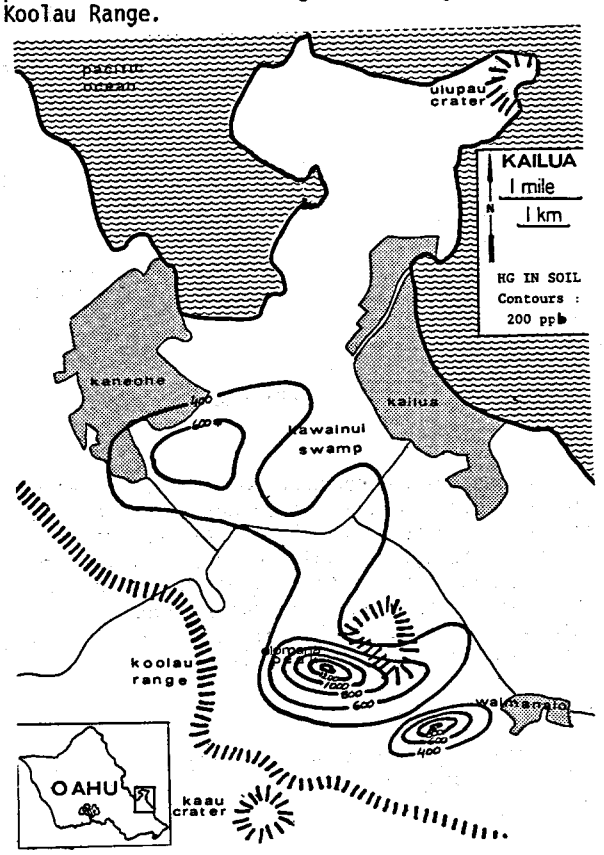


Fig. 3 Soil mercury content in the Koolau caldera. Contours in parts per million.

The presence of a geothermal reservoir can also be detected by measuring the mercury content of soil (Gutsalo, 1975),(Matlick, Bussek, 1975). Soil mercury analysis carried out in this island showed values as high as 1400 ppb in the Waimanalo Valley (Figure 3).

A microseismic survey was also carried out during 20 days in the Koolau area. High noise levels were encountered due mainly to cultural or human noise and surf action. No events were identified as occurring within either the Waianae or the Koolau calderas.

Conclusions

The geothermal surveys centered about the Koolau Range indicate a zone where low resistivities and high mercury content coincide. These anomalies lie southward the Koko Head fracture zone. The absence of microseismic activity must be considered a negative factor with respect to the possible existence of a geothermal system in the Koolau Range.

The possiblilties of latent heat at the roots of the Honolulu series events is supported by the electrical and geochemical surveys. These geothermal indicators should lead to further surface exploration on both Waianae and Koolau calderas, but the only way to confirm the geothermal potential of Oahu will be through the drilling of an exploratory well.

BIBLIOGRAPHY

Furumoto, A.S., 1976, Prospects for geothermal energy on the Island of Oahu, Hawaii: Geothermal Energy Mag., v. 4, June.

Gutsalo, L.K., 1975, Helium Isotopic Geochemistry in thermal waters of the Kuril Islands and Kamchatka, II UNSGD.

Keller, G.V., Furgerson, R., Lee, C.Y., Harthill, N., and Jacobson, J.J., 1975, The dipole mapping method: Geophysics, v. 40, no. 3, pp. 451-472.

MacDonald, G.A., and Abbot, A.T., 1970, Volcanoes in the sea: Univ. of Hawaii Press, Honolulu, 441 pp.

Matlick, J.S., III, and Buseck, P.R., 1975, Exploration for geothermal areas using mercury, a new geophysical technique: 2nd UN Symposium on the Development of Geothermal Energy, San Francisco.

Souto, J.M., 1977, Exploration for geothermal energy in Oahu, Hawaii, CSM thesis 1977, Golden, Colorado.

Strange, W.E., Machevsky, L.F., and Woollard, G.P., 1965, A gravity survey of the Island of Oahu, Hawaii: Pacific Science, v. 19, pp. 350-353.

Tasci, T., 1975, Exploration for a geothermal system in the Lualualei Valley, Oahu, Hawaii: CSM Thesis T-1743, Colorado School of Mines, Golden, Colorado.

SOIL COOLING FOR GEOTHERMAL ELECTRIC POWER PLANTS IN THE WESTERN UNITED STATES: THE RAFT RIVER EXPERIMENT

N. E. Stanley, D. L. Slegel and W. D. Gertsch

EG&G IDAHO, INC.
IDAHO NATIONAL ENGINEERING LABORATORY
IDAHO FALLS, IDAHO 83401

Increasingly, the availability of water through either new appropriations or purchase is being recognized as a constraint in Western energy development. Several oil shale and coal gasification projects have already confronted the questions of where and how to get the necessary water supplies to support commercial-sized plants. Since most of the known geothermal resources are located in Western areas which experience chronic water deficiencies, widespread implementation of geothermal technology in electric and direct-use applications must ultimately address the water supply question. In direct-use applications, every attempt must be made to use the geothermal fluid wisely following a primary heat extraction process. In electric applications, the issue of major importance concerns the rejection of from 85 to 90% of the total heat from power plants. Moderate-temperature geothermal electric power production is particularly handicapped compared to fossil-fueled or nuclear power plants, as indicated by this comparison:

Power Plant	Discharge Heat Electrical Output	Estimated Annual* Water Use (Cubic Meters/year)
Coal	1.5	18,500,000
Nuclear (LWR)	2.0	27,100,000
Geothermal (Geysers type)	4.0	61,700,000
Geothermal (Raft River 143°C binary cycle)	7.0	172,700,000

* 1000 MW plant, 80% load factor

Costs and power requirements of both conventional and fluidized-bed dry cooling towers suggest that neither will be cost effective or competitive in the foreseeable future.

A recent research effort to gauge the regional water use requirements of geothermal development presents a pessimistic conclusion.[1] The Department of Energy's "Forecast 2" energy-demand and fuel-supply scenario postulates the somewhat implausible possibility of about 30 GWe geothermal electric capacity in the 17 western states by 2000. More conservatively, Bloomster and Engle[2] used a linear programming-optimization technique under different competitive scenarios, estimating the installed geothermal electric capacity might be between 9 and 17 GWe by 1990 and between 28 and 65 GWe by 2015. Using these estimates, it is plausible to expect a 15 to 20 GWe geothermal electric production capacity sometime near the turn of the century, of which 20% might be of the Geysers and Roosevelt Springs quality, and the remainder from the moderate-temperature reservoirs identified throughout the West by USGS Circular 726. Assuming that evaporative cooling towers will be used, this suggests a regional annual water requirement of perhaps 2220.3 to 2960.4 million cubic meters. Without other intervening factors, this requirement by itself would seem to prsent an imposing constraint on geothermal electric development. Obviously, there is a necessity for new water-conservation measures and technological innovations.

Soil-cooling systems may be a viable alternative to evaporative cooling towers. While impractical for large fossil-fueled plants, buried pipe grids may be feasible for 50 to 100 MW geothermal power plants. In many locations, this alternative may be economically more attractive, use less water, yield a secondary income from surface crops, and offer environmental advantages.

EG&G Idaho, Inc. as part of its activities performed for the Department of Energy's Division of Geothermal Energy located at DOE's Idaho Operations Office, is conducting a three-year experiment to study the technical and economic feasibility of using heat dissipation-soil warming systems to reject heat from modular-sized geothermal power plants in cool desert regions. The project focuses on two areas of study. First, a computer program is being developed to model the performance of soil cooling systems. Second, field studies are being conducted to evaluate the performance of an underground pipe system installed at the Raft River Geothermal Test Site in south-central Idaho.

Direct extrapolation of the experimental field data to large-scale heat dissipation-soil warming systems would be difficult, at best. At Raft River, the approach taken is to use the experimental data to assess the accuracy of a computer program which models heat and mass transfer in soils. Given sufficient accuracy (or agreement between predictions and field data), the computer program would then be used to model proposed large-scale systems in order to assess their feasibility and potential benefits.

The computer program being developed for the Raft River experiment is similar to an existing program which was developed to model transient two-dimensional heat and mass transfer in soils and has been used to model continuous operation of soil warming systems using waste heat from nuclear power plants.[3] The program uses available information on soil type, depth and spacing of heat sources, heat source temperature, and climatological data to solve equations modeling heat and moisture transfer in soils. Results obtained to date have been predicted soil temperature and moisture-content distributions, estimates of increases in the length of the growing season for crops, design guidelines for soil warming systems,[4] and estimates of the total land surface required to dissipate a given amount of energy. Figure 1 presents a typical soil-temperature distribution.

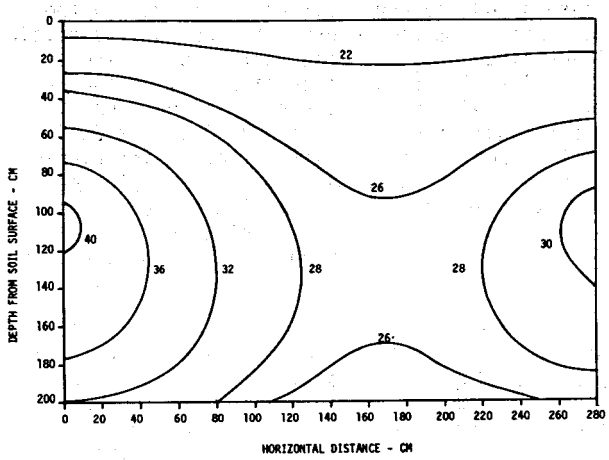


Fig. 1 Isotherms (°C) for August conditions, pipe spacing of 280 cm and pipe depth of 100 cm. The left pipe temperature was 41 °C, while the right was 31 °C.

Figure 2 presents a typical seasonal variation in predicted soil temperature, using the computer program. Once its accuracy is verified, the computer program will be used to predict soil temperatures and heat dissipation rates, thereby providing estimates of the size and potential benefits of heat dissipation-soil warming systems using rows of buried pipes to dissipate the heat from geothermal electric power plants. Results from the computer-program development, winter-spring system operation, and crop responses will be available for reporting at Hilo.

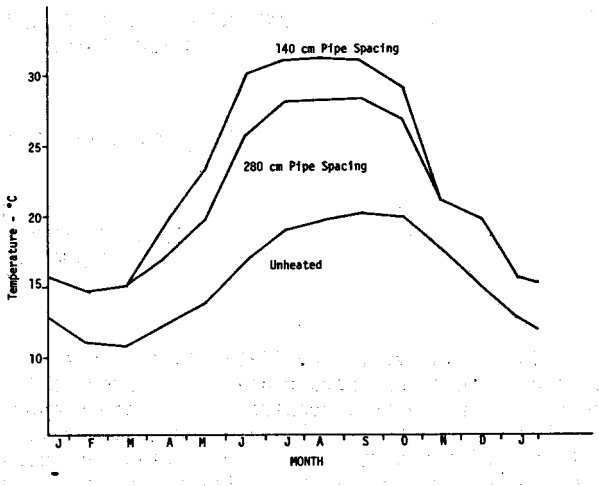


Fig. 2 Simulated annual temperature variation at 20 cm depth. Pipe depth is 50 cm.

The field layout involves three experimental plots, 24 meters wide by 152 meters long, two of which are heated by dissimilar configurations of PVC pipe, buried 0.6 meters beneath the soil surface. The remaining plot is unheated and serves as a control plot. Warm geothermal water, simulating power plant condenser discharge, circulates through the grid while heat dissipation rates and soil temperatures are monitored. In the near future, the heat-dissipation system will be linked to an operational 60-kW binary fluid geothermal power plant currently under construction.

Apparent soil thermal conductivity is influenced by properties of the solid materials, texture, temperature, and water content. In general, thermal conductivity increases with soil moisture content and particle size. In order to evaluate the heat transfer properties of different pipe-soil interfaces and to inhibit the formation of a "baked," insulating jacket of soil around the pipes, the soil heat-dissipation system incorporates the use of sand envelopes around some pipes and employs sub-surface irrigation tubes above several pipes in each configuration (Figure 3). The heat dissipation and soil temperature data will be used to validate the computer model and to correlate crop responses to warmed soils.

It has been demonstrated by Boersma[5], Mays[6], Allred[7], and others that selected field crops respond favorably to warmed soils in their root zones. In many locations, if geothermal power-plant waste-heat rejection were accomplished with soil warming systems, crop growth and development rates could be accelerated, and the water conserved would more than satisfy crop irrigation requirements.

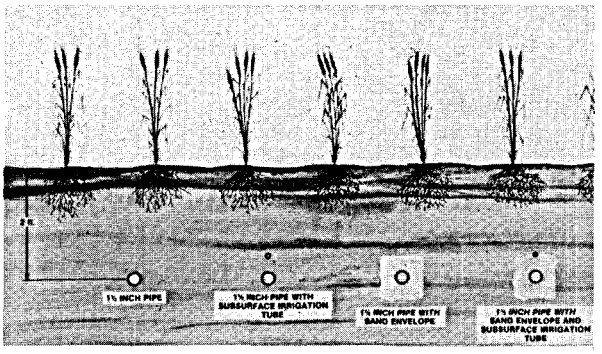


Fig. 3 Cross section of heat-dissipation soil warming plot showing the combinations of pipe-soil interfaces.

A variety of field, vegetable, and tree crops is being cultured on the experimental open-field plots. The crops are adapted to the Raft River climate and are tolerant of saline soils and water. Accepted intensive-management techniques are being used to culture barley, sugar beets, alfalfa, forage grasses, garden vegetables, and trees. Researchers are examining plant germination, emergence, growth rates, maturation, water requirements, plant-soil relationships, and yield data to assess the agricultural economics of the soil heat-dissipation concept and to develop appropriate management practices to maximize productivity.

The experiment will provide information useful to a variety of locations, especially those where the development of both agriculture and power plants are limited by the amount of available water.

REFERENCES

1. R. G. Palmer, W. D. Gertsch, et al, Water for Energy in the West: An Analysis of the Impact of Federal Energy Supply and Demand Projections, Los Alamos Scientific Laboratory (June 1977-draft), final report in preparation.

2. C. H. Bloomster and R. L. Engel, The Potential Benefits of Geothermal Electric Production from Hydrothermal Resources, BNWL-2001.

3. D. L. Slegel, L. R. Davis, "Transient Heat and Mass Transfer in Soils in the Vicinity of Heated Porous Pipes," ASME Journal of Heat Transfer, 99 (November 1977) pp 541-546.

4. D. L. Slegel, Design Guidelines for Agricultural Soil Warming Systems Utilizing Waste Heat, EPA-600/3-76-026 (March 1976).

5. L. Boersma, K. A. Rykbost, H. J. Mack, W. C. Schmisseur, Crop Response to Warming Soils Above Their Natural Temperature, Oregon State Univ. Ag. Exp. Station Special Rpt. 385 (1974) pp 98.

6. D. A. Mays, TVA's Experiences with Soil Warming, Oregon State Univ. Eng. Exp. Station Circular 49 (1975) pp 87-90.

7. E. R. Allred, V. R. Gilley, L. L. Boyd, P. E. Read, Use of Waste Heat for Soil Warming and Frost Protection of Field Crops in Northern Climates, Oregon State Univ. Eng. Exp. Station Circular 49 (1975) pp 90-96.

MAGMA AS A GEOTHERMAL RESOURCE - A Summary

H. M. Stoller
J. L. Colp

SANDIA LABORATORIES
ALBUQUERQUE, NM 87185

INTRODUCTION

The objective of the Magma Energy Research Project under way at Sandia Laboratories is to assess the scientific feasibility of extracting energy directly from deeply buried circulating magma sources. The USGS has estimated that the energy contained in molten and partially molten magma within 10 km of the surface within the U.S. at 5×10^{4} quads. Methods of energy extraction under consideration include: the insertion of a heat exchanger into a magma source with surface conversion to electric power; and utilizing the reducing nature of magma to produce transportable fuels such as hydrogen and methane. Technical elements of the Magma Energy Research Project include:

Source location and definition - the development, demonstration and verification of exploratory techniques for locating and defining molten rock sources.

Source tapping - the assessment of the deep-rock, near-magma environment and the technology to drill into molten rock sources.

Magma property and materials compatibility - the definition of in situ properties of magma and the evaluation of engineering materials subjected to that environment.

Energy extraction - the examination and development of processes and systems capable of extracting energy from magma sources.

SOURCE LOCATION AND DEFINITION

Critical to the project is developing the ability to locate and identify a source of molten rock in the subsurface. Characteristics of interest are its depth, its areal extent, and its general form (whether in a homogeneous pool or in a honeycomb of crevices filled with molten material). Although many methods have been developed for the remote sensing of various geologic structures, until recently none of these methods have been directed intentionally toward locating magma sources.

To evaluate the ability of a variety of geophysical sensing systems to identify buried molten rock, Sandia conducted a Molten Lava Sensing Experiment starting in March 1976. The still-molten lense in Kilauea Iki Lava Lake (a prehistoric pit crater located in the Hawaii Volcanoes National Park that was partially filled with lava during a 1959 eruption) is the only known location of buried molten rock in the U.S. and was selected as the experiment site.

The experiment was divided into three sections. The first used active and passive seismic sensing systems. A series of twenty active seismic observations were made. The second section evaluated electrical and electromagnetic sensing systems. The last section assessed an audio magnetotelluric sensing system.

Two supplemental sensing experiments were run. One was a fine mesh grid passive seismic survey of the northeast quadrant of the lava lake. The other was an active seismic survey using downhole sensors and explosive sources.

The data from the experiments are still being analyzed. Preliminary results from the various systems were in fairly general agreement on the definition of the areal extent of the molten lense. The evaluation of the depth and thickness of the molten lense was unclear. This lack of clarity results from not having accurate values of physical properties of the molten rock.

For an evaluation of the sensing systems, it is necessary to get data on the dimensions of the molten lense by drilling. In 1976, two holes were drilled with the cooperation of the Hawaiian Volcano Observatory. Conventional rotary drilling was used with diamond core bits and water as the drilling fluid. Each was drilled through the overlying crust to the molten rock interface at a depth of 149 feet. One hole penetrated the molten rock to a depth of 30 inches until it encountered a solid obstruction. While this constituted the farthest penetration ever achieved in magma, this drilling approach was unable to define the dimensions of the molten lens.

A Lava Lake Drilling Program was instituted. The objective was to design and develop a system capable of drilling through solid obstructions while the drill stem was surrounded by 1070°C molten rock. It should be emphasized that this study was aimed specifically at the conditions represented by Kilauea Iki.

Two drilling systems have been selected for the 1978 lava lake drilling experiment. The first uses a drag bit made of a high temperature resistant material so that it can drill uncooled

while being driven by an insulated drill stem. The outer part of the insulated drill stem remains at a temperature near that of the molten rock to minimize the amount of rock that is chilled onto its exterior. The inner pipe is air-cooled to permit it to carry the torque required to drive the bit. An alternate system that will be experimentally examined uses a high pressure, low volume water jet propelled ahead of a conventional bit and drill stem to solidify the molten rock.

SOURCE TAPPING

The Magma Energy Research Project as presently funded is not intended to develop deep-drilling methods in the high-temperature magma environment. It is focused on associated problems.

Little is known about the physical properties of rocks at elevated geostatic pressures and temperatures close to a magma source. Two basic questions must be answered: will a hole through such a hot plastic material stay open and are there methods for keeping it open so that the heat exchanger equipment can be inserted through it into the magma source?

To answer these questions, a research program at the Center for Tectonophysics at Texas A&M University to investigate the physical properties of rocks under dynamic stress conditions at pressures up to 5 kbar and at temperatures of approximately 1000°C is being conducted. Preliminary results indicate that for dry Mt. Hood andesite and dry Charcoal Granodiorite instantaneous failure-strengths and stresses likely at the walls of open and water-filled boreholes as deep as 10 km are not likely to fail under short-time loading even at 1000°C, unless the horizontal stress is $\geq$ vertical stress and the hole is open.

MAGMA PROPERTY AND MATERIAL COMPATIBILITY

Magma is a high-temperature, highly corrosive environment. Information must be obtained about the character of this environment and its effects on engineering materials. Three rock types were chosen as standards for magma/material compatibility laboratory tests. The simulants chosen were Hawaiian Tholeiite, Mt. Hood Andesite, and Newberry Rhyolite Obsidian.

Magmas contain volatile elements which can form a separate volatile-enriched gaseous phase at pressure appreciably above atmospheric pressure. A set of computer codes has been developed to calculate equilibrium distributions in multi-component gas mixtures characteristic of magmatic volatiles over a wide range of specifiable conditions. The calculations can be carried out treating the gas phase as an ideal or non-ideal mixture. Non-ideal properties are calculated from measured P-V-T data, if available, or from a corresponding state version of the Redlich-Kwong equation. The equilibrium distributions can be calculated at a specified temperature and pressure for a full set of mass balance constraints, or one or more mass balance constraints can be replaced by fixed fugacities or activities.

Early laboratory tests on the interaction of various representative alloys with degassified molten Hawaiian tholeiite indicated that a good correlation could be made between reactivity and the free energies of formation of the various metal oxides. These data further indicate that the Ni- and Co-based alloys may have special qualities in regard to survivability in the magma environment.

Metal samples have been exposed to fumarolic gases from various vents in Kilauea caldera, Hawaii, and Mt. Baker, Washington. In general, stainless steels are attacked fairly rapidly in the fumarole environment while nickel-base alloys such as Inconel, Rene-41, and Hastelloy-C are resistant.

The Magma Simulation Facility, an experimental apparatus capable of studying molten rock reactions and material compatibilities at pressures up to 4 kbar and temperature up to 1600°C, has been designed. The uniqueness of this facility is the size of its experimental chamber, $4\frac{1}{2}$ inches in diameter by $7\frac{1}{2}$ inches high. Start-up operations will be initiated in FY'80.

ENERGY EXTRACTION

The convection and heat transfer processes operational in molten rock at extremely high geodynamic pressures must be understood before suitable energy-extraction methods can be devised. A study of possible heat extraction rates from a magma reservoir has been completed. Estimates of the heat extraction rates ranged from a low of 1 kW/m^2 to a value of 175 kW/m^2. The 1 kW/m^2 figure corresponded to the rate expected from a conduction-dominated reservoir at the end of a 30-year period. The higher figure of 175 kW/m^2 was typical of a reservoir with convection.

A small, single-tube boiler to study heat extraction from a molten lava source has been tested in 0.2 m^3 of Hawaiian tholeiitic lava melted in an induction furnace. Two test runs showed that high heat extraction rates (100 kW/m^2 to 300 kW/m^2) could be obtained from a molten lava heat source. Corrosion or failure of the heat exchanger due to thermal effects was not a problem even though the temperature of the molten lava core (1450 to 1650°C) was well in excess of the melt temperature of the heat exchanger. The test data verified assumptions in the heat transfer calculations, particularly in the convection calculations and the calculations for the transient thermal insertion problem. The test demonstrated that useful amounts of thermal energy in the form of high-quality steam can be extracted from a molten lava heat source.

A Long Tube Heat Exchanger facility has been designed and constructed for larger scale tests. This facility consists of a 20-meter long vertical electrically heated furnace enclosing a single-tube boiler. The internal configuration can be changed to incorporate a number of experimental setups. The facility is being used to study the basic dynamics of long tube, vertical boiling.

The next step in the energy extraction studies is to move from the laboratory into field experiments in molten rock. A long-tube boiler experiment inserted into a lava lake is planned. The objectives are to measure (1) the dynamic mechanical and thermal changes on the buried molten rock body resulting from induced cooling (thermal energy extraction), and (2) the dynamic effects of the hostile environment of buried molten rock on the test (energy extraction) equipment.

Thermodynamic calculations and experimental studies of the potential of magma and hot rock for the production of fuels (H_2, CO, CH_4O) indicate that fluids containing one to three mole percent hydrogen are possible from the interaction of water with typical basaltic magmas or hot rocks in the temperature range 1300°C to 600°C. Fuel production can be enhanced by addition of organic matter to the injected aqueous fluid. If organic additions are sufficiently large, fuels can be generated directly from the fluid mixtures using only the thermal energy of the magma or hot rock. For example, thermodynamic calculations show that mixtures containing 10 weight percent cellulose ($C_6H_{10}O_5$) and 90 weight percent H_2O produce fluids with 5 percent CH_4 and H_2 at hot rock temperature (600°C) and 12 percent H_2 and CO at magmatic temperatures (1200°C).

The magma-fuel concept is considered as a part of the overall Magma Energy Research Program under way at Sandia Laboratories. If fuel production from magma can be made practicable, it could provide a sizable increment in the total energy extractible from magma.

THE ROLE OF THE U.S. GEOLOGICAL SURVEY IN THE FEDERAL GEOTHERMAL LEASING PROGRAM

Reid T. Stone, Henry L. Cullins, and Max D. Crittenden

U.S. Geological Survey, Menlo Park, CA

Introduction

The role of the Geological Survey in the Federal Geothermal Leasing Program is basically defined by the Geothermal Steam Act of 1970[1/], and precedents established by administration of the Mineral Leasing Act of 1920[2/]. The geothermal leasing program of the Department of the Interior has as its objectives: (1) orderly and timely resources development; (2) protection of the environment; and (3) receipt of fair market value for the leased mineral resources. Both the Geological Survey and the Bureau of Land Management have major responsibilities to ensure that those objectives are met.

The Bureau of Land Management as the Department's surface resource manager for Federal lands is responsible for issuing mineral leases and licenses to applicants. This responsibility includes maintaining the official records in leasing matters. A memorandum of understanding[3/] between Interior Bureaus defines each Bureau's responsibilities and advisory roles in the geothermal leasing program.

The Geological Survey as the Department's mineral resource manager for Federal lands is responsible for the geologic, engineering, economic value determinations, and supervision of lessee operations. These responsibilities include parcelling of leasing tracts, determination of bond values, establishment of royalty and rental rates, resource evaluations, and reserve calculations. Also included are reviews of investment costs for diligent development and minimum production requirements, and those actions relating to supervision over the area of operations within a lease. The responsibilities of the Geological Survey are both administrative and regulatory since the Federal government is both a landlord and a regulator.

The effect of the Department of Energy with its newly created legislative authority is yet to be determined through either regulation or mutual agreements between the involved agencies. At this time it does not appear that major changes will be made in Geological Survey responsibilities as that role relates to administration of the Geothermal Steam Act.

Figure 1 summarizes major agency coordination efforts in lease management responsibilities. Figure 2 identifies major Geological Survey elements and their relationship to leasing responsibilities.

GEOTHERMAL LEASING PROGRAM
AGENCY COORDINATION

RESOURCE CLASSIFICATION: LEAD - *U.S. Geological Survey*
SUPPORT - *U.S. Bureau of Land Management*

	PRE-LEASE	ISSUANCE	POST-LEASE
LEAD	*U.S. Bureau of Land Management (BLM)*	*BLM*	*U.S. Geological Survey (USGS)*
CONCURRENCE	*U.S. Geological Survey (USGS)* *U.S. Forest Service (USFS)* *Dept. of Energy (DOE)*	*USGS* *USFS*	*BLM* *USFS*
ADVICE AND SUPPORT	*U.S. Fish & Wildlife Service (USFWS)* *State Agencies (SA)* *Local Agencies (LA)* *Private & Public Interested Parties (PP)*		⊗ *GEAP* *DOE* *SA* *LA* *PP*

⊗ *GEAP - Dept. of Interior Geothermal Environmental Advisory Panel*

FIGURE 1.

1/ Geothermal Steam Act of 1970, Public Law 91-581, Dec 1970

2/ Mineral Leasing Act as amended, 30 U.S.C. 181 et seq., 1920

3/ Memorandum of Understanding for the Geothermal Program (Tripartite Agreement), USGS-BLM-USF&WS, June 1976

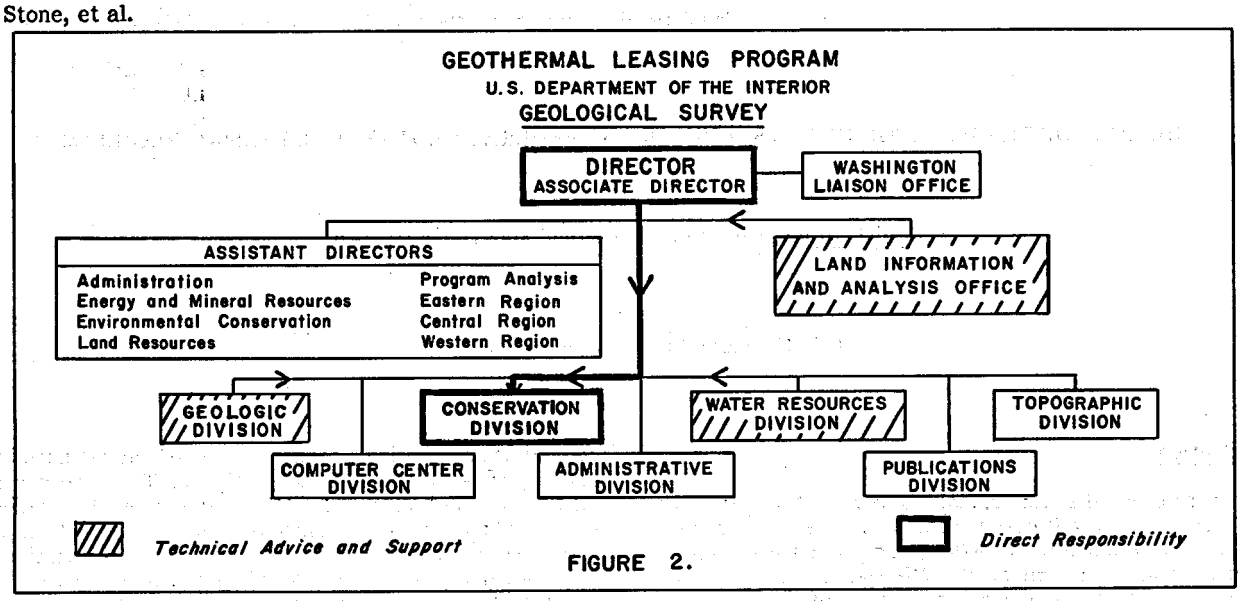


FIGURE 2.

Preleasing Activities

At annual planning workshops Federal agencies having significant program responsibilities determine leasing priorities with recommended schedules for leasing actions. The major agencies are the Department of the Interior (Bureau of Land Management, Geological Survey, U.S. Fish & Wildlife Service), Department of Agriculture (U.S. Forest Service), and Department of Energy. Criteria used in determining leasing priorities are geothermal potential, mineral land classification status, environmental considerations, legal constraints, and industry interest. The Bureau of Land Management, as the lead Bureau, establishes the leasing schedule and goals for the next planning (usually 3-year) period.

Even though unforeseen problems and conflicts alter many lease sale schedules, the establishment of such planning goals is basic to the efficient allocation of budget and manpower requirements for an effective leasing program. Other basic preleasing activities include: (1) the Geological Survey determination of the mineral land classification status, establishing the means of leasing; (2) establishment of the legal status of the lands and resources; and (3) preparation of the environmental analyses and related documents to meet the requirements of the National Environmental Policy Act of 1969 (NEPA).

The Geological Survey is responsible for classifying[4/] lands where the geothermal indicia or identified competitive interests require leasing by competitive procedures (sealed bidding). Land in this category is designated as a Known Geothermal Resources Area (KGRA). Land not in a KGRA may be leased by noncompetitive procedures. The mineral land classification function is delegated to the Area Geologist in consultation with the Geothermal Supervisor, with classification-action approval by the Regional Conservation Manager, Conservation Division, U.S. Geological Survey (Fig. 3). All

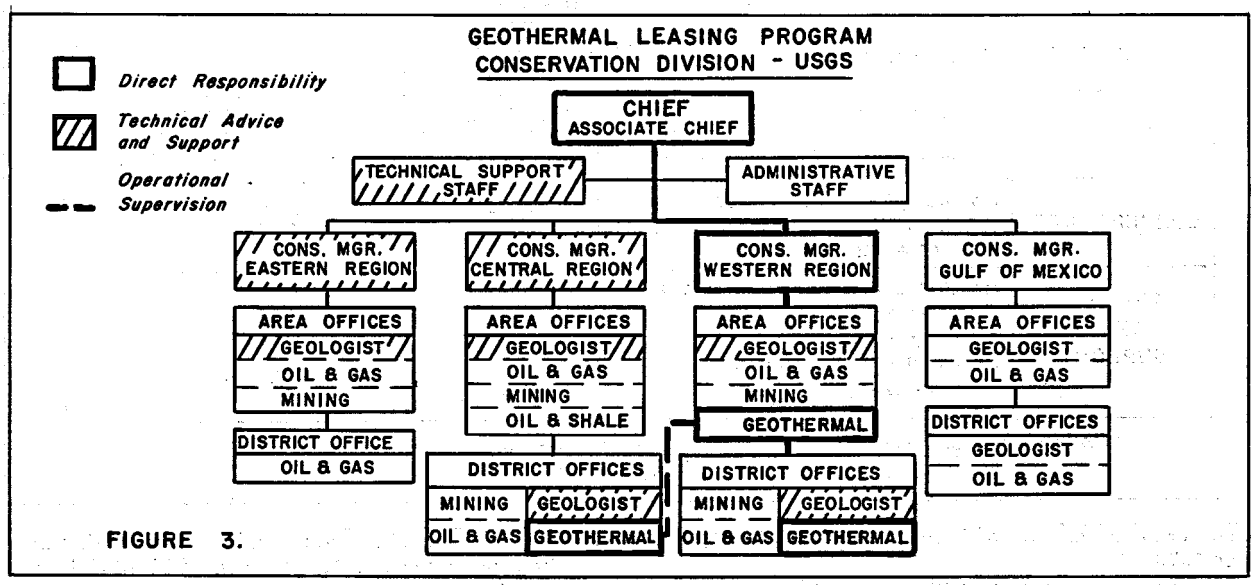


FIGURE 3.

4/ L. H. Godwin and others, 1971, Classification of Public Lands Valuable for Geothermal Steam and Associated Geothermal Resources: U.S. Geological Survey Circular #647, 18 p.

available information, both public and proprietary, including preliminary exploration activities, is evaluated prior to establishment of a mineral land classification action. Other Geological Survey staff members, such as those in the Geologic and Water Resources Divisions, frequently furnish geologic reconnaissance, field investigations, water analyses, and other data (Fig. 2) in support of the Conservation Division's responsibilities.

The Geological Survey also has the authority to revise KGRA classifications in those instances where resource data or competitive interest no longer justifies that classification. The Departments of Interior and Energy are now developing procedures and regulations for handling lands that have been removed from a KGRA classification. It is proposed that the Geological Survey will place a notice of the reclassification in the Federal Register. The Bureau of Land Management will then accept applications for leasing of those lands under a modification of their simultaneous filing procedures (43 CFR 3211) for processing previously leased non-KGRA lands.

Determination of the legal status of the geothermal resource is primarily a Bureau of Land Management function in regard to a clear title to the resource. Potential conflicts with the use of surface resources can involve other agencies, particularly the Forest Service. Those surface-managing agencies directly responsible for administration of any specific area must concur in any proposed action involving lands under joint jurisdiction. The Geological Survey's responsibility in dealing with legal matters involving other mineral values or the effect of potential geothermal development is advisory. The Geological Survey provides recommendations for appropriate leasing stipulations thus allowing multiple use or concurrent development of several resources. These recommendations are provided to the Bureau of Land Management by the Geothermal Supervisor with advice from the Area Geologist.

The Bureau of Land Management, as the lead Bureau, prepares the environmental assessments necessary for a decision as to lease issuance on lands under their jurisdiction. The Forest Service prepares the document for Forest Service lands. Generally, these documents are completed on a geographic area (for example Imperial Valley) and include both competitive and noncompetitive leasing areas. Where Forest Service and Bureau of Land Management lands are both involved, a joint evaluation is usually completed. The assessment may take the form of an Environmental Assessment Report (EAR) or an Environmental Impact Statement (EIS). An EIS is prepared when it is believed that a significant impact on the human environment will occur as a result of geothermal development in the proposed leasing area.

The Geological Survey's role in the preparation of these documents is to provide the surface manager with the geologic evaluation and interpretation of expected impacts on the environment resulting from the proposed geothermal development. The Area Geologist supplies the Geothermal Supervisor with the resource data for these studies.

During the prelease period, applicants for leases or other interested parties may conduct preliminary exploration programs (geological, geophysical, and geochemical surveys) on the public lands to determine their potential for geothermal development. Such activities are conducted under Notice of Intent applications filed with and approved by the appropriate District Office of the Bureau of Land Management, or under similar type permits issued by the local Forest Service Supervisors. The Geothermal Supervisor reviews such applications and recommends appropriate operating stipulations for protection of ground water, mineral resources, and public safety. Where requested, the Supervisor supports the land management agency in supervising the operations under the permit. Generally, these operations have limited surface impact. The testing and producing of geothermal resources are not allowed on lands not under lease.

Lease Issuance

The Bureau of Land Management is responsible for lease approval and issuance with the advice and/or concurrence of the Geological Survey on certain technical aspects. Leasing of the lands by the Department of the Interior is discretionary after review of all legal and environmental considerations.

The activities outlined above generally complete the leasing involvement of the Geological Survey on lands where noncompetitive leasing occurs. The Geothermal Supervisor must concur with any special stipulations contained in the lease. The mineral classification status of the lands applied for must also be confirmed by the Area Geologist at the time of lease issuance. If the classification has changed to a KGRA status, the application is voided and the lease may be issued only on a competitive basis.

The Geothermal Supervisor, in consultation with the Area Geologist, prepares an evaluation report on each tract offered for bid in competitive leasing areas. Geology, geophysics, geochemistry, engineering, and cost data are analyzed, using current state of the art techniques, to evaluate the fair market value of the resource and to assure attainment of the Department's objective in this regard. Frequently special geophysical or geochemical studies are made by other divisions of the Geological Survey for Conservation Division's use in lease sale evaluation. These special studies are made public prior to the sale.

Prior to the opening of bids, the Bureau of Land Management is advised of the results from the Geological Survey's pre-sale evaluation. After the bid opening, the bonus offers are reviewed in light of the pre-sale estimates, and the Geological Survey provides the Bureau of Land Management its recommendation as to bid acceptance or rejection on the basis of its fair market value estimates. The Bureau of Land Management then makes the final decision to accept or reject the offered bid. A bidder may appeal rejection of his bid to the Department of the Interior's Board of Land Appeals for administrative review.

Post-Lease Requirements

The Geological Survey assumes the lead role for approval and supervision of all activities relating to operations conducted on the lease by the lessee or his operator after a lease is issued. The Bureau of Land Management retains the original lease document, collects all rents, and finalizes all actions relating to termination, cancellation, relinquishment, transfer of

title, and bond recording. The Geological Survey advises the Bureau of Land Management as to lessee compliance regarding operational commitments on the leased lands. This assures that Federal interests are properly protected from any disturbance the lessee may have incurred on the leased lands. The interagency relationship during this phase of operations was shown on Figure 1.

The Geothermal Supervisor maintains annual reports on exploration or development expenditures which can be used as credit on portions of the annual rent, and on environmental activities by the lessee. Whenever the Geothermal Supervisor declares a lease to be in "productive" status, he must determine the royalty values and collect the appropriate amount from the lessee. All monies due the Federal government are collected by the Supervisor and royalties received are credited against the lease rental.

Casual-use entry on the leased lands by a lessee is defined as operations which create minimal or no surface disturbance. These activities can be approved under a Sundry Notice or Notice of Intent application, which is similar to the Bureau of Land Management's Notice of Intent. These applications cover most preliminary exploratory operations prior to deep drilling or testing of the resource. It is important that these documents be completed to ensure that proper financial credit is applied to the leasehold. Exploration activities, such as geophysical or shallow temperature gradient holes involving only limited surface disturbance, may be approved within 30 to 60 days, after consultation with the surface management agencies. Approval by the Geothermal Supervisor essentially requires a documented negative declaration of environmental impact.

Most operations on leased lands are carried out under a Plan of Operation. In the normal course of events, a series of such plans will be prepared beginning with exploration, and followed by plans for development, production, injection, and utilization as a field passes through successive phases. Prior to approval of these plans, the analysis of environmental impact (EA) and documentation of related decisions, in conformance with NEPA requirements, is made at each stage by the Geothermal Supervisor and his staff with advice from the surface management agency and the U.S. Fish and Wildlife Service. These documents are available for public review. An on-site field inspection for interested parties, including the public, is conducted unless all involved agencies agree that the inspection is unnecessary. This inspection when used as part of the NEPA process enables the Supervisor to review the widest spectrum of concerns, viewpoints, and comments.

Preparation of the necessary EA may take from 3 to 18 months depending on the information developed previously, extent of surface disturbance contemplated, and the environmental sensitivity of the area. Approval of Plans of Operation is the responsibility of the Geothermal Supervisor with the concurrence of the surface management agency (U.S. Bureau of Land Management or U.S. Department of Agriculture's Forest Service).

In the event that a proposed operation is of such magnitude or its environmental impact so significant that it is anticipated to become a major Federal action, preparation of an EIS may be required (an example might include an application to install one or more powerplants in an area not already covered by an EIS). Such an EIS is prepared by the Department of the Interior, using an interagency task force. The proposed operation is subject to the final approval of the Secretary of the Interior. This process normally takes 2-3 years, including the time necessary for completion of the EIS and Secretarial approval of the proposal.

In addition to the environmental analyses conducted internally by the surface management agency and the Geological Survey, the first proposed major exploration or development activity in each geologic or ecologic setting is reviewed by the Geothermal Environmental Advisory Panel (GEAP). GEAP is an interdepartmental panel established by Order 2962 of the Secretary of the Interior dated February 6, 1974. The panel consists of representatives from Interior Department agencies, together with representatives from the U.S. Forest Service, Environmental Protection Agency, the Department of Energy, and Department of Labor. Although formal membership on the panel is limited to representatives of Federal agencies, their discussions and consultations—always conducted in public meetings—include representatives of state, county, and local governments, conservation organizations, and representatives of the general public interested in the particular area under discussion.

The function of the panel is essentially threefold: (1) to review the first Plans of Operation for Exploration, Development, or Production in each new geological or ecological setting to determine whether the environmental constraints contained in the lease document and any attached stipulations, and in the Plans of Operation and any attached conditions, are adequate to provide appropriate levels of environmental protection; (2) to assure that the diverse technical expertise available within Federal agencies or other sources is considered and may be used, if necessary, to provide advice for mitigation of foreseeable impacts and to aid in developing appropriate remedial measures in the event of unforeseen consequences or accidents; and (3) to provide an additional interface between the Federal agencies involved in supervising lease activities, and relevant state, county, local agencies, industry, and the general public.

The Panel advises the Geothermal Supervisor or the surface management agencies, regarding the environmental impacts of proposed operations, including powerplants or other facilities for utilizing geothermal energy.

According to the type and scope of the activity, the lessee applies for final approval of operations to be conducted under the general framework of a Plan of Operation by filing a Sundry Notice or an Application to Drill. Individual permits and approval provide the Geological Survey flexibility in approving minor changes in plans, permitting activities not requiring Plans of Operation, scheduling work to ensure adequate supervision, and retaining the confidential nature of lease documents. A lessee should allow adequate leadtime for the Geological Survey's review and approval of technical data.

The Geological Survey is also responsible for the approval and supervision of all Federal cooperative or unit agreements and plans. Such plans and agreements

are, in essence, contracts between all the owners of interests in the property to cooperate or produce the resource in an agreed-upon manner. In accordance with Section 18 of the Geothermal Steam Act, the Department of the Interior may approve a Federal lessee's request to participate in cooperative or unit plans for purposes of conserving the natural resource. Conserving the resource in this instance refers to production management which enhances recovery and minimizes waste. Under conditions where drainage, loss, or damage to the Federal resources can be demonstrated, the government can require a Federal lessee to participate in such cooperative plans. Briefly, the company desiring to form a unit requests designation of an area as logically subject to development under a unit agreement. The application for designation of an area is submitted to the Geothermal Supervisor and must be approved by the Regional Conservation Manager. Upon commitment of the leases necessary to permit effective control of operation within the unit area, the Geothermal Supervisor may approve the unit agreement. Under terms of the unit agreement, specific exploration or development activities must be done within stated time frames. The Geothermal Supervisor notifies the Bureau of Land Management of the lease commitment, because unitized lands are not chargeable against the Federal limitation on maximum acreage holdings by any one party within any given state.

Permits or licenses for electrical generating plants or other energy conversion systems may be issued by the Geothermal Supervisor or by the Bureau of Land Management according to the size, length of permitting time, or facility ownership. For lessee operations on leased lands involving single well developments, the Geothermal Supervisor may issue a permit to operate the facility for the life of the project. He may also issue permits for research and development (R&D) operations of less than 20 Megawatt (MW) capacity for a period of 5 years. The Bureau of Land Management issues all other licenses for larger facilities or for commitments beyond the 5-year R&D period. The Geothermal Supervisor is responsible for supervision of all operations under either permit or license and authorizes construction and operations under Plans of Utilization, with appropriate Sundry Notices and similar types of approval.

Summary

Within its administrative responsibility, the Geological Survey must work closely with the Bureau of Land Management to assure that all commitments as the Federal resource landlord are satisfied. Under its regulatory responsibility the Geological Survey must satisfy the requirement that all lease operations comply with other Federal regulations and all state and local standards. This commitment in regulatory responsibility requires extensive liaison between various state and local jurisdictions to reduce duplication of permitting requirement and to be certain that the established standards for environmental controls are satisfied.

The foregoing description of the Geological Survey's role in the geothermal leasing program has focused primarily on the details of its administrative and regulatory role; however, an equally significant contribution lies in the ability to bring diverse earth science expertise to focus on geothermal development problems. The Geological Survey's research role in geochemistry, geophysics, hydrology, and volcanic processes is uniquely brought into focus by practical application and support of geothermal leasing and resolving development problems. Therefore, as the Geological Survey begins its centennial year, we along with others in the scientific and industrial community, will continue to expand our cumulative knowledge of the earth and its history and to utilize this knowledge in a dedicated effort to add to man's usable energy resources.

Geothermal Resources Council, TRANSACTIONS, Vol. 2 July 1978

PROGRESS IN THE WATER JET ASSISTED DRILLING OF ROCK

David A. Summers*
Ahmed A. El-Saie**

*University of Missouri-Rolla; Rolla, Missouri
**Ingersoll Rand Company; Princeton, New Jersey

INTRODUCTION

Conventional uses of fluid in drilling oil, gas and geothermal wells are severalfold. Primarily the fluid acts as a transport medium to carry the broken rock from the drilling surface, back up out of the hole. At the same time the fluid is directed onto the cutting surface with sufficient velocity that it will remove the broken rock from under the bit teeth. A third function, of increased importance in geothermal work, is the cooling of the bit and the bearings as the penetration continues.

Early work on the additional benefits which could accrue if the jets could cut the rock was carried out by the Carter Oil Company (Ref. 1). Because of the problems, in the late 1940's, of attaining high pressure in depth, their research examined the potential benefits of adding an abrasive to the flow. The abrasive used was sand and some performance gain was achieved in the trials, but the rapid erosion of the nozzles stopped this development.

In the early 1960's tungsten carbide was developed as a nozzle material and abrasive fluid jets were rapidly adopted for penetrating casing and slitting boreholes for hydrofracing (Ref. 2).

As a result of this successful development the Gulf Research Corporation began to investigate the use of abrasive particles as a means of enhancing the drilling rates for use in oil rigs. It was determined that, by increasing the fluid pressure to 10,000 psi and adding steel shot to the fluid, the penetration rate of the drill could be increased by a factor of up to five.

Laboratory test results were confirmed when the trials were repeated in the field and it was found possible to drill at rates of up to 80 ft/hr at depths of up to 14,000 ft with this method. Although the group appeared to solve many of the problems which have since bothered other investigators, the high cost of the experiments combined with the problems associated with the abrasives, led to the termination of the research. One problem which influenced the results was control of the mud weight, affected by the concentration of the abrasive steel shot. The steel shot could also instantaneously block the nozzle orifices and, when this occurred the drill steel became pressurized and stretched overloading the bit (Ref. 3).

The Exxon Research Corporation began field trials of a high pressure fluid system at about the time that the Gulf investigation was drawing to a close. High pressure flows were combined with conventional tricone bits and it was demonstrated that, in drilling of shallow deviated holes drilling rates of up to 200 ft/hr could be achieved in contrast to the conventional rate of 20 ft/hr (Ref. 4). This improvement was also found in straight hole drilling but the improvement was not as great as hole depth increased. Equipment problems particularly with the pumps, conventionally used for hydrofracing, slowed the development of the process. A series of four tests in depth were carried out in the mid 1970's but only one of these was carried out at the higher pressures of previous tests and this indicated, contrary to the findings of the Gulf group (who went to deeper levels), that as the depth of the hole increased so the improvement in performance which could be obtained by the addition of high pressure jets to the bits decreased and, at a depth of 6,000 ft there was no improvement. Since the addition of the jets is an expensive process, even though this continuing investigation was funded in the end by eight oil groups it was discontinued in 1976 (Ref. 5).

At about this time the Shell Research Corporation in the Netherlands, who has also been examining the advantages to be obtained by adding water jets to drilling moved the nozzles on the bits closer to the bottom of the bit and reduced the pressure 5,000 psi. This led to a breakthrough in 1977, when the Shell group became the first team to actually save money (some $140,000) in drilling a hole using high pressure water jet assistance on the bit (Ref. 6).

CURRENT RESEARCH AT UMR

In 1975 the University of Missouri-Rolla signed a contract with the U.S. Energy Research and Development Administration - Geothermal Division, to investigate the use of high pressure

water jets as a means of enhancing the drilling rate in geothermal wells. Much of the experience at the University has been in the application of water jets at slightly higher pressures than are normally, to date, considered for use in geothermal operations and at somewhat smaller diameters. The first objective of the research was therefore to determine if such small jets would be effective in drilling holes in depth.

After preliminary experimentation to determine an optimum cutting geometry for the water jet nozzles, which resulted incidentally in achieving advance rates of up to some 300 in./min in sandstone, the water jet drill was tested in a triaxial chamber in which the rock could be pressurized and pressure could also be applied within the borehole created to simulate back pressure within the hole. The results of these trials indicated that in relatively soft rock, such as sandstone, there was a considerable decrease in hole diameter as a result of applying stress to either the rock or the borehole of the order of some 40 percent. However, when the experiment was repeated in granite a diameter change of only some 12 percent was achieved. It was also noticed that the granite was broken out in larger fragments than the sandstone and penetration rates of up to 200 ft/hr could be achieved in the granite at jet pressures of approximately 15,000 psi, a pressure which had been achieved in field operations carried out by Exxon.

The results of this endeavor indicated that high pressure water jets at small diameter could practically operate in the configurations desired and it was therefore decided to examine the performance of the jets on large diameter bits. Because of the localized nature of the water jet cutting action, it is not practical to use water jets alone to remove all the material at the face of the drill and, as a result, it is necessary to combine the water jet cutting action with that of conventional roller bits.

In order to determine the practical effectiveness a new bit design has been developed which takes into consideration not only the use of high pressure water jets as a faster method of drilling but also the benefit which can be achieved by combining water jet and mechanical bit action together. The bit is shown in silhouette in Figure 1 in order to more clearly show the relative jet locations. The jets are located so as first to drill an access hole ahead of the main body of the bit along the central axis, using high pressure water jet action alone and into this leading hole to insert a water jet nozzle system to direct jets under the quadra-cone bit teeth at the point of their contact with the rock. In this manner the water jet and rock bits will work together and improve drilling rate. Where this has been tried in the field advance rate improvement by a factor of up to 8 has been achieved. The research is currently moving from the preliminary sandstone tests into dolomite and it is intended that the experiments will conclude in granite during the course of the summer of 1978.

While this research is continuing a continued investigation has been made of the effect of stress on drilling rate and, because of the small size of the samples which were used in the triaxial chamber, the water jet drill was mounted on a drilling jumbo and taken 1,000 ft down into a lead mine in southeastern Missouri where, during the winter of 1977-78 it drilled over 100 holes in a barrier pillar and demonstrated not only that the water jet will drill effectively in these confined conditions at a much lower noise level than existing rock drills, but also that the effect of stress is as marked in the field as was found to be the case in the laboratory. For example where a block of the rock was destressed there was a change in the hole diameter of approximately 1/2 in. from that drilled by the water jets in a stress zone and that achieved by the jets in an area that had been destressed.

The research has also examined the potential benefits of adding abrasive to the water as had been proposed by Gulf and also the potential benefits to be achieved by cavitating the jet stream as has been proposed by Hydronautics (Ref. 7). It has been found that at pressures of up to 10,000 psi in the drilling of granite it is more effective to use abrasives in the fluid flow than cavitation or plain water jets since at this pressure the threshold velocity of the granite has barely been reached (Ref. 8). At pressures of above 10,000 psi it is more effective to use cavitating water jets in drilling through granite (Figure 2). As the pressure increases plain water jets become more effective than abrasive laden jets. It is postulated that the reason for this is that the abrasive wears a smooth surface on the rock, less susceptible to the fluid wedging of jet attack than the broken surface left by the plain or cavitated flow attack. This theory is substantiated by other experiments which have shown that, at a pressure of 8,500 psi, the jet attack on a smooth surface only becomes effective in cutting once a preliminary pass over the surface has created a broken surface.

CONCLUSIONS

Evidence developed at the University of Missouri-Rolla has shown that, at pressures currently available with commercial equipment, advance rates up to 200 ft/hr can be achieved in drilling granite.

This rate is, however, diminished by the application of the pressures to be found in a borehole at depths up to 6,000 ft. However, this reduction is to a much lesser extent in granite than has been observed in sandstone. It has also been shown advantageous to use abrasives and/or cavitation of the fluid flow in order to enhance drilling rates. At fluid pressures below 10,000 psi abrasive laden jets

appear more effective while at fluid pressures above 10,000 psi cavitating jets would appear more effective.

ACKNOWLEDGEMENTS

This work was funded under U.S. Energy Research and Development Administration contract EY 76 S 02 2677.A002 with Mr. Cliff Carwile as the Technical Project Officer, Ms. June Wiinikka and Ms. Sheryl Povalish acted as Contracting Officers. We are pleased to acknowledge this assistance. The research was carried out with the assistance of Mr. J. Blaine, who made the nozzles, Mr. L.J. Tyler, and Mr. K. Davis of the Rock Mechanics and Explosives Research Center staff. We were also ably assited by Mr. B. Larkin, Mr. L. Ashby, and Mr. J. Carter of the St. Joe Research Department, this assistance and the help furnished by St. Joe under Mr. Casteel, Vice President - Mining of St. Joe Minerals is gratefully acknowledged.

REFERENCES

1. Ledgewood, L.W. (1960), J. Pet. Tech., 4, 61-74.

2. Weber, G. (1971), Oil & Gas Jl., July 26, 1977, p. 57.

3. Wyllie, R.J. (1972), Proc. 8th World Petroleum Congress, Moscow, 1972, 403-411.

4. Maurer, W.C., J.K. Heilhecker, and W.W. Love (1973), J. Pet. Tech., 7, 851-859.

5. Maurer, W.C. (1977), Drilling Research Report, 7, 87.

6. Van Strijp, A.J.R. and R. Feenstra (1977), Proc. 1977 Energy Tech. Conf., ASME, Houston, Texas.

7. Conn, A.F. and R.P. Radtke (1977), Proc. 1977 Energy Tech. Conf., Houston, Texas, paper 77-Pet. 54.

8. El-Saie, A.A. (1977), "Investigation of Rock Slotting by High Pressure Water Jet for Use in Tunnelling," Ph.D. thesis, Rolla, Missouri.

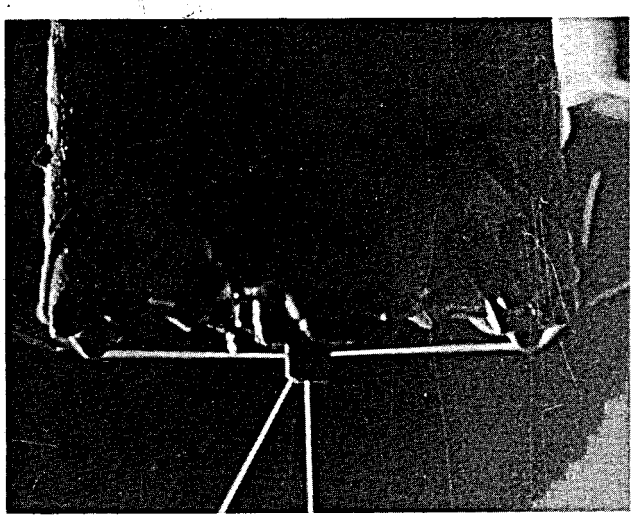


Figure 1. Hydromechanical drill bit showing the jet locations relative to the bit teeth.

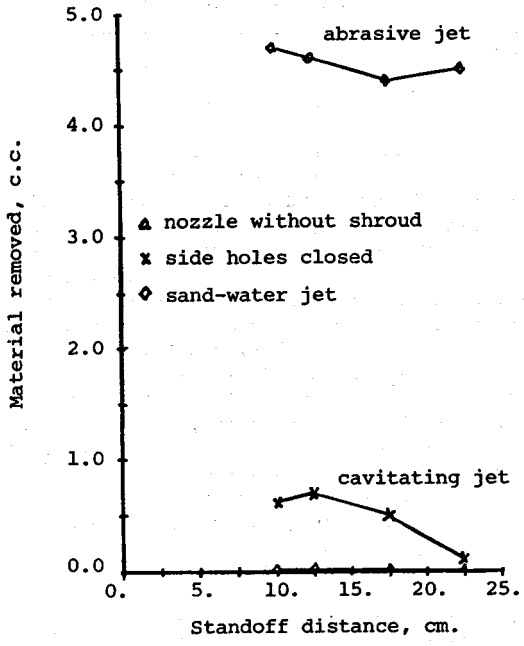


Figure 2a. Pressure = 51.7 MPa

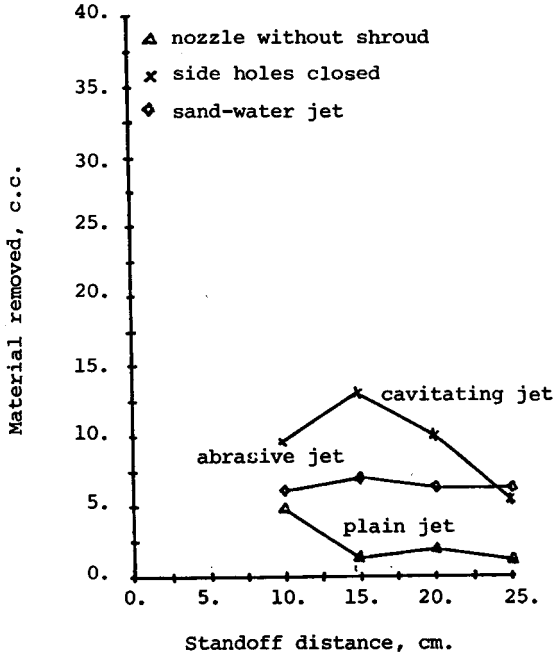


Figure 2b. Pressure = 69.0 MPa

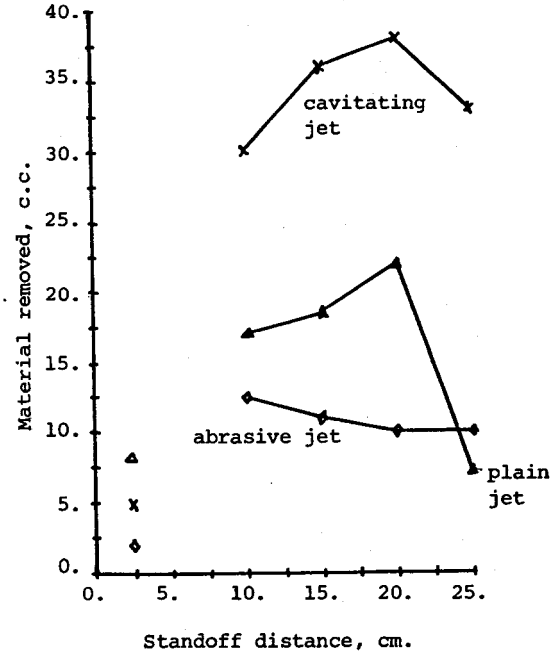


Figure 2c. Pressure = 13.80 MPa

Figure 2. Relative erosive capability of jets at various pressures, as a function of standoff distance.

Geothermal Resources Council, TRANSACTIONS, Vol. 2 July 1978

GEOTHERMAL DEVELOPMENT AND WILDLIFE BEHAVIOR

Glenn W. Suter II

Environmental Sciences Division
Oak Ridge National Laboratory
Oak Ridge, Tennessee 37830

ABSTRACT

Because of improved emissions control and tighter air and water quality regulations, disturbance of wildlife is replacing toxic emissions as the major ecological problem associated with hydrothermal development. This problem is discussed, using raptorial birds as an example. It is proposed that a 1 km buffer zone be observed around raptor nest sites in the arid, intermountain west. Suggestions are made for increased monitoring of wildlife behavior.

The geothermal industry prides itself on providing an environmentally sound energy alternative in the U.S.; today that contention would appear to be supportable. The available results of the Geysers vegetation and wildlife studies suggest that the ecological effects of the Geysers operation are roughly equivalent to those of any other project in that location which would require the same amount of land disturbance (earth moving).[1] Routine emissions to aquatic environments have ceased, and except for damage to boron sensitive vegetation near the cooling towers, the effects of atmospheric emissions are essentially aesthetic. Emissions at other resource areas appear to be similarly controllable, and state and federal air and water quality standards will ensure that they are controlled. This is not to suggest that toxic emissions, particularly from accidental releases, will never be an ecological problem or that subtle or long-term emission effects will not be found at the Geysers or elsewhere. Rather, the most serious ecological problem resulting from further hydrothermal development will be disruption of wildlife behavior. The effects of emissions from geopressured resource development may be more serious.

The resources at Geysers and the Imperial Valley having now been well established, the intermountain west is the current frontier of geothermal exploration and development. While no geothermal power plants currently exist in this region, development is underway at several locations. The predominate land use is natural pasturage with typical stocking rates of 10 or more acres per animal unit month. The human population density is low, and the vegetation has remained largely natural. As a result of this low intensity of land use, the density of wildlife has remained relatively high.

Superficially, geothermal development results in a small amount of habitat loss relative to other energy extractive industries. The operating 5 MWe Raft River Plant and associated facilities are expected to occupy about 8 ha (20 acres) within a 3,500 ha withdrawal area or 1.6 ha per MW. Development of the higher enthalpy resource at the Geysers requires disturbance of only 3.5 ha per 100 MW or approximately 8% of an average leasehold.[2] This appearance of minimal habitat loss is only real if critical habitat components are preserved. These include strutting grounds for sage grouse, kidding areas for antelope, cliffs and large trees for bird nests, and sources of water in arid areas. The environmentally conscientious resource developer must determine what wildlife species are present and where critical habitat components are located. For game species, this information is often available from the nearest office of the U.S. Fish and Wildlife Service or the state wildlife resource agency. Finally, the resource developer, realizing that wildlife disturbance by human presence and activity extends well beyond the area of vegetation disturbance, must determine the spatial and temporal extent of buffer zones necessary around these critical habitats.

The problem of critical habitat protection is particularly difficult when dealing with raptors (hawks, eagles, falcons and owls). Within the last decade these birds have gained roughly the same biopolitical significance as game species. This is a result of their increasing rarity (4 U.S. Falconiforme species are listed as endangered[3] and an additional 12 are listed as declining over a significant part of their range[4]), and a general reversal of the public's image of raptors from despicable murderers to beautiful symbols of wildness and freedom. Raptors are abundant and diverse in the vicinity of all of the intermountain known geothermal resource areas.

Raptors are notoriously sensitive to disturbance at their nest sites. Disturbance of nesting birds can result in complete desertion of the nest, eggs or young or temporary desertion resulting in damage to the eggs during a hasty

departure, overheating, chilling or desiccation of eggs or young, predation on eggs or young, or missed feedings. Eggs can be fatally chilled or heated in less than one half hour. The high pesticide concentrations in raptors have made them more sensitive to disturbance by thinning their egg shells, thus making the eggs more subject to damage by the adults and by decreasing attachment of adults to the nest. Three studies of golden eagles have found that 46%, 71% and 85% of nesting failures were due to human disturbance.[5,6,7] The effects of such disturbance range from loss of a year's reproduction to loss of the nest site if the disturbance is chronic.

Nest sites are at a premium in much of the intermountain west. Cliff nesting birds such as golden eagles and prairie falcons require a suitable ledge or pot hole in a cliff of sufficient height, preferably with overhead protection, while tree nesters require sufficiently tall and strong trees. Nest sites should adjoin good hunting areas. A forced move to a suboptimum site will result in reduced probabilities of successful reproduction. Suitable nest sites are at a particular premium because they tend to be clustered while raptors are territorial. Therefore, most alternate nest sites will not be available to a displaced pair because they lie within territories defended by other pairs.

The sensitivity of a particular pair of birds to disturbance depends on their species, their experience with humans, the time of the disturbance, the nature of the disturbance, the quality of the nest site and individual variance. The range of species characteristic behavior extends from the ferruginous hawk which may abandon a nest with eggs after a single human visit, to the osprey which will stay on a site while logging is carried on around the nest tree or rebuild after a nest has been repeatedly destroyed.

Human influence is a strong selective force on animal behavior. In Scotland, where golden eagles have been persecuted for centuries, eagles are extremely wary and have been observed to flush from a nest when an approaching human was over a mile away.[8] In the U.S. most hawks and eagles found shot are immature birds which are less experienced than adults and, therefore, less wary. Birds are most apt to abandon an empty nest, less apt to abandon eggs and least apt to abandon nestling young; dedication is related to investment. Temporary nest abandonment is most serious during hatching and in the weeks immediately following due to the extreme vulnerability of the young. Periods of extreme heat and cold (early morning and late afternoon) are critical.

The severity of disturbance seems to be related to its noise level (sudden, sharp noises such as those produced by pipe racking are particularly disturbing), visibility from the nest, familiarity, duration, and the number of people involved. Loyalty to a nest site may be dependent on the quality of the site. For cliff nesters this primarily means a large cliff, overlooking a good hunting area without strong downdrafts. Finally, some individual birds are more nervous than others. Camenzind found that most golden eagles in his study area left the nest when they become aware of his approach, but two females would allow him to come within touching distance.[5]

Despite these sources of variance it is possible to make some recommendations concerning buffer zones. Geothermal drilling and associated construction represent a serious disturbance involving high noise levels (approximately 90dBA), numerous personnel and continuous activity over a period of one to several months. In addition, tall, dense vegetation is seldom available to act as a screen. While numerous accounts exist of nest abandonment due to similar scale activities, the distances involved are seldom reported. Two relevant studies of nest site disturbance are planned, but the only completed studies known to the author concern recreational and research related disturbance of bald eagles.[9,10] The only existing U.S. Government guideline (no management activities within 132 ft of a nest and no activity within 660 ft during the nesting period on Forest Service land) applies to bald eagles, a moderately tolerant species nesting in forests. In the face of this problem, based on experience and the literature, a 1 km buffer zone was proposed for geothermal drilling near cliff nesting golden eagles and prairie falcons in southwestern Utah.[11] On similar bases, Richard Howard of the U.S. Fish and Wildlife Service has proposed 0.5 to 1 mile buffer zones for ferruginous hawks at Raft River, Idaho.[12] Since these figures were independently arrived at and are essentially equal, I would like to propose a standard 1 km buffer between geothermal drilling and nesting sites of arid land raptors until better information becomes available. Outside of the March 1 to July 1 period of egg laying and hatching, short term activities such as geophysical exploration could be carried out.

In arid areas tall perches are also rare habitat components. Transmission line towers should be designed to preclude raptor electrocution and should be placed away from roads so that perching raptors are not such tempting targets.

The geothermal industry can help to supply the basis for improved guidelines for protection of raptor nest sites and other critical wildlife habitat components by better use of ecological field time. Baseline wildlife data gathered for DOE geothermal loan applications consists primarily of species lists with some population size estimates. Field personnel should, when noting the presence of a species, also note behavior, including flight distance and habitat use relative to existing human activities. Behavioral information concerning important species can also be obtained by questioning local residents. Behavioral data are likely to be too sparse for formal analysis but is more important for impact analysis than most of the more readily gathered animal data. Finally, observations of changes in animal behavior in the vicinity of geothermal development, or the absence of changes, would probably be the most significant result to come out of an ecological monitoring program.

ACKNOWLEDGEMENTS

This research was sponsored by the Division of Geothermal Energy, U. S. Department of Energy, under contract W-7405-eng-26 with Union Carbide Corporation. Environmental Sciences Division Publication No. 1166, ORNL.

REFERENCES

1. The Geysers Wildlife Study: Interim Report October, 1977.
2. W. Chris Chouteau, "Loss of natural vegetation and wildlife habitat," talk presented at the Geysers Ecosystem Quality Workshop, Santa Rosa, Ca., October 26, 1977.
3. U.S. Department of the Interior, "Endangered and Threatened Wildlife and Plants," Fed. Regist. 41(208) (1976).
4. R. Arbib, "The Blue List for 1978," Am. Birds, 31(6) 1977.
5. F. J. Camenzind, Nesting ecology and behavior of the golden eagle in west central Utah. M.S. Thesis. Brigham Young U., Provo, 49 p. (1968).
6. D. O. D'Ostilio, Nesting status and food of the golden eagle in northern Colorado. M.A. Thesis. U. Colorado, Boulder, 48 p. (1954).
7. E. L. Boeker and T. D. Ray, "Golden Eagle Population Studies in the Southwest," Condor 73(4) 1971.
8. M. T. Jollie, The Golden Eagle, Its Life History, Behavior and Ecology, M.S. Thesis, U. Colorado, Boulder, 206 p. (1943).
9. J. W. Grier, "Bald eagle behavior and productivity responses to climbing to nests," J. Wildl. Mgmt. 33(4):961-966, 1969.
10. J. E. Mathisen, "Effects of human disturbance on nesting of bald eagles," J. Wildl. Mgmt. 32(1):1-6. 1968.
11. Energy Research and Development Administration, EIA for CUI Venture Application for Geothermal Loan Guarantry (Beryl and Lund, Utah), EIA/GE/77-8, September, 1977.
12. R. J. Fisher, "Biological Values in the Raft River Valley Geothermal Resource Area," Appendix A in: U.S. Department of Energy, Environmental Assessment, Raft River Geothermal Project, Thermal Test Loop, Cassia County, Idaho, DOE/EA-0008, March, 1978.

Geothermal Resources Council, TRANSACTIONS, Vol. 2 July 1978

WATER QUALITY MANAGEMENT FOR IMPERIAL VALLEY GEOTHERMAL DEVELOPMENT

Arthur Swajian
Gary L. Morris

CALIFORNIA REGIONAL WATER QUALITY CONTROL BOARD
COLORADO RIVER BASIN REGION

Palm Desert California 92260

Kenneth D. Pimentel
Lawrence Livermore Laboratory
Livermore, California 94550

The development of geothermal resources in the Imperial Valley of California poses the possibility of geothermal brine pollution of surface and subsurface waters. Control of pollution of Imperial Valley waters comes under the jurisdiction of the California Regional Water Quality Control Board, Colorado River Basin Region. Division 7 of the California Water Code requires that "Each regional board shall establish such water quality objectives in water quality control plans as in its judgment will insure the resonable protection of beneficial uses and the prevention of nuisance."

The "Water Quality Control Plan, West Colorado River Basin (7A), April 1975" establishes the following beneficial uses of Imperial Valley water supply canals:

1. Municipal and Domestic Water Supply
2. Noncontact Water Recreation
3. Industrial Water Service Supply
4. Agricultural Water Supply
5. Warm Freshwater Aquatic Habitat
6. Wildlife Habitat
7. Hydropower Generation

In order to protect the beneficial uses of Imperial Valley waters, it is essential that the characteristics of geothermal water quality pollution be understood and closely monitored by the Regional Water Quality Control Board.

The Regional Board has been working closely with the staff of Lawrence Livermore Laboratory in its Imperial Valley Environmental Project (IVEP) in the development of a geothermal water quality monitoring program in Imperial Valley. The water quality monitoring program is based on the belief that geothermal brines have a different chemical composition from the surface and subsurface waters of Imperial Valley.

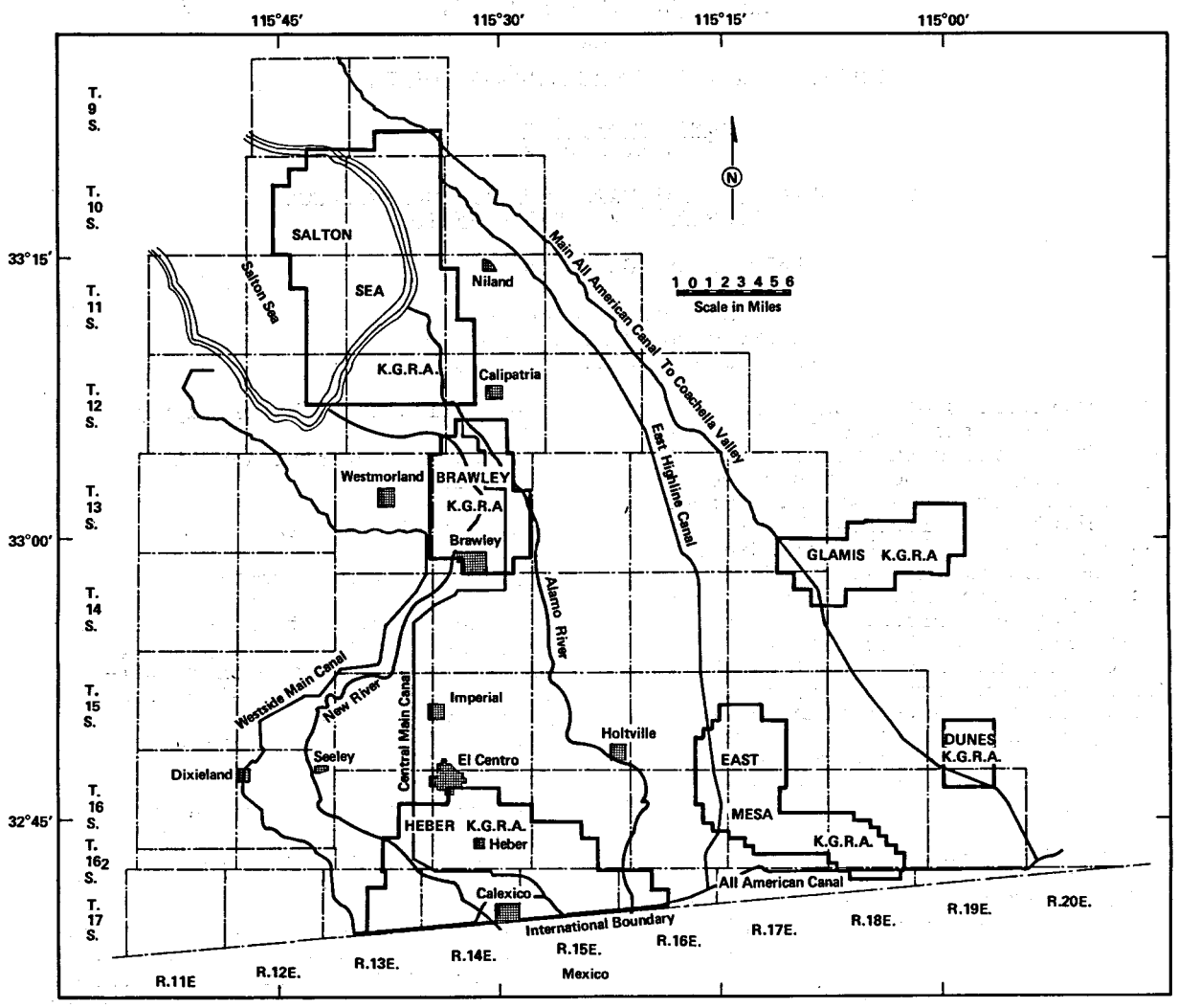


Fig. 1 Imperial Valley California showing Known Geothermal Resource Areas

A site-specific water sampling network was established by Lawrence Livermore Laboratory under a U.S. Department of Energy contract in the Salton Sea Geothermal Field of Imperial Valley near the San Diego Gas and Electric - U.S. Department of Energy Geothermal Test Facility. In the process of developing the sampling network a sump (Sump 116) was sampled near Sinclair #4 geothermal well on Boyle Road that indicated the possibility of geothermal brine pollution.

Table 1 gives a summary of chemical analyses of representative water samples compiled by Lawrence Livermore Laboratory from the sampling network. Table 2 gives a comparison of water sample constituents from the Salton Sea KGRA. The water samples from Sump 116 show high amounts of Boron (B), Lithium (Li), Manganese (Mn), Strontium (Sr), Zinc (Zn),

TABLE 1

CHEMICAL ANALYSES OF REPRESENTATIVE WATER SAMPLES FROM SALTON SEA KGRA

(All Values are in mg/l unless indicated)

Source	Vail 4A Canal	Vail 4A Drain	Sinclair No. 4 Geothermal Well	Sump 116	Salton Sea
Date	12/76	12/76	4/75*	12/76	12/76
Na	161	923	70,000	4,250	10,600
K	7	19	15,800	260	195
Ca	93	305	29,000	3,870	850
Mg	37	161	71	666	1,200
Cl	147	903	165,000	14,900	14,730
SO_4	357	1,866	20	1,686	8,100
TDS	970	4,560	290,000	29,200	38,600
SC($\frac{\mu mho}{cm}$)	1,130	6,000	-	43,900	40,000
pH	8.0	7.0	5.2	6.5	8.8
As	0.01	<0.01	2,700	<0.01	<0.01
B	0.23	0.95	140	16.9	6.8
Ba	0.06	0.07	3,000	0.72	0.07
Cd	<0.01	<0.01	9	0.03	<0.05
Cu	<0.01	<0.01	2.7	0.07	0.08
Li	0.09	0.30	350	22.2	3.2
Mn	0.01	0.19	1,900	66	0.08
Ni	0.01	<0.01	450	0.14	<0.2
Sr	1.60	3.4	3,700	72.8	13.5
Zn	0.03	0.03	2,200	12.2	0.03
Pb	<0.01	<0.01	60	0.37	<0.01

* Trace Element Data obtained by Spark Source mass spectography and may be good to only within an order of magnitude.

TABLE 2

CONSTITUENT COMPARISON OF WATER SAMPLES FROM SALTON SEA KGRA

Source	Vail 4A Canal	Vail 4A Drain	Sinclair No. 4 Geothermal Well	Sump 116	Salton Sea
Date	12/76	12/76	4/75	12/76	12/76
K/TDS	0.0072	0.0042	0.054	0.0089	0.0051
Cl/TDS	0.152	0.198	0.569	0.510	0.382
Na/K	23.0	48.6	4.4	16.3	54.4
K/Mg	0.189	0.118	222.5	0.390	0.163
SO_4/Cl	2.429	2.066	0.0001	0.113	0.550
Na/Ca	1.731	3.026	2.413	1.098	12.471

Lead (Pb) as does the geothermal brine in Sinclair No. 4 geothermal well. The water samples from sump 116 also showed a low Na/K ratio which occurred with the brines from Sinclair No. 4 geothermal well.

Although these data strongly suggest a definite relationship between geothermal brines and brine-polluted surface water in Sump 116, it should be noted that this is a limited observation and the Regional Water Quality Control Board needs to do additional analysis for verification and corrective action.

The results of the site-specific water sampling network in the Salton Sea KGRA indicate that "fingerprints" of the geothermal water pollution are available through chemical analysis. An Imperial Valley water quality network has been developed by the staff of Lawrence Livermore Laboratory and the Colorado River Basin Regional Water Quality Control Board. The recommended water quality monitoring program would consist of water samples obtained on a quarterly basis at 40 sites throughout Imperial Valley. Table 3 lists the recommended chemical analyses of water samples.

The recommended monitoring program will enable the Colorado River Basin Regional Water Quality Control Board to protect the beneficial water uses of Imperial Valley while the needed development of geothermal energy continues.

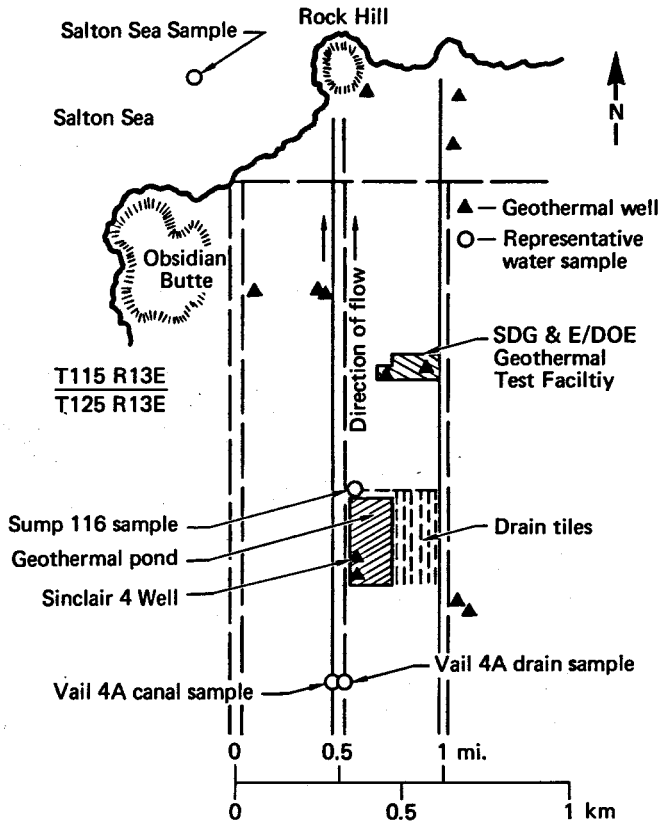


Fig. 2 Site - specific water samples in the Salton Sea KGRA

TABLE 3

RECOMMENDED CHEMICAL ANALYSES OF WATER SAMPLES

Field Analyses	Laboratory Analyses	
Specific Conductance (SC)	Na	TDS
	K	B
	Ca	NH_4
Temperature (°C)	Mg	SiO_2
	Cl	Li
pH	CO_3	Mn
	HCO_3	Sr
	SO_4	Zn
		Pb

The Use of the Random Groundwater Data from WATSTORE in Geothermal Exploration: An Example from the Imperial Valley, California

Chandler A. Swanberg Shari Alexander

New Mexico State University

ABSTRACT

On the basis of about 500 groundwaters from the Imperial Valley of California, supplemented by about 8,000 groundwaters from adjacent parts of the Basin and Range province, we have established the normal ranges of various chemical geothermal indicators and the criteria by which geothermal waters can be recognized. For the Imperial Valley and the southern Basin and Range province, we propose the following values as potentially signifying geothermal waters:

silica geotemperature	>100°C
Na-K-Ca geotemperature	>125°C
Fluoride	>2.5 ppm
In situ temperature	>35°C
Heat flow	>120 mWm^{-2}

Application of the above criteria to groundwater data from the Imperial Valley and the southern Basin and Range province has lead to the rediscovery of most known thermal areas and the delineation of an equal number of promising new target areas.

INTRODUCTION

The Water Resources Division of the U.S. Geological Survey maintains a centralized water quality data bank called WATSTORE. This computerized file represents both surface and groundwaters (wells and springs) for the entire United States, and includes such information as chemical analysis, well depth, temperature, date of sampling, location of the sample in latitude and longitude, and various other parameters. The entire file represents over a million individual waters and perhaps 20 million individual pieces of information. The present study, however, includes only the several thousand samples representing groundwaters from the Imperial Valley and southern Basin and Range province.

Since this large amount of chemical data exists in a computerized data bank, and since the chemical quality of groundwaters is such an important tool in the search for and evaluation of potentially valuable geothermal resources, it was decided to search the WATSTORE file for groundwaters whose chemical nature seemed to suggest that they might have originated within an active geothermal system. A summary of the chemical indicators of geothermal activity (geothermometers), the assumptions upon which they are based, and their applications to geothermal studies is given by Truesdell (1976).

DEFINING ANOMALOUS PARAMETERS

Our general approach in establishing the criteria for recognizing potential geothermal waters is to prepare histograms of the various geothermal indicators, calculate the mean and standard deviation, and to assume that a value greater than one deviation above the mean is anomalous. Waters which are anomalous on the basis of three or more parameters are considered to represent potential thermal waters. The details of the various geothermal indicators are discussed below:

Heat flow. Figure 1 presents the heat flow data for the Imperial Valley (Swanberg, unpl.) and the Basin and Range (Sass et al., 1976). The two histograms are quite similar if the thermal wells from the Imperial Valley are not considered. In defining anomalously high heat flow, it seems more appropriate to use the Basin and Range data set. A heat flow cutoff value of 120 mWm^{-2} follows from the data in Figure 1.

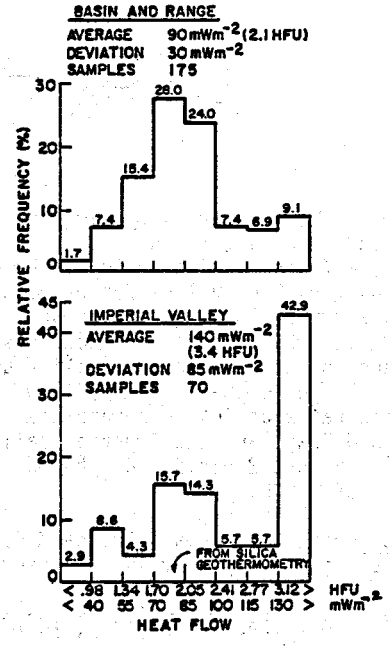


FIGURE 1

Silica Geotemperatures. The silica geothermometer is based on the temperature dependence of quartz solubility in water and is quantitatively expressed according to the conductive cooling equation of Truesdell (1976):

$$TS_iO_2 = \frac{1315}{5.205 - \log_{10} SiO_2} - 273.15 \qquad (2)$$

where TS_iO_2 is the silica geotemperature in degrees Celsius and silica is expressed in parts per million. Histograms of silica geotemperatures for the Basin and Range province and the Imperial Valley are shown in Figure 2.

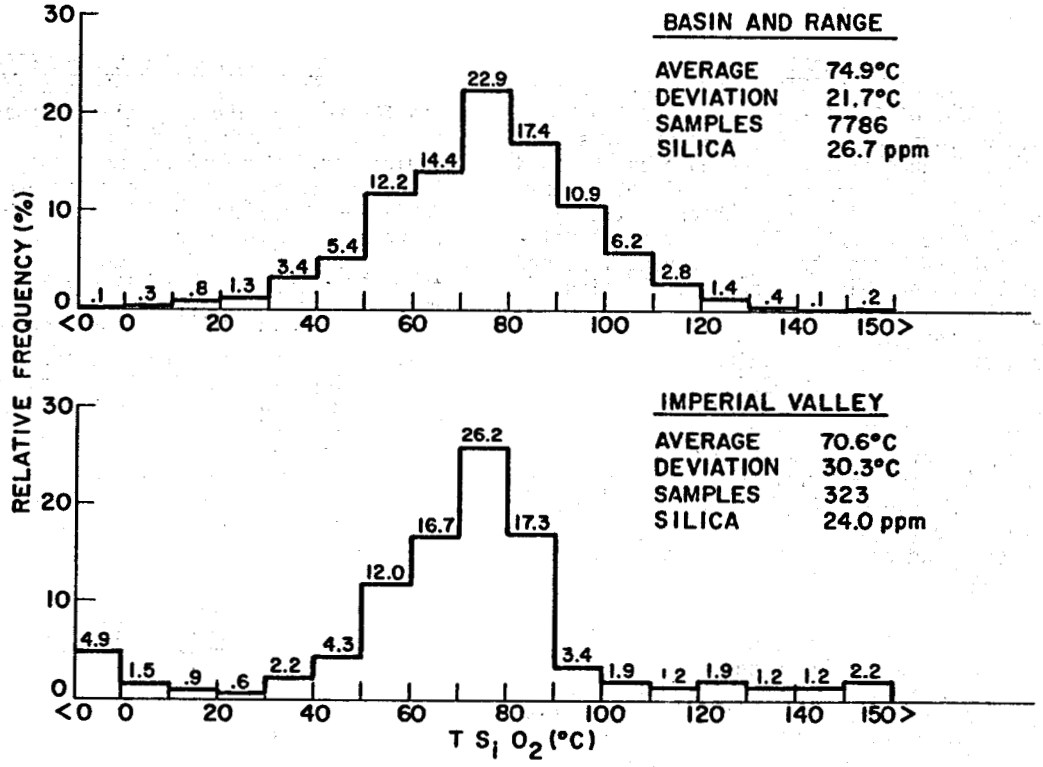


FIGURE 2

The two histograms are very similar except that the standard deviation is larger for the Imperial Valley, a feature which reflects the presence of numerous very high values representing geothermal waters and very low values representing Colorado River water which has circulated in shallow aquifers and never reached equilibrium with the host rock due to the extremely slow water-rock reaction rates at low temperatures. Both the Basin and Range and the Imperial Valley data sets shown in Figure 2 yield a geothermal cutoff temperature of 100°C.

Na-K-Ca Geotemperatures. The Na-K-Ca geothermometer can be quantitatively expressed as follows:

$$TNaKCa = \frac{1647}{\log_{10}(Na/K) + \beta \log_{10}(\sqrt{Ca}/Na) + 2.24} - 273.15 \qquad (3)$$

where TNaKCa is in degrees Celsius, Na, K, and Ca are expressed in molal concentrations, and the value of β is determined by the following tests (Truesdell, 1976):

$\beta = 4/3$ for $\sqrt{Ca}/Na > 1$ and $TNaKCa < 100^0C$

$\beta = 1/3$ for $\sqrt{Ca}/Na < 1$ or $TNaKCa(4/3) < 100^0C$

The histogram fro this geothermometer is shown in Figure 3. Using our standard criteria, geotemperatures greater than 125°C are considered to represent potential geothermal waters.

Fluoride. Fluoride appears to be concentrated in the Imperial Valley geothermal waters, particularly along the major fault zones, and may therefore be used as a qualitative geothermometer. The fluoride histogram is shown in Figure 4. Using our standard criteria of one deviation above the mean, fluoride concentrations greater than 2.5 ppm are taken as representing potential geothermal water.

In Situ Temperature. The use of in situ temperature is an obvious tool in geothermal exploration although its use in the present study is somewhat restricted because the depths of the wells are not always known. Thus, it may not always be possible to distinguish true geothermal waters from those waters which are heated by a normal geothermal gradient but were sampled from deep wells. In fact, the latter case may be quite prominent in the Imperial Valley because both the mean temperature (40.4°C, Figure 4) and modal temperature (30-40°C, Figure 4) are substantially

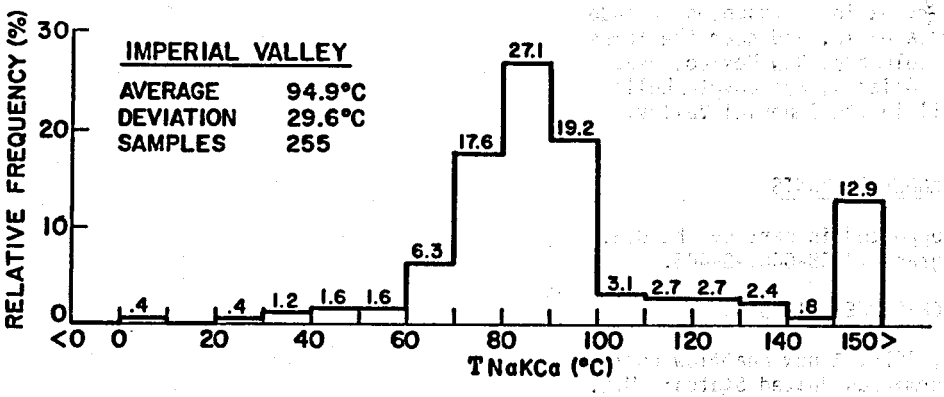


FIGURE 3

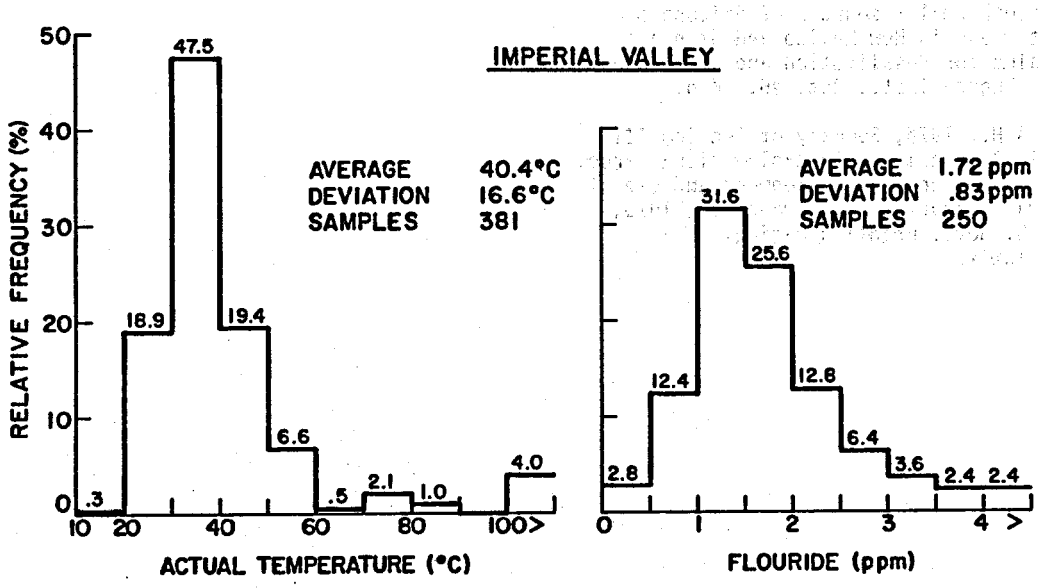


FIGURE 4

greater than the mean surface air temperature of 24°C reported for Yuma, Arizona. Thus, to select the criteria for recognizing thermal water on the basis of in situ temperature, it seems more appropriate to use the data set from the nearby Basin and Range province of southern Arizona.

Swanberg et al., (1975) have examined the in situ temperatures of nearly 2,000 wells in southern Arizona and found a mean temperature of 26.7°C and a standard deviation of 5.2°C. Making a small allowance for the finite depth of the wells studied, this mean value is in good agreement with the mean air temperature of Yuma, Arizona. Using our standard criteria of one deviation above the mean, waters greater than 32°C are potentially thermal. Interestingly enough, this is exactly the same temperature obtained by applying Waring's original definition of thermal water; i.e., 150°F above mean air temperature.

For the present study, the value of 32°C has been rounded up to 35°C.

ANOMALIES

Once the above criteria have been established, it is a simple matter to scan the WATSTORE file or any other set of groundwater chemical data for waters whose chemistry suggests that they might have originated within an active geothermal system. The general approach is to place most emphasis on areas having several waters which appear to be of geothermal origin on the basis of all the tests applied. Less emphasis is placed upon single station anomalies and upon waters giving contradictory results.

The principle geothermal anomalies which could be detected on the basis of the chemical data in WATSTORE include most known geothermal areas in the Imperial Valley and the southern Basin and Range province and this rediscovery underscores the potential value of WATSTORE in geothermal exploration. In addition, numerous new target areas have been delineated wich warrant detailed geophysical scrutiny. Most of these new target areas are

associated with either Quaternary volcanics or very deep sedimentary basins. Examples include the southern Tularosa Basin, and near the towns of White Sands and Columbus, New Mexico, near Bisbee and Safford, Arizona, and Coyote Wells and Hot Mineral Well in the Imperial Valley, California.

ACKNOWLEDGEMENTS

This work was supported in part by the U.S. Geological Survey grant 14-08-0001-G-406.

REFERENCES CITED

Sass, J.H., et al., 1976, A new heat-flow contour map of the conterminous United States: U.S. Geol. Sur. open file rpt. 76-756, 24 p.

Swanberg, C.A., et al., 1975, An appraisal study of the geothermal resources of Arizona and adjacent areas in New Mexico and Utah and their value for desalination and other uses: New Mex. Energy Inst., Rpt. #6, 76 p.

Truesdell, A.H., 1976, Summary of Section III: Geochemical Techniques in Exploration: Proc. 2nd U.N. Symp. on the development and use of geothermal resources, San Francisco, 1975, v. 1, U.S. Govt. Printing Office, p. liii lxxix.

Geothermal Resources Council, TRANSACTIONS, Vol. 2 July 1978

SAN DIEGO GAS & ELECTRIC COMPANY'S GEOTHERMAL PROGRAM

C. R. Swanson

San Diego Gas & Electric Company
San Diego, California 92112

Program Goal

SDG&E's current Geothermal Program is directed toward determining the technical and economic feasibility of generating electric energy from the liquid-dominated hydrothermal resources of the Imperial Valley. The goal of the program has been to accelerate the development of geothermal energy production as an alternative to present conventional power generation for the Company. This is in accordance with the national energy policy to reduce the current level of dependence on imported fuels.

Development Risks

The development of geothermal energy for purposes of electrical energy production has a number of significant potential advantages. However, due to its present state-of-the-art, the development of this resource is also not without significant risks. The major constraints to large-scale development of liquid-dominated geothermal resources for electrical energy production may be classified into technical, environmental and economic risk categories.

- Technical Risks

1. Scaling of geologic zones from which the brine is produced and scaling in production and reinjection well bores. Either of these problems could severely limit brine production.

2. Excessive scale formation in brine-handling pipelines and equipment.

3. Shorter than anticipated reservoir life-spans, leading to premature cooling of the reservoir, and hence, reduced efficiency of power plant operation.

4. Excessive corrosion of brine-handling equipment.

5. Construction and operation of the large hydrocarbon turbines proposed for use in binary cycles. For instance, SDG&E's Heber demonstration project will require a 65 MWe hydrocarbon turbine. The largest such turbine built to date has been about 8 MW.

- Environmental Risks

1. There may be inadequate supplies of water currently available in the Imperial Valley to utilize in rejecting the waste heat from power plants. Since geothermal power cycles operate at low temperatures, the amount of heat flow per kilowatt of power is very high. Geothermal plants may consume from two to four times as much cooling water as conventional thermal plants of the same capacity.

2. Withdrawal of geothermal fluids could cause subsidence of the land overlying the reservoir. This would adversely affect farming in the area, as the supply of irrigation water depends on small changes in surface elevation. Reinjection of the geothermal brine may be necessary to minimize or eliminate this problem; however, it is not known whether full reinjection will be required.

3. Production and reinjection of geothermal fluids may also cause increases in seismic activity. While some studies have shown that most seismic activity occurs beneath geothermal production zones, only long-term experience will provide definite answers.

- Economic Risks

The most important challenge of SDG&E's Geothermal Program is to design and construct plants that can produce power cheaply enough to compete with conventional alternatives. Geothermal plants must produce economically competitive power; otherwise, the utility would be running the risk of not receiving rate increase authorizations for its geothermal plant investments, since cost of power is a high priority criteria used by regulatory commissions in assessing applications for plant certification.

The fixed costs of geothermal plants are estimated to be relatively high. Hence, to make busbar costs competitive, a geothermal plant will have to be on-line a very high percentage of the time. High plant availability levels will hopefully be assured through experience with the pilot and demonstration projects. To further reduce the fixed costs associated with geofluid production, tax incentives in the form of

recovery of intangible drilling expenses, and a depletion allowance are needed.

Program Description

SDG&E's current Geothermal Program involves research, development and demonstration activities to address these risks which are presently serving as constraints to large-scale commercial geothermal development. Specific objectives of the Company's current Geothermal Program include the following:

1. To assess and delineate those reservoir characteristics which may impact power plant operations.

2. To develop brine handling methods and equipment.

3. To optimize the design of power plants and to test power plant systems and components.

4. To demonstrate and evaluate commercial-scale power plant and reservoir operations.

5. To assess busbar cost of power from geothermal plants.

Achievement of these objectives is being pursued through the following SDG&E geothermal projects:

1. The Geothermal Loop Experimental Facility (GLEF) at Niland.

2. The large-scale demonstration plant project at Heber.

3. Participation in a small-scale pilot plant project of Magma Power Company at East Mesa.

Niland Geothermal Loop Experimental Facility

The Company's early exploration drilling of the Niland field was conducted by NARCO with Magma Power Company beginning in 1971. Wells were tested to obtain such reservoir information as flow characteristics, resource temperature, stability and mineral content of the geothermal brine. The preliminary design of the GLEF was undertaken in 1972. In 1973 and 1974, heat exchangers, piping and other equipment were tested extensively to determine:

1. The amount and rapidity of mineral-deposit buildup caused by the brine and how to control it.

2. Procedures, frequency and costs of cleaning deposits from piping and equipment.

3. Plant design parameters.

4. Improved methods to separate steam from the geothermal brine.

In August 1975, the Department of Energy (DOE), then ERDA, entered into a contract with SDG&E to fund 50% of the costs of the design, construction and operation of the GLEF. The facility was first started up in May 1976 and is scheduled to continue operations and testing through 1978.

- Purpose

The purpose of the GLEF project is as follows:

1. To reduce the risks associated with commercial-scale geothermal power plant development at the Niland reservoir by identifying problems and determining solutions to problems through experimental testing.

2. To help assess the capacity and long-term characteristics of the Niland reservoir.

- Participation

SDG&E, the GLEF project manager and facility operator, owns the property and facility, and provides half of the project funding.

DOE contributes the balance of the funding, and provides technology support through its Lawrence Livermore and Lawrence Berkeley Laboratories in the areas of brine chemistry, reservoir assessment, and data acquisition. The contract with DOE provides for an option to construct and operate an additional component test facility adjacent to the Geothermal Loop Facility.

In addition, the U. S. Bureau of Mines has established a materials test facility on the site. Imperial Magma Company is the reservoir operator, and NARCO shares the cost of reservoir operations with Magma.

SDG&E and the other project participants are confident that most of the major GLEF objectives will be achieved by late 1978. The detailed results of GLEF operation are being covered by W. O. Jacobson, GLEF Project Manager, in a subsequent talk.

Magma Power's Pilot Plant at East Mesa

Magma Electric Company, a subsidiary of Magma Power Company, is proceeding with the construction of an 11.2 MWe (net) binary ("Magmamax") cycle geothermal pilot power plant at East Mesa at the present time.

A letter of understanding provides for Magma to construct and operate the plant, with SDG&E buying the power for resale to Imperial Irrigation District (IID). This will entail the purchase and installation of the main power transformer and interconnect facilities by SDG&E to deliver the power to the IID system. In return, SDG&E will have access to the engineering data from Magma in regard to the (1) design, construction and operation of a binary cycle turbine on a small scale, and (2) the characteristics of the East Mesa reservoir. SDG&E also has the option of acquiring the plant from Magma after initial plant startup, which is expected to occur in late 1978.

Heber Geothermal Demonstration Project

The Heber reservoir is located at the southern end of the Imperial Valley (Figure # 1).

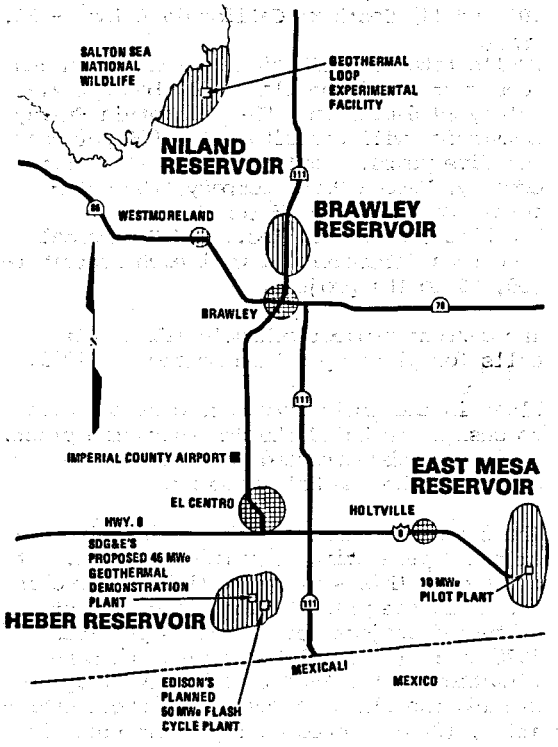


Figure 1

This reservoir was recommended as the site for a large-scale demonstration plant in a study completed in 1976 by The Ben Holt Company for the Electric Power Research Institute. Subsequently, SDG&E submitted a proposal to EPRI, and was contracted to continue the engineering design of the 65 MWe (gross), 45 MWe (net) demonstration plant and undertake its construction and operation if DOE cost-sharing support were obtained.

Tests conducted in 1973 by Chevron showed the reservoir to have a bottom-hole temperature of 360°F. Subsequent tests by SDG&E in 1974 for EPRI confirmed that the relatively clean brine would not cause significant scaling and corrosion problems.

- Purpose

The objective of the Heber Demonstration Project is to design, construct, operate and maintain a large-scale binary cycle geothermal power plant. Its purpose is to demonstrate the technical and economic feasibility of geothermal power generation from low salinity, moderate temperature, liquid-dominated resources. Such a demonstration plant would be the first large-scale power generating facility in the U.S. utilizing liquid-dominated geothermal resources, and the first large-scale plant in the world using the binary energy conversion process.

It is expected that information resulting from this demonstration will be applicable to a wide range of moderate temperature, low-salinity hydrothermal reservoirs. It is estimated that a large portion of liquid-dominated geothermal reservoirs in the U.S. fall into this category.

The binary energy conversion process (see Figure 2) to be employed in this plant has the potential advantage of converting a greater amount of geothermal heat into electrical energy than other thermal cycles.

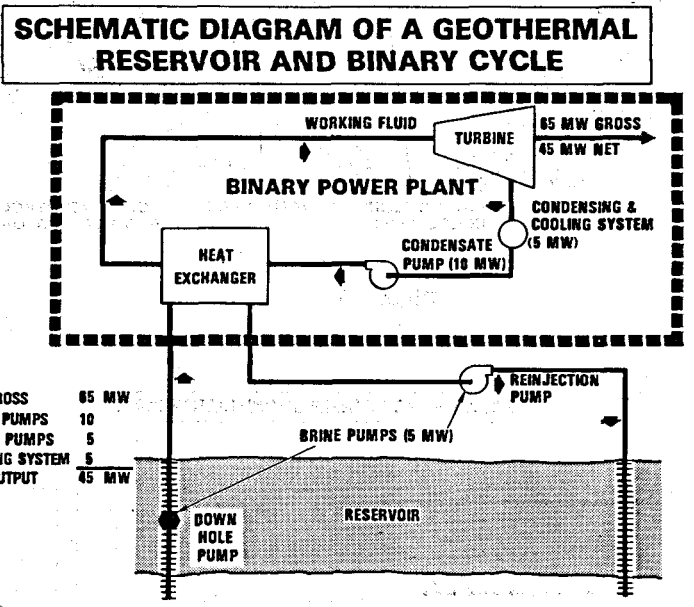


Figure 2

Much of the technology is now in existence, but it has not been proven on a large-scale. The major plant components, such as the hydrocarbon turbine, have never been constructed in this size.

An artists's rendering of the plant is shown in Figure 3. The major plant components include the cooling towers, turbine-generator and electrical equipment, brine working fluid heat exchangers, working fluid condensers, accumulators and condensate pumps. The production and injection well islands are also shown.

The project will be conducted in six separate phases. Phase I is the feasibility study discussed earlier, which was completed in late 1976. Phase II includes the preliminary engineering design. Work on this phase is currently underway. Phase III will involve the detailed engineering design, equipment procurement, and site preparation. Construction will be accomplished during Phase IV. Phase V will include plant startup and the initial test period. Phase VI will include long-term operation and performance evaluation.

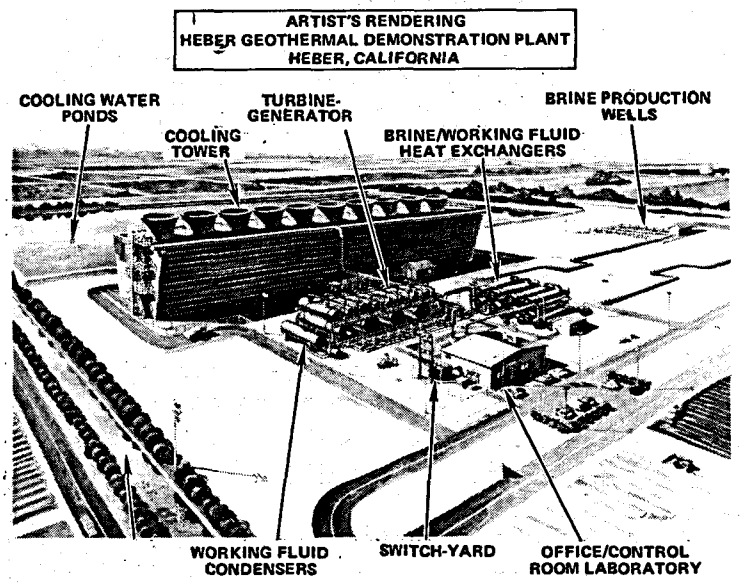


Figure 3

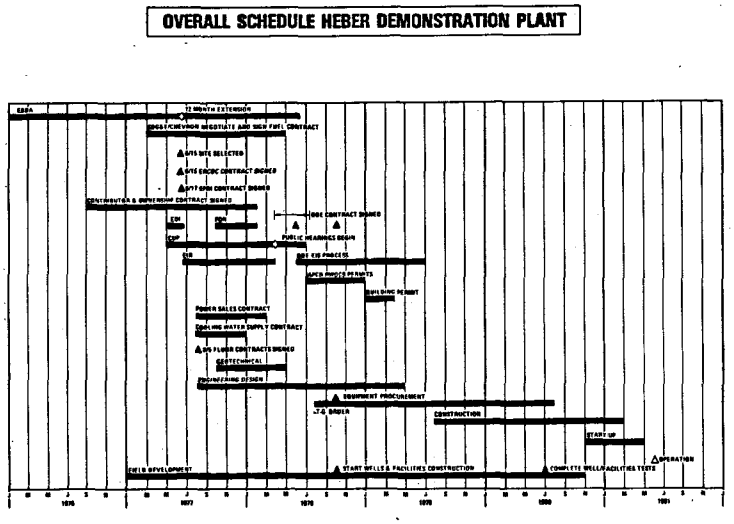


Figure 4

Phase II, now nearing completion, includes the following tasks: (1) obtain utility participants, (2) contract for (a) participation, (b) geothermal heat, (c) cooling water, (d) power sales and (e) engineering design (A/E), (3) obtain DOE funding support, (4) conduct preliminary engineering design, and (5) obtain permits and conduct environmental studies.

The project is being managed by SDG&E. EPRI, the California Energy Commission, the California Department of Water Resources, five other utilities and two resource companies have committed to participation. The plant owners include: (1) San Diego Gas & Electric Company - 77%, (2) Imperial Irrigation District - 10%, (3) Los Angeles Department of Water and Power - 10% and (4) Southern California Edison - 3%.

EPRI's total contribution to the design and construction of the plant will be approximately $4.6 million. The California Energy Commission will contribute $50,000 per year for five years. Portland General Electric Company, Nevada Power Company, the California Department of Water Resources, Republic Geothermal, Inc., and Geothermal Resources International will each contribute $50,000 to the project.

The current project schedule (Figure 4) calls for plant operation before mid-1981.

Fluor is the engineer/constructor selected to design and build the demonstration plant. Fluor has subcontracted portions of the design to The Ben Holt Company.

The detailed results of the engineering design and permitting activities to date, not covered in this summary, will be covered in detail in the presentation. The current status of project activities as of March 1978 are: (1) completed review and confirmation of the EPRI feasibility study including the flash versus binary cycle evaluation, (2) developed an implementation plan, a project design guide, and a procedures manual for the project. Will begin detailed engineering of plant on May 1st when preliminary engineering is scheduled to be completed and the project design guide is approved, (3) established the engineering schedule, (4) completed negotiations and executed contracts with owning and contributing project participants, (5) negotiations with the Imperial Irrigation District for the sale of power and the purchase of cooling water have been completed. We expect to execute these contracts in April 1978, (6) the Environmental Impact Report and Rezoning Application have been prepared and reviewed. Approval of these documents by the Imperial County Planning Commission was received on March 22, 1978. Hearings on the Conditional Use Permit are scheduled for early May 1978, (7) preliminary engineering is near completion and system optimization studies are currently underway, namely, the brine/hydrocarbon system and cooling water system, and (8) negotiations with Chevron Resources Company for the purchase of geothermal heat energy are continuing. We expect to conclude these negotiations and execute an agreement by May 1978. Among the early engineering tasks is the development of a specification for the turbine-generator. Vendors predict that 18 to 24 months will be required for turbine-generator lead time. This results in a purchase date of October 1978 for this item.

GEOTHERMAL ENERGY RESOURCES: EXPLORATION BUDGETS AND COSTS RECOVERY

Ronald T. Takashima

GeoThermal Services, Inc.
10072 Willow Creek Road
San Diego, California 92131

ABSTRACT

Increasing costs of geothermal exploration have made it a necessity that program managers be adequately trained to collect and analyze budgetary data. Exploration budgets should be used to monitor and control dollar expenditures. Furthermore, the program manager must properly utilize the available geothermal exploration techniques with an adequate economic and technical analysis of the acquired data in order to provide a supported determination to continue each exploration venture. Finally, appropriate utilization of cost information should allow geothermal exploration management to make proper decisions as to cost control and calculations of cost recovery.

INTRODUCTION

An important aspect of the economic development of geothermal resources is the fuel or energy price which represents the fair market price for a risk taking energy company in the private sector that explores for, drills, tests, and produces steam or hot water and delivers it through a system of gathering lines to the utility or other end product user. The major cost of exploring for, developing, and producing a geothermal resource is that of drilling and casing the large diameter, deep holes in hot formations that are needed to bring the geothermal fluids to the surface. Therefore, the intent and purpose of any geothermal exploration program is to minimize the number of unsuccessful deep tests, i.e., minimize the number of dry holes or maximize the number of productive wells. This can be most successfully acomplished by conducting a cost effective and technically decisive exploration program. Cost effective in the sense that the monies spent on an exploration program should not represent more than a small percentage of the total costs of the deep exploratory wildcat and development wells. Technically decisive in that most of the questions pertaining to the availability of a viable economic geothermal resource at depth can be adequately answered by the exploration effort.

Due to the increased costs of geothermal exploration, industry personnel must be adequately trained to collect and analyze cost information data to properly assess the program development. Appropriate utilization of the cost information should allow exploration management to make proper decisions as to cost control and calculations of cost recovery. Cost information on each prospect must be collected and compared to the initial prospect budget and then if necessary, budget updating can be prepared.

BASIC REQUIREMENTS OF EXPLORATION BUDGETS

Budgets and budgetary information tools have been used in several high risk industries and in many ventures where cost estimates have been useful in planning cash flow and investment strategies.

Typical budgets include such information as:

1. Total program funding
2. Task, function
3. Amount of contract or projected costs
4. Costs to date
5. Estimate to complete
6. Variance.

Exploration budgets should be used to monitor and control dollar expenditures. This monitoring of the program costs will be useful in determining the financial impact of program extensions or cut backs prior to initiating such changes. If properly updated, the budgetary information will produce a variance report upon which the program manager can analyze and make recommendations.

As shown in the example presented in Table 1, the committed costs include program changes which should be noted. These costs have been adjusted to reflect the changes. The total updated budget can then be used to help determine if the program economics are in line with the original projections.

Since the initial exploration costs should represent approximately 15 to 20 percent of a geothermal development program, including deep test drilling, it appears that the data collection prior to the citing and drilling of the first wildcat would be of a greater impact than the accumulation of costs expended on the initial program. It can be noted, however, that the program manager must keep in mind that the initial exploration tools, i.e., geology, geochemistry and geophysics, should be properly utilized in order to provide a

good economic and technical review of the program prior to committing the company to spending additional development funds on the prospect.

If the program manager properly uses the available geothermal exploration methods and techniques and adequately analyzes the resulting data, the final determination to continue his program can be supported. This will help in continuing his task of evaluating the balance of his prospect areas since the company will see that he is evaluating the exploration results on both an economic and technical basis.

dollar limitation on each geothermal exploration program.

Due to the number of influences which are generally outside of the expertise of the program manager, it appears that there should be a full utilization of the supporting departments such as accounting, tax and economic departments. With this type of approach, the program manager should develop his resources and be able to utilize all available tools to aid in the evaluation of each geothermal prospect.

TABLE 1. EXAMPLE GEOTHERMAL EXPLORATION BUDGET

PROSPECT AREA: _____
REPORT AS OF : _____
PREPARED BY : _____

TASK/FUNCTION	CONTRACTOR	CONTRACT OR PROJECTED COST	COST TO DATE	ESTIMATED COST TO COMPLETE	TOTAL COMMITTED COST	OVER (UNDER) BUDGET	COMMENTS
Geology	In-house	$ 15,000	$ 13,200	$	$ 13,200	$(1,800)	Additional mapping
Microseismics	In-house	18,000	23,400		23,400	5,400	Purchase additional equipment charged to prospect
Gravity	A company	23,000	22,700		22,700	(300)	
Resistivity	B company	28,000	14,000		14,000	(14,000)	Program decrease
Magnetotellurics	C company	62,000	57,000	5,000	62,000		Final report due
Geochemistry	In-house	8,000	9,500	1,200	10,700	2,700	Add outside lab fees
Temperature gradient/heat flow 25-500'	D company	146,000	50,368	132,240	184,608	38,608	Increase in program to 30-500' holes
3-1,500'	D company	142,500		95,000	95,000	(47,500)	Only two intermediate depth holes to be drilled
SUB-TOTAL		$442,500	$190,168	$235,440	$425,608	$(16,892)	

COST RECOVERY

One of the greatest influences on the program is the compilation of the potential for cost recovery. Companies must decide what rates of return, risk factors and total committments that are acceptable for them. It appears that these variables between companies must be understood and kept in mind by the program manager in order to properly assess the geothermal prospect.

Items such as income tax factors should be understood since the costs will be decreased by the tax impact, or the funds committed may greatly influence the company's position on timing of the expenditure. Items which are classified as "expense" rather than "capitized development" costs may be expended in a profitable period, but may be deferred in a low profit or loss period.

Overall, compilation of cost recovery should be made using the latest information on utility price schedules, required rates of return, income tax effect and estimated program life. This compilation will then be utilized to project available funds to be budgeted and establish a total

MODELING THE HEBER GEOTHERMAL RESERVOIR

Erdal O. Tansev
Chevron Resources Company

Mel L. Wasserman
Chevron Oil Field Research Company

Abstract

In this paper we briefly describe the lithology, temperature, and pressure of the Heber Geothermal Reservoir. This we base on the extensive data gathered in the past few years through well drilling and testing. We then describe our three-dimensional, heterogenous, single phase water flow simulator, including the equations solved, and the assumptions made. We present several applicatins of the numerical simulator, in predicting the reservoir behavior with time. Conclusions based on an analysis of simulator results are finally presented.

Introduction

The Heber Geothermal Anomaly, located in the Imperial Valley of California, could be the first commercial hot water power generation project in the United States. Chevron Resources Company will operate the proposed Heber Unit. Currently, plans are for developing a nearly circular area of 7500 acres, with each plant increment representing a pie-shaped segment. Producers will be placed at the temperature high which is at the center. The processed fluid will be reinjected at the periphery of the reservoir. Wells will be drilled from centrally located surface islands, most of them being directionally drilled. Production rates at Heber will ultimately reach several millions of barrels per day. This requires large surface facilities and large well equipment. Revenues cannot be realized until a power plant is constructed. Due to large initial investment, an accurate reservoir performance prediction becomes an important factor. The predictions in this paper are limited by the accuracy of the data collected and analyzed, and by our modeling assumptions.

Reservoir Description

The Heber Geothermal Anomaly is a circular shaped, moderate temperature, low salinity, water dominant reservoir. It is characterized by high heat flow, low electrical resistivity and high gravity. It is part of the Colorado River deltaic environment, consisting of interbedded sandstones and shales. Shales are thick and predominant from the surface to 2000 feet. Sand layers become predominant below 2000 feet, where shale layers become thinner.

At 8000 to 10,000 feet sands are predominant with minor shale breaks. A few faults have been identified, others are probably present; however, any occurring in the predominantly sandy section would not be significant barriers to fluid flow. Reservoir continuity of several sand layers have been confirmed by interference tests. Pressure drawdown and buildup tests have indicated a radius of investigation greater than 20,000 feet.

Porosity and horizontal permeability of the sand layers at Heber were determined by using available density logs and core analysis information. Good correlations were found between density log porosity and core porosity, also between core porosity and core permeability. Permeability of each sand was calculated from the latter correlation and the log derived porosity values. It was possible to correlate these permeabilities to permeabilities computed from flow test analysis. In general, sandstone layers demonstrated decreasing permeability and porosity with depth.

The Heber Geothermal Anomaly has a mushroom-shaped temperature profile. The maximum temperature at the center of the field is around 375°F. Conductive heat flow at shallow depths could be deduced from high temperature gradients and the presence of thick impermeable shales. Below this depth heat flow is naturally convective, as temperature gradients become small and sandstones dominate. To a reference temperature of 200°F, the heat in place under approximately 7500 acres, and between 2000 to 6000 feet is 5.4 quadrillion (10^{15}) BTU's. Heber could be classified as a normal pressured reservoir with measured static gradients of 0.42 psi/foot.

Reservoir Model

To predict Heber's performance under various development schemes, a three-dimensional, radial, heterogeneous, and single phase water flow simulator was used. The simulator basically solves the mass and the energy balances. The equation of continuity, expressing conservation of mass[1], is:

$$\frac{\partial(\rho_\ell \phi)}{\partial t} = -\nabla\cdot\rho_\ell \underset{\sim}{V}_\ell - Q \qquad \ldots.(1)$$

where:

ℓ denotes liquid, ρ_ℓ is liquid density, (lbm/ft^3), ϕ is porosity, t is time (days), $\nabla\cdot$ is divergence operator (1/ft), Q is mass production or injection. It is a function of position and time ($lbm/day\ ft^3$), a positive value denotes production. $\underset{\sim}{V}_\ell$ is the Darcy velocity vector of the fluid (ft/day) and expressed as:

$$\underset{\sim}{V}_\ell = -6.328 \frac{k}{\mu} \nabla\cdot\Phi \qquad \ldots.(2)$$

where:

k is permeability (Darcy), μ is viscosity (cp), Φ is the fluid potential (psi), = pressure + gravity correction.

The following assumptions were made:

Porosity is not a function of time; it can, however, be a function of position.

Viscosity is a function of temperature.

Liquid density is a function of temperature, but is independent of pressure, making the model "partially compressible." Zero fluid compressibility is satisfactory for single phase water systems.

Next we expand the density derivatives in equation (1).

$$\frac{\phi\partial\rho_\ell}{\partial T}\frac{\partial T}{\partial t} = -\rho_\ell\nabla\cdot\underset{\sim}{V}_\ell - \underset{\sim}{V}_\ell\cdot\nabla\rho_\ell - Q \qquad \ldots.(3)$$

where T is temperature. We also assume that the reservoir fluid volumes are locally in balance. Therefore:

$$\nabla\cdot\underset{\sim}{V}_\ell = -\frac{1}{\rho_\ell} Q \qquad \ldots.(4)$$

Without this assumption we could not let density vary with temperature without using a fully compressible two-phase model. The produced fluid at Heber will be initially at 360°F, the injected water will be at 200°F. In order to maintain a mass balance between production and injection, we assumed that the required mass came across the outer reservoir boundary at a temperature under 200°F. Thus, we avoided solving - complicated and costly - coupled mass and energy balances.

The equation for conservation of energy[1] is:

$$\frac{\partial}{\partial T}[(\rho C_V)^* T] = \phi C_{V_\ell}\frac{\partial}{\partial t}(\rho_\ell T) + (1-\phi)\rho_3 C_{V_S}\frac{\partial T}{\partial t} = \ldots.(5)$$

where: $\nabla\cdot(K^*\nabla T) - C_{V_\ell}\nabla\cdot(\rho_\ell T\underset{\sim}{V}_\ell) - QC_{V_\ell}T_N$

s denotes solid, C_V is specific heat at constant volume (BTU/lbm°F), K is thermal conductivity (BTU/ft day°F), T_N is injection fluid temperature if $Q<0$, T_N is produced fluid temperature if $Q>0$.

The left hand side of equation (5) represents heat accumulation; the terms on the right hand side are respectively, conduction, convection and injection and/or production.

In relation to equation (5) we have defined the following volumetric averages:

$$K^* = \phi K_\ell + (1-\phi)K_S$$

$$\rho C_V^* = \phi\rho_\ell C_{V_\ell} + (1-\phi)\rho_S C_{V_S} \qquad \ldots.(6)$$

And we made the following assumptions:

The solid and liquid are locally in thermal equilibrium.

The viscous dissipation energy losses are negligible.

Specific heats are independent of pressure, temperature, and position.

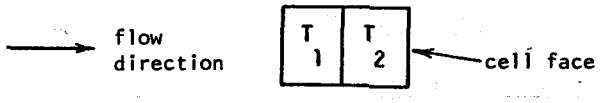
Thermal conductivities are independent of pressure and temperature.

Rock densities are constant.

Solution - We have independently solved equations (4) and (5). Equation (4) gave us a steady-state solution for pressure, and provided the velocity terms required by the energy balance, equation (5). We conservatively used two temperature time steps per pressure solution. The need for recomputing pressures arose when: (a) the temperature dependent viscosities materially changed, (b) injection and/or production rates changed with declining reservoir temperature in order to maintain constant energy. Time Dating of Terms - In equation (4) the latest temperatures were used to calculate liquid density and viscosity. In the finite difference form of equation (5), temperature was used implicitly in the conduction term, explicitly in the convection term. Densities were evaluated at start of time steps.

Overburden and Underburden - The first four and the last four layers of the model were used as overburden and underburden with zero fluid permeabilities.

Numerical Dispersion - In an effort to reduce smearing of the temperature profiles, a two-point-upstream approximation[2], for temperature, was used in the convection term. The illustration below shows two cell blocks.



In evaluating the temperature T in the $\rho_\ell T\underset{\sim}{V}_\ell$ term at the cell face, T_1 and T_2 are linearly extrapolated to the cell face. A one-point-upstream approximation uses only T_2 and results in excessive smearing of temperature. Averaging upstream

and downstream values gave temperature oscillations and was discarded.

Flow Splitting - Flow rates for production wells were supplied and were split among the layers according to the product of productivity index and pressure drawdown - difference between current cell and well bore pressure. Injection wells used either fixed pressures or supplied flow rates.

Applications

Based on lithological correlations and production constraints, we defined two zones: zone 1, 2000 to 4000 feet: zone 2, 4000 to 6000 feet. We then subdivided zone 1 into 15 and zone 2 into 13 horizontal sand and shale layers of field-wide averaged thickness. Figure 1 shows the geometry we used. We further divided Heber into 8 areal pies, each pie having 15 rows. Therefore, 1800 cells in zone 1, 1560 cells in zone 2 represented the reservoir. We also made the following assumptions:

> The sand and shale layers themselves are continuous, homogeneous and isotropic.
>
> The initial temperatures are a function of radial coordinate; they do not vary with vertical coordinate in a given zone.
>
> The regional northerly ground water movement is small, hence negligible.
>
> There is no heat recharge from the underburden.

Pies initially were chosen such that their boundaries coincided with stream lines as obtained from the previous streamtube model runs. Most 3-D simulator runs were made assuming no cross flow between the pies.

Figure 2 shows bottom hole temperatures at the producers versus time for 100 megawatts (MW) constant energy production from each zone. Equivalent starting rates are 1.24×10^6 barrels per day per zone. Also shown on this figure are the previous predictions using the streamtube model. The difference in predictions can be explained as follows: the 3-D simulator has the capability of solving a rigorous heat conduction equation, given the actual thicknesses of sand and shale layers. The streamtube model assumed vertical thermal equilibrium between sand and shale in each reservoir layer. It could handle the shales as thin layers of infinite thermal conductivity. The injected fluid, upon contacting these shales, absorbed all their heat. In zone 1, the streamtube model predicted a greater temperature decline and in zone 2 it predicted about the same temperature decline as the 3-D simulator. We think the small difference in zone 2 is due to the use of slightly less shale. The difference in general was due to a better vertical lithological description and a more rigorous heat conduction equation. The 3-D model shows a 30°F decline in thirty years for both zones.

Figure 3 shows the bottom hole temperature at the producers versus the cumulative water produced. This figure indicates the large volume of water required to produce 100 MW constant energy from each zone.

Figure 4 shows heat recovery from Heber versus bottom hole temperature at the producers. This plot is for two zones combined. The 200°F temperature is used as a lower bound in determining the heat in place. We have tentatively decided to place the injectors near the 265°F isotherm. If we use an economic temperature of 320°F for the power plant, as a cutoff point, Figure 4 shows a recovery of 30% of the heat in place.

Figure 5 shows the predicted average pressure drops between injectors and producers versus time.

The following case studies showed little or no difference in our predictions:

> Combining both zones - simultaneous injection and production in both zones.
>
> Introducing shale breaks - making 10% of the shale volume permeable to flow.
>
> Introducing a few "idle pies" - by partitioning the bigger ones, with no injection and production, and allowing crossflow between all pies.

Conclusions

As a result of our modeling studies to date, we conclude the following:

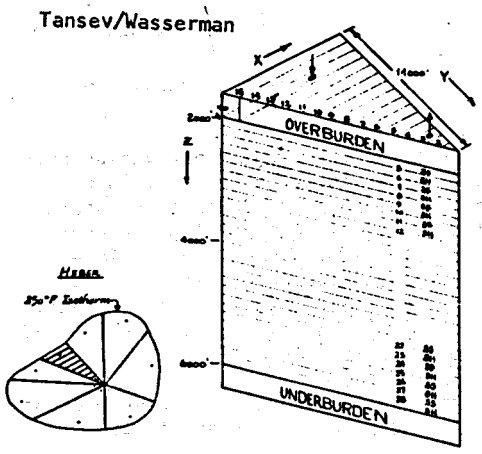
> Heber has 5.4 quadrillion (10^{15}) BTU's in place to a temperature of 200°F. This heat is under approximately 7500 acres within the 265°F isotherm, and between 2000 to 6000 feet.
>
> 30% of this heat in place is recoverable with respect to the plant economic temperature of 320°F.
>
> Heber Reservoir between 2000 to 6000 feet alone can support a 250 MW development.
>
> At Heber, development in general will be more restricted by pressure drops than by temperature decline.
>
> Economics will govern the power plant type and the development potential at Heber.

References

1. Bird, R.B.; Stewart, W. E.; and Lightfoot, E.N., Transport Phenomena, Wiley, 1960.

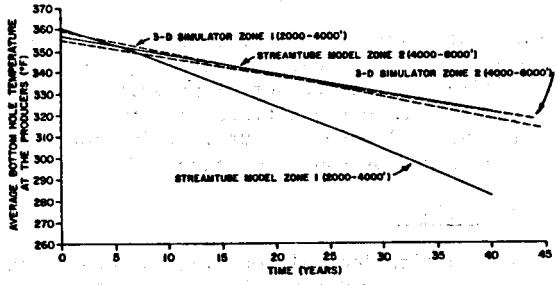
2. Todd, M. R.; O'Dell, P. M.; and Hirasaki, G.J., Methods for Increased Accuracy in Numerical Simulators, Society of Petroleum Engineers Journal (December 1972), pp 515-530.

Tansev/Wasserman



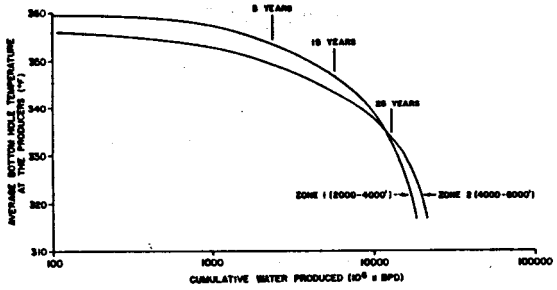
GEOMETRY OF 3-D RESERVOIR MODEL

FIGURE 1



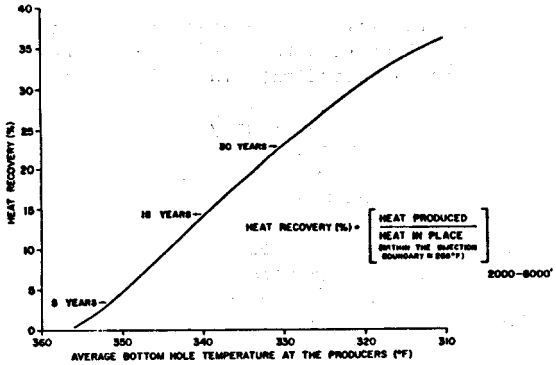
BOTTOM HOLE TEMPERATURE AT THE PRODUCERS VS.
TIME FOR 100 MW CONSTANT ENERGY PRODUCTION PER ZONE

FIGURE 2



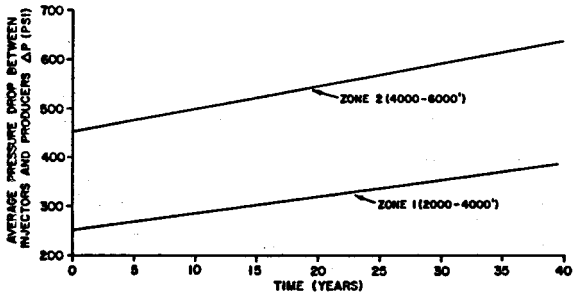
BOTTOM HOLE TEMPERATURE AT THE PRODUCERS VS.
CUMULATIVE PRODUCTION
(100 MW CONSTANT ENERGY FROM EACH ZONE)

FIGURE 3



HEAT RECOVERY VS. BOTTOM HOLE TEMPERATURE AT THE PRODUCERS
(200 MW CONSTANT ENERGY FROM TWO ZONES COMBINED)

FIGURE 4



AVERAGE PRESSURE DROP
BETWEEN INJECTORS AND PRODUCERS VS. TIME
(100 MW CONSTANT ENERGY FROM EACH ZONE)

FIGURE 5

DEVELOPMENT OF INJECTION CRITERIA FOR GEOTHERMAL RESOURCES

John D. Tewhey, Marjorie A. Chan, Paul W. Kasameyer and Lawrence B. Owen

University of California
Lawrence Livermore Laboratory
Livermore, California 94550

INTRODUCTION

The ability to inject large quantities of brine effluent will be an important factor in the development of liquid-dominated geothermal systems. Experimental studies have been conducted by the Earth Science Division of the Lawrence Livermore Laboratory (LLL) to evaluate injection of "spent" geothermal brine at the Salton Sea Geothermal Field (SSGF). The studies have dealt principally with the injectability of suspended solids that are produced in the brine during the energy conversion process. In the experimental plan, the subsurface medium was represented by membrane filters with pore diameters ranging from 0.4 to 10 microns and by sandstone core material. Changes in permeability with time were evaluated with respect to the following variables: (1) prefiltration of brine upstream from the core or membrane filter, (2) brine temperature (20°C to 100°C), (3) brine pH (Owen, 1977) and (4) confining pressure.

MATERIALS AND METHODS

All experiments were conducted at LLL's test facility at the SSGF utilizing brine production from the Magmamax #1 and #2 wells. The experimental apparatus and methodology of testing are described in detail by Netherton and Owen (1978, this volume). Subsurface cores from the SSGF were unavailable for testing. Analogues of reservoir rocks were chosen for testing from several well-characterized sandstones. Samples selected were Kayenta sandstone, a lithic quartz arenite (Triassic) from Colorado and Berea sandstone, an orthoquartzite (Miss.) from Ohio. The porosity of Kayenta and Berea sandstones are approximately 20% and 18%, respectively. Permeabilities were determined by means of the equation

$$k = \frac{\Lambda Q L}{A\,(P_2 - P_1)} \qquad \text{(Eq. 1)}$$

where k = permeability (darcy)
Λ = viscosity (centipoise)
Q = flow rate (cm^3/sec)
L = core length (cm)
A = core cross-sectional area (cm^2)
P_2 = incoming brine pressure (atm)
P_1 = outgoing brine pressure (1 atm)

MEMBRANE FILTER RESULTS

Membrane filtration tests are a standard tool in the petroleum industry to evaluate injection well performance. Analytical models are available (i.e., Barkman and Davidson, 1972) which relate filtration data to injection well longevity. Input data required in the models are suspended solids concentration (w) and filter cake permeability (k_c) as well as injection well and formation characteristics. For wells with characteristics of those of the SSGF, the water quality ratio (w/k_c) must be < 1 to insure that the injection has a half-life of greater than one year. The half-life is the time required for the injection rate to decline to one half of its initial value at constant differential pressure. The membrane filtration tests run with acidified brine ($pH \leq 4.6$) and unmodified brine ($pH = 5.8$) at 80°C resulted in w/k_c values ranging from 500 to 900,000, thereby predicting a short half-life for injection wells ($t_{1/2} < 0.01$ years). The analytical results are supported by observations of filters with the scanning electron microscope (SEM). The pores of a membrane filter are rapidly plugged by deposition of amorphous silica from acidified or unmodified brine that is supersaturated with respect to silica (Fig. 1). These results suggest that the effluents produced at the SSGF are unsuitable for direct injection into a porous medium.

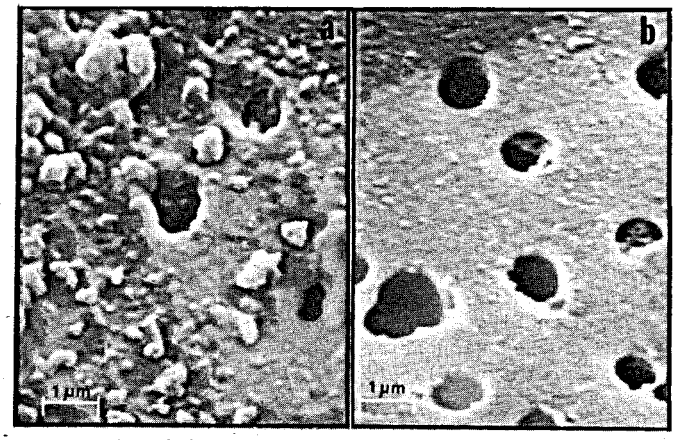


Figure 1. (a) Scanning Electron Micrograph of a portion of a 1 µm membrane filter partially plugged by amorphous silica deposited from silica supersaturated brine at 80°C. (b) Unused 1 µm membrane filter, same magnification as (a).

In developing the appropriate pre-injection treatment of a specific effluent, it is necessary to consider the effects of(1)suspended solids concentration, (2) particle size distribution of suspended solids and (3) the permeability characteristics of filtered solids. A suite of filtration tests were done on brine effluents from the Magmamax #1 and #2 wells in the SSGF and the results

are depicted in Fig. 2a-b. Magmamax #2 brine is produced from a lower interval in the reservoir (3784-4360 ft) than Magmamax #1 (1797-2264 ft) and contains higher dissolved silica, iron and total dissolved solids. A 10μm prefilter retained 91% of the suspended solids in Magmamax #1 brine whereas only 36% of the solids were retained by an 10 μm filter with Magmamax #2 effluent. The differences in the particle size distribution resulted in significant differences in filter cake permeability. It should also be noted that prefiltration to 1 μm permits substantial volumes of effluent to be passed through a 0.4 μm filter. Using the Barkman and Davidson analytical model (1972), the estimated half-life of an injection well accepting 1 μm prefiltered effluent at a rate of 320,000 lbs/hr (ρ = 1.15 g/cc) into a uniform porous medium 250 feet thick is one year or less, depending on formation permeability.

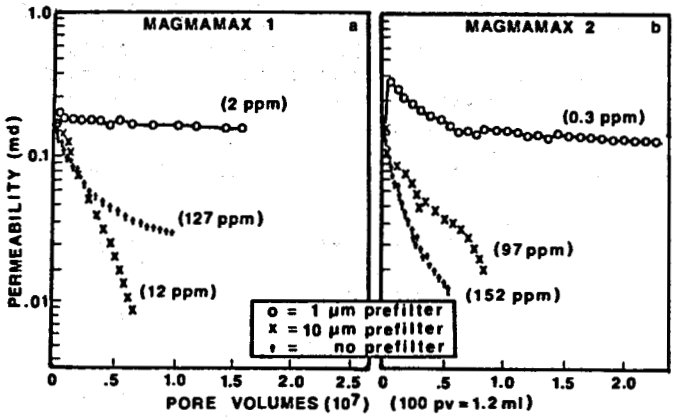


Figure 2. Results of filtration tests of Magmamax #1 and #2 effluents with 0.4 μm filters. Brines were subjected to 2.5 hours residence time in holding tanks at 85°C. Numbers in parentheses are suspended solids input to 0.4 μm filters.

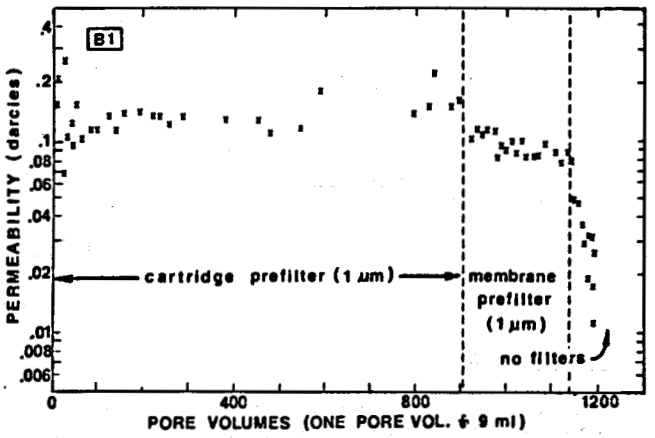


Figure 3. A plot of permeability versus brine throughput illustrating the effect of prefilters on core permeability. Brine temperature, 50°C; differential pressure, 45 psi; core confining pressure, 500 psi.

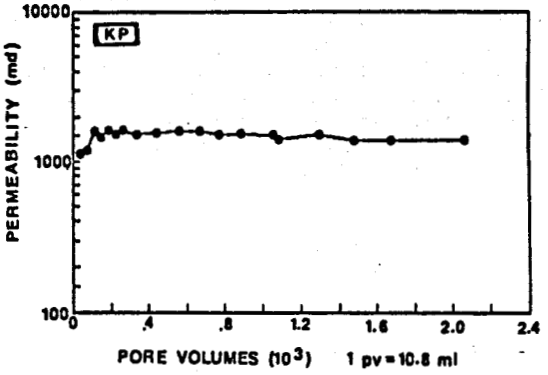


Figure 4. Permeability of Kayenta core KD with sand-column prefilter. Brine temperature, 62°C; differential pressure, 25 psi; core confining pressure, 500 psi.

CORE RESULTS

The Effect of Prefiltration on Core Permeability

All experimental core runs conducted as part of this study indicate that prefiltering of "spent" brine is essential for successful injection into porous media. Typical results of prefiltering are shown in Fig. 3. A core of Berea sandstone (B1) was flushed with brine overflow from an LLL-operated prototype clarifier. The effluent was pretreated with caustic prior to entry to the clarifier to provide a silica undersaturated effluent with approximately 150 ppm suspended solids. One micron cartridge and membrane filters were effective in removal of solids and, thereby, enabled the core permeability to be maintained. However, the core permeability degraded rapidly when the filters were removed. Similar results were obtained for runs with acidified brine.

Kayenta core KP (Fig. 4) was flushed with brine effluent from the LLL clarification-filtration system described by Quong et al. (1978, this volume). The mixed-media filter column (coal-sand-garnet) acted as a 1 μm prefilter and resulted in no degradation of permeability over the run duration.

The Effect of Brine Temperature on Core Permeability (Acidified Brine)

The permeability of core samples was found to be a strong function of the temperature of the incoming brine. The permeability-pore volume plots for four experimental runs of Kayenta sandstone (Fig. 5) show a systematic decrease in permeability corresponding to decreases in brine temperature. The temperature-dependent phenomena which influence core permeability are precipitation of solids from brine and disolution of calcite from the rock matrix. The extent of solids precipitation during the transit of brine through the core was determined by (1) chemical analysis of the brine upstream of the core and by (2) scanning electron microscopy (SEM) of the core subsequent to experimental runs. In all core runs, the amount of dissolved silica in the brine (as SiO_2) decreased while transiting the core and all cores showed evidence of precipitation of iron-rich amorphous silica on core surfaces and in the rock matrix. The precipitation of silica from acidified brine was found to be more prominent at lower brine temperatures. The quantitative data relating silica precipitation to brine temperature is presented in Fig. 6. SEM photographs (Figs. 7a-b) corroborate

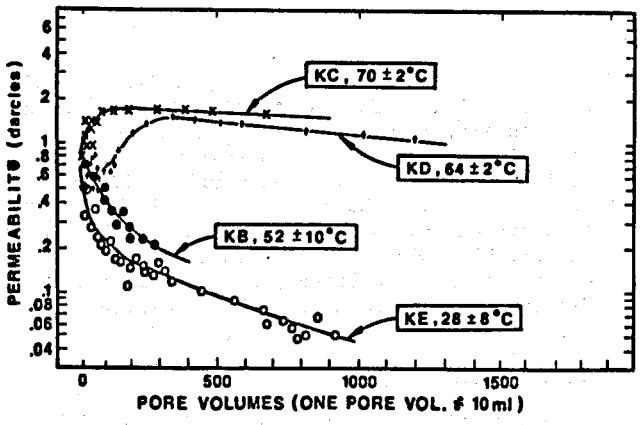


Figure 5. Plot of permeability versus volume of throughput for four cores of Kayenta sandstone at various brine temperatures. All runs were with prefiltered (1 μm) acidified (pH ≤ 4.6) brine and cores at 500 psi confining pressure.

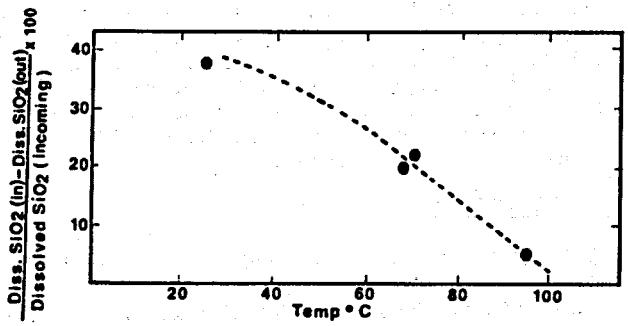


Figure 6. Percentage of dissolved silica precipitated in core for runs of Kayenta sandstone at various temperatures.

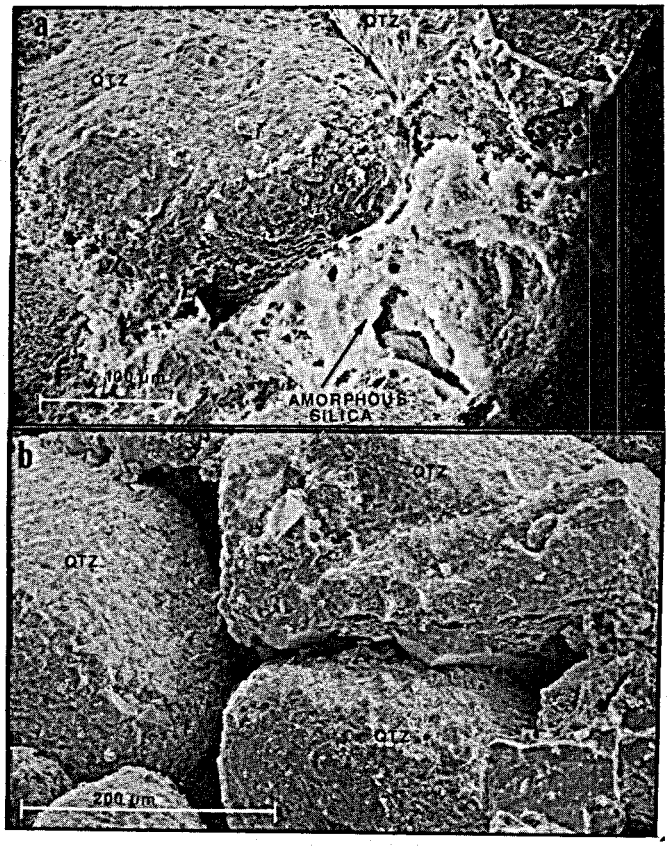


Figure 7. (a) SEM micrograph of silica deposition in upper portion of core KD run at 64°C. In this high temperature run, silica precipitation is less than in lower temperature runs and does not completely plug pore space. (b) Original Kayenta sandstone at same magnification as (a).

that silica deposition is more prominent in lower temperature runs. X-ray diffraction analyses of filter cake on the top surface of cores and SEM x-ray dispersive analysis of matrix deposition confirms that the pore-plugging substance is iron-rich amorphous silica. Calcite dissolution by acidified brine (avg. pH = 4.55) is a permeability-enhancing phenomenon that occurs principally in cores run with high-temperature brine. Only minor evidence of calcite dissolution was observed with the SEM in cores run at lower temperatures (60°C). Fig. 8 shows evidence of dissolution of calcite cement in core KD which was run at 64 ± 2°C. The initial increase in permeability exhibited by cores KC and KD (Fig. 5) may be due to calcite dissolution.

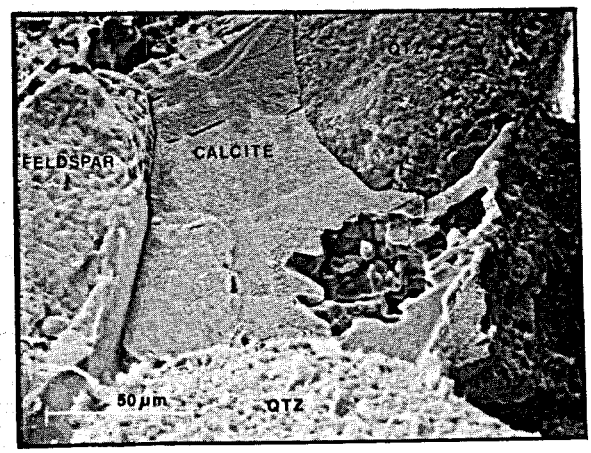


Figure 8. The prominent cavity in the calcite matrix from run KC (70°C) is interpreted as a dissolution phenomenon.

A Note on Brine Viscosity

The viscosity of brine produced from Magmamax 1 has been determined by Piwinskii et al., (1977). The viscosity-temperature plot in Fig. 9 shows that viscosities vary by a factor of two over the temperature range of the experimental runs shown in Fig. 5. The temperature-dependence of brine viscosity is accounted for in Eq. 1.

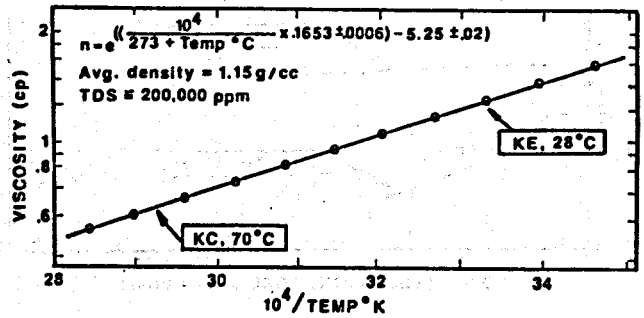


Figure 9. Plot of viscosity versus inverse temperature for acidified brine. Viscosity for runs KC and KE (see Fig. 5) are indicated.

The Effect of pH on Core Permeability (Acidified versus Unmodified Brine, Prefiltered)

Comparative core flooding experiments were made with acidified brine (avg. pH = 4.0) and unmodified brine, each with a 1 μm cartridge filter upstream from the core. Prior to entering the core, the unmodified brine was subjected to a 2.5 hour residence time in settling tanks operated by Magma Power Company. The data in Fig. 10 indicate that (1) there is essentially no difference in core permeability with acidified versus slightly supersaturated unmodified brine that has undergone a settling process and (2) in both cases, permeability is maintained with only minor degradation after the flow of several thousand pore volumes of brine.

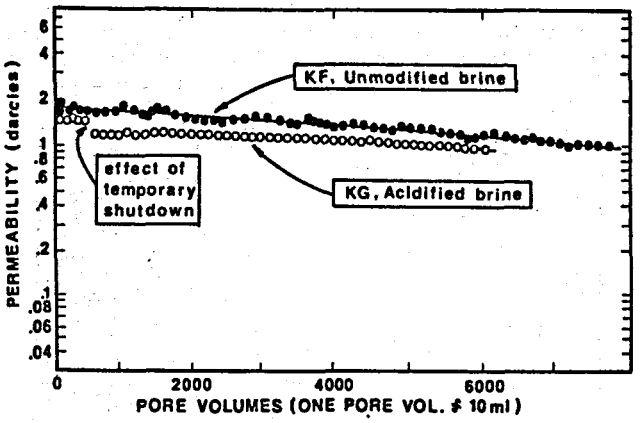


Figure 10. Results of a comparative study of prefiltered acidified brine and prefiltered unmodified brine that flowed through settling tanks. Run KF was at 70 ± 4°C and KG was at 94 ± 3°C. Both runs were at confining pressures of 500 psi.

The Effect of Confining Pressure on Core Permeability (Acidified Brine)

Assuming an overburden pressure gradient of 0.9 psi/ft. and a counteracting pore pressure of 0.45 psi/ft., a confining pressure 500 psi represents a depth of 1100 feet and 1550 psi, 3500 ft. A suite of early experimental runs were done at confining pressures of approximately 1550 psi whereas later runs were done at 500 psi. In Fig. 11, cores, KC and KA were run identically

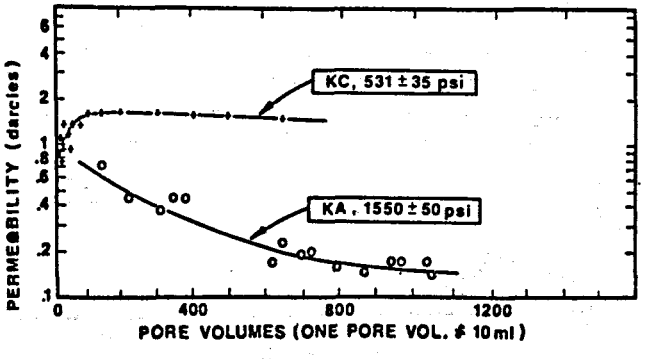


Figure 11. Plot of permeability versus brine throughput for runs or Kayenta with differing confining pressure. KC and KA are runs with acidified brine (pH ≤ 4.6). KA data from Piwinskii and Netherton, 1978.

with respect to temperature, pre-filtering and pH (acidified). The substantial difference in permeability is attributed to the effects of confining pressure. In single runs where confining pressure was varied, similar differences in permeability are observed. It should be pointed out that the Kayenta sandstone is loosely cemented and friable. Confining pressure is likely to have a more significant effect on the permeability of Kayenta than on the more highly cemented reservoir rocks in the SSGF (see Tewhey, 1977).

Conclusions

No significant degradation in permeability was observed when silica saturated and moderately oversaturated solutions, prefiltered to 1 μm, were flowed through core samples. The core flushing results indicate that half-life estimates for injection wells obtained from 0.4 μm membrane filters may be too conservative. The results with cores suggest that effluents with 1-2 ppm suspended solids are injectable at the SSGF. Such effluents can be obtained by a combination of reaction clarification and final filtration by means of mixed-media sand columns or pressure filters (Quong, et al., 1978, this volume).

ACKNOWLEDGMENTS

Ray Netherton provided fine support with data acquisition and equipment maintenance, Wayne Steele and Stan McInturff are responsible for the high quality SEM photographs and William Beiriger performed x-ray diffraction analyses of filter cake samples. Their contributions are greatly appreciated.

REFERENCES

Barkman, J. H. and Davidson, D. H., (1972), Measuring Water Quality and Predicting Well Impairment, Jour. Petroleum Technology, V. 24, p. 865-873.

Netherton, R. and Owen, L. B., (1978), Apparatus for the Field Evaluation of Geothermal Effluent Injection, Transactions of the Geothermal Resources Council Annual Meeting, V. 2 (this volume).

Owen, L. B., (1977), Properties of Siliceous Scale from the Salton Sea Geothermal Field, Transactions of the Geothermal Resources Council, V. 1, p. 235-237.

Piwinskii, A. J., Netherton, R., and Chan, M. A., (1977), Viscosity of Brines from the Salton Sea Geothermal Field, Imperial Valley, California, Lawrence Livermore Laboratory, Report UCRL-52344.

Piwinskii, A. J. and Netherton, R., (1978), An Experimental Investigation of the Permeability of Kayenta and St. Peter Sandstones to Hypersaline Brine in the Temperature Interval 70°-90°C at 10.3 MPa Confining Pressure, Lawrence Livermore Laboratory, Report UCRL-52382.

Tewhey, J. D., (1977), Geologic Characteristics of a Portion of the Salton Sea Geothermal Field, Lawrence Livermore Laboratory, Report UCRL-52267.

Quong, R., Schoepflin, F., and Stout, N. D., (1978), Processing of Geothermal Brine Effluents for Injection, Transactions of the Geothermal Resources Council, V. 2 (this volume).

Work performed under the auspices of the U.S. Energy Research & Development Administration under contract No. W-7405-Eng-48.

ISOTOPES AND GASES IN A HAWAIIAN GEOTHERMAL SYSTEM: HGP-A

Donald Thomas
Hawaii Institute of Geophysics, Univ. of Hawaii

Peter M. Kroopnick
Hawaii Institute of Geophysics, Univ. of Hawaii

Gases from the Hawaii Geothermal Project well-A (HGP-A) were sampled over the course of twelve months to determine their isotopic and chemical composition. Samples of steam and gas were collected and condensed at the well head through a twin cyclone steam/water separator during steam discharge of the well.

Gas separations were carried out on standard gas chromatographic columns with thermistor and mass spectrometric detection of the chromatogram peaks. Isotopic analyses were carried out on several individual components of the gas phase: CO_2 ($\delta^{13}C$), N_2, He, H_2O ($\delta^{18}O$).

Results. The results of the chemical analyses made for the geothermal gases sampled are summarized in Table 1. The most important aspect of the data presented here is that there appears to be a significant increase in the concentration of geothermal gases in the well output during each successive discharge of the well. Hydrogen and hydrogen sulfide appear to be increasing in concentration relative to the nitrogen and carbon dioxide fraction of the well gases. It is felt that these changes reflect the progressive maturation of the well toward a steady state composition of the geothermal fluids.

Helium analyses were also made on the well gases. It was found that the helium:nitrogen ratio in the well was at least six times the atmospheric concentration although analytical difficulties prevented an exact determination of the helium concentrations.

A summary of the isotopic analyses made on HGP-A gases is presented in Table 2. The carbon, nitrogen, and helium analyses were made on gases obtained during steam discharge while several oxygen analyses were made on downhole water samples.

The interpretation of the carbon isotope data is considerably complicated by the presence of ^{14}C at a concentration of 20% of modern carbon in the well gases, thus indicating that no less than 20% of the carbon dioxide in HGP-A is from atmospheric or biogenic sources. The origin, true age, and isotope composition of the biogenic fraction of the carbon in the well is presently unknown. Further testing of the well gases is presently planned in order to determine the relative contributions of the several possible sources of carbon in HGP-A.

The oxygen isotope data presented in Table 2 indicate only slight variations with depth in the well. This can be interpreted in one of two ways: either the water in the thermal reservoir (and the well bore) is very well mixed with depth, or one of the several possible fluid sources for HGP-A is providing nearly all the water in the well. It is presently felt that the latter possibility is the more likely.

The $\delta^{15}N$ values observed for HGP-A are richer in ^{15}N than any nitrogen ratios reported in the literature to date. Whether these values reflect the true isotopic composition of HGP-A nitrogen or whether they are an artifact of contamination is uncertain at present. Analyses by gas chromatography-mass spectrometry are presently underway to resolve this question.

The helium isotope ratios presented in Table 2 are seen to be quite high and are similar to values observed for helium in fumarole gases taken from the Kilauea summit. This is a very strong indication that there is a large component of magmatic gas in the geothermal well fluids. One can conclude from this that the heat source from which HGP-A taps its fluids is in close communication with the Kilauea volcanic system. It is believed that the inter-connection is laterally through the east rift zone rather than directly to the deep magma reservoir beneath Kilauea (R. Koyanagi, personal communication).

The conclusions which can be drawn from the above reported results are as follows: (1) There are at least 3, and possibly more, sources of geothermal fluids in HGP-A. The relative contributions of the fluids has been tentatively set at: ocean water, 10%; meteoric water, 65%; hydrothermal fluids, 25%. (2) The rift zone in which HGP-A is situated is in close contact with the Kilauea volcanic system. Thus it is possible that the exploitable lifetime of this heat source will be much longer than would be expected for an isolated geothermal system.

H. I. G. Contributor No. 886

TABLE 1
SUMMARY OF GAS ANALYSES FOR HGP-A

Date/Type of Sample	Sampling Pressure (psi)	Temp. (°C)	Total Gas Content (mg/kg of discharge)	Composition (wt %) CO_2	H_2S	N_2	H_2	Mole Ratio CO_2/H_2S	N_2/H_2
29 Jan. 1977; Total Condensate from Cooled Cyclone Separator	50	30	991*	72	10	18	0.1	5.5	19.5
5 April 1977; Steam from Cyclone Separator	165	185	1604	59	20	21	0.5	2.3	3.0
9 May 1977; Steam from Cyclone Separator	167	188	1912	57	21	21	1	2.1	2.4
	40	188	2697	65	24	10	.4	2.1	1.8
19 July 1977; Steam from Cyclone Separator	25	180	1337	71	18	11	.5	3.0	1.6
Best estimate for total gas content of HGP-A	-	180	2100	60.3	21.7	17.3	.6	2.1	2.1

*The 29 Jan. 1977 values most closely reflect the composition of the HGP-A stack emissions.

TABLE 2

Isotope Analysis Results

Date Sampled	$\delta^{13}C$ ‰ vs PDB (CO_2)	Comments
7-22-76	- 3.62	Carbon dioxide gas samples taken during steam discharge.
11-8-76	- 2.35	
11-16-76	- 3.28	
1-30-77	- 1.97	
2 - 77	- 2.29	
Mean	- 2.7	standard deviation 0.87

Date Sampled	Depth Sampled	$\delta^{18}O$ (H_2O)
8-19-76	1000 ft	- 3.79
8-19-76	4300 ft	- 4.5
8-19-76	5800 ft	- 4.2
8-19-76	6300 ft	- 4.56
10-30-76	2270 ft	- 4.14
10-30-76	5800 ft	- 3.83
2-9-77	top / steam	- 5.58
2-9-77	top / steam	- 3.60

Date Sampled	$\delta^{15}N$ (N_2)	Comments
5-8-77	+ 55.7	Nitrogen gas sampled during steam discharge--- all samples treated with CuO to remove CO and CH_2O.
5-8-77	+ 56.7	
7-19-77	+ 55.9	
7-19-77	+ 57.6	

Date Sampled	Depth Sampled	$^3He/^4He$
1-25-77	3500 ft	$>> 8.25 \times 10^{-6}$
1-25-77	5800 ft	8.25×10^{-6}
2-9-77	top / steam	1.7×10^{-5}
Kilauea fumarole gas		2.0×10^{-5}
Atmospheric Air		1.4×10^{-6}

Geothermal Resources Council, TRANSACTIONS, Vol. 2 July 1978

INVESTIGATION OF HEAT TRANSFER COEFFICIENTS OF WORKING FLUIDS IN GEOTHERMAL POWER CYCLES

B. W. Tleimat and A. D. K. Laird

Sea Water Conversion Laboratory
University of California
47th & Hoffman Blvd.
Richmond, California 94804

The objective of the binary fluid experiment described herein is to obtain data to determine baseline heat transfer data for working fluids being considered for binary cycle systems to produce power from hot geothermal brines. These data will be used to calculate film coefficients for heating, boiling, superheating, desuperheating as well as condensation for candidate working fluids.

In the binary system, the geothermal fluid is used to heat another, or secondary, fluid used as the working fluid of a turbo-generator power cycle.

Heat transfer equipment, principally to heat and cool the secondary fluid, accounts for approximately half the capital cost of a binary plant. That this cost is significant is shown by the cost estimate for a 10 MW Experimental Power Generation Facility, prepared jointly by the Lawrence Berkeley Laboratory (LBL) and the Rogers Engineering Co., Inc., of San Francisco, California. The installed cost of the plant, excluding brine production and injection wells, was estimated to be $12 million, of which the heat transfer equipment accounted for $6 million. On the same basis, for a 50 MW plant, the heat transfer equipment alone would cost about $30 million. In such cases, uncertainties in the estimate of the heat transfer coefficients can have serious effects. If the coefficients used in the design are too high, the plant may fail to meet its performance guarantee; if too low, the plant will be overdesigned and wastefully expensive.

Computer studies of power cycles using geothermal brines as the heat source, LBL's GEOTHM for example, indicate that operation of a binary system in the supercritical region will be the most efficient for isobutane. However, there is a real shortage of good heat transfer data for isobutane in this region.

The Binary Fluid Experiment (BFE) has been designed to provide experimental data on heat transfer coefficients of isobutane and other candidate fluids. Data to be gathered from the BFE on the heat transfer coefficients will include those expected to be appropriate for geothermal power plant applications.

Experimental Loop

The BFE is located at the University of California, Richmond Field Station. The experimental equipment consists of a stainless steel loop simulating a binary system with steam as the heating fluid and a throttling valve instead of the turbine. The loop consists of a heater, surface desuperheater, direct contact desuperheater, condenser, booster pump, a high pressure positive displacement pump and associated valving and control elements and instruments.

Figure 1 is a schematic flow diagram of the BFE apparatus. The pressurized secondary fluid is heated inside a single tube with steam condensing on the outside of the tube. After heating, the secondary fluid expands through a throttling valve and is introduced into a direct contact or a surface desuperheater by means of two three-way valves. After being desuperheated, the vapor enters the condenser, condenses on the outside of a single tube identical to that in the heater with cooling water inside the tube. The condensate is collected in the secondary fluid hotwell and enters the booster pump where it is slightly pressurized before entering the high pressure pump. During operation with the direct contact desuperheater, the three-way valves are oriented so that the secondary fluid enters the direct contact desuperheater and the separated vapor goes from this desuperheater to the condenser. Also in this mode of operation, a portion of the secondary fluid stream from the booster pump is diverted to the desuperheater and the excess fluid at the bottom is returned to the suction side of the booster pump.

The two tubes in the heater and condenser are made from a 31.8 mm (1.25 in. O.D.) and 19.1 mm (3/4 in. I.D.) type 316 stainless steel tube which was cut at its midpoint and honed to an inside diameter of 19.2 mm. In order to obtain uniform wall thickness, the two pieces were machined to an outside diameter of 30.2 mm. The concentricity was then checked by ultrasonic measurement of the tube wall thickness at 10 cm intervals along the axis. At each location, the wall thickness was measured at four points 90° apart. These measurements were used to precisely locate the thermocouples imbedded in the wall of the tubes.

Figure 2 shows the location of the imbedded thermocouples in the tube at five stations twenty-four inches apart. By measuring the temperature at these locations, one can determine the inside and outside surface temperatures of the tube regardless of the thermal conductivity of the

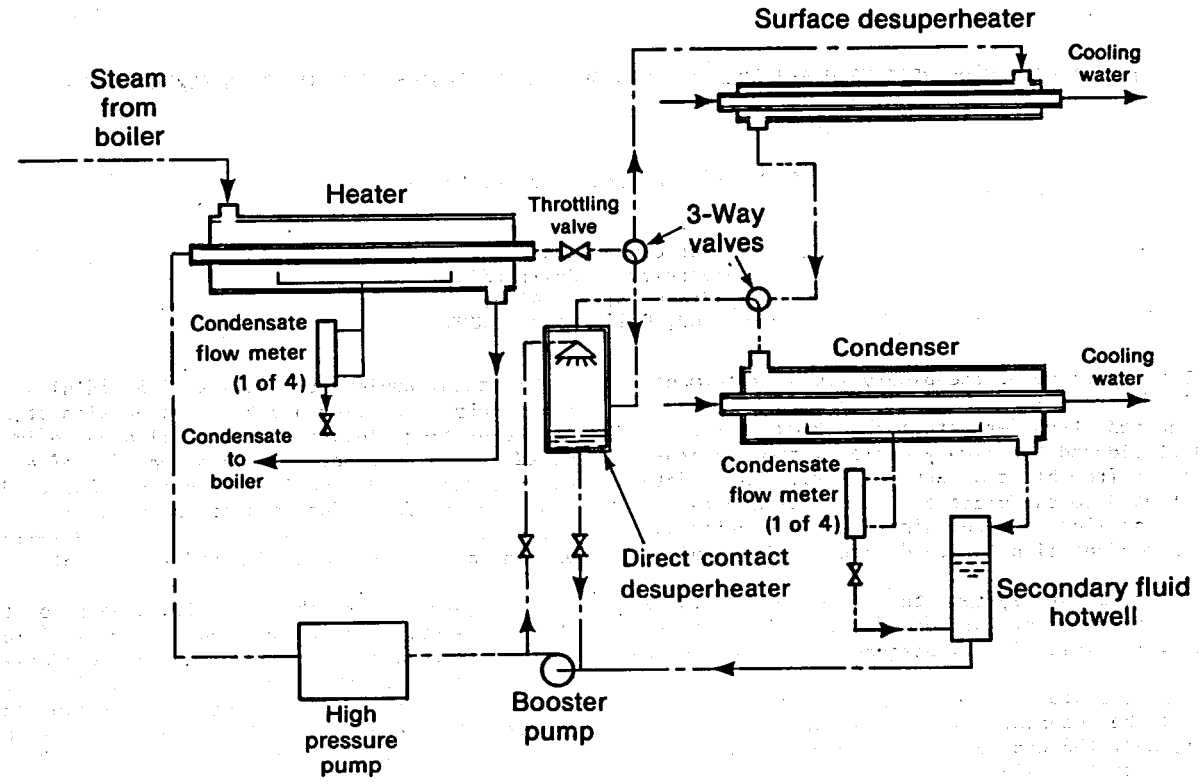


Fig. 1. Binary Fluid Experiment flow diagram (schematic)

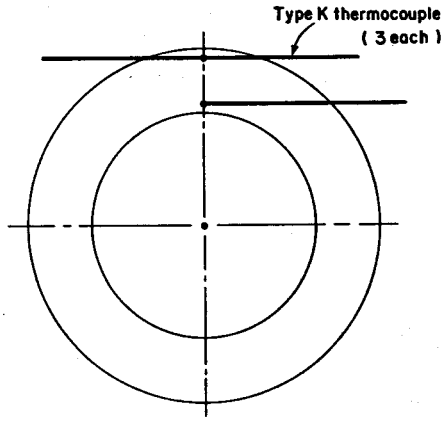


Fig. 2. Tube cross-section showing location of thermocouples

material of construction of the tube. Thus if one can determine the heat rate between the stations and measure the vapor temperature outside of the tube and the bulk temperature of the fluid inside the tube at the five stations, one can calculate the average inside and outside film coefficient of the four sections. Also by determining the heat rate in each section and measuring the bulk temperature at the stations, one can determine the state of the fluid inside the tube between the stations.

The rate of heat input to the secondary fluid in the heater and the heat released by the isobutane in the condenser are determined by measuring the rate of condensing vapor on the outside of the tubes at the four sections of each tube. This is done by placing a pan separated in four sections under the tube with the separations located under the thermocouples. The condensate formed on the outside of the tube drips into the separate sections of the pan and drains into four vapor traced condensate flow meters. Each condensate flow meter, specially designed for this experiment, consists of a calibrated volume and a timer to measure the time required for the condensate to fill this volume, operated by photocells to detect rising condensate surface between two predetermined levels. The temperature of the condensing vapor outside of the tube is measured

by means of calibrated platinum resistance temperature detectors (RTD) and thermocouples located in the vapor space. The pressure in the vapor space is measured by means of calibrated pressure tranducers. This pressure measurement is used as a check on the temperature of the vapor and also to detect presence of noncondensible gases in the vapor space. The bulk temperature of the secondary fluid in the heater is measured by a traveling platinum RTD inside the tube. In both heater and condenser, the bulk temperatures of the secondary fluid and cooling water at both inlet and outlet are measured by platinum RTD's.

Preliminary data were obtained on heating, condensation and desuperheating of isobutane. Overall heat transfer coefficients were calculated from the preliminary data. The overall heat transfer coefficient for heating the isobutane ranged from 280 - 1130 W/m^2C (50 - 200 Btu/hr ft^2F). The overall heat transfer coefficient for isobutane condensing on the outside of the tube ranged from 280 - 680 W/m^2C (50 - 120 Btu/hr ft^2F). The overall heat transfer for desuperheating the isobutane ranged between 120 - 600 W/m^2C (20 - 100 Btu/hr ft^2F).

Geothermal Resources Council, TRANSACTIONS, Vol. 2 July 1978

Dup

A Study of Alternative Reinjection Schemes for the Cerro Prieto Geothermal Field, Baja California, Mexico

Chin Fu Tsang, Gudmundur Bodvarsson, Marcelo J. Lippmann

Earth Science Division, Lawrence Berkeley Laboratory, Berkeley, California 94720

and

Jesus Rivera R.

Comision Federal de Electricidad, Mexico 5, D.F., Mexico

Introduction

It has become generally accepted that reinjection will be necessary for optimizing the exploitation of a geothermal field. Not only does this afford a way to solve the problem of disposal of cooled geothermal brine, but it also serves the purpose of maintaining reservoir pressure, thus reducing possible subsidence effects, and sustaining production flow rates. In addition, reinjection enhances thermal energy extraction from the reservoir rocks.

However, reinjection creates a zone of relatively cold water around each injection well that will grow with time and eventually reach the production wells. When the cold water appears ("breaks through") in the producing wells, the efficiency of the operation may be drastically reduced. It is therefore important to design the system of injection wells to prevent cold water breakthrough before a specified time. For a given production field, it is essential that both the location and flow rates of the injection wells be optimized.

In the present paper the results of an initial study of possible reinjection patterns for the Cerro Prieto geothermal field, Baja California, Mexico are discussed. First, the numerical model and assumptions made are described, then the various cases we studied are presented. The resulting data indicate what may be expected from different reinjection schemes and may provide useful guidelines for future reinjection operations at Cerro Prieto and other liquid-dominated geothermal fields.

Analytic Model Used

In this study a single two-dimensional steady-state flow model based on the work of Gringarten and Sauty[1] has been used. This model, which assumes constant fluid property parameters, is capable of simulating a system of many production and injection wells in a horizontal aquifer system. In such a system, steady-state fluid flow is expected within a relatively short time. Then the fluid velocity may be written down explicitly as a sum of contributions from each well. Natural regional flow in the reservoir can also be included very simply. Along each flow line thus constructed, the temperature is evaluated by considering heat transfer with bedrock and caprock, and by assuming instantaneous local thermal equilibrium between fluid and rock matrix. It is true that more sophisticated numerical models are available; but due to their complexity, nearly all of these are limited to the study of a small number of wells, or wells arranged in a highly symmetrical pattern. The simpler model adopted for the present work has the great advantage of being able to readily handle a system of many production and injection wells located throughout the field.

Calculations and Results

At Cerro Prieto around sixteen production wells are directing steam to the power plant and the separated brine is disposed to a large evaporation pond. This study explores the effect of reinjecting part of the produced water into the reservoir. At the present time a total of about 2750 m^3/hr of brine-steam mixture is being produced.

In our calculations we assume that 50% of the produced fluids, i.e. 1375 m^3/hr, will be reinjected into 3 or 4 wells. The thickness of the actual aquifer varies from place to place. We do not have sufficient data to obtain a typical average thickness. However, we assume a reasonable value of 250 m. The breakthrough time at the production wells, i.e. the time it takes for cold water to reach the production wells, is simply proportional to this thickness. Further field tests are now being performed at Cerro Prieto to establish the characteristics of this geothermal system. As more data come in and as the geological model of the field is improved, a more detailed analysis will be made.

Figure 1 shows the positions of all the wells used in the study. A well label beginning with M represents a currently existing well. A well label beginning with X represents a hypothetical reinjection well yet to be drilled and tested for injection. Only three or four of the wells are used for injection in any particular case. Thus not all the wells indicated are used at the same time. The production wells indicated in the figure are those currently used to supply steam to the Cerro Prieto power plant. They are located toward the northeast next to the railroad. Note that wells M-11 and M-42 are somewhat separated from the rest of the producing wells and are relatively closer to wells M-3 and M-7. This will have certain implications if M-3 and M-7 are used for reinjection, as is shown below.

Altogether 13 alternative reinjection schemes have been studied. Eight of these assume that we basically use the presently available wells outside the production region for reinjection. The other five cases assume a line of four injection wells southwest of the production area. The parameters assumed in these calculations are listed in Table 1, and the results are summarized in Table 2. The first and second breakthrough times shown in

Table 2 are the earliest times required for cold water to break through at any two production wells the numbers of which are indicated in brackets. A brief description of these runs is given as follows:

Run #1: Water is injected into the existing wells, M-3, M-6, M-7 and M-92, at the rate of 343.75 m^3/hr at each one. On the other hand, the 16 production wells, operating at the same rate, produce a total of 2750 m^3/hr. The results indicate that the first breakthrough of cold water will occur at well M-11 after about 32 years, due to cold water from well M-7. Note that the second breakthrough does not occur until 18 years later. Thus, if M-11 is discarded as an active production well after approximately 32 years, production from the other wells remains undisturbed for an additional 18 years. During these 18 years, M-11 will serve as a screening well[2].

Run #2: In this run the injection rates in wells M-7 and M-6 are smaller than in run #1, but the total injection rate of 1375 m^3/hr is maintained. As expected, this variation improves the breakthrough times from wells M-7 and M-6, but only by 5 and 2 years respectively.

Run #3 (Figure 2): In the first two runs, injection well M-7 was determined to be the critical well with respect to breakthrough times. Therefore, M-7 is omitted in this run and the total injection rate is maintained by doubling the injection rate at M-92. The results obtained show considerable improvement, as breakthrough occurs at well M-29 after 56 years.

Run #4 (Figure 3): For this run, a fourth injection well X-B is added to the three employed in run #3. The injection rates are unequally distributed, and the total injection rate is unchanged. Again, the first breakthrough occurs at M-29 as brine injected at M-6 arrives 62 years after injection began. Secondary breakthrough of brine from well M-6 arrives at M-25 7 years later.

Run #5: In this run, well M-6 is not used, and the brine is injected into M-3, X-B, and M-92 at rates of 343.75, 468.75, and 562.50 m^3/hr, respectively. The first breakthrough occurs at well M-11 after a 74 year period of injection, and the second occurs 15 years later at M-19A. Both breakthroughs are due to the injection at well M-3.

Run #6: For this run, the same injection-production scheme as in the previous run, is used. The only difference is the decrease of the injection rate at M-3. In this case, the breakthrough occurs at M-11, 80 years after injection begins, thus indicating some improvement in the breakthrough times.

Run #7: In this run, only 14 production wells are employed, the wells M-11 and M-42, are considerably closer to injection well M-7 than are the other 14 (see Figure 1) and have been omitted in this run to avoid early breakthrough times. However, the total production rate of 2750 m^3/hr remains unchanged. In all other aspects this run is identical to run #1. In a comparison between the two runs (#'s 1 and 7), the earliest breakthrough time is increased from 32 to 47 years.

Run #8: This run is identical to run #5, except that M-11 is omitted as a production well. Comparison with run #5 shows a 12 year improvement in the first breakthrough time, resulting in 86 years of undisturbed production.

Run #9: This case is the first of a series of runs in which injection is made along a line of wells southwest of the present production area. In this run wells X-1, M-6, X-2, and X-3 are injected at equal rates. The 16 production wells operate at a total rate of 2750 m^3/hr. Breakthrough occurs after 45 years of injection, as brine from wells X-1 and M-6 arrives at wells M-29 and M-30.

Run #10: The well pattern used in the previous run is repeated here. The injection rates at X-1 and M-6 are decreased, but increased at X-2 and X-3. However, the total injection rate is maintained. In this run there is minor improvement (5 years) in the breakthrough time.

Run #11: For this run, a new injection well, X-4, is introduced (see Figure 1), and injection well X-1 is dropped. Otherwise, run #11 is identical to run #10. The breakthrough occurs after 54 years, so only minor improvement is found in the breakthrough time (by 4 years).

Run #12 (Figure 4): In this run the use of injection wells X-5, X-6, X-7, and X-8, which are positioned farther from the production area than those of the last runs is considered. The breakthrough times are consequently longer, with the shortest breakthrough occuring 90 years after injection began.

Run #13: For this run, the conditions are the same as those of run #12, but different spacings are used between the injection wells. The results indicate minimal change in breakthrough times when compared with run #12

Summary and Conclusions

Under the assumptions adopted in these studies, the preliminary results suggest that reinjection of cold brines into the Cerro Prieto reservoir can be safely accomplished without a premature reduction in the temperature of the produced fluids. If the presently available wells, M-3, M-6, M-7, and M-92, are used for injection, the productive life of the field is strongly dependent upon well M-7. The use of M-7 would probably limit undisturbed production to approximately 30 years; whereas, replacing M-7 by an injection well further away from the production area would lengthen the productive life of the field to over 50 years.

The results from the runs involving brine injection into wells placed along a straight line southwest of the production area (including well M-6) indicate that breakthrough of cold water should not occur for at least 50 years. When the injection line is moved farther away from the production area, the productive life of the geothermal field is significantly increased. In general, cold water breakthrough time is strongly dependent on the distance of the production wells from the closest injection well. On the other hand, varying the relative flow rates among the injection wells does not change the breakthrough times by more than a few years. One point to note is that, as colder water is injected into the reservoir, it is heated by the rock-matrix through which it passes. Thus the hydrodynamic front, corresponding to the mass of injected water, precedes the thermal front across which the change of water temperature occurs. (The lag of the temperature front behind the injected fluid front depends on well distribution and reservoir properties.) Since the molecules of injected brine follow the hydrodynamic front, if one

tags the injected fluid with a tracer, the approach of the cold front may then be predicted by periodic chemical analysis of the produced waters. This would provide time for remedial actions if necessary.

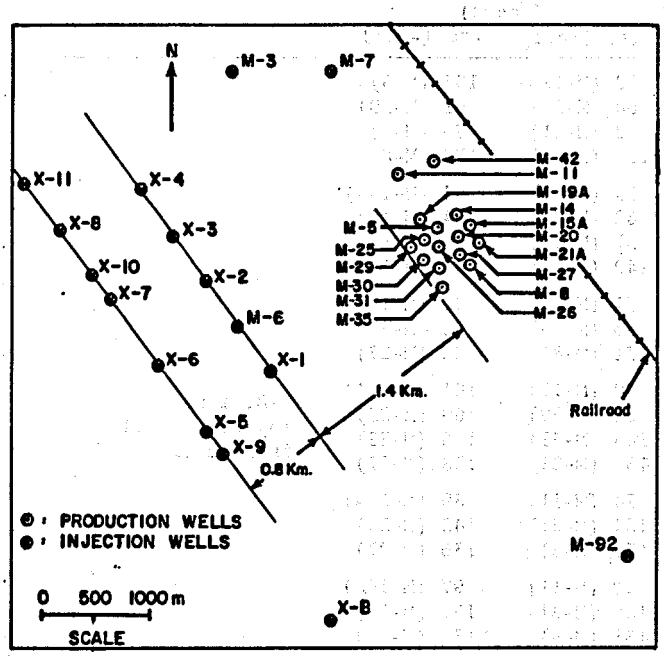
The results presented in this paper should be regarded as rough esitmates, since they are based on the assumption that the Cerro Prieto reservoir can be simulated by an homogeneous horizontal 250 meter-thick aquifer. They will be updated as a better understanding of the field is achieved. Furthermore, in practical cases, we need to consider (a) the injectibility of the reinjection wells, i.e. whether they are able to accept a given flow rate; and (b) the chemical compatibility of injected and native waters. Research to address these problems is underway.

†Work performed under the auspices of U.S. Department of Energy.

References

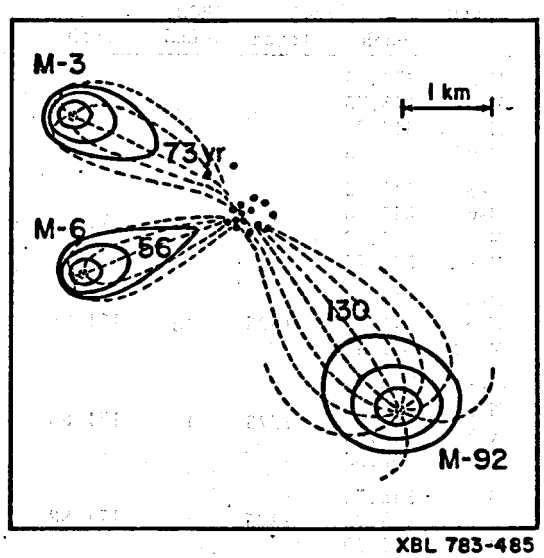
[1]Gringarten, A. C. and J. P. Sauty, Journal of Geophysical Research, Dec. 1975, pp. 4956-4962.

[2]Tsang, C. F. and P. A. Witherspoon, and A. C. Gringarten, Proceedings of the Workshop on Geothermal Reservoir Engineering, Stanford, Dec. 15-17, 1978, p. 62, Lawrence Berkeley Laboratory report #5914.



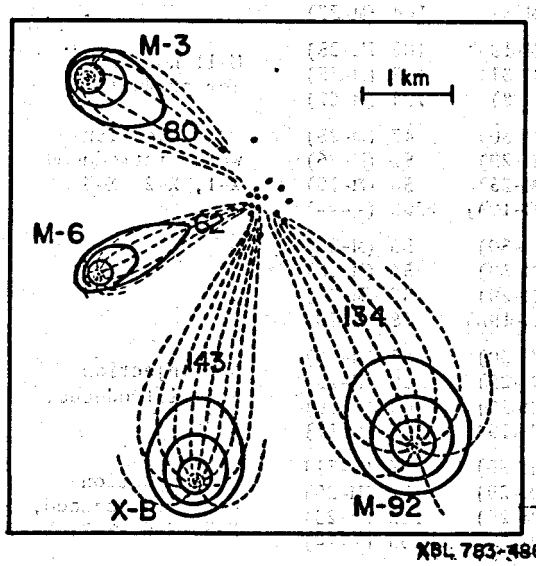
XBL 783-482

Figure 1: Relative locations of the production and injection wells used.



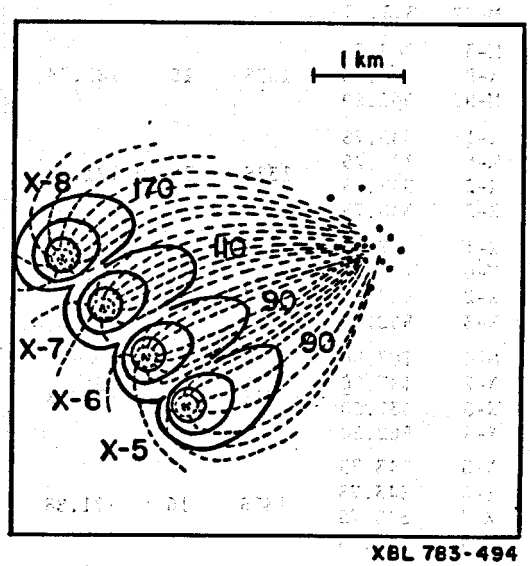
XBL 783-485

Figure 2: The brine flow characteristics for run #3. The dotted lines are streamlines and the solid lines are the thermal fronts, after 5, 20 and 50 years of injection. The numbers indicate the first breakthrough time in years.



XBL 783-486

Figure 3: The brine flow characteristics for run #4.



XBL 783-494

Figure #4: The brine flow characteristics for run #12.

Table I: CONSTANTS USED

Rock thermal conductivity = 0.006 $^{cal}/_{cm/sec/°C}$

Initial reservoir temperature = 300°C

Injected water temperature = 100°C

Aquifer thickness = 250 m

Aquifer porosity = 19%

Rock volumetric heat capacity = 0.5 $^{cal}/_{cm^3/°C}$

Density of brine = $1g/cm^3$

Table 2:

Summary of Reinjection Studies for the Cerro Prieto Geothermal Field

RUN	INJ. WEEKS	INJ. RATE (m^3/hr) each	total	No. PROD. WELLS	each	total	BREAKTHROUGH TIME (years) 1st (well)	2nd (well)	COMMENTS
1	M-3	343.75	1375	16	171.88	2750	82 (M-19A)	107 (M-5)	
	M-6	343.75					60 (M-30)	61 (M-29)	
	M-7	343.75					32 (M-11)	50 (M-5)	
	M-92	343.75					169 (M-25)	170 (M-8)	
2	M-3	343.75	1375	16	171.88	2750	79 (M-11)	84 (M-19A)	
	M-6	250.00					62 (M-29)	64 (M-25)	
	M-7	187.50					37 (M-11)	56 (M-5)	
	M-92	593.75					140 (M-8)	140 (M-27)	
3	M-3	343.75	1375	16	171.88	2750	73 (M-11)	92 (M-19A)	
	M-6	343.75					56 (M-29)	60 (M-25)	
	M-92	687.50					131 (M-8)	133 (M-27)	
4	M-3	250.00	1375	16	171.88	2750	80 (M-11)	101 (M-19A)	X-B, a new injection well introduced.
	M-6	187.50					62 (M-29)	69 (M-25)	
	X-B	375.00					143 (M-31)	146 (M-35)	
	M-92	562.50					137 (M-8)	138 (M-27)	
5	M-3	343.75	1375	16	171.88	2750	74 (M-11)	89 (M-19A)	
	X-B	468.75					134 (M-31)	143 (M-35)	
	M-92	562.50					133 (M-8)	136 (M-27)	
6	M-3	250.00	1375	16	171.88	2750	80 (M-11)	97 (M-19A)	
	X-B	562.50					126 (M-31)	132 (M-35)	
	M-92	562.50					131 (M-8)	136 (M-27)	
7	M-3	343.75	1375	14	196.43	2750	85 (M-19A)	89 (M-25)	M-11, M-42 not used for production.
	M-6	343.75					56 (M-30)	61 (M-26)	
	M-7	343.75					47 (M-19A)	48 (M-5)	
	M-92	343.75					163 (M-8)	164 (M-27)	
8	M-3	343.75	1375	15	183.33	2750	86 (M-19A)	102 (M-25)	M-11 not used for production.
	X-B	468.75					132 (M-31)	137 (M-35)	
	M-92	562.50					131 (M-8)	134 (M-27)	
9	X-1	343.75	1375	16	171.88	2750	45 (M-30)	47 (M-25)	New injection wells introduced X-1, X-2, X-3
	M-6	343.75					45 (M-29)	51 (M-26)	
	X-2	343.75					55 (M-25)	56 (M-29)	
	X-3	343.75					81 (M-19A)	>200 (----)	
10	X-1	187.50	1375	16	171.88	2750	53 (M-30)	56 (M-26)	
	M-6	187.50					50 (M-30)	54 (M-26)	
	X-2	437.50					49 (M-29)	53 (M-25)	
	X-3	562.50					68 (M-19A)	78 (M-20)	
11	M-6	187.50	1375	16	171.88	2750	54 (M-30)	87 (M-26)	New injection well introduced, X-4
	X-2	187.50					54 (M-29)	60 (M-25)	
	X-3	437.50					63 (M-25)	64 (M-29)	
	X-4	562.50					87 (M-19A)	97 (M-11)	
12	X-5	343.75	1375	16	171.88	2750	90 (M-30)	95 (M-31)	New injection wells introduced, X-5, X-6, X-7, X-8.
	X-6	343.75					88 (M-29)	90 (M-25)	
	X-7	343.75					110 (M-25)	112 (M-20)	
	X-8	343.75					168 (M-19A)	>200 (----)	
13	X-9	343.75	1375	16	171.88	2750	93 (M-30)	95 (M-31)	New injection wells introduced, X-9, X-10, X-11.
	X-6	343.75					91 (M-29)	93 (M-25)	
	X-10	343.75					125 (M-25)	144 (M-20)	
	X-11	343.75					>200 (----)	>200 (----)	

Geothermal Resources Council, TRANSACTIONS, Vol. 2 July 1978

A PRACTICAL HYDROGEN SULFIDE ABATEMENT PROCESS FOR AIR DRILLING AND VENTING GEOTHERMAL STEAM WELLS

Thomas A. Turner and Dr. R. W. Rex

Republic Geothermal, Inc.
Santa Fe Springs, California

ABSTRACT

A simple, economic process has been developed and applied to full scale operations for the abatement of hydrogen sulfide emissions while air drilling and venting geothermal steam wells. The process consists of blooie line injection of sodium hydroxide and hydrogen peroxide. 91-98% of hydrogen sulfide emissions can be abated during the drilling of a typical geothermal steam well for a cost of less than $10,000.

INTRODUCTION

Hydrogen sulfide is an odorous gaseous pollutant generally present in geothermal steam. When the first geothermal steam well was drilled at the Geysers in 1922, the presence of hydrogen sulfide odor was accepted as a naturally occurring phenomena associated with fumarolic activity. Most of the fumarolic activity has declined during the ensuing years due to man's modifications to harness this natural energy source for electrical power generation.

The majority of today's hydrogen sulfide emissions entering the atmosphere from the Geysers are from man-made devices. Increased environmental awareness in recent years has resulted in a legislative standard for hydrogen sulfide based on the threshold of smell. This standard of 30 ppb has been exceeded on occasion as a result of Geysers emissions. New source review rules promulgated by the California Air Resources Board were recently adopted as regulation in Lake County, CA. The rule requires that the respective air pollution control officer review any proposed new source of pollutant in excess of 20 pounds/hour and deny a construction permit if there is substantial evidence that the new source will prevent attainment of the ambient hydrogen sulfide standard.

Some geothermal well drilling activity, even though it constitutes a minor transitory source of emission, has been constrained as a result of these new regulations. The response has been the development of a process - using blooie line injection of hydrogen peroxide and sodium hydroxide to abate the hydrogen sulfide emissions during drilling, plant gathering line venting and well bleeding operations in order to prevent future violations of point source emission rules or the ambient air quality standard. From preliminary laboratory work performed by FMC Corporation, a manufacturer of hydrogen peroxide, at the request of Dr. R. W. Rex, it was determined that field drilling conditions could not, economically, be lab simulated. Republic Geothermal, in August of 1976, then designed and constructed a pilot sized geothermal muffler unit for use in California's high pressure steam field, the Geysers. The muffler unit was designed to dynamically simulate flow conditions present in conventional mufflers used to suppress noise and control particulates. Steam for the field trial was supplied by Magma Power Company and at Magma's request, field and technical assistance was furnished by their operator, Union Oil's Geothermal Division.

The process involves the continuous injection of aqueous hydrogen peroxide and sodium hydroxide solutions into the geothermal steam. Injection is made into the blooie line upstream from the muffler. The principal product of the oxidation is sodium sulfate, a neutral salt. During preliminary testing, sulfide abatement of 91% was achieved at a 4:1 weight ratio of hydrogen peroxide to hydrogen sulfide and 2.8:1 weight ratio of sodium hydroxide to hydrogen sulfide.

CHEMISTRY

The products of sulfide oxidation are controlled by pH and the chemical reactions that take place with hydrogen peroxide are illustrated by the simplified equations:

$$H_2S + H_2O_2 \xrightarrow[\text{solution}]{\text{acid or neutral}} \frac{1}{X} S_x + 2H_2O$$

$$S^{--} + 4H_2O_2 \xrightarrow[\text{solution}]{\text{alkaline}} SO_4^{--} + 4H_2O$$

At ambient temperatures a period of 5 to 20 minutes is generally needed for hydrogen peroxide to completely react with sulfide in aqueous solution. This range has led some investigators to conclude that indigenous catalysts are operating. At 122°F the reaction is complete in 15 seconds. Rates in water solutions at still higher temperatures should be extremely fast. The presence of heavy metal ions will increase reaction rates even further. Reactions in the pilot system proceeded

to completion in less than 4 seconds.

In detail the reactions proceed at more rapid rate in the liquid phase and H_2S assimilation into the liquid phase is accelerated by an increased liquid phase pH as follows:

$$2\ NaOH + H_2S \rightleftharpoons Na_2S + H_2O$$

$$\text{or } NaOH + H_2S \rightleftharpoons NaHS + H_2O$$

plus Peroxide

$$Na_2S + 4H_2O_2 \rightarrow Na_2SO_4 + 4\ H_2O$$

$$\text{or } NaHS + 4H_2O_2 \rightarrow Na\ HSO_4 + 4\ H_2$$

The reaction products Na_2SO_4 and $Na\ HSO_4$ are stable salts and will not revert to hydrogen sulfide in the sump during neutralization activities upon completion of drilling.

Analysis of test muffler condensate reaction products performed for Republic by Quality Water Laboratory, Inc. identified trace amounts of SO_3, SO_2 and elemental sulphur, and it is probably due to the catalytic action of iron and trace heavy metals that the reaction does not proceed in precise stoichiometric proportions as displayed in the simplified equations above. Although not field tested, many other combinations of oxidents, and pH modifiers can be utilized to effect similar results. However, since hydrogen peroxide is a readily available, inexpensive industrial chemical and strong reagent solutions can be prepared with NaOH, sodium is the preferred cation for creating a strong alkaline environment for the practical disassociation and oxidation of H_2S.

Measurements made of the resultant steam emitted to the atmosphere indicate no caustic or peroxide carryover to the atmosphere.

OPERATING PROCEDURES

In field practice, implementation of the system is very straightforward. Caustic and peroxide injection points should be separate and located as closely as practical to the banjo box in order to provide maximum system residence time for the reaction to proceed to completion and maximum exposure to high Reynolds, Froude, & Webber number flow regimes for optimal mixing. Vacuum sampling points should be provided both upstream of the injection point and on the muffler stack in order to control abatement levels and optimize process efficiencies.

Hydrogen peroxide storage and transfer lines should be 304 or 316 passified stanless steel using low volume positive displacement chemical metering pumps for injection such as Pulsa Feeder Model 7120 4.2 to 42 GPH electric driven pumps. Care should be taken that storage tanks are protected by anti-siphon valves and that all hydrogen peroxide handling equipment has been passified with 68% Nitric Acid for $\pm$ 24 hours.

Caustic storage and handling facilities can be mild steel and require no special handling procedures other than adequate containment provisions for personnel safety and anti-siphon valves to avoid storage contamination. If the system is to be utilized during cold weather conditions, a 25% aqueous solution of sodium hydroxide is recommended in that its freezing point is 0°F where 50% solutions freeze at 50°F.

For a typical geysers production well $\pm$ 2000 gallons of storage should be provided for each chemical depending on delivery problems at the specific location.

Injection points should be provided with high energy spray nozzles for improved mixing and dispersion in the blooie line. In line strainers are recommended in that the nozzles will tend to plug with foreign material. Provisions should be made for removal and cleaning of spray nozzles which provide minimum down time and personnel exposure.

The scope of this presentation is necessarily limited to the initial development phases of the abatement process and the construction aspects of full scale facilities. Republic Geothermal has not had the occasion to implement the process on a full scale operational basis, however, this sulfide abatement process has been utilized by other operators with reported attainable field abatement levels of up to 95% with per well costs averaging $6500. An additional important advantage of this blooie line abatement process is that atmospheric pollution can be mitigated continuously, independent of drilling operations. Previously tested systems, relying on drill string injection, necessarily preclude abatement during all rig operations other than drilling. This new method results in significant reductions in abatement efficiencies and undesirable pollution of the atmosphere.

Republic currently has its hydrogen sulfide process equipment leased to Phillips Petroleum Co. and it is being operated for Phillips by the R. F. Smith Corporation. The R. F. Smith Corp., a geological services corp. specializing in the provision of well mud logging services, also provides rig floor compressor breathing equipment, Scott Air Packs, blooie line vacuum sampling devices, hydrogen sulfide monitering equipment and intends to provide and operate the hydrogen sulfide abatement process described in this paper as a service to operators in the Geysers area.

REFERENCES

1. Castrantas, H. M., Rex, R. W., Turner T. A., "Hydrogen Sulfide Abatement at Geothermal Wells" Proceedings, Lake County Geothermal Environmental Conf. (1976)

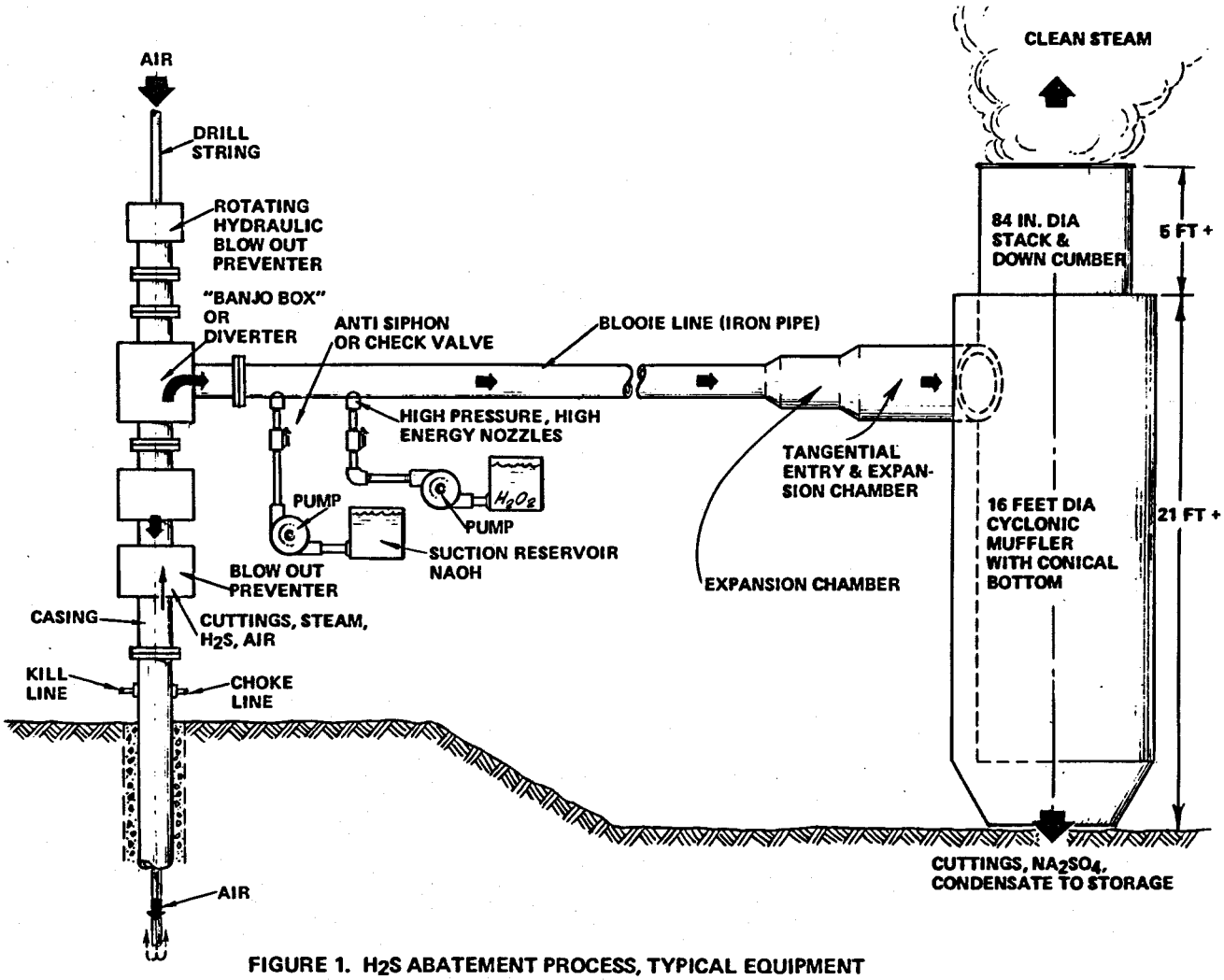


FIGURE 1. H_2S ABATEMENT PROCESS, TYPICAL EQUIPMENT

Geothermal Resources Council, TRANSACTIONS, Vol. 2 July 1978

EAST MESA GEOTHERMAL ANOMALY, IMPERIAL COUNTY, CALIFORNIA: SIGNIFICANCE OF TEMPERATURES IN A DEEP DRILL HOLE NEAR THERMAL EQUILIBRIUM

T. C. Urban, W. H. Diment and Manuel Nathenson

U. S. Geological Survey
Menlo Park, California 94025

Abstract. Precision temperature logs were obtained in U.S. Bureau of Reclamation drill hole Mesa 31-1 (32°48.6'N,115°15.7'W) at East Mesa to a depth of 1880 m. Comparison of logs taken some two months apart and nearly a year after the production testing suggests the hole is close to thermal equilibrium. The thermal regime of the hole is characterized (1) by high gradients which predominate in the conductive cap (0-840 m) and are affected by hydrologic disturbances to at least 150 m, (2) by a sharp decrease in gradient at the base of the cap (∿ 840 m), (3) by a uniformly low gradient (∿ 40°C/km) below the cap except near the perforated zones (below 1650 m), and (4) by small convective motions within the hole as indicated by temperature-time recordings. The observed low gradient below the cap does not necessarily imply convection in a thick permeable medium. Instead, simple numerical models suggest the gradient could be the result of conductive heating from a hot permeable zone maintained by horizontal water movement near the base of the cap.

Experimental Details. Temperature measurements were made using a glass-enclosed bead thermistor (50,000 ohms at 25°C) attached to a Teflon insulated cable. Resistances and depths were sampled at intervals of 0.6 m and recorded on punch-paper tape for later computer processing. The 20 cm cased hole was logged downward at 6 m/min through a lubricator (well-head pressure 4 bars).

Temperatures. The temperatures plotted in Figure 1 were used to calculate the gradients over 20-m intervals by a linear differencing of the observed data. A second log, taken 72 days later, indicates an average warming of the hole by ∿ 0.2°C. The scatter evident in the temperature differences (Fig. 2) probably reflects variations in conditions both inside and outside the casing.

High gradients (Fig. 1) predominate in the conductive cap and are affected by hydrologic disturbances to at least 150 m and possibly to as great a depth as 400 m (Diment, et al., 1977). The base of the cap (∿ 840 m) is marked by a sudden decrease in the gradient to ∿ 40°C/km. This low gradient persists throughout the remainder of the hole except near the perforated zones below ∿ 1650 m.

Time-temperature recordings at seventeen depths exhibit temperature oscillations of the type illustrated in Figure 3. The range (R) of the oscillation is roughly proportional to the temperature gradient (G) at the depth of recording; and R/G is on the order of 100 cm, a fact first noted by Diment (1967) and Gretener (1967) for holes of nearly the same diameter (∿ 25 cm) but of much lower gradients. Taken as a whole the oscillation data suggests that the principal convective motions in holes near this diameter take place over a vertical dimension on the order of a hole diameter, and that this observation is valid at least in the gradient range 10 to 300°C/km.

The temperature differences in Figure 2 are anomalously large in the interval below the cap and above the perforated zones. Moreover, each of the logs is "noisy" in this interval in the sense that variations of gradient with depth as measured over short intervals are entirely too large to be explained by variation in rock types or convective motions of the type discussed above. Perhaps the "noisy" interval is due to spurious electrical noise. Perhaps it represents a different flow regime within the hole that is caused by ascent of small quantities of gas from the perforated zone below 1650 m. All the deep USBR holes at East Mesa produce some CO_2 at the well head (Mathias, 1976).

Some other features of the difference plot (Fig. 2) may reflect changing conditions outside of the hole, but further speculation is unwarranted in view of the experimental uncertainties. For example, the leakage rate through the lubricator, although small, was not constant when either log was obtained. Thus, some of the differences are a consequence of small differences in the position of the fluid column.

Discussion. The temperatures observed in Mesa 31-1 (generalized as curve II in Figure 4) put constraints on the thermal-hydrologic regime in this part of the East Mesa KGRA. The region below 840 m has been referred to as a convective zone below the conductive cap (e.g., Swanberg, 1976). Examination of the geophysical logs made in the hole, however, indicates significant amounts of shale throughout the section below 840 m, which probably would restrict vertical flow to relatively small intervals. However, if it is assumed that vertical convection does occur below ∿ 840 m and that heat transfer is

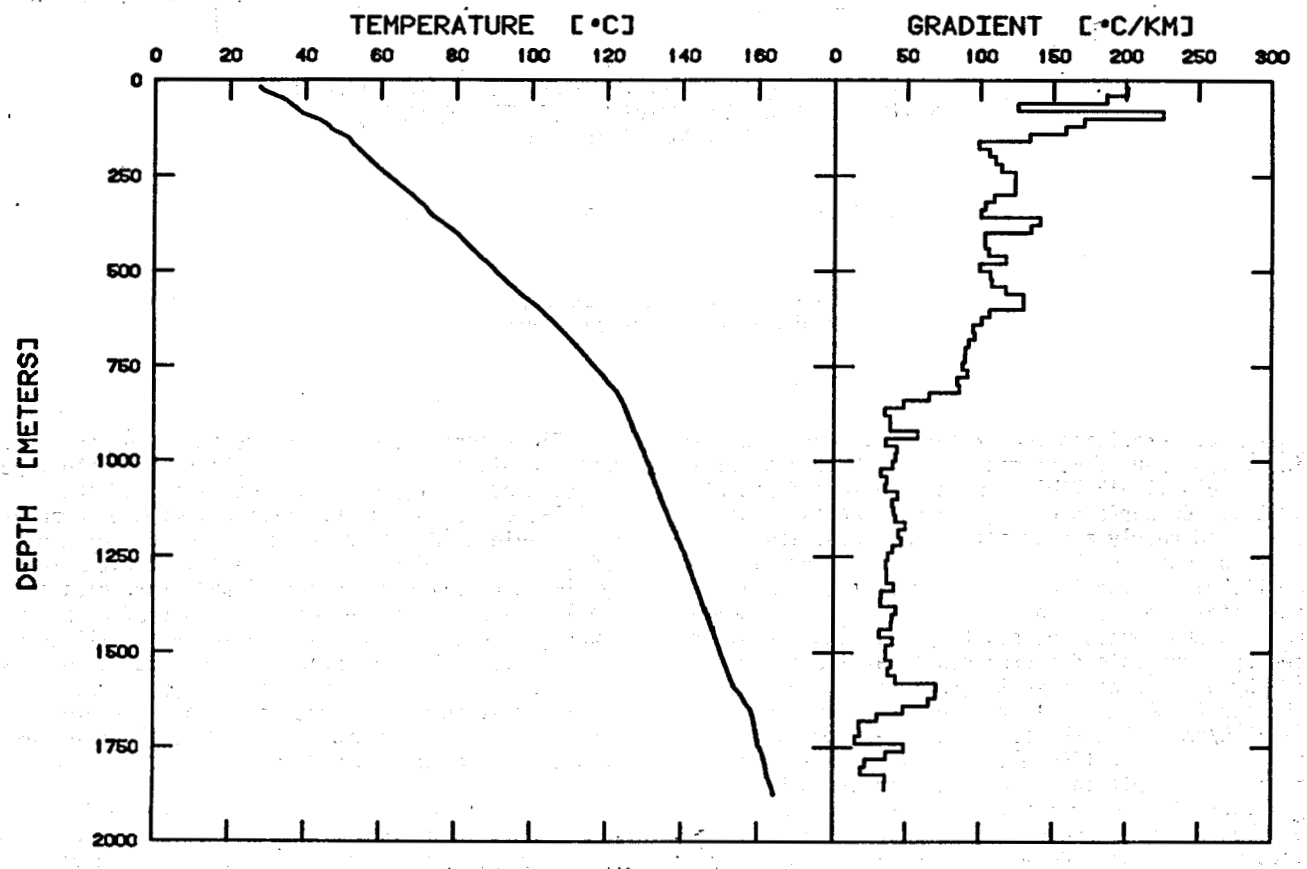


Figure 1. Temperatures and thermal gradients in Mesa 31-1 (April 14, 1977).

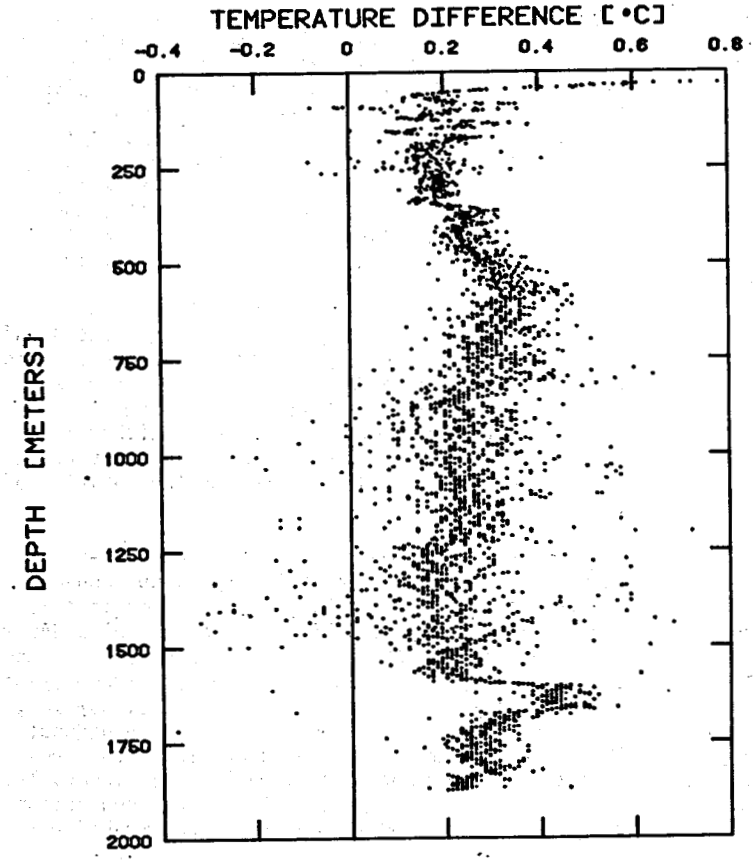


Figure 2. Temperature increase in Mesa 31-1 from April 14 to June 25, 1977. The apparent vertical alignment of the points below 600 m is due to rounding of the temperatures to 0.001°C above 600 m and to 0.01°C below 600 m.

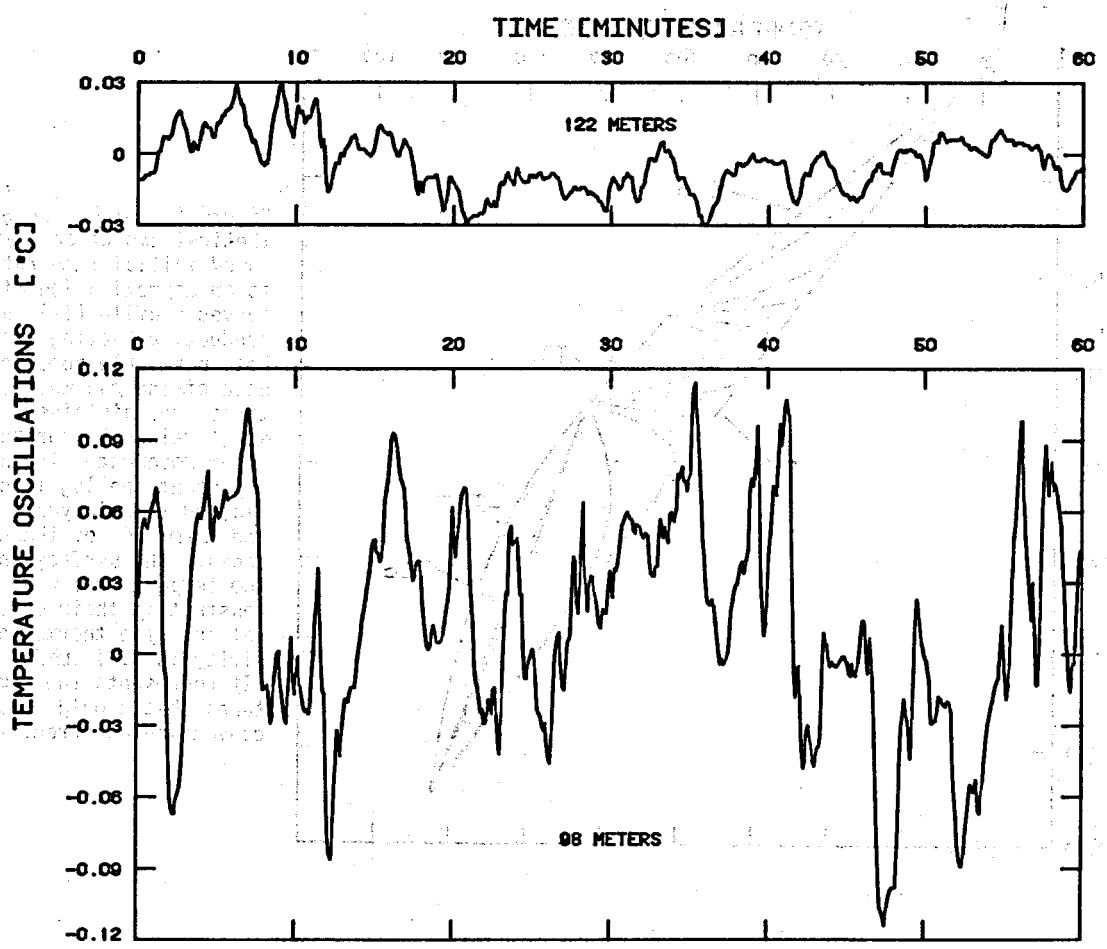


Figure 3. Temperature oscillations in Mesa 31-1. The gradient is 315°C/km at 98 m and 87°C/km at 122m.

by conduction above, then by balancing the energy flows in the "conductive" (curve IIb) and "convective" regions and applying the analysis of Bredehoeft and Papadopulos (1965), curve III in Figure 4 is obtained. The calculated temperatures (curve III) exhibit far more curvature than is observed (curve IIc) in Mesa 31-1. The calculations suggest that no vertical convection takes place at Mesa 31-1 but at the same time tell us nothing about the rest of the field. Indeed, convection could take place in a fault zone a few kilometers away and no curvature would probably be observed in Mesa 31-1.

The evolution of the system to the observed data may be modeled by conductive heating from two hot permeable zones maintained by horizontal water movement. The initial temperature distribution (curve I) is $T = 25^{\circ}C + 74.5Z$, where Z is in kilometers. The initial gradient (74.5°C/km) is obtained from the observed surface intercept and bottom hole temperature. Depending upon the thermal conductivity assumed for the section, this would correspond to a heat flow of 2 to 4 $\mu cal/cm^2$ s. The curves shown in Figure 4 were calculated assuming plane heat sources at 610 and 840 m (Carslaw and Jaeger, 1959, p. 100). Temperatures very close to those observed can be obtained with such a hypothetical model in about 10,000 years. Although the details of this model are probably incorrect, the important point is that many features of the temperature distribution in this and other wells can be produced by conduction from a hot zone near the base of the cap.

Acknowledgments. We thank the personnel at the U.S. Bureau of Reclamation, Boulder City, NV., for their assistance in many aspects of this investigation and for permission to log drill hole 31-1 at East Mesa. K.E. Mathias, USBR, was especially helpful in discussions concerning East Mesa. A.H. Lachenbruch and L.J.P. Muffler suggested many improvements in the manuscript.

References

Bredehoeft, J.D. and Papadopulos, I.S., 1965, Rates of vertical groundwater movement estimated from the earth's thermal profile: Water Resources Res., v. 1(2), p. 325-328.

Carslaw, H.S. and Jaeger, J.C., 1959, Conduction of heat in solids: London, Oxford University Press, 510 p.

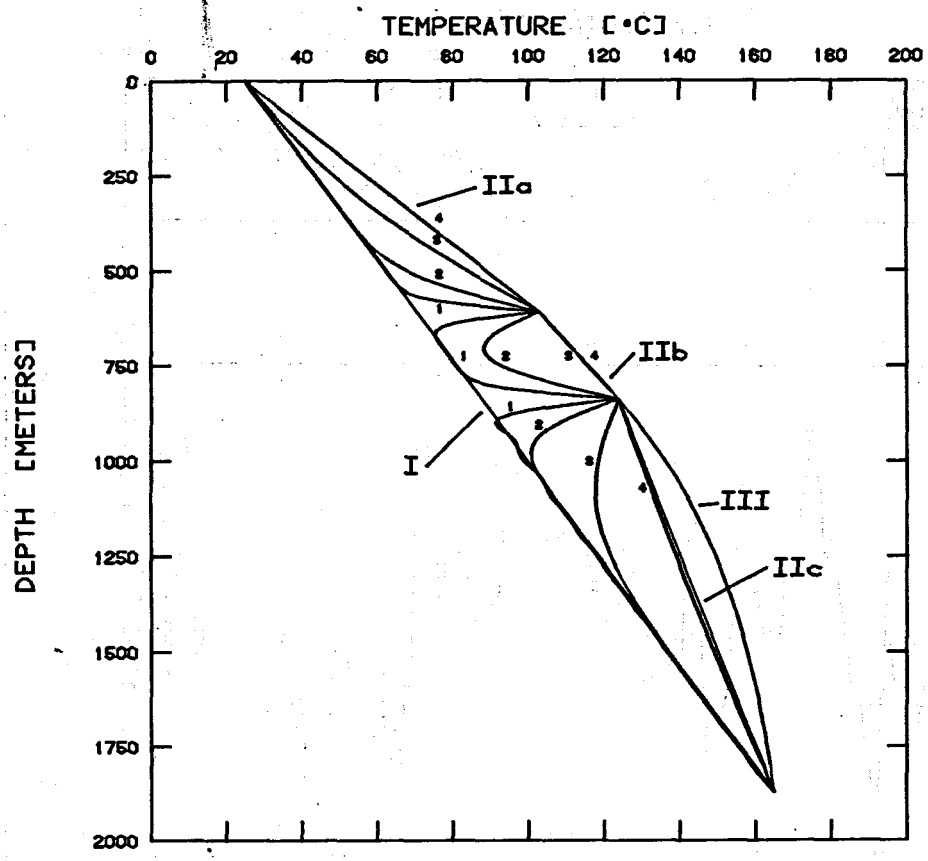


Figure 4. Graphs showing hypothetical evolution from an assumed initial temperature (I) to an approximation of the observed profile (II), assuming conductive heating from two hot, permeable zones near the base of the cap whose temperatures are maintained at constant values by horizontal water movement. The numbers represent the log 10 of the elapsed time in years since the formation of the hot zones. The surface and bottom temperatures were held constant at their observed values. The thermal diffusivity is 0.01 cm^2/s. Curve III represents the temperatures that should result if convection occurred.

Diment, W.H., 1967, Thermal regime of a large diameter borehole: Instability of the water column and comparison of air- and water-filled conditions: Geophysics, v. 32, p. 720-726.

Diment, W.H., Urban, T.C., Nathenson, M. and Mathias, K.E., 1977, East Mesa geothermal anomaly, Imperial County, California: Effects of canal leakage on shallow thermal regime (abs.): Trans. Amer. Geophys. Union, v. 58, p. 1241.

Gretener, P., 1967, On the thermal stability of large diameter wells--an observational report: Geophysics, v. 32, p. 727-738.

Mathias, K.E., 1976, The Mesa geothermal field--a preliminary evaluation of five geothermal wells: Second UN Symposium on the Development and Use of Geothermal Resources, San Francisco, Proceedings, Lawrence Berkeley Lab., Univ. of California, p. 1741-1747.

Swanberg, C.A., 1976, The Mesa geothermal anomaly, Imperial Valley, California: A comparison and evaluation of results obtained from surface geophysics and deep drilling: Second UN Symposium on the Development and Use of Geothermal Resources, San Francisco, Proceedings, Lawrence Berkeley Lab., Univ. of California, p. 1217-1228.

U.S. Bureau of Reclamation, 1974, Geothermal resource investigations, East Mesa test site, Imperial Valley, California, status report, November, 1974: Boulder City, NV, 64 p.

Geothermal Resources Council, TRANSACTIONS, Vol. 2 July 1978

COMPUTER PROGRAM FOR CALCULATING THEORETICAL CURVES AND IT'S APPLICATION TO VES DATA IN GEOTHERMAL AREAS

Keisuke USHIJIMA and Kazuo USHIJIMA

FACULTY OF ENGINEERING, KYUSHU UNIVERSITY 36
FUKUOKA 812, JAPAN

1. INTRODUCTION

In order to interpret Vertical Electrical Soundings (VES) data obtained in geothermal areas, a complete curve matching method may be used on the condition that the subsurface of the area is a horizontally layered structure. For this purpose, several albums of theoretical curves have been published by many authors, for instance, Mooney and Wetzel (1956), La Compagnie Generale de Geophysique (1955), Orellana and Mooney (1966), E.A.E.G. (1969) and others. However, these albums are frequently inadequate for interpreting field curves when several layers are present. They are applicable when the depth ratio of the bedrock to the thickness of the overburden is not greater than 30. This means that it is impossible to recognize the deepest structure if the thickness of the first layer is not great enough. In a geothermal field survey, it is usually encountered that the thickness of the first layer is of few meters and the depth to the bedrock is greater than 1000 meters. This is the reason why a set of theoretical curves having a maximum depth ratio of 300 or 500 must be calculated. The development of these curves requires the computations of the exact apparent resistivities for large electrode separations but these produce many difficulties in the numerical calculation.

The authors have already published two programs, PSH-A (1977a) and PSH-B (1977b), written in FORTRAN to compute theoretical curves for Wenner and Schlumberger electrode arrangements. These programs have been developed using a large scale computer (FACOM 230-45S) but they are so small in size that a geophysicist can easily make use of them on a mini-computer.

This paper describes the PSH-B program and it's practical application to the VES curves obtained in Otake (Lines L0 and L5) and Takenoyu (Lines M1 and M2) geothermal fields of Japan.

2. ALGORITHM OF THE PROGRAM

The apparent resistivity formulas for Wenner and Schlumberger arrangements are

$$\rho_{aW} = \rho_1 \left\{ 1 + \sum_{i=1}^{\infty} A(i) f_W(a,i) \right\} \quad (1)$$

$$\rho_{aS} = \rho_1 \left\{ 1 + \sum_{i=1}^{\infty} A(i) f_S(s,i) \right\} \quad (2)$$

where ρ_1 = resistivity of the first layer, a = electrode separation for Wenner array, s = electrode separation for Schlumberger array, A(i) = the i-th coefficient of series expansion of the kernel function, $f_W(a,i)$ and $f_S(s,i)$ = the distance factors expressed respectively as

$$f_W(a,i) = 2a\left\{ 2/(4i^2+a^2)^{1/2} - 1/(i^2+a^2)^{1/2} \right\} \quad (3)$$

$$f_S(s,i) = 2/(1+4i^2/s^2)^{3/2} \quad (4)$$

The summations of the eqs.(1) and (2) are computed up to a finite term. The error produced by truncating the series after N terms is estimated by Mooney et. al. (1966). According to their result, this error is no greater than $s^3/8N^2$ for Schlumberger array.

In order to minimize the errors produced during the summation process of the equation (3), it is better to rewrite as

$$f_W(a,i) = \frac{6a^3}{\sqrt{(4i^2+a^2)(i^2+a^2)}\left\{2\sqrt{i^2+a^2}+\sqrt{4i^2+a^2}\right\}} \quad (5)$$

The coefficients A(i) can be obtained recurrently (Argelo, 1967):

$$A(i) = p_{i+1} - \sum_{j=2}^{h_{n-1}} q_j A(i-j+1) \quad (6)$$

where h_{n-1} = depth to the bedrock, p_{i+1}, q_j are functions of the reflection coefficients $k_j = (\rho_{j+1} - \rho_j)/(\rho_{j+1} + \rho_j)$ and they are determined from the recursion formula for n-layer case (Flathe, 1955):

$$\left.\begin{aligned} P_n(u) &= P_{n-1}(u) + k_{n-1} u^{h_{n-1}} \left\{ P_{n-1}\left(\tfrac{1}{u}\right) + Q_{n-1}\left(\tfrac{1}{u}\right) \right\} \\ Q_n(u) &= Q_{n-1}(u) - k_{n-1} u^{h_{n-1}} Q_{n-1}\left(\tfrac{1}{u}\right) \end{aligned}\right\} \quad (7)$$

with $u = \exp(-2\lambda)$, λ = separation constant.

Since $P_1(u) = 0$, $Q_1(u) = 1$ (8)

eqs.(7) can be expressed as

$$\left.\begin{aligned} P_n(u) &= \sum_{i=2}^{n-1} p_i u^{i-1} \\ Q_n(u) &= \sum_{i=1}^{n-1} q_i u^{i-1} \end{aligned}\right\} \quad (9)$$

Therefore the apparent and relative resistivities can be calculated using equations (4), (5) and (6).

3. COMPUTER PROGRAM PSH

Argelo (1967) and Onodera (1969) have already published computer program which compute apparent resistivity curves for a general n-layer case. These programs are written in ALGOL.

The PSH program is written in FORTRAN. It is specially designed not to occupy a large memory and not to consume much time, so that field engineer can calculate theoretical curves by using a mini-computer. The PSH-A program has the following features:
(1) The computations are done in single precision arithmetic.
(2) The maximum number of polynomial coefficients is limited to 300.
(3) The summation process in equations (1) and (2) is stopped when the following condition is fullfilled:

$$\Delta \rho_{aN} = 0.00001 \cdot \rho_a \quad (10)$$

where $\Delta \rho_{aN}$ is the difference between the latest calculated apparent resistivity (for N terms) and the preceding one (for N-1 terms), ρ_a is the latest calculated apparent resistivity.

The convergence of the sums of eqs. (1) and (2) is fast for small electrode separation. For some models which converges fast, the PSH-A program is very adequate because the condition (10) is soon satisfied. However the VES curves obtained in geothermal areas do not show these characteristics, so that, the calculations are often performed to the maximum number of terms (N=300). Therefore in order to avoid the waste of time required by the condition (10), the test statement of PSH-A program should be removed. This modificated program is called PSH-B (see Appendix) and it finds its main application to the interpretation of VES curves obtained in geothermal areas. It has the follwing features:
(1) It is operated in a single precision arithmetic (7 decimal digits in length on FACOM 230-45S computer)
(2) It has not test statement given by the condition (10), so that the number of polynomial coefficients is always fixed to 300.
(3) Array variables in the DIMENSION statement (see Appendix) can be freely redimensioned to a large extent depending on the difficulty of convergence and the computer capacity.
(4) The computer output consists of 55 values of relative and apparent resistivities, calculated for 55 fixed values of electrode separations given to the program using DATA statements.
(5) All thickness of a multiple layer must be an integer value.

All executable statements in the PSH-B program are accompanied by execution numbers which are generated by FORTRAN Program Dynamic Analyzing system (Fujimura and Ushijima,1976). This execution profile shows that the total computing time is mainly dependent on the executions of eq. (6), which is proportional to N^2 and on the executions of eqs.(1) and (2) which are proportional to N. The former corresponds to 44850 executions which is nearly equal to $300^2/2$ while the latter corresponds to 16500 = 300 x 55 executions.

In many case studies, the total time required for computing one set of Wenner and Schlumberger curves is 14 seconds for N = 300 and 60 seconds for N = 1000 on FACOM 230-45S. Since the consumption of storage memory is directly proportional to the number of terms only, it does not mean a serious problem.

In order to keep the accuracy, the variables RWO and RSO which store the sums of the power series, are declared in double precission arithmetic. However, it is ascertained that for many cases, this declaration is not necessary.

As already pointed out, the PSH-B program can be directly executed on a mini-computer. Actually, it was tested on some mini-computers. For example, for a multiple layer model, the total computing time was 53 seconds when it was run on a mini-computer, FACOM U-200L, which has a floating point arithmetic system internally in the machine and about 9 minutes on another mini-computer, OKITAC-4300b, where the floating point arithmetic is carried out by subroutines.

4. APPLICATION OF PSH-B TO FIELD DATA

The PSH-B program was applied to 35 VES curves obtained in Otake area (Oita prefecture) and 29 VES curves obtained in Takenoyu area (Kumamoto prefecture) both in Kyushu Island.

4.1. CLASSIFICATION OF VES CURVES

The field VES curves can be classified according to their shape by the use of four types of three layer curves: type H($\rho_1 > \rho_2$

$< \rho_3$), type K($\rho_1 < \rho_2 > \rho_3$), type A($\rho_1 < \rho_2 < \rho_3$) and type Q($\rho_1 > \rho_2 > \rho_3$). The resume of the classification is shown in Figure 1, where it is also found that typical VES curves observed in geothermal areas are of type H for three-layer case, types KH and QH for four-layer case and types AKH, KHA, KQH, HKH, QHA, QQH for five-layer case.

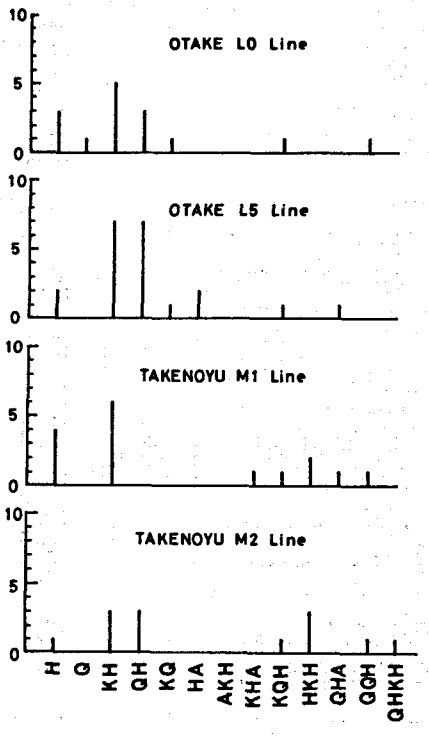


Fig. 1. Classification of VES curves

In Otake area, it is noticed that 73 % of the total curves are of types H, KH and QH on the surveying line L0 and 76 % of the total on the line L5. However, in Takenoyu area, the number of QH type curves decreases while that of HKH type does not exist. Such a classification might be very helpful and convenient for comparing geothermal areas.

4.2. RESULTS OF APPLICATION

It was found that 56 of the 64 VES curves show good shapes. The remaining 8 VES curves, which are four of the type KH, one of the type HA and one of the type QH, and two of the type KQH, showed a very bad shape of the apparent resistivity curve for large electrode separations. The program was applied to these 8 curves increasing the number of terms from 400 up to 1000. After these trials, it was concluded that N = 1000 gave the most satisfactory results.

4.3. INTERPRETATION PROCEDURES

In order to apply the PSH-B program for interpreting VES curves obtained at geothermal area, the following procedures are recommended.
(1) In order to detect faults and horizontal structures, obtain the horizontal resistivity mapping curves from the VES data.
(2) Make corrections on the VES curves if necessary, then they can be interpreted by conventional methods, for instance, using the partial curve matching method by means of the two layer standard curves and an auxilliary curve. Then rough estimations of the resistivities, number and thicknesses of the layers can be done.
(3) Input the estimated values of layer parameters to PSH-B program then theoretical curves are obtained. The field VES data are then compared with the new curves and reinterpreted.
(4) If good agreements are not reached, the procedure (3) is repeated until good fits between the theoretical and field curves are obtained.
(5) The determined subsurface structures are then drawn in the topographic section of the surveying line.
(6) The subsurface structures that indicate the possible existence of geothermal reservoirs are decided taking in considerations of various factors affecting the resistivity values.

5. CONCLUDING REMARKS

PSH-B program which compute the apparent and relative resistivities for a multiple layer model was presented and it was applied to 64 VES curves obtained in Otake and Takenoyu geothermal areas. It produced good theoretical curves for 56 cases, by only using 300 terms. For the remaining 8 cases, acceptable curves were obtained with the slight modification of increasing the maximum number of terms of polynomials to N = 1000.

The total computing time for the 64 curves was 64 x 14 seconds + 8 x 60 seconds = 23 minutes.

With these results, it is possible to conclude that the PSH-B program can be applied to the interpretation of the VES curves obtained in geothermal areas.

ACKNOWLEDGMENTS

The authors wish to express their thanks to Professor S. Onodera for his helpful discussions. They wish to express thanks to Enrique Lima, Graduate Course Student of Kyushu University, for his critically reading the manuscript.

REFERENCES CITED

Mooney, H. M., and Wetzel, W. W., 1956, The potentials about a point electrode and apparent resistivity curves for a two-, three- and four-layered earth: One volume and one atlas. University of Minnesota Press, Mineapolis, Minnesota.

La Compagnie Generale de Geophysique, 1955, Abaques de sondage electrique: Geophysical Prospecting, v.3, Supplement,no.3.

Orellana, E., and Mooney, H. M., 1966, Master tables and curves for vertical electrical sounding over layered structures: Interciencia, Madrid.

Rijkswaterstaat, The Netherlands, 1969, Standard graphs for resistivity prospecting, European Association of Exploration Geophysicists.

Keisuke USHIJIMA and Kazuo USHIJIMA, 1977a, Calculation of resistivity sounding curves for a horizontally layered earth: BUTSURI-TANKO, v.30, no.1, pp.1-11.

Keisuke USHIJIMA and Kazuo USHIJIMA, 1977b, Application of the computer program PSH to the interpretation of resistivity soundings in geothermal areas: BUTSURI-TANKO, v.30, no.4, pp.10-19.

Argelo, S. M., 1967, Two computer programs for the calculation of standard graphs for resistivity prospecting, Geophysical Prospecting, v.15, no.1, pp.71-91.

Seibe ONODERA, 1969, Interpretation of VES curves by digital computer, Journal of the Mining and Metallurgical Institute of Japan, v.85, no.976, pp.7-10.

Mooney, H. M., Orellana, E., Pickett, H., and Tornheim, L., 1966, A resistivity computation method for layered earth models: Geophysics, v.31, no.1, pp.192-203.

Flathe, H., 1955, A practical method of calculating geoelectrical model graphs for horizontally stratified media: Geophysical Prospecting, v.3, pp.38-44.

Naomi FUJIMURA and Kazuo USHIJIMA, 1976, On transferability of Fortran dynamic analyzing system, JYOHO-SHORI, v.17, no. 11, pp.1048-1055.

Keller, G. V., and Frischknecht, F. C., 1970, Electrical methods in geophysical prospecting: Pergamon press, pp.135-136.

Takashi NOGUCHI and Seibe ONODERA, 1969, Resistivity exploration for altered zone at Otake geothermal area - Japan: Bulletin Volcanologique, Tome 33-1, pp. 205-228.

APPENDIX

```
      FACOM 230-45S  OS2     FORDAP      -760805-      V-01  L-08       DATE 77-05-14     TIME
 * SOURCE STATEMENT *                EXECUTION TIME =      15643 MSEC          EXECUTIONS

      C**** WENNER AND SCHLUMBERGER RESISTIVITY SOUNDING CURVES FOR          PSH00000
      C****          HORIZONTALLY LAYERED EARTH                             PSH00001
      C                                                                     PSH00002
      C     PROGRAM PSH=B CODED BY KEISUKE USHIJIMA AND KAZUO USHIJIMA      PSH00003
      C     FACULTY OF ENGINEERING, KYUSHU UNIVERSITY, 6-10-1, HAKOZAKI     PSH00004
      C     FUKUOKA 812, JAPAN                                              PSH00005
      C     CRITICISM INVITED. TEL 092-641-1101 EXT.3218                    PSH00006
      C     VERSION OF MAY 10, 1977                                         PSH00007
      C                                                                     PSH00008
            INTEGER STAN                                                    PSH00009
            DIMENSION RHO(10),H(9),STAN(10)                                 PSH00010
      C                                                                     PSH00011
      C**** CHANGE FOLLOWING TWO STATEMENTS IF ADVANCED CALCULATION NEEDED. PSH00012
      C                                                                     PSH00013
            DIMENSION P( 301),Q( 301),COEF( 300)                            PSH00014
            N=300                                                           PSH00015          1
      C                                                                     PSH00016
            WRITE(6,10)                                                     PSH00017          1
         10 FORMAT(1H1,/,10X,'RESISTIVITY SOUNDING CURVES BY PROGRAM PSH',/) PSH00018
      C                                                                     PSH00019
      C**** INPUT OF LAYER PARAMETERS                                       PSH00020
      C                                                                     PSH00021
         20 READ(5,30)LAYER,STAN                                            PSH00022          2
         30 FORMAT(I10,10A2)                                                PSH00023
            IF(LAYER .EQ. 0) STOP                                           PSH00024          2
            READ(5,40)(RHO(I),I=1,LAYER)                                    PSH00025          1
         40 FORMAT(8F10.0)                                                  PSH00026
            LM1=LAYER-1                                                     PSH00027          1
            READ(5,50)(H(I),I=1,LM1)                                        PSH00028          1
         50 FORMAT(8I10)                                                    PSH00029
      C                                                                     PSH00030
            CALL PSH(LAYER,STAN,RHO,H,N,P,Q,COEF,N+1)                       PSH00031          1
      C                                                                     PSH00032
            GO TO 20                                                        PSH00033          1
            END                                                             PSH00034

 * SOURCE STATEMENT *                EXECUTION TIME =      15633 MSEC          EXECUTIONS

            SUBROUTINE PSH(LAYER,STAN,RHO,H,N,P,Q,COEF,NDIM)                PSH00035          1
            INTEGER TERM,STAN                                               PSH00036
            INTEGER*4 T1,T2,T3                                              PSH00037
            DOUBLE PRECISION RWO,RSO                                        PSH00038
            DIMENSION A(55),AO(55),RHO(10),RE(9),H(9),                      PSH00039
           *          P(NDIM),Q(NDIM),COEF(N),STAN(10)                     PSH00040
            DATA NA/55/                                                     PSH00041
      C                                                                     PSH00042
      C**** INPUT OF WENNER ELECTRODE SEPARATIONS                           PSH00043
      C                                                                     PSH00044
            DATA AO/0.1,   0.2,   0.3,   0.4,   0.5,   0.6,   0.7,   0.8,  PSH00045
           1       0.9,   1.0,   1.2,   1.4,   1.6,   1.8,   2.0,   2.2,  PSH00046
           2       2.4,   2.6,   2.8,   3.0,   3.4,   3.8,   4.2,   4.6,  PSH00047
           3       5.0,   6.0,   7.0,   8.0,   9.0,  10.0,  12.0,  14.0,  PSH00048
           4      16.0,  18.0,  20.0,  25.0,  30.0,  32.0,  40.0,  46.0,  PSH00049
           5      56.0,  64.0,  80.0,  96.0, 100.0, 120.0, 140.0, 200.0,  PSH00050
           6     240.0, 280.0, 320.0, 400.0, 480.0, 560.0, 640.0/         PSH00051
      C                                                                     PSH00052
      C**** INPUT OF SCHLUMBERGER ELECTRODE SEPARATIONS                     PSH00053
      C                                                                     PSH00054
            DATA AO/0.3,   0.4,   0.5,   0.6,   0.7,   0.8,   0.9,   1.0,  PSH00055
           1       1.2,   1.4,   1.6,   1.8,   2.0,   2.2,   2.5,   2.8,  PSH00056
           2       3.0,   3.4,   4.0,   4.4,   5.0,   6.0,   7.0,   8.0,  PSH00057
           3       9.0,  10.0,  12.0,  14.0,  16.0,  18.0,  20.0,  22.0,  PSH00058
           4      25.0,  28.0,  30.0,  34.0,  40.0,  44.0,  50.0,  60.0,  PSH00059
           5      70.0,  80.0,  90.0, 100.0, 120.0, 140.0, 160.0, 180.0,  PSH00060
           6     200.0, 220.0, 250.0, 280.0, 320.0, 380.0, 460.0/         PSH00061
      C                                                                     PSH00062
            CALL CLOCK(T1)                                                  PSH00063          1
      C                                                                     PSH00064
      C**** CALCULATION OF REFLECTION COEFFICIENTS                          PSH00065
      C                                                                     PSH00066
            LM1=LAYER-1                                                     PSH00067          1
            DO 60 I=1,LM1                                                   PSH00068          1
               RE(I)=(RHO(I+1)-RHO(I))/(RHO(I+1)+RHO(I))                    PSH00069          2
         60 CONTINUE                                                        PSH00070          2
      C                                                                     PSH00071
      C**** PRINT OF LAYER PARAMETERS                                       PSH00072
      C                                                                     PSH00073
            WRITE(6,65)STAN                                                 PSH00074          1
         65 FORMAT(1H0,20A1O42)                                             PSH00075
            WRITE(6,70)                                                     PSH00076          1
         70 FORMAT(1H0,8X,'LAYER',7X,'RHO',10X,'H',13X,'H*',/)              PSH00077
            WRITE(6,80)(I,RHO(I),H(I),H(I),I=1,LM1)                         PSH00078          1
         80 FORMAT(1H ,7X,I5,F15.8,F15.8,/10)                               PSH00079
            WRITE(6,90)LAYER,RHO(LAYER)                                     PSH00080          1
         90 FORMAT(1H ,7X,I5,F15.8,///)                                     PSH00081
      -                                                                     PSH00082
      C                                                                     PSH00083
      C**** DETERMINATION OF P(J) AND Q(J)                                  PSH00084
      C                                                                     PSH00085
            P(1)=0                                                          PSH00086          1
            Q(1)=1.0                                                        PSH00087          1
            DO 100 I=1,N                                                    PSH00088        300
               P(I+1)=0                                                     PSH00089        300
               Q(I+1)=0                                                     PSH00090        300
        100 CONTINUE                                                        PSH00091          1
            ID=1                                                            PSH00092          1
            DO 120 I=1,LM1                                                  PSH00093          2
               ID=ID+H(I)                                                   PSH00094          2
               JS=ID-10*H(I)+1                                              PSH00095          2
               DO 110 J=JS,ID                                               PSH00096          2
                  JE=ID-J+1                                                 PSH00097          3
                  P(J)=P(J)+RE(I)*(P(JE)+Q(JE))                             PSH00098          3
                  Q(J)=Q(J)-RE(I)*Q(JE)                                     PSH00099          3
        110    CONTINUE                                                     PSH00100          3
        120 CONTINUE                                                        PSH00101          2
      C                                                                     PSH00102
      C**** PRINT OF TITLE                                                  PSH00103
      C                                                                     PSH00104
            WRITE(6,130)                                                    PSH00105          1
        130 FORMAT(1H0,15X,'WENNER CURVE',30X,'SCHLUMBERGER CURVE',//,      PSH00106
           1    8X,'A',10X,'R(A)',10X,'G',10X,'AR(A)',13X,'AO',8X,         PSH00107
           2     'R(AO)',10X,'AR(AO)',10X,'TERM',//)                        PSH00108
      C                                                                     PSH00109
      C**** DETERMINATION OF COEFFICIENTS                                   PSH00110
      C                                                                     PSH00111
            COEF(1)=P(2)                                                    PSH00112          1
            DO 150 TERM=2,N                                                 PSH00113          1
               C=P(TERM+1)                                                  PSH00114        299
               DO 140 J=2,TERM                                              PSH00115        299
                  IJ=TERM+1-J                                               PSH00116      44850
                  C=C-Q(J)*COEF(IJ)                                         PSH00117      44850
        140    CONTINUE                                                     PSH00118      44850
               COEF(TERM)=C                                                 PSH00119        299
        150 CONTINUE                                                        PSH00120        299
      C                                                                     PSH00121
      C**** CALCULATION OF RESISTIVITY SOUNDING CURVES                      PSH00122
      C                                                                     PSH00123
            DO 190 I=1,NA                                                   PSH00124          1
               RWO=1.0                                                      PSH00125         55
               RSO=1.0                                                      PSH00126         55
               AA=A(I)*A(I)                                                 PSH00127         55
               SS=AO(I)*AO(I)                                               PSH00128         55
               DO 160 TERM=1,N                                              PSH00129         55
                  FJ=TERM                                                   PSH00130      16500
                  FFJ=FJ*FJ                                                 PSH00131      16500
                  FS=4.0*FFJ                                                PSH00132      16500
      C     WENNER CURVE                                                    PSH00133
                  AC=4.0*AA*A(I)                                            PSH00134      16500
                  SQA=SQRT(FS+AA)                                           PSH00135      16500
                  SQB=SQRT(FFJ*AA)                                          PSH00136      16500
                  WD=COEF(TERM)*AC/(SQA*SQB*(2.0*SQB+SQA))                  PSH00137      16500
                  RWO=RWO+WD                                                PSH00138      16500
      C     SCHLUMBERGER CURVE                                              PSH00139
                  SO=2.0*COEF(TERM)/(1.(*+S/SS)/SQRT(1.0*+S/SS)             PSH00140      16500
                  RSO=RSO+SO                                                PSH00141      16500
        160    CONTINUE                                                     PSH00142      16500
               TERM=N                                                       PSH00143         55
               RW=RWO*RHO(1)                                                PSH00144         55
               RS=RSO*RHO(1)                                                PSH00145         55
      C     PRINT OF WENNER AND SCHLUMPERGER CURVES                         PSH00146
            WRITE(6,180)A(I),RW,AO(I),RS,TERM                               PSH00147         55
        180    FORMAT(1H ,F10.1,2F15.8,F15.1,2F15.8,I10)                    PSH00148
        190 CONTINUE                                                        PSH00149         55
      C                                                                     PSH00150
      C**** TIME COUNT FOR ONE SET OF CURVE                                 PSH00151
      C                                                                     PSH00152
            CALL CLOCK(T2)                                                  PSH00153          1
            T3=T2-T1                                                        PSH00154          1
            WRITE(6,200)T3                                                  PSH00155          1
        200 FORMAT(1H0,///,5X,'TIME COUNT FOR MS CURVES=',I10,2X,'MS',///)  PSH00156
      C                                                                     PSH00157
      C**** PRINT OF COEFFICIENTS OF POWER SERIES                           PSH00158
      C                                                                     PSH00159
            WRITE(6,210)(JJ,COEF(JJ),JJ=1,TERM)                             PSH00160          1
        210 FORMAT(5(I5,F15.8))                                             PSH00161
            RETURN                                                          PSH00162          1
            END                                                             PSH00163
```

Dup

Geothermal Resources Council, TRANSACTIONS, Vol. 2 July 1978

GEOTHERMAL DRILLING AND COMPLETION TECHNOLOGY DEVELOPMENT

S. G. Varnado and H. M. Stoller

Sandia Laboratories
Albuquerque, New Mexico 87185

Abstract

The high cost of drilling and completing geothermal wells is an impediment to the development of geothermal energy resources. Technological deficiencies in rotary drilling techniques are evidenced when drilling geothermal wells. The Division of Geothermal Energy (DGE) of the U. S. Department of Energy has initiated a program aimed at developing new drilling and completion techniques for geothermal wells. The goals of this program are to reduce well costs by 25% by 1982 and by 50% by 1986. Sandia Laboratories has been selected to manage this technology development program, and this paper presents an overview of the program. Program justification which relates well cost to busbar energy cost and to DGE power-on-line goals is presented. Technological deficiencies in current rotary drilling techniques for geothermal wells are discussed. A program for correcting these deficiencies is described.

Work supported by the U. S. Department of Energy.

Introduction

The Division of Geothermal Energy (DGE) of the U. S. Department of Energy (DOE) has established geothermal power-on-line goals of 3,000 MW_e by 1985 and 20,000 MW_e by the year 2000[1] for the National Geothermal Energy Program. Achievement of these goals will be possible only if geothermal energy competes on a favorable economic basis with energy from conventional sources, e.g., fossil and nuclear. The cost of drilling and completing geothermal wells accounts for a significant portion of the cost of geothermally produced power. At the present time, the cost per foot of geothermal wells is about two to four times that of conventional oil and gas wells[2-4] (see Figure 1), and these costs must be reduced if DGE power-on-line goals are to be met.

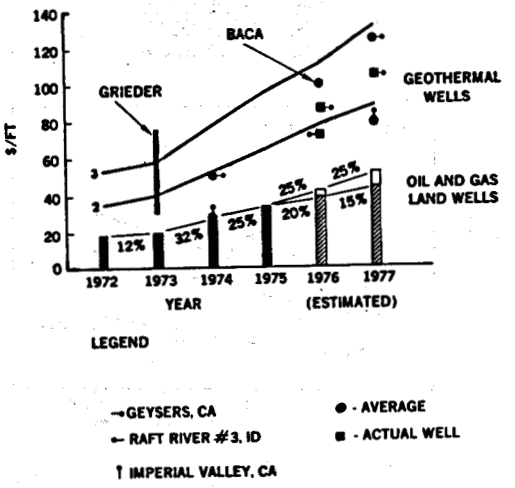


Fig. 1 Trend in footage costs for geothermal wells as compared to oil and gas land wells

Reductions in well cost will result in reduced busbar energy cost for geothermally-produced electricity. This will, in turn, improve the relative economic position of geothermal power in the marketplace and will lead to substitution of geothermal power for conventional power. For example, Bloomster[5] has estimated that a 6% reduction in geothermal busbar energy cost would lead to a 13% increase in geothermal power-on-line, and that reductions of 10 to 35% in busbar cost would effectively double the amount of geothermal energy that is economically attractive because large, lower temperature reserves become competitive. Therefore, the critical questions concerning geothermal drilling and completion technology development relate to the impact of well cost on busbar energy cost and to the effectiveness of technological improvements in reducing well costs.

Figure 2 indicates the sensitivity of busbar energy costs to well cost and reservoir temperature.[2] Assuming a base

cost of $500,000 per well, a 40% reduction in well cost, for example, would result in a decrease in busbar energy cost of from 15 to 23%, depending on reservoir temperature. Since geothermal power-on-line is sensitive to busbar energy cost, reductions in well cost have the potential for significantly accelerating the utilization of geothermal energy. Therefore, it is important to consider the role of technology development in reducing well cost.

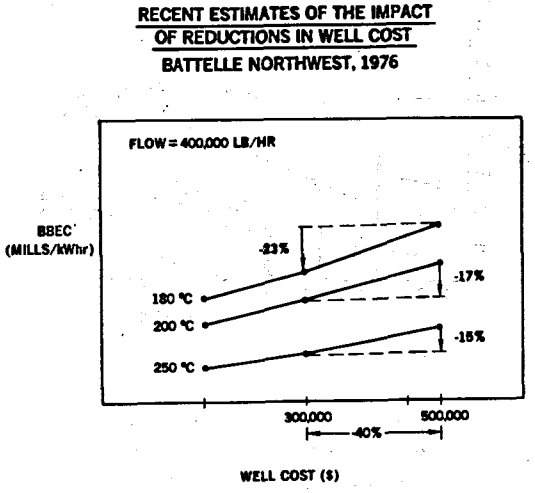


Fig. 2 Recent estimates of the impact of reductions in well cost

Present Difficulties in Drilling

The high cost associated with geothermal wells is due in part to a number of deficiencies in geothermal drilling and completion technology. These deficiencies are attributable to temperature, formation, and corrosion and erosion effects which are found uniquely or primarily in geothermal environments.

Temperature Effects

The high temperature environment encountered in geothermal wells produces adverse effects on drilling fluids, casing and cement, bits, and elastomeric materials.

Drilling-fluid-related difficulties form the single most frequently cited category of geothermal drilling problems. Lost circulation is a pervasive difficulty in the geothermal field because of the highly fractured formations in which geothermal resources are found. Fluids which remain stable at high temperature often do not have adequate filtration characteristics for control of lost circulation. Furthermore, conventional muds tend to gel when circulation is stopped for tripping, logging, and running casing. This can lead to induced problems such as stuck tools and failures of the drill string from differential sticking. Expensive procedures are required to correct these fluid-related failures.

Drilling fluids can also affect the quality of the cementing job, since they tend to contaminate the cement, and muds that have gelled and thickened leave excessive filter cake on the casing and formation. This filter cake inhibits good cement bonding. Also, a thickened mud can cause the cement to channel behind the casing and can result in large uncemented regions. These regions can fill with water which can vaporize at geothermal temperatures. The pressures which build up have the potential for causing collapse of the casing.

A further problem results from uncertainty in determining the temperature profile of the well. Geothermal cements must be formulated with the proper amount of retardants. Incorrect mixtures will fail to set up properly and may lead to expensive remedial cementing ("perf and squeeze"). Such operations are expensive in themselves and also increase non-rotating rig costs.

The predominant mode of bit failure in geothermal wells is through bearing failure. Unsealed bearings are normally used because elastomeric seals will not survive the high temperatures encountered. The bearings and races are lubricated only by the drilling fluid. High downhole temperature and increased friction cause these critical parts to experience much higher temperatures than the main bit body. Research at the Geysers,[6] where formation temperatures are about 240°C, has shown that temperatures up to 540°C are experienced at the friction pin, and that significant softening of the steel occurs at 260-316°C. The high temperature and resultant softening of the bearing surfaces reduces bit life at the Geysers to 1/4-1/5 normal. Costs are increased by the need for more bits, the greater number of round trips required, and reduced penetration rates while drilling.

Currently the best available elastomers fail at temperatures of 175-225°C depending upon use and environment. These materials cease to be elastomeric when subjected to high temperatures and pressures, and thus their value in geothermal applications is limited. Unfortunately, elastomers are important to

virtually every aspect of drilling. The best current designs of rock bits, downhole motors, blowout preventers, packers, and logging tools all contain elastomers. Most of this equipment either cannot be used or can be used only with frequent, costly inspection, repair, and special procedures.

Formation Effects

In addition to the extra costs due to high temperature, additional costs are often incurred in geothermal drilling because of the type and condition of the formations which must be penetrated. The fractured formations that predominate in most geothermal reservoirs (except the geopressured Gulf Coast) cause severe stresses on drilling equipment. Furthermore, many reservoirs exist in hard or medium-hard formations where penetration is slow and equipment wear is high.

Erosion and Corrosion Effects

Air is an attractive fluid for drilling into competent reservoirs because it will not damage the formations and generally improves rate of penetration. However, air drilling causes rapid erosion of downhole equipment.[7] At the Geysers, where the drill string is frequently inspected and hardbanded and where a special anti-erosion additive is used in the air stream, it is still necessary to junk one foot of drill pipe for each seven feet of hole.[8] These procedures require extra services and additional training for the rig crew, and the high discard rate for pipe requires advance planning to insure adequate supplies of replacements.

Completion problems can arise for those wells which produce wet stream because it can erode casing as the high speed fluid strips water film from the casing surface. Higher quality casing with flush joints must be used to reduce the problem.

When hot, acidic brines or H_2S are present, downhole equipment is subject to embrittlement and corrosion. These conditions also require special procedures and training for the crews. Also, more expensive, corrosion resistant materials are used, and additives may be required in the drilling fluid to help control corrosion.

Geothermal Well Technology Development Program

In view of the existing technological difficulties associated with drilling and completing geothermal wells, DOE/DGE has initiated a program directed at developing and commercializing the technology required to reduce the cost of geothermal wells. An analysis of existing geothermal well cost data indicates that technological developments such as higher penetration rate, longer life rock bits; high temperature drilling fluids; improved completion techniques; and improved directional drilling techniques have the potential for reducing the cost of geothermal wells drilled with conventional rotary technology by approximately 25%. Cost reductions in excess of 25% will require the use of new drilling techniques. Research in novel drilling techniques is presently underway, and the successful implementation of these new techniques could possibly reduce well costs by as much as 50%. Based on these facts, cost reduction goals of 25% by 1982 and 50% by 1986 have been set for the DOE/DGE Geothermal Well Technology Program.

In October of 1977, Sandia Laboratories was selected by DOE/DGE to manage the well technology development program. Since that time a detailed, ten-year program plan has been prepared, and technical management of contracted R&D activities has begun. In addition, in-house research is being conducted on novel bit designs, high temperature elastomers, and novel drilling systems. Drilling technology R&D efforts during 1978 are centered on three major areas: high temperature drilling fluids, high temperature downhole motors, and high performance rock bits. Completion technology efforts emphasize sand control methods in geopressured formations and analyses of reinjection well plugging problems in all reservoirs.

Research in high temperature drilling fluids is underway at Maurer Engineering, Baroid, and the University of Oklahoma. Maurer has performed high temperature laboratory tests of commercially available muds, and is presently involved in a study of high temperature drilling foams. Baroid has entered a cost sharing contract with DOE/DGE to design, fabricate, and test a 700°F, 20,000 psi mud flow loop to test rheology, filtration, density, and corrosion characteristics of muds at temperature and pressure. The University of Oklahoma is using a modified Magcobar mud flow loop for testing muds to 400°F.

Sandia is presently funding work at Terra Tek directed at the development of high temperature bearings, seals, and lubricants for use in bits and downhole motors. Under previous DOE funding, a seal tester has been developed and is available for general use. Temperatures and pressures representative of geothermal well borehole conditions can be

simulated in this tester. In addition, a twenty-five-foot-long borehole simulator suitable for testing the bearing and seal package for a geothermal downhole motor has been constructed. Extension of this simulator to allow full scale motor testing is underway.

Bit development includes investigation of sealed and unsealed bits at Terra Tek, of water jet erosion drilling at the University of Missouri, of cavitation assisted diamond bits at Hydronautics, of Stratapax[R] bits at General Electric, and of the continuous chain, downhole replaceable bit at Sandia. These efforts are directed at increasing penetration rate and bit life in the geothermal environment. Performance of these bits will be described in detail.

[R]Registered trademark for the General Electric synthetic diamond cutters

References

1. "Program Approval Document Fiscal Year 1977 -- Geothermal Energy Develment," Solar, Geothermal and Advanced Energy Systems Development, ERDA, January, 1977.
2. R. Grieder, "Economic Considerations for Geothermal Exploration in the Western United States," presented at Symposium, Colorado Department of Natural Resources, Denver, Colorado, December 6, 1973.
3. W. A. Glass, "1977 Drilling Methods and Costs at the Geysers," Geothermal Resource Council 1, 5/77.
4. D. Pyle, Union Oil Corporation, private communication.
5. C. H. Bloom, et al., "The Potential Benefits of Geothermal Electrical Production from Hydrothermal Resources," BNWL-2001, Battelle Pacific Northwest Laboratories, June, 1976.
6. L. M. Barker, S. J. Green, A. H. Jones, M. Skalka, "Geothermal Environment Effects on Drill Bit Life," 11th Intersociety Energy Conversion Engineering Conference, 1976.
7. J. H. Cromling, "Geothermal Drilling Procedures and Costs," J. Pet. Tech. 25, 1973 (1033-1038).
8. P. W. Fischer and D. E. Pyle, "Corrosion-Erosion Control of Tubulars in Geothermal Drilling," API Joint Meeting, Bakersfield, California, October, 1977.

Dup

Geothermal Resources Council, TRANSACTIONS, Vol. 2 July 1978

HIGH TEMPERATURE INSTRUMENTATION FOR GEOTHERMAL APPLICATIONS*

A. F. Veneruso
H. M. Stoller

SANDIA LABORATORIES
ALBUQUERQUE, NM 87185

INTRODUCTION

Instrumentation for making geothermal borehole measurements is limited by the temperature capabilities (~ 180°C) of existing logging equipment developed for the oil and gas industry. The Geothermal Logging Instrumentation Development Program being conducted by Sandia Laboratories for the Department of Energy (DOE), Division of Geothermal Energy is an industry based effort to develop and apply the high temperature instrumentation needed to make geothermal borehole measurements.[1] The near-term goal is to develop instrumentation for use at 275°C in pressures up to 48.3 MPa (7,000 psi); subsequent goals are to extend the capabilities to 350°C and 138 MPa (20,000 psi). Working closely with geothermal producers, logging service companies are conducting R&D to correct technical deficiencies so they may adequately serve the growing geothermal market. The basic impediments they face involve special technologies which are not normally required in their trade and for which there are insufficient incentives for them to develop. These technologies are precisely those which are being developed by this program; components development activities are directed toward stimulating industries' own inventions and field applications of geothermal logging instruments having improved reliability, appropriate size, reasonable cost and performance versatility which encompasses not only geothermal but conventional petroleum and hot, deep natural gas logging as well. Tools to be upgraded and/or developed include temperature, flow rate, high resolution downhole pressure, caliper and fracture mapping sondes.

GEOTHERMAL BOREHOLE MEASUREMENTS

In geothermal wells, temperatures frequently range up to 350°C while, at present, most of the commercially available logging tools, cables and seals are rated to only 180°C. Above their temperature rating and combined with the corrosive environment of a geothermal well, logging tools and cables have significantly reduced reliability and life expectancy.

The repertoire of tools needed to enhance geothermal development, their development priority and performance requirements are listed in Table 1 based on information compiled by the 1975 Geothermal Workshop[2] and updated by the industry based Geothermal Logging Instrumentation Steering Committee.

TABLE 1

PROTOTYPE GEOTHERMAL LOGGING TOOLS
(up to 275°C operation)

Tool	Performance Goal
Temperature	1.0°C accuracy, 0.5°C resolution
Pressure	0-7000 psi, 0.1 psi accuracy, 0.01 psi resolution
Flow	0-2000 gpm in diphasic flow
Caliper	6 arm borehole geometry, 0.1 in. accuracy with fracture indication
Casing Collar Locator	Detect standard collars
Formation Resistivity	To be determined
Fracture Mapping	To be determined
Casing & Cementing Inspection	To be determined
Directional Survey	To be determined
Sonde Refrigeration	50 watts cooling to 125°C for at least 100 hours

GEOTHERMAL LOGGING DEVELOPMENT

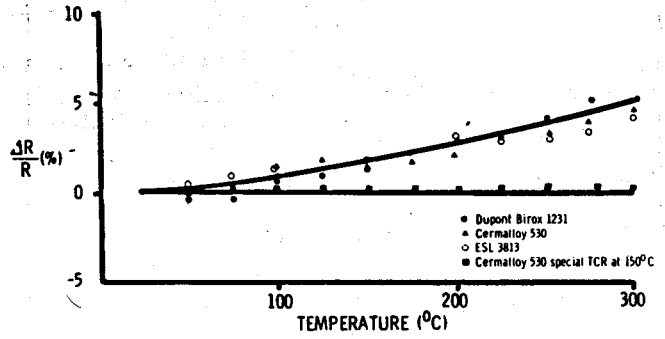
The technical development of geothermal borehole instrumentation is divided into three tasks: 1) severe environment components development, 2) prototype system development, and 3) borehole test and evaluation.

SEVERE ENVIRONMENT COMPONENTS DEVELOPMENT

Efforts in components development are directed toward alleviating existing technical deficiencies by identifying, testing and evaluating devices, materials, and components suitable for use in geothermal logging systems. Specific developments are under way in 275°C electronics, high temperature-high resolution pressure transducers, acoustic transducers, and high temperature corrosion resistant elastomers, ceramics and metals.

*Work performed under the auspices of the U.S. Department of Energy, Contract No. AT(29-1)-789 for the Division of Geothermal Energy (DGE).

High temperature Electronics - The thrust for a 275°C capability is the use of hybrid thick film microcircuits technology. This commercial technology is employed for small quantity production runs but typically limited to 125°C applications. The technology can be adapted to the required temperature range, has the necessary ruggedness and gives the desired level of miniaturization. Adaption of the hybrid thick film process to high temperature operation requires selection of resistor inks specially formulated for low values of thermal coefficient of resistivity as shown in Figure 1. Similarly, dielectric inks, for capacitors, are formulated to maintain stable low loss properties over a wide temperature range. Hundreds of these hybrid thick film resistor and capacitor devices have been laboratory tested for thousands of hours at 300°C.



THICK FILM RESISTANCE CHANGE AS A FUNCTION OF TEMPERATURE. THE THREE STANDARD INK SAMPLES THAT WERE EXTENSIVELY TESTED PERFORMED ROUGHLY THE SAME. THE SPECIAL TCR CERMALLOY 530 HAD A ΔR/R OF LESS THAN 0.2%.

Figure 1

For active devices in the 275-300°C range, the popular bipolar silicon transistors are intrinsically limited. However, a few commercially available silicon semiconductors have been found to operate satisfactorily at these high temperatures. The majority of these devices are junction field effect transistors (JFETs). JFETs operate by means of electrostatic control of majority carrier current. Figure 2 displays temperature performance curves for a commercially available JFTE specially selected for its high temperature qualified construction. Several have been qualified for 275°C operation through active circuit tests for 1000 hours at 300°C.

Through laboratory testing of active and passive electronic devices, a sufficient, though limited, line of commercial components and fabrication techniques is now available for 275°C

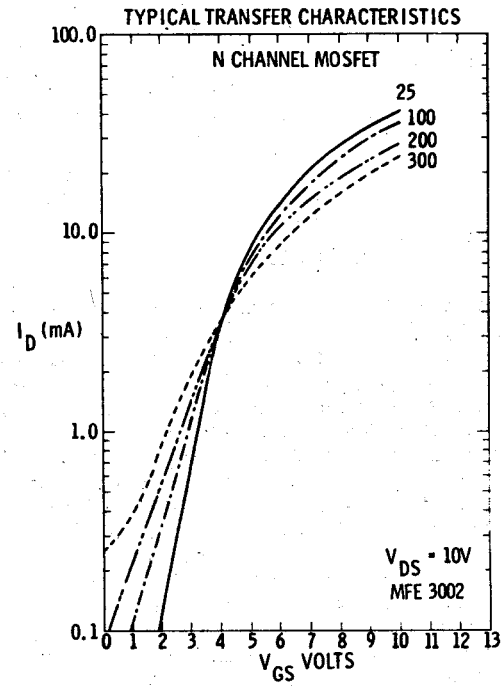


Figure 2

operation to fulfill basic circuit needs for amplification, switching and filtering. Development work is continuing toward expanding the repertoire of available devices suitable for 275°C operation.[4]

High Temperature Mechanical Components - Elastomers and seals capable of withstanding temperatures of at least 275°C and 7,000 psi in the presence of geothermal brine for up to 100 hours are required for geothermal well logging applications in seals, gaskets, connectors, cable sheathing, wire insulation, pressure controls, and borehole packers. The approach taken to develop high temperature mechanical components includes: 1) coordination of material needs and developments with DGE's Geochemical Engineering Program, 2) test and evaluation of available high temperature, steam resistant elastomers and metals as moisture barrier seals, and 3) investigation of special coatings to enhance the chemical and steam resistance of elastomers made from available polymers.

As shown in Tables 2 and 3, test and evaluation of available materials has identified several promising candidates for use in specific components such as seals and wire insulation. Other materials, along with specific prototype designs of cables, cableheads and tool seals will be tested in the coming months.

TABLE 2

HIGH TEMPERATURE ELASTOMERS

Trade Name	Type	Decomposition Temperature °C	Cost $/LB	Components
BUNA N	NITRILE	150	6	Good Oil Resistance Poor Resistance to H_2S and Steam
VITON E- -C	FLUORO ELASTOMER	290	35	Fair Resistance to Steam Poor for H_2S
VITON G (Peroxide Cure)	FLUORO ELASTOMER	290	40	Improved Steam Resistance Poor for H_2S
KALREZ	FLUORO ELASTOMER (Fully Fluorinated)	400	2000	Best for H_2S Fair for Steam
EPR	POLYOLEFIN	250	8	Excellent Steam Resistance H_2S Unknown
SILOXANE	SILICONE	300	17	Poor Steam and Poor H_2S Resistance

TABLE 3

HIGH TEMPERATURE SEALS

Type	Temperature Limitation		Components
Elastomeric O-Rings	Polymer Decomposition	300°C	Reuse Permitted Least Dirt Sensitive
Metal O-Rings	Metal Softening	500°C	Reuse Not Recommended Soft Plating Recommended Nick and Scratch Sensitive Minor Joint Motion Tolerated
Wave Rings	Metal Softening	500°C	Reuse Not Recommended Soft Plating Recommended Nick and Scratch Sensitive

PROTOTYPE SYSTEM DEVELOPMENT

Based on the priority of needs listed in Table 1, the temperature, pressure, flow, and caliper tools are being addressed first.

Temperature - Both printed circuit board and hybrid microcircuits have been completed and evaluated for a 275°C temperature tool. The design is based on a platinum resistance transducer with active downhole electronics. The design is compatible with both multi- and mono-conductor cables. A printed circuit board version has successfully completed 62 hours of testing at 275°C. A drift error of less than 0.28°C was obtained.

Fabrication of a complete tool including housing and interconnections has been accomplished. Test results are subsequently discussed.

Pressure - This development is directed toward a high resolution quartz crystal based pressure sensor which strives for 0.01 psi resolution in temperatures up to 275°C. Currently available, high resolution pressure gauges utilize quartz crystals but are temperature limited because of: crystal geometry employed; the bonding of the crystals to the substrate; and the temperature range of the associated electronics. The approach taken for the high temperature design begins with a new quartz crystal configuration that is specifically designed to operate optimally at 275°C rather than over a wide range of temperatures. The crystal is small enough to fit inside a miniature oven which precisely maintains the quartz crystal at the optimum temperature. Deficiencies in the associated electronics are corrected by utilizing the repertoire of high temperature hybrid thick film circuit components already developed.

Flow - A high temperature impeller type flux gate transducer signal feedthrough mechanism has been constructed. The associated hybrid electronics for 275°C operation are presently under development.

Caliper - A caliper tool is a necessary adjunct to the impeller type flow tool in order to compute flow rate. The caliper is also necessary to

identify open borehole geometry and thereby establish a basis for log instrumentation and well completion strategy. In addition, a caliper is also useful in gross fracture mapping where the fractures are at least 0.1 inches wide. Development efforts are directed at correcting major deficiencies in existing caliper's susceptibility to the corrosive, high temperature geothermal environment.

Fracture Mapping - Most liquid dominated hydrothermal reservoirs appear to be fracture dominated permeable zones rather than the intergranular dominated permeable zones common in petroleum reservoirs. The development of fracture mapping techniques for geothermal reservoir assessment is, therefore, of very high priority.

DOE/DGE is currently sponsoring Westinghouse Research Laboratory to improve and temperature harden transducers for a Borehole Televiewer (BHTV). The BHTV is patented by the Mobil Oil Corp. and incorporates a high frequency (1.5 MHz) acoustic transducer system which provides an acoustic image of the borehole wall to indicate cracks and associated fracture zones.

Activities in acoustic fracture mapping are directed toward further development of the BHTV because such development will complement industries' own efforts. Also, pioneering work by the USGS and Simplec Manufacturing Co. indicates that the BHTV has a high potential for satisfying geothermal needs.

Other Prototypes - Available thermal protection devices such as eutectic heat sink equipped dewar flasks are presently the industry's staple in packaging and protecting state-of-the-art electronics for logging geothermal wells. However, the best available dewars are limited to no more than 12 hours of operation in boreholes up to 275°C. A reliable instrumentation refrigerator, capable of operating for 100 hours or more, will enable long-term operation of existing downhole electronic packages and thereby open up the geothermal logging market to conventional logging services. Due to the high potential payoffs, this sonde refrigerator is currently being contracted to industry with appropriate technical support from Sandia.

BOREHOLE TEST AND EVALUATION

The above experimental prototypes will be tested in geothermal boreholes using a special trailer mounted skid unit, a 50 foot mast truck and auxiliary support equipment for long term experimental tests of prototype borehole instruments. The skid unit is equipped with 16,000 ft. of seven conductor and 15,000 ft. of monoconductor high temperature cables.

Two field tests have been conducted of the prototype temperature tool developed by Sandia and Gearhart-Owens, Inc. (GOI) which consisted of a printed circuit board version of the high temperature electronics design, a high temperature casing collar locator, and a GOI tool housing. The first test was conducted in the Hot Dry Rock Well, GT-2 of the Los Alamos Scientific Laboratory at the Jemez Mountains, NM.* Figure 3 presents the data from the test run conducted in this well.

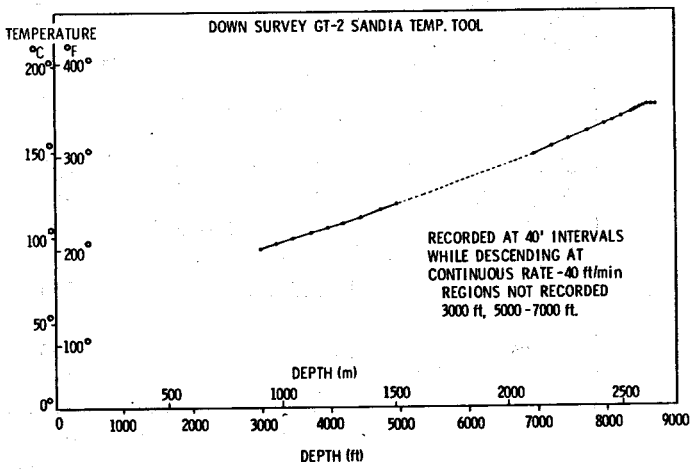


Figure 3

The second test was conducted in the COSO Geothermal Well CGEH-1 at the Chino Lake Naval Air Station, CA.* Data from this test run indicated a maximum borehole temperature of 189°C at 834 m. Performance of the instrument is considered excellent. Subsequent tests will be conducted to assess reliability and accuracy up to 275°C.

REFERENCES

1. A. F. Veneruso, "High Temperature Instrumentation," Proceedings of Well Testing Symposium, held at the Lawrence Berkeley Laboratories, October 1977.

2. L. E. Baker, R. P. Baker and R. L. Hughen, Report of the Geophysical Measurements in Geothermal Wells Workshop, Sandia Laboratories SAND75-0608, December 1975.

3. "Minutes of the First Meeting of the Geothermal Logging Steering Committee," Sandia Laboratories, June 28, 1977.

4. D. W. Palmer, B. L. Draper, J. D. McBrayer and K. R. White, Active Devices for High Temperature Microcircuitry, Sandia Laboratories, SAND77-1145, February 1978.

*The assistance of LASL personnel at GT-2 and Lawrence Berkeley Laboratories at CGEH-1 is gratefully acknowledged.

Geothermal Resources Council, TRANSACTIONS, Vol. 2 July 1978

PUMPING EXPERIENCE IN GEOTHERMAL WELLS AT EAST MESA

Robert V. Verity and Carl E. Fisher

Republic Geothermal, Inc.

ABSTRACT

Republic Geothermal, Inc. is presently carrying out extensive well testing in the East Mesa Field. The testing and development of geothermal well pumps is one important phase of this testing. The intent is two-fold: 1) to test the deliverability of the wells under high rate pumping conditions and 2) to guide the economic selection of well pumps for production to the future power plant. To date, two types of pumps have been tested, a lineshaft turbine pump and an electric submersible pump.

Testing Summary

The two types of pumps undergoing testing differ primarily in the means of transmitting power down the well to the pump. The lineshaft turbine is a downhole multistage turbine pump driven by a motor or engine on the surface through a rotating shaft. The pump is suspended from the surface on a pipe called the pump column through which fluids are pumped to the surface. Control of pump output is achieved by throttling the discharge at the surface or by rpm control with the prime mover or gearbox. The electric submersible is also a turbine pump; however, it is driven directly by a downhole motor(s). Power is transmitted to the motor(s) by an electric cable banded to the side of the pipe on which the pump and motor assembly is suspended. This pipe, or tubing, also conducts the pumped fluid to the surface. Control of pump output is achieved by throttling the discharge at the surface.

Table 1 is a summary of test conditions. The lineshaft turbine pump has been tested for 39 days and 27 days respectively in each of two wells. The pump completed both tests successfully but required extensive repairs after the first run. The electric submersible pump ran 4 days in one well, then failed, was pulled and repaired and is currently running in another well. In both cases the failures are attributable to factors which can be corrected and do not negate the basic ability of the systems to perform in the geothermal well environment.

In the case of the electric submersible, the principal question is whether or not the electric motors and cable will withstand the geothermal well temperatures for extended runs. The first test was terminated after 5 days by a nonelectrical failure, so the durability of the motors and cable in the high temperature environment has not been adequately tested. The failure was a bearing seizure in the seal assembly caused by excessive thrust loads when the producing rate fell below the recommended operating range for the pump.

The principal operating problems with the lineshaft turbine have been associated with the lineshaft bearings and bearing flush water. With results from two tests and competitor experience, the solutions to these problems appear to be virtually in hand. The pump is an enclosed lineshaft design of standard water well construction except that it has increased bearing clearances and carbon-filled Teflon lineshaft bearings. In the first test, in well No. 38-30, severe wear to the lineshaft, bearings and impellers resulted from the fact that initial bearing clearances were too small to offset thermal expansion and the filtered geothermal water used as bearing flush water, carried suspended solids and formed precipitates which abraded the bearings and shaft. In the East Mesa 56-30 installation, lineshaft bearing clearances were increased and a softened flush water filtered with 10-micron filters was used. Some carbonate scale was formed on the shaft because of hardness leakage through the softeners but bearing wear was minimal, i.e. 0.002-0.003 inches. Recent experience of another operator with water lubricated bronze bearings as well as the carbon-filled Teflon bearings has been good.

Technical Applicability of Pumping

In general, pumping is advantageous in a moderate temperature resource where a substantial gain in production over flashing flow can be achieved. Additional advantages of reduced well bore scaling and single-phase surface gathering lines may alone justify pumping in some projects.

East Mesa, a moderate temperature resource with a relatively low noncondensable gas content, is well suited to pumping production. Substantial production increases of 2-3 fold over flashing flow are economically achievable. Also, carbonate scale deposition, although not severe, has been observed to be primarily coincident with steam flash. Pumping with a surface discharge pressure above flash pressure appears to have virtually eliminated well bore scale deposition.

In order to evaluate the technical applicability of pumping to a hot water resource, one must

know the resource temperature, the free gas content and scaling tendency of the geothermal fluid as a function of pressure and the inflow performance of the wells, i.e., producing rate as a function of bottom-hole pressure. For acceptable pump life and efficiency, the pump intake must, of course, be set below the depth of steam flashing. Where substantial free noncondensable gas evolves below the flash point, the pump setting depth must be even deeper to avoid cavitation. Further, to avoid scaling in or above the pump, the surface discharge pressure must normally be above steam flash pressure, but in some cases much higher. Where a high surface discharge pressure is required, the energy requirement alone may rule out pumping as a means of controlling scale deposition.

The lineshaft turbine has the following specific advantages over the electric submersible pump:

1. It operates over a broader range of rates than electric submersibles at a given rpm. This advantage is further enhanced by the potential of rpm control at the surface which would allow matching well production to plant demand without wasteful throttling.
2. Its lower rpm probably makes it less susceptible to erosion than a submersible.
3. Its temperature capability is probably quite high since only metal parts are required downhole.

Its principal disadvantage is high capital cost for a deep-set pump due to the high cost of the column and lineshaft assembly.

The principal advantage of the electric submersible over the lineshaft turbine is that its capital cost is substantially lower for deep settings. Its principal disadvantages as mentioned above are susceptibility to erosion in the pump and its relatively narrow operating range. If sustained sand production is not a problem and if the pump capacity is properly matched to the well productivity, then these disadvantages become unimportant. The principal unknown is the ability of the electrical components to withstand the geothermal temperatures for long periods.

Based on published performance data, energy requirements for lineshaft turbine and submersible pumps are quite comparable. The goals of testing are to confirm the published performance in a geothermal application and to estimate the long-term repair and maintenance expense for the two types of pumps. The testing program is beginning to develop this information.

Pump Performance Monitoring

A nitrogen-filled "bubble" tube has been used to measure downhole pressure at the pump during production. (Refer to Figure 1.) These data are essential for monitoring pump performance and can be used to calculate the well productivity index (PI).

The first two attempts to install a bubble tube failed. In both these attempts, in East Mesa 38-30 and one previous well, a 1/4" O.D. stainless steel tube was banded to the outside of the lineshaft turbine pump column as it was being run in the well. In both cases, contact with the well casing crimped the tube and made it unusable. For the East Mesa 56-30 installation, the pump discharge head was modified so that a string of 1/4" line pipe could be run after the pump was installed. This procedure was successful.

In the submersible pump installations, a 1/8" O.D. stainless steel tube was banded to the outside of the 7" O.D. tubing on which the pump was run. The armored electrical cable (~1-1/4" O.D.) was then banded on beside the bubble tube, providing protection from contact with the well casing. Both installations were successful.

Surface bubble tube pressure readings, combined with normal flow rate, temperature and pressure data are used to calculate pump intake pressure, pump submergence, total pumping head and well PI. These calculations, assuming negligible kinetic energy effects, are outlined below.

Pump Intake Pressure

$$p_{in} = p_b + (z_{in} - z_b)\,\gamma_f$$

where

$$p_b = p_{bs} e^{\frac{G\,z_b}{53.3\ Tavg\ Z}} \qquad (1)$$

Pump Submergence

$$z_f = \frac{p_{bs} - p_a}{\gamma_f}$$

This assumes that the density of gas in the casing annulus equals that in the bubble tube. In fact, the densities of the two gases are probably not equal, but the calculation provides at least an estimate of submergence to protect the pump against cavitation.

Total Pumping Head

$$h = \frac{p_s - p_{in} + \Delta p_{f_c}}{\gamma_f} + z_p$$

Productivity Index

$$J = \frac{q}{p_e - p_{wf}} \qquad (2)$$

where

$$p_{wf} = p_{in} + \gamma_f\,(z_d - z_{in}) + \Delta p_{f_w}$$

Future Testing

Future pumping tests at East Mesa are aimed at testing the durability of lineshaft turbine and electric submersible pumps and projecting operating and maintenance expenses to guide the economic selection. Larger capactiy pumps capable of 800,000-900,000 lb/hr will be tested. One lineshaft turbine of this size is scheduled for delivery in June, 1978. If results with the present submersible pump are sufficiently encouraging, a larger submersible probably will be ordered and tested.

NOMENCLATURE

- G = gas gravity relative to air = 0.967 for nitrogen
- h = head, feet
- J = productivity index, lb/hr/psi
- p_a = casing annulus pressure at surface
- p_b = pressure at bottom of nitrogen-filled bubble tube, psia
- p_e = external boundary pressure in the reservoir, psia
- p_s = pump discharge pressure at surface, psia
- p_{in} = pump intake pressure, psia
- p_{bs} = surface bubble tube pressure, psia
- p_{wf} = bottom-hole flowing pressure at z_d, psia
- Δp_{f_c} = pressure loss due to friction in the column or tubing above the pump, psi
- Δp_{f_w} = pressure loss due to friction in the well casing below the pump, psi
- q = well producing rate, lb_m/hr
- T_{avg} = average temperature of nitrogen in bubble tube, ^{o}R. Assume equal to temperature of pumped fluid.
- z_b = depth to bottom of bubble tube, feet
- z_f = depth to liquid level, feet
- z_{in} = depth to pump intake, feet
- z_p = depth to top of pump, feet
- z_d = datum depth in producing interval
- Z = gas compressibility factor
- γ_f = static pressure gradient of the produced fluid at flowing conditions, psi/foot.

REFERENCES

1. Winkler, Herald Warren and Smith, Sydney, Camco Gas Lift Manual, Camco, Inc., Houston, Texas, p. 2-006.
2. Craft, B. C. and Hawkins, M. F., Applied Petroleum Reservoir Engineering, Prentice-Hall, Inc., Englewood Cliffs, N.J., p. 289.

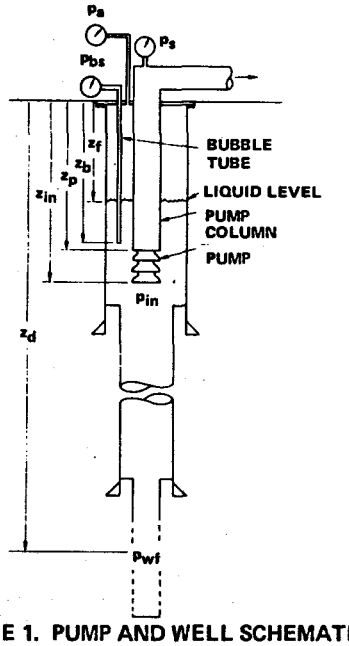


FIGURE 1. PUMP AND WELL SCHEMATIC

TABLE 1 - SUMMARY OF PUMPING TESTS

Well No.	Type of Pump	Pump Setting Depth (feet)(1)	Test Duration (days)	Range of Producing Rates (M lb/hr)	Optimum Capacity Range of Pump (M lb/hr)
38-30	lineshaft turbine	400	39	170-350	230-590(3)
56-30	lineshaft turbine	840	27	207-520	230-590(3)
78-30	electric submersible	1203	4	276-440	320-515(4)
16-29	electric submersible	1319	7+(2)	320-440	320-515(4)

(1) Depth from surface to top of pump.
(2) Test in progress
(3) Range for pump efficiency $\geq$ 70%
(4) Range in which thrust loads are properly balanced in pump

MUD SOLIDS CONTROL FOR MINIMUM LIQUID DISCHARGE DEMONSTRATED ON WYOMING WELL -- A POSSIBLE APPLICATION FOR GEOTHERMAL DRILLING

Don Vesely

NL Baroid

ABSTRACT

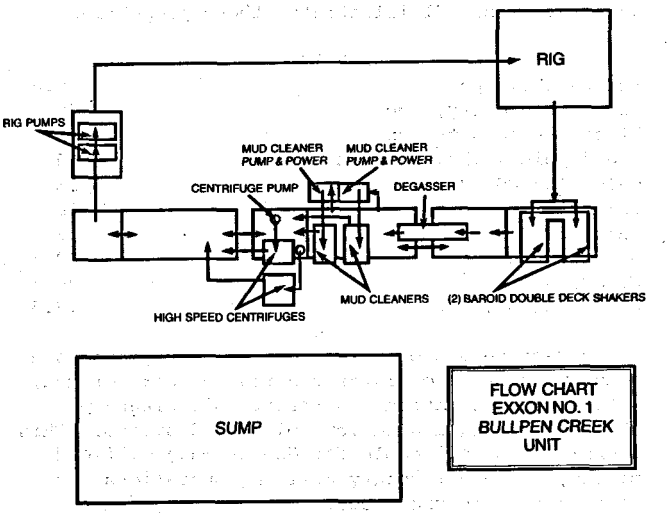
A 12,500 foot well was drilled in Wyoming with virtually no liquid discharge (jetting). This article explains how the solids control equipment was configured to achieve this objective and gives technical information regarding the percent solids removed by each piece of equipment.

Exxon Company, U.S.A. has completed its Bullpen Creek Unit #1 in Lincoln County, Wyoming. In March 1976 Exxon invited several service companies to submit drilling mud and solids processing programs for a wildcat well in southwestern Wyoming. Baroid was awarded the drilling mud, solids control equipment, and mud logging services on this project, which successfully utilized a closed mud system to a total depth of 12,500 feet. The Bullpen Creek unit was drilled by Parker Drilling Company's Rig 116 which was designated a special Bicentennial rig.

The mud processing equipment specification was a joint effort of Exxon Company, U.S.A., Exxon Production Research Company, and Baroid personnel in Denver and Houston. The unique design objective of the solids processing system was to minimize liquid discharge and, ultimately, to develop a closed mud system with dry solids discharge. Field research on this wildcat was conducted to provide insight and technology to handle ecological problems, reduce expense of reserve pit clean-up, and reduce water consumption and mud cost. The closed mud system used on the Bullpen Creek well would have application in areas such as the Beaufort Sea, the North Sea, or any other location where stringent regulations prohibit the discharge of solids and liquids, and where transporation of these materials from the rig site is very costly.

The Bullpen Creek solids control system utilized two specially manifolded BAROID DOUBLE DECK SHAKERS equipped with 50 mesh over 100 mesh screens to effect primary solids removal. Two BAROID MUD CLEANERS were utilized as an intermediate step in the control process. These mud cleaners which incorporate desilting and shaking operations, were equipped with 150 mesh screens to allow discarded fluid to be reclaimed and added back to the mud system.

The final solid-liquid separation stage was accomplished by the use of two high speed cylindrical contour shaped centrifuges operating at 2500-3000 RPM. This equipment combined with the DOUBLE DECK SHAKERS and MUD CLEANERS comprised the entire solids removal system.



Discarded solids from each piece of equipment were collected in specially prepared steel bins and transported to the reserve pit with a forklift.

A series of special tests and measurements was performed daily to monitor such variables as flow rate and density into and out of the equipment, weight of solids discarded per minute, and percentage of liquid associated with the discarded solids. Water and chemical additions were monitored to obtain a material balance. Table I shows the results of these field tests.

TABLE I

Time Interval	60 days
Depth Interval	1,044 to 9,212 feet
Calc. lb of drill solids (theoretical)	1,130,000
Solids removed by Shakers, lb	563,000(47%)
Solids removed by Mud Cleaners, lb	292,000(24%)
Solids removed by Centrifuges, lb	334,000(29%)
Total solids removed, lb	1,189,000
Estimated 60,000 lb bentonite equivalent removed by centrifuges (based on the Methylene Blue Test)	
Water addition	800 bbl

The percentage of solids removed from each piece of equipment did not vary appreciably during the complete test. Between May 20 and May 31, 1976, it is estimated that 5,800 barrels of mud would have been jetted to the sump to remove the same amount of solids discarded by the mud cleaners and centrifuges. To maintain the mud density of 8.8 ppg during this time interval, approximately 470 bbl of mud would have been built each day.

The mud system used on the Bullpen Creek unit included AQUAGEL Bentonite and CARBONOX^{R} Mud Thinner Mud properties at 12,383 feet were good in spite of the fact that no mud was jetted and the reserve pit was dry. Table II illustrates these properties.

TABLE II

Mud Weight, ppg	8.8
Funnel viscosity, sec	35
Plastic viscosity, cp	5
Yield point, lb/100 sq ft	4
Gels, lb/100 sq ft	6/16
Filtrate, ML/30 min	26
Cake, 32nd in	2
Solids, 0/0	3.7
Water, 0/0	96.3
Clay content, ppb	13.5

The effective use of solids control equipment is a means whereby an operator can reduce costs of mud, water, transportation and reserve pit clean-up, while obtaining a good low solids mud system. This technique is applicable for Geothermal, oilfield, mining, and other rotary drilling operations. It is essential to the success of such a system to have conscientious, able personnel present to supervise the operation. Such personnel were responsible to a great degree for the effectiveness of the closed mud system at Bullpen Creek.

Acknowledgements to Exxon Company, U.S.A., and Exxon Production Research Company for data used in this article.

THE AUTHOR

Don Vesely is Regional Technical Services Manager for NL Baroid's Western Region. He graduated from the University of Texas in 1965 with a degree in Mathematics. Vesely worked as a Sales Engineer on the Texas Gulf Coast and has been a Regional Engineer in Midland and Denver. Also, he was District Manager in Vernal, Utah.

Geothermal Resources Council, TRANSACTIONS, Vol. 2 July 1978

GEOTHERMAL FLUID INVESTIGATIONS AT REPUBLIC'S EAST MESA TEST SITE

by O.J. Vetter*, D.A. Campbell** and M.J. Walker**

* VETTER RESEARCH, COSTA MESA, CALIFORNIA

** REPUBLIC GEOTHERMAL, INC., SANTA FE SPRINGS, CALIFORNIA

ABSTRACT

This paper summarizes some of the experiments and tests performed thus far in the northern part of the East Mesa Geothermal Field operated by REPUBLIC GEOTHERMAL, INC. (RGI). The investigations described concern only the fluid characteristics pertinent to future power plant design and operation. Test facilities including test loops, fluid composition, scaling tendencies, pH control experiments and gas behavior ("noncondensables") are briefly reviewed. The data available thus far indicate that the geothermal fluids will present no significant technical problems in a conventional flashed steam power cycle.

1.0 INTRODUCTION

REPUBLIC GEOTHERMAL, INC. is currently conducting extensive test and evaluation work at its East Mesa site. A 48 Mw (net) power plant is now in the final design stage. The current work includes reservoir evaluation as well as a study of the fluid characteristics under simulated power plant conditions.

The present paper describes the fluid study in a summary form. Three additional detailed papers are being prepared under a Department of Energy (DOE) contract. These three reports[1,2,3] will be published within the next few months.

The study was performed jointly by RGI and VETTER RESEARCH. BATTELLE PNL[4] provided valuable support for some later phases of the study with expertise, manpower and instrumentation.

2.0 TEST OBJECTIVES

The main objectives of the tests were to: (1) Determine if there would be problems in a power plant due to scale formation; (2) Predict any problems in the planned flashed steam plant which might be caused by noncondensables; and (3) Suggest technically and economically feasible ways and means to overcome any scale and/or noncondensable problems indicated.

In order to achieve the above goals, it was necessary to conduct a comprehensive study of the geothermal fluids under actual field conditions. This required the design and construction of equipment at the well sites that allowed simulation of the flow conditions encountered in an actual power plant and also, measurements of the pertinent properties and characteristics of the fluids. Of particular interest were the fluid chemistry and phase separation data (e.g., the formation of noncondensables) at different temperature, pressure and flow conditions. In addition, the test equipment had to be designed so that it would not interfere with other concurrent field testing.

3.0 TEST LOOPS

In most geothermal testing, the critical fluid characteristics are supposedly determined by utilizing side streams. The main flow line is tapped and a small stream of fluid is diverted into a "test device" to evaluate a number of characteristics such as corrosion or scaling tendencies. It is then concluded that the reactions observed in the device can be related to similar reactions in the main stream. The general validity of these methods is questionable for the following reasons: (1) It is impossible - in most cases - to draw a representative portion of the fluid into the side stream. This would be possible only if the fluid in the main line is homogeneous, i.e., no separate phases are present (suspended particles, liquid drops, and/or gas bubbles); (2) The flow characteristics of the fluids in the main stream and those in the side stream may be different, leading to a change of the fluid properties; and, finally, (3) The devices themselves may not allow the proper evaluation of fluid properties for an actual power plant. For example, scaling and corrosion properties are different in the devices than they are in various components of a power plant. It is doubtful that even relative comparisons yield valid data, because it is almost impossible to duplicate all the pertinent flow conditions (thermodynamic and hydrodynamic) in such devices.

Pilot plants of any size offer similar problems in investigating fluid characteristics. In addition, a full-fledged pilot plant is much too expensive to build if valid data on the fluid characteristics are not available in advance.

In order to overcome many of these problems,

it was decided to add test loops to the standard test facilities. As shown in Figure 1 the test loop is simply an attachment to the flow line leading from the production well to the separator. This device, constructed of common valves and pipe fittings, allows the diversion or by-pass of the total geothermal fluid stream at various flow rates into an area where accurate pressure, temperature and fluid chemistry measurements can be obtained without affecting the well flow. Orifice plates of predetermined size are inserted at various points in the loop in order to simulate the desired pressure or temperature conditions. Valves are provided which allow the loop to be isolated from the well stream for modification, cleaning, and visual inspection.

Such facilities have a number of advantages in that: (1) Their cost of construction is relatively low: (2) They can be run with little extra expense; (3) They are portable and can be moved easily from well to well; (4) They can be operated without interfering with other reservoir or well test work; (5) They can simulate almost all operations of future power plants using flashed steam power cycles; (6) They can easily be adapted for evaluation of other power plant cycles; (7) They can be utilized to investigate scaling and corrosion; (8) They allow evaluation of the effects of fluid alteration by the addition of chemicals (continuous or batch) at any temperature and pressure; (9) They permit obtaining information on the fluid properties at various temperatures and pressures in order to extrapolate the measured data to reservoir conditions (producer or injector); (10) They can be used for evaluation work regarding mineral recovery; and, finally (11) They offer a means of evaluating various types of instrumentation and process control equipment under field conditons.

4.0 TEST FACILITY INSTRUMENTATION

Conventional liquid filled bourdon tube pressure gauges and bimetallic thermometers were used throughout the test loop. Two orifice meters and an automatic level controller are used to measure and control flow rates of the fluids in the liquid and steam exit lines of the separator. This type of instrumentation is generally adequate for evaluation of the data and control of the test facility. However, the accuracy of the gauges is inadequate for some purposes. During the later phases of testing, additional instrumentation was supplied by BATTELLE PNL; e.g., thermoelements, pressure transducers, conductivity cells and pH monitors. The signals from each of these instruments were fed into an automatic data logger. The conductivity cells need further improvement, but the other instrumentation provided valuable data.

5.0 FLUID COMPOSITION

Samples of fluids were collected from the test facility at various times and locations using a variety of sampling methods. These samples were collected in plastic bottles, glass containers and/or stainless steel bombs, with and without, sample preservation. Thousands of samples were analyzed for a large number of chemical constituents by VETTER RESEARCH. Instrumental methods (various types of AA, UV/VIS, GC) and wet procedures were used. The volume of the gathered data prohibits discussion in detail in this summary.

The composition of the unflashed liquid varies slightly from well to well. A typical example is given in Table I.

TABLE I
COMPOSITION OF UNFLASHED GEOTHERMAL WATER
(Well No. 38-30, September 1977)

CONSTITUENT	MG/LITER	CONSTITUENT	MG/LITER
Ag	<0.06	Ba	<0.20
Pb	<0.50	Al	<0.30
Mn	<0.06	Mg	0.06
Zn	0.50	SiO_2	172.0
Hg	0.0008	K	30.0
Fe	0.20	Na	660.0
Cd	<0.03	Ca	2.50
Li	0.92	Cl	535.0
Sr	0.80	TDS	1804.0
B	1.50		

Carbon dioxide constitutes 90± percent of the noncondensables present in the vapor phase. The balance is nitrogen, methane and traces of other gases. No H_2S has been detected. The CO_2 concentration in the single phase water is on the order of 1000 mg/liter. After flashing, noncondensables amount to approximately 0.5 percent of the vapor phase.

6.0 SCALING TENDENCY

The scaling tendency of the fluid is low, but could cause problems in a power plant if not handled properly. Two types of scale were found, calcium carbonate and silica. Approximately 1.5 mg $CaCO_3$ per liter of unflashed water can form. No measurable amounts of $CaCO_3$ are found if the pressure of the fluid is kept above 60 psig, even though a large percentage of the carbon dioxide is already flashed at this pressure. The majority of the $CaCO_3$ scale (more than 50 percent) is formed at pressures below 25 psig. The $CaCO_3$ deposited at these low pressures is a very fluffy porous material; whereas, the $CaCO_3$ formed between 25 and 60 psig is dense and exhibits well formed crystals. The silica forms in measureable amounts below pressures of 25 psig and is masked by the $CaCO_3$ scale. Approximately 1 percent SiO_2 is dispersed in the fluffy $CaCO_3$ scale. No other type of scale has been detected in the test facilities.

7.0 pH CONTROL OF SCALING

A major effort was made to investigate the feasibility of controlling the pH by continuous

injection of acid at various production rates. A pH of approximately 6.0 is considered sufficient to keep all the calcium carbonate in solution. A pH of 4.5 or lower may be sufficient to retard (not prevent) the silica precipitation. Figure 2 shows the effect of acid (HCl) addition on the water pH at approximately 25 psig pressure. This figure clearly indicates that the buffer capacity of this water - even at 25 psig - is still too high to make the continuous pH control with HCl an economical method. These pH control experiments proved that most of the acid is utilized to titrate the bicarbonate under line pressure, or, in other words, the first and major portion of the acid drives off the CO_2 instead of lowering the pH.

It should not be concluded that all fluids behave similarly when acid is added. Fluids having a different composition may act differently. These experiments show, however, that effective and economical pH control by continuous injection of acid is not possible at East Mesa.

In contrast, a batch addition of acid can be used to remove the formed $CaCO_3$ without a shutdown of the facilities. Small slugs of acid applied at regular intervals proved to be a much more economical method of scale control. The power plant design will incorporate appropriate provisions to allow for batch acid treatment if it proves to be the preferred method of control.

The cost of acid required to maintain scale-free lines and equipment by batch acid treatment would be less than 0.5 mills/kwh. This is a very small percentage of total plant operating costs and would be acceptable. Concurrently, high temperature scale inhibitors are being tested which may control scale at a cost even less than the batch acid treatment method. By contrast, continuous injection of acid, if it were feasible, would cost on the order of 33 mills/kwh.

8.0 CO_2 VENTING

Another problem in a flashed steam power cycle may be caused by the noncondensables. Gases (mainly CO_2, methane and nitrogen) will break out of solution and enter the turbines and condensers with the steam. The more gas there is, the more costly the power plant becomes due to the larger capital investment and power requirements for vacuum pumps and/or steam ejectors. The actual East Mesa plant design will utilize vacuum pumps to handle the relatively small amount of CO_2.

Field experiments also show that the CO_2 can be handled in another fairly simple and economical way. The main portion of all gases may be vented from the geothermal fluids before these fluids enter the first steam flash stage. Computer modeling of the East Mesa fluids show that almost 50 percent of the CO_2 (capable of forming non-condensables) can be vented by pressure decreases before a 0.1 percent steam flash is experienced. Thus, major portions of the gases can be kept from entering the turbines and condensers. This method of CO_2 venting is favored by economics in fields with high CO_2 content. At East Mesa the more straight forward use of vacuum pumps is preferred because of the low CO_2 content.

9.0 MAJOR CONCLUSIONS

It can be concluded from the collected data that: (1) The liquid in the reservoir is low in TDS and is not saturated with carbon dioxide; (2) Calcium carbonate and small amounts of silica scale can occur in surface installations unless preventive action is taken; (3) No scale problems are expected in pumped producing wells; (4) The boron, H_2S and heavy metal ion content are too low to cause any serious environmental or operational problems; (5) No significant corrosion will occur if oxygen is kept out of the system; (6) Continuous pH control of the fluids by the addition of acid to prevent scale deposition is not economically feasible; (7) Removal of deposited $CaCO_3$ at regular intervals by batch acid treatment is economically feasible; (8) Scale control by chemical inhibitors may be a viable alternative to batch acid treatment; (9) Venting of the CO_2 before steam flash occurs can prevent a major portion of the noncondensables from entering the turbines and is feasible in fields with high CO_2 content; (10) The test facilities with the test loops proved to be an excellent means of studying the behavior of the geothermal fluid.

10.0 REFERENCES

1. O.J. Vetter and V. Kandarpa, "Study of CO_2 Behavior in Geothermal Operations." DOE report being prepared.

2. O.J. Vetter and M.J. Walker, "Test Loops for Geothermal Brines." DOE report being prepared.

3. O.J. Vetter and D.A. Campbell, "pH Control of Geothermal Brines." DOE report being prepared.

4. Sampling and Analysis Methods for Geothermal Fluids and Gases. BATTELLE PNL. Prime contract with DOE (DGE); Contract Number EY-76-C-06-1830.

11.0 ACKNOWLEDGEMENT

We wish to express our thanks to RGI, BATTELLE PNL and the U.S. Department of Energy (DGE) for their support of this work.

Figure 1

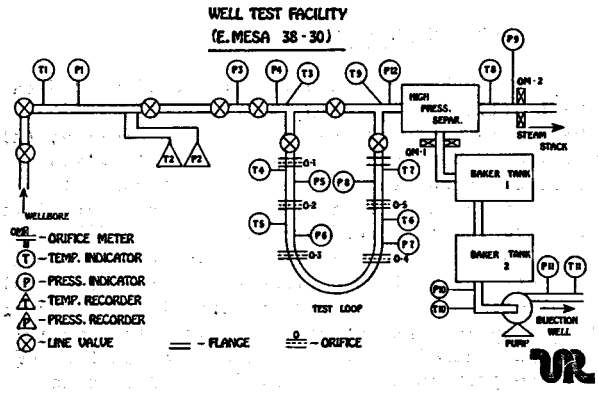
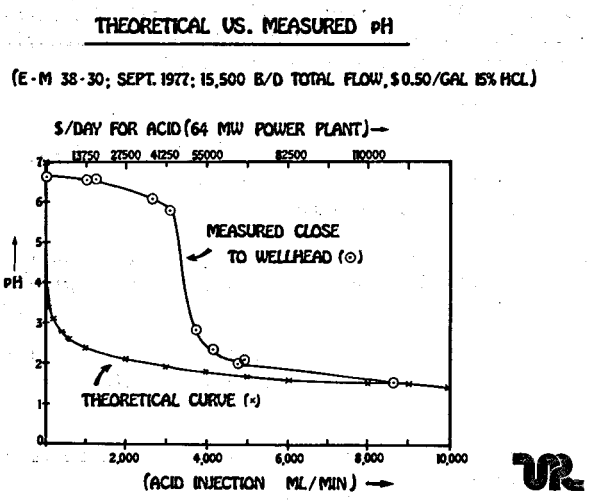


Figure 2



Geothermal Resources Council, TRANSACTIONS, Vol. 2 July 1978

SAMPLING IN GEOTHERMAL OPERATIONS-PHILOSOPHY AND REALITY

O. Vetter*, E. Woodruff**, J. Watson**, D. Shannon**

* VETTER RESEARCH, 3189C Airway Avenue, Costa Mesa, California 92626

**BATTELLE PACIFIC NORTHWEST LABORATORIES, Richland, Washington 99352

1.0 INTRODUCTION

The sampling and analysis (chemical or other) of geothermal fluids, i.e., liquids, gases and suspended particles, is being done today by different investigators using methods of their own choice. It is a wide-spread opinion among chemists and engineers involved in geothermal operations that sampling and analysis is filled with "pitfalls for the unwary". In the majority of the cases, the analytical numbers reported are not truly representative of the geothermal systems. Sampling problems are compounded by two-phase flows (or even flows with more than two phases present), gas flashing (and/or losses), and chemical reaction and precipitation processes occuring during sampling.

The problem of sampling and analyzing geothermal fluids is further compounded by the fact that many wells produce fluids which can change their composition at various times as a function of changing reservoir and operational conditions.[1]

It seems clear that unless positive action is taken, the literature of geothermal energy will soon be filled with published chemical analyses of dubious quality at best.

Recent comprehensive studies on the chemical characterization of geothermal brines[2] revealed that the reported data on a large number of brines can not be compared due to the contradictions between data reported by different authors and the lack of details describing when, where and how the samples were taken in any given instance. Battelle PNL[3] is presently undertaking a new and comprehensive study of sampling and analytical methods used in geothermal operations. This study does not involve sampling for suspended or deposited solids.

What is needed is an assessment of the state-of-the-art, a selection of candidate methods and a verification of various sampling procedures.

This paper describes the reasoning behind Battelle's efforts. The final goal of this study is to evaluate the possibility of standardizing the sampling methods in geothermal operations.

Solutions to sampling problems in any geothermal field play a major role in solving field problems. A large variety of field operations are based on data retrieved from the analysis of specific samples. Therefore, the importance of sampling procedures can not be over-emphasized. One can say - without exaggeration - that the entire investment of a geothermal field, its numerous stages of development and operation will depend on the proper collection and analyses of samples.

The need for a manual listing the possible candidate methods for sampling and containing a critical evaluation of the various methods together with suggestions for future developments seems to be unquestionable. This need is also indicated by various attempts of industry and government supported organizations to gather and collect the ideas on sampling procedures used or suggested by all parties interested or involved in geothermal operations.[4]

One must also be aware of the fact that a number of geothermal fluid characteristics can not be determined through the examination of samples collected in the system. These fluid characteristics must be measured in situ.[2]

2.0 REASONS AND OBJECTIVES FOR SAMPLING

Unfortunately, there are many reasons and motivations for collecting and analyzing samples in geothermal operations at various locations and times in the field. Table I lists some typical examples of objectives and reasons for sampling. Table I is not an exhaustive treatment of the subject; there can be many more, sometimes very specific reasons to collect samples.

Arbitrarily, we divided the type of samples into three major groups:

1) Samples of Reservoir Fluids

2) Samples of Wellbore Fluids

3) Samples in Surface Equipment

Battelle PNL's present contract calls for a study and evaluation of the numerous methods used in todays geothermal fields. Only the third sample category (surface operations) is presently considered. However, the reasons and objectives for collecting samples and many of the basic sampling problems are similar in all three catagories.

The large number of reasons or objectives for collecting samples and the numerous technical problems encountered during any sampling process create a complicated situation: None of the present sampling methods fullfills the need of all objectives: There is no ideal sampling procedure. In addition, only a very few methods take all the sampling problems into proper account.

The present and future sampling methods could be divided into two major groups:

1) Standardized Methods

2) Special Methods

Both groups must consider the objectives of the sampling and the special properties and problems of geothermal fluids at the location and time of sampling.

3.0 STANDARDIZED METHODS

No standardized sampling or analytical methods exist in the geothermal industry despite the apparently strong need for standardizing various sampling methods. Battelle PNL's recent studies and field experiments indicate that some of the more frequently used methods and some of the newly developed or conceived methods could be raised to the rank of a standardized method. One of the suggestions to be considered could be the standardizing of components used in various sampling methods instead of standardizing entire methods. The components could be combined into various equipment (component) arrangements to fullfill the need for the large number of sample types to be collected. The components as well as the arrangements could be standardized.

It is felt that some of the more frequently used components could fall into these catagories: 1) Hardware used to connect sampling devices to field equipment, 2) Stationary and traversing sample probes, 3) Connectors to combine components, 4) Cooling coils, 5) Physical separators, 6) Chemical separators, 7) Components measuring the critical parameters of fluids in sampling devices 8) Components controlling the critical parameters of fluids during sampling, 9) Sample containers used as component, 10) Storing and shipping containers, 11) Sample treatment, preservations, shipping and storing.

Each of these components must handle and control certain parameters of the sampled fluid during the sampling process. In addition, each component will offer problems of its own and can have a serious effect on the composition of the final sample.

These parameters and problems for a component system are described by using the cooling coils as an example (See Table II).

4.0 SPECIAL SAMPLING METHODS

All methods presently being used must be considered "special sampling methods" because of a total lack of standardized methods. Many methods being used have major "flaws" and are in need of changes. In addition, there are a number of objectives for which no sampling methods have been described in the open literature.

We believe that a large number of special methods will be used even after the development of standardized methods. The reasons are:

1) The objectives are too manifold to allow standardization of all methods (components or arrangements).
2) Quite often, the sampling methods may require too costly instrumentation and/or the collected data may be an "overkill" for a specific objective. Therefore, a number of different methods should be developed for similar purposes or objectives to allow more cost-effective collecting and analyzing of samples. There is already a considerable complaint in the industry because of the exorbitant cost of some sampling and analytical methods.

5.0 MAJOR PROBLEMS ENCOUNTERED DURING SAMPLING

There are two major problems encountered during sampling in geothermal operations: (1) The fluids to be sampled may behave in an absolutely unexpected or unknown way and, therefore, the wrong approach to the sampling may be chosen, (2) the entire sampling method or certain components of the sampling equipment does not take into account the very special properties of the fluids within the sampling equipment itself.

Basically, both problems have the same effect: The geothermal fluids will change their chemical and physical behavior if any of the thermodynamic or kinetic conditions are changed. Sampling per se, will change both sets of conditions in most cases. Therefore, the sampling itself will exhibit properties quite different from those of the sampled fluid. For example, the fluid to be sampled may be steam, whereas, the actually retrieved sample may be a liquid and a gas.

The basic differences between actual sample and sampled fluid caused by the process of sampling itself quite often need an elaborate and sophisticated interpretation of the final analytical data. The lack of reporting the sampling methods and conditions in papers listing analytical data are one of the two major reasons for the questionable reliability of the information.

The other reason lies with the flow of the fluids in geothermal installations. Drawing a sample from a truely single phase fluid into a sample port is fairly easy if detrimental phase changes

are avoided. However, many fluids in these installation represent two or more phase systems which can also be multicomponent systems. Quite often, it is required to sample these multiphase systems. In this case, it may become extremely difficult to draw a "representative" sample. Quite often, the flow regimes at the sample port are not even known. We may encounter mist flow, bubble flow, slug flow, annular flow, etc. Without knowing the flow regime it becomes impossible to collect a "representative" sample. The only conceivable methods for two-phase sampling seem to be: 1) Proper instrumentation is installed in the lines to allow the precise measuring or calculation of the flow profile or 2) Various samples are drawn from the cross-sectional area of the fluid line and analyzed separately. This latter information can than be used to calculate either the flow profile itself or to calculate the composition of the "recombined" fluid.

Battelle PNL's effort is pointed in the direction of clarifing all these problems comparing presently used or suggested sampling methods for single-phase and two-phase geothermal fluids in the East Mesa area. The main objectives are 1) To point out the problems encountered during the comparison of the sampling methods and 2) To suggest the development of more appropriate sampling methods to properly characterize the liquids and gases that flow in a geothermal operation.

REFERENCES

1. O.J. Vetter, "Some Basic Chemical Problems in Geothermal Operations", Workshop on Thermodynamics and Electrochemistry, ERDA Workshop Recommending Future Direction in Energy Related Basic Materials Research, Argonne National Laboratory, May 18 - 20, 1977.

2. J.W. Cobble, V. Bertucci, S.C. Creason, H.P. Eugster, L.B. Rogers, M. Sato and O.J. Vetter, "Assessment of the Characterization (In Situ-Downhole) of Geothermal Brines", National Academy of Sciences, Report No. NMAB 344, January, 1978.

3. D.W. Shannon, E.M. Woodruff, J.C. Watson, J.G. Douglas, S.J. Thompson and R.J. Jerne, "Sampling and Analysis Methods for Geothermal Fluids and Gases", U.S. Department of Energy, Division of Geothermal Energy, Utilization Branch, Contract No. EY-76-C-06-1830 to Battelle Pacific Northwest Laboratories.

4. Proceedings of EPA Conference on "Sampling in Geothermal Operations, February 1977, Las Vegas, Nevada.

Table I. TYPICAL EXAMPLES OF REASONS AND OBJECTIVES FOR TAKING SAMPLES IN GEOTHERMAL OPERATIONS.

OBJECTIVE-PROFESSION	REASON
Formation Fluids	
- Geologist	Geology of Area and/or Reservoir
- Geochemist	Geothermometry
- Reservoir Engineer	Reservoir Evaluation and Characteristics
- Drilling Engineer	Mud Design and Drilling Method Wellbore Completion
- Production Engineer	Wellbore Equipment Design
Wellbore Fluids	
- Production Engineer	Surface Equipment Design Well/Surface Equipment Monitoring Reservoir and/or Wellbore Stimulation
Surface Equipment Fluids	
- Production Engineer	Reservoir and/or wellbore Stimulation
- Power Plant Engineer	Power Plant Design
- Environmental Engineer	Emission Control
- Field Engineer	Reinjection
- Reservoir Engineer	Reinjection

Table II. COOLING COILS AS A COMPONENT IN SAMPLING DEVICES.

A. PARAMETERS:
   1. Geometry
      (A) Tubing (Diameters, Length)
      (B) Coil (Diameters, Shape)
      (C) Orientation of Coil
   2. Material
   3. Temperature
   4. Flow Rate of Fluids

B. PROBLEMS:
   1. Slug Flow of Fluids (e.g., Gas-Liquid)
   2. Slip of Fluids in Horizontal Parts
   3. Condensation Profiles
   4. Time Delay Between Line Fluid and Sample
   5. Averaging of Composition
   6. Deposition of Scale
   7. Corrosion and Corrosion Products

MAGNETOTELLURIC OBSERVATIONS AT THE ROOSEVELT HOT SPRINGS KGRA AND MINERAL MTS, UTAH

Philip E. Wannamaker, William R. Sill, and Stanley H. Ward

Dept. of Geology and Geophysics, University of Utah

Twenty-five magnetotelluric soundings in the Roosevelt Hot Springs area indicate a very complicated, three-dimensional electrical environment. The assembly of a profile of one-dimensional transverse electric inversion interpretations yields a calculated 2-D apparent resistivity-frequency pseudosection far removed from the observed data. Trial-and-error modeling improves the fit only a little. The most notable difficulty, the presence in both TE and TM pseudosections of pronounced contrasts in ρ_a persisting to the lowest observed frequency, may be explained by the discontinuities in electric field that are found for all directions of wave excitation for 3-D geometries.

The estimation of electrical strike is also difficult in the 3-D case since the total fields do not decompose into the two principal excitation modes. Whenever a plane of symmetry exists, the estimated electrical strike will be normal to it; otherwise an oblique estimation results. The observed consistency of strike estimation at Roosevelt is likely due to the gross, elongate, resistive horst structure of the Mineral Mts. in surrounding conductive valley fill.

Mode identification and the effects of near-surface 3D inhomogeneities pose potential major limitations to the magnetotelluric method.

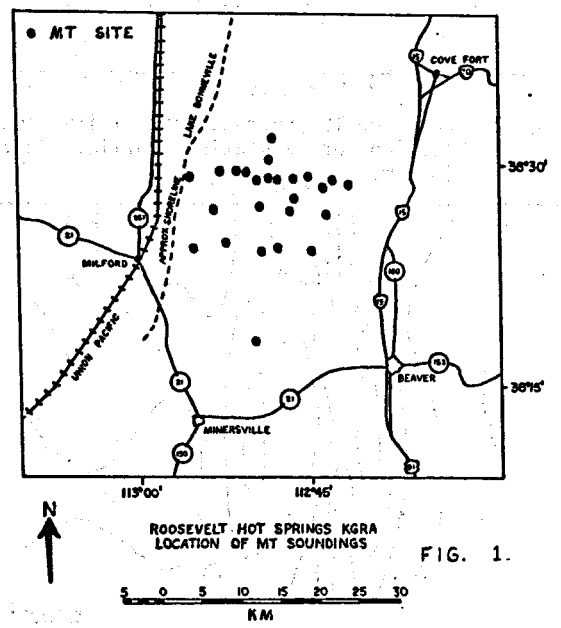


FIG. 1.

Previous active source electrical and electromagnetic measurements show a range of interpreted true resistivities spanning 3 to 10^3 Ω-m at the Roosevelt Hot Springs KGRA. Contour pattern lows of first separation dipole-dipole apparent resistivity values are roughly coincident with highs of near-surface thermal gradient measurements. During the summer of 1976, twenty-five magnetotelluric (MT) soundings were obtained in the vicinity of the Roosevelt Hot Springs in an attempt to describe any possible deep convective heat source for the conductive hydrothermal system (see Figure 1).

Sources of electrical conductivity to consider are electrolytic conduction through pore passages, surface conduction along mineral surfaces, thermally activated semiconduction, and electrolytic conduction in wet, partial melts. The Basin and Range tectonic province conductivity model of W. F. Brace in the AGU Monograph 14 (1971) is used as a rough standard by which to judge the observed MT results. Petrological work on the Mineral Mts. rhyolitic volcanics indicated substantial magma chambers existed at depths of 1.6 to 12 kms as little as 0.5 m.y. ago. Any present-day partially molten magmas may be detected electrically.

As is the standard procedure, 1-D layered and continuous inversions of the transverse electric (TE) data for several individual sites were performed. In the conductive Milford Valley graben, values of apparent resistivity drop to 0.10 Ω-m for the lowest frequencies of observation and interpreted true resistivities are low by a factor of 5 to 10 while interface depths are too shallow by a factor of 2 or more.

Multifrequency apparent resistivity data for a profile of 12 MT stations is presented in the form of frequency-distance pseudosections for both TE and TM modes of wave excitation (see Figs. 2 and 3). The major difference between the two pseudosections involves the overall level of ρ_a values. Except perhaps for the westernmost stations on conductive valley fill, the TM values generally exceed those of TE by a factor of about ten. One important common characteristic is the presence of pronounced, station-to-station apparent resistivity contrasts enduring to the lowest frequency of observation at two of the sites. For use as an interpretational starting point, the best-fit discrete-layer inversion results for each of the twelve stations in the profile were stitched together to form a crude,

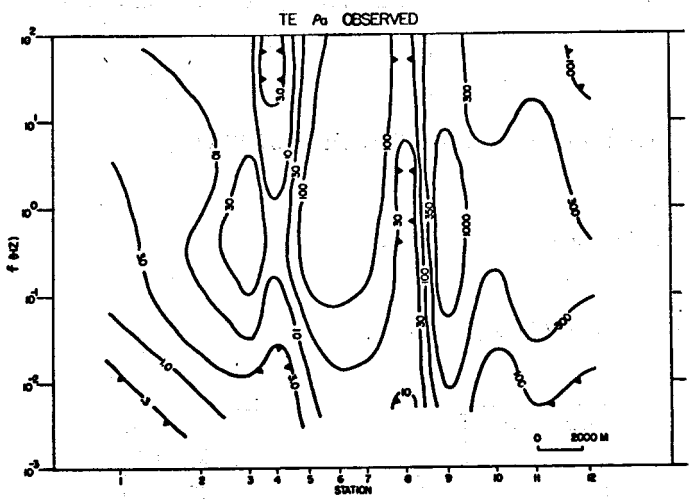


Fig. 2: Observed TE apparent resistivity pseudosection for 12-station profile. Contours in Ω-m.

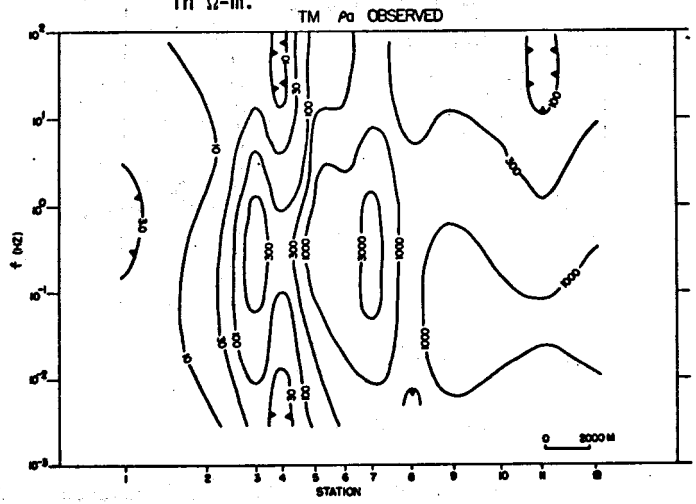


Fig. 3: Observed TM apparent resistivity pseudosection for 12-station profile. Contours in Ω-m.

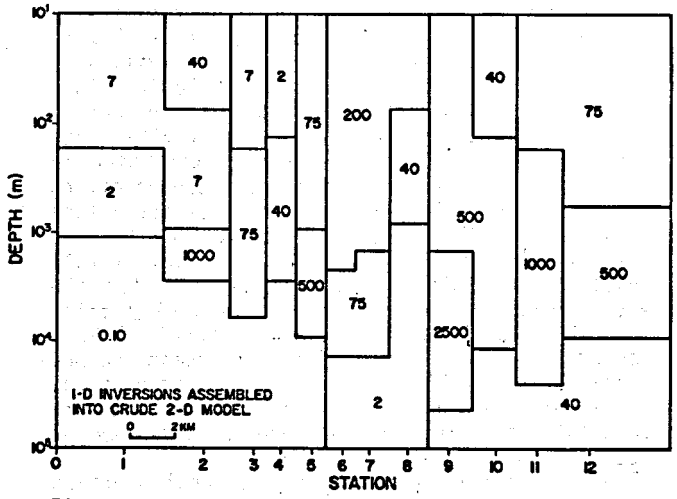


Fig. 4: Discrete-layer, 1-D inversion stitch model for 12-station profile. Values in Ω-m.

initial 2-D estimate of the resistivity structure (see Fig. 4). The computed TE, 2-D pseudosection for this ensemble matches the observed ρ_a section only for the stations in the conductive graben and for the very high frequency values for the rest of the stations (Fig. 5). Trial-and-error attempts at improving the basic model yield an adequate fit only down to about 0.5 Hz whereafter the degeneration of agreement is marked (see Figs. 6 and 7). A TM pseudosection calculation for the 1-D assembly agrees very well with the observed TE contours however TE modelled does not agree whatsoever with TM observed so a mere mode misidentification is not the answer (Fig. 8).

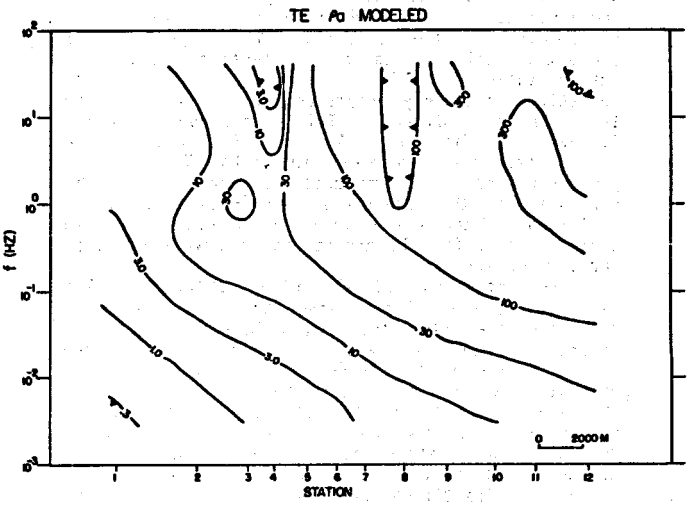


Fig. 5: Computed, 2-D, TE pseudosection for 1-D stitch model. Contours in Ω-m.

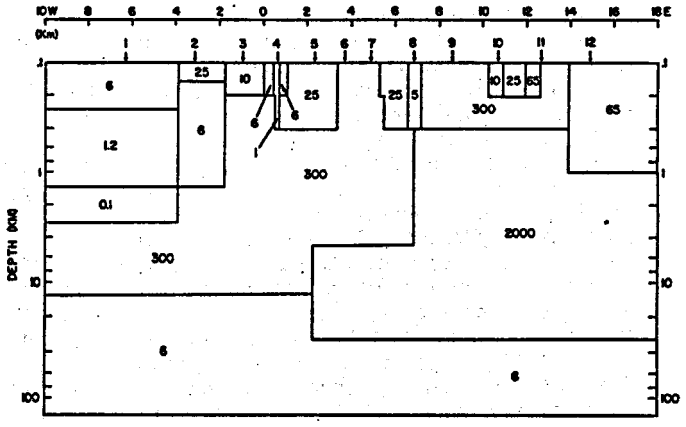


Fig. 7: Best-fit TE resistivity model for 12-station profile. Values in Ω-m.

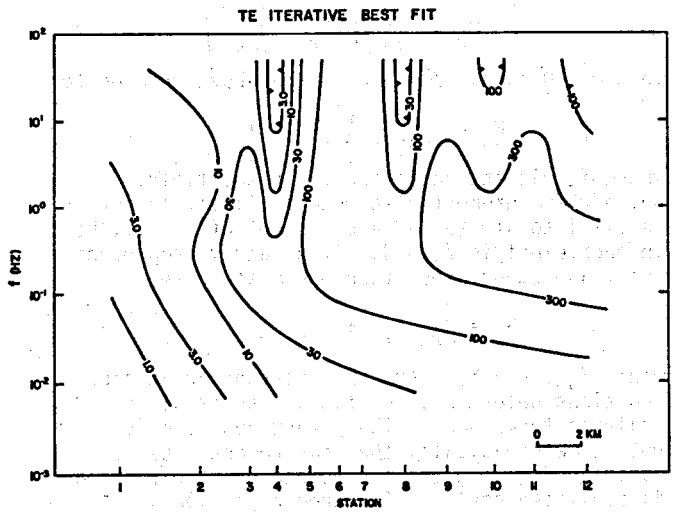


Fig. 6: Trial-and-error best-fit 2-D TE pseudosection for 12-station profile. Contours in Ω-m.

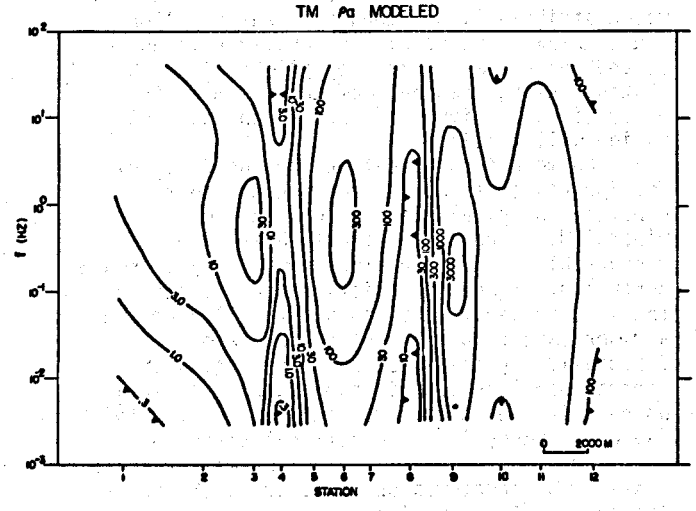


Fig. 8: Computed, 2-D, TM pseudosection for 1-D stitch model. Contours in Ω-m.

Some outcropping, single conductor, multifrequency, TE and TM model results may explain some of the problems in terms of 3-D effects (Fig. 9). In the 2-D, TE model, continuity of tangential electric field (E_t) parallel to media boundaries requires a continuous apparent resistivity function for all frequencies. In the TM model, the electric vector is orthogonal to the media contacts, normal current density (J_n) must be continuous, and so the total electric vector at the contacts will be discontinuous by a factor of (ρ_1/ρ_2). For the TM case, $\rho_a \sim E^2$ so one expects and observes a $(\rho_1/\rho_2)^2$ discontinuity at vertical contacts for all frequencies. Please note that the apparent resistivity values within the prism are greatly depressed below the true value while those outside are only slightly elevated w.r.t. the true resistivity. The anomaly for a simple, outcropping, conductive 3-D prism will possess

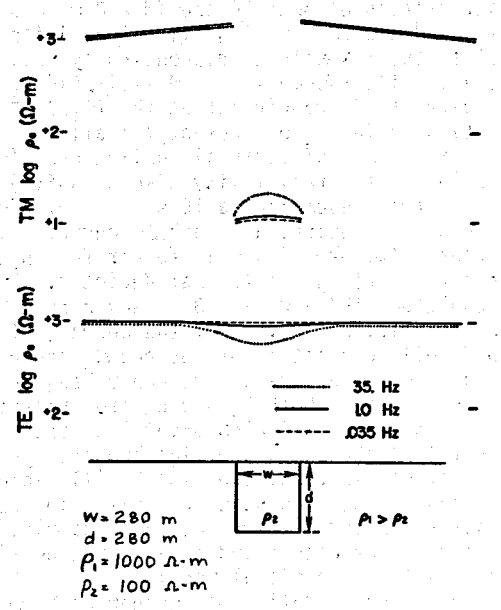


Fig. 9: TM and TE multifrequency profiles for single, outcropping, shallow, 2-D conductor.

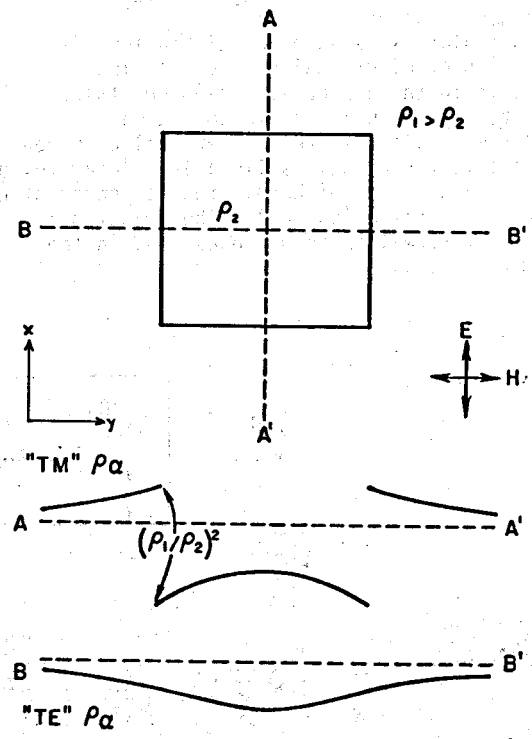


Fig. 10: Conductive rectangular prism in resistive environment plus proposed apparent resistivity signatures for single polarization of electric vector.

characteristics of both TE and TM 2-D models (see Fig. 10). Measurements along line A-A' (with E normal to the resistivity discontinuity) will yield a profile resembling a TM excitation. Continuity of J_n requires that the $(\rho_1/\rho_2)^2$ discontinuity in ρ_a be present for all frequencies. Measurements along line B-B' (with E parallel to the resistivity discontinuity) will give a profile resembling a TE situation. Continuity of E_t requires a smooth ρ_a curve. Analogous $\rho_a(\omega)$ profiles will appear for an E polarization orthogonal to that depicted. Line A-A' would be "TE" and line B-B' would be "TM". Hence, finally, a map view of the anomaly of this 3-D body will consist of pronounced ρ_a contours lasting down to the lowest frequency measured. Since in the field both E_x and E_y are present, then regardless of which observed pseudosection (TE or TM) is chosen, a profile across a conductive prism of finite strike length will exhibit such exaggerated, persisting contrasts in ρ_a. The enclosed pseudosections contain examples of this very phenomenon and they cannot be fit by any purely two-dimensional model.

Depth of exploration is another problem in 3-D environments. A 2-D, TM model of a deeply extending conductive model is very similar to the previous shallow model and one may reason as above that the 3-D anomalies will also be very similar. MT soundings within such 3-D conductive prisms may provide no meaningful information about deeper structures.

The plane wave mode identification (ie. estimation of electrical strike) is also difficult in the 3-D case. Standard strike estimation procedures assume approximate two-dimensionality where the vertical component of magnetic field, Hz, is linearly related to, or completely coherent with only the component of E parallel to strike (say E_x). The relation is defined by Maxwell's second equation, in the general case, as

$$H_z = \frac{-1}{i\omega\mu_o}\left[\frac{\partial E_x}{\partial y} - \frac{\partial E_y}{\partial x}\right]$$

In the 2-D case, $\partial/\partial x = 0$ so the above reduces to

$$H_z = \frac{-1}{i\omega\mu_o}\frac{\partial E_x}{\partial y} = Y_{zx}E_x$$

where Y_{zx} is the admittance. In the field, neither measurement electrode is likely to be parallel to strike and a component of E_x will be in each electric record. If x' and y' represent the measurement axes, then one must write

$$H_z = Y_{zx'}E_{x'} + Y_{zx'}E_{y'}$$

where $Y_{zx'}$ and $Y_{zy'}$ are the relevant admittance functions determined by standard spectral analysis techniques. The patent approach is to rotate mathematically the measurement axes to maximize $Y_{zx'}$ and the corresponding x'-direction is estimated strike. In three dimensions, however, Hz no longer depends on a single direction of electric vector. Referring to Fig. 9, from symmetry observe that along A-A', $\partial/\partial y = 0$, Hz will be wholly related to E_y and the estimated strike will be along the y-axis. Along B-B', $\partial/\partial x = 0$, Hz will be wholly related to E_x and the estimated strike will be along the x-axis. Along diagonals of the prism, both derivatives are important and an oblique estimation will result.

The mode identification for the Roosevelt Hot Springs stations is pretty consistent, however, and parallels the long axis of the Mineral Mts. Regional structure is likely responsible. The mountains form a very elongate, north-south trending resistive body flanked on the west by deep, very conductive alluvium and to a minor extent on the east by the same. Especially for east-west profiles across the central portions of this range, $\partial/\partial y >> \partial/\partial x$ where x is the north-south axis of the mountains. The consistency in the electrical strike estimation does not appear related to smaller-scale hot-spring structures but instead to the gross topography of the region.

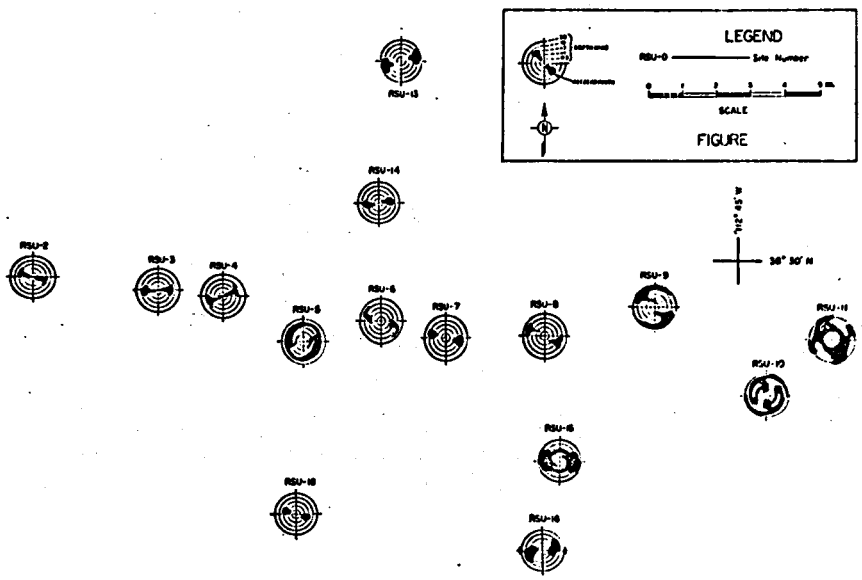


Fig. 11: Dip-axis estimates (A(YZ) is contractor's notation) as a function of depth for several stations in Roosevelt area. Dip-axis is normal to estimated strike and blackened area indicates scatter in calculated axes. Depth is a product of continuous inversion algorithm which provides approximate depth-frequency correspondence listing.

THE CHARACTERIZATION OF CRACK STRUCTURE CONTROLLING PERMEABILITY USING VELOCITY-PRESSURE DATA

Nick Warren

University of California
Institute of Geophysics and Planetary Physics
Los Angeles, California 90024

Work performed under grants from the U.S. Energy Research and Development Administration (contract no. EY-76-S-03-0034) and the Los Alamos Scientific Laboratory (contract no. RFQ NP8-14780).

Expressions for permeability and elastic moduli can be derived. Such expressions provide a means of modeling the microstructure controlling permeability and velocity and they elucidate the feasibility of predicating the functional dependence of permeability on pressure from independent determination of microstructure, such as from ultrasonic data.

An equation for the diffusion of fluid through cracked rock has been derived by H. Fisher [1], and involves explicitly the permeability k, and the pressure derivative of a "conduit porosity" θ, with respect to pore pressure P_h.

$$\nabla \cdot (k \cdot \nabla P_h) = \mu \frac{d\theta}{dP_h} \frac{\delta P_h}{\delta t} \qquad (1)$$

In equation (1) μ is viscosity and t is time. The porosity is defined by its total derivative

$$\frac{d\theta}{dP_h} = \frac{1}{V} \frac{dV_h}{dP_h} \qquad (2)$$

where V is the bulk volume and V_h is the pore volume at any pressure and temperature. Difficulty arises in evaluating equation (1). As Fisher notes: "The related quantities k, θ, and $d\theta/dP$ and in particular the dependence on pressure cannot be exactly determined since they also depend on the pore volumes." However, it is possible to approach this problem by seeking to characterize the manner in which the microstructures that form the conduits for fluid flow can be related to elastic properties such as a compliance through their effects on bulk strain and velocities.

In sufficient generality, a normalized elastic compliance ϕ/ϕ_o, (such as compressibility) can be expressed in terms of a "referred porosity" ω and its pressure derivative [2].

$$\omega = 1 - V_o/V \qquad (3)$$

where V_o is the reference solid material and

$$-\frac{d\omega}{dR} = (1 - \omega)\phi_o \cdot [\phi/\phi_o - 1] \qquad (4)$$

where R is the applied stress state which is used in defining ϕ (for example, R is applied pressure in the case of compressibility). All the porosity affecting the elastic deformation is involved. This is an "elastic porosity" to distinguish it from the conduit porosity.

The expression for $(\phi/\phi_o - 1)$ can be obtained from velocity data or from modeling theory [2,3]. Velocity-pressure data for rocks show systematics which are related to microstructure and which can be inverted into model microstructure by expressing equation (4) in terms of distributions over partial porosities ($_i\eta$, given by $_iV_h/V$) and pore strains ($_ie_h/e_o$).

$$\phi/\phi_o - 1 + \eta \frac{dP_h}{dP} = \frac{1}{1 - \eta} \sum_i {}_i\eta \left(\frac{{}_ie_h}{e_o}\right) \qquad (5)$$

The question arises, can the conduit porosity be related to the elastic porosity? At present this question requires experiments to be answered. One cannot tell yet whether the two porosities are numerically equal, but the pressure derivatives may well be relatable. The quantity $d\theta/dP_h$ can be stated in terms of $d\omega/dR$ through the expressions for the pore strains. In equation (5) the geometries of the pores and their closure laws are not restricted. For cracks, the approximate form of the solution follows, using the distributions in a form involving a pore number density.

If the crack network is characterized by some distributions in length a and width b, then the number density distribution satisfies

$$\int_a \int_b \frac{d^2W}{dadb}\, dadb = N \qquad (6)$$

where N is the total crack number density and

$$(\phi/\phi_o - 1) \sim \int_a \int_b a^3 \frac{d^2W}{dadb}\, dadb \qquad (7)$$

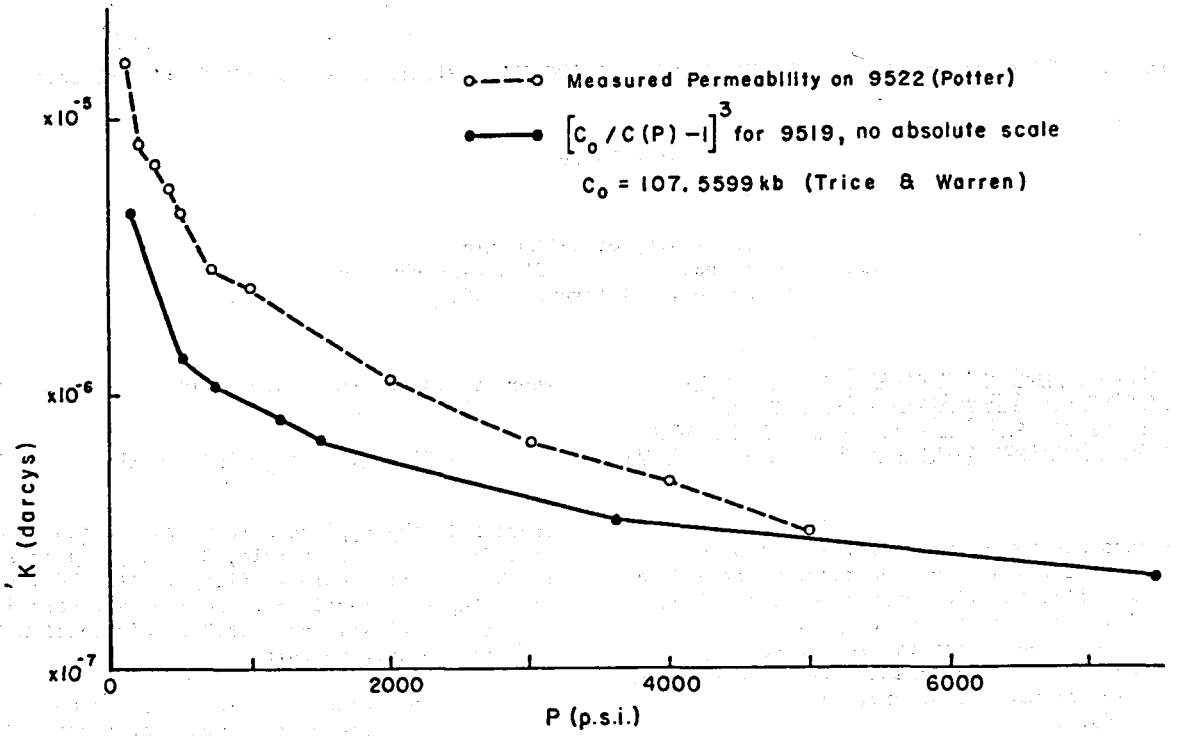


Fig. 1 Permeability and the cubic function of acoustic data versus pressure for GT-2-9522/9519 (permeability data on 9522) from J. Potter, personal communication.

If the Kozenzy relation is assumed for permeability

$$k = c \cdot \theta \bar{b}^2 \tag{8}$$

where c is a constant and $\bar{b}$ is the characteristic crack width given by the ratio of pore volume to surface area

$$\bar{b} = \int_a \int_b a^2 b \frac{d^2W}{dadb}\, dadb \Big/ \int_a \int_b a^2 \frac{d^2W}{dadb}\, dadb \tag{9}$$

and can be obtained for a model crack spectrum fitting the velocity data. The pressure dependence of k is thus expressible as a function of the pressure dependence of the density distribution.

Two conclusions that can be drawn are: 1) that various pressure laws are equally admissible, which may help explain why published power laws fit to permeability have shown such a wide range of exponents (from 2 or 3 to 6), and 2) that comparison of acoustic data or model-crack spectra to permeability-pressure data may elucidate the effects of tortuosity and pinch-off on the conduit porosity. Figure 1 illustrates these points. The figure shows a comparison of permeability data to a cubic function of the compressional wave velocity data for a sample of granodiorite from LASL's Fenton Hills HDR geothermal site, New Mexico [4]. The velocity-pressure data can be modeled assuming cracks with linear closure laws. The parallelness of these curves indicates that the same microcrack network controls both permeability and acoustic properties and that, based on the model, permeability goes as the average crack width (over all pores) cubed.

References

[1] Fisher, H., "An interpretation of the pressure and flow data for the two fractures of the Los Alamos hot dry rock (HDR) geothermal system," Energy Resource and Excavation Technology Proceedings: 18th U.S. Symposium on Rock Mechanics, June, 1977.

[2] Warren, N. and R. Nashner, "Theoretical calculation of the compliance of a porous medium," in The Physics and Chemistry of Minerals and Rocks, John Wiley & Sons, 1976.

[3] Warren, N., "Characterization of Modulus-Pressure Systematics of Rocks: Dependence on Microstructure," published in Monograph-20 of the American Geophysical Union, 1977.

[4] Trice, R. and N. Warren, "Preliminary Study on the Correlation of Acoustic Velocity and Permeability in Two Granodiorites from LASL Fenton Hill Deep Borehole, GT-2, Near the Valles Caldera, New Mexico," July, 1977.

Geothermal Resources Council, TRANSACTIONS, Vol. 2 July 1978

BUSBAR ECONOMICS OF LIQUID-DOMINATED GEOTHERMAL POWER

Johan A. Wassenaar

Fugro, Inc.

The state-of-the-art of electrical power generation using hot-water geothermal resources as opposed to geothermal steam, has yet to be developed to where an accurate prognosis of busbar cost can be made. There are many uncertainties that are responsible for this, and until an empirical data base is brought into being through long-term operation of commercial-scale power plants using liquid-dominated hydrothermal resources, no exact economic projections will be possible.

However, the body of knowledge about the use of hot-water resources is expanding rapidly, and through conjectural analyses, it is becoming increasingly possible to draw a fairly tight bead on the prospective busbar costs of power generated from such resources.

It appears fairly certain, for instance, that liquid-dominated geothermal power could generally be cheaper than oil-fired power, but would not be able to compete with nuclear or coal-fired power in areas where the physical and political climates would still permit such power plants to be built.

The main causes of uncertainty about the cost of hot-water geothermal power are variations in the following:

- Plant utility (availability) factor
- Conversion cycle efficiency
- Fuel (heat) price
- Capital cost
- Resource decay characteristics
- Plant cooling provisions
- Operations and Maintenance cost (O&M)
- Power transmission cost

Plant Utility Factor:

A very large portion of the busbar cost of a hot-water geothermal power plant will be fixed. The capital component of busbar cost associated with the power plant is in the order of one-third. However, the fuel (heat) cost which represents more than half of overall busbar cost, also contains a large capital component associated with the drilling and completion costs of production and injection wells. Even the operations and maintenance portion of busbar cost, which is in the order of 10-13%, is mostly fixed as a function of the irreducible staffing and equipment requirements to deal effectively with scale prevention from the saline geothermal brines.

Early indications for a family of 50-100 MWe plants are that a fixed busbar cost component in the order of 80-85% may be expected. This very clearly classifies geothermal power from hot-water resources as base load capacity with very high cost susceptibility to plant utilization. To compete with the cost of conventional or new (combined cycle) oil-fired power, such geothermal power plants would have to be kept on-line at least 75-80% of the time. This could be a serious challenge at reservoirs where the salinity of the geothermal brines is high, such as, for instance, at Niland in Imperial Valley (250,000-300,000 ppm). A substantial amount of redundancy in the brine flow circuits may be justified in such cases to permit off-line cleaning without plant shut-down.

Experience in Mexico at Cerro Prieto, while not involving brine reinjection as yet, nevertheless provides the basis for some optimism that high geothermal power plant availabilities will be achievable.

Conversion Cycle Efficiency:

By definition, the low heat intensity of geothermal power from hot-water resources severely limits the thermal efficiency achievable in the power conversion cycle. This reflects in a high heat flow rate per kilowatt of power which varies substantially as a function of the reservoir down-hole temperature. For example, as shown in figure 1., a flash steam cycle plant at Niland (550°F) would typically use about 16 lb. of steam per kilowatt-hour whereas its counterpart at Heber (360°F) would use as much as 27 lb. per

kilowatt-hour. We are, therefore, dealing with conversion cycle efficiencies in the range of 10-15%, which has a great impact on the fuel (heat) component of busbar cost, and which constitutes something in the range of 55-60% of overall busbar cost.

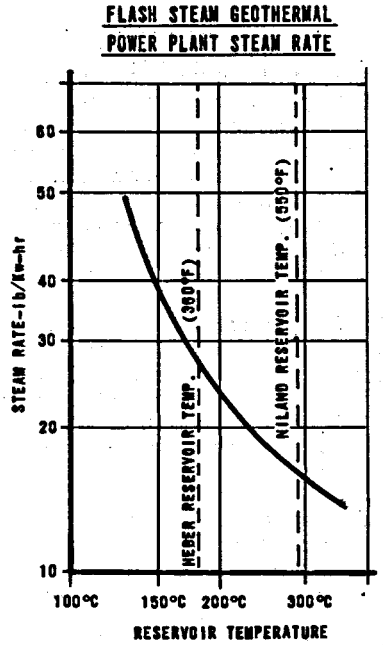


FIGURE 1

Much will be said about the relative merits of different conversion cycles for use at certain reservoirs. For instance, the prospects of using a hydrocarbon binary cycle approach at reservoirs in the 350°F temperature range to attain improved conversion efficiencies over that possible with a flash steam cycle, will hopefully be tested on a commercially comparative scale if the Heber Demonstration Binary Project and other comparable flash steam plants get underway in parallel.

Later prospects for efficiency improvement through use of total flow impulse turbines, or with the introduction of heat augmentation of geothermal steam by fossil-fuel, nuclear or solar energy means will undoubtedly follow. However, the economics of these approaches will be suspect for quite some time.

Fuel (Heat) Price:

During this early evolutionary phase of liquid-dominated geothermal power, it would be unreasonable to expect free market forces to set the price of geothermal heat. There are only so many resource companies involved in the development of the reservoirs, and they are understandably skeptical about the consistency of demand for their geothermal heat product.

Initial heat supply contracts for geothermal power plants will, therefore, tend to contain guarantees for certain minimum heat use rates to ensure reasonable recovery of fixed reservoir development costs. Such guarantees effectively render a large part of the fuel cost of a geothermal power plant invariable, as pointed out before.

The resource operator also still faces many uncertainties that could impact his production costs. Unexpected decay of the resource temperature, deteriorating steam quality, if a flash process is used, and clogging of injection wells and geologic dispersal zones by disassociating mineral salts from the cooled brines, are but a few of the possibilities as yet unproven.

Capital Cost:

No one knows exactly what the capital cost per kilowatt of a series of like geothermal plants, replicated in a region of multiple reservoirs such as Imperial Valley would be. It depends on the choice of optimum power plant designs for the different reservoirs, and could also be seriously impacted by power plant cooling provisions. It appears that initial commercial-scale (50-100 MWe) plants will cost in the range of $750-800 per kilowatt, but the learning curve effect of a construction program involving a series of very similar (or identical) plants should reduce this to something in the $500-700 per kilowatt range (1978 constant dollars).

Resource Longevity:

Until substantial generating capacity is installed and operated for long periods of time at the prime reservoirs, their characteristic behavior in terms of temperature and pressure decay will be left to scientific conjecture. The fingerprint of each reservoir in the sense of convective thermal recharge will not be known with certainty before then. Also, the possible modification of reservoir permeability by the circulation of injected spent brines with high salt contents will not be fully understood without empirical data on a suitably large scale.

The effects of reservoir decay on power plant economics are significant. Heat flow rates of flash steam plants rise rapidly with reducing reservoir temperatures, and binary cycle plants require adjustments in

heat transfer surface areas, and in working fluid composition to compensate for temperature drops.

Power Plant Cooling:

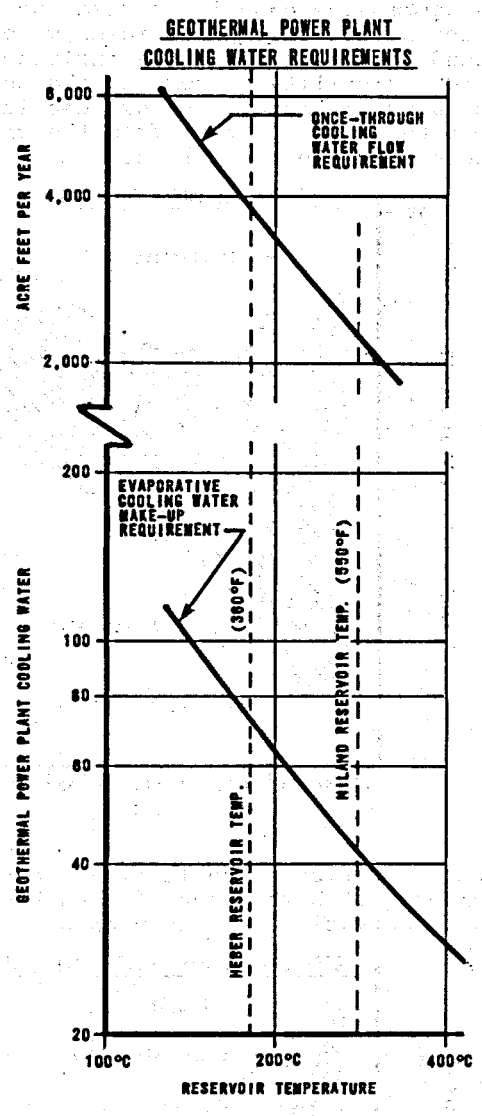


FIGURE 2

Because of their low thermal efficiency, geothermal power plants are gargantuan users of cooling water (see figure 2). In all but a few possible cases, once-through cooling would be economically unfeasible. Evaporative cooling seems to be the best near-term solution, but it requires a substantial supply of cooling tower make-up water (100 acre feet/yr./MWe). While flash steam plants could use their own condensate for this purpose, they still require an equivalent alternative water supply for injection into the reservoir to replace the withdrawn steam, and so avoid the possibility of land subsidence as a result of ultimate fluid depletion.

For instance, Imperial Valley, agricultural drain water would appear to be the best source of plant cooling-related water at upstream locations such as Heber. However, diversion of drain water reduces dilution and replenishment of the Salton Sea, which is already increasing each year in salinity. To obtain water rights, this effect may have to be mitigated by injecting compensating amounts of Salton Sea water into the Niland reservoir in association with power plants at that location. However, the effects on Salton Sea water injection on the reservoir would first have to be investigated.

With large-scale commercial development of geothermal power plants in arid areas such as Imperial Valley and Roosevelt Hot Springs, it seems likely that wet/dry cooling tower methods may ultimately have to be used. This could bring about a 50% reduction in annual make-up water consumption, but would impact busbar cost to the extent of about 10 mills/kw-hr. (in 1977 dollars).

Operations and Maintenance Cost:

Geothermal power plant (liquid-dominated) O&M costs appear to be four to six times more than for equivalent oil or nuclear generation methods. Much of this is occasioned by the small unit sizes of geothermal plants, and by the requirement for flow circuit cleaning and descaling. However, O&M costs still only make up about a tenth of overall geothermal busbar costs, and since the O&M procedures will have a great influence on plant utility factor, compromises to reduce O&M costs will have to be carefully considered. One approach to reduce O&M charges without compromise, may be to improve maintenance efficiency by grouping geothermal plants in clusters.

Power Transmission:

Many geothermal resources are remote from major population centers, and the cost of transmitting power from geothermal power plants could be considerable. This problem is compounded by the fact that economical transmission lines have capacities that would require many geothermal units in the 50-100 MWe size range to fill.

Transmission costs during the initial period of a commercial geothermal plant construction program, when a mismatch between generating and transmission capacities could be expected would, therefore, be high. A potential solution may be the sharing of transmission facilities between different power plant owners, or between different generation plant types within one utility.

While it may be imprudent to risk specific forecasts of liquid-dominated geothermal

busbar costs in this uncertain environment, the following preliminary assessment is offered to stimulate thought and discussion. Two hypothetical cases of commercial hot water geothermal power plant development are presented as depicted in figure 3.

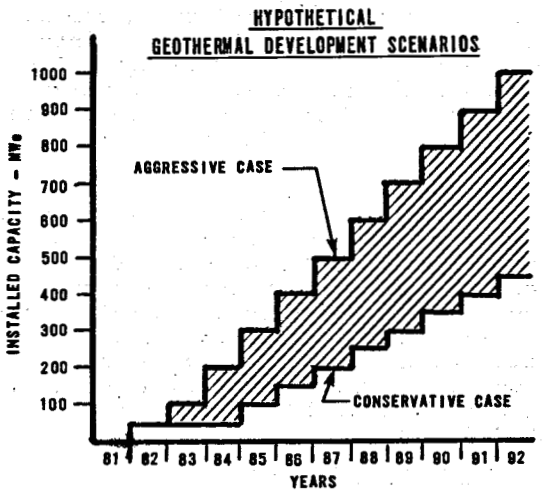


FIGURE 3

The conservative case assumes a cautious construction program resulting in an installed capacity of only 450 MWe by 1991. No government funding aid is postulated, limited tax and rate incentives, and a sharing of transmission facilities with other generation alternatives are assumed.

The aggressive case assumes a bolder construction program yielding 1000 MWe capacity by 1991. A 50% government participation initially in two 50 MWe demonstration plants at different reservoirs, and liberal tax and rate incentives are assumed.

Figure 4 shows the plant utility factors that would result from an 80% learning curve, starting at a 40% utility factor and peaking at 80% with ultimate experience.

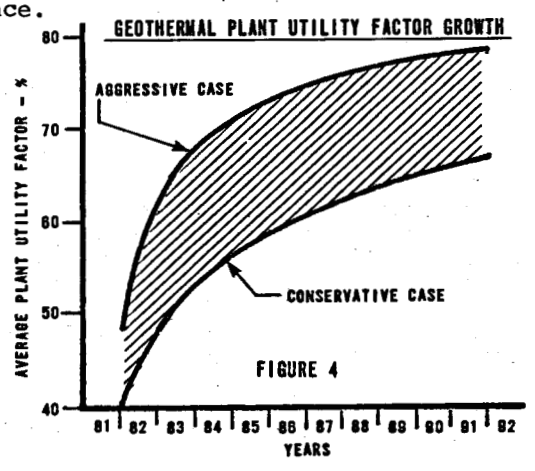


FIGURE 4

Figure 5 illustrates the fuel cost components of busbar cost for the two cases. The conservative case assumed achievement of 10.8% thermal efficiency for half the plants and 12% for the other half. The aggressive case is premised upon achieving 15% thermal efficiency for the second half. The opposite influences of improving utility factors on the one hand, and labor and materials cost escalation on the other, are apparent from the change in gradient of the two curves.

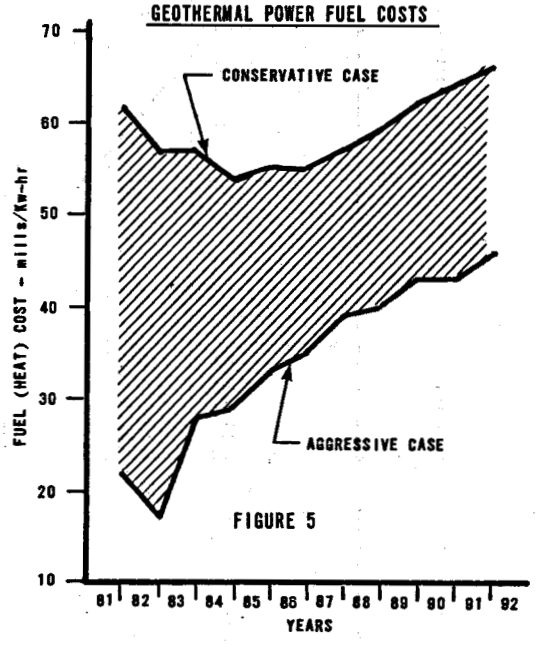


FIGURE 5

Figure 6 reflects the levelized capital component of busbar cost for each case. The conservative case assumes no demonstration grants from public sources, and assigns a 25-year book life to commercial plants, with a 16-year tax life for Federal purposes, and a 20-year tax life for State purposes. The aggressive case assumes a 30-year book life for commer-

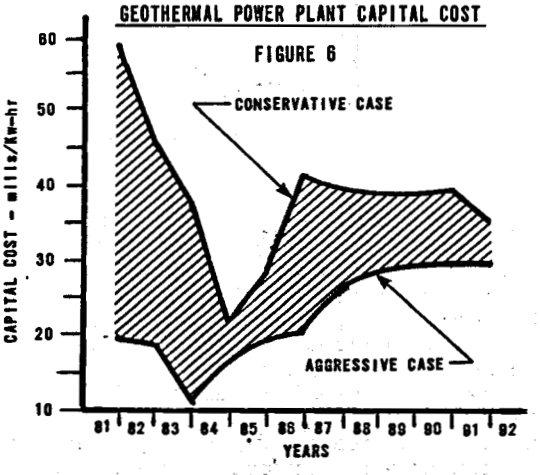


FIGURE 6

cial units, and provides for 50% public funding in support of two demonstration plants, including government participation in the first five years of operation.

Figure 7 shows the O&M portion of busbar cost for each case. Figure 8 summarizes overall busbar cost for both cases and compares them with the busbar costs of an oil-fired plant in a coastal setting, and a nuclear plant inland in the desert. It will be seen that the optimistic (aggressive) case competes successfully on a cost basis with the oil-fired alternative. However, the range of geothermal busbar costs, as represented by the shaded area between the curves, is still much too wide to feel confident about any conclusions. Nevertheless, it will not escape your notice that geothermal power from hot-water resources will have to be undertaken on a large scale in order to make it competitive with other forms of power generation at the busbar. This may come as a surprise to those who may have viewed geothermal power as a small incremental electrical growth opportunity consistent with the constrained industrial expansion ethic espoused by some.

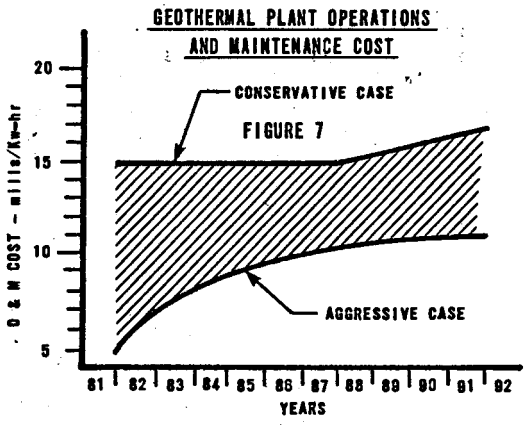


FIGURE 7

More refined economic analyses, using conjectural probabilistic techniques should narrow the range of economic uncertainty about geothermal power substantially in the near future.

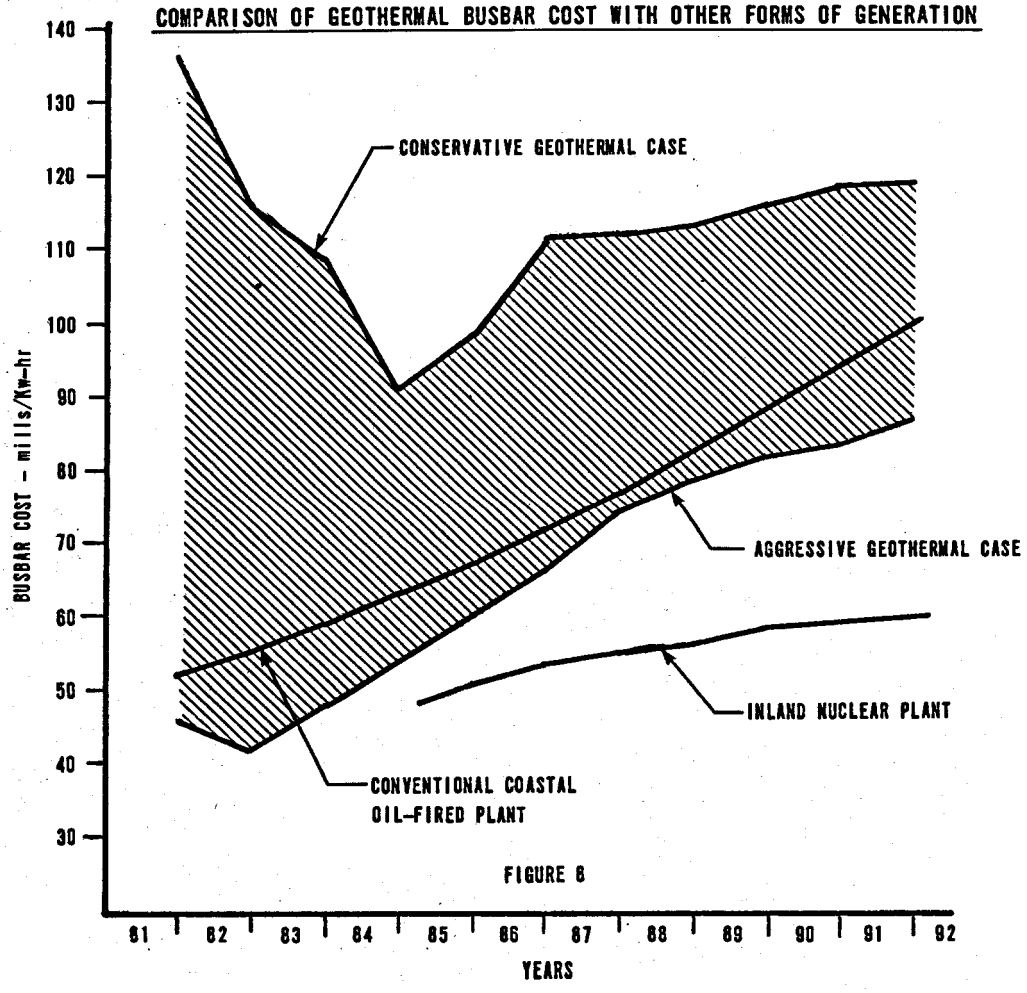


FIGURE 8

GROUND WATER MONITORING METHODOLOGY FOR GEOTHERMAL DEVELOPMENT

Richard Weiss
Project Geologist

Harding-Lawson Associates
San Rafael, California 94902

ABSTRACT

The proposed ground water monitoring methodology for geothermal development specifies a seven-step monitoring system development and evaluation procedure consisting of (1) definition of baseline conditions and projected development; (2) forecast of aquifer conditions; (3) definition of necessary detection limits; (4) evaluation of alternative ground water and disposal facility monitoring techniques; (5) proposal of monitoring system and alternatives; (6) implementation of monitoring system; and (7) continuation of monitoring program and modification as necessary.

INTRODUCTION

This study, sponsored by the U.S. E.P.A., emphasizes a philosophy of "preventive monitoring" as an integral and essential component of a "detective monitoring" methodology since ground water degradation is often an essentially irreversible process and case histories of ground water contamination due to injection of waste show that many of them could have been prevented by appropriate study and planning beforehand. By utilizing this proposed methodology and by enforcing rigid specifications for injection well construction prior to injection ground water degradation can be avoided. If the preventive monitoring study shows that the injected fluid will interfer with any useful aquifer, then the initial design, location and production schedules of the offending wells must be modified before production and injection begin.

Injection of geothermal effluent into the ground is a somewhat special case of deep well injection. Some of the distinctive characteristics include effluent chemistry, quantity and temperature, and injection depth. Fluid composition may vary from a few hundred ppm to well over 250,000 ppm TDS. Within each geothermal reservoir the chemistry of the injected fluid may also vary considerably. For example, at East Mesa, California the total dissolved solids (TDS) from different wells range from less than 2,000 parts per million (ppm) in Mesa 5-1 to about 30,000 ppm in Mesa 6-1 (USBR, 1974). For most geothermal operations the quantity of fluid processed and injected will be enormous. For example, in the Otake, Japan fields 1,350 tons of fluid per hour are injected into three wells (Kubota and Aosaki, 1976). This is 10 to 100 times the quantity generally injected for oil production. Injection will generally take place in the deeper geothermal aquifer system usually more than 1,000 meters deep. The injected fluid will be significantly hotter than ambient air and may be hotter or cooler than the receiving aquifer.

Several potential pollution mechanisms must be considered in deep well injection of any waste fluid, and the proposed methodology must be able to monitor potential leaks from these mechanisms, which include: (a) surface-accidental spills; (b) cement failure; (c) casing corrosion; (d) hydrofracturing of confining formations due to high pressure injection; (e) percolation from evaporation ponds (enhanced by higher temperatures); (f) differential pore pressure resulting in intrusion of waste or simple disruption of near-surface hydraulic gradients; (g) percolation from discharge of mineralized fluid to land surfaces or drains; (h) escape of injected fluid through unknown structural or stratigraphic pathways; (i) escape of water from sheared well casings, for example, slope failure at The Geysers, California.

An additional objective of this study is to develop possible uses of borehole geophysics in ground water monitoring for potential geothermal development that may be coordinated with other more traditional monitoring approaches. Geophysical well logging may

be applied in two aspects of the monitoring system. First, prior to injection it may be used for detailed definition of geologic and hydrologic properties of the strata, such as permeability, porosity, thickness of individual layers, clay content and other important structural and stratigraphic characteristics. Secondly, it may be used to monitor ground water characteristics during and prior to injection.

GENERAL METHODOLOGY

Figure 1 is a flow chart illustrating the proposed methodology. Each of the steps shown in the figure is described below.

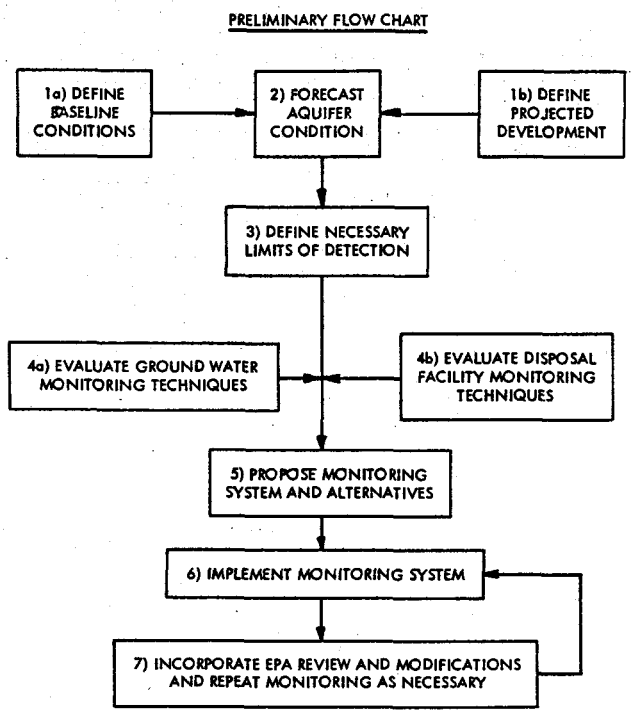


Fig. 1 Proposed Ground Water Monitoring Methodology for Geothermal Development

Define Baseline Conditions

Baseline conditions are those that exist prior to injection. To determine hydrologic changes that may occur during injection, baseline conditions must be established, including:

a. chemical characteristics of nongeothermal ground water and surface waters;
b. chemical characteristics of geothermal ground water;
c. geology and hydrology of the area;
d. location and well completion data for all wells around the geothermal site;
e. land use and sensitivity;
f. mechanics and characteristics of the geothermal system.

Determining the chemical characteristics of nongeothermal ground water and surface water will include, in addition to standard chemical analyses, available historic data which will be synthesized to identify changes with time, location or depth. A characteristic "chemical signature" for each water type from each recharge source will be sought.

In determining the chemical characteristics of the geothermal water, we must sample geothermal wells, as well as springs, and insure that we have a representative sample of the reservoir. Data analyses should cover the possibility of mixing with nongeothermal waters.

Geologic descriptions should include potential structural and stratigraphic pollutant pathways and boundaries, aquifer locations, depths, and areal extents. Well pumping tests and geologic data can provide information on the transmissivity and permeability of the aquifers. Contour maps of ground water depths and elevations for each aquifer can be prepared from water level and topographic data. Precipitation, evapotranspiration, soils, land use and water level data can be combined to describe natural ground water recharge. Irrigation and recharge data can be used to describe artificial ground water recharge. Stream flow and water level data can be used to define natural ground water discharge. Water level and transmissivity data can be used to determine directions and velocities of ground water flow. A hydrologic budget can be prepared to get an overview of the magnitude of water movement in the area.

A water well canvass will establish locations, owners, perforated intervals, well construction, water and well use, the amount of pumping and any other relevant well data for all wells around the site. Each well's suitability for use as a monitoring well, or as a potential conduit for cross aquifer pollution due to poor well construction will be evaluated. Land use and particular land sensitivities will be observed, e.g. ecologic, agricultural, subsidence, or slope stability factors as they may relate to the ground water program.

The hydraulics, temperature gradient, reservoir characteristics of the geothermal system will be defined and the system will be modeled. Of particular importance is the determination of how the geothermal ground water system is related to the nongeothermal ground water system.

To finalize the baseline data acquisition phase we would evaluate each data category for completeness. For example, are the hydrologic characteristics adequately defined? is the geographic and depth distribution of wells sufficient for adequate monitoring? is the temporal distribution of historic chemical data sufficient to establish patterns of temporal variation in water quality? Determination of data completeness will include consideration of current EPA or other regulations as well as considerations of current and potential ground water use in the area. If necessary, further data acquisition to insure an adequate baseline would be recommended. The limitations of the data that exists would be explicitly defined.

Define Projected Development

The type and magnitude of potential development will be defined, including descriptions of the heat extraction and waste disposal processes. Chemical effects of these processes such as silicification or carbonate deposition on potential pollutant pathways must be considered along with potential ground water pollution. The proportions of potential geothermal water production and injection to natural ground water system flow should be determined. The chemical characteristics of the post-process geothermal fluids must be compared with those of natural geothermal fluid and nongeothermal ground water. Local geologic and hydrologic factors at the site must also be defined. For example, landsliding has been a major consideration in planning geothermal facilities at The Geysers.

Forecast Aquifer Condition

Forecasting the interaction between geothermal and nongeothermal aquifers before production and injection begin may enable us to avoid potential problems. By incorporating possible pollutant mechanisms and pathways in our ground water and geothermal model, we would aim to predict the water quality and quantity changes in the geothermal reservoir and in the ground water system due to the production and injection of varying quantities and qualities of fluid. Hopefully, many of the geologic and hydrologic parameters necessary for this model would be supplied by detailed geophysical borehole logging.

Limits of Detection

The monitoring system will be designed to detect chemical changes in the ground water. These changes will occur in a spatial and temporal matrix. The necessary sensitivity of detection in chemistry, time and space must be specified for each area and is a function of:

a. Chemical contrast of geothermal and nongeothermal fluids
b. Environmental sensitivity to particular constituents
c. Natural variations in water characteristics
d. Hydrologic factors
e. The relative size of the development
f. Characteristics of potential pollutant pathways
g. Water use and well distribution density in the area
h. Available analytic techniques
i. EPA and other regulatory constraints

Analysis of these parameters will aid in determining sampling frequency, distribution and density of sample points, significant chemical and physical parameters, and sampling and analysis methods to be utilized. Where ground water is used extensively, we would be more concerned about rapidly detecting minute changes in quality, whereas where ground water quality is poor and it is not used we may accept larger variations and less frequent sampling.

Ground Water and Disposal Facility Monitoring Techniques

Once the monitoring parameters have been defined the most appropriate monitoring techniques must be selected, e.g. standard water sampling and analyses, geophysical well logging, electromagnetic probes, surface geophysics, etc. The applications, sensitivities, accuracy and cost of these techniques, taken individually or in combination will be considered.

For the water sampling we want to specify field determination of volatile constituents and evaluate standard lab chemical analysis techniques; e.g. wet chemical, atomic absorption, mass spectrography, pH, specific conductance.

The techniques and parameters which most closely reflect our needs and our budget will be determined.

Geophysical well logs can be interpreted to determine the lithology, geometry, resistivity, formation factor, bulk density, porosity, permeability, moisture content and specific yield of water bearing rocks and to define the source, movement and chemical and physical characteristics of ground water. However, log interpretation techniques used for geothermal wells often provide inaccurate answers since log interpretation technology has been developed for petroleum reservoirs which generally have different physical characteristics than geothermal reservoirs. One aspect of this particular study is to define how geophysical well logs can accurately and economically be used in ground water monitoring for geothermal systems development. A few sample applications are briefly noted below.

One important capability of geophysical well logging is continuous vertical profiling of water quality with depth. With this vertical profile temporal changes in water quality and rates of dispersion in individual layers could be detected. Salinity of the formation water can be determined from electrical resistivity and SP logs in uncased holes or it can be calculated from pulsed neutron logs in cased holes. Disposal of geothermal waste water may be monitored using temperature logs which detect the movement of a fluid which is either hotter or cooler than the aquifer. Gamma ray logs may be used to detect movement of contaminated water behind well casings.

Most monitoring of deep well disposal has been done through monitoring of the disposal facility itself as opposed to monitoring the area around the disposal facility. This type of monitoring has included measuring the volume of disposed fluid, chemical and physical properties of the fluid, and fluid pressures at the wellhead and annulus, as well as periodic inspection of surface and subsurface facilities, determination of permeable boundaries and periodic geophysical well logging.

Propose Monitoring System and Alternatives

Detecting temporal and spatial changes in ground water characteristics within the established limits of detection is the goal of the proposed monitoring system. Designing a site specific monitoring system may be done using a matrix evaluation technique specifying an algorithm or relative weighting for each factor and parameter to arrive at an optimum balance of cost versus confidence.

Generally, sample points will be more concentrated around and down-gradient from potential pollutant sources, i.e., disposal wells. Sample frequency should be greater near and down-gradient from the source than further away. Initially, some comprehensive chemical analysis (e.g. multispectrographic analysis) of sample water should be done to determine which trace minerals need to be specified for detailed wet chemical or atomic absorption analysis.

Recommendations to achieve the proposed monitoring system may include installing additional observation holes, specifications for the sampling frequency and pattern, specifications for sampling and analysis techniques to be used and chemical constituents to analyze for. We may find that adequate detection limits can be achieved economically by carefully selecting frequency, density and types of sampling and analysis.

Implement Monitoring System

Implementing the monitoring system will involve data collection at specified frequency and locations, and data synthesis, interpretation and display. Past data will be reviewed and correlated with the new data. Modifications will be recommended for the system as necessary.

References

Kubota, K., and Aosaki, K., Reinjection of Geothermal Hot Water at the Otake Geothermal Field, Proceedings Second U.N. Symposium on the Development and Use of Geothermal Resources, pp. 1379-1384, 1976.

U.S. Bureau of Reclamation, Geothermal Resource Investigations, East Mesa Test Site, Imperial Valley, California - Status Report, November 1974.

Geothermal Resources Council, TRANSACTIONS, Vol. 2 July 1978

COMBINED ELECTROMAGNETIC AND GALVANIC (d.c.) ELECTRICAL RESISTIVITY SOUNDINGS

Richard C. West and James I. Pritchard

Electrodyne Surveys
P.O. Box 1522
Sparks, NV 89431

The problem often encountered in the exploration for geothermal resources by any geophysical method is the complexity of the geologic setting. Because the known geothermal fields of the world are associated with crustal block movement, volcanic activity, faulting and fracturing systems, (Combs, 1975) two and three dimensional geologic structures are normally encountered and have to be considered when planning an exploration program. Electrical resistivity methods have been very successful in locating areas of low resistivity associated with geothermal resources, but resolving the complexity of the geoelectric structure is difficult because of the high cost of detailed surveys or because of weaknesses inherent in some of the less expensive methods, such as galvanic or telluric current methods. Dissatisfaction with the magnetotelluric method as a detailing tool has been expressed (Goldstein, 1978) because two dimensional structures, such as near surface inhomogeneities, strongly affect the tensor impedances.

A new combination of three of the basic electrical methods, galvanic, controlled source electromagnetic and telluric profiling methods, is suggested as an alternative detailing tool which can provide less ambiguous results at a reasonable cost. This combined method will be referred to as Electro-Sonde Profiling (ESP).

A plan view of the ESP scheme is shown in Figure 1. A grounded source bipole is located in conjunction with at least one parallel ESP profile, such that the center of the profile is located along the perpendicular bisector of the bipole and is separated from the bipole by a distance "r". A receiver unit traverses the profile and records on magnetic tape the electric field measurements obtained at the twelve adjacent sites utilizing a receiver dipole $\overline{MN}$ and source bipole $\overline{AB}$. At every second or at least every fourth receiver site, the vertical and radial (horizontal) components of the magnetic field generated by the subordinate source bipoles $\overline{AC}$ or $\overline{CB}$ are recorded. Bipole $\overline{AC}$ is energized only when the magnetic field is required along the left-hand half of the profile and dipole $\overline{CB}$ is energized only when the magnetic field is required along the right-hand half of the profile. Utilization of the shorter bipoles provides a better approximation of a dipole source as required by the theory of electromagnetic soundings (Vanyan, 1967). A schedule of alternating periods of power on (source bipole energized) and power off (source bipole not energized) allows recording of both the actively and passively generated electric fields at the surface of the earth. The ratio of the passive electric fields (end-on-end tellurics) can then be determined (Beyer, 1977). A summary of the six parameters measured along the profile are given on Figure 1.

The distribution of the frequency and the relative depth of penetration of each of these six measurements in an H-type geoelectric section is shown in Figure 2. Given that the profile separation "r" is large, a nearly complete probing of a conductive basin is accomplished by this combined technique as opposed to tensor magnetotelluric soundings which may show incomplete sounding curves in the 0.1-5hz frequency band due to low coherency between orthogonal electric and magnetic fields. Lateral and vertical resistivity variations are readily determined along the profile because of the continuous set of electromagnetic soundings and telluric electric field ratios. Multiple profile coverage in an area of complex geologic structures will aid in the determination of the three dimensionality of the exploration problem.

Interpretation of the electromagnetic soundings can be accomplished by curve-matching techniques, (Banyan, 1967) comparison of field curves with computer generated sounding curves, and inversion techniques (Anderson, 1974; Anderson, 1977).

In addition to the profiles, a set of modified Schlumberger depth soundings are obtained along the source bipole $\overline{AB}$ (see Figure 1). This is done by expanding a short receiver dipole collinearly from both source electrodes towards the center of the bipole. The depth of penetration of the array is equivalent the distance from the closest electrode to the center of the dipole. This array is much more sensitive to lateral resistivity variations than a Schlumberger sounding so vertical and horizontal resistivity variations can be observed in the determined sounding curves. Equatorial soundings constructed from the static parallel electric field along the profiles extends the depth of penetration of the galvanic sounding.

The advantages of this detailing scheme can be briefly stated as:

(1) The collective use of galvanic and electromagnetic depth soundings provides definition of the longitudinal and transverse resistivity of layers within a multi-layered earth. These can be an important set of parameters in many geophysical problems.

(2) The controlled source electromagnetic soundings provide definition of the electrical resistivity variation beneath and in the vicinity of the receivers, but are less affected by lateral resistivity variations than passive electromagnetic soundings or galvanic soundings.

(3) ESP field logistics are simpler than for galvanic profiling or sounding techniques that attempt to achieve similar depths of penetrations, especially in moderately difficult terrain.

(4) The end-on-end telluric profiles and electromagnetic soundings are inductive techniques that provide better definition of conductive layers and are not screened by near surface resistive layers as galvanic methods are.

(5) The sub-audio EOE tellurics will be more definitive in mapping basement structure because the upper section conductance will be determined by the electromagnetic soundings.

(6) This combined method is not as dependent upon the existance of suitable natural electromagnetic field amplitudes since only the peak energy in the spectrum is required.

(7) ESP is less expensive and more definitive than telluric-magnetotelluric surveys in complex areas.

Several detailed field surveys have been conducted in the Western United States utilizing ESP profiles and more definitive results were obtained than from conventional electrical resistivity surveys that could have been completed at a similar cost (Pritchard and Zebal, 1978). This was especially true in those areas which contained a considerable thickness of moderately resistive material above the conductive layer.

The versatility of this technique lends itself to solving both geothermal and petroleum problems where complex geologic settings occur. However, it must be remembered that while less ambiguous results can be obtained from this type of survey, a certain degree of ambiguity will exist in the interpretation of any geophysical data obtained in complex areas.

REFERENCES

Anderson, Walter, 1974, Electromagnetic fields about a finite electric wire source: available only from U.S. Dept. Commerce Natl. Tech. Inf. Service, Springfield, VA 22161, as U.S. G.S. Rept. GD-74-041, PB 238 199.

Anderson, Walter, 1977, Marquardt inversion of vertical magnetic field measurements from a grounded wire source: available only from . . . "same as above" . . ., as U.S.G.S. Rept. GD-77-001 PB 263 924.

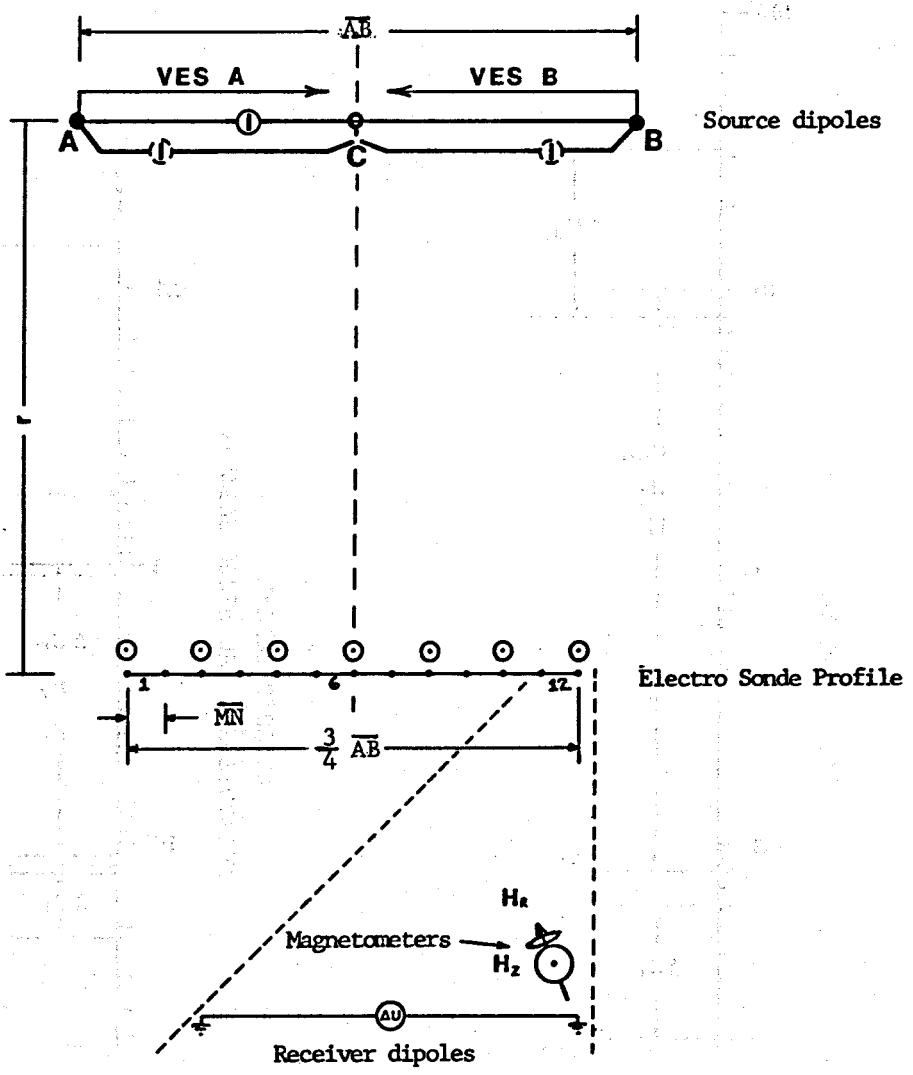
Beyer, H., 1977, Telluric and d.c. resistivity techniques applied to the geophysical investigation of Basin and Range geothermal systems, Part I: The E-field ratio telluric method, LBL-6325-1/3: Lawrence Berkeley Lab., Univ. of CA, Berkeley.

Combs, Jim, 1975, Summary of Section IV, geophysical techniques in exploration: Proceedings, Second U.N. Symp. on the Development and Use of Geothermal Resources, Vol. 1, lxxxi-lxxxvi.

Goldstein, N. E., 1977, Northern Nevada geothermal exploration strategy analysis: Lawrence Berkeley Lab., Univ. of CA, Berkeley, p. 16-17.

Pritchard, J. I. and Zebal, G. P., 1978, Honey Lake KGRA geophysical survey and drilling tests: presented at Geothermal Resource Council Meeting in Hilo, Hawaii, July 25-28.

Vanyan, L. L., 1967, Electromagnetic depth sounding: selected and translated by Keller, G. V., New York, Consultants Bureau.



LEGEND

H_Z Time domain vertical magnetic field response (0.08-10hz equiv.)
H_R Time domain horizontal radial magnetic field response (0.08-10hz equiv.)
ΔU_{AT} End-on-end audio-telluric response (8-32hz)
ΔU_{EMP} Parallel electric field time domain response (0.8-10hz equiv.)
ΔU_T End-on-end telluric response (0.02-0.06hz)
ΔU_{DCP} Parallel static electric field response (0.0hz equiv.)
VES A Modified Schlumberger sounding

Figure 1. Electro Sonde Profile scheme.

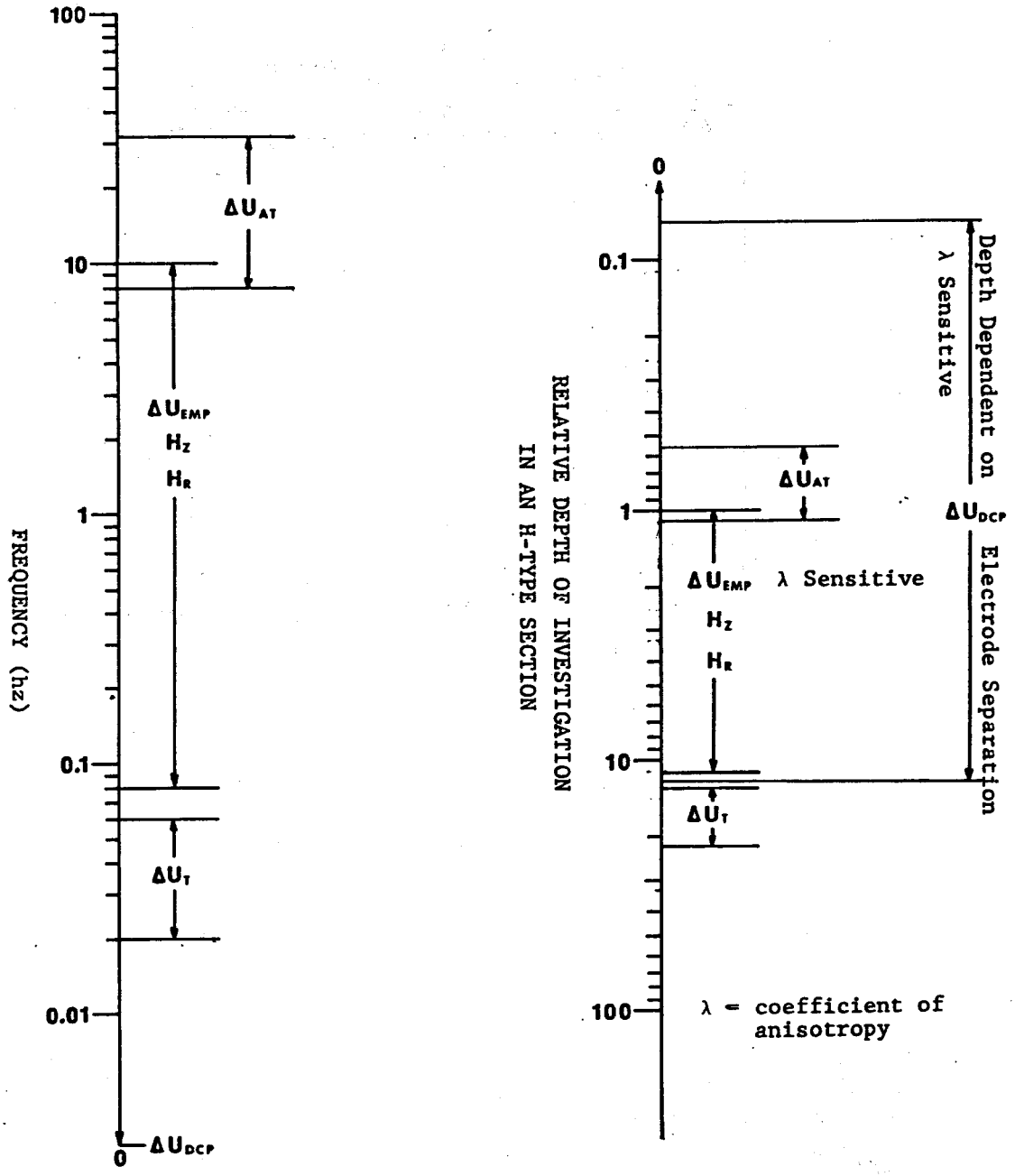


Figure 2. Frequency distribution and relative depth of investigation of the various Electro Sonde Profiling measurements. See Figure 3 for definition of the abbreviations.

Geothermal Resources Council, TRANSACTIONS, Vol. 2 July 1978

STATUS REPORT - GEOTHERMAL OPERATIONS RESEARCH PROJECT FOR CALIFORNIA AND HAWAII

Jeffery W. Wiegand*, and
Craig Cummings**

*Science Applications, Inc.
**U.S. Department of Energy

The purpose of this paper is to present a status report on a U.S. Department of Energy Geothermal Contract No. ET-78-C-03-1529. The objective of the Geothermal Operations Research Project is to develop, update and refine realistic scenarios for the development and commercial utilization of geothermal energy resources in California and Hawaii. To ensure achievement of the potential of the regional scenarios, it is necessary to evaluate the potential regional contributions to the national energy goals, as well as identify the type, magnitude, and scheduling of Federal, State and local, public, industrial and commercial actions needed at the present time and in the future.

During the initial period of the contract, the primary effort has been concentrated in the following activities:

- developing a site-specific electric scenario at Heber, CA, and Puna, HI;
- making contacts and participating in meetings within the geothermal community; and
- developing a technical basis and rationale for approaching direct use scenarios.

At the Project Review Meeting in Sacramento on March 6th, the first-order electric scenario for Heber was presented. The purpose of this scenario is to:

1. provide a planned time sequence for bringing power on-line;
2. lay groundwork for monitoring;
3. bring all pertinent parties into the planning process; and
4. identify actions needed by all parties in order to actualize the potential of the prospect.

Under present industry planning, the Heber area is likely to be the first liquid-dominated resource at which commercial scale power production begins (50 MW or more). The first power plant on-line can be expected at Heber in early 1981. Ideally, additional power plants on the order of 50 MW in size should be achieved in 1982 and thereafter, leading to the installation of up to 300 MW by the end of 1985, and full development of the field to 1000 MW installed capacity in the mid 1990's. One thousand MW is taken as a conservative figure for full field development in view of resource potential estimates of 100 to 2000 MW for 30 years.

In developing this scenario, geophysical, technical, environmental, regulatory, economic and financial requirements for development have been examined. Certain key requirements for achievement of this scenario have been identified and programmatic recommendations prepared accordingly. Without these, delays in the completion of power plants will begin to develop in the 1979-1980 time frame and amount to 2 to 3 years in duration by the late 1980's.

The preliminary recommendations resulting from the analysis of the Heber scenario are shown in Table I, including the beneficial impact on the scenario of each recommendation and the date by which each action is necessary to avoid delaying the scenario. Further analysis and refinements of the scenario are likely to result in additional suggestions; however, the items in Table I will remain as major needs requiring action fairly soon if geothermal development at Heber is to progress rapidly.

In addition to completing the Heber electric scenario, work is continuing on the direct use scenario and an electric scenario for Puna, HI (results to be presented at meeting).

Some of the pertinent highlights of the Puna scenario are resource assessment, utilization of the power produced,

Table I. Summary of Heber Programmatic Needs

RECOMMENDED ACTION	BENEFIT IN HEBER SCENARIO	DOE ROLE	SUGGESTED LEAD AGENCY	DATE NEEDED
EXPAND IMPERIAL COUNTY PLANNING OFFICE CAPABILITIES.	ELIMINATION OF DELAYS OF UP TO TWO YEARS.	FUNDING GRANT OF IMPERIAL COUNTY	DOE AND CERCDC	LATE 1978 TO TO EARLY 1979
DEFINE CERCDC ROLE	REDUCE INDUSTRY UNCERTAINTY. PREVENT CREATION OF NEW DELAYS.	N/A	CERCDC	1979
PROVIDE TAX INCENTIVES	ENCOURAGE NECESSARY INDUSTRY COMMITMENT.	SUPPORT NECESSARY LEGISLATION	CONGRESS	EARLY 1979
- INVESTMENT CREDIT	GREATEST IMPACT IN THE NEAR-TERM BENEFITS BOTH UTILITY AND FIELD DEVELOPER.			
- DEPLETION ALLOWANCE	STRONG IMPACT. ENCOURAGES FIELD DEVELOPERS TO ACCEPT RISKS.			
- INTANGIBLE COSTS WRITEOFF	SMALL IMPACT. PRIMARILY BENEFITS FIELD DEVELOPER.			
SETTLE MAJOR QUESTIONS REGARDING PROVISION OF COOLING WATER	ESSENTIAL FOR PERMITTING OF POWER PLANTS.	INITIATE DISCUSSIONS WITH ALL AGENCIES INVOLVED.	DOE	MID-1980
PROVIDE FOR IMPROVED SEISMIC BASELINE FOR HEBER	PREVENT POSSIBLE LONG DELAYS IN FUTURE.	PROVIDE FUNDS IF NECESSARY	USGS	1978 OR 1979

Jeffery W. Wiegand
Craig Cummings

permitting requirements, recently enacted State geothermal regulations, county-State aspects, the current state of pertinent projects such as the wellhead generator, possible direct uses, and the environmental and sociological aspects of the development of geothermal energy.

Seven tasks have been identified which constitute the scope of the Geothermal Operations Research Project. They are:

1. refining and updating the preliminary regional geothermal energy development scenarios;
2. developing a regional progress monitor;
3. performing market analysis;
4. constructing institutional and financial profiles;
5. generating cost/benefit analyses and cost-effectiveness analyses of Federal and State government measures;
6. developing a local area cost/benefit analysis; and
7. providing support to DOE-DGE, the regional systems development contractor and the national operations research contractor.

A status report providing an update of the activities of the SAI Geothermal Research Staff will be available at the Geothermal Resources Council meeting to be held in Hilo, HI, on July 25-28, 1978.

Geothermal Resources Council, TRANSACTIONS, Vol. 2 July 1978

Dup

GEOTHERMAL DRILLING IN HOT GRANITIC ROCK

R. E. Williams

UNIVERSITY OF CALIFORNIA
LOS ALAMOS SCIENTIFIC LABORATORY
LOS ALAMOS, NEW MEXICO 87545

Geothermal drilling has largely followed the methods of the oil well drilling industry. It has used the techniques, tools, and indeed the personnel and equipment used by this older industry. This is natural and certainly justified as the most cost effective method.

Some extension of the methods used in oil well drilling is now being required in order to penetrate the hotter zones and the harder rocks from which geothermal energy can be obtained. Fortunately, some of the established producers of oil field equipment see the possibilities of an expanding, though presently small, market for their equipment in the geothermal area. They also see that many of the developments of equipment for geothermal use also have an application in the drilling of deeper and hotter holes for hydrocarbons. Therefore, while we in the geothermal field are continuing to learn and obtain valuable information from the older drillers, we are now in a position to share in the advancement of some techniques and equipment development which will be of use in the drilling for hydrocarbons.

In the hot dry rock program, we see the most urgent techniques and equipment problems as those shown in Tables I and II which list the problems and their present status.

An elaboration of the status of each of these various problem areas is as follows:

Mud Motors. Because of the temperature limitations of presently available mud motors, a new turbodrill has been designed for our needs by Maurer Engineering, Inc. of Houston, Texas. The first unit is now being manufactured. This unit is required to meet the high temperatures we will encounter and is designed with special blades which will cause it to rotate more slowly than presently-available downhole motors. Characteristics are as follows for the version of this motor which is especially designed for use in directional drilling with button-type roller bits: rotary speed 150 rpm; diameter 7-3/4-in.; length 21 ft; power output 36 hp; flow rates 400 gpm; temperature limit 350°C (662°F); and bearing life 50 h at 275°C (527°F). Unfortunately, we will have only one of these units, plus replacement parts, for our next drilling program. The only backup is the Dyna-Drill or similar mud motors which have temperature limitations of

TABLE I

HEAT-RELATED PROBLEMS

Item	Problem	Solution or Status
Mud Motors	Temperature limitations of elastomers used in these units.	A new all-metal turbodrill with a slower speed has been designed and is being fabricated.
	Inability to run at slow speeds for efficient use of button-type bits.	
Steering Tools	Heat limit of internal components.	Suppliers are providing heat shields to protect equipment for limited time down hole.
Open-Hole Packers	Temperature limitations of elastomers used extensively in these units.	Suppliers are experimenting with higher temperature elastomers and asbestos-type compression packers.
Cementing	Emplacement difficulties.	Testing closely controlled samples at downhole temperatures.
	Deterioration of cement at high temperatures and under cyclic conditions.	Possible use of polymeric cements or viscous epoxy fluids. No good solution now appears evident.

TABLE II

HARD ROCK-RELATED PROBLEMS

Item	Problem	Solution or Status
Sidetracking in Granitic Rock	Neither special diamond bits or standard button-type bits cut satisfactorily into hard walls.	Use of special button-type bits with extremely hard "gage" buttons.
Coring	Sub-marginal cutting of diamond coring bits in fractured granitic formation.	Use of hybrid button-stratapax bits.
Standard	Low bearing and button life.	Use of hard-rock type mining bits altered for use with water.

about 196°C (385°F) but which may be utilized at somewhat higher temperatures by hole cooling and cutting back on bit loading.

Steering Tools. Two companies, Eastman Whipstock and Sperry-Sun, have agreed to improve the temperature capabilities of their directional steering tools to meet our needs in the 250 to 275°C (482 to 527°F) temperature range. It is expected that these tools will be required for much of the directional drilling that is performed below a depth of 8000 ft or at temperatures greater than 166°C (330°F). Heat shielding will increase the tool diameters to about 3 in., which will necessitate a limitation on the minimum inside diameter of the drill string and particularly on the non-magnetic drill collar. The expected limit on the time the tools can spend downhole in a 250°C (482°F) environment is 6 h. In order to cut down on the cost of steering tool services, the old method of directional drilling using single-shot orientation tools will be used when it is practical.

Open-Hole Packers. In the early fracturing work at the Fenton Hill site, many commercial packers were tried and found to be inadequate for our temperature requirements. However, for the last redrilling program, Lynes Services, Inc. provided inflatable packers which had been designed for temperatures of 195°C (383°F) and pressures of 2000 psi. These packers were used successfully downhole at 187°C (368°F) and 1830 psi. At these conditions, the elastomer coatings of the packers became bonded to the walls of the formation and were stripped from the packer as it was removed from the holes. The packers were not reusable. They performed adequately in packing off the formation and continued to function during inflations of as long as 20 h.

The 195°C rated packers used previously will not be adequate for our next fracturing job. Therefore, we have interested Guiberson and Brown Oil Tools, as well as Lynes, in providing us with high-temperature packers for this work. Lynes and Brown Oil Tools are planning, as far as we now know, to propose their standard products modified by the use of high-temperature elastomeric compounds for this work. Guiberson is proposing an asbestos compression-type packer modeled after a unit which they have not marketed since the 1940's. These packers are all being tested at high-temperatures.

Our requirement for these packers is perhaps unique since they will not be subjected to any petroleum products. This undoubtedly will ease the problem of locating materials which will withstand the 250°C (482°F) or greater temperatures we expect to encounter.

Cementing. Pumping and emplacement problems have been eliminated by closely monitoring the cement batching and by testing samples of each batch prior to pumping. Samples, mixed with water from our local well, are tested at temperature by the cementing service company prior to pumping the cement into the hole.

Standard cements which are available are not able to withstand the high temperature now encountered (200°C) and the temperature cycling which is the result of intermittent flow thru the system. With the higher temperatures we expect to obtain at greater depths (250°C), this problem will be more severe. It is suspected that these standard cements crack and do not satisfactorily seal off the water flow in the annulus around the casings. Polymeric cements have been suggested as solutions to this problem and we are now beginning to investigate the possibilities of using these cements. Also the use of very viscous epoxy fluids to seal cracks in the standard cements is another possibility. Hopefully, one of these methods will appear sufficiently promising by the time we conduct our next casing cementing operation.

Drill Bits. For drilling holes in hot, hard granitic rock we have found that tungsten carbide insert bits are doing an excellent job. The bits we have used are mining-type bits (Security Type H-100 and Smith Tool Type 9JA). When using unsealed air-type bits, the air passages were sealed off to prevent the drilling mud from fouling the bearings. These bits are used in rotary drilling at 40 rpm and 40,000-lb load; they are also used in directional drilling with the Dyna-Drill at speeds of 400 rpm but with reduced life. No problems are expected in using these bits at temperatures up to 250°C (482°F). Hopefully they will continue to function well at even higher temperatures.

Sidetracking Bits. During our last drilling operation, a 9-5/8-in. hole was sidetracked twice. The first of these operations required 2-1/2 weeks and was performed with both specially-designed diamond bits and standard-type tungsten-carbide button bits. These bits were used with a Dyna-Drill and a kick sub or with a Dyna-Drill with a

bent housing. The diamond bits were successful in cutting only a few feet of hole at best and often the side-cutting surfaces appeared to have been badly worn by scraping the side of the hole before the bits reached bottom. Diamond bits were preferred at the beginning of this operation as specially-designed bits could be procured in about 36 h, whereas the procurement time of specially-designed button bits was prohibitative. The second sidetracking operation was performed using only the standard button bits and was accomplished in 2-1/2 days. This improvement in time was probably due to improvement in the drilling techniques, but as it was performed inexpensively with button bits, we plan to use this general type of bit for any future sidetracking attempts. For this purpose, we have ordered two special bits from Smith Tool with extra hard buttons on the "gage" surfaces. We are also looking for any other bit which appears to have the capability of side cutting into granitic formations.

Coring Bits. Our coring bit experience has been quite similar to the sidetracking bit experience. In our last drilling operation, five attempts were made with diamond bits to obtain granitic cores. From these attempts, only one core about 2 ft long was obtained. One coring run was made using a Smith hybrid-type bit with both tungsten-carbide roller cones and stratapax snythetic diamonds. This run produced 4 ft of core. We are ordering an improved version of these hybrid bits for use in the next drilling program.

THE UTILIZATION OF HOT DRY ROCK
- A Scenario -

Ralph E. Williams

Denver Research Institute
Denver, Colorado 80208

ABSTRACT

A scenario is a statement of what could possibly happen, based upon a knowledge of what currently exists and upon what may be reasonable assumed. A scenario is not a prediction of what is likely to occur.

Portions of this work were sponsored by the Los Alamos Scientific Laboratories.

The year 1990 was realized to have been the harbinger of scarce traditional energy supplies. Twenty years earlier, energy economists and visionary scientists had forecast that the 1990's into the year 2000 would be severe in terms of oil and gas shortages. True, coal had made an impact on the energy scene, and its use had helped to alleviate some of the unpleasant times over the past years, such as the OPEC oil embargoes of 1979 and 1986, and the closing of the Alaskan pipeline in 1893 due to a major structural flaw. However, coal burning brought its own problems, especially in air pollution. A greater than ever amount of sulphur, sulphuric acid and particulates hovered over many cities. Because of the relatively large coal reserve, many industries and utility companies switched over entirely to coal; yet these industries were now facing strict new federal legislation limiting coal burning in dangerous highly polluted areas. It came as a surprise to no one that citizens were desperately urging their congressmen to pass immediate "crash" programs to develop alternate energy sources such as solar, wind, and geothermal. If government had been responsive to industry by providing, for example, geothermal exploration with the same intangible drilling expense tax break allotted to the oil industry, much of the needed exploration incentive would have spurred development and production at an earlier time.

The city of Saddle Creek in the Rocky Mountains with a population of 22,000 and about 6,000 houses initiated a plan in 1977 that would make them energy independent by the turn of the century. The motivation for the action was precipitated from the oil embargo of 1974 which left Saddle Creek with a three weeks' supply of fuel oil and a bankrupt oil distributor. Located within a potential KGRA (Known Geothermal Resource Area) the citizens of Saddle Creek voted for a bond that would help finance preliminary geological/geophysical exploration of their energy potential.

A local geothermal exploration company was hired for the initial exploration work that was structured to meet the following criteria:

1. To determine if the geothermal resource (if any) was adequate to support converting the buildings of Saddle Creek for long-term utilization of geothermal fluids for space heating purposes.

2. To determine the costs and practicality of remodeling the existing heating systems using low temperature (80°C) water.

3. To prepare a design model of the geothermal distribution system that would be adequate for the intended purpose.

4. To examine environmental questions.

5. To build and test the proposed geothermal system to accurately demonstrate construction and operation costs. (Schmitt et al, 1976).

A brief breakdown of the results of the geothermal consulting firm was the following:

A. Geological Studies

1. Remote sensing of the area helped in locating faults and in the mapping of surface features around Saddle Creek.

2. Hand samples of rock enabled a detailed petrographic study of the area so that a prediction of the rock type at depth could be made.

3. A detailed study was made to determine the fracture orientations of the rock because the analyzed basement rock is believed to be crystalline and impermeable, therefore perhaps necessitating future fracturing for water circulation.

B. Geophysical

1. Heat flow studies - These revealed the existence of a large regional conductive heat flow, and it was suspected that this was associated with an active magma chamber.

2. Seismic refraction and magnetometer surveys - These determined that the basement rock was within two kilometers of the surface and that minor indications of active fault zones or dormant faults existed in the target area.

3. Geoelectromagnetic studies - These were helpful in locating and determining subsurface heat flows and useful resistivity parameters.

C. Exploratory Drilling

1. Four wells were drilled to measure temperature gradients with depth, as well as a sampling well, which would have been used had any fluid been present to sample.

2. The exploratory wells revealed that a high temperature of 160°C was found at the bottom of an 8,000 foot well.

These limited geological and geophysical investigations of the Saddle Creek area pointed to the evidence of a geothermal resource, and especially a hot dry rock resource, these criteria being:

1. An attractive temperature at an economic drilling depth,

2. Impermeable basement rock,

3. A lack of active faults, (Laughlin and West, 1976).

Economic factors are also essential in the development of any enterprise and the City of Saddle Creek decided that it should commission a study of a proposed geothermal system amortized over a reasonable length of time (20-30 years) vs. the present cost of fuel oil escalated through the same period of time. Figure 1 presents graphically the results of this study.

Motivated by the long term value of geothermal exploration and space-heating production, the important consideration of degree days was investigated. Saddle Creek has less than 6000°F degree days per year. If the proposed system was exclusively geothermal, (based on a usable temperature of 120°F) then the system would have to be efficient in the winter low range of -12°F. However, in this range, the system would operate at 20%-22% efficiency, and it would be difficult to justify such a cost intensive project for such a relatively low utilization factor. The consideration was then proposed to design the geothermal system in the 20°F-30°F range in order to maximize utilization during most of the heating season months. If temperatures over a given month dropped below the efficiency of the geothermal system, a backup fossil fuel system would then become operable. The graphs in Figure 2 help to justify this rational.

Comments that are applicable to the graph are the following:

1. Designing the system for twice the load is made by halving the normal temperature design.

2. With fossil fuel peaking for colder days, fossil fuels need to supply only 6% of the total energy requirements.

3. Overall economics of geothermal heating is improved by about 35%. (Kunze et al; 1977).

With geologic and economic analysis showing favorable signs for hot dry rock geothermal development, an adequate source of water was needed. The nearby Menick River with its near drinking quality water was chosen as a source. As the proposed system would be an elongated circulation loop, a volume of water equal to the carrying capacity of the pipe network as well as the cross-sectional area of circulation loop within the fractured reservoir would be needed. A reservoir was built for this purpose by damming the river with an added volume of water to serve as a built-in reserve to compensate for water loss due to subsurface loss and surface evaporation.

Other necessary factors were considered and the town decided on the following plan of action.

1. A legal advisor was hired to interpret and recommend State and Federal laws that would guide the resource development.

2. An application to the Department of Energy was made for an approved guaranteed loan where up to 75% of the costs toward geothermal energy development up to a value of fifty million dollars would be covered.

3. The solicitation of advice in the exploration and development of the hot dry rock resource was sought from the national scientific laboratories.

4. The establishment of a watchdog committee to oversee any potential insurmountable environmental problems such as micro-earthquakes caused by hydrofracturing, subsidence, air pollution, or ground water pollution.

Eventually, Saddle Creek subcontracted many aspects of development and production to qualified firms, and the city was using geothermal energy to meet all of its heating needs at a substantial reduction over traditional fuel costs by 1990.

References:

Schmitt, R. C., Donovan, L. E., Spencer, S. G., Keller, J. G., and Stoker, R. C., 1976, Report to the Idaho Governor-Project Summary for the Boise Space Heating Project: Idaho National Engineering Laboratory.

Laughlin, A. W., and West, F. G., 1976, The Zuni Mountains, New Mexico, as a Potential Dry Hot Rock Geothermal Energy Site: Los Alamos Scientific Laboratory, LA-6197-MS.

Kunze, J. G., Donovan, L. E., and Griffith, J. L., 1977, The Size Effect for Distant Space Heating in Boise, Idaho: In Geothermal: State of the Art, Transactions, Geothermal Resources Council, Vol. 1, 1977.

Rowley, J., LASL, Personal Communication, 1978.

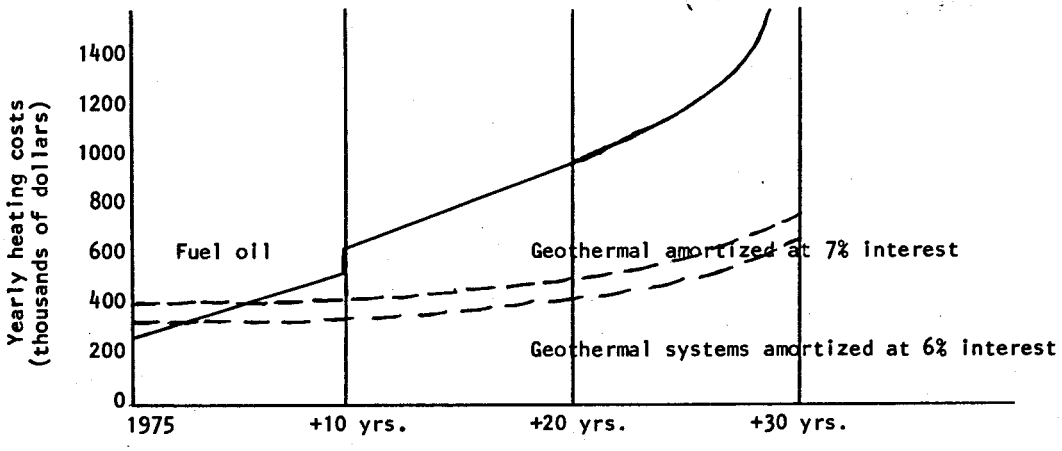
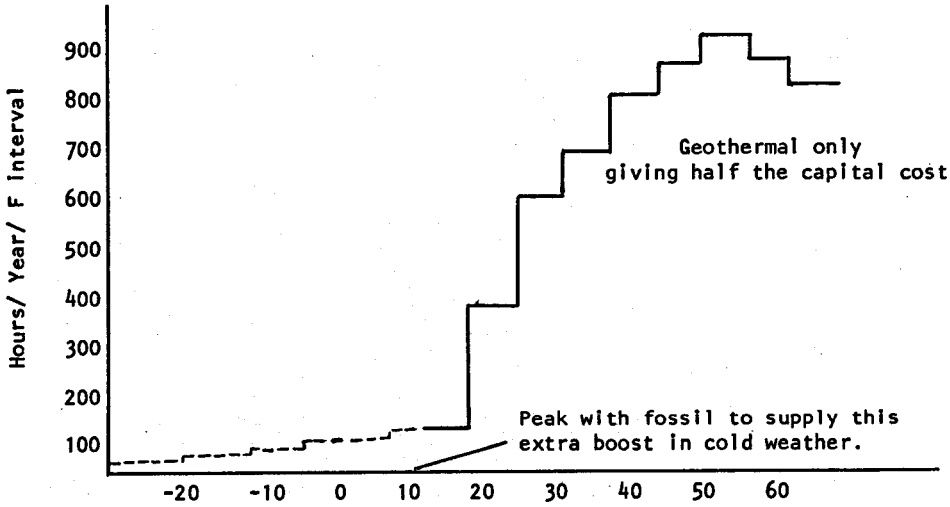


FIGURE 1

(Adapted)
(Schmitt, et al, 1976)



(After Kunze, Donovan & Griffith - 1977)

FIGURE 2

Geothermal Resources Council, TRANSACTIONS, Vol. 2 July 1978

WELL PENETRATION AND STIMULATION

Ralph E. Williams

Denver Research Institute
Denver, Colorado 80208

ABSTRACT

Two aspects of explosive fracturing--depth of penetration and degree of fracturing were investigated. A study was made of penetrators employing designs other than typical conical shaped charges. Configurations included linear, hemispherical and "dished" designed shaped charges. Through the mechanism of wave shaping as a technique for shock enhancement, fracturing of a host rock was investigated. These two elements, depth of penetration and degree of fracturing, were used as criteria for the design of a single package which generally consists of simultaneously initiated perforators closely followed by a main driver charge(s) which is (are) wave-shaped to cause fracturing in a rock media. The device was successfully field tested in five marginal oil wells and indicates an applicability to geothermal stimulation.

The research was sponsored by Pene-frac Inc. of Houston, Texas.

Explosives have been used in fracturing to generate high pressure shock waves. When initiated, an explosive decomposes by detonation and a radially expanding shock wave is generated which places the host rock in compression--both by the shock wave and by the expanding gases. The compression wave is followed by a tensile reflection which can shatter the rock. While less "brute force" methods such as acidization or hydraulic fracturing tend to produce fractures in a definitive pattern; explosively generated fractures tend to produce a more random and interconnecting system of fractures. The degree of success for explosive fracturing is very dependent on the pressures produced and the positive duration of the overpressure. To improve explosive fracturing, techniques will be necessary to develop and test prototypes designed to enhance the positive duration by at least one order of magnitude.

In general, an explosive device is lowered into a well to a predetermined depth near the producing zone and detonated. One of these techniques achieves penetration through the application of shaped charge explosive devices. The basis for shaped charge action was first noted by Munroe, but little use was made of this effect until 1940. During and after World War II, specialized shaped charges were developed for use against specific military targets to a high level of sophistication. Also, the effectiveness of such directed explosive energy found wide application in various industrial processes. Shaped charges are manufactured to a degree of sophistication such that they are now off-the-shelf stock items. However, the bulk of information available at this moment of these items is relevant to the penetration of some homogeneous* target media in air, with few exceptions. That is, the penetration of a heterogeneous** media such as water, well casing (steel), and concrete has not been studied to the depth that the homogeneous target has. It could be expected that in the case of the heterogeneous target, that when a longitudinal stress wave strikes the boundary between the steel casing and the concrete grout, part of the stress will be transmitted through the concrete and part will be reflected back through the steel well casing. The same conditions will hold true for the stress wave striking the concrete-rock boundary. This "impedence mismatching" was characterized as much as possible from available physical properties of the target materials.

Other available data on penetration of heterogeneous media shows the effect of the liquid layer to be detrimental even though additional confinement of the explosive is available when the test charges are submerged. A reduction in the penetration that can be expected in air by a factor of the order of two has been observed.

In similar fashion, shaped charge penetration of siliceous materials is notably poor. This observed fact has been a major factor limiting the use of shaped charges in such applications as rock drilling, well stimulation, etc. Consequently, the effective use of shaped explosive charges for the penetration of heterogeneous media required the development of specialized configurations of explosive and liner to achieve not only crack initiation, but also propagation. Discussion of two basic approaches that indicate promise in the case of a water-steel target are presented:

* A homogeneous target is defined as one comprising only one phase, usually a solid or solids, with little or no separation by vapor fluid phases.

**A heterogeneous target is defined as being comprised of two or more phases, interspersed.

The two basic approaches consider first the mechanisms that will permit the reliable penetration of the system directly by the energy focusing characteristic of shaped charges. The second approach will consider mechanisms by which the explosive energy can be coupled to the liquid medium in such fashion that the liquid becomes a primary damage agent, e.g., explosive forming and punching operations using water as a transfer medium and the well-known fact that bubble collapse and/or bubble cycling is normally the primary damage mechanism in the instance of conventional depth charges applied against submarines.

The theory of shaped charge action is based on the control of the detonation wave front, or wave-shaping. In the case of lined conical cavity charges, a jet or slug is formed from the liner material which is propelled along the axis of the conical cavity at high velocity, of the order of 30,000 feet per second. When this jet impacts a target, e.g., a steel well casing, pressures of the order of 3.75×10^6 psi are created--far in excess of the yield strengths of common materials--and the casing behaves like a liquid. An elementary prediction of the penetration, based on hydrodynamic theory, states that

$$P \propto \ell \sqrt{\frac{\rho_j}{\rho}}$$

in which P is penetration, ρ_j the average density of the jet, ρ the density of the target and ℓ the length of the jet. The reason for the reduction in penetration of a charge fired in, say, water as compared to air, is evident, The rate at which the jet is used up is proportional to $\sqrt{\rho}$. On this basis, the penetration in air, water, and steel is as 1:0.036:0.013 and it appears that water is approximately one-third as difficult for the jet to penetrate as steel.

It is evident that penetration can be improved by a design of a charge that will act to first reduce the amount of liquid in the path of the penetration element--usually a jet or wedge. This is difficult to accomplish with charges that weigh only a few pounds because, at these 120,000-360,000 in. sec.$^{-1}$ velocities (of detonation) the time available for the "special actions" to aid the penetration by "clearing the path" of water is only of the order of ten microseconds or less. Inertia effects, etc., make it difficult to obtain good penetration with simple systems under these conditions.

However, on effect that may prove useful in "clearing a path" for the shaped charge slug is the exploitation of induced cavitation. For example, it was discovered by the German Research Establishment during World War II that as much as thirty percent of the explosive energy of air-dropped devices, e.g., torpedoes, depth charges, and bombs, was lost through "venting" along the cavitated entry path into the water. One general concept is to first initiate an annular ring of explosive or several separate charges simultaneously. Extremely intense, high speed shock waves due to mutual shock reinforcement have been observed in seismic studies using the concept.*** The resulting cavitation path which should develop at velocities in excess 5,000 per second, should materially assist in "clearing a path" to the second target plate for the shaped charge jet. In the above concept, it is not intended (as will be discussed later) to perform perforations by any device other than the shaped charge.

In regard to the water environment explosive forming and depth charge studies have indicated that the water itself can be used very effectively as an energy transfer and focusing medium. The detonation of a spherical charge next to a target tends to emit its energy in an isotropic fashion and the direct energy applied to the target plate may not perform sufficient work on the target plate to produce rupture. However, on collapse, the target itself inhibits the symmetrical collapse of the gas bubble and a significant proportion of the initial explosive energy is thereby directed at a local area of the target. This effect has been studied photographically and target damage was observed to occur during bubble collapse.

The DRI concept, therefore, includes two facets--first, penetration and second, fracturing. Conceptually, the design package may be considered to be cylindrical with linear shaped charges located around the cylinder. The ends of the cylinder may be a conventional explosive or a metalized explosive. The cylinder may be a solid explosive or may have an air or water cavity. Upon initiation, the shaped-charges penetrated the casing and rock formation. Microseconds after the shaped-charges are fired, simultaneous initiation of the main "driver" charge will occur. Through wave-shaping, a high pressure pulse will be driven radially from the axis of the charge. It is expected that this shock enhancement will cause fractures to extend and by placing the rock in alternate compression and tension will cause massive fracturing around the perforations.

Several of these devices were fabricated and field tested in marginal oil wells. Depths to producing zones ranged from 900 feet to 11,000 feet. In all cases production was increased substantially.

We feel that by suitable design for high temperatures, this novel device can be of benefit to the geothermal industry.

***Reference Project WHITE TRIBE, Ballistic Research Laboratories, APG, Aberdeen, Maryland.

ST LUCIA GEOTHERMAL PROJECT

K.H. WILLIAMSON E. P. WRIGHT

Institute of Geological Sciences, London SW7 2DE, U.K.

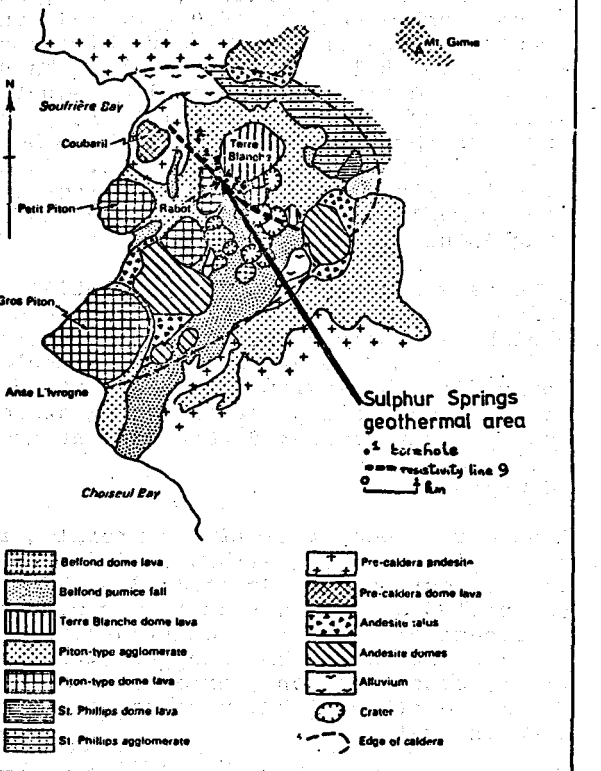
The St. Lucia Project is the first geothermal study overseas undertaken by the Institute of Geological Sciences. It was commissioned by the Ministry of Overseas Development (U.K.) and carried out in conjunction with Merz and McLellan, Consultant Engineers. The University of the West Indies also participated in studies of the geology and seismicity of the areas. The object of the investigations was to develop geothermal steam for electric power.

St. Lucia is one of the islands of the Lesser Antilles which is a chain linking the northeast of Venezuela with Puerto Rico and the Greater Antilles. It has a roughly elliptical shape 45 x 22 km. The island is entirely volcanic with ages ranging from Lower Miocene to fairly Recent (40,000 years B P). Steam fumaroles and boiling pools, known as Sulphur Springs, occur in the Soufriere area in S. W. St. Lucia, and are associated with the Qualibou Caldera, the youngest of the volcanic centres (figure 1). The caldera is about 6 km in diameter and is thought to have collapsed during the mid Pleistocene with the peripheral fault having a throw of the order of 250 meters. Sulphur Springs is an area of fumaroles and boiling pools located in a narrow valley between the domes of Rabot and Terre Blanche. The area of present activity extends over some 20,000 sq.m and the surface valley fill in the vicinity is intensely altered and kaolinised with formation of sulphur and gypsum. During the recent investigations, pool water temperatures showed a range from 63-96°C and the maximum temperature of the fumaroles was 185°C.

Boiling mudpools, steam vents, thermal springs and a number of cold springs and waterwells within the Qualibou Caldera were sampled and analysed for major elements, some minor elements (Si, B, Sr) stable isotopes of oxygen and hydrogen, and tritium levels.

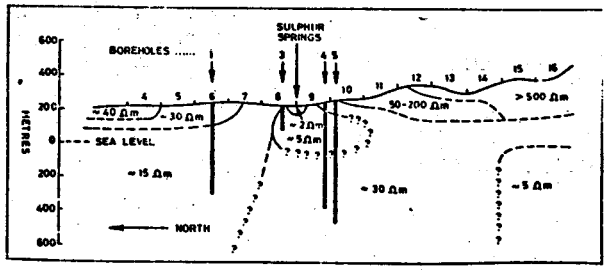
Recently developed mudpools were found to be acid sulphate type (pH 3.0) while older ones were slight acid or neutral (pH around 5-7) and sodium calcium sulphate type. Temperatures within the mudpools

Figure 1 Qualibou Caldera



ranged from 66-96°C. The highest reported temperature from a steam vent was 185°C, and noncondensable gas associated with this steam contained 92% CO_2 and 2% H_2S. Low tritium levels in the steam condensate indicated that the turnover time for the reservoir fluids was in excess of twenty years. The stable isotope compositions of oxygen and hydrogen showed a considerable enrichment in ^{18}O relative to surface to meteoric water, which suggested that extensive steam-wallrock reaction had occured. Boron levels within the mudpools (up to 1000 mg/1) were anomalously high with respect to a background level of less than 0.1 mg/1.

Thermal springs sampled in the area typi-



LINE 9 ESTIMATED TRUE RESISTIVITY SECTION

Fig 2. Line 9 Resistivity model

cally had low flow rates (5 - 100 1/min), were roughly neutral (6.0 - 8.0 pH) and could be classified as sodium bicarbonate type with low mineralisation. This water is derived from a shallow aquifer within pyroclastic debris infilling the Sulphur Springs Valley, contained between the massive dacitic domes. Boron levels within these thermal springs (up to 14 mg/1) were also well above the background level.

The very high levels of the volatile element boron in mudpools, their acid sulphate composition, and the occurence of steam in a fumarole with an enthalpy exceeding the maximum enthalpy of saturated steam, all point to the existence of a vapour dominated reservoir at depth.

GEOPHYSICS

A number of deep resistivity profiles in the region of the Qualibou Caldera were carried out using a Scintrex 2.5 kW commutated direct current system with the dipole-dipole electrode configuration. A total of 50 line - km of apparent resistivity cross-sections, extending to a maximum depth of 1 km, were constructed from the data.

Throughout the survey area, apparent resistivity values were low (3-500Ωm) and typically less than 50Ωm. The most interesting anomalies occurred on survey line 9 which passed close to the Sulphur Springs emanations. On this line the apparent resistivity cross-section in the vicinity of the Springs suggested a zone of low resistivity (<5Ωm) near the surface and another of comparatively high resistivity at depth. This was consistent with a model for a vapour-dominated geothermal reservoir in which a low resistivity upper zone of condensing steam overlies a comparatively high resistivity zone where rock pores are vapour filled. However, computer modelling studies showed that the apparent high resistivity zone at depth was probably due to near surface lateral variations in resistivity. (figure 2). The geological complexity, coupled with severe topography in this area, made the resistivity method difficult to carry out in the field and difficult to interpret. HOwever an area of generally low resistivity (5Ωm) surrounding a very low resistivity (2Ωm) zone was identified at Sulphur Springs. Deeper anomalies (say below 400 m) would probably not be detectable in this environment.

A total of seven holes were drilled (figure 1), ranging in depth from 116 to 726 meters. Steam was produced from four of these and it is hoped that the two most successful can be utilised for producing electricity. Holes 1 (527 m) and 2 (116 m) were drilled to the north of Sulphur Springs and sited mainly on the evidence of the northerly extension of kaolinised rocks and on the presence of hot springs to the north, particularly near Terre Blanche. Both holes were cold. Hole 3 (133 m) was drilled very close to the emanations and as was feared, low pressure, low volume steam was encountered at shallow levels requiring the hole to be terminated at an uneconomic depth. Hole 4 (610 m) and 5 (726 m) were both good steam producers although 5 had eventually to be plugged because of surface blow-outs. Hole 6 (692 m) drilled only 100 m from Hole 5 had comparable high temperatures but did not produce steam. Hole 7 (254 m) was finally drilled closed to Hole 4 and is a good producer. The main steam zone yet encountered in the vicinity of 4, 5, 7 is between 250/300 m below ground level. Hydrothermally altered material corresponding with the steam producing zone occurs within the basal dacites overlying the Pre-Caldera rocks.

A number of physical and chemical tests were performed on the discharge from Holes 4 and 7, to determine their output characteristics over a range of operationg pressures and to determine the chemical and isotopic composition of the steam and associated gases. Hole 4 produced 2.1 kg. s^{-1} of steam with 10°C superheat at 10 bars (gauge) wellhead pressure, while Hole 7 produced 4.5 kg.s^{-1} with 40°C superheat of 10 bars (gauge).

Back pressure curves were constructed using bottom hole pressures deduced theoretically from wellhead values. Analysis, of the curves indicated turbulent flow in the formation around well 7, laminar flow around well 4 and kh (intrinsic permeability x formation thickness) values of 10-20 darcy.meters for well 7 and 2-5 darcy.meter for well 4. Pressure build-up tests were also conducted on the wells and similar kh values obtained from HOrner build-up plots.

Chemical and isotopic analyses were carri-

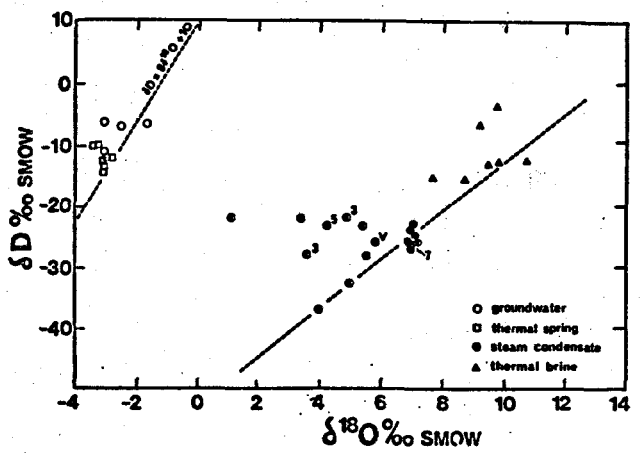


Figure 3

Conventional Delta-Diagram for waters in Sulphur Springs geothermal area.

Stable isotope compositions of hydrogen and oxygen are shown.

Steam condensate samples are from borehole 4, or boreholes 3, 5, 7 where indicated. "V" denotes a natural steam vent.

ed out on the steam condensates, entrained liquids (on Hole 4) and noncondensable gases. A very high noncondensable gas content, 21% by weight, was measured consistently on both holes throughout the test period. The gas composition was approximately 90% CO_2, 2% H_2S, 6% H_2, 1%N_2, 0.5% CH_4. Although this gas content may have been expected to diminish slowly with time, no significant change was detected over an eight month observation period. Large quantities of concentrated brine were discharged from well 4 during wet/dry cycling. The salinities of the samples varied up to levels of Cl at 70,000 mg/1, although 25000 mg/1 was probably a more reasonable figure for the reservoir itself. A likely origin for the chloride is from leaching from the volcanic host rock which the drilling had shown to be extensively altered.

The stable isotope compositions of oxygen and hydrogen for the thermal fluids provide further evidence of extensive reaction with deep reservoir rocks. In figure 3, these compositions are plotted using the δ notation in per mil (‰) variation from a standard (SMOW - Standard Mean Ocean Water).

The samples representing shallow groundwater (open symbols in figure 3) are seen to plot on the isotopic trend ($\delta D = 8\delta^{18}O$ + 10) representing equilibrium fractionation processes in meteoric waters. On the other hand, steam condensates and thermal brines (from Well 4 only) have isotopic compositions which are considerably enriched in ^{18}O relative to the meteoric waters : up to + 13‰ $\delta^{18}O$ heavier. The δD values for brine samples are roughly similar to those for shallow groundwater samples. This coupled with the measured Cl/Br ratio, 60,000 approx. by weight (c.f.marine Cl/Br = 290) suggest that the source of deep fluids is meteoric and not marine. The trend, represented by the dashed line in figure 3, and having a slope of 5, between brine and steam samples demonstrates the evolution of the latter by non-equilibrium evaporation from the thermal brine. The shift of 13‰ in $\delta^{18}O$ of water implies a low proportion of water to rock (supporting the earlier hypothesis of brine evolution from rock leaching alone) and also a high temperature of interaction.

The extent of the reservoir and the location of the heat source have not yet been established. Further information on the heat source will be obtained from a microearthquake study recently completed, and future pressure transient tests using downhole recorders in the producing boreholes may help to define the limits of the reservoir. It is hoped that a back pressure turbo-generator capable of producing 1 MW can be installed to utilise steam produced from wells 4 and 7.

ACKNOWLEDGMENTS

The work presented here was a collaborative effort between Merz and McLellan Consultant Engineers, Institute of Geological Sciences and the Seismic Research Unit of the University of the West Indies. Within the Institute of Geological Sciences, major contributions came from D. K. Buckley, A. H. Bath, P. G. Greenwood and M. K. Lee. This paper is presented with the permission of the Director, Institute of Geological Sciences.

ACOUSTIC SENSOR DEVELOPMENT FOR GEOTHERMAL BOREHOLE TELEVIEWER

J. W. Wonn

Westinghouse R&D Center, Pittsburgh, Pa.

INTRODUCTION

The Borehole Televiewer[1] (BHTV) is a well logging tool which provides an acoustic image of the borehole surface, delineating such important features as wall discontinuities, formation dip, fracture patterns, vugs, and washouts. Demonstrated capabilities include mapping of fracture zones, bedding planes, and other borehole manifestations of the geology. BHTV has also been used in cased wells as an inspection tool to map cavitation, pitting, perforation plugging or enlargement, casing breaches, and other production-related parameters. It is generally agreed that BHTV would be extremely useful during many phases of geothermal resource development.

USGS/Water Resources Department[2] has been conducting field evaluations of BHTV in geothermal reservoirs for some time. Their cooperative efforts with Simplec[3] have resulted in an improved BHTV with extended temperature tolerance. However, efforts to operate the improved tool at temperatures as high as 500°F have been largely unsuccessful to date. The most serious geothermal tool deficiencies appear to be concentrated in the acoustic sensor portion of the tool, as it must withstand direct exposure to the borehole fluid.

Westinghouse[4] is currently under contract with DOE/DGE to develop a geothermal BHTV sensor. Environmental design goals are operation at 275°C (525°F) and 7000 psi and sufficient tolerance to the corrosive borehole fluid. The primary project objective is to demonstrate the operation of a BHTV sensor under simulated geothermal borehole conditions. The developed sensor configuration will follow that of the improved BHTV sensor package so that the resulting technology can be readily incorporated into an experimental geothermal BHTV design.

The basic approach selected is to provide geothermal replacement components for the improved BHTV embodiment rather than completely redesigning the tool. This decision was made for several reasons 1.) sensor problems are essentially materials problems and solutions are considered to be realizable, 2.) the basic BHTV configuration is believed to be functionally effective in geothermal logging, 3.) an improved BHTV tool is available for experimentation, 4.) the approach facilitates relatively low-cost investigation of the usefulness of BHTV in the geothermal environment.

GEOTHERMAL BHTV SENSOR PROBLEMS

The cross section diagram of Figure 1 indicates the various components comprising the sensor. The lead metaniobate piezoceramic disc used to transmit and receive acoustic pulses provides good electro-acoustic performance at temperatures exceeding 275°C and therefore is not a problem. The piezoceramic disc is mounted on a damping material to minimize structural reverberation within the tool which could mask weak received signals. The commonly used damping material is absorptive rubber which is unsatisfactory at 275°C and 7000 psi and must be replaced. Efficient acoustic communication between the piezoceramic and the borehole fluid is accomplished through a protective acoustic window and an intermediate coupling fluid. Traditional BHTV windows are fabricated from temperature intolerant elastomers. Recent efforts toward a high temperature window have focused on polyimide plastics such as Vespel by DuPont. While this material has permitted

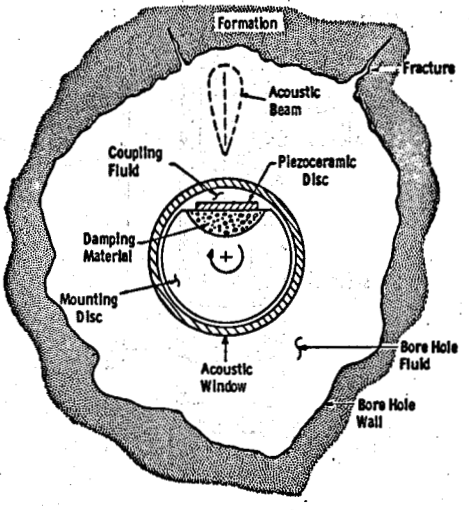


Figure 1 - BHTV Sensor Cross-section

1. Patented by Mobil Research & Development Corp.
2. U.S. Geological Survey-Water Resources, Denver.
3. Simplec Manufacturing Co., Inc., Dallas, Texas.
4. Westinghouse R&D Center, Pittsburgh, Pa.

logging in hotter wells, frequent window failure is reported and the window is initially viewed as a likely problem. A typical internal coupling fluid is synthetic lubricating oil formulated for jet engines. The performance of this fluid is considered questionable under geothermal conditions and is therefore viewed as a potential problem.

BHTV SENSOR DEVELOPMENT PROGRAM PLAN

Three phases of 275°C, 7000 psi, simulated borehole fluid autoclave tests are planned. The final phase involves comprehensive performance testing of a working BHTV sensor package. Prior to this, a sensor replica is to be tested to demonstrate all non-acoustic functional requirements. The initial phase consists of screening candidate materials, components, and fabrication methods necessary to conduct the test program.

Supportive investigation and development of appropriate acoustic materials and location of critical mechanical components are to be conducted in parallel with initial autoclave work. Earlier project work had included a detailed study of two improved Simplec BHTV tools. The major purpose was to establish acoustic performance reference data against which our experimental sensor could be compared. The exercise also provided familiarization with tool embodiment and operation.

Phase I - Screening Tests: A special capsule (Figure 2) was designed to expose candidate sensor materials and components to service-simulative conditions. Capsules were fabricated from 6-inch lengths of 1-inch, Schedule 80, SS 316 pipe, threaded on both ends to accept threaded caps. The end caps compress the perimeter of the candidate window material against a series of concentric sealing grooves machined in the pipe end faces. 1-inch diameter axial holes through the center of the end caps provide simultaneous exposure of window materials to internal coupling fluid on one face and autoclave fluid on the other. The capsule interior is charged with various samples of candidate sensor internal components and then filled with a candidate coupling fluid. Total fluid volume was minimized to reduce volume expansion and the accompanying risk of window rupture. This was done by charging the capsule interior with tabular alumina before installing the coupling fluid.

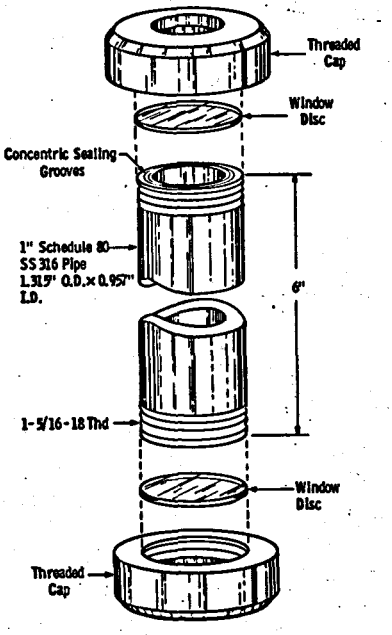


Figure 2 - Assembly diagram of screening test capsule.

Free-flooding capsules were also constructed by replacing the window disc with a perforated stainless steel disc. These capsules were used to evaluate survivability of numerous items requiring direct exposure to the corrosive fluid.

Phase II - Non-acoustic Sensor Tests: Tests are to be accomplished using a replica of the envisioned final form sensor. The replica design is shown in Figure 3 and consists of a SS 316 spool enveloped by a cylindrical shell window. The window will be sealed around the circumference of both end flanges of the spool using a SS hose clamp or equivalent device. The resulting interior chamber will be charged with prototypical transducer assemblies and a coupling fluid. An Inconel bellows will be used to minimize pressure differential across the window as the fluid volume changes. Fill-hole sealing will be accomplished using a metallic or elastomeric o-ring or a Bal-seal. Overall integrity and durability of the replica will be evaluated by testing several versions in the subject autoclave environment.

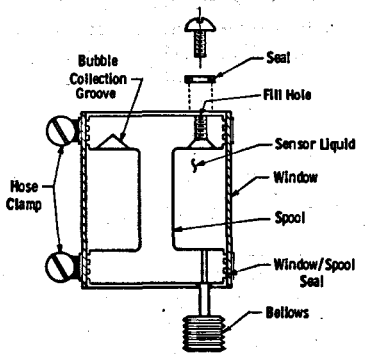


Figure 3 - Cross-sectional view of cylindrical structure comprising sensor replica.

Phase III - Acoustic Sensor Tests: Final tests will be accomplished by providing a special replacement autoclave agitator shaft. This hollow shaft will penetrate the existing packing seal in the autoclave head and will support an operating BHTV sensor package designed around previously demonstrated methods, materials, and components. Sensor leads will be brought out through a special electrical penetration. One or more arrays of stationary acoustic targets (reflectors) will be attached to the autoclave internals. The test concept is indicated in Figure 4.

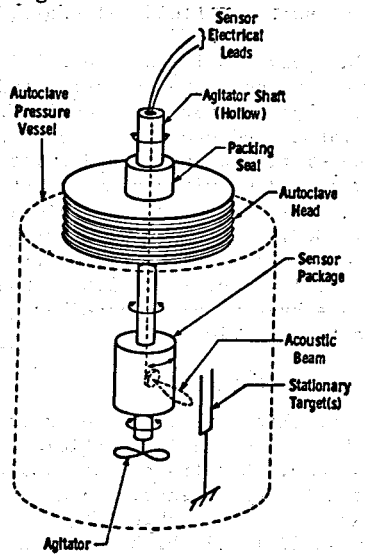


Figure 4 - BHTV sensor evaluation concept.

Since the support shaft permits rotation of the sensor, this apparatus will provide a complete analysis of sensor operation including beam pattern, resolution, and sensitivity measurements. The experimental sensor will be evaluated by comparison with the reference characteristics previously measured on actual BHTV tools.

Satisfactory sensor performance will provide the basis for incorporating the developed technology into an experimental geothermal BHTV tool.

FACILITIES

Autoclave: Fundamental to the development program is availability of specialized autoclave facilities. A commercial autoclave service was located, having a 316 stainless steel vessel capable of achieving 275°C, 7000 psi, and tolerant to simulated geothermal brine. The 10 gallon vessel (Figure 5) is cylindrical with interior dimensions of 11-½" diameter and 19" height. The vessel is resistance-heated from the outside and the internal temperature is controlled by circulating a moderating fluid through spiral wound tubing coils suspended inside the vessel. Continuous or intermittent mixing of autoclave fluid is provided by an agitator affixed to a rotary shaft which penetrates the autoclave head. Temperature and pressure within the vessel can be continuously monitored.

An argon cover gas is being used to pressurize the autoclave fluid. Exact volumes of brine and cover gas under room conditions are noted to permit computation of dissolved gas liquid-vapor phase partition at elevated temperature and pressure.

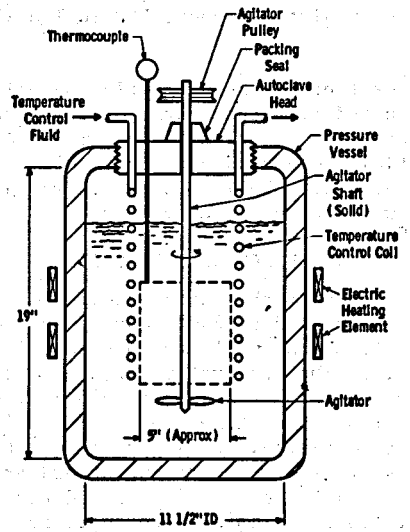


Figure 5 - Cross-section diagram of autoclave.

Simulated Geothermal Brine: Of similar importance was formulating an autoclave fluid representative of the borehole environment. DOE/DGE provided the essentials of a recipe developed for similar evaluations of other geothermal components (elastomers). The following composition is being used:

H_2O	=	990 g/l	
NaCl	=	25.4 g/l	
$NaHCO_3$	=	1.94 g/l	(0.023 M)
$Na_2S \cdot 9H_2O$	=	2.15 g/l	(0.00895 M)
HCl(1M)	=	41.0 ml/l	(0.041 M)

MATERIALS AND COMPONENTS EVALUATED

Acoustic Windows: 1.) Kalrez high-temperature elastomer by DuPont, 2.) ALFAS-150 high-temperature elastomer by ASAHI Glass Co., 3.) Vespel polyimide by DuPont, 4.) TFE Teflon by DuPont, 5.) Graphite-carbon-glass-filled TFE Teflon supplied by Bal-Seal Engineering, 6.) PFN phosphazene supplied by Firestone Tire and Rubber.

Coupling Fluids: 1.) Mobil Jet Oil II, synthetic jet engine lubricant, 2.) Dow Corning DC-210H Silicone oil, 3.) DC-550 high-phenyl silicone oil, 4.) DC-710 high-phenyl silicone oil.

Transducer Assemblies: Rudimentary transducers were constructed consisting of pieces of silver-electroded lead metaniobate bonded to three candidate damping materials using EPOTEK H-20E electrically conductive epoxy. Candidate backing materials were tungsten-filled Stycast 2762FT epoxy, tungsten-filled Duralco 700 epoxy, and a novel tungsten-filled refractory cement. All three materials exhibit excellent damping properties.

Potting/Encapsulating Materials: Cubical samples of two high-temperature epoxies were fabricated, Stycast 2762FT and Duralco 700.

Insulated Wire: Specimens included Mica-glass insulated nickel, silicone dioxide insulated nickel, TFE Teflon insulated copper, FEP Teflon insulated copper.

An assortment of other interesting materials were also evaluated over the course of the screening tests: ethylene propylene (elastomer), Astrel 360 (3M-plastic), Polybutadiene, doryl-glass-mica, 304 SS, Inconel 718, a bellows sample, two Bal-Seals, and 316 Swagelok tubing couplings.

AUTOCLAVE TEST CYCLE

The temperature of the autoclave-liquid system is first slowly raised to 250°F during an overnight period of 12 hours, while the pressure is maintained at 100 psig. The temperature of the autoclave-liquid system is next raised to 525°F over a 7 hour period, during which time the autoclave liquid is continuously stirred. During this time the autoclave pressure rises of its own accord from 100 to 1200 psig. With the autoclave fluid temperature at 525°F, argon gas is used to increase pressure from 1200 to 7000 psig. The total elapsed time from the start of initial heating to the attainment of 525°F, 7000 psig test conditions is 19 hours. The next three hours of testing can best be described as a test-condition stabilization period. The last 14-½ hours of testing can be described as being the specified test period itself. During this time the pressure and temperature are maintained at 7000 psi and 525°F, respectively.

PROJECT STATUS AND RESULTS

Two iterations of screening tests have provided sufficient data for design of the sensor replica. At this time, replica design is complete and components are being fabricated. The following materials, components, and fabrication techniques have been selected for the sensor replica.

Acoustic Window: TFE Teflon, selected for its superior retention of mechanical properties combined with attractive acoustic properties. Carbon- and graphite-carbon-glass-filled TFE Teflon is also being considered but is expected to be more porous.

Coupling Fluid: All four fluids tested appear to be equally satisfactory. Mobil Jet Oil II is slightly favored since it has been successfully used at elevated temperature in direct contact with auxiliary sensor components such as the motor and slip rings. The four subject coupling fluids will be carried over into sensor replica testing.

Transducer Assembly: Lead metaniobate piezoceramic will be used exclusively with silver electrodes replaced by gold. Damping material will be tungsten-loaded refractory cement, selected for its inherent immunity to the environment, its excellent acoustic loss characteristics, and machineability. Piezoceramic elements will be bonded to damping blocks using EPOTEK H-20E electrically conductive epoxy.

Miscellaneous: An Inconel bellows is being incorporated into the replica design to minimize differential pressure across the acoustic window. The bellows will be connected to the replica housing using 316 SS Swagelok tubing fittings. A stainless steel hose clamp is being used to provide the sealing force between the Teflon window and concentric grooves around the housing. TFE Teflon Bal-Seal will be used to seal the fluid fill-hole.

Other screening test results of general interest are as follows: Vespel, the acoustic window material presently used for improved BHTV, virtually disintegrated over the subject test cycle. All non-Teflon plastics and elastomers evaluated are judged unsuitable as acoustic windows. Kalrez sheet exposed to autoclave fluid swelled approximately 100%. Astrel 360 was totally consumed. The two epoxies tested varied from partially to totally consumed. 316 SS Swagelok tubing couplings have provided excellent seals against the autoclave fluid.

CONCLUSIONS

The objective of this work is to demonstrate feasibility of a BHTV sensor having sufficient durability for geothermal use. Results to date indicate that suitable materials, components, and construction methods are available for achieving that goal. Confidence is sufficiently high to permit preliminary design of the Phase III test apparatus. Figure 6 indicates a cross-section of the apparatus which is expected to provide the final sensor verification tests.

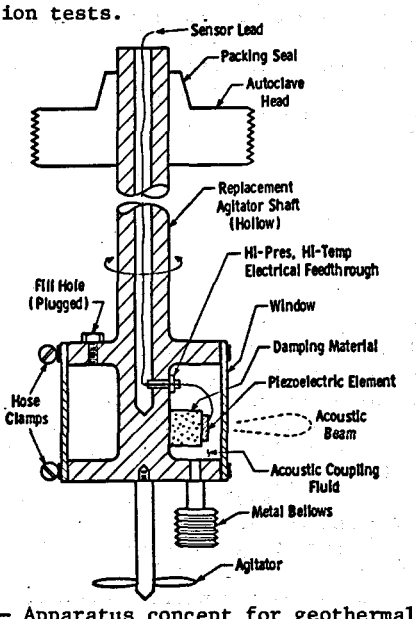


Figure 6 - Apparatus concept for geothermal BHTV sensor feasibility tests.

WESTERN STATES COOPERATIVE DIRECT HEAT GEOTHERMAL PROGRAM OF DOE

Phillip M. Wright and Duncan Foley
Earth Science Laboratory, University of Utah Research Institute, Salt Lake City, Utah

Clayton R. Nichols
U.S. Department of Energy, Division of Geothermal Energy, Washington, D.C.

Paul J. Grim
National Geophysical and Solar-Terrestrial Data Center, NOAA, Boulder, Colorado

Objectives and Scope of Program

The objectives of the Western States Cooperative Direct Heat Geothermal Program are 1) to assist the U.S. Geological Survey in extending the inventory of geothermal resources to include the low temperature ($\pm 20^{\circ} < T < 90^{\circ}$) resources most suitable for direct heat application[1], and, 2) to stimulate reservoir confirmation studies at sites with an apparent but unquantified potential for direct heat application development. It is the belief of the participants that development of direct-heat geothermal resources will have a significant near-term impact by helping to fulfill U.S. energy requirements.

The Program will be conducted separately but concurrently in each of about 15 western states by interdisciplinary groups of people from state agencies, the Division of Geothermal Energy, the U.S. Geological Survey, the University of Utah Research Institute, the National Oceanic and Atmospheric Administration, and Los Alamos Scientific Laboratory. Each state project will be carried out in two phases, which may or may not operate concurrently.

Phase I:
1. Compilation of available data and possibly collection of new data on temperature, temperature gradient, water quality, aquifer productivity, and related peripheral geoscience items as specified further below;
2. Submission of the basic data from (1) above for inclusion in the U.S. Geological Survey computer file GEOTHERM;
3. Publication of maps and reports based on detailed interpretation of the above data compilation.

Phase II:
1. Selection of specific sites for detailed testing by use of the Phase I data base;
2. Geoscience investigations of the above specific sites to select drill test locations;
3. Drill testing for reservoir confirmation and assessment;
4. Publication of site-specific results, including distribution of maps and reports to potential developers of direct-heat geothermal resources.

A summary of the responsibilities of the participating organizations is as follows:

State Agency: Project management within the state, data compilation and interpretation, site-specific geoscience studies and drill-testing, publication of reports and maps, and preparation of resource maps for NOAA publication.

Division of Geothermal Energy: Technical and administrative management of contracts, liaison with U.S. Geological Survey and with other Federal and State organizations.

U.S. Geological Survey: Technical assistance to the state agencies as requested, liaison with other USGS geothermal programs, updating of file GEOTHERM and delivery to NOAA of geothermal data in digital form, and delivery to NOAA of digitized base data for state maps.

University of Utah Research Institute: Management assistance to DGE, technical advice on all phases of the project to the state agency as requested, and project coordination.

National Oceanic and Atmospheric Administration: Publication of state maps showing low temperature geothermal resources.

Los Alamos Scientific Laboratory: For the states of Arizona and New Mexico, management assistance to DGE and technical advice on all phases of the project to the state agencies as requested.

Present Knowledge of Low Temperature Geothermal Resources

Low-and moderate-temperature geothermal resources are relatively plentiful in the western United States. The recently published (1977) map "Geothermal Energy Resources of the Western United States" (produced by Paul J. Grim, NOAA) shows approximately 950 geothermal sites, about

[1]The presently existing geothermal resource inventory published in the U.S. Geological Survey Circular 726 tabulates resources where $T \geq 90^{\circ}C$.

700 of which have measured or geochemically indicated reservoir temperatures less than 100°C. Typically plots of frequency of occurrence vs temperature for these geothermal resources show increasing frequency as temperature decreases, as illustrated in Fig. 1 (data from White, D.E., and Williams, D.L., 1975, Assessment of Geothermal Resources of the United States-1975: U.S. Geol. Surv. Circ. 726, Tables 3, 4, 5) and Fig. 2 (data from Mundorff, J.C., 1970, Major Thermal Springs of Utah: Utah Geol. and Mineral Surv. Water Resources Bull. 13, Table I). The relatively small number of occurrences in the range 90°C -120°C in Fig. 1 is likely due to present lack of an adequate data base.

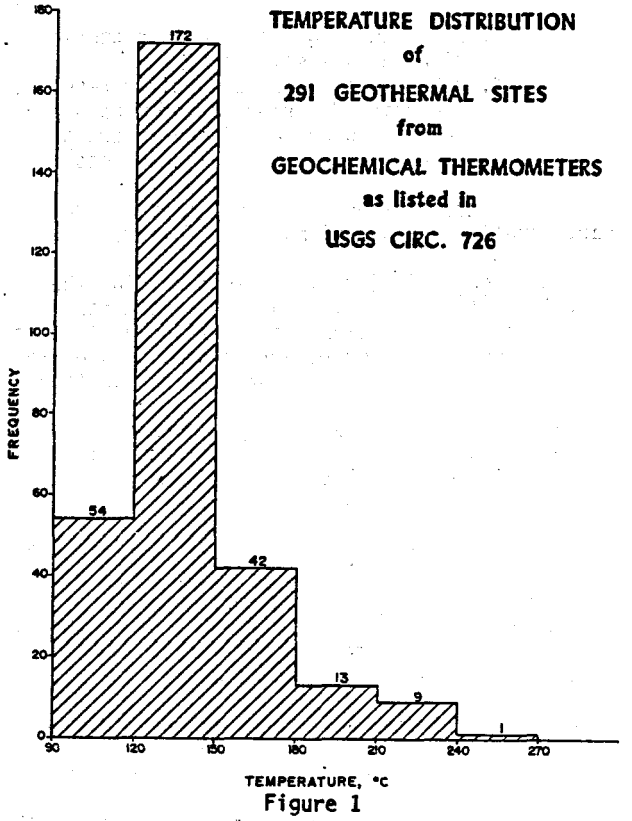


Figure 1

Known occurrences of low-and moderate-temperature geothermal resources in the West seem to be predominantly of two kinds: 1) resources associated with heating of water by recent igneous activity, illustrated by the Geysers, Roosevelt Hot Springs and others, and 2) resources associated with deep circulation of meteoric water, illustrated by the many fault-controlled springs in the Basin and Range. There is good reason to believe that the known resources are only a small portion of the total resource population, and that many discoveries remain.

There are no presently existing, up-to-date maps or reports which give the location and pertinent facts for all known direct-heat geothermal resources for the Western states. Only pieces of the total picture exist. The authors believe that it is very important to compile and interpret existing geothermal resource data, and to present these data in map and report form. It is anticipated that this will be one of the principal methods for promoting the use of this neglected alternate form of energy.

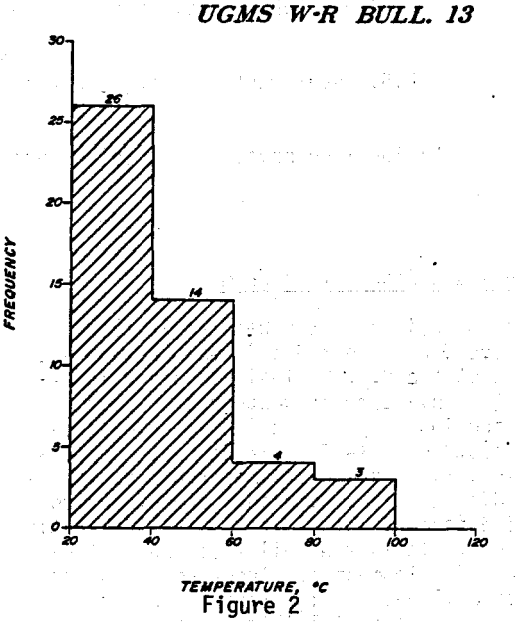


Figure 2

It is also important that collection of new data, especially temperature data in drill holes, be encouraged, both on a regional and on a local scale. A better understanding of crustal temperature distribution will be very important to discovery of new geothermal resources.

Maps and Reports Resulting from Phase I of this Program

One purpose of Phase I of this Program is to produce maps and reports illustrating on a state-by-state basis the location and characteristics of anomalously warm groundwater. The lower cutoff temperature for data compilation is stated as ±20°C only for purposes of discussion. It is apparent that the practical cutoff varies with shallow groundwater temperature, which usually approximates mean annual air temperature. Because focus will be on shallow or otherwise easily available resources, depth information will be important and will be integrated with temperature information. Present plans therefore call for outlining on maps interpreted areas of anomalously warm groundwater, where specifications of what is anomalously warm are determined after considering mean shallow groundwater temperatures, depth of temperature measurement, geothermal gradient, and perhaps other data. Thus, the exact methods of illustration will vary from state-to-state or region-to-region.

A selection of other pertinent geoscience data will be shown on the maps along with geothermal data. The list of these peripheral items includes water quality data, geochemical thermometry data, areas of young igneous activity, faults and lineaments, spring deposits, geochemical indicators, and earthquake epicenters. The primary use of these peripheral geoscience data will be in facilitating interpretation of the geothermal data in terms of probable reservoir location and extent.

The primary results of Phase I will be maps and reports aimed at the public at large, not necessarily at the geoscience community. The many inquiries from the public sector for information on direct-heat geothermal resource location and utilization indicate that potential exists for rapid, significant development using mainly private capital. It is anticipated that by making the results easily understandable to the general public, significant new interest in development of geothermal energy will be stimulated.

Acknowledgements

This work is being sponsored by the U.S. Department of Energy, Division of Geothermal Energy under Contract EG-78-C-07-1701 to the University of Utah and under numerous contracts with state agencies.

2-D INVERSION OF SEISMIC ATTENUATION OBSERVATIONS IN COSO HOT SPRINGS, KGRA

Chi-Yuh Young and Ronald W. Ward

CENTER FOR ENERGY STUDIES
UNIVERSITY OF TEXAS AT DALLAS
RICHARDSON, TEXAS 75080

ABSTRACT

Seismograms from over sixty teleseismic events recorded by a sixteen element vertical component telemetered seismograph array installed by the U. S. Geological Survey in the Coso Hot Springs, Known Geothermal Resource Area (KGRA) have been analyzed to determine the lateral variation of seismic attenuation using the reduced spectral ratio technique. Seismograms of events from the SE and NW azimuths observed at a five station linear array have been used to infer a 2-D Q^{-1} model across the center of the geothermal system. A constrained generalized linear inversion algorithm was used to infer the Q^{-1} model. The model contains 15 cells with boundaries at depth of 5, 20, and 33 km and Q variation from 32 to 890. The zone of high attenuation dips from the surface between Coso Hot Springs and Airport Lake toward the northwest beneath Devil's Kitchen.

Introduction

The thermal state and concentration of partial melting present within a geothermal system are known to contribute to high attenuation of seismic waves. The relationship between observed seismic attenuation and temperature within a geothermal system are not well understood, though there are several proposed mechanisms to explain the observations (Jackson and Anderson 1970). Partial melting (Walsh, 1968, 1969), grain boundary relaxation, "high temperature internal friction background" (Jackson and Anderson, 1970) and vapor domination of porous rocks (White, 1975) are all mechanisms that can be acting within a geothermal system to produce the observed seismic attenuation. Mapping the lateral variation of seismic attenuation has proved to be an effective tool in locating and estimating the potential of a geothermal system. This study is oriented toward the development of quantitative inversion techniques for the observed lateral variation of δt^*.

The area of study is the Coso Hot Springs, Known Geothermal Resource Area (KGRA) located in the southwestern part of the Basin and Range Province of the western U. S. The Basin and Range Province exhibits high heat flow (Blackwell, 1970). The Coso Hot Springs KGRA is underlain principally by Mesozoic granitic and metamorphic units that are covered by upper Cenozoic volcanic flows including basaltic flows, dacitic flows, tuff, and ryholitic domes. A Pleistocene age for most of the basaltic and rhyolitic flows has been determined by K-Ar dating. Fumaroles and hot springs are associated with these flows.

The geothermal system is bounded by a N-NW trending normal fault that borders the eastern scarp of the Sierra Nevada Mountains. On the south a W-NW trending Wilson Canyon fault is the terminus of the geothermal activity. Arcuate ring faults center on the geothermal system.

Extensive geophysical surveys have been conducted across the Coso KGRA including seismic background noise survey, resistivity, magnetotelluric, gravity, aeromagnetic, heat flow, microearthquake, teleseismic P-wave traveltime delays, and seismic refraction. The focal depth of the microearthquakes range from 4 to 8 km with depth increasing toward the northwest. The teleseismic traveltime delays observed at the Coso Hot Springs KGRA are much smaller than those observed above other geothermal systems such as Long Valley, Yellowstone, or Geysers-Clear Lake KGRA's. They are generally less than 0.4 sec. Significant seismic attenuation has been reported by one group based on seismic refraction data (Combs and Jarzabeck, 1977) though a second group found a much lower level of attenuation (Weaver, personal communication).

Data

In September 1975, the U. S. Geological Survey installed a sixteen element vertical component telemetered seismograph array in the Coso Hot Springs, KGRA. About one hundred events were judged suitable for attenuation analysis and were digitized using the facilities of the U. S. Geological Survey in Menlo Park, California. The majority of the events occurred in three different azimuths from the array, SW (Tonga, Fiji, Kermadec), SE (Central and South America), and NW (Aleutians, Kurile Islands, Japan). This study will be limited to those events occurring in NW and SE azimuths from the array. The lateral variation of the seismic attenuation along a NW-SE trending cross section will be used to infer a 2-D Q^{-1} model as illustrated in Fig. 1.

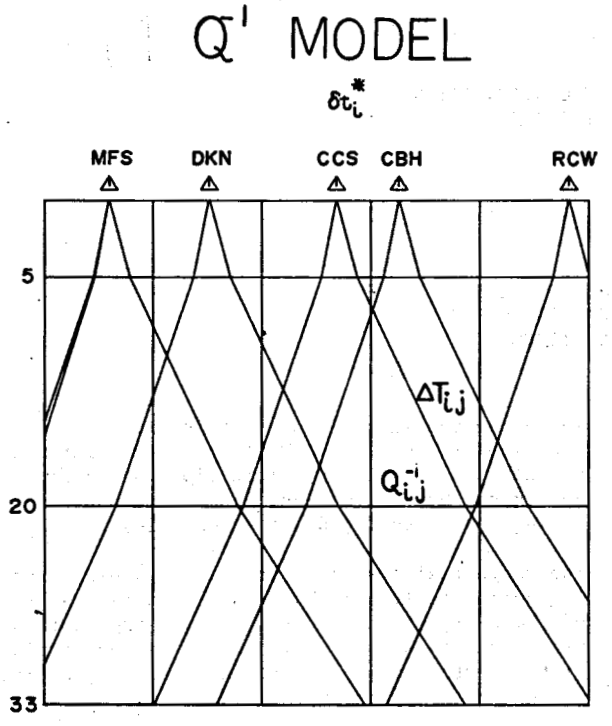


Fig. 1. Ray tracing to 5 stations through a discrete 2-D Q^{-1} model. Depth is in km. ΔT_{ij} is the traveltime of the ray from each event to a station through each cell. Q_{ij}^{-1} will be obtained from generalized linear inversion.

Differential Attenuation

Lateral variation of seismic attenuation exhibits itself in the amplitude, frequency content, and the coda duration of a seismic wave. This information is extracted by applying the reduced spectral ratio technique over a local area (Young and Ward, 1978) such as the Coso Hot Springs, KGRA. The amplitude spectrum of a seismic P-wave is estimated using the Maximum Entropy Method (Burg, 1967; Ulrych and Bishop, 1974).

It has been argued elsewhere (Young and Ward, 1978) that the ratio of the amplitude spectra of teleseismic event observed at two stations can be related to the differential attenuation δt* by

$$R_{ij}(f) = A_i(f)/A_j(f)$$
$$= C_{ij}\exp\{-f(\delta t_i^* - \delta t_j^*\}$$

We assume δt* for the reference stations is zero, which gives

$$\ln R_{ij} = \ln C_{ij} - f\delta t_i^*$$

The δt_i^* is calculated for each station and each of these events. The events are separated into two groups NW and SE, which approach from opposite azimuths.

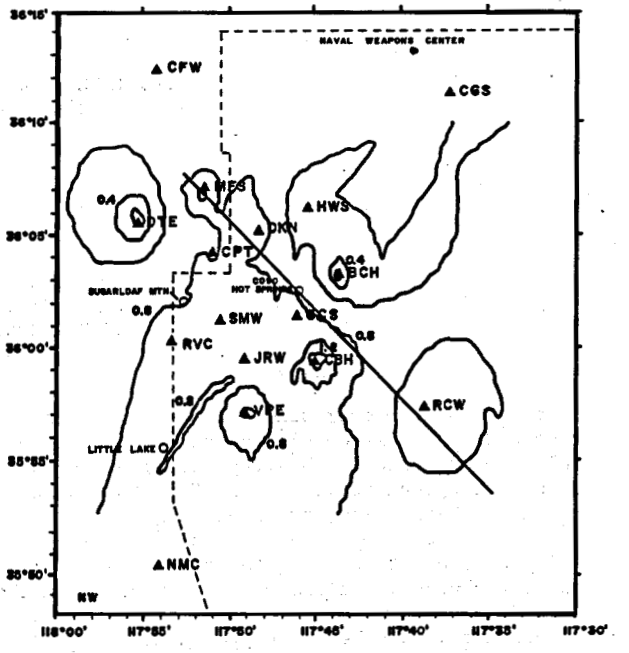


Fig. 2a

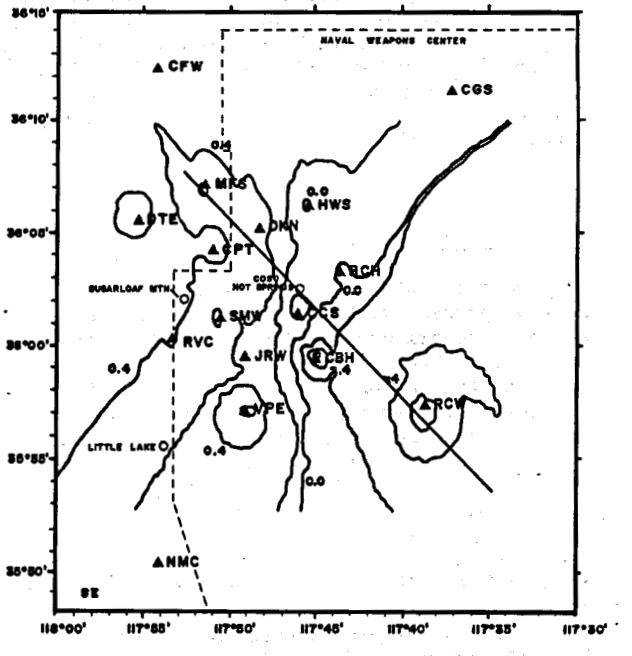


Fig. 2b

Fig. 2. 2-D contours of the averaged differential attenuation factor δt* for events from a) NW and b) SE

As a first step toward inferring a 2-D Q^{-1} model, we compute the average δt* of the events from the SE and NW for each station. Since the P-waves from most events are incident within 15° of the vertical, the observed δt* between events from

the same azimuth should not vary greatly. A contour map of δt^* values appears in Fig. 2a for events from the NW and Fig. 2b for events from the SE.

The attenuation anomalies for events from the NW are greatest near stations VPW (Volcano Peak) and CBH (in the north end of the Coso Basin). The anomalies in the Coso Basin shifts toward the northwest for events from the SE indicating that it is buried at depth. The anomaly above the Volcano Peak is independent of the azimuth of the events indicating a very shallow anomaly.

The qualitative interpretation of these δt^* observations must be improved if a quantiative Q^{-1} model is to be constructed, which gives the value of Q, the depth, and horizontal position within the geothermal system of the zones of low Q. In the following section we outline the mathematics for inverting this data to obtain a discrete Q^{-1} model.

Inversion of δt^* Data

A spherical layer earth model is assumed for the velocity variation. The velocity is a function of the radius only, and varies according to $v=ar^b$ (Julian and Anderson, 1968; Bullen, 1965), where a and b are constant for each layer. The velocity model of Herrin et al (1968) is used. The traveltime of the ray through each cell of a 2-D Q^{-1} model (Fig. 1) is calculated as outlined by Julian and Anderson (1968). The differential attenuation factor observed at a station for each event can be written

$$\delta t_j^* = \pi \sum_{ray} \Delta T_{ij} \, (Q^{-1})_i \qquad 1$$

where the summation is taken over the cells through which the ray passes and ΔT_{ij} is the traveltime to the jth station through the ith cell.

A generalized linear inversion algorithm is developed for discrete cells based on equation 1, and Wiggins (1972) and Jackson (1972). The inversion formulation assumes that Q^{-1} is an unknown parameter in each cell of the model. The first order perturbation of the unknown parameter is given by:

$$AX=\pi \begin{bmatrix} \Delta T_{11} & \cdots & \Delta T_{n1} \\ \vdots & & \vdots \\ \Delta T_{1m} & \cdots & \Delta T_{nm} \end{bmatrix} \begin{bmatrix} \Delta(Q_1^{-1}) \\ \vdots \\ \Delta(Q_n^{-1}) \end{bmatrix} =$$

$$= \begin{bmatrix} \Delta\delta t_1^* \\ \vdots \\ \Delta\delta t_m^* \end{bmatrix} = Y \qquad 2$$

The original traveltime matrix, A, is weighted by the observational errors, such that $A=S^{-\frac{1}{2}}AW^{\frac{1}{2}}$, where W is a constant weighting factor. The goal of the inversion iteration is to minimize $X^TW^{-1}X$. The generalized inverse matrix, H, the resolution matrix, R, and information density matrix S are given by:

$$H = V\Lambda^{-1}U^T \qquad 3$$

$$R = HA = VV^T \qquad 4$$

$$S = AH = UU^T \qquad 5$$

where U contains k data eigenvectors of length m associated with the observation δt_j^*,

Λ is a diagonal eigenvalue matrix, and

V contains k model eigenvectors of length n associated with the unknown parameters $\Delta(Q_i^{-1})$.

If eigenvalues fall below a threshold of 1% of the maximum they are omitted from the calculation.

This formalism permits the inversion of δt^* observations to obtain a Q^{-1} model for any geometry. In the present case a 2-D Q^{-1} model is inferred.

Q^{-1} Model

Seismogram from sixteen events occurring in NW and SE azimuths and observed at a NW-SE trending array of five stations (MFS, DKN, CCS, CBH, and RCW) were analyzed to obtain δt^* assuming a constant Q^{-1}. These observations formed the input data to a generalized inversion algorithm to determine a 2-D discrete Q^{-1} model for the Coso Hot Springs, KGRA. Layer boundaries were at depths of 5, 20 and 33 km for this preliminary model. A total of 15 cells of constant Q^{-1} were used. The model eigenvectors indicated that the Q^{-1} value was resolved accurately in every cell except the deepest cell beneath station RCW.

The 2-D Q^{-1} model derived (see Fig. 3) from teleseismic P-waves observed at the Coso Hot Springs, KGRA has a very low Q of 34 (high attenuation) in the near surface layer (upper 5 km) extending from the Coso Hot Springs toward the SE into the Airport Lake. This area is covered by Quaternary volcanics which are quite "lossy". The attenuation effect of surficial layers must be separated from the effect of partially molten zones. Both effects are probably operating near the surface. The zone of high attenuation dips toward the NW beneath Devil's Kitchen and then reverses itself moving back toward the SE. The attenuation decreases with depth.

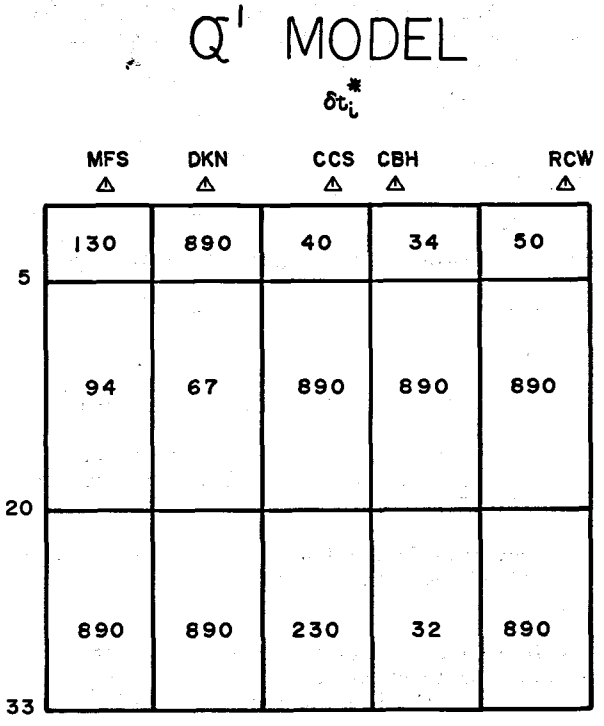


Fig. 3. 2-D Q^{-1} model derived from generalized linear inversion of δt* observations from sixteen events observed at 5 stations. Numbers in the cells are the value of Q.

In future studies these techniques will be extended to 3-D models using additional events and stations from the δt* observations at the Coso Hot Springs, KGRA. The resolution of these observations will be investigated by determining Q^{-1} models with different layer boundaries and many times the number of cells.

Research supported by the National Science Foundation, NSF Grant AER75-23619 and by the U. S. Geological Survey, Department of the Interior, under the USGS Grant No. 14-08-001-G-426.

References

Blackwell, D. D., (1970), The thermal structure of the continental crust, AGU, Geophysical Monograph, v. 14, p. 169-184.

Bullen, K. E., (1965), An introduction to the theory of seismology, 3rd ed., Cambridge Univ. Press, London

Burg, J. P., (1967), Maximum entropy spectral analysis: Paper presented at the 17th Annual Internation Meeting, Soc. of Exploration Geophysicists, Oklahoma City, Oklahoma, October 31, 1967.

Combs, J. and D. Jarzabeck, (1977), Preliminary seismic wave attenuation and Poisson's ratio studies at the Coso Geothermal Area, Calif.: The Coso Geothermal Project. Technical Report #5, Center for Energy Studies, U. T. at Dallas, Richardson, Texas.

Jackson, D. D., (1972), Interpretation of inaccurate, insufficient and inconsistent data, Geophys. J. R. astr. Soc., v. 28, p. 97-109

Jackson, D. D. and D. L. Anderson, (1970), Physical mechanism of seismic wave attenuation, Review of Geophy. and Space Physics v. 8, p. 1-63.

Julian, B. R. and D. L. Anderson, (1968), Traveltimes, apparent velocities and amplitudes of body waves, Bull. Seism. Soc. Am., v. 58, p. 339-366.

Ulrych, T. J. and T. N. Bishop, (1975), Maximum entropy spectral analysis and autoregressive decomposition, Review of Geophys. and Space Physics, v. 13, p. 183-200.

Walsh, J. B., (1968), Attenuation in partially melted material, J. Geophys. Res., v. 73, p. 2209-2216.

Walsh, J. B., (1969), A new analysis of attenuation in partially melted rock, J. Geophys. Res., v. 74, p. 4333-4337.

White, J. E., (1975), Computed seismic speeds and attenuation in rocks with partial gas saturation: Geophysics, v. 40, p. 224-232.

Wiggins, R. A., (1972), The general linear inverse problem: Implication of surface waves and free oscillations for earth structure, Review of Geophys. and Space Physics, v. 10, p. 251-285.

Young, Chi-Yuh and Ward, R. W., (1978), Attenuation of teleseismic P-waves in Geysers-Clear Lake Region, California, to be published in U. S. Geol. Survey Prof. Paper.

STREAMING POTENTIALS RESULTING FROM THE DESCENT OF METEORIC WATER--A POSSIBLE SOURCE MECHANISM FOR KILAUEAN SELF-POTENTIAL ANOMALIES

Charles J. Zablocki

U.S. GEOLOGICAL SURVEY
BOX 25046, DENVER FEDERAL CENTER
DENVER, COLORADO 80225

From extensive self-potential (SP) surveys made on Kilauea Volcano, Hawaii, Zablocki (1976) concluded that all of the mapped positive SP anomalies, upwards to 1.5 volts in magnitude, could be related unambiguously and exclusively to subsurface localizations of heat. This conclusion was the basis for recommending the siting of a geothermal test hole for the Hawaii Institute of Geophysics in the vicinity of a prominent SP anomaly in Puna, Hawaii (Zablocki, 1977). The subsequently drilled hole (HGP-A) encountered high-temperature fluids at depth. Various reservoir tests are currently underway to assess its potential as a viable source for electric power generation.

The apparent success of the Puna SP survey has further increased the desire to understand the principal source mechanism responsible for these distinct and large-magnitude anomalies. If the mechanism were clearly understood, then the SP data might ultimately be helpful in quantifying the configuration of the heat sources and the mode of distribution of the associated hydrothermal fluids.

No definitive mechanism has as yet been established. Various types of evidence, however, appeared to favor an electrokinetic phenomenon as the primary source. The potentials were thought to result from the differential displacement of certain ion species in the waters that overlie deeper-seated hot zones. Other potential-generating sources such as isothermal diffusion-adsorption or oxidation/reduction were discounted as probable primary sources on the basis of their limited electric potential capacity or the many restrictive conditions required to produce them. Thermoelectric processes, involving the direct interaction between liquid and subsolidus lava, also were discounted because of the unrealistically shallow depths to magma inferred from analysing some of the SP anomalies.

A thermoelectric process that was considered a possibility is thermal diffusion, a process that gives rise to a potential gradient whenever a temperature gradient exists in an electrolyte. This potential gradient arises from the tendency of the ions to diffuse at different speeds, the polarity and magnitude being such as to equalize their diffusion rates. Reported values of thermal potential coefficients of common electrolytes are of the order of 0.2 to 0.5 millivolt/C° (Tyrrell and Colledge, 1954). However, a major inconsistency of this process with some mapped dipolar anomalies is the impractically shallow depths and short lateral distances at which a reversal in a large temperature gradient would be required to explain large magnitude negative potentials on the immediate flanks of similarly large magnitude positive potential anomalies.

It is reasonable to expect that all of the large SP anomalies on Kilauea result from a common principal mechanism. A phenomenological model that would hold up to explain one type of anomaly should also be expected to hold up for another. To this end, a mechanism that seemed to be generally compatible with the observed anomalies and which required a thermally-induced, ion-displacement process was electrofiltration. Electrofiltration (streaming) potentials can arise when a differential fluid pressure exists in the pore-water system of a rock (Dakhnov, 1959). Ions of the same polarity in the pore water are absorbed preferentially along the pore walls, leaving an excess of opposite-charged ions in the pore water. Charge separation occurs when the water flows. Most rocks absorb cations, so that the mobile anions will effect a potential gradient that is positive in the direction of the fluid flow. The magnitude of the potentials is directly proportional to the differential pressure, the ion-adsorption efficiency of the rock (zeta potential), and the dielectric constant and resistivity of the pore water; it is inversely proportional to the fluid viscosity.

The possibility of large streaming potentials arising in a hydrothermal convection cell that might be formed above a magma body or high temperature lavas would depend largely on the dynamic pressures developed and the nature of the convecting interstitial fluids. It seemed reasonable that the high rock permeabilities, abundant ground water, and the shallow heat sources in Kilauea would be adequate to support fluid convection. Further, if the pore fluid at some depth existed partially in a vapor phase, then the electrical conductivity and viscosity of the fluid might be markedly reduced. Accordingly, these factors would tend to produce larger electrofiltration coefficients than those commonly reported for moderately conductive electrolytes (a few to tens of millivolts per atmosphere).

Notwithstanding the qualitative merits that this model has for explaining the source for Kilauean anomalies, a recent critical evaluation of a few anomalies has brought out some inconsistencies. The wavelength of some anomalies suggest top-of-source depths to be as shallow as 30 meters. Resistivity sounding measurements made in these areas indicated that the flanking lavas are undersaturated in water to depths of about 600 meters (Zablocki, 1976; 1978). Below these depths, lower resistivities were ascribed to the local water table. It is difficult to envision, therefore, how a well-developed convection cell could occur at such shallow depths in the undersaturated medium. Another inconsistency, or enigma, that is confronted when applying this, or any other model in which the potentials are assumed to be derived from a buried localized source, is the virtual absence of perturbations of the surface potentials due to some nearby large-scale topographic features. For example, a large magnitude (1.5 volts) and broad (1.5 x 1.0 km) anomaly is associated with a correspondingly broad fumarolic area located on the north rim of Kilauea Caldera (Zablocki, 1976). Surprisingly, however, the large potentials remain essentially constant right up to the edge of the caldera rim where the near-vertical scarp is about 100 meters above the caldera floor. Similarly, large and steep potential gradients that are developed on the flanks of some anomalies indiscriminately transect several large, deep pit craters with no apparent deviations that one might expect if there was a lateral component to the potential-derived currents. The lack of such deviations has probably contributed more to the exceptional smoothness of the mapped potential distributions in Kilauea than any other single factor.

The foregoing observations have prompted me to seek yet another mechanism that would be compatible with all observations as well as be hydrogeologically reasonable. In the Puna SP survey mentioned earlier, it was observed that a large, smooth, potential gradient tended to conform with the topography. The potentials were more negative upslope than toward the shoreline (water table). The linear gradient in this area was about -2 mv/m. In a research hole drilled near Kilauea's summit, the potential difference measured between the surface and the local water table (488 m deep) was -655 mv (-1.35 mv/m). An SP borehole log, made in conjunction with electrical logs, showed that the gradient was fairly constant in the zone above the water table.

These observations strongly indicate that the vertical descent of abundant meteoric water through the vadose zone can give rise to significantly large streaming potentials. Resistivity soundings made in non-thermal areas around Kilauea's summit (elevation $\sim$ 1 km above sea level) indicate great depths to the water table. Even the anomalously shallow water table encountered in the summit drill hole (610 m above sea level) represents a substantially thick vadose zone.

The proposed mechanism, then, involves the assumption that the surface potential intensities are directly proportional to the thickness of the vadose zone. Accordingly, the apparent positive anomalies developed over thermal areas may simply reflect the shallow depths to which cool meteoric water may descend before encountering higher temperature fluids rising above a deeper heat source. The flanking cool lavas would allow the water to descend to greater depths (i.e., to water table). The thicker vadose zone (200-700 m) would result in large negative potentials at the surface whereas the thinner zone directly over the thermal area would be significantly less negative. A resulting potential profile across the thermal feature would therefore appear as a positive polarity anomaly.

This model would explain the shallow depths noted for some of the anomalies, and because the potentials are generated essentially in a vertical direction, the model would explain the virtual absence of perturbations in the vicinity of local topographic features. Also, this model does not require an unusually large potential-generation scheme to account for some of the largest magnitude anomalies that have ever been reported. Enhancement of the anomalies may result from the ascending water vapor over the thermal area and from a large flux of liquid-phase water diverted laterally and downward along the immediate flanks of the thermal zone.

Unlike some of the other proposed mechanisms, this new scheme should be amenable to testing by some theoretical and experimental studies. If such studies should support this concept, then we can begin to assess the quantitative utility of SP measurements in Hawaii.

References Cited

Dakhnov, V. N., 1959, Geophysical well logging: translated in English in Colorado School Mines Quart., v. 57, no. 2, April 1962.

Tyrrell, H. J. V., and Colledge, R., 1954, Thermal diffusion potentials in non-isothermal electrolytic systems-part 3: Trans. of Faraday Soc., v. 50, part 10, no. 382, pp. 1056-1066.

Zablocki, C. J., 1976, Mapping thermal anomalies on an active volcano by the self-potential method, Kilauea, Hawaii, in Proceedings of the Second U.N. Symposium on the development and use of geothermal resources, San Francisco, Calif., May 1975, v. 2: pp. 1299-1309.

Zablocki, C. J., 1977, Self-potential studies in East Puna in Geoelectric studies on the east rift, Kilauea Volcano, Hawaii Island: Hawaii Inst. Geophys., Univ. of Hawaii Tech. Rept. HIG-77-15, pp. 175-195.

Zablocki, C. J., 1978, Applications of the VLF induction method for studying some volcanic processes of Kilauea Volcano, Hawaii: Journ. of Volcan. and Geotherm. Res., v. 3 (in press).